
Electronic Thesis and Dissertation Repository

2-12-2016 12:00 AM

Reframing the Mammoth Steppe: Examining Mammoth Steppe Ecology Using Carbon and Nitrogen Isotopic Compositions of Megafauna Collagen

Rachel E. Schwartz-Narbonne
The University of Western Ontario

Supervisor
Dr. Fred Longstaffe
The University of Western Ontario

Graduate Program in Geology
A thesis submitted in partial fulfillment of the requirements for the degree in Doctor of Philosophy
© Rachel E. Schwartz-Narbonne 2016

Follow this and additional works at: <https://ir.lib.uwo.ca/etd>

 Part of the [Biogeochemistry Commons](#)

Recommended Citation

Schwartz-Narbonne, Rachel E., "Reframing the Mammoth Steppe: Examining Mammoth Steppe Ecology Using Carbon and Nitrogen Isotopic Compositions of Megafauna Collagen" (2016). *Electronic Thesis and Dissertation Repository*. 3495.
<https://ir.lib.uwo.ca/etd/3495>

This Dissertation/Thesis is brought to you for free and open access by Scholarship@Western. It has been accepted for inclusion in Electronic Thesis and Dissertation Repository by an authorized administrator of Scholarship@Western. For more information, please contact wlsadmin@uwo.ca.

Abstract

The Pleistocene mammoth steppe was a vast biome that stretched from northwestern Europe to central Canada. A diverse set of megaherbivore and megacarnivore species lived within this biome and there was significant ecosystem faunal and floral homogeneity. At the end of the Pleistocene, this biome disappeared, with the extinction or extirpation of many of the megafaunal species that inhabited it. This thesis reconstructs the ecology of the mammoth steppe using the isotopic compositions of carbon and nitrogen from megafaunal collagen. The reconstruction is done at a variety of ecological scales, beginning with individual animal- and season-specific isotopic studies of antlers, and then comparison to bones from the same species. This provides a framework to understand the habitat and diet of antlered species through the Pleistocene and into the Holocene. Non-ruminant species ecology is assessed using the carbon and nitrogen isotopic compositions of the individual amino acids that comprise their bulk collagen. The compound-specific technique allows metabolic and habitat or dietary effects to be separated and diets to be classified. These studies indicate woolly mammoths ate a distinct diet, likely comprising decayed plants, and that some horses shared this dietary niche. The Pleistocene giant beaver consumed aquatic plants, while the mastodon consumed unmodified terrestrial plant material. Finally, the bulk collagen isotopic compositions measured in this work as well as reviewed from the literature are compiled and the mathematical tool SIBER (Stable Isotope Bayesian Ellipses in R) is used to define the isotopic niche for multiple megaherbivore species at different times and sites across the mammoth steppe. This, combined with the dietary and habitat information gleaned from the antler and amino acid isotopic measurements, allows an in-depth analysis of mammoth steppe ecology. Before the LGM (Last Glacial Maximum), most species occupied consistent isotopic niches between sites across the mammoth steppe, suggesting consistent diets or habitats during the pre-LGM period. These isotopic niche patterns changed during the LGM, and the patterns were not re-established post-LGM or in the Holocene. These changes suggest that the ecosystem suffered a major disturbance during the LGM, before the extinctions that occurred at the end of the Pleistocene.

Keywords

mammoth steppe, Pleistocene, stable isotopes, carbon isotopes, nitrogen isotopes, collagen, amino acid isotopes, SIBER, serial sampling, paleoecology

Co-Authorship Statement

Chapter 3 of this thesis was co-authored by Dr. Fred J. Longstaffe, Dr. Jessica Z. Metcalfe and Dr. Grant Zazula. F.J.L. funded the study, participated in study conception, sample collection, data reduction and interpretation and revised the manuscript. J.Z.M. participated in sample collection, data interpretation and provided substantive comments on the manuscript. G.Z. provided access to the samples and substantive comments on the manuscript.

Artwork for figures was commissioned from Katherine Allan, and her work is acknowledged in the figure captions.

Epigraph

*This isotope is so dope
I got hope
Lookin' through my microscope
On high power,
Get a glower
They're supervising; I'm socializing, minimizing the work that I'm doing
And I'm reviewing my data, but my results are nada.
I won't listen to the hate,
Those who can't appreciate,
Say this field ain't yo' fate,
So I'll be showin' defiance with a paper in Science
Yeah*

- By Heather Schwartz-Narbonne

Acknowledgments

Thank you to my supervisor, Fred Longstaffe, for his support, guidance and wisdom in every aspect of my studies and in my academic life.

I'd like to thank the lab staff who helped so much with my lab work, and who guided me in troubleshooting the inevitable complications. Kim Law, Li Huang, Grace Yau and Lisa LeClair all helped me navigate lab work. I had invaluable assistance and collaboration in the amino acid protocol implementation from Karyn Olsen, Nadia Dildar and Joanne Potter. Tessa Plint was my assistant in serial sampling antlers, and her technical and visual abilities were invaluable. I also want to thank Farnoush Tahmasebi who took me on as a field assistant for her work, and let me experience sample collection from the field – and to thank her for always being available for a scientific discussion at a moment's notice! Jessica Metcalfe was my peer mentor and guide through this project, and her advice and expertise was invaluable.

Sample collection was an integral part of this thesis, and I'd like to thank the institutions that provided samples as well as the people who helped me with the sampling. I'd like to thank Grant Zazula at the Yukon Government Palaeontology Program. I'd like to thank Chris Jass and Peter Milot at the Royal Alberta Museum. I'd like to thank Patrick Druckenmiller and his team at the University of Alaska Museum Earth Sciences. I'd like to thank the American Museum of Natural History.

Funding for this research was provided by a Natural Sciences and Engineering Research Council of Canada (NSERC) Discovery Grant (F.J.L.), an NSERC Canada Graduate Scholarship (R.S.N.), an NSERC Postgraduate Scholarship (R.S.N.) and an Ontario Graduate Scholarship (R.S.N.). Laboratory infrastructure was funded by the Canada Foundation for Innovation (F.J.L.) and the Ontario Research Fund (F.J.L.). Funding for radiocarbon dating and travel was provided in part by the Western Graduate Thesis Research Award (R.S.N.) Additional time for research was funded through the Canada Research Chairs program (F.J.L.).

I had an amazing opportunity to learn the techniques of radiocarbon dating at the University of Arizona, and I'd like to thank Greg Hodgins and all the staff at the NSF Arizona AMS Laboratory for making that possible.

The artwork for my figures was drawn by Katherine Allan, who has the ability to turn my words into beautiful and informative diagrams. Tessa Plint, Andrea Prentice and Nicolle Bellissimo had magic abilities to make my figures informative, and thank you for your help.

I'd like to thank all my officemates in B&G 1031, past and present, for their support and friendship throughout the years. You've made my workspace into a second home. I'd like to thank Marie for her help and friendship. I'd also like to thank all the members of the LSIS group, past and present, who have given me invaluable insights into my project as well as friendship. In particular, I'd like to thank Andrea Prentice for everything she's done to keep me going. I can't possibly list all the ways she's helped me.

I have an incredibly supportive family, both scientifically and emotionally. Thank you for everything. I'd also like to thank my partner, Tim, for his incredible support and love. I couldn't have done it without you. And I'd like to thank Nimmy and Malk Harington for their love.

Table of Contents

Abstract.....	i
Co-Authorship Statement.....	iii
Epigraph.....	iv
Acknowledgments.....	v
Table of Contents.....	vii
List of Tables.....	xii
List of Figures.....	xiii
List of Appendices.....	xxi
Chapter 1.....	1
1 Introduction.....	1
1.1 Thesis objectives.....	1
1.2 The mammoth steppe.....	1
1.2.1 The mammoth steppe ecosystem.....	1
1.2.2 Megafaunal extinctions on the mammoth steppe.....	4
1.3 Stable isotopes.....	6
1.3.1 Carbon isotopes.....	6
1.3.2 Nitrogen isotopes.....	10
1.3.3 Combined carbon and nitrogen isotopic analysis.....	12
1.4 Previous isotopic investigations of collagen on the mammoth steppe.....	13
1.5 Dissertation.....	15
1.5.1 Goals of the dissertation.....	15
1.5.2 Organization of the dissertation.....	18
1.6 References.....	19
Chapter 2.....	34

2	Carbon and nitrogen isotopic analysis of antlers as a tool to investigate seasonal shifts in ecology	34
2.1	Introduction.....	34
2.1.1	Importance of investigating seasonal variation.....	34
2.1.2	Antler and bone growth	36
2.1.3	Modern seasonal diet and habitat.....	38
2.1.4	Stable Isotopes	40
2.2	Methods.....	46
2.2.1	Sample selection	46
2.2.2	Collagen extraction	46
2.2.3	Stable isotope measurements	47
2.2.4	Radiocarbon dating	48
2.2.5	Mathematical treatment	48
2.3	Results.....	49
2.3.1	Preservation.....	49
2.3.2	Collagen stable isotope compositions.....	49
2.3.3	Isotopic variation over time	54
2.4	Discussion.....	54
2.4.1	Antler-specific physiological factors	54
2.4.2	Seasonal, yearly, and inter-annual variation	59
2.5	Conclusion	63
2.6	References.....	64
	Chapter 3.....	76
3	Solving the woolly mammoth conundrum: amino acid ¹⁵ N-enrichment suggests a distinct forage or habitat.....	76
3.1	Introduction.....	76
3.2	Methods.....	78

3.2.1	Bulk collagen nitrogen isotope analysis	78
3.2.2	Amino acid nitrogen isotope analysis	80
3.2.3	Radiocarbon dating	81
3.3	Results.....	81
3.4	Discussion and conclusion.....	82
3.5	References.....	85
Chapter 4	89
4	Ecology of Pleistocene Old Crow revealed by amino acid carbon and nitrogen isotopic compositions	89
4.1	Introduction.....	89
4.1.1	Mammoth steppe ecology	89
4.1.2	Nitrogen isotopic compositions	90
4.1.3	Carbon isotopic compositions.....	95
4.1.4	Inter-tissue variation	100
4.1.5	Site	101
4.2	Methods.....	102
4.2.1	Sample selection	102
4.2.2	Collagen extraction and measurement	102
4.2.3	Hydrolysis, derivatization and measurement of amino acid isotopic compositions	103
4.2.4	Amino acid profiles.....	107
4.2.5	Radiocarbon dating	110
4.2.6	Mathematical treatment	110
4.3	Results.....	110
4.3.1	Evaluation of collagen extraction and hydrolysis technique	110
4.3.2	Sample preservation.....	111
4.3.3	Bulk collagen stable isotope compositions.....	111

4.3.4	Inter-tissue differences	113
4.3.5	Amino acid $\delta^{15}\text{N}$	115
4.3.6	Amino acid $\delta^{13}\text{C}$	117
4.4	Discussion.....	123
4.4.1	Inter-tissue variation	123
4.4.2	Dietary patterns suggested by $\delta^{15}\text{N}$	124
4.4.3	Dietary patterns suggested by $\delta^{13}\text{C}$	127
4.5	Conclusion	131
4.6	References.....	132
Chapter 5	145
5	Insights from mathematical analysis of isotopic niche on the mammoth steppe.....	145
5.1	Introduction.....	145
5.1.1	The Pleistocene mammoth steppe.....	145
5.1.2	Stable isotopes	148
5.2	Methods.....	154
5.2.1	Sample selection	154
5.2.2	Sample preparation and analysis.....	155
5.2.3	Mathematical treatment	157
5.3	Results.....	158
5.3.1	Age binning approaches.....	158
5.3.2	Species proportions at each site	160
5.3.3	Variation between species at a given site and time period	161
5.3.4	Variation between sites for a given species and time period	173
5.3.5	Variation between time periods for a given species and site	184
5.4	Discussion.....	187
5.4.1	Pre-LGM mammoth steppe.....	187

5.4.2	Response of the mammoth steppe to environmental changes over time	193
5.5	Conclusion	196
5.6	References	197
Chapter 6	209
6	Conclusions	209
6.1	Summary of the thesis	209
6.2	Mammoth steppe ecology and extinction	210
6.3	Future work	212
6.4	Concluding remarks	213
6.5	References	214
Appendices	217
Curriculum Vitae	393

List of Tables

Table 2.1 Comparison of the isotopic composition of bone and antler in a population for various species and sites. The difference in carbon isotopic composition between bone and antler for one species at one site, or $\delta^{13}\text{C}_{\text{Bone}} - \delta^{13}\text{C}_{\text{Antler}}$, is given as $\Delta^{13}\text{C}_{(\text{Bone-Antler})}$. The significance of a Mann-Whitney-Wilcoxon test between the two tissues is given as p value (Bone, Antler), with differences $p \leq 0.05$ treated as significant and shown in bold..... 53

Table 4.1 $\delta^{15}\text{N}$ for bulk collagen and individual amino acids. The nitrogen isotopic compositions of the specimens' amino acids (Ala = alanine, Val = valine, Gly = glycine, Leu = leucine, Thr = threonine, Pro = proline, Glu = glutamate, Phe = phenylalanine and Hyp = hydroxyproline) and bulk collagen are listed for all samples, along with the standard deviation (SD) for triplicate measurements of each amino acid. The average $\delta^{15}\text{N}$ (and SD) for each species or group of animals is also provided. Peaks that did not give reliable isotopic compositions are listed as ND (not determined). Except for sample YT83, the phenylalanine, glutamate and bulk collagen isotopic compositions were previously reported (Metcalf, 2011; Metcalfe et al., 2010; Schwartz-Narbonne et al., 2015). RD = root dentin, D = crown dentin, B = bone, C = cementum and T = tusk. 106

Table 4.2 $\delta^{13}\text{C}$ for bulk collagen and individual amino acids. The carbon isotopic compositions of the specimens' amino acids and bulk collagen are listed for all samples, along with the SD of duplicate measurements for the amino acids. Amino acids and tissues are labelled as in Table 1. The average $\delta^{13}\text{C}$ (and SD) for each species or group of animals is also provided. The bulk collagen isotopic compositions of the mammoths and mastodons were previously reported (Metcalf, 2011; Metcalfe et al., 2010)..... 109

Table 4.3 $\Delta^{13}\text{C}$ of individual amino acids normalized to bulk collagen $\delta^{13}\text{C}$. $\Delta^{13}\text{C}_{\text{Normalized}} = \delta^{13}\text{C}_{\text{Amino Acid}} - \delta^{13}\text{C}_{\text{Bulk}}$. The average $\Delta^{13}\text{C}$ and SD for each species or group of animals is also listed. The average SD of the average $\Delta^{13}\text{C}$ for each species is also listed. 122

Table 4.4 Linear discriminant analysis (LDA) classification of herbivore and carnivore diets. The most probable diet of each specimen is indicated, along with the posterior probabilities of these classifications. 125

List of Figures

Figure 1.1 The traditional boundaries of the mammoth steppe are shown in red. Higher altitudes are represented by darker shades of grey. Artwork by Katherine Allan.	2
Figure 1.2 Conceptual diagram illustrating the relative carbon and nitrogen isotopic compositions of common modern terrestrial tundra vegetation.	7
Figure 2.1 Sites included in this study: ED. Edmonton; HI. Herschel Island; KD. Klondike; NS. North Slope; SK. Selawik. Darker shades of grey represent higher altitudes. Art by Katherine Allan.	35
Figure 2.2 Sampling strategy: a. Conceptual model of the timing of tissue formation in cranial bone (right occipital condyle) versus antler. Art by Katherine Allan; b. Outermost, outer and inner antler tissue; c. An example of the sampling pattern (arrows) for a caribou skull and antler. Photograph by Tessa Plint.	37
Figure 2.3 (left) Carbon isotopic compositions of serially sampled antler collagen (Herschel Island; Klondike): a. caribou antler, post-bomb; b. caribou antler; c. caribou antler, >41,100 ¹⁴ C BP; d. caribou antler, 29,570±970 ¹⁴ C BP; e. elk antler, 11,675±45 ¹⁴ C BP and h. moose antler, 1,363±35 and 1,197±27 ¹⁴ C BP. Black stars represent samples from Herschel Island; blue diamonds represent samples from the Klondike.	50
Figure 2.4 (right) Nitrogen isotopic compositions of serially sampled antler collagen. Description as in Figure 2.3.	50
Figure 2.5 Isotopic compositions of antler and bone collagen: a. caribou; b. elk, and c. moose. Paired antler and bone samples for a single individual are joined by a line. The number of specimens in each group is listed in parentheses in the legend.	52
Figure 2.6 Isotopic compositions of caribou collagen from specimens younger than 45,000 ¹⁴ C BP: a. $\delta^{13}\text{C}$; b. $\delta^{15}\text{N}$. The number of specimens in each group is listed in parentheses in the legend.	55

Figure 2.7 Isotopic compositions of elk collagen from specimens younger than 15,000 ¹⁴C BP: a. $\delta^{13}\text{C}$; b. $\delta^{15}\text{N}$. The number of specimens in each group is listed in parentheses in the legend..... 56

Figure 2.8 Isotopic compositions of dated moose collagen from specimens younger than 15,000 ¹⁴C BP: a. $\delta^{13}\text{C}$; b. $\delta^{15}\text{N}$. The number of specimens in each group is listed in parentheses in the legend. 57

Figure 3.1 Simplified pathway for nitrogen incorporation from soil to animal protein. Arrows represent: uptake (dashed line), chemical transformations (solid line), and metabolic processes (solid curves). a. Plant NO_3^- uptake; b. NO_3^- converted to glutamine (Styring et al., 2014); c. NH_4^+ uptake; d. NH_4^+ converted to glutamine by attachment to glutamate (Styring et al., 2014); e. Glutamine supplies nitrogen for synthesis of other amino acids. The associated shift in $\delta^{15}\text{N}$ depends on the specific amino acid, plant part and plant type (Styring et al., 2014); f. Consumption of amino acids by the animal; g. Source amino acids are minimally involved in metabolic processes, undergoing small changes in $\delta^{15}\text{N}$ (e.g. increases in $\delta^{15}\text{N}_{\text{Phe}}$ from diet to consumer tissue are commonly $\leq 2\%$; (McClelland and Montoya, 2002); h. Trophic amino acids are heavily involved in metabolic processes, undergoing enrichment in ¹⁵N (e.g. increases in $\delta^{15}\text{N}_{\text{Glu}}$ from diet to consumer tissue are commonly 6-7 %; McClelland and Montoya, 2002). Katherine Allan drew the images of grass and mammoth. 79

Figure 3.2 Nitrogen isotopic compositions of Pleistocene Old Crow megafauna: a. Bulk collagen nitrogen isotopic compositions ($\delta^{15}\text{N}_{\text{Bulk}}$). Results for woolly mammoths are displayed in blue, other herbivores in purple, and carnivores in red; b. Phenylalanine (source) amino acid nitrogen isotopic compositions ($\delta^{15}\text{N}_{\text{Phe}}$) of each species; c. Difference between the nitrogen isotopic composition of glutamate and phenylalanine ($\Delta^{15}\text{N}_{\text{Glu-Phe}}$) for each species. 83

Figure 4.1 Location of samples. Samples were collected in Old Crow (OC), Yukon Territory, Canada. Higher altitudes are represented by darker shades of grey. The map was drawn by Katherine Allan. 92

Figure 4.2 Simplified pathway for carbon incorporation from plant biochemicals to animal protein. Arrows represent: uptake (solid lines) and metabolic processes (solid curves). a. Typical plant $\delta^{13}\text{C}$ fingerprint for each plant type. The specific fingerprint for the essential and non-essential amino acids depends on the biosynthetic pathways used by the plant to produce and store amino acids. The amino acid carbon isotopic fingerprints are adapted from Larsen et al. (Larsen et al., 2013, 2012, 2009); b. Essential amino acids are taken up from the plant to animal; c. Non-essential amino acids are taken up from the plant to animal. d. Plant lipids are taken up from the plant to animal; e. Carbohydrates are taken up from the plant to animal; f. Animals can synthesize lipids from their diet; g. These lipids can be used by the animal during times of nutritional stress; h. Essential amino acids are generally routed directly from the diet with minimal changes in their isotopic composition (Jim et al., 2006); i. Non-essential amino acids can be routed directly from the diet. They can also be synthesized out of the entire diet, from precursors such as proteins, plant carbohydrates, plant lipids and animal lipids. The difference in $\delta^{13}\text{C}$ of a nonessential amino acid in the diet and in the body depends on the degree of routing versus *de novo* synthesis, the difference in isotopic composition between the amino acid in the diet and the portion of the diet from which the amino acid is synthesized, and the isotopic shift induced by biochemical synthesis. Katherine Allan drew the grass, aquatic plant, giant beaver and mastodon images. The grass image was published previously (Schwartz-Narbonne et al., 2015)..... 99

Figure 4.3 Amino acid profiles of samples after a variety of treatments. The modern bone measured was a cow femur. The archeological bone is a human rib bone and its amino acid profile was presented previously by (Olsen et al., 2010). The average mammal bone amino acid profile and SD is taken from (Szpak, 2011). Amino acid profiles are presented as the percentage of the tissue comprising each amino acid. 112

Figure 4.4 $\delta^{13}\text{C}$ and $\delta^{15}\text{N}$ of bulk collagen for all samples. Values in parentheses in the legend indicate the number of specimens. 113

Figure 4.5 Amino acid profiles for various mammalian tissue types from Old Crow samples. Amino acid profiles are presented as the percentage of the tissue comprising each amino acid. The average mammal bone amino acid profile and SD is taken from (Szpak, 2011).. 114

Figure 4.6 Amino acid: a. $\delta^{13}\text{C}$; b. $\delta^{15}\text{N}$ in a variety of woolly mammoth tissues. Values in parentheses in the legend are the number of tissues measured. Error bars (whiskers) show SD. 115

Figure 4.7 Nitrogen isotopic compositions of amino acids and amino acid pairs. Results for woolly mammoths are displayed as blue circles, other herbivores are displayed as purple triangles, and carnivores are displayed as red squares: a. Phenylalanine (source) amino acid nitrogen isotopic compositions ($\delta^{15}\text{N}_{\text{Phe}}$) of each species. These data have been presented previously (Chapter 3; Schwartz-Narbonne et al., 2015); b. Threonine (source) amino acid nitrogen isotopic compositions ($\delta^{15}\text{N}_{\text{Thr}}$) of each species; c. Glycine (source) amino acid nitrogen isotopic compositions ($\delta^{15}\text{N}_{\text{Gly}}$) of each species; d. Difference between the nitrogen isotopic composition of glutamate and phenylalanine ($\Delta^{15}\text{N}_{\text{Glu-Phe}}$) for each species. These data have been presented previously (Chapter 3; Schwartz-Narbonne et al., 2015); e. Difference between the nitrogen isotopic composition of glutamate and threonine ($\Delta^{15}\text{N}_{\text{Glu-Thr}}$) for each species; f. Difference between the nitrogen isotopic composition of glutamate and glycine ($\Delta^{15}\text{N}_{\text{Glu-Gly}}$) for each species. 119

Figure 4.8 $\delta^{15}\text{N}$ of individual amino acids versus $\delta^{15}\text{N}_{\text{Bulk}}$ for all herbivores: a. $\delta^{15}\text{N}_{\text{Phe}}$; b. $\delta^{15}\text{N}_{\text{Thr}}$; c. $\delta^{15}\text{N}_{\text{Gly}}$. Trendline, R^2 and p value include data for all herbivores. Individual herbivores have distinct symbols and colours so that species-specific deviations from linearity can be observed. 120

Figure 4.9 Normalized carbon isotopic compositions of amino acids ($\Delta^{13}\text{C}_{\text{Amino acid-Bulk}} = \delta^{13}\text{C}_{\text{Amino acid}} - \delta^{13}\text{C}_{\text{Bulk}}$): a. Average for species or groups of species; b. woolly mammoth; c. horse; d. carnivore. 121

Figure 4.10 LDA Dietary classifications versus: a. $\delta^{13}\text{C}_{\text{Bulk}}$ for each herbivore species; b. $\delta^{13}\text{C}_{\text{Bulk}}$ for all species; c. $\delta^{15}\text{N}_{\text{Bulk}}$ for each herbivore species; d. $\delta^{15}\text{N}_{\text{Bulk}}$ for all species. Values in parentheses in the legend indicate the number of samples analyzed. 130

Figure 5.1 Location of sites across the mammoth steppe. ‘Red’ represents the mammoth steppe as defined by Guthrie (1982). ‘Yellow’ represents areas where woolly mammoth, horse and bison remains are present in an environment hypothesized to have had steppe

elements. ‘Blue’ represents areas where woolly mammoth, horse and bison remains are present, but in an environment hypothesized to be primarily forested. Darker shades represent higher elevations. Sites are lettered: SP. Spain; EU. NW Europe; RP. Russian Plain; GP. Gydan Peninsula; SB. south central Siberia; TP. Taymyr Peninsula; YK. Yakutia; WI. Wrangel Island, SK. Selawik; NS. North Slope; FB. Fairbanks; HI. Herschel Island; OC. Old Crow; KD. Klondike; AB. Alberta; GL. Great Lakes Area. Artwork by Katherine Allan. . 146

Figure 5.2 Conceptual model of hypothetical niche differences: a. Variation in carbon and nitrogen isotopic position between the isotopic niche of two species; b. Variation in the size of two isotopic niches; c. Variation between isotopic niches with an overlap and without an overlap..... 152

Figure 5.3 Conceptual model of isotopic niche based on hypothetical points and groupings: a. The outer edge, or convex hull, of the group of data points for each species; b. Same data as for (a), but showing a standard ellipse corrected for small sample-size. The ellipses encompass 40% of the dataset for each group. 153

Figure 5.4 Graphs of $\delta^{13}\text{C}$ and $\delta^{15}\text{N}$ of pre-LGM Albertan megafauna produced in SIBER: a. Individual data; b. Small-sample-size corrected ellipses encompassing 40% of the data for each species; c. Convex hulls encompassing the total area of all data for each species; d. Density plots of the most probable sizes of the standard ellipses for each species, based on Bayesian statistical analysis. The most probable size predicted by Bayesian statistical analysis for each species is shown by a black diamond (SEA_b), while the size of the small sample-size corrected ellipse (SEA_c) is shown by a red square. 159

Figure 5.5 Herbivore species proportions at sites across the mammoth steppe. Sites lettered as in Figure 5.1. Proportions are shown for sites known to represent pre-LGM species abundances (Alberta and North Slope), sites that are primarily composed of pre-LGM samples (Selawik and Taymyr Peninsula), and sites for which there is no dating control (Fairbanks and Yakutia). Higher altitudes are represented by darker shades of grey. Artwork by Katherine Allan..... 162

Figure 5.6 Changes in herbivore species proportions over time at Alberta and the North Slope. Sites lettered as in Figure 5.1. Higher altitudes are represented by darker shades of grey. Artwork by Katherine Allan. 163

Figure 5.7 Small-sample size corrected ellipses (SEAc) of species at two periods at two sites: a. Alberta species during the pre-LGM period; b. Alberta species during the post-LGM period; c. North Slope species during the pre-LGM period; d. North Slope species during the post-LGM period. 164

Figure 5.8 Typical carbon and nitrogen isotopic ranking of species at pre-LGM sites. From lowest to highest, average $\delta^{13}\text{C}$ tended to follow the order: mammoth < mastodon = horse < bison < muskox < caribou. From lowest to highest, the average $\delta^{15}\text{N}$ tended to follow the order: mastodon < caribou < bison < horse < muskox < mammoth. Artwork by Katherine Allan. Mammoth drawing from Chapter 3 and Schwartz-Narbonne et al. (2015). Mastodon drawing from Chapter 4. 165

Figure 5.9 Average and nitrogen isotopic rankings of species from at all pre-LGM site having sufficient data for qualitative analysis. Sites lettered as in Figure 5.1. Higher altitudes are represented by darker shades of grey: a. Pre-LGM isotopic rankings; b. LGM isotopic rankings; c. Post-LGM isotopic rankings; d. Holocene isotopic rankings. Artwork by Katherine Allan. Mammoth drawing from Schwartz-Narbonne et al. (2015). Mastodon drawing from Chapter 4. 169

Figure 5.10 Small-sample size corrected ellipses (SEAc) of sites at two periods for two species: a. Bison during the pre-LGM period; b. Bison during the post-LGM period; c. Horse during the pre-LGM period; d. Horse during the post-LGM period..... 174

Figure 5.11 Typical isotopic ranking of sites across the mammoth steppe based on the δ -values of multiple species, incorporating results from quantitative analysis. Sites are presented from west to east; note x-axis spacing is not proportional to geographic separation: a. Average pre-LGM $\delta^{13}\text{C}$: Fairbanks = Yakutia = Selawik = Taymyr Peninsula (Taymyr) < NW Europe = North Slope < Alberta = Klondike; b. Average pre-LGM $\delta^{15}\text{N}$: Fairbanks = Klondike = Selawik < North Slope < NW Europe < Yakutia = Alberta; c. Average post-LGM

$\delta^{13}\text{C}$: North Slope = NW Europe < Alberta. d. Average post-LGM $\delta^{15}\text{N}$: Alberta < NW Europe < North Slope. 178

Figure 5.12 Typical isotopic ranking of sites across the mammoth steppe based on the δ -values of multiple species, incorporating results from both qualitative and quantitative analysis. Sites are presented from west to east; note x-axis spacing is not proportional to geographic separation: a. Average pre-LGM $\delta^{13}\text{C}$: Fairbanks = Yakutia = Selawik = Taymyr Peninsula (Taymyr) < NW Europe = North Slope < Spain < Alberta = Klondike < Russian Plain = south central Siberia (SC Siberia); b. Average LGM $\delta^{13}\text{C}$: Yakutia < Fairbanks < NW Europe < SC Siberia = Selawik = North Slope = Old Crow < Klondike; c. Average post-LGM $\delta^{13}\text{C}$: Yakutia < Old Crow < Selawik = Fairbanks = North Slope = NW Europe = Gydan Peninsula (Gydan) < SC Siberia < Klondike < Russian Plain = Great Lakes = Alberta; d. Average Holocene $\delta^{13}\text{C}$: Yakutia < Taymyr = Selawik < North Slope = Klondike = Fairbanks; e. Average pre-LGM $\delta^{15}\text{N}$: Fairbanks = Klondike = Selawik < North Slope < SC Siberia = NW Europe < Yakutia = Alberta < Russian Plain < Spain; f. Average LGM $\delta^{15}\text{N}$: SC Siberia = Selawik = NW Europe = Fairbanks < Yakutia < North Slope < Old Crow; g. Average post-LGM $\delta^{15}\text{N}$: Alberta = SC Siberia = Klondike < Russian Plain < NW Europe = Fairbanks < Great Lakes = Selawik < Yakutia = North Slope = Old Crow = Taymyr = Gydan; h. Average Holocene $\delta^{15}\text{N}$: Fairbanks < North Slope < Klondike = Taymyr = Yakutia. 183

Figure 5.13 Small-sample size corrected ellipses (SEAc) of multiple time periods for two species at two sites: a. Bison in Alberta; b. Horse in Alberta; c. Bison in the North Slope; d. Horse in the North Slope..... 185

Figure 5.14 Typical isotopic ranking of time periods in the mammoth steppe: a. Rankings based on quantitative observations. Average $\delta^{13}\text{C}$: Holocene < post-LGM < pre-LGM; average $\delta^{15}\text{N}$: post-LGM < pre-LGM = Holocene; b. Rankings based both on qualitative and quantitative observations. Average $\delta^{13}\text{C}$: Holocene < post-LGM < pre-LGM < LGM. Average $\delta^{15}\text{N}$: post-LGM < Holocene = pre-LGM = LGM. 186

Figure 6.1 Typical carbon and nitrogen isotopic pattern observed for collagen of pre-LGM mammoth steppe megaherivores, as well as the hypothesized diets of these animals.

Megaherbivores images drawn by Kate Allan. Spruce from
<https://en.wikipedia.org/wiki/Spruce>. Lichen from <https://en.wikipedia.org/wiki/Lichen>.
Grass from <https://en.wikipedia.org/wiki/Grass>. Decayed plants from
<http://biogrounds.org/category/life-in-soils/> 211

List of Appendices

Appendix A: Sample information for specimens whose isotopic compositions were included in this study. Previously reported radiocarbon dates are taken from literature sources (Druckenmiller, 2008; Mann et al., 2013; Meiri et al., 2014, Zazula, pers. comm., 2015)..	217
Appendix B: Carbon and nitrogen isotopic compositions of serially sampled antlers, as well as information about sample size and antler beam completeness.	226
Appendix C: Carbon and nitrogen isotopic data for collagen from specimens described in this study.	231
Appendix D: Comparison of the $\delta^{13}\text{C}$ and $\delta^{15}\text{N}$ of lipid-extracted versus unextracted tissues.	237
Appendix E Sample Information for Old Crow megafauna analyzed in Chapter 3.	238
Appendix F Nitrogen isotopic data and preservation information.	240
Appendix G Typical gas chromatogram (sample YT51T) of N-acetyl-methyl ester derivatized amino acids from collagen.	242
Appendix H Sample information for additional specimens used in this study.	243
Appendix I Gas chromatogram arising from compound-specific carbon isotopic measurements of amino acids from collagen extracted from sample YT51T following derivatization to their N-acetyl-methyl ester.	244
Appendix J Amino acid profiles of collagenous tissues determined in this study and previous work.	245
Appendix K Relative abundances of megafaunal herbivores from various sites across the mammoth steppe.	247
Appendix L Sample information for megafaunal herbivores from Alberta.	251
Appendix M Sample information for megafaunal herbivores from Fairbanks.	258

Appendix N Sample information for megafaunal herbivores from the Great Lakes Area. ..	265
Appendix O Sample information for megafaunal herbivores from the Gydan Peninsula....	268
Appendix P Sample information for megafaunal herbivores from Herschel Island.....	269
Appendix Q Sample information for megafaunal herbivores from the Klondike area.....	271
Appendix R Sample information for megafaunal herbivores from the North Slope.....	279
Appendix S Sample information for megafaunal herbivores from NW Europe.	301
Appendix T Sample information for megafaunal herbivores from Old Crow.....	341
Appendix U Sample information for megafaunal herbivores from the Russian Plain.	344
Appendix V Sample information for megafaunal herbivores from the Selawik area.....	346
Appendix W Sample information for megafaunal herbivores from south central Siberia. ..	349
Appendix X Sample information for megafaunal herbivores from Spain.....	351
Appendix Y Sample information for megafaunal herbivores from the Taymyr Peninsula. .	352
Appendix Z Sample information for megafaunal herbivores from Wrangel Island.	358
Appendix AA Sample information for megafaunal herbivores from Yakutia.	359
Appendix BB Results of the mathematical analysis on groups for each site and time period, with the time periods defined using binning approach A.	367
Appendix CC Results of the mathematical analysis on groups for each site and time period, with the time periods defined using binning approach B.	371
Appendix DD Results of the mathematical analysis on groups for each species and time period, with the time periods defined using binning approach A.	374
Appendix EE Results of the mathematical analysis on groups for each species and time period, with the time periods defined using binning approach B.	379

Appendix FF Results of the mathematical analysis on groups for each species and site, with the time periods defined using binning approach A.	384
Appendix GG Results of the mathematical analysis on groups for each species and site, with the time periods defined using binning approach B.....	387
Appendix HH Results of the normality tests on all groups of data.	390
Appendix II Copyright release.....	392

Chapter 1

1 Introduction

1.1 Thesis objectives

During the Pleistocene, a vast biome existed, known as the mammoth steppe. The mammoth steppe was home to a wide array of megaherbivore and megacarnivore species. At the end of the Pleistocene, many of these species went extinct or were extirpated, and leading to the loss of the ecosystem as a whole. Understanding the individual-, population- and species-level behaviours that allowed this ecosystem to be maintained is vital to reconstructing Pleistocene ecology, as well as to understanding modern ecosystems that are facing significant changes from climate and anthropogenic effects. This thesis uses isotopic analysis of collagen in bone, teeth, tusk and antler to investigate megaherbivore and megacarnivore ecology. This is first studied over short time scales, such as a single season or a few years of life, to understand individual animal responses to changing environmental conditions. Species' diet and physiology are then investigated using the isotopic compositions of the individual amino acids that compose collagen. Finally, population-level responses are examined by comparing isotopic compositions of various species at multiple sites and time periods. This allows for a deeper understanding of the ecology of the mammoth steppe, and potentially the factors that might have contributed to its disappearance.

1.2 The mammoth steppe

1.2.1 The mammoth steppe ecosystem

The Pleistocene mammoth steppe was a highly diverse biome, with a range of megafaunal and floral elements that are not seen in association in modern ecosystems (Guthrie, 2001, 1990, 1982). The Pleistocene mammoth steppe has been reconstructed to have had animal and plant productivity similar to the African savannah (Zimov et al., 2012), and to have had more ecological connectivity than the modern African savannah (Pires et al., 2015). The mammoth steppe was the largest biome on Earth during the Pleistocene, spanning from Spain to the Yukon (Fig. 1.1; Guthrie, 2001, 1990, 1982).

Understanding the mammoth steppe is key to understanding Pleistocene paleoecology. Such insight also holds value for anticipating the ecological outcomes of modern climate change, as it can help to elucidate how species adapt to differences in climate and anthropogenic effects, both by comparing geographic locations across the mammoth steppe and examining ecosystem changes over time. Given the potential consequences of modern, anthropogenic climate change, and the prediction that the future will hold an increasing number of non-analogue faunal communities (Williams and Jackson, 2007), understanding the functioning of past ecosystems has become of growing importance.

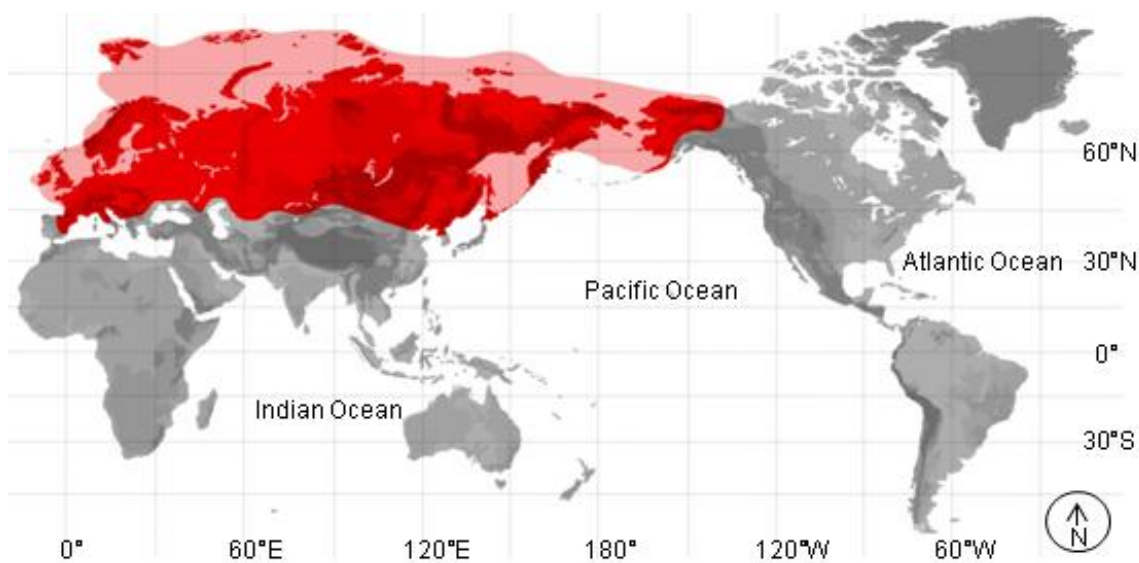


Figure 1.1 The traditional boundaries of the mammoth steppe are shown in red. Higher altitudes are represented by darker shades of grey. Artwork by Katherine Allan.

The mammoth steppe biome was characterized by woolly mammoth, horse and bison dominated ecosystems (Druckenmiller, 2008; Guthrie, 1968; Mann et al., 2013; Mol et al., 2006; Zimov et al., 2012), as well as by herb-steppe-tundra flora (Bocherens, 2003; Guthrie, 2001, 1990, 1982). Pollen, ancient DNA and plant macrofossil studies have identified the mammoth steppe plants as primarily graminoids and forbs, with some willow present. Few records of trees were found during most of the Pleistocene (Blinnikov et al., 2011; Goetcheus and Birks, 2001; Höfle et al., 2000; Schweger et al., 2011; Willerslev et al., 2014). Rather than floral species being evenly distributed across the mammoth steppe, they formed a “vegetational mosaic” (Guthrie, 1982). However,

similar floral characteristics were seen at a broad scale between different sites on the mammoth steppe (Willerslev et al., 2014). Similar megaherbivore and megacarnivore species were also present across the mammoth steppe, including muskox, caribou, brown bear and grey wolf (Bocherens, 2015; Druckenmiller, 2008; Guthrie, 1968; Mann et al., 2013; Mol et al., 2006; Zimov et al., 2012). There were some differences between regions. For example, woolly rhinoceros has not been found in North America and short-faced bear has not been found in Eurasia, suggesting that some species were unable to cross the Bering Land Bridge and fully disperse (Guthrie, 2001). Others co-existed only during specific time intervals. For example, elk was present in Europe throughout the Pleistocene, but did not migrate to North America until around 13,000 ^{14}C years BP (Guthrie, 2006; Meiri et al., 2014).

A combination of environmental factors generated a large, highly productive plant biomass on the mammoth steppe. The mammoth steppe was more arid than those regions are today (Edwards et al., 2001; Elias, 2000; Guthrie, 2001; Schweger et al., 2011). This led to decreased snowfall and thus an early spring melt, which increased the length of the growing season (Guthrie, 2001, 1982). Decreased precipitation promoted the growth of arid-adapted plants, which do not form a summer-season insulating cover over soil. This lack of insulating cover meant that the soil warmed more rapidly and warmer soils promoted nutrient turnover and soil fertility (Guthrie, 1982). The Pleistocene flora had an extended growing season causing increased plant productivity. Warmer soils also meant a deeper permafrost layer, so a significant proportion of plant biomass could be stored underground and the plants faced decreased risk from grazing herbivores. This meant they did not develop strong anti-herbivore defence mechanisms such as production of various alkaloids (Guthrie, 1990, 1982). The decreased snowfall also made the plants more accessible to several Pleistocene herbivores (Guthrie, 2001). The high plant biomass levels were also promoted by nutrient-rich soils (Goetcheus and Birks, 2001; Guthrie, 1982). Many Pleistocene soils were composed of loess, a fine-grained material that forms when glacial flow erodes the underlying rock. This glacial dust was carried by outwash streams and deposited by wind kilometres from the original glacier, forming the basis of a new soil layer (Goetcheus and Birks, 2001; Guthrie, 1990, 1982). These newly formed soils were rich in potassium, phosphate and calcium, which are necessary for

plant nutrition. The megafauna are suggested to have encouraged plant growth by trampling and grazing, both of which promoted the growth of fast-growing flora (Blinnikov et al., 2011; Guthrie, 1982; Willerslev et al., 2014; Zimov et al., 2012).

The Pleistocene had repeated cycles of glaciations and deglaciation, and the accompanying climatic changes had significant effects on the mammoth steppe. Woodlands became more prevalent in parts of the mammoth steppe during warmer periods (interglacials and interstadials; Castaños et al., 2014; Elias, 2000; Schweger et al., 2011). During the last glacial maximum (LGM), several species are posited to have been extirpated from parts of the mammoth steppe. For example, there are no post-LGM dates for the scimitar-tooth cat or the short-faced bear in central Alaska (Fox-Dobbs et al., 2008). The floral compositions of sites on the mammoth steppe changed during the LGM as well, with fewer species and less similarity of plant species among sites (Willerslev et al., 2014). The post-LGM warming and increase in mesic conditions may have been the factor that allowed elk to enter North America (Meiri et al., 2014).

1.2.2 Megafaunal extinctions on the mammoth steppe

A number of extinctions occurred at the terminal Pleistocene (12,000-10,000 ^{14}C BP). In North America alone, 35 genera of animals went extinct locally, and 29 of those went extinct globally (Faith and Surovell, 2009). The majority of the megaherbivore and megacarnivore species on the mammoth steppe were extirpated or went extinct. The exact timing of the extinctions is disputed and needs to be resolved on a species-by-species basis (Faith and Surovell, 2009; Gill et al., 2009; Grayson and Meltzer, 2003; Guthrie, 2006). However, while the precise timing is not fully resolved, many of these extinctions were approximately synchronous with widespread climatic and vegetation change (Guthrie, 2006). The extinctions were also approximately synchronous with some of the earliest evidence for human habitation in North America, which is provided by the Clovis spear points (Faith and Surovell, 2009; Guthrie, 2006). Humans and their predecessors coexisted with Pleistocene megafaunal species for approximately 2 million years in the mammoth steppe in Eurasia, though anatomically modern humans likely arrived in Eurasia around 45,000 years ago (Barnosky et al., 2004; Koch and Barnosky, 2006). It is generally accepted that human hunting, climate change or a combination of

these two factors led to the extinctions and that the extent to which each of those factors is responsible varied globally (Barnosky et al., 2004; Cooper et al., 2015; Koch and Barnosky, 2006).

Overkill models are based on the concept that species were removed from the mammoth steppe by human hunting, leaving empty ecological niches (Barnosky et al., 2004; Koch and Barnosky, 2006; Sandom et al., 2014). The structure of mammoth steppe ecology may have made the ecosystem particularly vulnerable to disruption by human hunting (Pires et al., 2015). Some authors further suggest that the terminal Pleistocene vegetation change occurred because of the removal of mammoths, a keystone herbivore (Gill et al., 2009; Koch and Barnosky, 2006), and that these changes led to the extinction of further herbivore species. Radiocarbon dating of megafaunal remains, however, suggests that – in Alaska and the Yukon – mammoth extinctions followed rather than preceded the extinctions of most megafauna species (Guthrie, 2006), and this likely occurred at other places as well (Barnosky et al., 2004).

At the terminal Pleistocene, the climate changed to warmer, moister conditions (Edwards et al., 2001; Guthrie, 2006). Vegetation shifted from herb-steppe-tundra to bogs, wetlands, and forests (Guthrie, 2001, 1982). Mammoth steppe flora was replaced with highly zoned, low diversity floral communities, with high levels of anti-herbivore defences. Ungulates in general are unable to digest significant quantities of woody tissues, and non-ruminants (e.g. horse, mammoth) in particular require a diverse set of forage types. This vegetation shift is hypothesized to have disrupted the ability of these species to obtain the diverse types and quantity of forage that they required (Barnosky et al., 2004). This conclusion is supported by evidence that several species of megafauna experienced population decline or environmental stress as a result of climatic changes before the terminal Pleistocene, suggesting that while the extinction event occurred at the terminal Pleistocene, the species may have already been in decline (Faith, 2011; Guthrie, 2003; Shapiro et al., 2004).

1.3 Stable isotopes

1.3.1 Carbon isotopes

Plants can take up and fix carbon using a variety of mechanisms, each of which has implications for the $\delta^{13}\text{C}$ of the plant. The three major photosynthetic pathways are C_3 , C_4 and CAM (Crassulacean Acid Metabolism). C_3 plants tend to have much lower $\delta^{13}\text{C}$ (average -27‰ ; Koch, 2007), than C_4 plants (average -13‰ ; Koch, 2007), though in some circumstances, such as low $p\text{CO}_2$, C_3 plants may utilize pathways more similar to C_4 plants, which may cause their isotopic compositions to increase (Busch et al., 2013; Way et al., 2014). CAM plants tend to have isotopic compositions between the two (average -11‰ ; Marshall et al., 2007). No evidence for CAM plants has been found on the mammoth steppe. There is a limited quantity of modern C_4 plants on the area that was the Pleistocene mammoth steppe (Wooller et al., 2007). However, studies of the Pleistocene mammoth steppe have found only C_3 plants (Bocherens, 2015, 2003; Gaglioti et al., 2011; Kristensen et al., 2011; Wooller et al., 2007).

In modern tundra, shrubs generally have the lowest $\delta^{13}\text{C}$, followed by forbs, graminoids, fungi and then lichens (Fig. 1.2; Barnett, 1994; Ben-David et al., 2001; Drucker et al., 2010; Kristensen et al., 2011). There is commonly significant overlap in the range of $\delta^{13}\text{C}$ of different plant types. Some of this overlap occurs because of varying isotopic compositions of different plant parts. For example, in trees there is a tendency for needles and leaves to have lower $\delta^{13}\text{C}$ than twigs (Ehleringer et al., 1992; Gebauer and Schulze, 1991; Tischler, 2004). Algae and C_3 macrophytes have a wide range of $\delta^{13}\text{C}$ (-47 to -8‰) encompassing the entire range of C_3 terrestrial plants (-32 to -22‰ ; Farquhar, 1989; Finlay and Kendall, 2007). While terrestrial plants use only atmospheric carbon, aquatic plants take up carbon from a variety of sources including dissolved inorganic carbonate from carbonate rocks, respiring organic matter and detritus, and atmospheric CO_2 , and each of these can impart a distinct $\delta^{13}\text{C}$ to the plant (Farquhar, 1989; Finlay and Kendall, 2007; Keeley and Sandquist, 1992; LaZerte and Szalados, 1982; Osmond et al., 1981). While several site-specific studies have found consistent differences between terrestrial and aquatic plants (Doucett et al., 1996; Fry, 1991; Tischler, 2004), these

cannot be generalized to global differences among plant types (Finlay and Kendall, 2007; France, 1995; Keeley and Sandquist, 1992).

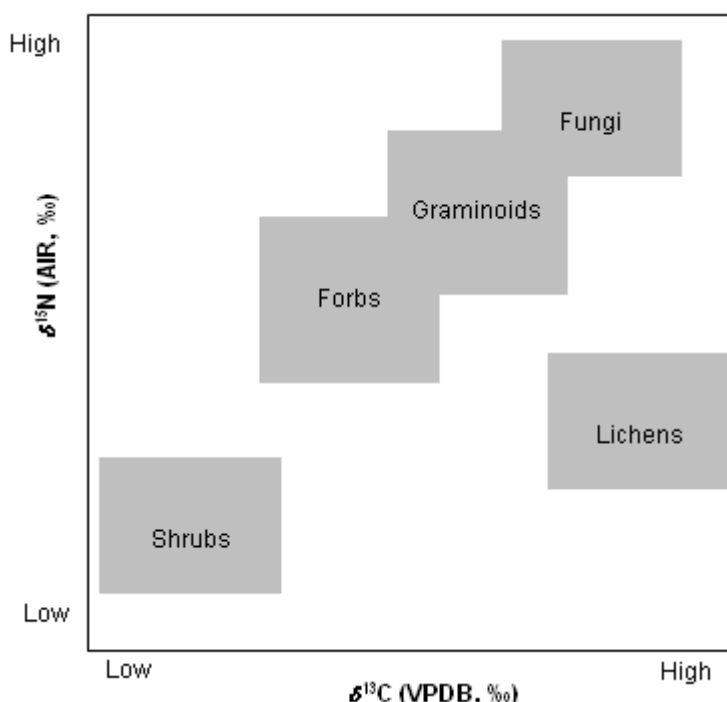


Figure 1.2 Conceptual diagram illustrating the relative carbon and nitrogen isotopic compositions of common modern terrestrial tundra vegetation.

Climatic differences between habitats affect the $\delta^{13}\text{C}$ of terrestrial plants. When aridity increases, plants have higher water use efficiency, leading to higher $\delta^{13}\text{C}$ (de Bello et al., 2009; Farquhar, 1989; Tieszen, 1991; Wooller et al., 2007). An increase in altitude and temperature can also cause higher $\delta^{13}\text{C}$, though these effects are disputed (de Bello et al., 2009; Diefendorf et al., 2010; Ehleringer and Cooper, 1988; Ehleringer et al., 1987; Farquhar, 1989; Heaton, 1999; Kohn, 2011, 2010; Stevens et al., 2006; Tieszen, 1991; Wooller et al., 2007). The role of temperature may vary with landscape, and temperature has been reported as a significant factor in plant $\delta^{13}\text{C}$ in Arctic environments (Iacumin et al., 2006). Plants that grow underneath a dense canopy obtain less light, and more recycled CO_2 from respiring plant tissue, than plants that grow in open areas. For this reason, they tend to have lower $\delta^{13}\text{C}$ (Adams and Grierson, 2001; Bocherens et al., 2011; Bonafini et al., 2013; Buchmann et al., 1997; Farquhar, 1989; Garten Jr and Taylor Jr,

1992; Heaton, 1999; Kohn, 2010; Tieszen, 1991). Sea spray can increase the $\delta^{13}\text{C}$ of plants (see Sykes et al., 2011 and references therein), as can higher levels of nutrients such as nitrogen or phosphorus (Heaton, 1999; Tieszen, 1991; Toft et al., 1989). Some authors have suggested during periods when the Earth had lower $p\text{CO}_2$, plants had higher $\delta^{13}\text{C}$, and vice versa (Schubert and Jahren, 2015), but this has not been consistently observed in multiple studies (see discussions in Bocherens, 2003; Richards and Hedges, 2003; Stevens and Hedges, 2004). Once a plant has died, its carbon isotopic composition can also be changed by decay processes (Gleixner et al., 1993; Wynn, 2007).

The biochemical components within a plant have consistent differences in their $\delta^{13}\text{C}$. Within a plant, lipids have the lowest $\delta^{13}\text{C}$, followed by carbohydrates and then proteins (Boutton, 1996; Gleixner et al., 1993; Tieszen, 1991). The patterns of isotopic compositions of the amino acids that compose proteins vary with plant type, plant part, and kingdom (Fogel and Tuross, 2003; Larsen et al., 2013, 2012, 2011, 2009; Lynch et al., 2011; Smallwood et al., 2003). Since there are clear differences in the $\delta^{13}\text{C}$ patterns among groups such as aquatic plants, terrestrial plants, bacteria and fungi, linear discriminant analysis can be used to classify the group from which a protein originated by determining common trends in the $\delta^{13}\text{C}$ of the amino acids between groups (Larsen et al., 2013, 2012, 2009).

Bone, tooth, tusk and antler are composed of organic and inorganic components. The organic material consists primarily of the protein collagen and the inorganic component comprises bioapatite (Szpak, 2011). Collagen can be preserved over archaeological and paleontological time scales. There are well-defined criteria to assess the extent of collagen preservation prior to accepting its isotopic composition as representative of primary processes (Ambrose, 1990; DeNiro, 1985; van Klinken, 1999). The isotopic composition of an animal's collagen derives from the isotopic composition of the diet that it consumed. Because of a number of metabolic effects, however, an animal's collagen typically has a higher carbon isotopic composition ($\delta^{13}\text{C}_{\text{Bulk}}$) than the dietary materials from which it formed. Large herbivores are typically enriched in ^{13}C by $5.1\text{‰} \pm 0.3\text{‰}$ from diet to bone collagen (Drucker et al., 2008). The increase in $\delta^{13}\text{C}_{\text{Bulk}}$ from prey to predator is typically $1.2 \pm 0.3\text{‰}$ (Bocherens, 2015).

Collagen is composed of both essential and nonessential amino acids (Howland et al., 2003). Essential amino acids are routed directly from the diet, while nonessential amino acids can either be directly routed, or can be synthesized from the carbohydrate or lipid portion of the diet (Jim et al., 2006; Newsome et al., 2014). Which nonessential amino acids are routed and which are synthesized depends in part on the quantity of those amino acids in the diet (McMahon et al., 2010). When nonessential amino acids are synthesized, their isotopic composition depends on the isotopic composition of the biochemical portion of the diet from which they are synthesized (e.g. lipids, carbohydrates or protein) and on the isotopic separation induced by the metabolic process (Jim et al., 2006; Newsome et al., 2014). Amino acids that are directly routed with minimal changes in their $\delta^{13}\text{C}$, such as essential amino acids, can be used to classify the dietary source of a consumer using linear discriminant analysis (LDA). In LDA, the characteristic $\delta^{13}\text{C}$ signatures of amino acids from defined groups such as terrestrial plants, aquatic plants, bacteria and fungi are entered into a program such as the MASS package in R (R Core Team, 2014; Venables and Ripley, 2002). This program defines the linear combination of features that vary between groups, and so is able to create a set of expected isotopic trends between amino acids for each group. These expected isotopic differences, or prediction functions, can then be used to classify unknown samples by checking the samples against the expected trends. This can be used to classify the diet of consumers by inputting amino acids from consumers and testing which dietary source they most closely resemble (Larsen et al., 2013, 2012, 2009). Herbivores consume significantly less protein than carnivores, and so some, or all, of their nonessential amino acids are expected to reflect the $\delta^{13}\text{C}$ of non-protein portions of the diet. Care must be taken, therefore, in selecting which amino acids are used in LDA to create the predictive functions.

The $\delta^{13}\text{C}_{\text{Bulk}}$ can also be affected by metabolic effects specific to an animal's physiology. For example, a nursing animal consumes a diet rich in lipids, which have lower $\delta^{13}\text{C}$ (Metcalf et al., 2010). An animal suffering from winter starvation may rely on its fat reserves to survive, which again could cause it to have lower $\delta^{13}\text{C}_{\text{Bulk}}$ (Szpak et al., 2010). Hibernation may also have an effect on a species' $\delta^{13}\text{C}_{\text{Bulk}}$, but it is difficult to distinguish this from the effect of consuming body lipids to survive the winter (Bocherens, 2015; Nelson et al., 1998). Ruminant species produce and release large quantities of methane,

which has low $\delta^{13}\text{C}$. This means that their $\delta^{13}\text{C}_{\text{Bulk}}$ may be higher than those of non-ruminant species (Coltrain et al., 2004). Finally, different tissues are grown over different time periods. Teeth form at a single point in an animal's life, while bone is continuously remodelled and thus its isotopic composition reflects diet and metabolic and physiological processes over several years of an animal's life (Bocherens, 2015; Koch et al., 1994; Metcalfe et al., 2010). Antler forms over a single season (Chapman, 1975). Hence, the isotopic compositions of different tissues from the same individual can provide information on the physiology, diet and habitat at different points in the animal's life. Conversely, the isotopic composition of bone, a tissue that provides an averaged isotopic composition over several years, can be invaluable to look at population-level ecology.

1.3.2 Nitrogen isotopes

Nitrogen used for plant amino acid synthesis can come from one of four sources: (i) direct uptake of soil amino acids, although most plants compete poorly for amino acids compared to soil microbes (Styring et al., 2014); fixation of atmospheric nitrogen by plants or associated microorganisms, and (iii) nitrate or (iv) ammonium uptake from soil (Amundson et al., 2003). Plants then convert this nitrogen into an amino acid by attaching it as an amide group to glutamate, forming glutamine. Glutamine can then be used a precursor to form the rest of the amino acids in the plant (Styring et al., 2014). The isotopic composition of a terrestrial plant partly depends on the source and $\delta^{15}\text{N}$ of the nitrogen used (Gannes et al., 1998; Nadelhoffer et al., 1996). Plants that fix nitrogen have $\delta^{15}\text{N}$ close to 0 ‰ (Amundson et al., 2003). If nitrogen is obtained from associated mycorrhizal fungi, the plant often has lower $\delta^{15}\text{N}$ than if it had obtained nitrogen directly from soil (Bocherens, 2003; Craine et al., 2009; Nadelhoffer et al., 1996). The rooting depth of a plant also affects its $\delta^{15}\text{N}$; deeper soil tends to have higher $\delta^{15}\text{N}$, which are passed on to the plant (Barnett, 1994; Handley and Raven, 1992; Kelly, 2000; Nadelhoffer et al., 1996). Nitrogen can also be lost from a plant by root exudations, or as gaseous nitrogen emissions from leaves, with an associated nitrogen isotopic fractionation (Dawson et al., 2002). All of these factors combine to produce the pattern of modern terrestrial plant isotopic compositions in tundra environments illustrated in

Figure 1.2. Fungi have the highest $\delta^{15}\text{N}$, followed by graminoids, forbs, lichens and shrubs (Ben-David et al., 2001; Drucker et al., 2010; Finstad and Kielland, 2011; Kristensen et al., 2011; Nadelhoffer et al., 1996). There is significant overlap in the $\delta^{15}\text{N}$ of different plant types, making clear differentiation based solely on the nitrogen isotopic composition of the plant difficult. There are also differences in the $\delta^{15}\text{N}$ of different plant parts. For examples, tree stems commonly have lower $\delta^{15}\text{N}$ than leaves or needles (Gebauer and Schulze, 1991; Kielland, 2001).

Global studies of aquatic plants report a wide range of $\delta^{15}\text{N}$, since there are a variety of sources that such plants can access, including dissolved inorganic nitrogen in lakes and rivers or nitrogen drawn from soils (Finlay and Kendall, 2007). The global range of aquatic plant $\delta^{15}\text{N}$ overlaps that of terrestrial plants (France, 1995). However, studies at specific sites commonly find higher $\delta^{15}\text{N}$ for aquatic than adjacent terrestrial plants (Delong and Thorp, 2006; Finstad and Kielland, 2011; Fry, 1991; Milligan et al., 2010; Tischler, 2004). This pattern, however, is not universally observed (Ben-David et al., 2001; McArthur and Moorhead, 1996).

Terrestrial habitats can be divided into “open” and “closed” ecosystems. An open habitat is usually warmer and more arid, and significant quantities of nitrogen are lost to the atmosphere or in removal of water from the system such as in run-off. Nitrogen is preferentially lost as ^{14}N , causing the remaining nitrogen to be enriched in ^{15}N , and the plants that grow in that habitat to have higher $\delta^{15}\text{N}$. Plants that grow in colder and more mesic environments tend to have lower $\delta^{15}\text{N}$ (Ambrose, 1991; Amundson et al., 2003; Drucker et al., 2003a; Heaton, 1987; Stevens and Hedges, 2004; Stevens et al., 2008). Salinity can increase the $\delta^{15}\text{N}$ of an ecosystem that experiences significant quantities of sea spray (see Sykes et al., 2011). Deeper winter snow can cause higher $\delta^{15}\text{N}$ in the plants that grow there (Blok et al., 2015). Finally, fertilization with organic material such as dung can increase the $\delta^{15}\text{N}$ of plants (Szpak et al., 2012).

The $\delta^{15}\text{N}$ of animal bone collagen ($\delta^{15}\text{N}_{\text{Bulk}}$) reflect the $\delta^{15}\text{N}$ of its diet plus an increase of $3.6 \pm 0.9 \text{ ‰}$ (Bocherens, 2015). The isotopic composition of an animal’s collagen derives from a combination of the $\delta^{15}\text{N}$ of source amino acids, which tend to retain the isotopic

composition of the diet, and trophic amino acids, which are strongly influenced by metabolic effects and therefore increase in $\delta^{15}\text{N}$ with trophic level (McCarthy et al., 2007; McClelland and Montoya, 2002; Popp et al., 2007). Source amino acids can be used to determine the isotopic composition of food from the base of the food web, while trophic amino acids provide an indication of the trophic level and degree of metabolic isotopic enrichment occurring within an animal.

There are some physiological effects that can cause an increase in $\delta^{15}\text{N}_{\text{Bulk}}$. A nursing individual consumes tissue from its mother, and so nursing animals have a $\delta^{15}\text{N}_{\text{Bulk}}$ one trophic level higher than their mother (Metcalf et al., 2010). Extreme nutritional stress has been posited to cause an animal to recycle its own tissues, causing an increase in $\delta^{15}\text{N}_{\text{Bulk}}$ (Gannes et al., 1998; Hobson et al., 1993; Kelly, 2000; Koch, 2007; Polischuk et al., 2011), although some research suggests that this only occurs at an extreme threshold of nutritional stress (Kempster et al., 2007). Aridity has also been suggested to cause increases in $\delta^{15}\text{N}_{\text{Bulk}}$ (Kelly, 2000; Koch et al., 1994; Sealy et al., 1987; Sponheimer et al., 2003). Hibernation has also been suggested to cause increases in $\delta^{15}\text{N}_{\text{Bulk}}$ of hibernators such as bears (see discussion in Bocherens, 2015).

1.3.3 Combined carbon and nitrogen isotopic analysis

A number of mathematical tools have been created that use the combination of $\delta^{13}\text{C}_{\text{Bulk}}$ and $\delta^{15}\text{N}_{\text{Bulk}}$ to better understand species' ecology. When considering a species at a single trophic level, evaluation of its carbon and nitrogen isotopic compositions in combination allows an "isotopic niche" to be defined. This isotopic niche can be defined to include the total area in isotopic space on a graph of $\delta^{13}\text{C}$ versus $\delta^{15}\text{N}$ (measured in per mil) covered by the all the isotopic compositions of a species (Layman et al., 2007), or it can be defined to include the core 40% of the isotopic compositions of the species on the graph (Jackson et al., 2011). Either method provides a distinctly shaped and sized isotopic niche for each species. The relative size of two isotopic niches can also be compared using Bayesian statistics. These statistics use a probabilistic framework to determine how likely it is that a species' niche is a given size. They can then compare the likelihood of each niche size for two groups to determine which species has a higher

proportion of expected niche sizes, and so is most probable to have the larger niche. (Jackson et al., 2011; Parnell et al., 2010). The size of the isotopic niche can provide information about the generalist versus specialist tendencies of a species. For example, a larger isotopic niche may indicate a species feeding on a more diverse set of resources or in a wider range of habitats, so a more generalist species. The amount of isotopic niche overlap is informative about the extent of competition for resources. SIBER (Stable Isotope Bayesian Ellipses in R) is one of the mathematical programs that perform this analysis (Jackson et al., 2011; Parnell et al., 2010).

Bayesian analysis can be used to elucidate the diet of a species when the isotopic compositions of plants and animals, and/or animals from multiple trophic levels are known. The isotopic compositions of potential dietary resources and the consumer can be used as the input to mixing models such as SIAR (Stable Isotope Analysis in R) to provide estimates of the most probable combination of dietary resources used (Parnell et al., 2010).

1.4 Previous isotopic investigations of collagen on the mammoth steppe

Isotopic compositions of collagen have been used in numerous studies to reconstruct the ecology of the mammoth steppe (e.g. Bocherens et al., 2011, 1994; Drucker et al., 2003a, b; Fizet et al., 1995; Fox-Dobbs et al., 2008; Iacumin et al., 2010; Mann et al., 2013; Metcalfe, 2011; Metcalfe et al., 2013; Raghavan et al., 2014; Stevens et al., 2009; Szpak et al., 2010). Reviews of isotopic results across the mammoth steppe have noted that the patterns of $\delta^{13}\text{C}_{\text{Bulk}}$ and $\delta^{15}\text{N}_{\text{Bulk}}$ among herbivores at a site tend to be relatively consistent (Bocherens, 2015, 2003), suggesting specific dietary niches for each species. For example, caribou are reconstructed as having consumed lichen (Bocherens, 2015; Castaños et al., 2014), and horse and bison as consuming graze (graminoids and forbs; Fox-Dobbs et al., 2008), with horses eating the shorter grasses and bison eating the taller grasses (Britton et al., 2012). Woolly mammoth had unusually high $\delta^{15}\text{N}_{\text{Bulk}}$, more similar to coeval carnivores than herbivores (Bocherens, 2003), which made their isotopic compositions difficult to interpret. This “woolly mammoth conundrum” suggests

that they had a distinct diet, habitat or physiological mechanism. A variety of explanations have been suggested, including consumption of plants that grew in more arid environments, consumption of plants that had been previously fertilized by dung, selection for specific plants or plant parts, seasonal starvation that caused ^{15}N -enrichment and/or consumption of their own feces (Bocherens, 2003; Iacumin et al., 2000; Koch, 1991; Kuitens et al., 2012; Metcalfe et al., 2013; Szpak et al., 2010). The low $\delta^{15}\text{N}_{\text{Bulk}}$ of mastodon, by comparison, are suggested to reflect consumption of browse such as spruce trees (Metcalfe et al., 2013).

Changes have been noted in the isotopic compositions of herbivore species, both over time and between sites. Higher $\delta^{15}\text{N}_{\text{Bulk}}$ have been measured for woolly mammoths in Russia than in Alaska or the Yukon (Szpak et al., 2010), suggesting that Pleistocene Russia was more arid than the two other sites. A decline in the average $\delta^{15}\text{N}_{\text{Bulk}}$ of 2-3 ‰ in several herbivore species was observed in southwestern Europe and in Alaska after the LGM (Bocherens et al., 2011; Fox-Dobbs et al., 2008; Mann et al., 2013; Stevens et al., 2008), which may have been caused by changes in aridity and/or temperature. Variations in the $p\text{CO}_2$ of the atmosphere may have also affected the $\delta^{13}\text{C}$ of plants between glacial and interglacial cycles, and thus the animals that consumed these plants (Bocherens, 2003; Iacumin et al., 2006; Stevens and Hedges, 2004), though this difference is not observed at all sites (Fox-Dobbs et al., 2008). Alternatively, changes in $\delta^{13}\text{C}_{\text{Bulk}}$ between the post-LGM period and the Holocene in France have been posited to reflect an increase in canopy vegetation (Drucker et al., 2003a, 2008). Overlapping $\delta^{15}\text{N}_{\text{Bulk}}$ have been observed for horse and woolly mammoth in Ukraine and Germany during certain time periods, which may suggest that these species shifted their diet depending on resource availability and competition with other herbivores (Bocherens, 2015).

Fewer studies have been performed on carnivore isotopic compositions for the mammoth steppe megafauna, likely because fewer carnivore than herbivore specimens have been found (e.g. Mann et al., 2013). Bocherens (2015) and Yeakel et al. (2013) have reviewed the isotopic compositions of carnivore collagen from multiple mammoth steppe sites. Bocherens (2015) focussed on identifying the diet of individual species, and comparing those diets at differing sites or time periods across the mammoth steppe. Several species,

such as cave lion and brown bear, varied their diet among sites, potentially in response to competition with other carnivores for prey, as had been observed in similar studies of individual species (Barnes et al., 2002; Bocherens, 2015; Bocherens et al., 2011). Yeakel et al. (2013) used a Bayesian mixing model to identify the diets of carnivores at two sites over multiple time periods, and then compared the structure of the ecosystems based on this interpretive approach to collagen isotopic data. They found that the Alaskan site had more resource segregation between carnivores, consistent with the interpretation that this ecosystem was more isolated from neighbouring animal communities.

1.5 Dissertation

1.5.1 Goals of the dissertation

There is a growing body of work using isotopic compositions of megafauna to understand the ecology of the mammoth steppe. The majority of work on collagen in the mammoth steppe has focused on single sampling of bone or adult teeth. Bone provides a time-averaged signal of the last several years of an animal's life (Balasse et al., 1999; Koch et al., 1994).

Teeth and tusk, by comparison, provide a "snapshot" view of an animal's life, as the collagen in teeth and tusk is deposited once and not remodelled over an animal's lifetime (Koch et al., 1994; Metcalfe et al., 2010). Measuring the isotopic composition of an adult tooth or tusk is also commonly used to assess the isotopic composition of the adult diet of the animal, in the same manner that bone collagen is used (e.g. Mann et al., 2013; Metcalfe et al., 2013; Szpak et al., 2010). This approach, however, is made more powerful by taking multiple samples, typically of smaller size, from an individual tusk or tooth to investigate seasonal or yearly changes. This approach is invaluable for investigating signals that are not generated year-round – for example, weaning happens once in an animal's lifetime, pregnancy occurs seasonally for species such as caribou (Finstad and Kielland, 2011) and many dietary resources are population-limiting seasonally rather than year-round (Adamczewski et al., 1988; Heggberget et al., 2002). In situations such as these, isotopic compositions can reveal dietary switching over time (Peterson and Fry, 1987). One study has examined the differences in the isotopic

composition of woolly mammoth teeth formed at different ages to assess the timing of nursing and weaning (Metcalf et al., 2010), and another studied serially sampled increments of a juvenile mammoth's tusk to assess age of weaning (Rountrey et al., 2007). Moving beyond collagen as the tissue examined, still other studies have serially sampled woolly mammoth hair (Iacumin et al., 2006, 2005), horse tooth enamel (Bellissimo, 2013) and tusk enamel of woolly mammoths (Fox et al., 2007) to investigate seasonal changes in the species.

There remain, however, a number of unresolved questions concerning the ecology of the mammoth steppe:

- (1) Extensions of the serial sampling approach to other tissues, such as antler, and to other species should allow more exploration of seasonal changes within the mammoth steppe.
- (2) Isotopic work to date on the mammoth steppe has focused on bulk tissue isotopic analysis. While the isotopic compositions of both carbonate and phosphate components of bioapatite from mammoth steppe animals are now routinely measured and interpreted (e.g. Bellissimo, 2013; Fox et al., 2007), only bulk protein from keratin and collagen has been analysed for these animals. Individual amino acid analysis, by comparison, has proven invaluable for elucidating an individual's trophic level and the major components of their diet in a number of modern (e.g. Hannides et al., 2009; Miller et al., 2012; Popp et al., 2007; Sherwood et al., 2011) and archeological studies (e.g. Fogel and Tuross, 2003; Naito et al., 2010; Styring et al., 2010). This method has the potential to provide insight into the diet of several species from the mammoth steppe, and to better resolve their ecology. For example, its application to woolly mammoth collagen could resolve the "woolly mammoth conundrum". It could also help to better resolve the diet of a variety of herbivores, using the $\delta^{15}\text{N}$ of source amino acids (McCarthy et al., 2007; McClelland and Montoya, 2002; Popp et al., 2007) and linear discriminant analysis classification of amino acid $\delta^{13}\text{C}$ (Larsen et al., 2013, 2012, 2009).

- (3) While there have been numerous studies of bulk collagen isotopic compositions of megaherbivores from the mammoth steppe (e.g. Bocherens et al., 2011, 1994; Drucker et al., 2003a, b; Fizet et al., 1995; Fox-Dobbs et al., 2008; Iacumin et al., 2010; Mann et al., 2013; Metcalfe, 2011; Metcalfe et al., 2013; Raghavan et al., 2014; Stevens et al., 2009; Szpak et al., 2010), reviews that integrate and explain the metadata arising from these studies are few (Bocherens, 2015, 2003). Several studies investigate multiple species, time periods or sites across the mammoth steppe. However, no single study has simultaneously examined the changes in published $\delta^{13}\text{C}_{\text{Bulk}}$ and $\delta^{15}\text{N}_{\text{Bulk}}$ for all megaherbivore species among different sites and time periods. As well, overlaps in the isotopic composition of species, such as those observed for the $\delta^{15}\text{N}$ of horse and mammoth in Germany and Ukraine (Bocherens, 2015), have not been quantified using models of isotopic niche. Mathematical tools such as SIBER (Jackson et al., 2011; Parnell et al., 2010) are being increasingly used in ecological work to provide insight into niche size and the degree of niche overlap between species, and thus the way that different species use and share resources (Layman et al., 2012). These tools could help to understand ecological patterns and changes over time, and between geographic areas.

To understand the mammoth steppe, the ecology of the species that inhabited it must be understood on both the individual and population levels. This thesis will accomplish this through applications of ecological techniques that have not been previously used in the mammoth steppe:

- (1) I examine seasonal changes and individual animal responses through changes in the isotopic composition over the length of an antler and comparison between this tissue and bone.
- (2) I use amino acid $\delta^{13}\text{C}$ and $\delta^{15}\text{N}$ to separate dietary and metabolic isotopic signals, allowing me to better understand and classify herbivore and carnivore diets.
- (3) I use SIBER analyses to understand the resource use of animal populations and competition between them.

Using these techniques, I am able to assess the typical megafaunal ecology of the mammoth steppe, as well as to assess ecological responses to climatic and anthropogenic changes over time and between geographic locations.

1.5.2 Organization of the dissertation

This thesis is composed of four distinct research chapters (Chapters 2 through 5), each of which is prepared as a stand-alone article for publication, plus this introduction (Chapter 1) and some broader conclusions (Chapter 6). Supplementary tables and figures for Chapters 2-5 are contained in the appendices.

Chapter 1 provides a general introduction to the mammoth steppe, carbon and nitrogen isotopic systematics of plants and animals, and a review of relevant previous isotopic investigations, with a focus on animal collagen.

Chapter 2 examines the carbon and nitrogen isotopic compositions of collagen from elk, moose and caribou antler and bone. As these tissues that have different growth periods, their isotopic compositions can provide a seasonal signal (antler) and an annual signal (bone). We serially sampled antler to investigate the changes in its isotopic composition over a single season, and compared antler isotopic compositions with those of bone to determine seasonal ecological differences as well as differences through the Late Pleistocene and Holocene. We establish that the isotopic compositions of antlers cannot be directly compared to those of bone when reconstructing a species' diet, and that each tissue provides a distinct set of ecological information concerning that species.

Chapter 3 examines the characteristic but anomalously high woolly mammoth bulk collagen $\delta^{15}\text{N}$ using a source (phenylalanine) and trophic (glutamate) amino acid. Using this approach, we established that the woolly mammoth ate a distinct diet or lived in a distinct habitat within the mammoth steppe. In some cases, this habitat may have been shared with horse. Understanding that the woolly mammoth's high $\delta^{15}\text{N}_{\text{Bulk}}$ arose from a dietary or habitat source provides insight into the ecology of a keystone herbivore of the mammoth steppe, which provides a starting point to investigate the rest of the megafaunal species.

Chapter 4 further investigates the isotopic compositions of amino acids in mammoth steppe herbivores and carnivores. The $\delta^{15}\text{N}$ of 8 amino acids are used to establish the trophic position of a variety of megaherbivores and megacarnivores, and to establish that there likely were differences in the plant types consumed by certain species or individuals. These differences are further evaluated using the $\delta^{13}\text{C}$ of 9 amino acids. We use LDA of the $\delta^{13}\text{C}$ for 7 of these amino acids to classify the diets of each herbivore individual, and of the herbivores consumed by the carnivores. Differences in $\delta^{13}\text{C}_{\text{Bulk}}$ and $\delta^{15}\text{N}_{\text{Bulk}}$ are linked to differences in diet, such as the consumption of aquatic plants by the giant beaver and decayed plants by horse and woolly mammoth.

Chapter 5 integrates data for $\delta^{13}\text{C}_{\text{Bulk}}$ and $\delta^{15}\text{N}_{\text{Bulk}}$ of megaherbivores from numerous sites across the mammoth steppe. Using SIBER (Jackson et al., 2011), isotopic niche spaces were defined for each herbivore at each site for four time periods (pre-LGM, LGM, post-LGM and Holocene). Species are shown to have had consistent niche positions and niche overlaps across the mammoth steppe before the LGM. These niches were disrupted during the LGM, and were not re-established post-LGM. This analysis suggests that a major ecosystem shift occurred during the LGM that weakened the ecosystem's stability as a whole, and made it more susceptible to changes from other climatic or anthropogenic effects.

Chapter 6 summarizes the previous chapters and discusses the implications of these new data for our understanding of the mammoth steppe as a whole.

1.6 References

- Adamczewski, J., Gates, C.C., Soutar, B.M., Hudson, R.J., 1988. Limiting effects of snow on seasonal habitat use and diets of caribou (*Rangifer tarandus groenlandicus*) on Coats Island, Northwest Territories, Canada. *Can. J. Zool.* 66, 1986–1996.
- Adams, M., Grierson, P., 2001. Stable isotopes at natural abundance in terrestrial plant ecology and ecophysiology: an update. *Plant Biol.* 3, 299–310.
- Ambrose, S., 1990. Preparation and characterization of bone and tooth collagen for isotopic analysis. *J. Archaeol. Sci.* 17, 431–451.
- Ambrose, S., 1991. Effects of diet, climate and physiology on nitrogen isotope abundances in terrestrial foodwebs. *J. Archaeol. Sci.* 18, 293–317.

- Amundson, R., Austin, A., Schuur, E.A.G., Yoo, K., Matzek, V., Kendall, C., Uebersax, A., Brenner, D., Baisden, W.T., 2003. Global patterns of the isotopic composition of soil and plant nitrogen. *Glob. Biogeochemical Cycles* 17. doi:10.1029/2002GB001903
- Balasse, M., Bocherens, H., Mariotti, A., 1999. Intra-bone variability of collagen and apatite isotopic composition used as evidence of a change of diet. *J. Archaeol. Sci.* 26, 593–598.
- Barnes, I., Matheus, P., Shapiro, B., Jensen, D., Cooper, A., 2002. Dynamics of Pleistocene population extinctions in Beringian brown bears. *Science* 295, 2267–70. doi:10.1126/science.1067814
- Barnett, B., 1994. Carbon and nitrogen isotope ratios of caribou tissues, vascular plants, and lichens from northern Alaska. Master's Thesis. University of Alaska, Fairbanks.
- Barnosky, A.D., Koch, P.L., Feranec, R.S., Wing, S.L., Shabel, A.B., 2004. Assessing the causes of late Pleistocene extinctions on the continents. *Science* 306, 70–75. doi:10.1126/science.1101476
- Bellissimo, N.S., 2013. Origins of stable isotopic variations in late Pleistocene horse enamel and bone from Alberta. Master's Thesis. University of Western Ontario.
- Ben-David, M., Shochat, E., Adams, L., 2001. Utility of stable isotope analysis in studying foraging ecology of herbivores: examples from moose and caribou. *Alces* 37, 421–434.
- Blinnikov, M.S., Gaglioti, B. V., Walker, D.A., Wooller, M.J., Zazula, G.D., 2011. Pleistocene graminoid-dominated ecosystems in the Arctic. *Quat. Sci. Rev.* 30, 2906–2929. doi:10.1016/j.quascirev.2011.07.002
- Blok, D., Weijers, S., Welker, J.M., Cooper, E.J., Michelsen, A., Löffler, J., Elberling, B., 2015. Deepened winter snow increases stem growth and alters stem $\delta^{13}\text{C}$ and $\delta^{15}\text{N}$ in evergreen dwarf shrub *Cassiope tetragona* in high-arctic Svalbard tundra. *Environ. Res. Lett.* 10, 044008. doi:10.1088/1748-9326/10/4/044008
- Bocherens, H., 2003. Isotopic biogeochemistry and the paleoecology of the mammoth steppe fauna. *Deinsea* 9, 57–76.
- Bocherens, H., 2015. Isotopic tracking of large carnivore palaeoecology in the mammoth steppe. *Quat. Sci. Rev.* 117, 42–71. doi:10.1016/j.quascirev.2015.03.018
- Bocherens, H., Drucker, D.G., Bonjean, D., Bridault, A., Conard, N.J., Cupillard, C., Germonpré, M., Höneisen, M., Münzel, S.C., Napierala, H., Patou-Mathis, M., Stephan, E., Uerpman, H.-P., Ziegler, R., 2011. Isotopic evidence for dietary ecology of cave lion (*Panthera spelaea*) in North-Western Europe: prey choice, competition and implications for extinction. *Quat. Int.* 245, 249–261. doi:10.1016/j.quaint.2011.02.023

- Bocherens, H., Fizet, M., Mariotti, A., Gangloff, R., Burns, J., 1994. Contribution of isotopic biogeochemistry (^{13}C , ^{15}N , ^{18}O) to the paleoecology of mammoths (*Mammuthus primigenius*). *Hist. Biol.* 7, 187–202.
- Bonafini, M., Pellegrini, M., Ditchfield, P., Pollard, A.M., 2013. Investigation of the “canopy effect” in the isotope ecology of temperate woodlands. *J. Archaeol. Sci.* 40, 3926–3935. doi:10.1016/j.jas.2013.03.028
- Boutton, T.W., 1996. Stable carbon isotope ratios of soil organic matter and their use as indicators of vegetation and climate change, in: Boutton, T.W., Yamasaki, S.I. (Eds.), *Mass Spectrometry of Soils*. Marcel Dekker Inc., New York, pp. 47–82.
- Britton, K., Gaudzinski-Windheuser, S., Roebroeks, W., Kindler, L., Richards, M.P., 2012. Stable isotope analysis of well-preserved 120,000-year-old herbivore bone collagen from the Middle Palaeolithic site of Neumark-Nord 2, Germany reveals niche separation between bovids and equids. *Palaeogeogr. Palaeoclimatol. Palaeoecol.* 333–334, 168–177. doi:10.1016/j.palaeo.2012.03.028
- Buchmann, N., Kao, W.-Y., Ehleringer, J., 1997. Influence of stand structure on carbon-13 of vegetation, soils, and canopy air within deciduous and evergreen forests in Utah, United States. *Oecologia* 110, 109–119. doi:10.1007/s004420050139
- Busch, F.A., Sage, T.L., Cousins, A.B., Sage, R.F., 2013. C_3 plants enhance rates of photosynthesis by reassimilating photorespired and respired CO_2 . *Plant. Cell Environ.* 36, 200–212. doi:10.1111/j.1365-3040.2012.02567.x
- Castaños, J., Zuluaga, M.C., Ortega, L.Á., Murelaga, X., Alonso-Olazabal, A., Rofes, J., Castaños, P., 2014. Carbon and nitrogen stable isotopes of bone collagen of large herbivores from the Late Pleistocene Kiputz IX cave site (Gipuzkoa, north Iberian Peninsula) for palaeoenvironmental reconstruction. *Quat. Int.* 339–340, 131–138. doi:10.1016/j.quaint.2013.10.006
- Chapman, D., 1975. Antlers – bones of contention. *Mamm. Rev.* 5, 121–172.
- Coltrain, J.B., Harris, J.M., Cerling, T.E., Ehleringer, J.R., Dearing, M.-D., Ward, J., Allen, J., 2004. Rancho La Brea stable isotope biogeochemistry and its implications for the palaeoecology of late Pleistocene, coastal southern California. *Palaeogeogr. Palaeoclimatol. Palaeoecol.* 205, 199–219. doi:10.1016/j.palaeo.2003.12.008
- Cooper, A., Turney, C., Hughen, K.A., Brook, B.W., McDonald, H.G., Bradshaw, C.J.A., 2015. Abrupt warming events drove Late Pleistocene Holarctic megafaunal turnover. *Science* 349, 602–606. doi:10.1126/science.aac4315
- Craine, J., Craine, J.M., Elmore, A.J., Aidar, M.P.M., Bustamante, M., Dawson, T.E., Hobbie, E.A., Kahmen, A., Mack, M.C., Mclauchlan, K.K., Michelsen, A., Nardoto, G.B., Pardo, L.H, Peñuelas, J., Reich, P.B., Schuur, E.A.G., Stock, W.D., Templer, P.H., Virginia, R.A., Welker, J.M., Wright, I.J., 2009. Global patterns of foliar

- nitrogen isotopes and their relationships with climate, mycorrhizal fungi, foliar nutrient concentrations, and nitrogen availability, *New Phytologist* 183, 980-992.
- Dawson, T.E., Mambelli, S., Plamboeck, A.H., Templer, P.H., Tu, K.P., 2002. Stable isotopes in plant ecology. *Annu. Rev. Ecol. Syst.* 33, 507–559.
doi:10.1146/annurev.ecolsys.33.020602.095451
- de Bello, F., Buchmann, N., Casals, P., Lepš, J., Sebastià, M.-T., 2009. Relating plant species and functional diversity to community $\delta^{13}\text{C}$ in NE Spain pastures. *Agric. Ecosyst. Environ.* 131, 303–307. doi:10.1016/j.agee.2009.02.002
- Delong, M.D., Thorp, J.H., 2006. Significance of instream autotrophs in trophic dynamics of the Upper Mississippi River. *Oecologia* 147, 76–85.
doi:10.1007/s00442-005-0241-y
- DeNiro, M., 1985. Postmortem preservation and alteration of in vivo bone collagen isotope ratios in relation to palaeodietary reconstruction. *Nature* 317, 806–809.
doi:10.1038/317806a0
- Diefendorf, A., Mueller, K., Wing, S.L., Koch, P.L., Freeman, K.H., 2010. Global patterns in leaf ^{13}C discrimination and implications for studies of past and future climate. *Proc. Natl. Acad. Sci.* 107, 5738–5743.
- Doucett, R.R., Barton, D.R., Guiguer, K., Power, G., Drimmie, R.J., 1996. Comment: Critical examination of stable isotope analysis as a means for tracing carbon pathways in stream ecosystems. *Can. J. Fish. Aquat. Sci.* 53, 1913–1915.
doi:10.1139/f96-114
- Druckenmiller, P.S., 2008. Survey of Pleistocene (Ice Age) vertebrates from the Selawik and Kobuk River areas of Northwestern Alaska. Intern. Rep. U.S. Fish Wildl. Serv. 1–56.
- Drucker, D.G., Bocherens, H., Bridault, A., Billiou, D., 2003a. Carbon and nitrogen isotopic composition of red deer (*Cervus elaphus*) collagen as a tool for tracking palaeoenvironmental change during the Late-Glacial and Early Holocene in the northern Jura (France). *Palaeogeogr. Palaeoclimatol. Palaeoecol.* 195, 375–388.
doi:10.1016/S0031-0182(03)00366-3
- Drucker, D.G., Bocherens, H., Billiou, D., 2003b. Evidence for shifting environmental conditions in Southwestern France from 33 000 to 15 000 years ago derived from carbon-13 and nitrogen-15 natural abundances in collagen of large herbivores. *Earth Planet. Sci. Lett.* 216, 163–173. doi:10.1016/S0012-821X(03)00514-4
- Drucker, D.G., Bridault, A., Hobson, K. a., Szuma, E., Bocherens, H., 2008. Can carbon-13 in large herbivores reflect the canopy effect in temperate and boreal ecosystems? Evidence from modern and ancient ungulates. *Palaeogeogr. Palaeoclimatol. Palaeoecol.* 266, 69–82. doi:10.1016/j.palaeo.2008.03.020

- Drucker, D.G., Hobson, K.A., Ouellet, J.-P., Courtois, R., 2010. Influence of forage preferences and habitat use on ^{13}C and ^{15}N abundance in wild caribou (*Rangifer tarandus caribou*) and moose (*Alces alces*) from Canada. *Isotopes Environ. Health Stud.* 46, 107–21. doi:10.1080/10256010903388410
- Edwards, M., Mock, C., Finney, B., Barber, V.A., Bartlein, P.J., 2001. Potential analogues for paleoclimatic variations in eastern interior Alaska during the past 14,000 yr: atmospheric-circulation controls of regional temperature. *Quat. Sci. Rev.* 20, 189–202.
- Ehleringer, J., Comstock, J., Cooper, T., 1987. Leaf-twig carbon isotope ratio differences in photosynthetic-twig desert shrubs. *Oecologia* 71, 318–320.
- Ehleringer, J., Cooper, T., 1988. Correlations between carbon isotope ratio and microhabitat in desert plants. *Oecologia* 76, 562–566.
- Ehleringer, J., Phillips, S., Comstock, J., 1992. Seasonal variation in the carbon isotopic composition of desert plants. *Funct. Ecol.* 6, 396–404.
- Elias, S. a., 2000. Late Pleistocene climates of Beringia, based on analysis of fossil beetles. *Quat. Res.* 53, 229–235. doi:10.1006/qres.1999.2093
- Faith, J., 2011. Late Pleistocene climate change, nutrient cycling, and the megafaunal extinctions in North America. *Quat. Sci. Rev.* 30, 1675–1680.
- Faith, J.T., Surovell, T.A., 2009. Synchronous extinction of North America's Pleistocene mammals. *Proc. Natl. Acad. Sci.* 106, 20641–20645.
- Farquhar, G., 1989. Carbon isotope discrimination and photosynthesis. *Annu. Rev. Plant Biol.* 40, 503–537.
- Finlay, J., Kendall, C., 2007. Stable isotope tracing of temporal and spatial variability in organic matter sources to freshwater ecosystems, in: Michener, R., Lajtha, K. (Eds.), *Stable Isotopes in Ecology and Environmental Science*. Blackwell Publishing Ltd, Hong Kong, pp. 283–333.
- Finstad, G.L., Kielland, K., 2011. Landscape variation in the diet and productivity of reindeer in Alaska based on stable isotope analyses. *Arctic, Antarct. Alp. Res.* 43, 543–554. doi:10.1657/1938-4246-43.4.543
- Fizet, M., Mariotti, A., Bocherens, H., Lange-Badré, B., Vandermeersch, B., Borel, J.P., Bellon, G., 1995. Effect of diet, physiology and climate on carbon and nitrogen stable isotopes of collagen in a Late Pleistocene anthropic palaeoecosystem: Marillac, Charente, France. *J. Archaeol. Sci.* 22, 67–79.
- Fogel, M., Tuross, N., 2003. Extending the limits of paleodietary studies of humans with compound specific carbon isotope analysis of amino acids. *J. Archaeol. Sci.* 30, 535–545.

- Fox, D.L., Fisher, D.C., Vartanyan, S., Tikhonov, A.N., Mol, D., Buigues, B., 2007. Paleoclimatic implications of oxygen isotopic variation in late Pleistocene and Holocene tusks of *Mammuthus primigenius* from northern Eurasia. *Quat. Int.* 169–170, 154–165. doi:10.1016/j.quaint.2006.09.001
- Fox-Dobbs, K., Leonard, J., Koch, P., 2008. Pleistocene megafauna from eastern Beringia: paleoecological and paleoenvironmental interpretations of stable carbon and nitrogen isotope and radiocarbon records. *Palaeogeogr. Palaeoclimatol. Palaeoecol.* 261, 30–46.
- France, R., 1995. Critical examination of stable isotope analysis as a means for tracing carbon pathways in stream ecosystems. *Can. J. Fish. Aquat. Sci.* 52, 651–656.
- France, R.L., 1995. Source variability in $\delta^{15}\text{N}$ of autotrophs as a potential aid in measuring allochthony in freshwaters. *Ecography* 18, 318–320. doi:10.1111/j.1600-0587.1995.tb00134.x
- Fry, B., 1991. Stable isotope diagrams of freshwater food webs. *Ecology* 72, 2293–2297.
- Gaglioti, B. V., Barnes, B.M., Zazula, G.D., Beaudoin, A.B., Wooller, M.J., 2011. Late Pleistocene paleoecology of arctic ground squirrel (*Urocitellus parryii*) caches and nests from Interior Alaska's mammoth steppe ecosystem, USA. *Quat. Res.* 76, 373–382. doi:10.1016/j.yqres.2011.08.004
- Gannes, L., del Rio, C., Koch, P., 1998. Natural abundance variations in stable isotopes and their potential uses in animal physiological ecology. *Comp. Biochem. Physiol. Part A Mol. Integr. Physiol.* 119, 725–737.
- Garten Jr, C.T., Taylor Jr, G.E., 1992. Foliar $\delta^{13}\text{C}$ within a temperate deciduous forest: spatial, temporal, and species sources of variation. *Oecologia* 90, 1–7.
- Gebauer, G., Schulze, E., 1991. Carbon and nitrogen isotope ratios in different compartments of a healthy and a declining *Picea abies* forest in the Fichtelgebirge, NE Bavaria. *Oecologia* 87, 198–207.
- Gill, J.L., Williams, J.W., Jackson, S.T., Lininger, K.B., Robinson, G.S., 2009. Pleistocene megafaunal collapse, novel plant communities, and enhanced fire regimes in North America. *Science* 326, 1100–1103. doi:10.1126/science.1179504
- Gleixner, G., Danier, H.J., Werner, R.A., Schmidt, H.L., 1993. Correlations between the ^{13}C content of primary and secondary plant products in different cell compartments and that in decomposing Basidiomycetes. *Plant Physiol.* 102, 1287–1290. doi:10.1104/pp.102.4.1287
- Goetcheus, V.G., Birks, H.H., 2001. Full-glacial upland tundra vegetation preserved under tephra in the Beringia National Park, Seward Peninsula, Alaska. *Quat. Sci. Rev.* 20, 135–147. doi:10.1016/S0277-3791(00)00127-X

- Grayson, D.K., Meltzer, D.J., 2003. A requiem for North American overkill. *J. Archaeol. Sci.* 30, 585–593. doi:10.1016/S0305-4403(02)00205-4
- Guthrie, R.D., 1968. Paleoeology of the large-mammal community in interior Alaska during the late Pleistocene. *Am. Midl. Nat.* 79, 346–363.
- Guthrie, R.D., 1982. Mammals of the mammoth steppe as paleoenvironmental indicators, in: Hopkins, D.M., Matthews, Jr., J.V., Schweger, C.E., Young, S.B. (Eds.), *Paleoecology of Beringia*. Academic Press, New York, pp. 307–326.
- Guthrie, R.D., 1990. *Frozen fauna of the mammoth steppe: the story of Blue Babe*. The University of Chicago Press, Chicago.
- Guthrie, R.D., 2001. Origin and causes of the mammoth steppe: a story of cloud cover, woolly mammal tooth pits, buckles, and inside-out Beringia. *Quat. Sci. Rev.*
- Guthrie, R.D., 2003. Rapid body size decline in Alaskan Pleistocene horses before extinction. *Nature* 426, 169–171. doi:10.1038/nature02070.1.
- Guthrie, R.D., 2006. New carbon dates link climatic change with human colonization and Pleistocene extinctions. *Nature* 441, 207–209. doi:10.1038/nature04604
- Handley, L.L., Raven, J.A., 1992. The use of natural abundance of nitrogen isotopes in plant physiology and ecology. *Plant, Cell Environ.* 15, 965–985. doi:10.1111/j.1365-3040.1992.tb01650.x
- Hannides, C.C.S., Popp, B.N., Landry, M.R., Graham, B.S., 2009. Quantification of zooplankton trophic position in the North Pacific Subtropical Gyre using stable nitrogen isotopes. *Limnol. Oceanogr.* 54, 50–61. doi:10.4319/lo.2009.54.1.0050
- Heaton, T.H.E., 1987. The $^{15}\text{N}/^{14}\text{N}$ ratios of plants in South Africa and Namibia: relationship to climate and coastal/saline environments. *Oecologia* 74, 236–246.
- Heaton, T.H.E., 1999. Spatial, species, and temporal variations in the $^{13}\text{C}/^{12}\text{C}$ ratios of C_3 plants: implications for palaeodiet studies. *J. Archaeol. Sci.* 26, 637–649.
- Heggberget, T., Gaare, E., Ball, J., 2002. Reindeer (*Rangifer tarandus*) and climate change: importance of winter forage. *Rangifer* 22, 13–31.
- Hobson, K.A., Alisauskas, R.T., Clark, R.G., 1993. Stable-nitrogen isotope enrichment in avian tissues due to fasting and nutritional stress: implications for isotopic analyses of diet. *Condor* 95, 388–394.
- Höfle, C., Edwards, M.E., Hopkins, D.M., Mann, D.H., Ping, C.-L., 2000. The full-glacial environment of the northern Seward Peninsula, Alaska, reconstructed from the 21,500-year-old Kitluk paleosol. *Quat. Res.* 53, 143–153. doi:10.1006/qres.1999.2097

- Howland, M.R., Corr, L.T., Young, S.M.M., Jones, V., Jim, S., Van Der Merwe, N.J., Mitchell, A.D., Evershed, R.P., 2003. Expression of the dietary isotope signal in the compound-specific $\delta^{15}\text{N}$ values of pig bone lipids and amino acids. *Int. J. Osteoarchaeol.* 13, 54–65. doi:10.1002/oa.658
- Iacumin, P., Davanzo, S., Nikolaev, V., 2005. Short-term climatic changes recorded by mammoth hair in the Arctic environment. *Palaeogeogr. Palaeoclimatol. Palaeoecol.* 218, 317–324. doi:10.1016/j.palaeo.2004.12.021
- Iacumin, P., Davanzo, S., Nikolaev, V., 2006. Spatial and temporal variations in the $^{13}\text{C}/^{12}\text{C}$ and $^{15}\text{N}/^{14}\text{N}$ ratios of mammoth hairs: Palaeodiet and palaeoclimatic implications. *Chem. Geol.* 231, 16–25. doi:10.1016/j.chemgeo.2005.12.007
- Iacumin, P., Matteo, A. Di, Nikolaev, V., Kuznetsova, T., 2010. Climate information from C, N and O stable isotope analyses of mammoth bones from northern Siberia. *Quat. Int.* 212, 206–212.
- Iacumin, P., Nikolaev, V., Ramigni, M., 2000. C and N stable isotope measurements on Eurasian fossil mammals, 40 000 to 10 000 years BP: herbivore physiologies and palaeoenvironmental reconstruction. *Palaeogeogr. Palaeoclimatol. Palaeoecol.* 163, 33–47.
- Jackson, A.L., Inger, R., Parnell, A.C., Bearhop, S., 2011. Comparing isotopic niche widths among and within communities: SIBER - Stable Isotope Bayesian Ellipses in R. *J. Anim. Ecol.* 80, 595–602. doi:10.1111/j.1365-2656.2011.01806.x
- Jim, S., Jones, V., Ambrose, S.H., Evershed, R.P., 2006. Quantifying dietary macronutrient sources of carbon for bone collagen biosynthesis using natural abundance stable carbon isotope analysis. *Br. J. Nutr.* 95, 1055–1062. doi:10.1079/BJN20051685
- Keeley, J., Sandquist, D., 1992. Carbon: freshwater plants. *Plant. Cell Environ.* 15, 1021–1035.
- Kelly, J., 2000. Stable isotopes of carbon and nitrogen in the study of avian and mammalian trophic ecology. *Can. J. Zool.* 78, 1–27.
- Kempster, B., Zanette, L., Longstaffe, F.J., MacDougall-Shackleton, S.A., Wingfield, J.C., Clinchy, M., 2007. Do stable isotopes reflect nutritional stress? Results from a laboratory experiment on song sparrows. *Oecologia* 151, 365–71. doi:10.1007/s00442-006-0597-7
- Kielland, K., 2001. Stable isotope signatures of moose in relation to seasonal forage composition: a hypothesis. *Alces* 37, 329–337.
- Koch, P., 1991. The isotopic ecology of Pleistocene proboscideans. *J. Vertebr. Paleontol.* 11, 40A.

- Koch, P., 2007. Isotopic study of the biology of modern and fossil vertebrates, in: Michener, R., Lajtha, K. (Eds.), *Stable Isotopes in Ecology and Environmental Science*. Blackwell Publishing Ltd, Hong Kong, pp. 99–154.
- Koch, P., Fogel, M., Tuross, N., 1994. Tracing the diets of fossil animals using stable isotopes, in: Lajtha, K., Michener, R. (Eds.), *Stable Isotopes in Ecology and Environmental Science*. Blackwell Scientific Publications, pp. 63–92.
- Koch, P.L., Barnosky, A.D., 2006. Late Quaternary extinctions: state of the debate. *Annu. Rev. Ecol. Evol. Syst.* 37, 215–250. doi:10.1146/annurev.ecolsys.34.011802.132415
- Kohn, M.J., 2010. Carbon isotope compositions of terrestrial C₃ plants as indicators of (paleo)ecology and (paleo)climate. *Proc. Natl. Acad. Sci. U. S. A.* 107, 19691–5. doi:10.1073/pnas.1004933107
- Kohn, M.J., 2011. Reply to Freeman et al.: Carbon isotope discrimination by C₃ plants. *Proc. Natl. Acad. Sci.* 108, E61–E61. doi:10.1073/pnas.1103222108
- Kristensen, D.K., Kristensen, E., Forchhammer, M.C., Michelsen, A., Schmidt, N.M., 2011. Arctic herbivore diet can be inferred from stable carbon and nitrogen isotopes in C₃ plants, faeces, and wool. *Can. J. Zool.* 89, 892–899. doi:10.1139/z11-073
- Kuitens, M., van Kolschoten, T., van der Plicht, J., 2012. Elevated $\delta^{15}\text{N}$ values in mammoths: a comparison with modern elephants. *Archaeol. Anthropol. Sci.* 1–7. doi:10.1007/s12520-012-0095-2
- Larsen, T., Taylor, D.L., Leigh, M.B., O'Brien, D.M., 2009. Stable isotope fingerprinting: a novel method for identifying plant, fungal, or bacterial origins of amino acids. *Ecology* 90, 3526–35.
- Larsen, T., Ventura, M., Andersen, N., O'Brien, D.M., Piatkowski, U., McCarthy, M.D., 2013. Tracing carbon sources through aquatic and terrestrial food webs using amino acid stable isotope fingerprinting. *PLoS One* 8, e73441. doi:10.1371/journal.pone.0073441
- Larsen, T., Ventura, M., O'Brien, D.M., Magid, J., Lomstein, B.A., Larsen, J., 2011. Contrasting effects of nitrogen limitation and amino acid imbalance on carbon and nitrogen turnover in three species of Collembola. *Soil Biol. Biochem.* 43, 749–759. doi:10.1016/j.soilbio.2010.12.008
- Larsen, T., Wooller, M.J., Fogel, M.L., O'Brien, D.M., 2012. Can amino acid carbon isotope ratios distinguish primary producers in a mangrove ecosystem? *Rapid Commun. Mass Spectrom.* 26, 1541–1548. doi:10.1002/rcm.6259
- Layman, C., Arrington, D., Montaña, C., Post, D., 2007. Can stable isotope ratios provide for community-wide measures of trophic structure? *Ecology* 88, 42–48.

- Layman, C.A., Araujo, M.S., Boucek, R., Hammerschlag-Peyer, C.M., Harrison, E., Jud, Z.R., Matich, P., Rosenblatt, A.E., Vaudo, J.J., Yeager, L.A., Post, D.M., Bearhop, S., 2012. Applying stable isotopes to examine food-web structure: an overview of analytical tools. *Biol. Rev. Camb. Philos. Soc.* 87, 545–62. doi:10.1111/j.1469-185X.2011.00208.x
- LaZerte, B., Szalados, J., 1982. Stable carbon isotope ratio of submerged freshwater macrophytes. *Limnol. Oceanogr.* 27, 413–418.
- Lynch, A.H., McCullagh, J.S.O., Hedges, R.E.M., 2011. Liquid chromatography/isotope ratio mass spectrometry measurement of $\delta^{13}\text{C}$ of amino acids in plant proteins. *Rapid Commun. Mass Spectrom.* 25, 2981–8. doi:10.1002/rcm.5142
- Mann, D.H., Groves, P., Kunz, M.L., Reanier, R.E., Gaglioti, B. V., 2013. Ice-age megafauna in Arctic Alaska: extinction, invasion, survival. *Quat. Sci. Rev.* 70, 91–108. doi:10.1016/j.quascirev.2013.03.015
- Marshall, J.D., Brooks, J.R., Lajtha, K., 2007. Sources of variation in the stable isotopic composition of plants, in: Michener, R., Lajtha, K. (Eds.), *Stable Isotopes in Ecology and Environmental Science*. Blackwell Publishing Ltd, Hong Kong, pp. 22–60.
- McArthur, J.V., Moorhead, K.K., 1996. Characterization of riparian species and stream detritus using multiple stable isotopes. *Oecologia* 107, 232–238. doi:10.1007/BF00327907
- McCarthy, M.D., Benner, R., Lee, C., Fogel, M.L., 2007. Amino acid nitrogen isotopic fractionation patterns as indicators of heterotrophy in plankton, particulate, and dissolved organic matter. *Geochim. Cosmochim. Acta* 71, 4727–4744. doi:10.1016/j.gca.2007.06.061
- McClelland, J., Montoya, J., 2002. Trophic relationships and the nitrogen isotopic composition of amino acids in plankton. *Ecology* 83, 2173–2180.
- McMahon, K.W., Fogel, M.L., Elsdon, T.S., Thorrold, S.R., 2010. Carbon isotope fractionation of amino acids in fish muscle reflects biosynthesis and isotopic routing from dietary protein. *J. Anim. Ecol.* 79, 1132–41. doi:10.1111/j.1365-2656.2010.01722.x
- Meiri, M., Lister, A.M., Collins, M.J., Tuross, N., Goebel, T., Blockley, S., Zazula, G.D., van Doorn, N., Guthrie, R.D., Boeskorov, G.G., Baryshnikov, G.F., Sher, A., Barnes, I., 2014. Faunal record identifies Bering isthmus conditions as constraint to end-Pleistocene migration to the New World. *Proc. Biol. Sci.* 281, 20132167. doi:10.1098/rspb.2013.2167
- Metcalf, J.Z., 2011. Late Pleistocene climate and proboscidean paleoecology in North America: insights from stable isotope compositions of skeletal remains. Doctoral Thesis. University of Western Ontario.

- Metcalfe, J.Z., Longstaffe, F.J., Hodgins, G., 2013. Proboscideans and paleoenvironments of the Pleistocene Great Lakes: landscape, vegetation, and stable isotopes. *Quat. Sci. Rev.* 76, 102–113. doi:10.1016/j.quascirev.2013.07.004
- Metcalfe, J.Z., Longstaffe, F.J., Zazula, G.D., 2010. Nursing, weaning, and tooth development in woolly mammoths from Old Crow, Yukon, Canada: implications for Pleistocene extinctions. *Palaeogeogr. Palaeoclimatol. Palaeoecol.* 298, 257–270. doi:10.1016/j.palaeo.2010.09.032
- Miller, M.J., Chikaraishi, Y., Ogawa, N.O., Yamada, Y., Tsukamoto, K., Ohkouchi, N., 2012. A low trophic position of Japanese eel larvae indicates feeding on marine snow. *Biol. Lett.* 9, 20120826.
- Milligan, H.E., Pretzlaw, T.D., Humphries, M.M., 2010. Stable isotope differentiation of freshwater and terrestrial vascular plants in two subarctic regions. *Ecoscience* 17, 265–275. doi:10.2980/17-3-3282
- Mol, D., Tikhonov, A., van der Plicht, J., Kahlke, R.-D., Debruyne, R., van Geel, B., van Reenen, G., Pals, J.P., de Marliave, C., Reumer, J.W.F., 2006. Results of the CERPOLEX/Mammuthus Expeditions on the Taimyr Peninsula, Arctic Siberia, Russian Federation. *Quat. Int.* 142-143, 186–202. doi:10.1016/j.quaint.2005.03.016
- Nadelhoffer, K., Shaver, G., Fry, B., Giblin, A., 1996. ¹⁵N natural abundances and N use by tundra plants. *Oecologia* 107, 386–394.
- Naito, Y.I., Chikaraishi, Y., Ohkouchi, N., Mukai, H., Shibata, Y., Honch, N. V., Dodo, Y., Ishida, H., Amano, T., Ono, H., Yoneda, M., 2010. Dietary reconstruction of the Okhotsk culture of Hokkaido, Japan, based on nitrogen composition of amino acids: implications for correction of ¹⁴C marine reservoir effects on human bones. *Radiocarbon* 52, 671–681.
- Nelson, D.E., Angerbjörn, A., Lidén, K., Turk, I., 1998. Stable isotopes and the metabolism of the European cave bear. *Oecologia* 116, 177–181. doi:10.1007/s004420050577
- Newsome, S.D., Wolf, N., Peters, J., Fogel, M.L., 2014. Amino acid $\delta^{13}\text{C}$ analysis shows flexibility in the routing of dietary protein and lipids to the tissue of an omnivore. *Integr. Comp. Biol.* 54, 890–902. doi:10.1093/icb/icu106
- Osmond, C., Valaane, N., Haslam, S., Uotila, P., Roksandic, Z., 1981. Comparisons of $\delta^{13}\text{C}$ values in leaves of aquatic macrophytes from different habitats in Britain and Finland; some implications for photosynthetic processes in aquatic plants. *Oecologia* 50, 117–124.
- Parnell, A.C., Inger, R., Bearhop, S., Jackson, A.L., 2010. Source partitioning using stable isotopes: coping with too much variation. *PLoS One* 5, e9672. doi:10.1371/journal.pone.0009672

- Peterson, B., Fry, B., 1987. Stable isotopes in ecosystem studies. *Annu. Rev. Ecol. Syst.* 18, 193–320.
- Pires, M.M., Koch, P.L., Farina, R.A., de Aguiar, M.A.M., dos Reis, S.F., Guimaraes, Paulo R., J., 2015. Pleistocene megafaunal interaction networks became more vulnerable after human arrival. *Proc R Soc B* 282, 20151367. doi:10.1098/rspb.2015.1367
- Polischuk, S., Hobson, K., Ramsay, M., 2011. Use of stable-carbon and -nitrogen isotopes to assess weaning and fasting in female polar bears and their cubs. *Can. J. Zool.* 79, 499–511.
- Popp, B., Graham, B., Olson, R., Hannides, C., Lott, M.J., López-Ibarra, G.A., Galván-Magaña, F., Fry, B., 2007. Insight into the trophic ecology of Yellowfin Tuna, *Thunnus albacares*, from compound-specific nitrogen isotope analysis of proteinaceous amino acids. *Terr. Ecol.* 1, 173–190.
- R Core Team, 2014. R: A language and environment for statistical computing. R Foundation for Statistical Computing, Vienna, Austria.
- Raghavan, M., Espregueira Themudo, G., Smith, C.I., Zazula, G., Campos, P.F., 2014. Musk ox (*Ovibos moschatus*) of the mammoth steppe: tracing palaeodietary and palaeoenvironmental changes over the last 50,000 years using carbon and nitrogen isotopic analysis. *Quat. Sci. Rev.* 102, 192–201. doi:10.1016/j.quascirev.2014.08.001
- Richards, M.P., Hedges, R.E.M., 2003. Variations in bone collagen $\delta^{13}\text{C}$ and $\delta^{15}\text{N}$ values of fauna from Northwest Europe over the last 40 000 years. *Palaeogeogr. Palaeoclimatol. Palaeoecol.* 193, 261–267. doi:10.1016/S0031-0182(03)00229-3
- Rountrey, A.N., Fisher, D.C., Vartanyan, S., Fox, D.L., 2007. Carbon and nitrogen isotope analyses of a juvenile woolly mammoth tusk: evidence of weaning. *Quat. Int.* 169–170, 166–173. doi:10.1016/j.quaint.2006.08.002
- Sandom, C., Faurby, S., Sandel, B., Svenning, J.-C., 2014. Global late Quaternary megafauna extinctions linked to humans, not climate change. *Proc. Biol. Sci.* 281, 20133254–. doi:10.1098/rspb.2013.3254
- Schubert, B.A., Jahren, A.H., 2015. Global increase in plant carbon isotope fractionation following the Last Glacial Maximum caused by increase in atmospheric $p\text{CO}_2$. *Geology* 43, 435–438. doi:10.1130/G36467.1
- Schweger, C., Froese, D., White, J.M., Westgate, J.A., 2011. Pre-glacial and interglacial pollen records over the last 3 Ma from northwest Canada: why do Holocene forests differ from those of previous interglaciations? *Quat. Sci. Rev.* 30, 2124–2133. doi:10.1016/j.quascirev.2011.01.020
- Sealy, J., van der Merwe, N., Thorp, J.A.L., Lanham, J.L., 1987. Nitrogen isotopic

- ecology in southern Africa: implications for environmental and dietary tracing. *Geochim. Cosmochim. Acta* 51, 2707–2717.
- Shapiro, B., Drummond, A.J., Rambaut, A., Wilson, M.C., Matheus, P.E., Sher, A. V., Pybus, O.G., Gilbert, M.T.P., Barnes, I., Binladen, J., Willerslev, E., Hansen, A.J., Baryshnikov, G.F., Burns, J. a, Davydov, S., Driver, J.C., Froese, D.G., Harington, C.R., Keddie, G., Kosintsev, P., Kunz, M.L., Martin, L.D., Stephenson, R.O., Storer, J., Tedford, R., Zimov, S., Cooper, A., 2004. Rise and fall of the Beringian steppe bison. *Science* 306, 1561–5. doi:10.1126/science.1101074
- Sherwood, O.A., Lehmann, M.F., Schubert, C.J., Scott, D.B., McCarthy, M.D., 2011. Nutrient regime shift in the western North Atlantic indicated by compound-specific $\delta^{15}\text{N}$ of deep-sea gorgonian corals. *Proc. Natl. Acad. Sci. U. S. A.* 108, 1011–1015. doi:10.1073/pnas.1004904108
- Smallwood, B.J., Wooller, M.J., Jacobson, M.E., Fogel, M.L., 2003. Isotopic and molecular distributions of biochemicals from fresh and buried *Rhizophora mangle* leaves. *Geochem. Trans.* 4, 38–46. doi:10.1039/b308902a
- Sponheimer, M., Robinson, T., Ayliffe, L., Roeder, B., Hammer, J., Passey, B., West, A., Cerling, T., Dearing, D., Ehleringer, J., 2003. Nitrogen isotopes in mammalian herbivores: hair $\delta^{15}\text{N}$ values from a controlled feeding study. *Int. J. Osteoarchaeol.* 13, 80–87. doi:10.1002/oa.655
- Stevens, R., Lister, A., Hedges, R., 2006. Predicting diet, trophic level and palaeoecology from bone stable isotope analysis: a comparative study of five red deer populations. *Oecologia* 149, 12–21.
- Stevens, R.E., Germonpré, M., Petrie, C.A., O’Connell, T.C., 2009. Palaeoenvironmental and chronological investigations of the Magdalenian sites of Goyet Cave and Trou de Chaleux (Belgium), via stable isotope and radiocarbon analyses of horse skeletal remains. *J. Archaeol. Sci.* 36, 653–662. doi:10.1016/j.jas.2008.10.008
- Stevens, R.E., Hedges, R.E., 2004. Carbon and nitrogen stable isotope analysis of northwest European horse bone and tooth collagen, 40,000 BP–present: palaeoclimatic interpretations. *Quat. Sci. Rev.* 23, 977–991. doi:10.1016/j.quascirev.2003.06.024
- Stevens, R.E., Jacobi, R., Street, M., Germonpré, M., Conard, N.J., Münzel, S.C., Hedges, R.E.M., 2008. Nitrogen isotope analyses of reindeer (*Rangifer tarandus*), 45,000 BP to 9,000 BP: palaeoenvironmental reconstructions. *Palaeogeogr. Palaeoclimatol. Palaeoecol.* 262, 32–45. doi:10.1016/j.palaeo.2008.01.019
- Styring, A.K., Fraser, R.A., Bogaard, A., Evershed, R.P., 2014. Cereal grain, rachis and pulse seed amino acid $\delta^{15}\text{N}$ values as indicators of plant nitrogen metabolism. *Phytochemistry* 97, 20–9. doi:10.1016/j.phytochem.2013.05.009
- Styring, A.K., Sealy, J.C., Evershed, R.P., 2010. Resolving the bulk $\delta^{15}\text{N}$ values of

- ancient human and animal bone collagen via compound-specific nitrogen isotope analysis of constituent amino acids. *Geochim. Cosmochim. Acta* 74, 241–251. doi:10.1016/j.gca.2009.09.022
- Sykes, N.J., Baker, K.H., Carden, R.F., Higham, T.F.G., Hoelzel, A.R., Stevens, R.E., 2011. New evidence for the establishment and management of the European fallow deer (*Dama dama dama*) in Roman Britain. *J. Archaeol. Sci.* 38, 156–165. doi:10.1016/j.jas.2010.08.024
- Szpak, P., 2011. Fish bone chemistry and ultrastructure: implications for taphonomy and stable isotope analysis. *J. Archaeol. Sci.* 38, 3358–3372. doi:10.1016/j.jas.2011.07.022
- Szpak, P., Gröcke, D.R., Debruyne, R., MacPhee, R.D.E., Guthrie, R.D., Froese, D., Zazula, G.D., Patterson, W.P., Poinar, H.N., 2010. Regional differences in bone collagen $\delta^{13}\text{C}$ and $\delta^{15}\text{N}$ of Pleistocene mammoths: implications for paleoecology of the mammoth steppe. *Palaeogeogr. Palaeoclimatol. Palaeoecol.* 286, 88–96. doi:10.1016/j.palaeo.2009.12.009
- Szpak, P., Millaire, J., White, C., Longstaffe, F., 2012. Influence of seabird guano and camelid dung fertilization on the nitrogen isotopic composition of field-grown maize (*Zea mays*). *J. Archaeol. Sci.* 39, 3721–3740.
- Tieszen, L., 1991. Natural variations in the carbon isotope values of plants: implications for archaeology, ecology, and paleoecology. *J. Archaeol. Sci.* 18, 227–248.
- Tischler, K., 2004. Aquatic plant nutritional quality and contribution to moose diet at Isle Royale National Park. Master's Thesis. Michigan Technological University.
- Toft, N.L., Anderson, J.E., Nowak, R.S., 1989. Water use efficiency and carbon isotope composition of plants in a cold desert environment. *Oecologia* 80, 11–18.
- van Klinken, G., 1999. Bone collagen quality indicators for palaeodietary and radiocarbon measurements. *J. Archaeol. Sci.* 26, 687–695.
- Venables, W.N., Ripley, B.D., 2002. *Modern applied statistics with S*, Fourth Edition. Springer, New York.
- Way, D.A., Katul, G.G., Manzoni, S., Vico, G., 2014. Increasing water use efficiency along the C_3 to C_4 evolutionary pathway: a stomatal optimization perspective. *J. Exp. Bot.* 65, 3683–3693. doi:10.1093/jxb/eru205
- Willerslev, E., Davison, J., Moora, M., Zobel, M., Coissac, E., Edwards, M.E., Lorenzen, E.D., Vestergård, M., Gussarova, G., Haile, J., Craine, J., Gielly, L., Boessenkool, S., Epp, L.S., Pearman, P.B., Cheddadi, R., Murray, D., Bråthen, K.A., Yoccoz, N., Binney, H., Cruaud, C., Wincker, P., Goslar, T., Alsos, I.G., Bellemain, E., Brysting, A.K., Elven, R., Sønstebø, J.H., Murton, J., Sher, A., Rasmussen, M., Rønn, R., Mourier, T., Cooper, A., Austin, J., Möller, P., Froese, D., Zazula, G., Pompanon,

- F., Rioux, D., Niderkorn, V., Tikhonov, A., Savvinov, G., Roberts, R.G., MacPhee, R.D.E., Gilbert, M.T.P., Kjær, K.H., Orlando, L., Brochmann, C., Taberlet, P., 2014. Fifty thousand years of Arctic vegetation and megafaunal diet. *Nature* 506, 47–51. doi:10.1038/nature12921
- Williams, J.W., Jackson, S.T., 2007. Novel climates, no-analog communities, and ecological surprises. *Front. Ecol. Environ.* 5, 475–482. doi:10.1890/070037
- Wooller, M., Zazula, G., Edwards, M., Froese, D.G., Boone, R.D., Parker, C., Bennett, B., 2007. Stable carbon isotope compositions of Eastern Beringian grasses and sedges: investigating their potential as paleoenvironmental indicators. *Arctic, Antarct. Alp. Res.* 39, 318–331.
- Wynn, J.G., 2007. Carbon isotope fractionation during decomposition of organic matter in soils and paleosols: implications for paleoecological interpretations of paleosols. *Palaeogeogr. Palaeoclimatol. Palaeoecol.* 251, 437–448. doi:10.1016/j.palaeo.2007.04.009
- Yeakel, J.D., Guimarães, P.R., Bocherens, H., Koch, P.L., 2013. The impact of climate change on the structure of Pleistocene food webs across the mammoth steppe. *Proc. R. Soc. B Biol. Sci.* 280, 20130239.
- Zimov, S.A., Zimov, N.S., Tikhonov, A.N., Chapin, F.S., 2012. Mammoth steppe: a high-productivity phenomenon. *Quat. Sci. Rev.* 57, 26–45. doi:10.1016/j.quascirev.2012.10.005

Chapter 2

2 Carbon and nitrogen isotopic analysis of antlers as a tool to investigate seasonal shifts in ecology

2.1 Introduction

2.1.1 Importance of investigating seasonal variation

Understanding modern and ancient ecology at multiple time scales is key for biological, archeological and paleontological work. Such information is particularly important in high latitude regions, where climate change can have significant impacts. For example, climate change has effects on caribou ecology that are an integral part of high latitude food webs, including food webs that contain humans (Heggberget et al., 2002; Sharma et al., 2009). Carbon and nitrogen isotopic studies of collagen have proven to be valuable methods for investigating Holocene and Pleistocene ecology (e.g. Bellissimo, 2013; Bocherens et al., 2011, 2005, 2001, 1997, 1996, 1994; Drucker and Henry-Gambier, 2005; Drucker et al., 2003a, b; Drucker et al., 2011; Fizet et al., 1995; Fox-Dobbs et al., 2008; Iacumin et al., 2010, 2000; Mann et al., 2013; Metcalfe et al., 2013, 2010; Stevens and Hedges, 2004; Stevens et al., 2009; Szpak et al., 2010). The majority of studies have focused on bone collagen, which provides an isotopic signal representing the past several years of an animal's life, but does not provide discrete information over a shorter time scale (Koch et al., 1994). Interspecies interactions and the level of ecological niche overlap can change seasonally, and a yearly average may not fully represent the variations within the system (Hansen and Reid, 1975; Leslie et al., 1984). Many resources are scarcer during the winter, and may be population-limiting only during this season (Adamczewski et al., 1988; Heggberget et al., 2002). As well, metabolic changes are commonly coordinated seasonally (e.g. pregnancy, birth). Knowing the specific conditions at these times is therefore important to understanding the long-term health of a population (Finstad and Kielland, 2011). Examining the isotopic compositions of tissues with different growth periods and turnover rates than bone provides such a tool.

Here, we focus on antlers, which have a short growth period and do not remodel, and hence should record and retain the isotopic signal of the diet and environment during this tissue's formation. Antlers are cast naturally, making it possible to sample this tissue in modern settings without injuring the animal. As well, antler material is found in some archeological and paleontological contexts (e.g. Madgwick et al., 2013; Miller et al., 2014; Stevens et al., 2008), and thus it has the potential to be valuable for zooarcheological and paleoecological reconstruction. In the present study, antler from elk (*Cervus elaphus*), moose (*Alces alces*) and caribou (*Rangifer tarandus*) was serial-sampled to investigate the extent of isotopic variation along the growth length of this tissue. The isotopic compositions of coexisting antler and bone from several sites in Alaska and Yukon Territory (Fig. 2.1) were also determined to gain insight into seasonal and annual ecology and how it might have changed over several time periods during the Late Pleistocene and Holocene. These results were then compared with the ecological variation expected based on previous investigations in order to evaluate the viability of antler as a tool for investigating seasonal ecology and paleoecology.

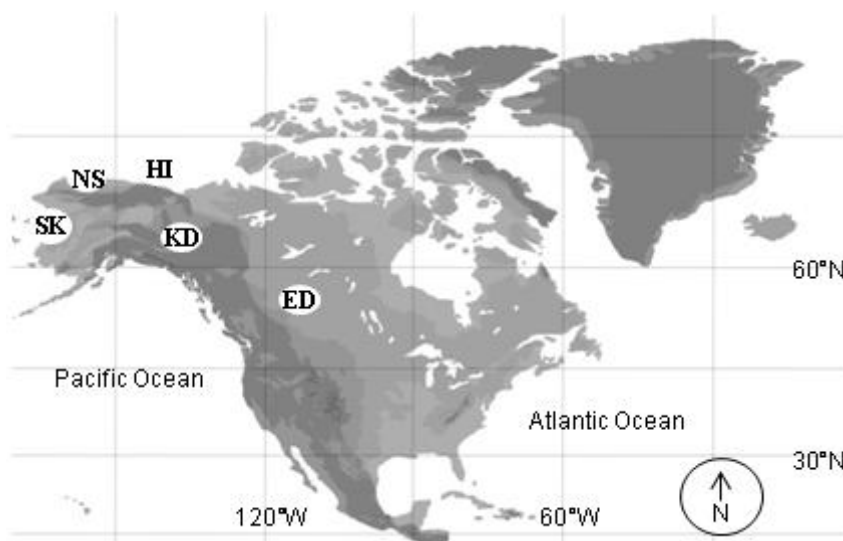


Figure 2.1 Sites included in this study: ED. Edmonton; HI. Herschel Island; KD. Klondike; NS. North Slope; SK. Selawik. Darker shades of grey represent higher altitudes. Art by Katherine Allan.

2.1.2 Antler and bone growth

Antler growth is a continuous process, with multiple deposition stages spatially overlapping in the tissue (Banks and Newbrey, 1983). As a result, growth lines are not visible in the antler. Nonetheless, the general pattern of deposition occurs from the base to the tip of the antler (Fig. 2.2a; Banks and Newbrey, 1983). The inner tissue of an antler is composed of trabecular bone, and is composed of younger tissue, while the outer tissue is denser and represents a signal from later in the growth season (Fig 2.2b; Finstad and Kielland, 2011). The final stage of collagen deposition involves a layer of woven bone that is deposited over the outside of the basal portions of the antler (Gomez et al., 2013), but this layer is extremely thin (Fig. 2.2b; Kierdorf et al., 2013). During growth, nutrients are supplied through the antler skin, known as velvet. Once this skin is shed, the antlers become dead appendages and there is no remodelling of tissue material (Gomez et al., 2013; Wislocki, 1942). Antler growth does not occur at a continuous pace. On a cellular level, primary osteons in the lower and middle third of elk antlers take 30-40 days to complete growth, while those in the upper third take 20-30 days (Gomez et al., 2013). On a larger scale, antler growth in south-central Alaskan moose was observed to be slow until the first green forage became available in late May; antler development then accelerated, with 50% of antler growth occurring in June (Ballenberghe, 1983). Finstad and Kielland (2011) also note that more rapid caribou antler growth corresponds to months with higher nutrient availability. The precise timing of antler growth initiation and cessation varies between individuals, especially of different age groups, between populations of a species and between species (Chapman, 1975). In males, antler growth typically begins in the late spring and summer, and velvet is shed in the early autumn or late summer before the rut (Ballenberghe, 1983; Chapman, 1975). Caribou are the only species where females as well as males have antlers. The timing of female antler growth is delayed relative to males in some populations, although it tends to fall in the same general seasonal time frame (Chapman, 1975; Leader-Williams, 1988).

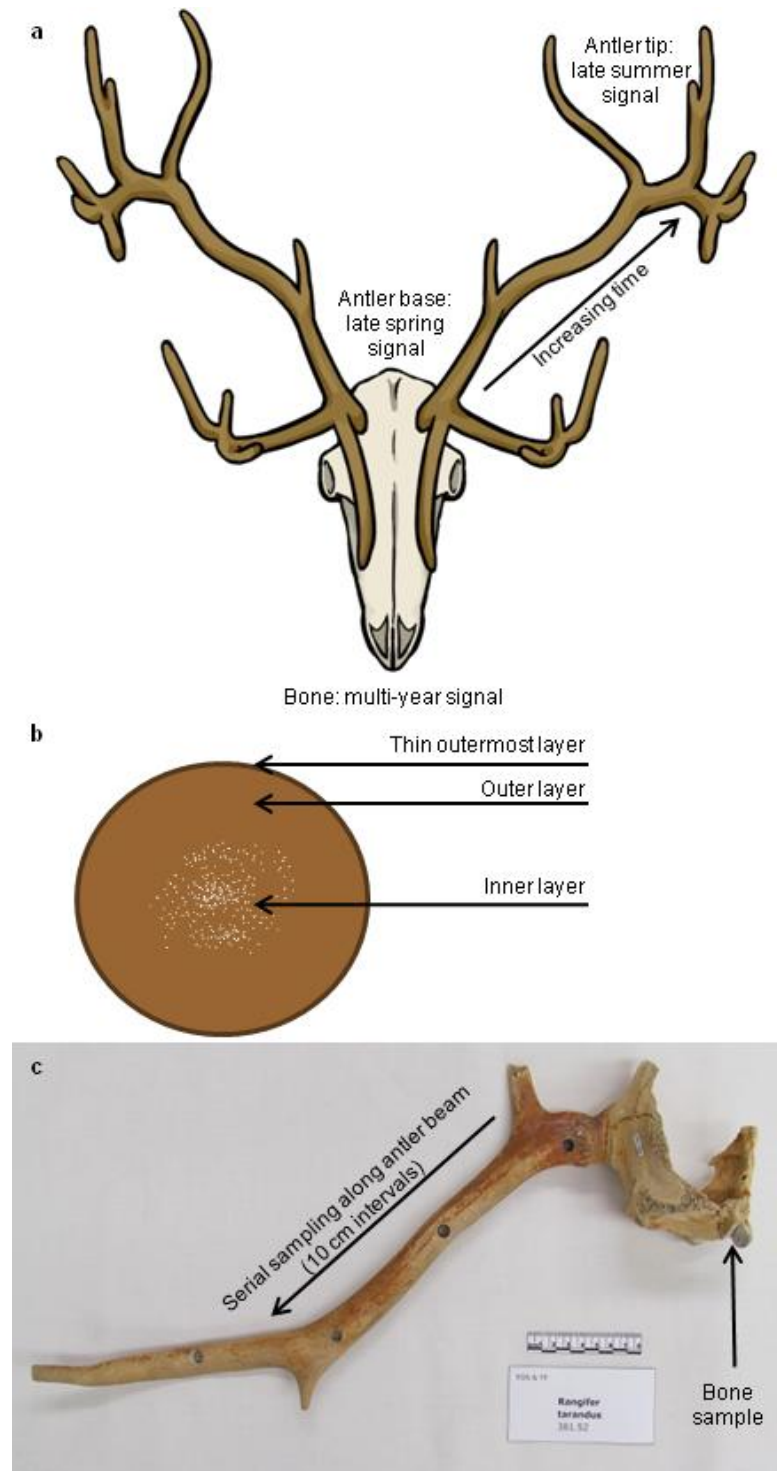


Figure 2.2 Sampling strategy: a. Conceptual model of the timing of tissue formation in cranial bone (right occipital condyle) versus antler. Art by Katherine Allan; b. Outermost, outer and inner antler tissue; c. An example of the sampling pattern (arrows) for a caribou skull and antler. Photograph by Tessa Plint.

In contrast to antler, bone forms by either endochondral or intramembranous ossification. Once formed, bone is then remodelled over a period of years, with the exact timing depending on the species. For this reason, bone records an isotopic signal averaged over many years of an individual's life (Balasse et al., 1999; Koch et al., 1994).

2.1.3 Modern seasonal diet and habitat

2.1.3.1 Caribou

Caribou (also known as reindeer) occupy an extremely diverse set of habitats, including forest, alpine and tundra environments. Within each of those regions, there are both migratory and sedentary populations of caribou (Sharma et al., 2009). The seasonal diets and habitats of caribou vary considerably depending on their habitat. Numerous studies have highlighted the role of lichen in caribou diet, both as a year-round food source and as the dominant, though never sole, forage during the winter (Boertje, 1984; Heggberget et al., 2002; Thomas et al., 1996; Thompson and McCourt, 1981). If snow is not overly deep, caribou are able to dig to access lichen (Guthrie, 1990). In areas with tree-cover, they can also access lichen growing on tree bark. Willow is often a large component of spring and summer diets, possibly because it helps caribou to recover their body protein after winter losses (Adamczewski et al., 1988; Bjørkvoll et al., 2009; Boertje, 1984; Shank et al., 1978; Thomas et al., 1996). Herbs, sedges and graminoids are also eaten in large quantities in the spring and summer in some environments (Bjørkvoll et al., 2009; Bjune, 2000; Thompson and McCourt, 1981). In caribou herds that migrated seasonally between tundra and forested environments, calving grounds, used during the spring, are commonly found in tundra regions, and the caribou then migrated into forests during the fall (Kelsall, 1968; Sharma et al., 2009).

2.1.3.2 Elk

Elk (also known as red deer or wapiti) are opportunistic mixed feeders that inhabit habitats ranging from steppe to boreal or temperate forests. Their diets vary with habitat, with the animals consuming graze in prairies and browse in dense forest, or migrating between the two habitats (Christianson and Creel, 2007; Drucker et al., 2008; Dumont et al., 2005; Gebert and Verheyden-Tixier, 2001; Hofmann, 1989; Jenkins and Starkey,

1991; Kufeld, 1973; Morgantini and Hudson, 1989; Prokešová, 2004). In addition to choosing their habitat to obtain the best quality forage, elk also choose dense forest rather than open steppe (i) when they face higher predation risk, (ii) for thermal cover in the winter, and (iii) to obtain forage not covered by heavy snowfall in harsh winters (Christianson and Creel, 2007; Jones and Hudson, 2002).

As elk inhabit highly varied habitats, it is difficult to assign a single diet type to all elk populations for each season. Commonly, spring and fall diets consist mainly of grasses (Jenkins and Starkey, 1991; Morgantini and Hudson, 1989; Stevens, 1966), and summer diets contain a high proportion of shrubs and forbs (Jenkins and Starkey, 1991; Morgantini and Hudson, 1989). Some populations consume higher proportions of conifers during the winter than during the rest of the year (Jenkins and Starkey, 1991), while others consume mainly grasses (Christianson and Creel, 2007; Morgantini and Hudson, 1989), and some shift from graze to browse (graminoids and forbs to trees and shrubs; Hobbs et al., 1981). Some elk populations consume winter diets sufficient to meet maintenance requirements (Hobbs et al., 1981) while others do not (Christianson and Creel, 2007; Morgantini and Hudson, 1989).

2.1.3.3 Moose

Moose (also called Eurasian elk) are browse specialists (Hofmann, 1989; Hörnberg, 2001; Stevens, 1970; Wam and Hjeljord, 2010), and the bulk of their diet is commonly composed of a small number of deciduous or coniferous browse, such as willow, birch, rowan and aspen (Hörnberg, 2001; Wam and Hjeljord, 2010). They tend to eat bark and new twigs and leaves of trees in the spring, and eat primarily dormant twigs during the winter (Belovsky, 1981; Edwards, 1983; MacCracken et al., 1997; Wam and Hjeljord, 2010). When aquatic plants are available in the moose's range, they tend to be a major part of the animal's diet from spring to midsummer (Fraser et al., 1982; MacCracken et al., 1993). Aquatic plant consumption generally declines by midsummer, though in some populations it continues until the fall (Fraser et al., 1982; MacCracken et al., 1993; Peek, 2007). Some studies report substantial forb consumption by moose in the spring and summer (Knowlton, 1960; LeResche and Davis, 1973). Winter maintenance diets have

lower nutrient levels and hence moose are at much higher risk of starvation during the winter than during the rest of the year (Edwards, 1983).

2.1.4 Stable Isotopes

Stable isotope compositions are reported using the δ -notation, which compares sample isotopic ratios to internationally accepted standard isotopic ratios, in units of per mil (‰). The reference standards are VPDB for carbon (Coplen et al., 2006), and AIR for nitrogen (Mariotti, 1983).

2.1.4.1 Plant $\delta^{13}\text{C}$

Plants utilizing the C_3 photosynthetic pathway comprised the vast majority, and at times the entirety, of the vegetation in North American high latitude regions during the late Pleistocene and Holocene (Gaglioti et al., 2011; Kristensen et al., 2011; Wooller et al., 2007). There is significant overlap in the range of C_3 plant carbon isotopic compositions. Nonetheless, there is a difference in the average $\delta^{13}\text{C}$ of various plant groups of ≥ 1.5 ‰ (Barnett, 1994). From lowest to highest, the average $\delta^{13}\text{C}$ of terrestrial plants tended to follow the order: shrubs, forbs, graminoids, fungi, lichens (see conceptual model Fig. 1.2; Barnett, 1994; Ben-David et al., 2001; Drucker et al., 2010; Kristensen et al., 2011). Isotopic compositions can also vary among tissues in a plant. In spruce trees, twigs were found to have higher $\delta^{13}\text{C}$ than needles, likely because of differences in their chemical makeup (Gebauer and Schulze, 1991). This pattern has also been observed for twigs and leaves of deciduous plants (Ehleringer et al., 1992; Tischler, 2004). This can have a seasonal effect on dietary carbon isotopic composition, as twigs of deciduous plants are more likely to be consumed in the winter when leaves are not available.

Evergreen trees usually have higher $\delta^{13}\text{C}$ than deciduous trees, but this is not universal (Brooks et al., 1997; Kloeppe et al., 1998). Variability in the carbon isotopic composition of a plant can also result from environmental effects. Increased aridity, higher altitudes and higher temperatures can all cause an increase in the $\delta^{13}\text{C}$ of a plant (de Bello et al., 2009; Diefendorf et al., 2010; Ehleringer and Cooper, 1988; Ehleringer et al., 1987; Farquhar, 1989; Kohn, 2010; Tieszen, 1991; Wooller et al., 2007). Plants growing under a dense canopy tend to have lower $\delta^{13}\text{C}$ than those growing in open

grasslands, deserts or tundra (Bocherens et al., 2011). Sea spray can also cause increases in the $\delta^{13}\text{C}$ of plants (see Sykes et al., 2011 and references therein); however, as this study compares populations within a site rather than between sites, it is unlikely to be a factor.

Freshwater aquatic plants have a much wider range of $\delta^{13}\text{C}$ (-47 to -8 ‰) than terrestrial C_3 plants (-32 to -22 ‰; Finlay and Kendall, 2007). This wide range occurs because freshwater algae and macrophytes take up carbon from a variety of sources including atmospheric CO_2 and dissolved inorganic carbon. Dissolved inorganic carbonate can originate from a wide range of sources including carbonate minerals, atmospheric carbon dioxide, respiring organic matter and detritus, each of which imparts a distinct $\delta^{13}\text{C}$ to the plant (Finlay and Kendall, 2007; Keeley and Sandquist, 1992; LaZerte and Szalados, 1982; Osmond et al., 1981). As well, the degree of isotopic fractionation between DIC and freshwater plants varies with species, the type of carbon taken up, and water velocity, though water velocity does not play a significant role in $\delta^{13}\text{C}$ of plant material in ponds (Finlay and Kendall, 2007; Finlay et al., 1999; Keeley and Sandquist, 1992; Osmond et al., 1981).

Although there is considerable overlap in the global $\delta^{13}\text{C}$ of terrestrial and aquatic plants (Finlay and Kendall, 2007; France, 1995; Keeley and Sandquist, 1992), several studies have demonstrated that they can have distinct carbon isotopic compositions at specific sites (Doucett et al., 1996; Fry, 1991; Tischler, 2004). Since moose consume aquatic plants and attached algae from lentic (still-water) systems, isotopic differences between these aquatic plants and terrestrial plants should be reflected in moose' tissues. At Isle Royale National Park, Michigan, aquatic plants have higher $\delta^{13}\text{C}$ than terrestrial plants, although the degree of ^{13}C -enrichment varies because the aquatic plants exhibit a wide range of $\delta^{13}\text{C}$ (Tischler, 2004). Higher average $\delta^{13}\text{C}$ for aquatic than terrestrial plants has also been found in rivers and lakes in the Old Crow flats of the Yukon, the James Bay region of Quebec (Milligan et al., 2010), and the tundra and associated rivers and lakes at Koroc River, Quebec (Bunn et al., 1989). The same pattern is known for several other lakes (Chikaraishi and Naraoka, 2003; LaZerte and Szalados, 1982), although it is not

universal (France, 1995; Fry, 1991; Rau, 1980). At the majority of sites studied to date, however, aquatic plants consumed by herbivores have higher $\delta^{13}\text{C}$ than terrestrial browse.

There is also a large overlap in the C/N ratios of terrestrial and aquatic plants (Finlay and Kendall, 2007), but the situation is variable from site to site. At Isle Royale National Park, for example, aquatic plants have lower C/N ratios, and thus more protein, than terrestrial plants (Tischler, 2004). Among terrestrial plants, lichen are particularly poor in protein (Chapin and Shaver, 1988; Drucker et al., 2001).

2.1.4.2 Herbivore collagen $\delta^{13}\text{C}$

Herbivores have a higher $\delta^{13}\text{C}$ than the food they eat. For large herbivores, there is generally an increase of ~ 5 ‰ between their bulk diet and their bone collagen (Drucker et al., 2008). Starvation and nursing can both affect the isotopic composition of an animal. Both involve greater utilization of lipids, either from the animal's own fat reserves (Szpak et al., 2010) or mother's milk (Metcalf et al., 2010). Lipids have low $\delta^{13}\text{C}$ relative to other biological macromolecules, and their preferential utilization may be the cause of the low $\delta^{13}\text{C}$ of woolly mammoth collagen, given the cold environments with harsh winters inhabited by these animals (Szpak et al., 2010). It is possible that the species sampled in this study might have been similarly affected. Bones from juvenile individuals were not sampled in the present study, and extremely young animals would be unlikely to grow large antlers. Nursing effects are therefore not considered further in this study.

2.1.4.3 Plant $\delta^{15}\text{N}$

The typical pattern of average $\delta^{15}\text{N}$ for terrestrial plants encountered in tundra environments, from lowest to highest, is: shrubs, lichens, forbs, graminoids and fungi (Fig. 1.2; Ben-David et al., 2001; Drucker et al., 2010; Finstad and Kielland, 2011; Kristensen et al., 2011; Nadelhoffer et al., 1996). There is a large degree of overlap among them. Forbs in particular have a wide variety of nitrogen isotopic compositions, likely resulting from a large number of possible growth forms, and the existence of nitrogen-fixing forbs with $\delta^{15}\text{N}$ close to 0 ‰ (Nadelhoffer et al., 1996; Stewart et al., 2003). Some tissue-based differences have been observed for $\delta^{15}\text{N}$. In spruce trees, twigs

have lower $\delta^{15}\text{N}$ than needles (Gebauer and Schulze, 1991). Lower $\delta^{15}\text{N}$ for stems versus leaves are also known for several deciduous species (Kielland, 2001). Similarly to the pattern observed in carbon, therefore, the isotopic composition of plants consumed could vary seasonally, as browsing herbivores' winter diets consist of twigs rather than leaves. Environmental factors can also affect the $\delta^{15}\text{N}$ of a plant. When nitrogen is lost from an ecosystem, it tends to be lost as ^{14}N , causing the plants to become enriched in ^{15}N . The quantity of nitrogen lost from an ecosystem relates to the degree of nitrogen cycling, which is higher in an arid, hot ecosystem than a mesic, cool ecosystem (Ambrose, 1991; Amundson et al., 2003; Drucker et al., 2003a; Heaton, 1987; Stevens and Hedges, 2004; Stevens et al., 2008). Increased salinity, and sea spray, can also lead to higher $\delta^{15}\text{N}$ in plants (as discussed in Sykes et al., 2011), but is unlikely to be important in this study.

The $\delta^{15}\text{N}$ of aquatic plants is less well understood than their carbon isotopic compositions (Finlay and Kendall, 2007). Typical undisturbed freshwater ecosystems have a wide range of $\delta^{15}\text{N}$ from -1 to $+7$ ‰, with the higher and lower values associated with anthropogenic effects (Finlay and Kendall, 2007). Variations occur because of differences in the type and $\delta^{15}\text{N}$ of nitrogen dissolved in the water or available in the sediment, and differences in the isotopic fractionation during nitrogen uptake (Finlay and Kendall, 2007). Globally, the mode $\delta^{15}\text{N}$ of aquatic plants ($+3$ ‰) is higher than that of terrestrial plants (-1 ‰), but there is extensive overlap in nitrogen isotopic compositions (France, 1995). Discrete differences are evident at some sites, and in the majority of those cases, aquatic plants have higher $\delta^{15}\text{N}$ than terrestrial plants (Ben-David et al., 2001; Delong and Thorp, 2006; Finstad and Kielland, 2011; Fry, 1991; McArthur and Moorhead, 1996; Milligan et al., 2010; Tischler, 2004).

2.1.4.4 Herbivores collagen $\delta^{15}\text{N}$

There is an increase of $+2$ to $+5$ ‰ in the $\delta^{15}\text{N}$ from diet to consumer collagen (Gannes et al., 1998; Koch, 2007; Koch et al., 1994). Physiological changes can also affect the nitrogen isotopic composition of an animal, and $\delta^{15}\text{N}$ are expected to be higher for animals undergoing nutritional stress (Gannes et al., 1998; Hobson et al., 1993; Kelly, 2000; Koch, 2007; Polischuk et al., 2011), though this may only occur when animals

experience a threshold level of extreme starvation (Kempster et al., 2007). Increases in $\delta^{15}\text{N}$ are likewise expected for animals living in arid environments (Kelly, 2000; Sealy et al., 1987; Sponheimer et al., 2003). Nursing young also experience an increase in $\delta^{15}\text{N}$ (Metcalf et al., 2010), but this trophic effect is not expected to be encountered in the present study.

There is some concern that antlers, being a rapidly growing tissue, would have a smaller nitrogen isotopic spacing ($\Delta^{15}\text{N}_{\text{Tissue-Diet}} = \delta^{15}\text{N}_{\text{Tissue}} - \delta^{15}\text{N}_{\text{Diet}}$) between antler collagen and diet than exists between bone and diet (Finstad and Kielland, 2011). Waters-Rist and Katzenberg (2010) reviewed previous studies that found such a decrease for several types of rapidly growing tissues, but did not observe it in their own investigation of bone, and it is unknown if this phenomenon occurs in antlers. Antler-specific studies have suggested other tissue-specific effects may occur. Towards the end of antler growth, there may be increased mobilization of protein from bones to the antler. In this case, the $\delta^{15}\text{N}$ of antler tips would trend towards the $\delta^{15}\text{N}$ of bone. As well, if the protein mobilized from the bone is recycled through the body before being deposited in the antler, then a metabolic effect could cause an additional increase in antler $\delta^{15}\text{N}$ (Madgwick et al., 2013; Osborne, 2013).

2.1.4.5 Isotopic analysis of shifting diets

Changes in diet can be recognized when distinct differences in isotopic compositions exist among dietary sources, and animal tissues preserve this seasonal or life stage record (e.g. Peterson and Fry, 1987). Such changes in animal tissue $\delta^{13}\text{C}$ and $\delta^{15}\text{N}$ have been used previously to study caribou, moose and elk dietary and habitat change over seasons and years. Studies of moose using hoof keratin and blood isotopic compositions have confirmed higher aquatic plant and shrub- and tree-leaf consumption in summer, and higher twig consumption in winter, based on lower $\delta^{13}\text{C}$ and lower $\delta^{15}\text{N}$ during summer than winter (Ben-David et al., 2001; Kielland, 2001; Tischler, 2004). Temporal variations in the amplitudes of isotopic changes of hoof keratin, however, suggest a high degree of dietary mixing and individual dietary choice (Kielland, 2001). In the absence of substantial consumption of aquatic plants, moose hair showed no distinctive seasonal

isotopic shifts (Drucker et al., 2010). The study of caribou using the isotopic composition of tooth dentin has revealed that individual caribou within a population ate distinct diets with a high level of individual dietary choice (Drucker et al., 2012) and increased nitrogen recycling and lichen consumption during winter, which caused higher tissue $\delta^{13}\text{C}$ and $\delta^{15}\text{N}$ in winter and spring than summer or fall (Drucker et al., 2001). Higher $\delta^{13}\text{C}$ was also found for blood and hoof keratin that corresponded to winter, again suggesting more lichen consumption in winter and more vascular plant consumption during the rest of the year (Barnett, 1994; Ben-David et al., 2001). Caribou hoof keratin, however, had the highest $\delta^{15}\text{N}$ in fall, suggesting consumption of a forage source with high $\delta^{15}\text{N}$, such as mushrooms.

Archaeological and palaeontological studies have previously employed antler isotopic compositions, alongside those of bone, to understand species ecology and to construct an isotopic herbivore baseline (France et al., 2007; Kuitens et al., 2015; Madgwick et al., 2013; Osborne, 2013; Stevens et al., 2010, 2008; Sykes et al., 2011), while noting potential pitfalls in the comparison of different tissues. Some studies have used these differences to investigate the origin of deer antler in Roman times (Madgwick et al., 2013; Miller et al., 2014), though limited work has been undertaken to expressly compare the isotopic compositions of archaeological bone and antler (Miller et al., 2014; Osborne, 2013).

Isotopic variability within antler has been investigated previously for modern animals. A feeding study found no isotopic variation along the length of the antler for deer fed a consistent diet (Darr and Hewitt, 2008). The $\delta^{15}\text{N}$ of inner and outer antler tissues of Alaskan female caribou were used to investigate the timing and proportion of shrub use (Finstad and Kielland, 2011). Lower $\delta^{15}\text{N}$ for spring than summer antler tissue was related to a higher proportions of shrubs in the spring diet. Higher shrub use in spring correlated to poorer body condition at the end of the winter, making this a potential technique to investigate the health of a population. A study of wild deer investigated the extent to which a single sample of antler could be used to assess the isotopic composition of the whole (Miller et al., 2014; Osborne, 2013). Within the limited isotopic variability that was observed, changes in $\delta^{13}\text{C}$ were attributed to dietary shifts during the growing

season, and higher $\delta^{15}\text{N}$ towards the tip of the antler to increased nitrogen supply from bone. These studies found that deer antler had higher $\delta^{13}\text{C}$ and lower $\delta^{15}\text{N}$ than bone (Miller et al., 2014; Osborne, 2013).

2.2 Methods

2.2.1 Sample selection

Caribou, elk and moose specimens were obtained from the Edmonton area (Edmonton), the Klondike area (Klondike), Herschel Island (Herschel Island) and the Selawik Wildlife Refuge and Surround Areas (Selawik) (Fig. 2.1). Information about sample location and age is summarized in Appendix A. Stable isotopic data for antlers that were serially sampled (sampled several times along the growing length) are listed in Appendix B. The dimensions of the antler are also listed in Appendix B, as well as whether the antler was broken along the length that that it was sampled, or was a complete specimen. All stable isotopic data, including previously reported data for antler and bone for the North Slope (Mann et al., 2013) and Selawik (Druckenmiller, 2008), are also summarized in Appendix C.

2.2.2 Collagen extraction

For specimens from which only a single sample was taken, this tissue was removed using a Dremel[®] cutting wheel. Sampling along the length of an antler specimen was performed using a 0.625 cm drill core attached to a drill press. These samples were taken every 10 cm along one side of one beam of the antler, with the base of the antler designated as 0 cm (Fig. 2.2b). Cancellous bone was removed from bone samples to allow for sampling of purely cortical bone. Outer antler tissue was preferentially sampled when the antler was thick. The surfaces of antler and bone were removed using a carbide burr attachment to the Dremel[®], and the new surface then washed with deionised water and dried at room temperature.

Lipid extraction was performed on a subset of seven samples using a modified Bligh and Dyer method (Bligh and Dyer, 1959). Prior to collagen extraction, these samples were treated three times each with a 2:1 chloroform:methanol solution (v:v) for 15 minutes.

The samples were then dried at room temperature. Comparison of unextracted versus lipid-extracted fractions showed that the isotopic compositions obtained from the two approaches differ by a maximum of ± 0.1 ‰ (SD) for both $\delta^{13}\text{C}$ and $\delta^{15}\text{N}$ (Appendix D). For this reason, unextracted and lipid-extracted fractions are considered to be isotopically equivalent in any discussion that follows.

Collagen extraction was performed at room temperature following the modified Longin method (see method in Metcalfe et al., 2010). Samples were dissolved for 24 hours in 0.25 M and subsequently in 0.5 M HCl with the acid changed every 1-3 days until the samples were demineralized. Samples were then rinsed 3 times with deionized water. Humic substances were removed by treatment with 0.1 M NaOH for 20 minutes at room temperature, which was repeated until the liquid remained colourless. The samples were then rinsed seven times with deionized water, and the pH was adjusted to less than 3. They were then placed in a 90°C oven for approximately 16 hours to solubilise the collagen. The solubilised collagen was decanted and dried at 90°C before being weighed for analysis.

2.2.3 Stable isotope measurements

The carbon and nitrogen isotopic compositions of the collagen were measured using a Costech elemental combustion system (ECS 4010) attached to a Thermo-Scientific Delta V stable isotope ratio mass spectrometer (IRMS) operated in continuous-flow mode. The results are presented in Appendices B (serial samples) and C (single samples). The samples were measured over a total of eleven analytical sessions. The carbon isotopic data were calibrated to VPDB using a two-point scale anchored by either NBS-22 (± 0.0 ‰ one standard deviation (SD), $n = 24$; accepted $\delta^{13}\text{C} = -30.03$ ‰; Coplen et al., 2006), and IAEA-CH-6 (± 0.1 ‰ SD, $n = 37$; accepted $\delta^{13}\text{C} = -10.45$ ‰; Coplen et al., 2006) or USGS-40 (± 0.1 ‰ SD, $n = 44$; accepted $\delta^{13}\text{C} = -26.39$ ‰; Coplen et al., 2006) and USGS-41 (± 0.2 ‰ SD, $n = 35$; accepted $\delta^{13}\text{C} = +37.63$ ‰; Coplen et al., 2006). The nitrogen isotopic data were calibrated to AIR using a two-point scale anchored by USGS-40 (± 0.1 ‰ SD, $n = 43$; accepted $\delta^{15}\text{N} = -4.52$ ‰; Qi et al., 2003) and either IAEA-N2 (± 0.2 ‰ SD, $n = 35$; accepted $\delta^{15}\text{N} = +20.39$ ‰; Qi et al., 2003) or USGS-41 (± 0.4 ‰

SD, $n = 33$; accepted $\delta^{15}\text{N} = +47.57 \text{ ‰}$; Qi et al., 2003). These standards were also used for calibration of the carbon and nitrogen contents and C/N ratio of each sample. When these standards were not used in the calibration curve, they were used measured as unknowns. IAEA-CH-6 (measured $\delta^{13}\text{C} = -10.5 \text{ ‰}$), USGS-40 (measured $\delta^{13}\text{C} = -26.4 \text{ ‰}$), USGS-41 (measured $\delta^{13}\text{C} = +37.8 \text{ ‰}$, measured $\delta^{15}\text{N} = +47.0 \text{ ‰}$), IAEA-N1 (measured $\delta^{15}\text{N} = +0.5 \text{ ‰}$; accepted $\delta^{15}\text{N} = +0.43 \text{ ‰}$; Qi et al., 2003) and IAEA-N2 (measured $\delta^{15}\text{N} = +20.4 \text{ ‰}$) all had similar isotopic compositions to their accepted values. Every analytical session also included an internal keratin laboratory standard (MP Biomedicals Inc., Cat. No. 90211, Lot No. 9966H) for which the following average results (SD) were obtained ($n = 72$): $\delta^{13}\text{C} = -24.1 \pm 0.1 \text{ ‰}$, $\delta^{15}\text{N} = +6.4 \pm 0.1 \text{ ‰}$, $\text{C} = 48 \pm 2 \text{ wt.}\%$, $\text{N} = 15 \pm 1 \text{ wt.}\%$, and atomic C/N ratio = 3.7 ± 0.2 . These compare well with accepted values of $\delta^{13}\text{C} = -24.0 \text{ ‰}$, $\delta^{15}\text{N} = +6.4 \text{ ‰}$, $\text{C} = 46.8 \text{ wt.}\%$, $\text{N} = 14.6 \text{ wt.}\%$ and atomic C/N = 3.7. A subset of samples ($n = 25$) were analyzed in duplicate or triplicate; reproducibility (SD) ranged from ± 0.0 to $\pm 0.2 \text{ ‰}$ for $\delta^{13}\text{C}$, and from ± 0.0 to $\pm 0.3 \text{ ‰}$ for $\delta^{15}\text{N}$, with an average for both of $\pm 0.1 \text{ ‰}$.

2.2.4 Radiocarbon dating

Radiocarbon dates were obtained for a subset of samples. Collagen was extracted, combusted, graphitized and dated at the University of Arizona Accelerator Mass Spectrometry (AMS) Laboratory. Dates are presented as uncalibrated radiocarbon years before present (1950), and are listed in Appendices A, B and C alongside previously published dates (Druckenmiller, 2008; Kristensen and Heffner, 2011; Mann et al., 2013; Meiri, 2010; Zazula, pers. comm., 2015).

2.2.5 Mathematical treatment

Antler-bone pairs were tested to determine if the populations were statistically identical using the Mann-Whitney-Wilcoxon test, as this test does not assume parametric populations (Bauer, 1972). Carbon and nitrogen isotopic compositions were tested separately, and the data sets were assumed to be independent. A p -value of 0.05 was selected. The test was run in R version 3.1.1 (R Core Team, 2014) using the R Studio interface version 0.98.1083, and the results are summarized in Table 2.1.

The Herschel Island caribou bone and antler samples postdate the Industrial Revolution (post-bomb period; Appendix A). A Suess effect correction was therefore made for the lower carbon isotopic composition of the atmosphere resulting from the burning of fossil fuels following the method of Long et al. (2005). Because the exact date for this specimen is not known, the mid-point (1987) between the start of the post-bomb time period (1964) and the time of collection (2009) was used to make the Suess effect correction.

2.3 Results

2.3.1 Preservation

Applying the preservation criterion for bone to both bone and antler samples, all samples are considered well preserved (see Appendices B and C). The collagen extraction yield ranges from 5.7 to 19.4 % for bone, and 1.4 to 44.2 % for antler, above the 1% limit below which original isotopic compositions may be affected (van Klinken, 1999). A higher yield of collagen from antler than bone was expected, as antler contains more organic matter than bone (Chapman, 1975). The sample with the lowest yield was obtained midway along the length of a serially sampled antler, and its $\delta^{13}\text{C}$ and $\delta^{15}\text{N}$ are consistent with other samples from the same antler. The C/N ratios of the samples range from 3.0 to 3.4, within the accepted range of 2.9-3.6 for well-preserved bone samples (Ambrose, 1990; DeNiro, 1985; van Klinken, 1999). The carbon and nitrogen contents range from 33-46 wt.% and 12-17 wt.%, respectively, which also meet the preservation criterion of ≥ 13 wt.% for carbon and ≥ 4.8 wt.% for nitrogen (Ambrose, 1990; DeNiro, 1985; van Klinken, 1999).

2.3.2 Collagen stable isotope compositions

2.3.2.1 Intra-tissue variation

Carbon and nitrogen isotopic compositions have been measured along the length of an antler for eight specimens (one Herschel Island caribou, three Klondike caribou, two Klondike elk and two Klondike moose; see Figs. 2.3; 2.4; Appendix B). For all antlers, the observed isotopic variation is greater than typical analytical error for at least one of

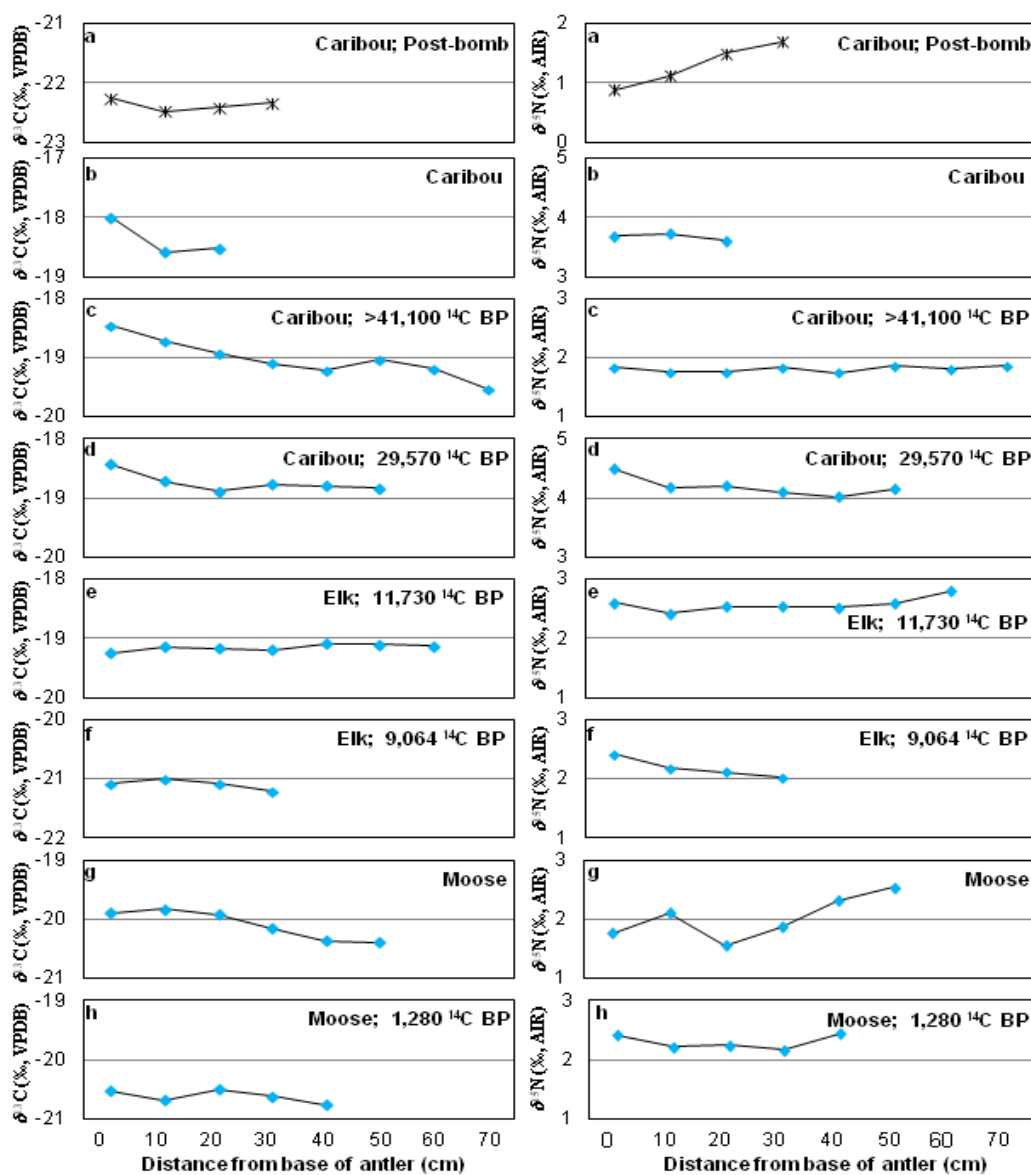


Figure 2.3 (left) Carbon isotopic compositions of serially sampled antler collagen (Herschel Island; Klondike): a. caribou antler, post-bomb; b. caribou antler; c. caribou antler, >41,100 ^{14}C BP; d. caribou antler, 29,570 \pm 970 ^{14}C BP; e. elk antler, 11,675 \pm 45 ^{14}C BP and h. moose antler, 1,363 \pm 35 and 1,197 \pm 27 ^{14}C BP. Black stars represent samples from Herschel Island; blue diamonds represent samples from the Klondike.

Figure 2.4 (right) Nitrogen isotopic compositions of serially sampled antler collagen. Description as in Figure 2.3.

the two isotopic systems considered (± 0.2 ‰ for $\delta^{13}\text{C}$, ± 0.3 ‰ for $\delta^{15}\text{N}$, as estimated using the maximum SD of sample replicates).

Four of the antlers (three Klondike caribou and one moose) exhibit generally decreasing $\delta^{13}\text{C}$ from the base of the antler to its tip, with the total change ranging from -0.4 ‰ to -1.1 ‰ between the base and the tip of the antler (Figs. 2.3b-d, g). Two antlers (one Herschel Island caribou and one moose) have $\delta^{15}\text{N}$ that increases by 0.8 ‰ from the antler base to its tip (Figs. 2.4a, g) and two antlers (one Klondike caribou, one elk) have $\delta^{15}\text{N}$ that decreases by 0.4 ‰ from the base to the tip (Figs. 2.4d, f). Two antlers (Klondike caribou and moose) display variations both in $\delta^{13}\text{C}$ and $\delta^{15}\text{N}$ (Figs. 2.3d, g; 2.4d, g) and two antlers (moose and elk) show no isotopic variation along the length of the antler (Figs. 2.3e, h; 2.4e, h). The change in isotopic composition with length along the antler is not always smooth, but a between-serial sample variation from the general isotopic trend that is larger than analytical error occurs for only once specimen (Fig. 2.4g). While the majority of the antlers are not complete tissues (Appendix B), sufficient tissue was preserved for isotopic shifts to be observed in the majority of antlers, even in cases where much of the antler was lost (e.g. Fig. 2.4f). The two antlers without isotopic shifts from base to tip both have long sampling lengths intact. While it is possible that isotopic shifts occurred during antler growth but were lost when the specimen was broken, it is more likely that the individuals had consistent diet and habitat during the period of antler growth.

2.3.2.2 Inter-tissue variation

Paired antler and bone specimens were available for one Klondike moose and one Herschel Island caribou. To allow for more analysis, comparisons were also made between antler and bone of populations composed of multiple individuals from a single site (see Fig. 2.5 and Appendix C). The difference in average carbon or nitrogen isotopic compositions between bone and antler for a population of one species at one site was calculated as $\delta_{\text{Bone}} - \delta_{\text{Antler}}$ ($\Delta_{\text{Bone-Antler}}$). The Mann-Whitney-Wilcoxon test was also used to check for significant differences between the isotopic compositions of bone and antler for a population (Table 2.1).

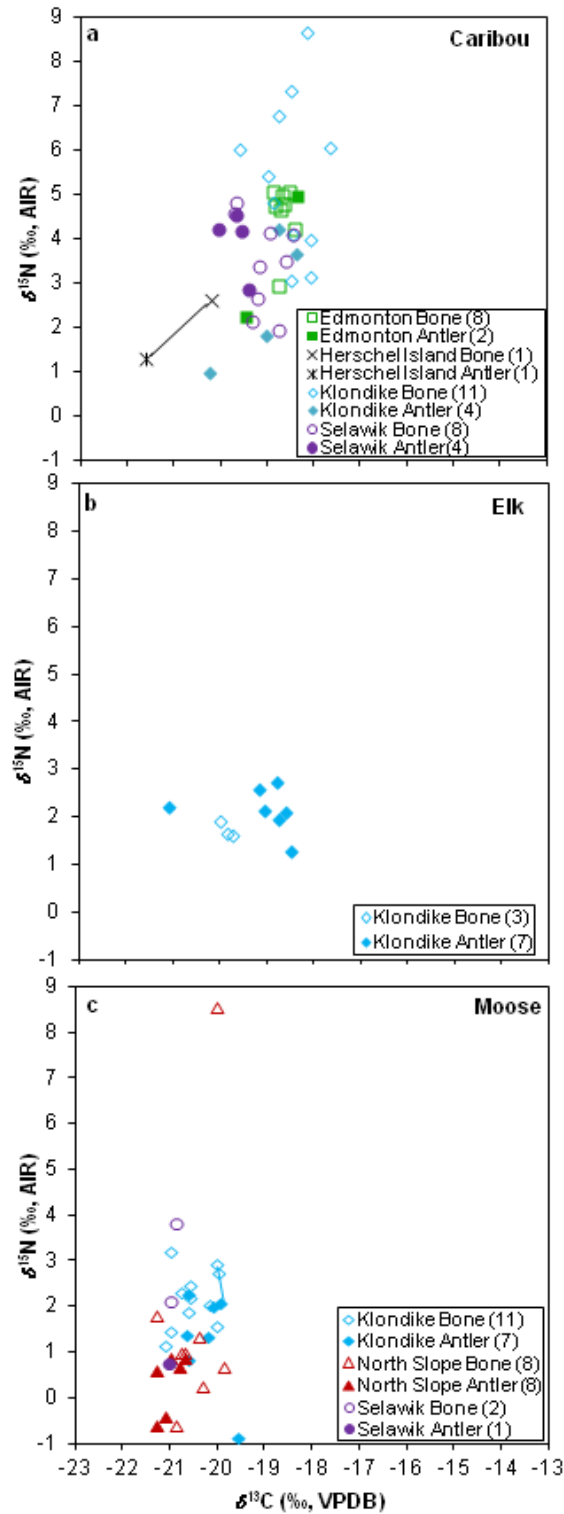


Figure 2.5 Isotopic compositions of antler and bone collagen: a. caribou; b. elk, and c. moose. Paired antler and bone samples for a single individual are joined by a line. The number of specimens in each group is listed in parentheses in the legend.

Species	Site	$\Delta^{13}\text{C}_{(\text{Bone}-\text{Antler})}$	p -value (Bone, Antler)	$\Delta^{15}\text{N}_{(\text{Bone}-\text{Antler})}$	p -value (Bone, Antler)
Caribou	Edmonton	0.2	1.00	1.0	0.51
Caribou	Herschel Island	1.4	N/A	1.3	N/A
Caribou	Klondike	0.6	0.21	2.7	0.04
Caribou	Selawik	0.6	0.05	-0.5	0.39
Elk	Klondike	-0.7	0.12	-0.4	0.13
Moose	Klondike	-0.3	0.17	0.9	0.06
Moose	North Slope	0.7	0.07	1.6	0.12
Moose	Selawik	0.1	N/A	2.2	N/A

Table 2.1 Comparison of the isotopic composition of bone and antler in a population for various species and sites. The difference in carbon isotopic composition between bone and antler for one species at one site, or $\delta^{13}\text{C}_{\text{Bone}} - \delta^{13}\text{C}_{\text{Antler}}$, is given as $\Delta^{13}\text{C}_{(\text{Bone}-\text{Antler})}$. The significance of a Mann-Whitney-Wilcoxon test between the two tissues is given as p value (Bone, Antler), with differences $p \leq 0.05$ treated as significant and shown in bold.

The $\delta^{15}\text{N}$ of Klondike caribou and the $\delta^{13}\text{C}$ of the Selawik caribou are the only groups that have significantly different isotopic compositions between bone and antler at $p \leq 0.05$. Despite the lack of statistical significance, however, there appears to be some trends in the data, which are generally consistent within a species. The Herschel Island caribou specimen has higher $\delta^{13}\text{C}$ and $\delta^{15}\text{N}$ in bone than antler, as is also observed for the populations of caribou at Edmonton and the Klondike and carbon isotopic compositions at Selawik. The Klondike elk specimens have lower $\delta^{13}\text{C}$ and $\delta^{15}\text{N}$ in bone than antler. Moose show no strong pattern of $\Delta^{13}\text{C}_{\text{Bone}-\text{Antler}}$ across the Klondike, North Slope and Selawik sites. Moose bone, however, has higher $\delta^{15}\text{N}$ than antler at all three of these sites. These patterns are generally consistent with the result for the Klondike moose bone-antler pair (Appendix C).

2.3.3 Isotopic variation over time

There are several dated specimens for each site and species considered here (see Appendices A and C and Figs. 2.6-2.8). Caribou specimens span an age range from >41,100 ^{14}C BP (infinite) to post-bomb. Elk specimens have dates ranging from 12,100 to 9,064 ^{14}C BP, which spans the transition from the Pleistocene to the Holocene. Radiocarbon dates for the moose specimens range from 10,790 to 80 ^{14}C BP, with the majority of the specimens being younger than 3,000 ^{14}C BP.

Statistical testing for changes in stable isotopic composition of antler or bone over the time periods considered here is impossible without additional dated specimens.

Nonetheless, the existing data can still be examined for general trends. No strong patterns in $\delta^{13}\text{C}$ are observed for caribou or moose; instead, the majority of isotopic variation appears to be site- or tissue-specific, rather than time-dependent (Figs. 2.6a; 2.8a).

Collagen $\delta^{13}\text{C}$ for elk antler and bone appear to decrease from oldest to youngest during the Terminal Pleistocene to Holocene transition (Fig. 2.7a). Caribou $\delta^{15}\text{N}$ reaches a maximum between 25,000-30,000 ^{14}C BP, and decreases thereafter (Fig. 2.6b). No time-dependent trend is apparent in $\delta^{15}\text{N}$ for elk or moose (Figs. 2.7b; 2.8b).

2.4 Discussion

2.4.1 Antler-specific physiological factors

There is general agreement that the $\delta^{13}\text{C}$ of antlers relates to the isotopic composition of the food consumed by the animal during the antler growth period (Darr and Hewitt, 2008; Osborne, 2013). Some authors suggest that dietary changes during antler growth are also a main control on their nitrogen isotopic compositions (Finstad and Kielland, 2011).

Antler-specific physiological factors, however, may also play a defining role in determining antler $\delta^{15}\text{N}$. Increasing levels of resorption and routing of bone protein to antler during the growth season would cause antler isotopic compositions to be more similar to bone towards the antler tip (Osborne, 2013). If routing was the primary control on the nitrogen isotopic composition of antlers, however, the observed shifts would all be of a similar magnitude and direction within a species, as was observed previously (Miller et al., 2014; Osborne, 2013). In the present study, one Klondike caribou antler has

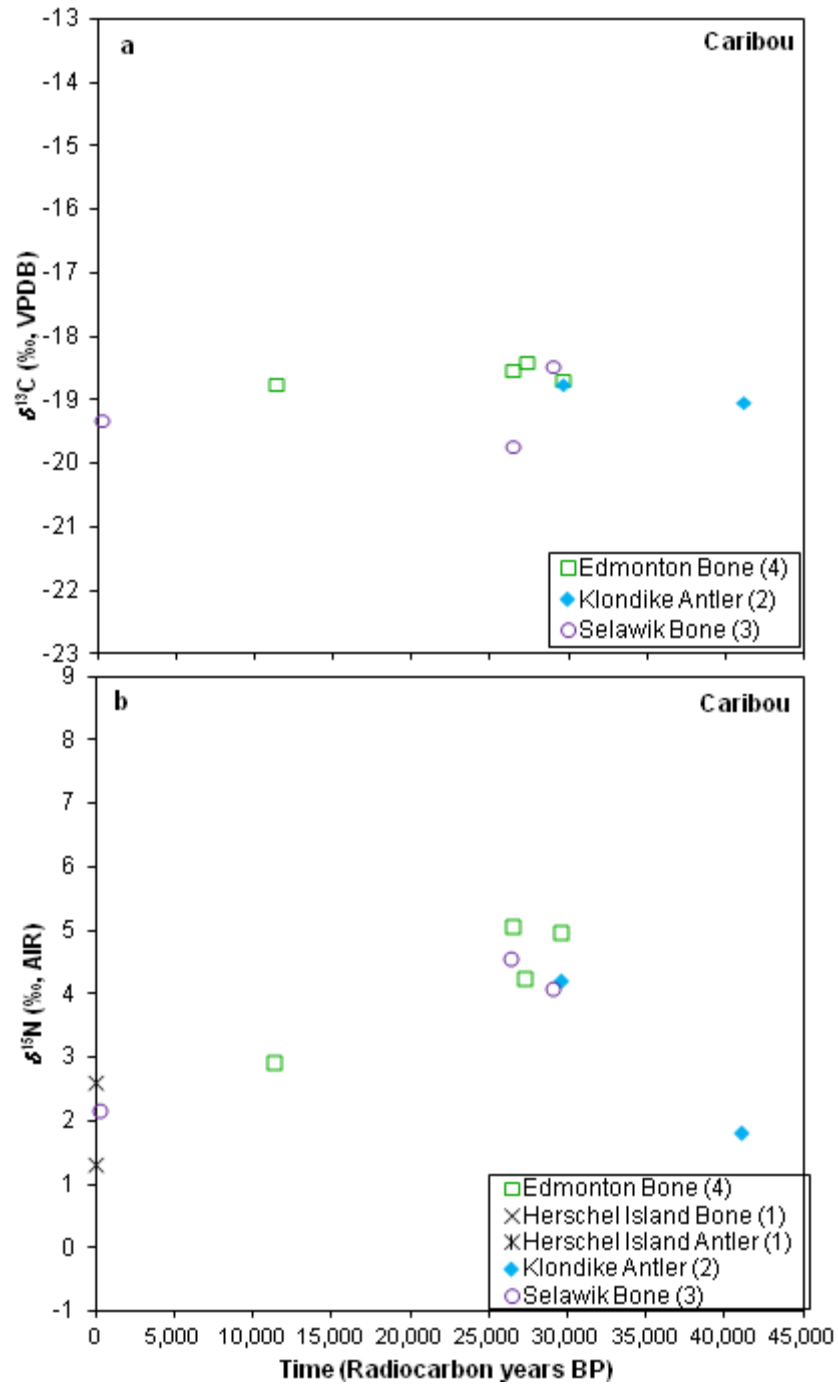


Figure 2.6 Isotopic compositions of caribou collagen from specimens younger than 45,000 ^{14}C BP: a. $\delta^{13}\text{C}$; b. $\delta^{15}\text{N}$. The number of specimens in each group is listed in parentheses in the legend.

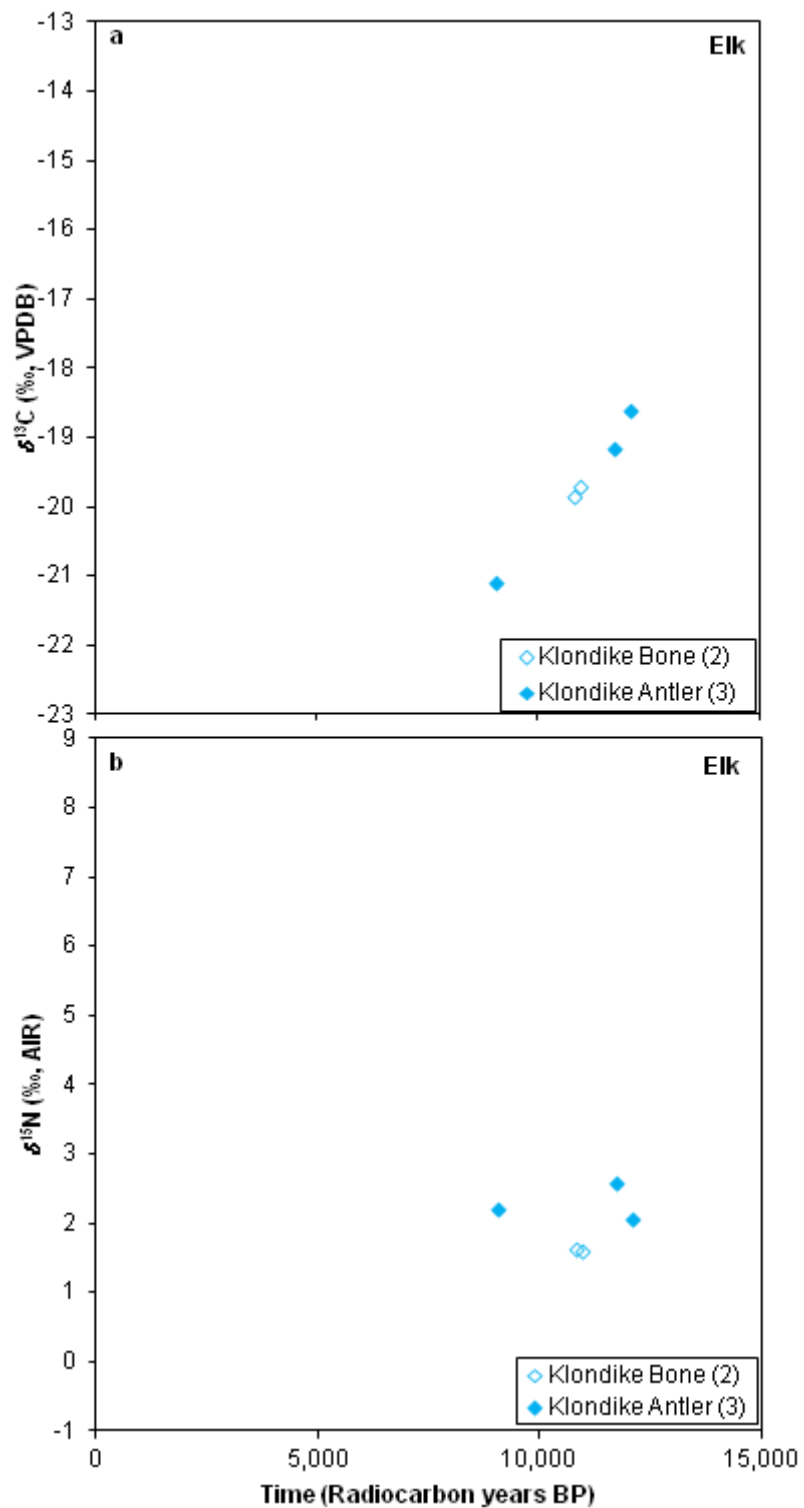


Figure 2.7 Isotopic compositions of elk collagen from specimens younger than 15,000 ^{14}C BP: a. $\delta^{13}\text{C}$; b. $\delta^{15}\text{N}$. The number of specimens in each group is listed in parentheses in the legend.

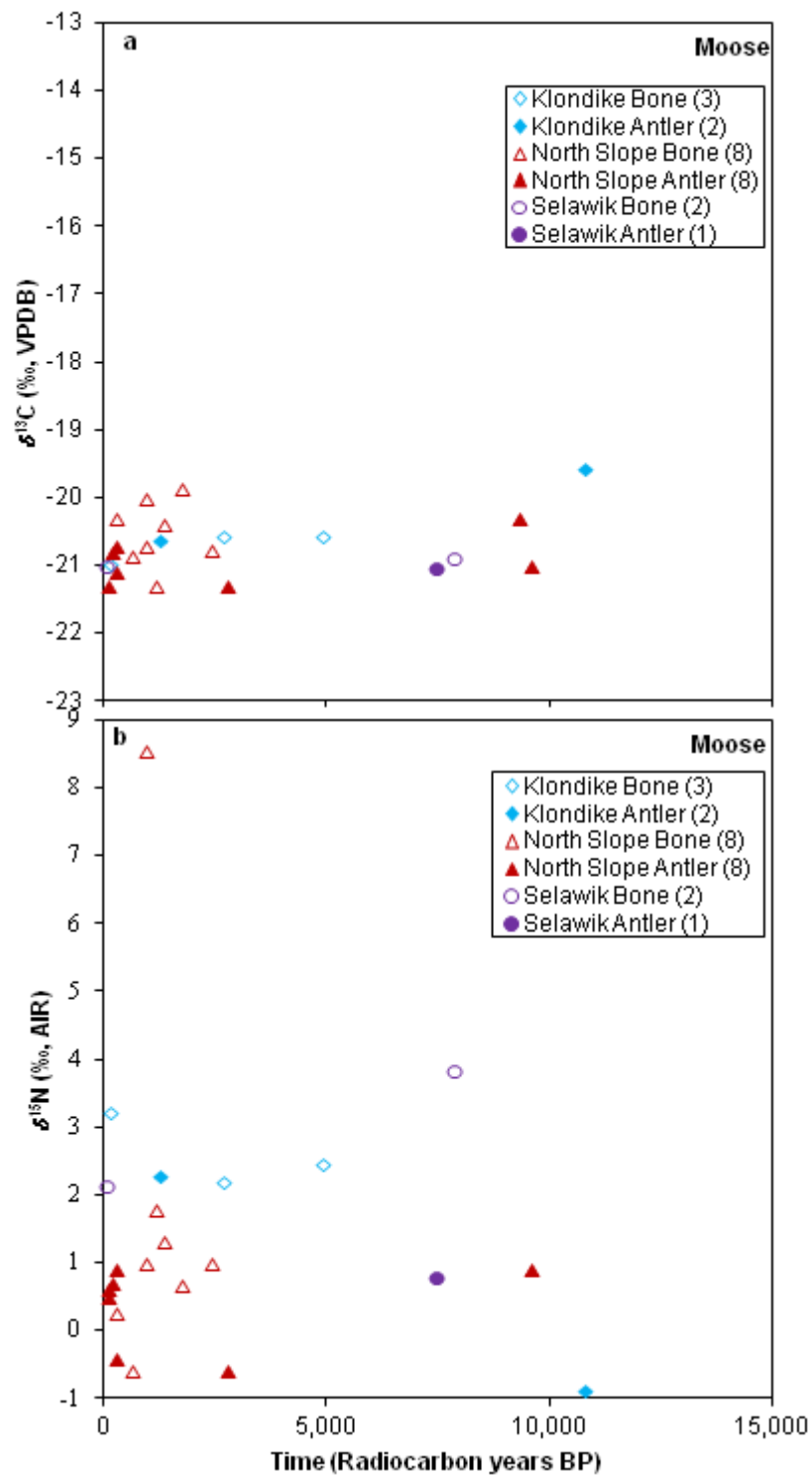


Figure 2.8 Isotopic compositions of dated moose collagen from specimens younger than 15,000 ^{14}C BP: a. $\delta^{13}\text{C}$; b. $\delta^{15}\text{N}$. The number of specimens in each group is listed in parentheses in the legend.

decreasing nitrogen isotopic compositions from the base to the tip of the antler (Fig. 2.4d), other Klondike specimens have unchanging nitrogen isotopic compositions along the antler length (Figs. 2.4b, c), and Herschel Island caribou antler has pattern of increasing $\delta^{15}\text{N}$ (Fig. 2.4a). In both Klondike and Herschel Island populations, caribou bone has higher average $\delta^{15}\text{N}$ than antler. Collectively, these data suggest that routing from bone is not a primary control on the nitrogen isotopic composition within antler.

We suggest instead that isotopic changes in diet are the main control on antler $\delta^{15}\text{N}$. Nonetheless, the differences between the isotopic composition of bone and antler observed in this study are generally not statistically significant, and in the case of the $\delta^{15}\text{N}$ of Selawik caribou, do not always follow the same pattern for a species. This may reflect the lack of strong temporal control on these specimens. Previous work has suggested that the isotopic compositions of plants have changed over the Pleistocene and Holocene (Bocherens et al., 2011; Drucker et al., 2003a; Fox-Dobbs et al., 2008; Mann et al., 2013; Stevens and Hedges, 2004; Stevens et al., 2008), and the specimens analysed here do not all date to the same time period. Some of the variation may also relate to individual dietary choices within a population, as observed by the differences in the amount of variation observed along the length of an antler within a species. Future feeding studies are needed to elucidate the exact controls on the isotopic compositions of each species. In general, however, it appears that the model shown in Figure 2.2a fairly represents the isotopic signals that can be obtained from antler and bone tissue.

The typically non-linear change in carbon and nitrogen isotopic compositions of serially sampled antler along the antler length has been observed previously (Miller et al., 2014; Osborne, 2013). There are a number of possible explanations for this behaviour. (1) There may be increased dietary routing from if forage is less available. As discussed earlier, however, this is unlikely to be the main process, since the Klondike moose antler for which this change is most prominent (Fig. 2.5g) shifts away from the average $\delta^{15}\text{N}$ of Klondike moose bone as growth continued. (2) Depending on the forage available in an animal's habitat, multiple shifts in diet could occur. Also, antler growth does not occur at a continuous pace. Shifts in diet, therefore, will be less represented during slower than faster growth by evenly spaced serial sampling. (3) Collagen deposition occurs both

along the length and across the width of the antler. Differences in the amounts of inner tissue included in the sample, either because of changes in antler width or variations in the extent of weathering of outer antler tissue, could affect the bulk isotopic signal. More detailed sampling of antler from a population with a known diet, and guided by histological mapping of the tissue, is needed to evaluate these possibilities more fully.

2.4.2 Seasonal, yearly, and inter-annual variation

2.4.2.1 Caribou

The caribou antler from Herschel Island, which increases in $\delta^{15}\text{N}$ along the length of the antler (Fig. 2.4a), is likely from a female or a juvenile male, based on the relatively small antler size. Modern studies of caribou highlight the importance of browse as one component of spring and summer diets, in conjunction with herbs, sedges and graminoids (Adamczewski et al., 1988; Bjørkvoll et al., 2009; Bjune, 2000; Boertje, 1984; Shank et al., 1978; Thomas et al., 1996; Thompson and McCourt, 1981). However, the proportion of each dietary source used may have changed over the antler growth period. Finstad and Kielland (2011) previously reported female Alaskan caribou to have increasing antler $\delta^{15}\text{N}$ over the growth period, which they attributed to consumption of less browse and more graminoids and forbs. While there are no trees on Herschel Island, this caribou may have consumed substantial amounts of ground shrubs during the late spring, but decreased its use of this forage over the summer.

Of the three caribou antlers from Klondike, two show decreases in $\delta^{13}\text{C}$ from antler base to tip, with no shift in $\delta^{15}\text{N}$ (Figs. 2.3b-c; 2.4b-c). One was from a female or juvenile male (Figs. 2.3b; 2.4b) and the other was from an adult male which dated to $>41,100$ ^{14}C BP (Figs. 2.3c; 2.4c), as identified based on their size (Appendix B). This $\delta^{13}\text{C}$ pattern may arise from reduced consumption of lichen as other, more nutrient-rich forage became available, but as lichen is protein-poor (Chapin and Shaver, 1988; Drucker et al., 2001), it may not have contributed substantially to the $\delta^{15}\text{N}$ signal. The decreasing $\delta^{13}\text{C}$ and $\delta^{15}\text{N}$ along the length of the third antler (Figs. 2.3d; 2.4d), which is from an adult male, likely indicates a dietary shift to consumption of more browse (ground shrubs) and fewer graminoids and forbs, and, perhaps for carbon, lichen (see Fig. 1.2).

The lower $\delta^{13}\text{C}$ is unlikely to indicate a canopy effect; this antler was dated to $\sim 29,570$ ^{14}C BP, at which time there was limited tree cover in the Klondike (Zazula et al., 2014). The decreasing $\delta^{13}\text{C}$ and $\delta^{15}\text{N}$ could also indicate an increase in aridity during antler growth. Isotopic analysis of modern antlers for years of known seasonal changes in aridity could be used to test this idea. The higher $\delta^{15}\text{N}$ and $\delta^{13}\text{C}$ of bone than antler in the paired caribou specimen from Herschel Island and more generally for this species (Fig. 2.5a; Table 2.1) mirrors that reported by (Drucker et al., 2001) and likely has the same cause, that is, bone acquires higher $\delta^{13}\text{C}$ from lichen in their winter diet and higher $\delta^{15}\text{N}$ from winter food shortages that led to increasing nitrogen recycling. In short, these data support the idea that lichen use was most important during the winter and decreased during the rest of the year.

Caribou were present in North American high latitude environments over the entirety of the time measurable using radiocarbon methods (Guthrie, 2006; Mann et al., 2013), and sampled over this range in the present study (Fig. 2.6). The Herschel Island caribou samples are not included in these comparisons because of the uncertainty associated with the Suess effect correction. The caribou collagen $\delta^{13}\text{C}$ for this limited number of samples is relatively constant over time (Fig. 2.6a). The peak in caribou $\delta^{15}\text{N}$ at $\sim 30,000$ to $25,000$ ^{14}C BP and subsequent decrease towards the Pleistocene/Holocene transition and into the Holocene (Fig. 2.6b) have been observed in multiple studies of megafaunal herbivore bone (Bocherens et al., 2011; Drucker et al., 2003b; Fox-Dobbs et al., 2008; Mann et al., 2013; Stevens and Hedges, 2004; Stevens et al., 2008) and may indicate a difference in available forage, such as an increase in browse, or an increase in moisture from the melting of permafrost (Guthrie, 2006; Stevens and Hedges, 2004; Stevens et al., 2008; Zazula et al., 2014).

2.4.2.2 Elk

The decrease in $\delta^{15}\text{N}$ of the elk antler from $9,064$ ^{14}C BP over the growth period potentially corresponds to a shift from a graze to a browse diet (Fig. 2.4f), as has been observed for several modern elk populations (Hobbs et al., 1981). Given that the collagen $\delta^{13}\text{C}$ did not change (Fig. 2.3f), this animal may have consumed a range of plant types

that grew in similar habitats. The elk antler from 11,675 ^{14}C BP, which shows no notable changes in collagen isotopic composition along the length of the antler (Figs. 2.3e; 2.4e), may have had a smaller range that limited access to wide a variety of plant or habitat types. Variability in the diet of ancient elk individuals is not unexpected, given the opportunistic and varied feeding patterns of modern populations (Christianson and Creel, 2007; Drucker et al., 2008; Dumont et al., 2005; Gebert and Verheyden-Tixier, 2001; Hofmann, 1989; Jenkins and Starkey, 1991; Kufeld, 1973; Morgantini and Hudson, 1989; Prokešová, 2004).

The higher average nitrogen isotopic compositions of antler than the bone in elk from the Klondike (Fig. 2.5b; Table 2.1) likely relate to seasonal differences in diet. As elk are mixed-feeders, they may consume more graminoids and forbs than browse during the fall and winter than during the spring and summer, consistent with some modern elk populations (Christianson and Creel, 2007; Morgantini and Hudson, 1989). It is interesting that the spring and summer diets have lower $\delta^{15}\text{N}$ than the fall and winter diets, opposite to that generally observed for caribou and moose (Fig. 2.5; Table 2.1). The caribou and moose nitrogen isotopic variation may indicate winter starvation, as discussed earlier. The lack of such an isotopic signal in elk may suggest they did not experience high levels of winter starvation in the Klondike during the Pleistocene/Holocene transition. Winter diets that meet maintenance requirements have been observed for some modern elk populations (Hobbs et al., 1981).

Elk are suggested to have entered North America across the Bering Land Bridge around 13,000 ^{14}C years BP and to have moved southward after the Pleistocene/Holocene transition (Guthrie, 2006; Meiri et al., 2014). This is consistent with the dated individuals examined in the present study (Fig. 2.7). There is a strong pattern of decreasing $\delta^{13}\text{C}$ in elk bone and antler collagen from ~15,000 to 10,000 ^{14}C BP (Fig. 2.7a), whereas no pattern is apparent in $\delta^{15}\text{N}$ (Fig. 2.7b). The change in $\delta^{13}\text{C}$ may relate to increasing consumption of plants that grew in dense canopy cover, consistent with the rise of boreal forests in these environments at this time (Zazula et al., 2014), as has been suggested to have occurred in other environments (Drucker et al., 2003a; Drucker et al., 2008). Alternatively, it may reflect variations in the $p\text{CO}_2$ of the atmosphere, which caused

changes in the $\delta^{13}\text{C}$ of the plants at the base of the food web (see discussions in Bocherens, 2003; Iacumin et al., 2006; Stevens and Hedges, 2004). As there are limited dated specimens available, and the dated specimens include both antler and bone, this pattern may also arise in part from seasonal differences between the two tissues, as we suggested for the differences in average elk $\delta^{15}\text{N}$. This seems a less parsimonious explanation, however, as both antler and bone show the same trend of decreasing $\delta^{13}\text{C}$ values over time, and no such temporal trend was seen in $\delta^{15}\text{N}$.

2.4.2.3 Moose

The increase in collagen $\delta^{15}\text{N}$ from base to tip of the moose antler dated to 1,197 ^{14}C BP (Fig. 2.4g) likely corresponds to a seasonal increase in the consumption of aquatic plants, which often have distinct isotopic compositions from terrestrial plants, as hypothesized in previous isotopic studies of moose (Kielland, 2001; Tischler, 2004). Aquatic plants typically have higher protein contents than browse, which would further accentuate the increase in $\delta^{15}\text{N}$. The concomitant decrease in $\delta^{13}\text{C}$ (Fig. 2.3g) could indicate a habitat where aquatic plants had lower $\delta^{13}\text{C}$ than browse, or a diet involving increased consumption of leaves relative to twigs (Tischler, 2004). The lack of significant variation in collagen $\delta^{13}\text{C}$ or $\delta^{15}\text{N}$ between the base and tip of the antler of the other moose specimen (Figs. 2.3h; 2.4h) suggests invariant forage over the antler growth period, and perhaps the lack of access to aquatic plants within this individual's range.

Higher $\delta^{15}\text{N}$ was observed for bone than antler both for the paired moose specimen and for the populations at all sites (Fig. 2.5c; Table 2.1). None of the typical dietary or habitat shifts of the moose are expected to produce a higher $\delta^{15}\text{N}$ for fall and winter than spring and summer. For example, an increase in aquatic plant or leaf consumption (rather than twigs) in spring and summer would be expected to increase the $\delta^{15}\text{N}$ of the antler. The higher $\delta^{15}\text{N}$ of the bone may be a metabolic signal, indicating that moose are undergoing sufficient winter dietary restrictions to cause increased nitrogen recycling that drove $\delta^{15}\text{N}$ to higher values in their bones.

The dated moose specimens cover the range expected for entry into North American high latitude environments at the end of the Pleistocene (Guthrie, 2006; Mann et al., 2013).

There is no significant pattern of isotopic variation from ~10,000 ^{14}C BP to pre-industrial revolution times, despite a larger dataset than for caribou or elk. This time period may have undergone fewer changes in the isotopic composition of plants, moose might have selected plants whose isotopic compositions tended not to change over time, or the wider range of isotopic compositions known for aquatic plants may obscure other variation that has occurred.

2.5 Conclusion

The main controls on the carbon and nitrogen isotopic composition of antler collagen are diet and the physiological state of the animal. Antler-specific metabolic effects do not exert a primary control on antler collagen isotopic composition. Such isotopic measurements of antler are therefore useful for investigating seasonal ecology. At a minimum, sampling of the base and tip of an antler can provide information about the spring and summer ecology of that animal. Isotopic variation over the length of the antler can have multiple causes: (1) individual dietary choice, potentially related to the relative nutrient levels of available forage, as reflected in decreased lichen consumption of some caribou during summer; (2) habitat differences such as access to aquatic plants during summer, as suggested for one moose, and (3) environmental differences, such as increased levels of aridity over summer, as was suggested for one caribou.

Comparisons between bone and antler collagen isotopic compositions demonstrate differences in the ecology of the species between summer and the rest of the year. The carbon isotopic compositions of bone versus antler highlight the varied diet between the summer and the rest of the year, in particular, the substantial contribution of lichen to the winter diet of caribou. The nitrogen isotopic compositions of the Holocene moose and Holocene and Pleistocene caribou both suggest that these species faced high levels of winter stress, almost certainly from starvation. Interestingly, elk from the Pleistocene/Holocene transition did not seem to have faced the same high levels of winter starvation.

The ability to pinpoint ecological differences over annual time periods is particularly useful for ecological reconstruction. Hence further investigation of the information held by the isotopic composition of antler tissues represents a fruitful direction for learning more about seasonal variations in diet and habitat, and more broadly climate-related changes that may have contributed to the extirpation or extinction of Pleistocene and Holocene megaherbivores.

2.6 References

- Adamczewski, J., Gates, C.C., Soutar, B.M., Hudson, R.J., 1988. Limiting effects of snow on seasonal habitat use and diets of caribou (*Rangifer tarandus groenlandicus*) on Coats Island, Northwest Territories, Canada. *Can. J. Zool.* 66, 1986–1996.
- Ambrose, S., 1990. Preparation and characterization of bone and tooth collagen for isotopic analysis. *J. Archaeol. Sci.* 17, 431–451.
- Ambrose, S., 1991. Effects of diet, climate and physiology on nitrogen isotope abundances in terrestrial foodwebs. *J. Archaeol. Sci.* 18, 293–317.
- Amundson, R., Austin, A., Schuur, E.A.G., Yoo, K., Matzek, V., Kendall, C., Uebersax, A., Brenner, D., Baisden, W.T., 2003. Global patterns of the isotopic composition of soil and plant nitrogen. *Glob. Biogeochemical Cycles* 17. doi:10.1029/2002GB001903
- Balasse, M., Bocherens, H., Mariotti, A., 1999. Intra-bone variability of collagen and apatite isotopic composition used as evidence of a change of diet. *J. Archaeol. Sci.* 26, 593–598.
- Ballenberghe, V. Van, 1983. Growth and development of moose antlers in Alaska, in: Brown, R.D. (Ed.), *Antler Development in Cervidae*. Caesar Kleberg Wildlife Research Institute, Kingsville, Texas, pp. 37–48.
- Banks, W., Newbrey, J., 1983. Light microscopic studies of the ossification process in developing antlers, in: Brown, R. (Ed.), *Antler Development in Cervidae*. Caesar Kleberg Wildlife Research Institute, Kingsville, Texas, pp. 231–260.
- Barnett, B., 1994. Carbon and nitrogen isotope ratios of caribou tissues, vascular plants, and lichens from northern Alaska. University of Alaska, Fairbanks.
- Bauer, D., 1972. Constructing confidence sets using rank statistics. *J. Am. Stat. Assoc.* 67, 687–690.
- Bellissimo, N.S., 2013. Origins of stable isotopic variations in late Pleistocene horse enamel and bone from Alberta. Master's Thesis. University of Western Ontario.

- Belovsky, G., 1981. Food plant selection by a generalist herbivore: the moose. *Ecology* 62, 1020–1030.
- Ben-David, M., Shochat, E., Adams, L., 2001. Utility of stable isotope analysis in studying foraging ecology of herbivores: examples from moose and caribou. *Alces* 37, 421–434.
- Bjørkvoll, E., Pedersen, B., Hytteborn, H., Jónsdóttir, I.S., Langvatn, R., 2009. Seasonal and interannual dietary variation during winter in female Svalbard reindeer (*Rangifer tarandus platyrhynchus*). *Arctic, Antarct. Alp. Res.* 41, 88–96. doi:10.1657/1938-4246(07-100)
- Bjune, A., 2000. Pollen analysis of faeces as a method of demonstrating seasonal variations in the diet of Svalbard reindeer (*Rangifer tarandus platyrhynchus*). *Polar Res.* 19, 183–192.
- Bligh, E.G., Dyer, W.J., 1959. A rapid method of total lipid extraction and purification. *Can. J. Biochem. Physiol.* 37, 911–917. doi:10.1139/o59-099
- Bocherens, H., 2003. Isotopic biogeochemistry and the paleoecology of the mammoth steppe fauna. *Deinsea* 9, 57–76.
- Bocherens, H., Billiou, D., Mariotti, A., Toussaint, M., Patou-Mathis, M., Bonjean, D., Otte, M., 2001. New isotopic evidence for dietary habits of Neandertals from Belgium. *J. Hum. Evol.* 40, 497–505. doi:10.1006/jhev.2000.0452
- Bocherens, H., Billiou, D., Patou-Mathis, M., Bonjean, D., Otte, M., Mariotti, A., 1997. Paleobiological implications of the isotopic Signatures (^{13}C , ^{15}N) of fossil mammal collagen in Scladina Cave (Sclayn, Belgium). *Quat. Res.* 48, 370–380. doi:10.1006/qres.1997.1927
- Bocherens, H., Drucker, D.G., Billiou, D., Patou-Mathis, M., Vandermeersch, B., 2005. Isotopic evidence for diet and subsistence pattern of the Saint-Césaire I Neanderthal: review and use of a multi-source mixing model. *J. Hum. Evol.* 49, 71–87. doi:10.1016/j.jhevol.2005.03.003
- Bocherens, H., Drucker, D.G., Bonjean, D., Bridault, A., Conard, N.J., Cupillard, C., Germonpré, M., Höneisen, M., Münzel, S.C., Napierala, H., Patou-Mathis, M., Stephan, E., Uerpmann, H.-P., Ziegler, R., 2011. Isotopic evidence for dietary ecology of cave lion (*Panthera spelaea*) in North-Western Europe: prey choice, competition and implications for extinction. *Quat. Int.* 245, 249–261. doi:10.1016/j.quaint.2011.02.023
- Bocherens, H., Fizet, M., Mariotti, A., Gangloff, R., Burns, J., 1994. Contribution of isotopic biogeochemistry (^{13}C , ^{15}N , ^{18}O) to the paleoecology of mammoths (*Mammuthus primigenius*). *Hist. Biol.* 7, 187–202.
- Bocherens, H., Pacaud, G., Lazarev, P.A., Mariotti, A., 1996. Stable isotope abundances

- (^{13}C , ^{15}N) in collagen and soft tissues from Pleistocene mammals from Yakutia: implications for the palaeobiology of the Mammoth Steppe. *Palaeogeogr. Palaeoclimatol. Palaeoecol.* 126, 31–44.
- Boertje, R., 1984. Seasonal diets of the Denali caribou herd, Alaska. *Arctic* 37, 161–165.
- Brooks, J., Flanagan, L., Buchmann, N., Ehleringer, J., 1997. Carbon isotope composition of boreal plants: functional grouping of life forms. *Oecologia* 110, 301–311.
- Bunn, S., Barton, D., Hynes, H.N., Power, G., Pope, M.A., 1989. Stable isotope analysis of carbon flow in a tundra river system. *Can. J. Fish. Aquat. Sci.* 46, 1769–1775.
- Chapin, F.S., Shaver, G.R., 1988. Differences in carbon and nutrient fractions among arctic growth forms. *Oecologia* 77, 506–514. doi:10.1007/BF00377266
- Chapman, D., 1975. Antlers – bones of contention. *Mamm. Rev.* 5, 121–172.
- Chikaraishi, Y., Naraoka, H., 2003. Compound-specific δD – $\delta^{13}\text{C}$ analyses of n-alkanes extracted from terrestrial and aquatic plants. *Phytochemistry* 63, 361–371. doi:10.1016/S0031-9422(02)00749-5
- Christianson, D., Creel, S., 2007. A review of environmental factors affecting elk winter diets. *J. Wildl. Manage.* 71, 164–176.
- Coplen, T., Brand, W., Gehre, M., Gröning, M., Meijer, H.A., Toman, B., Verkouteren, R.M., 2006. New guidelines for $\delta^{13}\text{C}$ measurements. *Anal. Chem.* 78, 2439–2441.
- Darr, R., Hewitt, D., 2008. Stable isotope trophic shifts in white-tailed deer. *J. Wildl. Manage.* 72, 1525–1531. doi:10.2193/2006-293
- de Bello, F., Buchmann, N., Casals, P., Lepš, J., Sebastià, M.-T., 2009. Relating plant species and functional diversity to community $\delta^{13}\text{C}$ in NE Spain pastures. *Agric. Ecosyst. Environ.* 131, 303–307. doi:10.1016/j.agee.2009.02.002
- Delong, M.D., Thorp, J.H., 2006. Significance of instream autotrophs in trophic dynamics of the Upper Mississippi River. *Oecologia* 147, 76–85. doi:10.1007/s00442-005-0241-y
- DeNiro, M., 1985. Postmortem preservation and alteration of in vivo bone collagen isotope ratios in relation to palaeodietary reconstruction. *Nature* 317, 806–809. doi:10.1038/317806a0
- Diefendorf, A., Mueller, K., Wing, S.L., Koch, P.L., Freeman, K.H., 2010. Global patterns in leaf ^{13}C discrimination and implications for studies of past and future climate. *Proc. Natl. Acad. Sci.* 107, 5738–5743.
- Doucett, R.R., Barton, D.R., Guiguer, K., Power, G., Drimmie, R.J., 1996. Comment: Critical examination of stable isotope analysis as a means for tracing carbon

- pathways in stream ecosystems. *Can. J. Fish. Aquat. Sci.* 53, 1913–1915.
doi:10.1139/f96-114
- Druckenmiller, P.S., 2008. Survey of Pleistocene (Ice Age) vertebrates from the Selawik and Kobuk River areas of Northwestern Alaska. *Intern. Rep. U.S. Fish Wildl. Serv.* 1–56.
- Drucker, D.G., Hobson, K.A., Münzel, S.C., Pike-Tay, A., 2012. Intra-individual variation in stable carbon ($\delta^{13}\text{C}$) and nitrogen ($\delta^{15}\text{N}$) isotopes in mandibles of modern caribou of Qamanirjuaq (*Rangifer tarandus groenlandicus*) and Banks Island (*Rangifer tarandus pearyi*): implications for tracing seasonal and temporal changes in diet. *Int. J. Osteoarchaeol.* 22, 494–504.
- Drucker, D.G., Bocherens, H., Bridault, A., Billiou, D., 2003a. Carbon and nitrogen isotopic composition of red deer (*Cervus elaphus*) collagen as a tool for tracking palaeoenvironmental change during the Late-Glacial and Early Holocene in the northern Jura (France). *Palaeogeogr. Palaeoclimatol. Palaeoecol.* 195, 375–388.
doi:10.1016/S0031-0182(03)00366-3
- Drucker, D.G., Bocherens, H., Billiou, D., 2003b. Evidence for shifting environmental conditions in Southwestern France from 33 000 to 15 000 years ago derived from carbon-13 and nitrogen-15 natural abundances in collagen of large herbivores. *Earth Planet. Sci. Lett.* 216, 163–173. doi:10.1016/S0012-821X(03)00514-4
- Drucker, D.G., Bocherens, H., Pike-Tay, A., Mariotti, A., 2001. Isotopic tracking of seasonal dietary change in dentine collagen: preliminary data from modern caribou. *Comptes Rendus l'Académie des Sci. - Ser. IIA - Earth Planet. Sci.* 333, 303–309.
doi:10.1016/S1251-8050(01)01640-8
- Drucker, D.G., Bridault, A., Cupillard, C., Hujic, A., Bocherens, H., 2011. Evolution of habitat and environment of red deer (*Cervus elaphus*) during the Late-glacial and early Holocene in eastern France (French Jura and the western Alps) using multi-isotope analysis ($\delta^{13}\text{C}$, $\delta^{15}\text{N}$, $\delta^{18}\text{O}$, $\delta^{34}\text{S}$) of archaeological remains. *Quat. Int.* 245, 268–278. doi:10.1016/j.quaint.2011.07.019
- Drucker, D.G., Bridault, A., Hobson, K.A., Szuma, E., Bocherens, H., 2008. Can carbon-13 in large herbivores reflect the canopy effect in temperate and boreal ecosystems? Evidence from modern and ancient ungulates. *Palaeogeogr. Palaeoclimatol. Palaeoecol.* 266, 69–82. doi:10.1016/j.palaeo.2008.03.020
- Drucker, D.G., Henry-Gambier, D., 2005. Determination of the dietary habits of a Magdalenian woman from Saint-Germain-la-Rivière in southwestern France using stable isotopes. *J. Hum. Evol.* 49, 19–35. doi:10.1016/j.jhevol.2005.02.007
- Drucker, D.G., Hobson, K.A., Ouellet, J.-P., Courtois, R., 2010. Influence of forage preferences and habitat use on ^{13}C and ^{15}N abundance in wild caribou (*Rangifer tarandus caribou*) and moose (*Alces alces*) from Canada. *Isotopes Environ. Health*

Stud. 46, 107–21. doi:10.1080/10256010903388410

- Dumont, B., Renaud, P., Morellet, N., Mallet, C., Anglard, F., Verheyden-Tixier, H., 2005. Seasonal variations of red deer selectivity on a mixed forest edge. *Anim. Res.* 54, 369–381.
- Edwards, J., 1983. Diet shifts in moose due to predator avoidance. *Oecologia* 60, 185–189.
- Ehleringer, J., Comstock, J., Cooper, T., 1987. Leaf-twig carbon isotope ratio differences in photosynthetic-twig desert shrubs. *Oecologia* 71, 318–320.
- Ehleringer, J., Cooper, T., 1988. Correlations between carbon isotope ratio and microhabitat in desert plants. *Oecologia* 76, 562–566.
- Ehleringer, J., Phillips, S., Comstock, J., 1992. Seasonal variation in the carbon isotopic composition of desert plants. *Funct. Ecol.* 6, 396–404.
- Farquhar, G., 1989. Carbon isotope discrimination and photosynthesis. *Annu. Rev. Plant Biol.* 40, 503–537.
- Finlay, J., Kendall, C., 2007. Stable isotope tracing of temporal and spatial variability in organic matter sources to freshwater ecosystems, in: Michener, R., Lajtha, K. (Eds.), *Stable Isotopes in Ecology and Environmental Science*. Blackwell Publishing Ltd, Hong Kong, pp. 283–333.
- Finlay, J., Power, M., Cabana, G., 1999. Effects of water velocity on algal carbon isotope ratios: implications for river food web studies. *Limnol. Oceanogr.* 44, 1198–1203.
- Finstad, G.L., Kielland, K., 2011. Landscape variation in the diet and productivity of reindeer in Alaska based on stable isotope analyses. *Arctic, Antarct. Alp. Res.* 43, 543–554. doi:10.1657/1938-4246-43.4.543
- Fizet, M., Mariotti, A., Bocherens, H., Lange-Badré, B., Vandermeersch, B., Borel, J.P., Bellon, G., 1995. Effect of diet, physiology and climate on carbon and nitrogen stable isotopes of collagen in a Late Pleistocene anthropic palaeoecosystem: Marillac, Charente, France. *J. Archaeol. Sci.* 22, 67–79.
- Fox-Dobbs, K., Leonard, J., Koch, P., 2008. Pleistocene megafauna from eastern Beringia: paleoecological and paleoenvironmental interpretations of stable carbon and nitrogen isotope and radiocarbon records. *Palaeogeogr. Palaeoclimatol. Palaeoecol.* 261, 30–46.
- France, C.A.M., Zelanko, P.M., Kaufman, A.J., Holtz, T.R., 2007. Carbon and nitrogen isotopic analysis of Pleistocene mammals from the Saltville Quarry (Virginia, USA): implications for trophic relationships. *Palaeogeogr. Palaeoclimatol. Palaeoecol.* 249, 271–282. doi:10.1016/j.palaeo.2007.02.002

- France, R., 1995. Critical examination of stable isotope analysis as a means for tracing carbon pathways in stream ecosystems. *Can. J. Fish. Aquat. Sci.* 52, 651–656.
- France, R.L., 1995. Source variability in $\delta^{15}\text{N}$ of autotrophs as a potential aid in measuring allochthony in freshwaters. *Ecography* 18, 318–320. doi:10.1111/j.1600-0587.1995.tb00134.x
- Fraser, D., Thompson, B.K., Arthur, D., 1982. Aquatic feeding by moose: seasonal variation in relation to plant chemical composition and use of mineral licks. *Can. J. Zool.* 60, 3121–3126.
- Fry, B., 1991. Stable isotope diagrams of freshwater food webs. *Ecology* 72, 2293–2297.
- Gaglioti, B. V., Barnes, B.M., Zazula, G.D., Beaudoin, A.B., Wooller, M.J., 2011. Late Pleistocene paleoecology of arctic ground squirrel (*Urocitellus parryii*) caches and nests from Interior Alaska's mammoth steppe ecosystem, USA. *Quat. Res.* 76, 373–382. doi:10.1016/j.yqres.2011.08.004
- Gannes, L., del Rio, C., Koch, P., 1998. Natural abundance variations in stable isotopes and their potential uses in animal physiological ecology. *Comp. Biochem. Physiol. Part A Mol. Integr. Physiol.* 119, 725–737.
- Gebauer, G., Schulze, E., 1991. Carbon and nitrogen isotope ratios in different compartments of a healthy and a declining *Picea abies* forest in the Fichtelgebirge, NE Bavaria. *Oecologia* 87, 198–207.
- Gebert, C., Verheyden-Tixier, H., 2001. Variations of diet composition of red deer (*Cervus elaphus L.*) in Europe. *Mamm. Rev.* 31, 189–201.
- Gomez, S., Garcia, A.J., Luna, S., Kierdorf, U., Kierdorf, H., Gallego, L., Landete-Castillejos, T., 2013. Labeling studies on cortical bone formation in the antlers of red deer (*Cervus elaphus*). *Bone* 52, 506–15. doi:10.1016/j.bone.2012.09.015
- Guthrie, R.D., 1990. Frozen fauna of the mammoth steppe: the story of Blue Babe. The University of Chicago Press, Chicago.
- Guthrie, R.D., 2006. New carbon dates link climatic change with human colonization and Pleistocene extinctions. *Nature* 441, 207–209. doi:10.1038/nature04604
- Hansen, R., Reid, L., 1975. Diet overlap of deer, elk, and cattle in southern Colorado. *J. Range Manag.* 28, 43–47.
- Heaton, T.H.E., 1987. The $^{15}\text{N}/^{14}\text{N}$ ratios of plants in South Africa and Namibia: relationship to climate and coastal/saline environments. *Oecologia* 74, 236–246.
- Heggberget, T., Gaare, E., Ball, J., 2002. Reindeer (*Rangifer tarandus*) and climate change: importance of winter forage. *Rangifer* 22, 13–31.

- Hobbs, N., Baker, D., Ellis, J., Swift, D., 1981. Composition and quality of elk winter diets in Colorado. *J. Wildl. Manage.* 45, 156–171.
- Hobson, K.A., Alisauskas, R.T., Clark, R.G., 1993. Stable-nitrogen isotope enrichment in avian tissues due to fasting and nutritional stress: implications for isotopic analyses of diet. *Condor* 95, 388–394.
- Hofmann, R., 1989. Evolutionary steps of ecophysiological adaptation and diversification of ruminants: a comparative view of their digestive system. *Oecologia* 78, 443–457.
- Hörnberg, S., 2001. Changes in population density of moose (*Alces alces*) and damage to forests in Sweden. *For. Ecol. Manage.* 149, 141–151.
- Iacumin, P., Davanzo, S., Nikolaev, V., 2006. Spatial and temporal variations in the $^{13}\text{C}/^{12}\text{C}$ and $^{15}\text{N}/^{14}\text{N}$ ratios of mammoth hairs: palaeodiet and palaeoclimatic implications. *Chem. Geol.* 231, 16–25. doi:10.1016/j.chemgeo.2005.12.007
- Iacumin, P., Matteo, A. Di, Nikolaev, V., Kuznetsova, T., 2010. Climate information from C, N and O stable isotope analyses of mammoth bones from northern Siberia. *Quat. Int.* 212, 206–212.
- Iacumin, P., Nikolaev, V., Ramigni, M., 2000. C and N stable isotope measurements on Eurasian fossil mammals, 40 000 to 10 000 years BP: herbivore physiologies and palaeoenvironmental reconstruction. *Palaeogeogr. Palaeoclimatol. Palaeoecol.* 163, 33–47.
- Jenkins, K.J., Starkey, E.E., 1991. Food habits of Roosevelt elk. *Rangelands Arch.* 13, 261–265.
- Jones, P., Hudson, R., 2002. Winter habitat selection at three spatial scales by American elk, *Cervus elaphus*, in west-central Alberta. *Can. Field-Naturalist* 116, 183–191.
- Keeley, J., Sandquist, D., 1992. Carbon: freshwater plants. *Plant. Cell Environ.* 15, 1021–1035.
- Kelly, J., 2000. Stable isotopes of carbon and nitrogen in the study of avian and mammalian trophic ecology. *Can. J. Zool.* 78, 1–27.
- Kelsall, J., 1968. The migratory barren-ground caribou of Canada. Queen's Printer, Ottawa.
- Kempster, B., Zanette, L., Longstaffe, F.J., MacDougall-Shackleton, S.A., Wingfield, J.C., Clinchy, M., 2007. Do stable isotopes reflect nutritional stress? Results from a laboratory experiment on song sparrows. *Oecologia* 151, 365–71. doi:10.1007/s00442-006-0597-7
- Kielland, K., 2001. Stable isotope signatures of moose in relation to seasonal forage composition: a hypothesis. *Alces* 37, 329–337.

- Kierdorf, U., Flohr, S., Gomez, S., Landete-Castillejos, T., Kierdorf, H., 2013. The structure of pedicle and hard antler bone in the European roe deer (*Capreolus capreolus*): a light microscope and backscattered electron imaging study. *J. Anat.* 223, 364–84. doi:10.1111/joa.12091
- Kloepfel, B.D., Treichel, I.W., Kharuk, S., Gower, S.T., 1998. Foliar carbon isotope discrimination in *Larix* species and sympatric evergreen conifers: a global comparison. *Oecologia* 114, 153–159. doi:10.1007/s004420050431
- Knowlton, F., 1960. Food habits, movements and populations of moose in the Gravelly Mountains, Montana. *J. Wildl. Manage.* 24, 162–170.
- Koch, P., 2007. Isotopic study of the biology of modern and fossil vertebrates, in: Michener, R., Lajtha, K. (Eds.), *Stable Isotopes in Ecology and Environmental Science*. Blackwell Publishing Ltd, Hong Kong, pp. 99–154.
- Koch, P., Fogel, M., Tuross, N., 1994. Tracing the diets of fossil animals using stable isotopes, in: Lajtha, K., Michener, R. (Eds.), *Stable Isotopes in Ecology and Environmental Science*. Blackwell Scientific Publications, pp. 63–92.
- Kohn, M.J., 2010. Carbon isotope compositions of terrestrial C₃ plants as indicators of (paleo)ecology and (paleo)climate. *Proc. Natl. Acad. Sci. U. S. A.* 107, 19691–5. doi:10.1073/pnas.1004933107
- Kristensen, D.K., Kristensen, E., Forchhammer, M.C., Michelsen, A., Schmidt, N.M., 2011. Arctic herbivore diet can be inferred from stable carbon and nitrogen isotopes in C₃ plants, faeces, and wool. *Can. J. Zool.* 89, 892–899. doi:10.1139/z11-073
- Kristensen, T., Heffner, T., 2011. Heritage resources impact assessment of the Yukon Hospital Corporation proposed Dawson City multi-level care facility conducted under Permit 10-02ASR. Whitehorse, YT.
- Kufeld, R., 1973. Foods eaten by the Rocky Mountain elk. *J. Range Manag.* 26, 106–113.
- Kuitemans, M., van der Plicht, J., Drucker, D.G., van Kolfschoten, T., Palstra, S.W.L., Bocherens, H., 2015. Carbon and nitrogen stable isotopes of well-preserved Middle Pleistocene bone collagen from Schöningen (Germany) and their palaeoecological implications. *J. Hum. Evol.* doi:10.1016/j.jhevol.2015.01.008
- LaZerte, B., Szalados, J., 1982. Stable carbon isotope ratio of submerged freshwater macrophytes. *Limnol. Oceanogr.* 27, 413–418.
- Leader-Williams, N., 1988. *Reindeer on South Georgia*. Cambridge University Press, Cambridge.
- LeResche, R., Davis, J., 1973. Importance of nonbrowse foods to moose on the Kenai Peninsula, Alaska. *J. Wildl. Manage.* 37, 279–287.

- Leslie, D.J., Starkey, E., Vavra, M., 1984. Elk and deer diets in old-growth forests in western Washington. *J. Wildl. Manage.* 48, 762–775.
- Long, E.S., Sweitzer, R.A., Diefenbach, D.R., Ben-David, M., 2005. Controlling for anthropogenically induced atmospheric variation in stable carbon isotope studies. *Oecologia* 146, 148–156. doi:10.1007/s00442-005-0181-6
- MacCracken, J., Ballenberghe, V. V., Peek, J.M., 1993. Use of aquatic plants by moose: sodium hunger or foraging efficiency? *Can. J. Zool.* 71, 2345–2351.
- MacCracken, J., Ballenberghe, V. Van, Peek, J., 1997. Habitat relationships of moose on the Copper River Delta in coastal south-central Alaska. *Wildl. Monogr.* 136, 3–52.
- Madgwick, R., Sykes, N., Miller, H., Symmons, R., Morris, J., Lamb, A., 2013. Fallow deer (*Dama dama dama*) management in Roman South-East Britain. *Archaeol. Anthropol. Sci.* 5, 111–122. doi:10.1007/s12520-013-0120-0
- Mann, D.H., Groves, P., Kunz, M.L., Reanier, R.E., Gaglioti, B. V., 2013. Ice-age megafauna in Arctic Alaska: extinction, invasion, survival. *Quat. Sci. Rev.* 70, 91–108. doi:10.1016/j.quascirev.2013.03.015
- Mariotti, A., 1983. Atmospheric nitrogen is a reliable standard for natural ¹⁵N abundance measurements. *Nature* 303, 685–687. doi:10.1038/303685a0
- McArthur, J.V., Moorhead, K.K., 1996. Characterization of riparian species and stream detritus using multiple stable isotopes. *Oecologia* 107, 232–238. doi:10.1007/BF00327907
- Meiri, M., 2010. The role of environmental change in species range shifts – analysis of Quaternary deer using ancient DNA. Doctoral Thesis. University of London.
- Meiri, M., Lister, A.M., Collins, M.J., Tuross, N., Goebel, T., Blockley, S., Zazula, G.D., van Doorn, N., Guthrie, R.D., Boeskorov, G.G., Baryshnikov, G.F., Sher, A., Barnes, I., 2014. Faunal record identifies Bering isthmus conditions as constraint to end-Pleistocene migration to the New World. *Proc. Biol. Sci.* 281, 20132167. doi:10.1098/rspb.2013.2167
- Metcalf, J.Z., Longstaffe, F.J., Hodgins, G., 2013. Proboscideans and paleoenvironments of the Pleistocene Great Lakes: landscape, vegetation, and stable isotopes. *Quat. Sci. Rev.* 76, 102–113. doi:10.1016/j.quascirev.2013.07.004
- Metcalf, J.Z., Longstaffe, F.J., Zazula, G.D., 2010. Nursing, weaning, and tooth development in woolly mammoths from Old Crow, Yukon, Canada: implications for Pleistocene extinctions. *Palaeogeogr. Palaeoclimatol. Palaeoecol.* 298, 257–270. doi:10.1016/j.palaeo.2010.09.032
- Miller, H., Carden, R.F., Evans, J., Lamb, A., Madgwick, R., Osborne, D., Symmons, R., Sykes, N., 2014. Dead or alive? Investigating long-distance transport of live fallow

- deer and their body parts in antiquity. *Environ. Archaeol.*
doi:<http://dx.doi.org/10.1179/1749631414Y.0000000043>
- Milligan, H.E., Pretzlaw, T.D., Humphries, M.M., 2010. Stable isotope differentiation of freshwater and terrestrial vascular plants in two subarctic regions. *Ecoscience* 17, 265–275. doi:10.2980/17-3-3282
- Morgantini, L., Hudson, R., 1989. Nutritional significance of wapiti (*Cervus elaphus*) migrations to alpine ranges in western Alberta, Canada. *Arct. Alp. Res.* 21, 288–295.
- Nadelhoffer, K., Shaver, G., Fry, B., Giblin, A., 1996. ^{15}N natural abundances and N use by tundra plants. *Oecologia* 107, 386–394.
- Osborne, D.A., 2013. Fallow deer in Iron Age and Roman Britain: a study of fallow deer antlers using stable isotopes. Master's Thesis. The University of Nottingham.
- Osmond, C., Valaane, N., Haslam, S., Uotila, P., Roksandic, Z., 1981. Comparisons of $\delta^{13}\text{C}$ values in leaves of aquatic macrophytes from different habitats in Britain and Finland; some implications for photosynthetic processes in aquatic plants. *Oecologia* 50, 117–124.
- Peek, J., 2007. Habitat relationships, in: Franzmann, A.W., Schwartz, C.C. (Eds.), *Ecology and Management of the North American Moose*. The University Press of Colorado, Boulder, p. 351.
- Peterson, B., Fry, B., 1987. Stable isotopes in ecosystem studies. *Annu. Rev. Ecol. Syst.* 18, 193–320.
- Polischuk, S., Hobson, K., Ramsay, M., 2011. Use of stable-carbon and -nitrogen isotopes to assess weaning and fasting in female polar bears and their cubs. *Can. J. Zool.* 79, 499–511.
- Prokešová, J., 2004. Red deer in the floodplain forest: the browse specialist. *Folia Zool.* 53, 293–302.
- Qi, H., Coplen, T.B., Geilmann, H., Brand, W., Böhlke, J.K., 2003. Two new organic reference materials for $\delta^{13}\text{C}$ and $\delta^{15}\text{N}$ measurements and a new value for the $\delta^{13}\text{C}$ of NBS 22 oil. *Rapid Commun. Mass Spectrom.* 17, 2483–2487. doi:10.1002/rcm.1219
- R Core Team, 2014. *R: A language and environment for statistical computing*. R Foundation for Statistical Computing, Vienna, Austria.
- Rau, G., 1980. Carbon-13/carbon-12 variation in subalpine lake aquatic insects: food source implications. *Can. J. Fish. Aquat. Sci.* 37, 742–746.
- Sealy, J., van der Merwe, N., Thorp, J.A.L., Lanham, J.L., 1987. Nitrogen isotopic ecology in southern Africa: implications for environmental and dietary tracing.

- Geochim. Cosmochim. Acta 51, 2707–2717.
- Shank, C., Wilkinson, P., Penner, D., 1978. Diet of Peary caribou, Banks Island, NWT. Arctic 31, 125–132.
- Sharma, S., Couturier, S., Côté, S.D., 2009. Impacts of climate change on the seasonal distribution of migratory caribou. Glob. Chang. Biol. 15, 2549–2562. doi:10.1111/j.1365-2486.2009.01945.x
- Sponheimer, M., Robinson, T., Ayliffe, L., Roeder, B., Hammer, J., Passey, B., West, A., Cerling, T., Dearing, D., Ehleringer, J., 2003. Nitrogen isotopes in mammalian herbivores: hair $\delta^{15}\text{N}$ values from a controlled feeding study. Int. J. Osteoarchaeol. 13, 80–87. doi:10.1002/oa.655
- Stevens, D., 1966. Range relationships of elk and livestock, Crow Creek Drainage, Montana. J. Wildl. Manage. 30, 349–363.
- Stevens, D., 1970. Winter ecology of moose in the Gallatin Mountains, Montana. J. Wildl. Manage. 34, 37–46.
- Stevens, R.E., Germonpré, M., Petrie, C.A., O’Connell, T.C., 2009. Palaeoenvironmental and chronological investigations of the Magdalenian sites of Goyet Cave and Trou de Chaleux (Belgium), via stable isotope and radiocarbon analyses of horse skeletal remains. J. Archaeol. Sci. 36, 653–662. doi:10.1016/j.jas.2008.10.008
- Stevens, R.E., Hedges, R.E., 2004. Carbon and nitrogen stable isotope analysis of northwest European horse bone and tooth collagen, 40,000 BP – present: palaeoclimatic interpretations. Quat. Sci. Rev. 23, 977–991. doi:10.1016/j.quascirev.2003.06.024
- Stevens, R.E., Jacobi, R., Higham, T., 2010. Reassessing the diet of Upper Palaeolithic humans from Gough’s Cave and Sun Hole, Cheddar Gorge, Somerset, UK. J. Archaeol. Sci. 37, 52–61.
- Stevens, R.E., Jacobi, R., Street, M., Germonpré, M., Conard, N.J., Münzel, S.C., Hedges, R.E.M., 2008. Nitrogen isotope analyses of reindeer (*Rangifer tarandus*), 45,000 BP to 9,000 BP: palaeoenvironmental reconstructions. Palaeogeogr. Palaeoclimatol. Palaeoecol. 262, 32–45. doi:10.1016/j.palaeo.2008.01.019
- Stewart, K., Bowyer, R., Kie, J., Dick, B., Ben-David, M., 2003. Niche partitioning among mule deer, elk, and cattle: Do stable isotopes reflect dietary niche? Ecoscience 10, 297–302.
- Sykes, N.J., Baker, K.H., Carden, R.F., Higham, T.F.G., Hoelzel, A.R., Stevens, R.E., 2011. New evidence for the establishment and management of the European fallow deer (*Dama dama dama*) in Roman Britain. J. Archaeol. Sci. 38, 156–165. doi:10.1016/j.jas.2010.08.024

- Szpak, P., Gröcke, D.R., Debruyne, R., MacPhee, R.D.E., Guthrie, R.D., Froese, D., Zazula, G.D., Patterson, W.P., Poinar, H.N., 2010. Regional differences in bone collagen $\delta^{13}\text{C}$ and $\delta^{15}\text{N}$ of Pleistocene mammoths: implications for paleoecology of the mammoth steppe. *Palaeogeogr. Palaeoclimatol. Palaeoecol.* 286, 88–96. doi:10.1016/j.palaeo.2009.12.009
- Thomas, D., Edmonds, E., Brown, W., 1996. The diet of woodland caribou populations in west-central Alberta. *Rangifer* 16, 337–342.
- Thompson, D., McCourt, K., 1981. Seasonal diets of the Porcupine caribou herd. *Am. Midl. Nat.* 105, 70–76.
- Tieszen, L., 1991. Natural variations in the carbon isotope values of plants: implications for archaeology, ecology, and paleoecology. *J. Archaeol. Sci.* 18, 227–248.
- Tischler, K., 2004. Aquatic plant nutritional quality and contribution to moose diet at Isle Royale National Park. Master's Thesis. Michigan Technological University.
- van Klinken, G., 1999. Bone collagen quality indicators for palaeodietary and radiocarbon measurements. *J. Archaeol. Sci.* 26, 687–695.
- Wam, H.K., Hjeljord, O., 2010. Moose summer and winter diets along a large scale gradient of forage availability in southern Norway. *Eur. J. Wildl. Res.* 56, 745–755. doi:10.1007/s10344-010-0370-4
- Waters-Rist, A., Katzenberg, M., 2010. The effect of growth on stable nitrogen isotope ratios in subadult bone collagen. *Int. J. Osteoarchaeol.* 20, 172–191.
- Wislocki, G., 1942. Studies on the growth of deer antlers. I. On the structure and histogenesis of the antlers of the Virginia deer (*Odocoileus virginianus borealis*). *Am. J. Anat.* 71, 371–415.
- Wooller, M., Zazula, G., Edwards, M., Froese, D.G., Boone, R.D., Parker, C., Bennett, B., 2007. Stable carbon isotope compositions of Eastern Beringian grasses and sedges: investigating their potential as paleoenvironmental indicators. *Arctic, Antarct. Alp. Res.* 39, 318–331.
- Zazula, G.D., Personal communication (e-mail), 2015
- Zazula, G.D., MacPhee, R.D.E., Metcalfe, J.Z., Reyes, A. V, Brock, F., Druckenmiller, P.S., Groves, P., Harington, C.R., Hodgins, G.W.L., Kunz, M.L., Longstaffe, F.J., Mann, D.H., McDonald, H.G., Nalawade-Chavan, S., Southon, J.R., 2014. American mastodon extirpation in the Arctic and Subarctic predates human colonization and terminal Pleistocene climate change. *Proc. Natl. Acad. Sci. U. S. A.* 111, 18460–18465. doi:10.1073/pnas.1416072111

Chapter 3

3 Solving the woolly mammoth conundrum: amino acid ^{15}N -enrichment suggests a distinct forage or habitat¹

3.1 Introduction

Woolly mammoths (*Mammuthus primigenius*) were keystone herbivores in the Pleistocene mammoth steppe (Owen-Smith, 1987; Zimov et al., 1995). This megacontinental biome was inhabited by a now-extinct community of mammals, dominated by woolly mammoth, horse and bison. The mammoth steppe reached from north-western Canada, across the exposed Bering Isthmus, to Western Europe (Bocherens, 2003; Guthrie, 1982). The ecological role of woolly mammoths within this ecosystem has been a subject of vigorous investigation (Bocherens, 2003; Haynes, 1991; Putshkov, 2003). Reconstructions of woolly mammoth behaviour and physiology have been largely based on morphology (Haynes, 1991). Isotopic studies of bulk tissues have provided independent tests of morphology-based hypotheses, as well as suggesting new ones (Bocherens, 2003; Bocherens et al., 1994; Iacumin et al., 2010, 2000; Szpak et al., 2010). Compound-specific isotopic studies can provide a further level of understanding of ecosystem functioning within the mammoth steppe.

Bulk collagen nitrogen isotopic compositions ($\delta^{15}\text{N}_{\text{Bulk}}$) are commonly used in ecological studies to reveal the diet and trophic level of a species, as these values typically reflect the isotopic compositions of the plants at the base of the food web plus a 2-5 ‰ increase with each trophic level (Koch et al., 1994). As a result, the $\delta^{15}\text{N}_{\text{Bulk}}$ of mammoth-steppe herbivore collagen are commonly $\sim+6$ ‰ where the values of carnivores ($\sim+9$ ‰) are

¹ A version of this chapter has been published: Schwartz-Narbonne, R., Longstaffe, F.J., Metcalfe, J.Z., Zazula, G., 2015. Solving the woolly mammoth conundrum: amino acid ^{15}N -enrichment suggests a distinct forage or habitat. *Sci. Rep.* 5, 9791. doi:10.1038/srep09791

higher, reflective of this trophic enrichment (Bocherens, 2003). The carnivore- rather than herbivore-like $\delta^{15}\text{N}_{\text{Bulk}}$ of woolly mammoth collagen ($\sim+8\text{‰}$; Bocherens, 2003), known as the “woolly mammoth conundrum” are seemingly problematic and therefore require examination. The various hypotheses to explain this phenomenon (unique diet, niche feeding in a special habitat or distinct metabolic processes; Bocherens, 2003; Bocherens et al., 1996, 1994; Fox-Dobbs et al., 2008; Iacumin et al., 2010, 2000; Koch, 1991; Metcalfe et al., 2013; Szpak et al., 2010; Tahmasebi, 2015) have different implications for our understanding of the now-vanished mammoth steppe ecosystem, woolly mammoth ecology, and related factors that contributed to extirpation of the woolly mammoth in this region.

Woolly mammoths may have consumed plants with higher $\delta^{15}\text{N}$, such as graminoids and herbs rather than woody vegetation (Koch, 1991; Metcalfe et al., 2013; Szpak et al., 2010), as suggested by the morphology of their enamel plates (Haynes, 1991). However, an herbaceous diet alone is not sufficient to fully explain the woolly mammoth’s high $\delta^{15}\text{N}$; some further form of habitat or plant selection is also required (Matheus et al., 2003). While modern Arctic graminoids and forbs from some sites have a $\delta^{15}\text{N}$ range of -0.3 to $+10\text{‰}$, the average value of these species ranges from $\sim+1$ to $\sim+4\text{‰}$ (Barnett, 1994), and still other studies have reported maximum $\delta^{15}\text{N}$ for sedges of $+2\text{‰}$ (Nadelhoffer et al., 1996) and for herbs of $+5.3\text{‰}$ (Ben-David et al., 2001). The majority of these plants, therefore, are not sufficiently enriched in ^{15}N to explain the woolly mammoth $\delta^{15}\text{N}_{\text{Bulk}}$. Plants growing in drier habitats, however, have higher $\delta^{15}\text{N}$ than plants from a more mesic environment (Szpak et al., 2010), and woolly mammoths may have eaten plants experiencing water-stress (Bocherens, 2003; Iacumin et al., 2000). Water stress can also cause ^{13}C -enrichment of plants (Wooller et al., 2007). This enrichment, however, is unlikely to be directly observable in woolly mammoth collagen, because its carbon isotopic composition is likely dominated by the low $\delta^{13}\text{C}$ of fat reserves used to survive the winter (Szpak et al., 2010).

Several other factors could also have contributed to high $\delta^{15}\text{N}$ for woolly mammoth collagen. Woolly mammoths that had small ranges, or repeatedly travelled the same routes, could have deposited significant quantities of faeces in those areas (Metcalfe et

al., 2013), thus causing ^{15}N -enrichment in plants arising from this dung fertilization (Szpak et al., 2012). Partially decayed plant material can also have higher $\delta^{15}\text{N}$ than the original living plant (Tremblay and Benner, 2006). Woolly mammoths may have removed snow and ice cover by trampling and (or) with their tusks (Putshkov, 2003), allowing them to forage on winter-killed plants generally not utilized by other large herbivores that did not share the mammoth ecological niche (Tahmasebi, 2015). It has also been proposed that woolly mammoths had distinct metabolic processes, such as increased levels of nitrogen recycling associated with winter starvation (Hobson et al., 1993; Polischuk et al., 2011) or poor quality food with low protein levels (Bocherens, 2003; Bocherens et al., 1996, 1994; Fox-Dobbs et al., 2008; Iacumin et al., 2010, 2000; Koch, 1991; Szpak et al., 2010), or that woolly mammoths engaged in coprophagy (Metcalf et al., 2013).

The nitrogen isotopic compositions of the individual amino acids in collagen, as opposed to bulk collagen, enable discrimination between ^{15}N -enrichment occurring at the base of the food chain prior to consumption (source amino acids) versus that associated with mammoth metabolic processes (trophic amino acids) (Fig. 3.1). Phenylalanine (Phe) and glutamate (Glu) have been identified as characteristic of source and trophic amino acids, respectively (McClelland and Montoya, 2002; Styring et al., 2010). The $\delta^{15}\text{N}_{\text{Phe}}$ reflects the isotopic composition of those amino acids in plants at the base of the food web, while the $\Delta^{15}\text{N}_{\text{Glu-Phe}}$ spacing ($\delta^{15}\text{N}_{\text{Glu}} - \delta^{15}\text{N}_{\text{Phe}}$) serves as a proxy for metabolic enrichment of ^{15}N in the consumer's body (Styring et al., 2010).

3.2 Methods

3.2.1 Bulk collagen nitrogen isotope analysis

Collagen for $\delta^{15}\text{N}_{\text{Bulk}}$ analysis was extracted at the Laboratory for Stable Isotope Science (LSIS) following previously published methods (Metcalf et al., 2010), or was previously extracted and analyzed for another study (see Appendix F; Metcalfe, 2011; Metcalfe et al., 2010). The $\delta^{15}\text{N}_{\text{Bulk}}$ was obtained using a Costech Elemental Combustion System (ECS 4010) attached to a Thermo-Scientific Delta Plus XL IRMS or to a

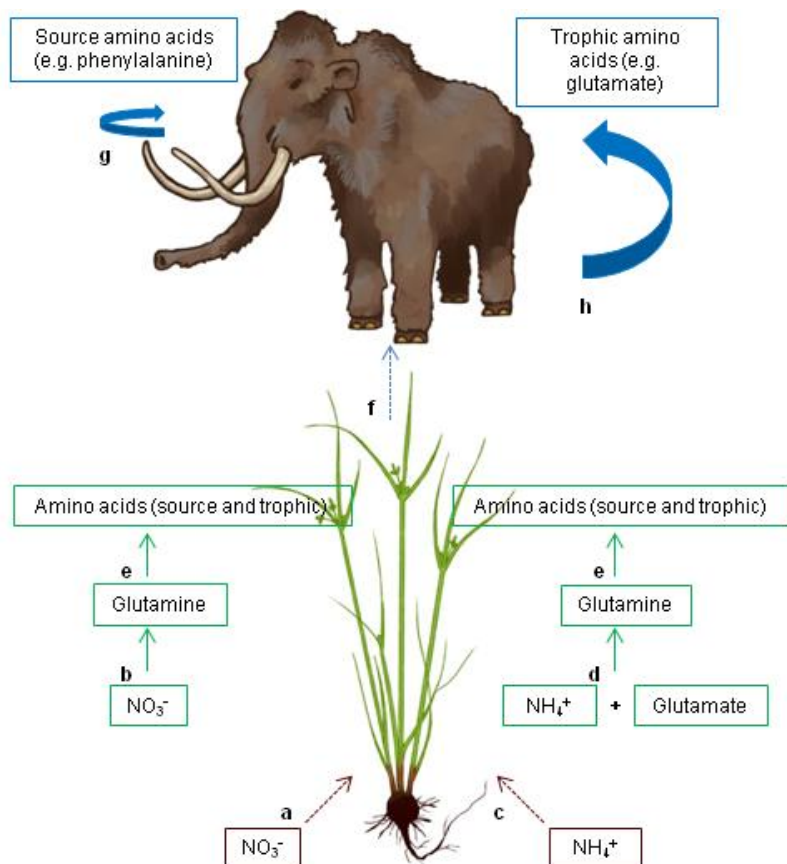


Figure 3.1 Simplified pathway for nitrogen incorporation from soil to animal protein. Arrows represent: uptake (dashed line), chemical transformations (solid line), and metabolic processes (solid curves). a. Plant NO₃⁻ uptake; b. NO₃⁻ converted to glutamine (Styring et al., 2014); c. NH₄⁺ uptake; d. NH₄⁺ converted to glutamine by attachment to glutamate (Styring et al., 2014); e. Glutamine supplies nitrogen for synthesis of other amino acids. The associated shift in $\delta^{15}\text{N}$ depends on the specific amino acid, plant part and plant type (Styring et al., 2014); f. Consumption of amino acids by the animal; g. Source amino acids are minimally involved in metabolic processes, undergoing small changes in $\delta^{15}\text{N}$ (e.g. increases in $\delta^{15}\text{N}_{\text{Phe}}$ from diet to consumer tissue are commonly $\leq 2\%$; (McClelland and Montoya, 2002); h. Trophic amino acids are heavily involved in metabolic processes, undergoing enrichment in ^{15}N (e.g. increases in $\delta^{15}\text{N}_{\text{Glu}}$ from diet to consumer tissue are commonly 6-7%; McClelland and Montoya, 2002). Katherine Allan drew the images of grass and mammoth.

Thermo-Scientific Delta V Plus IRMS. The $\delta^{15}\text{N}_{\text{Bulk}}$ was measured over three analytical sessions. In the first two analytical sessions, $\delta^{15}\text{N}$ was calibrated to AIR using USGS40 (L-glumatic acid; accepted value -4.52‰ ; Qi et al., 2003) and IAEA-N2 (ammonium sulfate; accepted value $+20.3\text{‰}$; Brand et al., 2014), while the third analytical sessions substituted USGS41 (L-glumatic acid; accepted value $+47.57\text{‰}$; Qi et al., 2003) for IAEA-N2. The same standards were used to create calibration curves for determining carbon and nitrogen contents (wt%) of each sample, from which C/N ratios were calculated. Keratin (MP Biomedicals Inc., Cat No. 90211, Lot No. 9966H) was used as an internal standard in each analytical session. For a total of 18 keratin measurements over the three analytical sessions, average values (mean \pm 1 SD) were $\delta^{15}\text{N} = +6.4 \pm 0.2\text{‰}$ (accepted value = $+6.4\text{‰}$), and $\text{C/N} = 3.6 \pm 0.4$ (accepted value = 3.7). The standard deviation of a sample analyzed as an instrumental duplicate was $\delta^{15}\text{N}_{\text{Bulk}} = \pm 0.0\text{‰}$, and $\text{C/N} = \pm 0.1$ (1 SD). The standard deviations (1 SD) for method duplicates of $\delta^{15}\text{N}_{\text{Bulk}}$ ranged from 0.0 to 0.2 ‰, and for C/N ratios, from 0.0 to 0.3. All samples were considered to be well preserved based on their extraction yields, C/N ratios, and carbon and nitrogen contents (Ambrose, 1990; van Klinken, 1999). Eight samples had high carbon and/or nitrogen contents, but this anomaly likely arises from a weighing error as they were well preserved by other measures.

3.2.2 Amino acid nitrogen isotope analysis

Using collagen first extracted for $\delta^{15}\text{N}_{\text{Bulk}}$ measurements, amino acids were hydrolysed, derivatized to their N-acetyl-methyl ester derivative, and their individual $\delta^{15}\text{N}_{\text{Amino Acid}}$ measured using an Aligent 6890N-Thermo-Scientific Gas Chromatograph-Combustion 3-Thermo-Scientific Delta Plus XL IRMS. An Agilent Technologies VF-23MS column was used in the GC. We followed published methods (Corr et al., 2007; Styring et al., 2010) with only slight modifications: (i) the quantity of collagen hydrolysed was increased from 2 to 6 mg, and the quantity derivatized was increased from 0.25 to 1.5 mg; and (ii) the initial GC column temperature was set at 60 °C instead of 40 °C, and its final temperature of 250 °C was held for 15 min instead of 20 min. A representative chromatogram is shown in Appendix G. Three reference gas pulses were introduced into the IRMS at the beginning of each analytical session and one pulse was introduced at the end of each

session. The isotopic composition of the reference gas was calibrated using four amino acid standards. Three of these standards, alanine, leucine and phenylalanine, were purchased as their NACME derivative from Sigma Aldrich. The fourth, proline, was purchased as an amino acid and derivatized in-house. The nitrogen isotopic compositions of the derivatized standards were established by multiple measurements performed in the same manner as used for isotopic analysis of bulk collagen, and calibration to AIR using international standards. The amino acid reference standards were injected every three to five runs. All samples were analyzed a minimum of three times, and the average variation was ± 0.7 ‰ (1 SD) for phenylalanine, and ± 0.7 ‰ (1 SD) for glutamate, with a range of 0.0-3.9 ‰. An internal standard, norleucine, was also analyzed. Its nitrogen isotopic compositions were offset from expected values by an average of +1.3 ‰.

3.2.3 Radiocarbon dating

Radiocarbon dates for six woolly mammoths discussed here have been published previously (Metcalf, 2011; Metcalf et al., 2010). A further subset of samples was dated for this study; these included two other herbivores and two carnivores (see Appendix E). Collagen was extracted, combusted, graphitized and radiocarbon dated at the University of Arizona Accelerator Mass Spectrometry (AMS) Laboratory. All dates are presented as uncalibrated radiocarbon years before present (mean \pm 1SD).

3.3 Results

Eight Pleistocene megafauna species were analyzed in this study. These included four herbivore species: woolly mammoth (*Mammuthus primigenius*), mastodon (*Mammut americanum*), horse (*Equus* sp.) and giant beaver (*Castoroides ohioensis*), and four carnivore species: brown bear (*Ursus arctos*), scimitar cat (*Homotherium serum*), wolf (*Canis lupus*), and short-faced bear (*Arctodus simus*) (see Appendix E). All samples were obtained from specimens collected near Old Crow, Yukon, Canada (latitude: 67.6; longitude: -139.8). A subset of these specimens was dated, including both herbivores and carnivores. Two horse specimens were dated to 18,370 and 27,180 ^{14}C years BP. The rest of the specimens yielded effectively non-finite radiocarbon dates $\geq 37,200$ ^{14}C yr BP, and one specimen was dated by context to $\sim 140,000$ years BP (see Appendix E; Metcalf,

2011; Metcalfe et al., 2010). All collagen samples were considered well preserved based on their collagen yields, C/N ratios, and carbon and nitrogen contents (see Appendix F; van Klinken, 1999).

The $\delta^{15}\text{N}_{\text{Bulk}}$ for the Old Crow samples follows the pattern previously observed for Pleistocene megafauna (Bocherens, 2003; Fox-Dobbs et al., 2008; Iacumin et al., 2000); woolly mammoth collagen generally has $\delta^{15}\text{N}_{\text{Bulk}}$ similar to the carnivores and higher than the other herbivores, with some overlap with horses (Fig. 3.2a). The $\delta^{15}\text{N}_{\text{Phe}}$ of woolly mammoth collagen, however, is higher than those of the carnivores and most of the other herbivores (Fig. 3.2b); horses with high $\delta^{15}\text{N}_{\text{Bulk}}$ for collagen show the most overlap with the $\delta^{15}\text{N}_{\text{Phe}}$ of woolly mammoths. Woolly mammoth $\Delta^{15}\text{N}_{\text{Glu-Phe}}$ spacings overlap those of the other herbivores but are lower than the $\Delta^{15}\text{N}_{\text{Glu-Phe}}$ spacings of the carnivores, extending to negative values for most samples (Fig. 3.2c). Negative $\Delta^{15}\text{N}_{\text{Glu-Phe}}$ spacings have been observed in terrestrial herbivores previously (Chikaraishi et al., 2011; Styring et al., 2010) and may be the result of relatively high $\delta^{15}\text{N}_{\text{Phe}}$ in vascular plants (Styring et al., 2014).

3.4 Discussion and conclusion

The high $\delta^{15}\text{N}_{\text{Phe}}$ of the woolly mammoth implies that they selectively consumed plants more enriched in ^{15}N than forage consumed by most of the other herbivores. The fact that the $\delta^{15}\text{N}_{\text{Phe}}$ of woolly mammoths is higher than those of carnivores suggests that the latter consumed herbivores subsisting on less ^{15}N -rich forage than consumed by woolly mammoths. In short, the carnivores did not consume significant quantities of woolly mammoth. Partial overlap between horse and woolly mammoth $\delta^{15}\text{N}_{\text{Bulk}}$ and $\delta^{15}\text{N}_{\text{Phe}}$ likely indicates that horses exploited a similar niche to the woolly mammoth in some cases. The low $\Delta^{15}\text{N}_{\text{Glu-Phe}}$ spacings of woolly mammoths indicate that their $\delta^{15}\text{N}_{\text{Bulk}}$ arises from the higher $\delta^{15}\text{N}$ of the plants they consumed, and not from a specialized metabolic process.

It seems that woolly mammoths occupied a specialized dietary or habitat niche. A dietary niche implies that woolly mammoths selected particular herbaceous plants or consumed

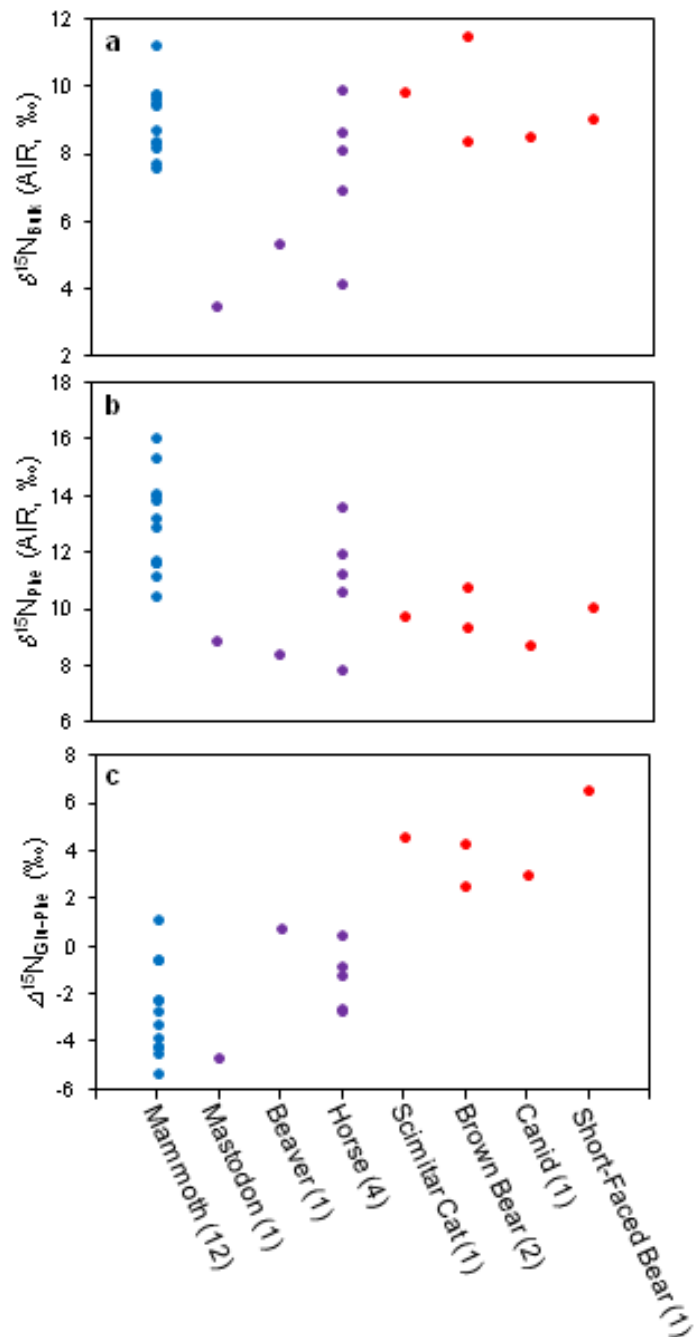


Figure 3.2 Nitrogen isotopic compositions of Pleistocene Old Crow megafauna: a. Bulk collagen nitrogen isotopic compositions ($\delta^{15}\text{N}_{\text{Bulk}}$). Results for woolly mammoths are displayed in blue, other herbivores in purple, and carnivores in red; b. Phenylalanine (source) amino acid nitrogen isotopic compositions ($\delta^{15}\text{N}_{\text{Phe}}$) of each species; c. Difference between the nitrogen isotopic composition of glutamate and phenylalanine ($\Delta^{15}\text{N}_{\text{Glu-Phe}}$) for each species.

large quantities of decayed plants in winter, while a habitat niche suggests that woolly mammoths occupied more arid habitats, or lived in distinct ranges where they left considerable quantities of dung that fertilized the plants growing there. While some Old Crow horses appear also to have exploited such a niche, it was not generally shared by other mammoth steppe megafauna. The Old Crow samples likely represent various time intervals through the late Pleistocene and potentially varied climate regimes. The fact that the relative differences in average $\delta^{15}\text{N}_{\text{Bulk}}$ among herbivore species are generally consistent across the mammoth steppe (Bocherens, 2003) suggests that most herbivore species ate the same forage types regardless of climatic differences or time period. This implies that mammoth steppe herbivores targeted specific forage types.

Two significant conclusions arise from these observations. First, the woolly mammoth occupied a distinct niche from other contemporaneous herbivores. This unique habitat or forage existed across the entirety of the mammoth steppe, although its size may have varied with changing climate across geographic or temporal zones. Other evidence of the woolly mammoth's dependence on a specialized niche may be provided by the retraction of woolly mammoth populations into small, isolated refugia during the last interglacial warm period (MIS 5e, 130-116 kyr BP), and the subsequent re-expansion upon return to glacial conditions (Palkopoulou et al., 2013). An investigation of the isotopic compositions of woolly mammoths from a variety of time periods and sites across the mammoth steppe could reveal the extent of adaptability of the woolly mammoth to disruptions in its niche, such as may have occurred with the onset of climatic shifts at the end of the Pleistocene (Willerslev et al., 2014).

Second, the horse $\delta^{15}\text{N}_{\text{Bulk}}$ and $\delta^{15}\text{N}_{\text{Phe}}$ overlap those of the woolly mammoth and the other herbivores. This implies that horses fed from a wide diversity of habitats or forage types, including the woolly mammoths' niche. Such behaviour would suggest that the mammoth steppe ecosystem supported herbivores with a variety of ecological adaptations, and that even in the Pleistocene Arctic, resources were sufficiently abundant to support both specialist and generalist strategies.

3.5 References

- Ambrose, S., 1990. Preparation and characterization of bone and tooth collagen for isotopic analysis. *J. Archaeol. Sci.* 17, 431–451.
- Barnett, B., 1994. Carbon and nitrogen isotope ratios of caribou tissues, vascular plants, and lichens from northern Alaska. University of Alaska, Fairbanks.
- Ben-David, M., Shochat, E., Adams, L., 2001. Utility of stable isotope analysis in studying foraging ecology of herbivores: examples from moose and caribou. *Alces* 37, 421–434.
- Bocherens, H., 2003. Isotopic biogeochemistry and the paleoecology of the mammoth steppe fauna. *Deinsea* 9, 57–76.
- Bocherens, H., Fizet, M., Mariotti, A., 1994. Diet, physiology and ecology of fossil mammals as inferred from stable carbon and nitrogen isotope biogeochemistry: implications for Pleistocene bears. *Palaeogeogr. Palaeoclimatol. Palaeoecol.* 107, 213–225. doi:10.1016/0031-0182(94)90095-7
- Bocherens, H., Fizet, M., Mariotti, A., Gangloff, R., Burns, J., 1994. Contribution of isotopic biogeochemistry (^{13}C , ^{15}N , ^{18}O) to the paleoecology of mammoths (*Mammuthus primigenius*). *Hist. Biol.* 7, 187–202.
- Bocherens, H., Pacaud, G., Lazarev, P.A., Mariotti, A., 1996. Stable isotope abundances (^{13}C , ^{15}N) in collagen and soft tissues from Pleistocene mammals from Yakutia: implications for the palaeobiology of the Mammoth Steppe. *Palaeogeogr. Palaeoclimatol. Palaeoecol.* 126, 31–44.
- Brand, W., Coplen, T., Vogl, J., Rosner, M., Prohaska, T., 2014. Assessment of international reference materials for isotope-ratio analysis (IUPAC Technical Report). *Pure Appl. Chem.* 86, 425–467. doi:10.1515/pac-2013-1023
- Chikaraishi, Y., Ogawa, N.O., Doi, H., Ohkouchi, N., 2011. $^{15}\text{N}/^{14}\text{N}$ ratios of amino acids as a tool for studying terrestrial food webs: a case study of terrestrial insects (bees, wasps, and hornets). *Ecol. Res.* 26, 835–844. doi:10.1007/s11284-011-0844-1
- Corr, L., Berstan, R., Evershed, R., 2007. Development of N-acetyl methyl ester derivatives for the determination of $\delta^{13}\text{C}$ values of amino acids using gas chromatography-combustion-isotope ratio mass spectrometry. *Anal. Chem.* 79, 9082–90. doi:10.1021/ac071223b
- Fox-Dobbs, K., Leonard, J., Koch, P., 2008. Pleistocene megafauna from eastern Beringia: paleoecological and paleoenvironmental interpretations of stable carbon and nitrogen isotope and radiocarbon records. *Palaeogeogr. Palaeoclimatol. Palaeoecol.* 261, 30–46.
- Guthrie, R.D., 1982. Mammals of the mammoth steppe as paleoenvironmental indicators,

- in: Hopkins, D.M., Matthews, Jr., J.V., Schweger, C.E., Young, S.B. (Eds.), *Paleoecology of Beringia*. Academic Press, New York, pp. 307–326.
- Haynes, G., 1991. *Mammoths, mastodons, and elephants*. Cambridge University Press, Cambridge.
- Hobson, K.A., Alisauskas, R.T., Clark, R.G., 1993. Stable-nitrogen isotope enrichment in avian tissues due to fasting and nutritional stress: implications for isotopic analyses of diet. *Condor* 95, 388–394.
- Iacumin, P., Matteo, A. Di, Nikolaev, V., Kuznetsova, T., 2010. Climate information from C, N and O stable isotope analyses of mammoth bones from northern Siberia. *Quat. Int.* 212, 206–212.
- Iacumin, P., Nikolaev, V., Ramigni, M., 2000. C and N stable isotope measurements on Eurasian fossil mammals, 40 000 to 10 000 years BP: herbivore physiologies and palaeoenvironmental reconstruction. *Palaeogeogr. Palaeoclimatol. Palaeoecol.* 163, 33–47.
- Koch, P., 1991. The isotopic ecology of Pleistocene proboscideans. *J. Vertebr. Paleontol.* 11, 40A.
- Koch, P., Fogel, M., Tuross, N., 1994. Tracing the diets of fossil animals using stable isotopes, in: Lajtha, K., Michener, R. (Eds.), *Stable Isotopes in Ecology and Environmental Science*. Blackwell Scientific Publications, pp. 63–92.
- Matheus, P., Guthrie, R., Kunz, M., 2003. Isotope ecology of late Quaternary megafauna in eastern Beringia, in: *3rd International Mammoth Conference*. Dawson City, pp. 80–83.
- McClelland, J., Montoya, J., 2002. Trophic relationships and the nitrogen isotopic composition of amino acids in plankton. *Ecology* 83, 2173–2180.
- Metcalf, J.Z., 2011. *Late Pleistocene climate and proboscidean paleoecology in North America: insights from stable isotope compositions of skeletal remains*. University of Western Ontario.
- Metcalf, J.Z., Longstaffe, F.J., Hodgins, G., 2013. Proboscideans and paleoenvironments of the Pleistocene Great Lakes: landscape, vegetation, and stable isotopes. *Quat. Sci. Rev.* 76, 102–113. doi:10.1016/j.quascirev.2013.07.004
- Metcalf, J.Z., Longstaffe, F.J., Zazula, G.D., 2010. Nursing, weaning, and tooth development in woolly mammoths from Old Crow, Yukon, Canada: implications for Pleistocene extinctions. *Palaeogeogr. Palaeoclimatol. Palaeoecol.* 298, 257–270. doi:10.1016/j.palaeo.2010.09.032
- Nadelhoffer, K., Shaver, G., Fry, B., Giblin, A., 1996. ^{15}N natural abundances and N use by tundra plants. *Oecologia* 107, 386–394.

- Owen-Smith, N., 1987. Pleistocene extinctions: the pivotal role of megaherbivores. *Paleobiology* 13, 351–362.
- Palkopoulou, E., Dalén, L., Lister, A.M., Vartanyan, S., Sablin, M., Sher, A., Edmark, V.N., Brandström, M.D., Germonpré, M., Barnes, I., Thomas, J.A., 2013. Holarctic genetic structure and range dynamics in the woolly mammoth. *Proc. Biol. Sci.* 280, 20131910. doi:10.1098/rspb.2013.1910
- Polischuk, S., Hobson, K., Ramsay, M., 2011. Use of stable-carbon and -nitrogen isotopes to assess weaning and fasting in female polar bears and their cubs. *Can. J. Zool.* 79, 499–511.
- Putshkov, P., 2003. The impact of mammoths in their biome: clash of two paradigms. *Deinsea* 9, 365–379.
- Qi, H., Coplen, T.B., Geilmann, H., Brand, W., Böhlke, J.K., 2003. Two new organic reference materials for $\delta^{13}\text{C}$ and $\delta^{15}\text{N}$ measurements and a new value for the $\delta^{13}\text{C}$ of NBS 22 oil. *Rapid Commun. Mass Spectrom.* 17, 2483–2487. doi:10.1002/rcm.1219
- Styring, A.K., Fraser, R.A., Bogaard, A., Evershed, R.P., 2014. Cereal grain, rachis and pulse seed amino acid $\delta^{15}\text{N}$ values as indicators of plant nitrogen metabolism. *Phytochemistry* 97, 20–9. doi:10.1016/j.phytochem.2013.05.009
- Styring, A.K., Sealy, J.C., Evershed, R.P., 2010. Resolving the bulk $\delta^{15}\text{N}$ values of ancient human and animal bone collagen via compound-specific nitrogen isotope analysis of constituent amino acids. *Geochim. Cosmochim. Acta* 74, 241–251. doi:10.1016/j.gca.2009.09.022
- Szpak, P., Gröcke, D.R., Debruyne, R., MacPhee, R.D.E., Guthrie, R.D., Froese, D., Zazula, G.D., Patterson, W.P., Poinar, H.N., 2010. Regional differences in bone collagen $\delta^{13}\text{C}$ and $\delta^{15}\text{N}$ of Pleistocene mammoths: implications for paleoecology of the mammoth steppe. *Palaeogeogr. Palaeoclimatol. Palaeoecol.* 286, 88–96. doi:10.1016/j.palaeo.2009.12.009
- Szpak, P., Millaire, J., White, C., Longstaffe, F., 2012. Influence of seabird guano and camelid dung fertilization on the nitrogen isotopic composition of field-grown maize (*Zea mays*). *J. Archaeol. Sci.* 39, 3721–3740.
- Tahmasebi, F., 2015. Carbon and nitrogen isotopic investigations of the late Pleistocene paleoecology of eastern Beringia, Yukon Territory, using soils, plants and rodent bones. University of Western Ontario.
- Tremblay, L., Benner, R., 2006. Microbial contributions to N-immobilization and organic matter preservation in decaying plant detritus. *Geochim. Cosmochim. Acta* 70, 133–146. doi:10.1016/j.gca.2005.08.024
- van Klinken, G., 1999. Bone collagen quality indicators for palaeodietary and radiocarbon measurements. *J. Archaeol. Sci.* 26, 687–695.

- Willerslev, E., Davison, J., Moora, M., Zobel, M., Coissac, E., Edwards, M.E., Lorenzen, E.D., Vestergård, M., Gussarova, G., Haile, J., Craine, J., Gielly, L., Boessenkool, S., Epp, L.S., Pearman, P.B., Cheddadi, R., Murray, D., Bråthen, K.A., Yoccoz, N., Binney, H., Cruaud, C., Wincker, P., Goslar, T., Alsos, I.G., Bellemain, E., Brysting, A.K., Elven, R., Sønstebo, J.H., Murton, J., Sher, A., Rasmussen, M., Rønn, R., Mourier, T., Cooper, A., Austin, J., Möller, P., Froese, D., Zazula, G., Pompanon, F., Rioux, D., Niderkorn, V., Tikhonov, A., Savvinov, G., Roberts, R.G., MacPhee, R.D.E., Gilbert, M.T.P., Kjær, K.H., Orlando, L., Brochmann, C., Taberlet, P., 2014. Fifty thousand years of Arctic vegetation and megafaunal diet. *Nature* 506, 47–51. doi:10.1038/nature12921
- Wooller, M., Zazula, G., Edwards, M., Froese, D.G., Boone, R.D., Parker, C., Bennett, B., 2007. Stable carbon isotope compositions of Eastern Beringian grasses and sedges: investigating their potential as paleoenvironmental indicators. *Arctic, Antarct. Alp. Res.* 39, 318–331.
- Zimov, S., Chuprynin, V., Oreshko, A., Chapin III, F.S., Reynolds, J.F., Chapin, M.C., 1995. Steppe-tundra transition: a herbivore-driven biome shift at the end of the Pleistocene. *Am. Nat.* 146, 765–794.

Chapter 4

4 Ecology of Pleistocene Old Crow revealed by amino acid carbon and nitrogen isotopic compositions

4.1 Introduction

4.1.1 Mammoth steppe ecology

The Pleistocene mammoth steppe was a megacontinental biome stretching from northwestern Canada to western Europe. It supported a highly diverse ecosystem, with faunal associations not seen in modern ecosystems (Guthrie, 2001, 1990, 1982). Understanding the diets of these species is a key part of understanding species interactions, and thus how this vast ecosystem was able to thrive throughout the Pleistocene. The climatic and environmental change from the Pleistocene to the Holocene is known to have caused changes in plant species across the mammoth step (e.g. Willerslev et al., 2014). There is also significant interest in understanding the responses of megafauna species to this change, including those that survived the Pleistocene-Holocene transition, and how their diet and habitat use may have changed over this time.

Previous work on this topic has interpreted the diet of herbivores and carnivores using a variety of techniques including direct analysis of plant remains in digesta and teeth of frozen animals (e.g. Guthrie, 2001; Ukraintseva, 2013), macro and microwear analysis of teeth (e.g. Rivals and Solounias, 2007; Rivals et al., 2007) and isotopic studies of animal tissues (e.g. Bocherens, 2003; Bocherens et al., 1996; Fizet et al., 1995; Fox-Dobbs et al., 2008; Iacumin et al., 2000). These studies have revealed a number of dietary traits. Horse and mammoth were grazers, feeding on some combination of grasses, sedges and herbs (Bocherens, 2003; Fox-Dobbs et al., 2008). Mastodons were browsers, consuming trees and shrubs (Metcalf, 2011; Metcalfe et al., 2013). The North American Pleistocene giant beaver may have consumed primarily aquatic plants, unlike the modern beaver's primarily browse diet (Perkins, 2009; Stirton, 1965; Stuart-Williams et al., 1997). The diet of the carnivore species varied with location and time period. At Fairbanks, Alaska, the gray wolf ate a wide range of prey (Feranec et al., 2010; Fox-Dobbs et al., 2008)

leading Fox-Dobbs et al. (2008) to speculate that it was a scavenging species. However, in Marillac, France, wolves were found to specialize on caribou (Fizet et al., 1995). The brown bear was generally omnivorous or herbivorous (Barnes et al., 2002; Feranec et al., 2010; Fox-Dobbs et al., 2008; Matheus, 1995), with some populations specializing on caribou at some points in time (Fox-Dobbs et al., 2008). Most morphological and all isotopic studies of the short-faced bear classify it as a hypercarnivore or scavenger (Barnes et al., 2002; Bocherens et al., 1995; Burns and Young, 1994; Matheus, 1995), and isotopic dietary reconstructions determined that short-faced bears were caribou specialists in the region near Fairbanks, Alaska (Fox-Dobbs et al., 2008). Previous work has classified various North American felid predators as generalists consuming multiple prey types (Coltrain et al., 2004; Fox-Dobbs et al., 2008).

Examining the carbon and nitrogen isotopic compositions of individual amino acids, rather than the bulk protein collagen, can reveal environment, physiology and diet of a species masked using other methods. Previous work on woolly mammoths from this site (Schwartz-Narbonne et al., 2015; Chapter 3) used amino acid $\delta^{15}\text{N}$ of two amino acids, phenylalanine and glutamate, to determine that the woolly mammoth consumed a diet drawn from a distinct habitat or forage niche. Several hypotheses were suggested for what made the diet distinct, such as extreme aridity, dung fertilization, consumption of decayed plants, plant selection for distinct plants, or a combination of these signals. The use of $\delta^{15}\text{N}$ in a greater number of amino acids, in combination with amino acid $\delta^{13}\text{C}$, has the potential to discriminate among these possibilities, thus shedding further light on the diets of mammoth steppe animals.

4.1.2 Nitrogen isotopic compositions

4.1.2.1 Plant $\delta^{15}\text{N}$

Within a trophic level, differences in $\delta^{15}\text{N}$ can arise from the plant type consumed, as seen in Figure 1.2. In a tundra environment, $\delta^{15}\text{N}$ of plants tends to vary, from lowest to highest in the following order: shrubs, lichens, forbs, graminoids, fungi (Ben-David et al., 2001; Drucker et al., 2010; Finstad and Kielland, 2011; Kristensen et al., 2011; Nadelhoffer et al., 1996). There is a great deal of overlap between categories. As well,

different parts of the same plant can have different $\delta^{15}\text{N}$. For examples, stems and twigs commonly have lower $\delta^{15}\text{N}$ than needles or leaves of trees (Gebauer and Schulze, 1991; Kielland, 2001). The $\delta^{15}\text{N}$ of aquatic plants are not as well understood as terrestrial plants (Finlay and Kendall, 2007). In general, the global average $\delta^{15}\text{N}$ of aquatic plants is higher than that of terrestrial plants (France, 1995), and higher values have been found for aquatic plants than terrestrial plants at several specific sites (DeLong and Thorp, 2006; Finstad and Kielland, 2011; Fry, 1991; Milligan et al., 2010; Tischler, 2004). Many of these studies, however, compared the nitrogen isotopic composition of browse to aquatic plants and did not compare the $\delta^{15}\text{N}$ of aquatic plants to graminoids or forbs.

The $\delta^{15}\text{N}$ of plants can also be affected by climatic conditions. A site with a more open nitrogen cycle – one with greater nitrogen lost – will tend to have higher $\delta^{15}\text{N}$ in the plants that grow there. Warmer and drier environments tend to have more open nitrogen cycles (Ambrose, 1991; Amundson et al., 2003; Drucker et al., 2003; Heaton, 1987; Stevens and Hedges, 2004; Stevens et al., 2008).

4.1.2.2 Bulk collagen $\delta^{15}\text{N}$

Physiological factors can influence the $\delta^{15}\text{N}$ of an animal's collagen ($\delta^{15}\text{N}_{\text{Bulk}}$). As there is a 2-5 ‰ increase in the $\delta^{15}\text{N}$ of collagen with trophic level (Koch et al., 1994), higher $\delta^{15}\text{N}$ can commonly be used to distinguish carnivores from herbivores. Nutritional stress can also cause an increase in $\delta^{15}\text{N}_{\text{Bulk}}$ (Gannes et al., 1998; Hobson et al., 1993; Kelly, 2000; Koch, 2007; Polischuk et al., 2011), as can living in arid environments (Kelly, 2000; Sealy et al., 1987; Sponheimer et al., 2003). Nursing can also increase the $\delta^{15}\text{N}$ value of an infant's tissue (Metcalf et al., 2010); however, samples of juvenile megafauna were not examined in this study.

Within the mammoth steppe, the “woolly mammoth conundrum” arose because of seemingly inconsistent evidence from woolly mammoths $\delta^{15}\text{N}_{\text{Bulk}}$, which is more similar to coeval carnivores than herbivores (Bocherens, 2003; Schwartz-Narbonne et al., 2015). This conundrum underscores a general problem in ecological and paleoecological isotopic studies when using $\delta^{15}\text{N}_{\text{Bulk}}$ to understand the isotopic compositions of an

animal. Environmental, dietary and metabolic factors can affect $\delta^{15}\text{N}_{\text{Bulk}}$, making it difficult to pinpoint which factor is responsible for any observed isotopic variation. For this reason, this study examines the isotopic compositions of the individual amino acids that comprise collagen. Previous work (Schwartz-Narbonne et al., 2015; Chapter 3) examined two amino acids, glutamate and phenylalanine, and determined that the cause of high mammoth bulk collagen $\delta^{15}\text{N}$ was a distinct dietary or habitat niche, and that this niche was shared by some horses on the mammoth steppe. However, Schwartz-Narbonne et al. (2015) were not able to determine if this niche resulted from mammoths consuming: (i) plants that grew in more arid environments, (ii) plants that were fertilized by dung, (iii) specific plants or plant parts, or (iv) partially decayed plants. The present study examines the nitrogen and carbon isotopic compositions of multiple amino acids to help answer these remaining questions, and to provide further insight into the diet, habitat and trophic level of several megafaunal species from the Old Crow site, Yukon Territory, Canada (Fig. 4.1).

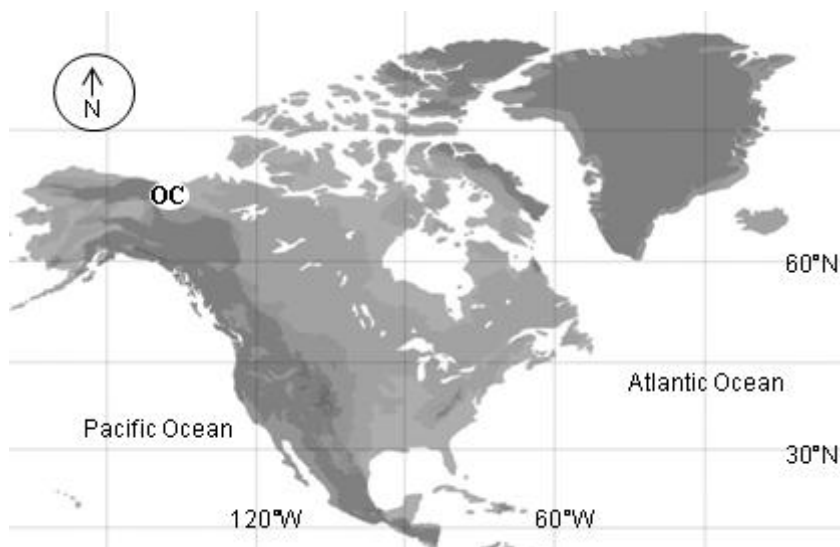


Figure 4.1 Location of samples. Samples were collected in Old Crow (OC), Yukon Territory, Canada. Higher altitudes are represented by darker shades of grey. The map was drawn by Katherine Allan.

4.1.2.3 Amino acid $\delta^{15}\text{N}$

Nitrogen used for plant amino acid synthesis can be drawn from several sources. It can come from direct uptake of soil amino acids, although most plants compete poorly for amino acids compared to soil microbes, and so this is not a primary mechanism of acquiring nitrogen for most plants (Styring et al., 2014). Plants, or associated microorganisms, can fix nitrogen, or plants can uptake nitrate or ammonium ions from soil. Plants then convert the nitrogen compound into an amino acid by attaching it as an amide group to glutamate, thus forming glutamine (Styring et al., 2014). Two of these processes are illustrated in Figure 3.1.

Since different plants synthesize and use amino acids with varied enzymes and in varied reactions, the pattern of amino acid $\delta^{15}\text{N}$ can vary among different plant types. This pattern has been referred to as the amino acid isotopic “fingerprint” (Larsen et al., 2009), though it has primarily been used for interpretation of carbon isotopic rather than nitrogen isotopic compositions (Arthur et al., 2014; Larsen et al., 2013, 2012, 2009). Chikaraishi et al. (2010) found the amino acid nitrogen fingerprint varied among aquatic, C_3 and C_4 plants, but did not propose a mechanism for this difference. Differences among plants’ growth environments and nitrogen uptake strategies may be responsible. Bol et al. (2002) suggested that differences in amino acid $\delta^{15}\text{N}$ of plants may be related to their functional nitrogen strategy, which means there is potential for them to distinguish the source of nitrogen in an ecosystem. As one of the plant types studied by Bol et al. (2002) lived in a particularly wet environment with less access to inorganic nutrients, environmental factors may also play a role. Other studies have also found amino acid-specific differences in $\delta^{15}\text{N}$ of plants that correlate with environmental effects such as the limiting nutrient in an environment (Smallwood et al., 2003). There may also be plant-part differences. Styring et al. (2014) suggested that nitrogen is transported to certain plant tissues, such as legume seeds, in the form of asparagine rather than as glutamine, which could lead to different $\delta^{15}\text{N}$ fingerprints in different tissues of the same plant. Decayed plants may have a different nitrogen isotopic amino acid fingerprint than the living plant. Several studies have investigated the potential of degradation to change the $\delta^{15}\text{N}$ of amino acids, particularly glycine, in primary producers (Calleja et al., 2013;

Fogel and Tuross, 1999; Smallwood et al., 2003). More work is necessary to be able to interpret with confidence the plant amino acid $\delta^{15}\text{N}$ fingerprint in terms of plant type, plant part or ecosystem. Once this is done, such data may be more useful in helping to characterize the diet or habitat of consumers.

When considering the nitrogen isotopic composition of individual amino acids in consumers, the amino acids can be divided into two groups: source and trophic amino acids (McCarthy et al., 2007; Popp et al., 2007). The source amino acids measured in this study are glycine (Gly), phenylalanine (Phe) and threonine (Thr). The trophic amino acids measured are alanine (Ala), glutamate (Glu), leucine (Leu), proline (Pro) and valine (Val). Source amino acids experience little nitrogen isotopic variation from diet to the consumer's tissues. The feeding study of McClelland and Montoya (2002) found a 0 to +2 ‰ variation in the $\delta^{15}\text{N}$ of phenylalanine moving up one trophic level; this shift was smaller than the change in $\delta^{15}\text{N}$ observed in the bulk material. Threonine was found to have a slightly lower $\delta^{15}\text{N}$ with increasing trophic level (Chikaraishi et al., 2007; Popp et al., 2007). Trophic amino acids undergo larger ^{15}N -enrichments (e.g. +6 to +7 ‰ for glutamate) upon moving up a trophic level (McClelland and Montoya, 2002). This process is illustrated in Fig. 3.1. Glutamate, which showed the largest trophic enrichment in feeding studies (Hare et al., 1991; McClelland and Montoya, 2002), plays a substantial role in nitrogen transport through the body (McCarthy et al., 2013), likely accounting for its significant enrichment in ^{15}N during metabolic processes.

Since source amino acids experience little ^{15}N -enrichment over their isotopic compositions at the base of the food web, they have been used to identify differences in dietary preferences and to track the changing isotopic compositions of plants with time or location (Hannides et al., 2009; Lorrain et al., 2009; McClelland et al., 2003; Ogawa et al., 2012; Pakhomov et al., 2004; Popp et al., 2007; Ruiz-Cooley et al., 2013; Seminoff et al., 2012; Sherwood et al., 2011). Source amino acids have the potential to be used to examine the nitrogen amino acid fingerprint of plants that were consumed, though this has not yet been done. The trophic amino acids have also been used to determine the degree of trophic enrichment of an organism. This measurement is typically performed by subtracting the $\delta^{15}\text{N}$ of a source amino acid from a trophic amino acid ($\Delta^{15}\text{N}_{\text{Trophic-}}$

Source), which accounts for varying $\delta^{15}\text{N}$ at the base of the food chain (e.g. Chikaraishi et al., 2014, 2007).

4.1.3 Carbon isotopic compositions

4.1.3.1 Plant $\delta^{13}\text{C}$

North American high latitude regions have been found to contain almost entirely C_3 plants, and no C_4 plants have been found for these regions from the Pleistocene (Gaglioti et al., 2011; Kristensen et al., 2011; Wooller et al., 2007). There are some isotopic differences among plant types of C_3 plants, as displayed in Figure 1.2. From lowest to highest, the carbon isotopic composition of plant types rank as follows: shrubs, forbs, graminoids, fungi and lichens (Barnett, 1994; Ben-David et al., 2001; Drucker et al., 2010; Kristensen et al., 2011). As for plant nitrogen isotopic compositions, there are differences in the $\delta^{13}\text{C}$ of plant parts, with twigs having higher $\delta^{13}\text{C}$ than needles or leaves (Ehleringer et al., 1992; Gebauer and Schulze, 1991; Tischler, 2004). Typical $\delta^{13}\text{C}$ for aquatic plants are difficult to define, as these plants have a much wider range of isotopic compositions than terrestrial C_3 plants (Finlay and Kendall, 2007).

Environmental factors can play a role in changing the $\delta^{13}\text{C}$ of a plant. For example, factors such as decreased aridity, lower altitudes, lower temperatures and growing underneath a dense canopy all tend to cause lower $\delta^{13}\text{C}$ in plants (Bocherens et al., 2011; de Bello et al., 2009; Diefendorf et al., 2010; Ehleringer and Cooper, 1988; Ehleringer et al., 1987; Farquhar, 1989; Kohn, 2010; Tieszen, 1991; Wooller et al., 2007).

4.1.3.2 Bulk collagen $\delta^{13}\text{C}$

Higher trophic levels, nutritional stress and nursing can all change the carbon isotopic composition of an animal's collagen. The collagen of large herbivores has been found to have ~5‰ higher $\delta^{13}\text{C}$ than their diet (Drucker et al., 2008). For carnivores, the increase in collagen $\delta^{13}\text{C}$ ($\delta^{13}\text{C}_{\text{Bulk}}$) with trophic level ranges from 0 to 2 ‰ (Bocherens and Drucker, 2003). During periods of nutritional stress, an animal may rely on stored lipids, which have a relatively low $\delta^{13}\text{C}$ (Szpak et al., 2010). Milk produced during nursing also has a large quantity of lipids, and so could also cause collagen from a juvenile animal to

have lower than expected $\delta^{13}\text{C}_{\text{Bulk}}$ (Metcalf et al., 2010). As described earlier, however, none of the specimens sampled in this study are expected to show a nursing signal.

There are a number of environments where conventional isotopic analysis is not sufficient to determine the dietary sources for humans or animals. For example, understanding food webs in C_3 plant-only environments using carbon isotopes is challenging because of the relatively narrow range of C_3 plant $\delta^{13}\text{C}$ (e.g. Fox-Dobbs et al., 2008). As well, isotopic modelling studies that attempt to separate the dietary sources utilized by a carnivore using bulk collagen compositions are hindered by the fact that one cannot uniquely determine the proportions of $n + 1$ diet sources using n isotopes (Fox-Dobbs et al., 2008). Bayesian statistics such as used in SIAR (Stable Isotope Analysis in R) are helping to overcome these limitations (e.g. Parnell et al., 2010; Yeakel et al., 2013). These incorporate the isotopic compositions of the diet and of the consumer into a probabilistic model and produce estimates of the most likely diet, or combination of resources, used by the consumer.

Woolly mammoths generally had slightly lower collagen $\delta^{13}\text{C}_{\text{Bulk}}$ than the other herbivores at a site (e.g. Bocherens, 2003; Bocherens et al., 1996; Iacumin et al., 2010; Mann et al., 2013; Matheus et al., 2003). Mastodons tended to have similar or slightly higher $\delta^{13}\text{C}_{\text{Bulk}}$ than mammoths (Mann et al., 2013; Metcalfe, 2011; Metcalfe et al., 2013). Stomach content and teeth morphology suggest that their diets were distinct, with mammoths eating graminoids and forbs, and mastodons eating browse (Haynes, 1991). Proboscideans are nonruminants, and so produce less methane than ruminant species. Methane tends to have low $\delta^{13}\text{C}$. The preferential loss of ^{12}C via methane emissions from the body would reduce the available ^{12}C reservoir for incorporation into collagen. This process could explain the higher $\delta^{13}\text{C}_{\text{Bulk}}$ of ruminant species such as caribou and bison compared to mammoth and mastodon, although it would not explain differences between proboscidean and horse $\delta^{13}\text{C}_{\text{Bulk}}$ (Mann et al., 2013). Alternatively, animals relied on fat reserves in order to survive the low forage levels available during the Pleistocene Arctic winter, and mammoths had thick fat deposits (Guthrie, 1990). Fat tends to be depleted of ^{13}C , and so extensive use of fat reserves by Pleistocene proboscideans could explain their low $\delta^{13}\text{C}_{\text{Bulk}}$ values (Szpak et al., 2010). This explanation, however, requires that

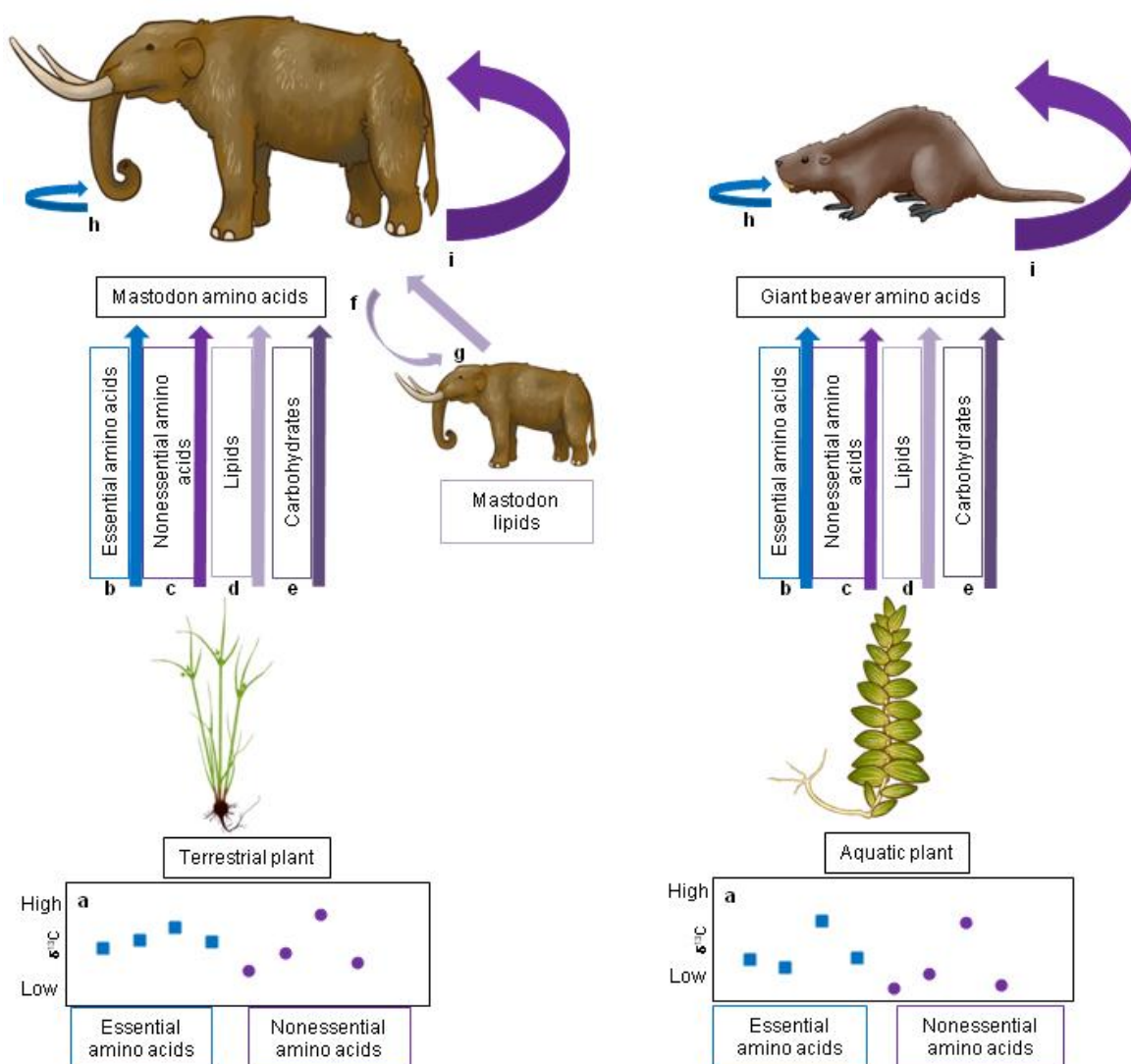
proboscideans relied more heavily on their fat reserves than did other Pleistocene animals. In a different explanation, Iacumin et al. (2010, 2000) suggested that differences between the $\delta^{13}\text{C}_{\text{Bulk}}$ of reindeer and mammoths are related to dietary differences, such as incorporation of lichens into reindeer diets and woody vegetation into some mammoths' winter diets. A combination of these factors may be responsible for the $\delta^{13}\text{C}_{\text{Bulk}}$ of Pleistocene herbivores.

4.1.3.3 Amino acid $\delta^{13}\text{C}$

While plants can uptake amino acids from soil, amino acids are generally synthesized *de novo* from organic compounds produced as intermediates in the plant's metabolic cycle (Styring et al., 2014). Organisms synthesize amino acids by specific pathways associated with particular enzymes. Accordingly, several studies have focused on determining $\delta^{13}\text{C}$ for individual amino acids of a specific plant type, leading to a carbon isotopic "fingerprint". Different kingdoms, plant species, and even different plant parts have been shown to have different amino acid carbon isotopic fingerprints (Fogel and Tuross, 2003; Larsen et al., 2013, 2012, 2011, 2009; Lynch et al., 2011; Smallwood et al., 2003). While these fingerprints can vary with environmental conditions, they are useful as a baseline (Fig. 4.2). Further work is necessary to determine the amino acid carbon isotopic variation between plant types and plant parts in more detail. Lynch et al. (2011) was able to find differences between the $\delta^{13}\text{C}$ fingerprints of tree and nettle leaves, and grain seeds. At present, only limited research has been conducted on the carbon isotopic fingerprints of plant or bacterial types that would have been found on the mammoth steppe. Some carbon isotopic fingerprints are available for aquatic plants, bacteria, fungi and terrestrial plants (Larsen et al., 2012, 2009), but further differences likely exist among graminoids, forbs and trees, and among types of bacteria.

When considering the carbon isotopic composition of a consumer's amino acids, the amino acids can be divided into two broad categories: essential and nonessential. Essential amino acids cannot be produced by the animal, while nonessential amino acids can be biosynthesized by the animal or taken directly from the diet, depending on their availability in the diet and metabolic demand (Fig. 4.2; Jim et al., 2006). The essential amino acids analyzed in this study are leucine, phenylalanine, threonine and valine, and

the nonessential amino acids measured are alanine, glutamate, glycine, hydroxyproline and proline (Howland et al., 2003), though the classification of an amino acid into one of these categories can vary among species and age groups (Jim et al., 2006). As essential amino acids are taken directly from the diet, limited isotopic fractionation is expected to occur when they are incorporated into body proteins. In particular, the essential amino acids leucine and phenylalanine tend to retain isotopic compositions characteristic of diet, with leucine showing ^{13}C enrichment of $+0.5 \pm 1.2 \text{ ‰}$, and phenylalanine varying from the diet by $-0.6 \pm 0.6 \text{ ‰}$ (Howland et al., 2003).



Caption on facing page.

Figure 4.2 Simplified pathway for carbon incorporation from plant biochemicals to animal protein. Arrows represent: uptake (solid lines) and metabolic processes (solid curves). a. Typical plant $\delta^{13}\text{C}$ fingerprint for each plant type. The specific fingerprint for the essential and non-essential amino acids depends on the biosynthetic pathways used by the plant to produce and store amino acids. The amino acid carbon isotopic fingerprints are adapted from Larsen et al. (Larsen et al., 2013, 2012, 2009); b. Essential amino acids are taken up from the plant to animal; c. Non-essential amino acids are taken up from the plant to animal. d. Plant lipids are taken up from the plant to animal; e. Carbohydrates are taken up from the plant to animal; f. Animals can synthesize lipids from their diet; g. These lipids can be used by the animal during times of nutritional stress; h. Essential amino acids are generally routed directly from the diet with minimal changes in their isotopic composition (Jim et al., 2006); i. Non-essential amino acids can be routed directly from the diet. They can also be synthesized out of the entire diet, from precursors such as proteins, plant carbohydrates, plant lipids and animal lipids. The difference in $\delta^{13}\text{C}$ of a nonessential amino acid in the diet and in the body depends on the degree of routing versus *de novo* synthesis, the difference in isotopic composition between the amino acid in the diet and the portion of the diet from which the amino acid is synthesized, and the isotopic shift induced by biochemical synthesis. Katherine Allan drew the grass, aquatic plant, giant beaver and mastodon images. The grass image was published previously (Schwartz-Narbonne et al., 2015).

Linear discriminant analysis (LDA) can be used to classify the diet of consumers based on the $\delta^{13}\text{C}$ of amino acids whose isotopic compositions are similar to those in the diet. The $\delta^{13}\text{C}$ of those amino acids in a variety of dietary sources were measured in previous work (Larsen et al., 2013, 2012, 2009). The common isotopic trends within a dietary group, or the linear combination of features for each dietary group (e.g. aquatic plants, bacteria, terrestrial plants) are defined based on the inputs from previous work. When an unknown sample is input, it can be compared to the linear combinations of features of each dietary group and it can be classified as most similar to one of the dietary groups. If the isotopic compositions of the amino acids in a consumer are similar to their isotopic composition in the diet, this technique can be used to identify what a consumer is eating

(Larsen et al., 2013, 2012, 2009).

When nonessential amino acids are synthesized *de novo* in the body, the biochemical processes involved can result in significant differences in the amino acid isotopic composition from diet to bone collagen. The feeding study of Jim et al. (2006), for example, was able to induce a glutamate variation of -7 to $+13$ ‰ from the diet to the consumer tissue. This variation occurred partially because of metabolic fractionations associated with the synthesis and degradation of amino acids, but largely because the nonessential amino acids were synthesized out of a carbon pool that was experimentally designed to have an extremely different isotopic composition to that of the essential amino acids. Some variation would also be expected in a natural system, as nonessential amino acids can be synthesized from carbohydrates, lipids or protein depending on the diet and metabolic state of the animal. Each of these compounds has a distinct $\delta^{13}\text{C}$ that will affect the $\delta^{13}\text{C}$ of the resulting amino acid, as has been demonstrated both for lipids (Newsome et al., 2014) and carbohydrates (Jim et al., 2006). The situation is further complicated by the fact that nonessential amino acids can also be routed directly from the diet. The degree of routing depends on the diet's protein content. An animal consuming a diet containing more than 5-12% protein will route some of their nonessential amino acids directly from the diet, and more routing appears to occur as the quantity of protein in the diet increases (Jim et al., 2006; Newsome et al., 2014, 2011). Which amino acids are routed, and which are *de novo* synthesized, seems to depend on the amino acid requirements of the consumer (McMahon et al., 2010). For extremely low protein diets, it has been suggested that the amino acid $\delta^{13}\text{C}$ are overprinted by the isotopic compositions introduced by enzymatic reactions of gut microflora (Arthur et al., 2014; Newsome et al., 2011). This process might be particularly pertinent for ruminants, as they digest a large portion of their food using gut microflora.

4.1.4 Inter-tissue variation

Previous work has observed some variation in $\delta^{13}\text{C}_{\text{Bulk}}$ and $\delta^{15}\text{N}_{\text{Bulk}}$ between different tissues of Old Crow mammoths (Metcalf, 2011). Dentin from adult mammoths had higher $\delta^{15}\text{N}_{\text{Bulk}}$ (on average by 1.2 ‰), and slightly higher $\delta^{13}\text{C}_{\text{Bulk}}$ (on average by 0.2 ‰), than cementum. Mammoths from other locations, however, did not consistently

display the same offsets among their tissues, and some inter-tissue variation observed for mammoths from other locations, such as higher $\delta^{15}\text{N}_{\text{Bulk}}$ for tooth dentin than tusk dentin or bone in mammoths from Ontario, was not observed in the Old Crow mammoths (Metcalf, 2011). Metcalfe (2011) suggested several explanations for these tissue-specific isotopic differences, including metabolism, diet, and age-related isotopic shifts resulting from variations in growth rates between tissues.

Amino-acid specific measurements have been used to examine tissue-specific differences in isotopic composition, with varying results and interpretations. In one study, the bulk protein of various non-collagen tissue types had different isotopic compositions but the individual amino acids did not, suggesting that variations among the amino acid profiles (relative abundances of individual amino acids) of the different tissues were responsible for the isotopic differences (Chikaraishi et al., 2011). Another study examined two tissues that had the same amino acid profile but different turnover rates and different amino acid $\delta^{13}\text{C}$, and related the difference to a shift in diet over time (Corr et al., 2009). A third study (Schmidt et al., 2004) found differences in both the amino acid profile and the amino acid isotopic compositions of the krill digestive gland region, abdominal segment and remaining body tissues, which were related to internal metabolic processes. The present study examines the existence and origin of differences in the isotopic composition of the woolly mammoth using both the amino acid profiles and the differences in $\delta^{13}\text{C}_{\text{Bulk}}$ and $\delta^{15}\text{N}_{\text{Bulk}}$ of various collagenous tissues.

4.1.5 Site

A number of aquatic and semi-aquatic species, as well as tree trunks, suggest that there were shallow pools and lakes, and a spruce-larch forest in the Beringian Old Crow Basin region during the last interglacial (Fig. 4.1; Harington, 2011). Isotopic studies of mammoth collagen have suggested that the Old Crow was as colder and more arid than Alaskan and Yukon sites during the Late Pleistocene, although warmer and wetter than Siberian sites of similar ages (Metcalf et al., 2010; Szpak et al., 2010). Appendix E and H present the longitude and latitude of sample collection for those specimens for which this information is available.

4.2 Methods

4.2.1 Sample selection

The herbivore species analysed include woolly mammoth (*Mammuthus primigenius*), mastodon (*Mammuthus americanus*), horse (*Equus* sp.) and giant beaver (*Castoroides ohioensis*). The carnivore species analysed are brown bear (*Ursus arctos*), scimitar cat (*Homotherium serum*), wolf (*Canis lupus*), and short-faced bear (*Arctodus simus*). The majority of the samples used in this work have been utilized for other purposes in previous studies (Chapter 3; Metcalfe, 2011; Metcalfe et al., 2010; Schwartz-Narbonne et al., 2015). Two additional specimens, bones from a brown bear and a giant beaver, were added to this study, and are described in Appendix H.

4.2.2 Collagen extraction and measurement

Samples were taken using a Dremel tool equipped with a cutting wheel. Surfaces and cancellous bone were removed using a burr Dremel attachment and then the remaining sample was cleaned with deionised water and dried in air. A test lipid extraction was performed on one sample using a modified Bligh and Dyer method (Bligh and Dyer, 1959). A 2:1 chloroform:methanol solution (v:v) was applied for 15 minutes 3 times. As was the case for test samples reported elsewhere (Chapters 2 and 5), the $\delta^{13}\text{C}_{\text{Bulk}}$ and $\delta^{15}\text{N}_{\text{Bulk}}$ were similar for this sample before and after lipid-extraction (an absolute difference of 0.0 ‰ for $\delta^{13}\text{C}$ and 0.5 ‰ for $\delta^{15}\text{N}$ was found in this study). Accordingly, the isotopic results for lipid-extracted and untreated collagen samples described below are considered to be equivalent.

The collagen utilized for the majority of the samples reported here was extracted in previous work (Chapter 3; Metcalfe, 2011; Metcalfe et al., 2010; Schwartz-Narbonne et al., 2015). Collagen from the two additional samples described above was extracted using the same modified Longin method (Longin, 1971). The $\delta^{13}\text{C}_{\text{Bulk}}$ and $\delta^{15}\text{N}_{\text{Bulk}}$ for the mammoth and mastodon collagen have been reported previously (Metcalfe, 2011; Metcalfe et al., 2010), and the $\delta^{15}\text{N}_{\text{Bulk}}$ of all but the two additional samples were also reported in (Chapter 3; Schwartz-Narbonne et al., 2015).

The additional bulk collagen isotopic compositions were measured in continuous flow mode using a Costech elemental combustion system (ECS 4010) connected to a Thermo-Scientific Delta V stable isotope ratio mass spectrometer (IRMS) over a total of four analytical sessions. The carbon isotopic compositions were calibrated to VPDB using a two-point curve anchored either by NBS-22 (accepted value -30.03 ‰, (Coplen et al., 2006) and IAEA-CH-6 (accepted value -10.45 ‰, (Coplen et al., 2006), or USGS-40 (accepted value -26.39 ‰, (Coplen et al., 2006) and USGS-41 (accepted value $+37.63$ ‰, (Coplen et al., 2006). Calibration of $\delta^{15}\text{N}$ to AIR was performed using a two point curve anchored by USGS-40 (accepted value -4.52 ‰, (Qi et al., 2003) and either IAEA-N2 (accepted value $+20.3$ ‰) or USGS-41 (accepted value $+47.57$ ‰, (Qi et al., 2003). Elemental compositions were calculated with the same standards (NBS-22, C = 86.3 %; IAEA-CH-6, C = 42.1 %; USGS-40, C = 40.7%, N = 9.5 %; USGS-41, C = 40.7%, N = 9.5%; IAEA-N2, N = 21.5%). Keratin (MP Biomedicals Inc., Cat No 90211, Lot No. 9966H) was used as an internal standard. Over 24 measurements, average values (\pm standard deviation, SD) were: -24.0 ± 0.1 ‰ for $\delta^{13}\text{C}$; $+6.3 \pm 0.1$ ‰ for $\delta^{15}\text{N}$; 48 ± 1 % for C wt.%; 16 ± 1 % for N wt.%, and 3.6 ± 0.4 for C/N ratio. These results compared well with accepted values of $\delta^{13}\text{C} = -24.0$ ‰, $\delta^{15}\text{N} = +6.4$ ‰, C wt.% = 46.8%, N wt.% = 14.6% and C/N = 3.7. Precision was also assessed for each standard. Over 8 to 14 measurements, the $\delta^{13}\text{C}$ of NBS-22, IAEA-CH-6, USGS-40 and USGS-41 varied by ± 0.1 to 0.2 ‰ (SD). Over 12 to 14 measurements, the $\delta^{15}\text{N}$ of USGS-40, IAEA-N2 and USGS-41 varied by ± 0.1 to 0.3 ‰ (SD). For 3 samples analyzed in duplicate or triplicate, the variation (SD) ranged from 0.0 to ± 0.1 ‰ for $\delta^{13}\text{C}$, 0.0 to ± 0.5 ‰ for $\delta^{15}\text{N}$, 0 to ± 3 % for C wt.%, 0.0 to ± 1 % for N wt.%, and 0.0 to ± 0.3 for C/N.

4.2.3 Hydrolysis, derivatization and measurement of amino acid isotopic compositions

The majority of samples were hydrolysed, derivatized to their N-acetyl-methyl ester derivative, and their amino-acid specific nitrogen isotopic compositions were measured for a previous study (Chapter 3; Schwartz-Narbonne et al., 2015). A typical gas chromatogram of the nitrogen isotopic measurements is found in Appendix G. The additional brown bear sample (YT83) was treated using the same method and analysed

using an Agilent 6890N-Thermo-Scientific Gas Chromatograph-Combustion 3-Thermo-Scientific Delta Plus XL IRMS, equipped with an Agilent Technologies VF-23MS column.

The present study reports $\delta^{15}\text{N}$ for 8 amino acids (Ala, Glu, Gly, Hyp, Phe, Pro, Thr and Val; Table 4.1). Peaks with intensities less than 100 mV are not reported. Samples were injected in triplicate, and the standard deviation (SD) of the triplicate measurement for all amino acids ranged from 0.0 to ± 3.9 ‰, with an average standard deviation of ± 0.7 ‰. Norleucine was used as an internal standard, for which an average isotopic composition of $+13.3 \pm 1.0$ ‰ was obtained, as compared to a $\delta^{15}\text{N}$ of $+14.5$ ‰ as measured using a Costech elemental combustion system (ECS 4010) connected to a Thermo-Scientific Delta V IRMS. Two amino acids produced $\delta^{15}\text{N}$ that should be considered with caution. Threonine was regularly determined to have very low $\delta^{15}\text{N}$, down to -22.0 ‰, whereas the four in-house standards used for calibration to AIR (Ala, Leu, Pro and Phe) had a minimum value of -4.6 ‰. This means that the threonine data lie outside of the range of the calibration curve. This is the only amino acid for which this situation arose. Second, the glycine peak partially overlapped with the leucine peak, as is visible from the gas chromatogram (Chapter 3; Schwartz-Narbonne et al., 2015). This overlap is more significant for measurements of nitrogen isotopic composition than carbon isotopic composition. Each amino acid has fewer nitrogen atoms than carbon atoms, and the IRMS system is less sensitive to nitrogen than to carbon, so more sample has to be injected than when measuring carbon isotopic composition, leading to more overlap of the amino acid peaks. The overlap is generally $< 25\%$, for which reliable isotopic compositions can still be obtained, but it is recommended that such peaks are measured at multiple amplitudes (Evershed et al., 2007), which was not possible for all samples.

The $\delta^{13}\text{C}$ of 9 amino acids are reported in this paper (Ala, Glu, Gly, Hyp, Leu, Phe, Pro, Thr and Val; Table 4.2). The same methods were used as for measurement of the nitrogen isotopic compositions, except that a liquid nitrogen trap was not used to trap the CO_2 , and samples were analyzed in duplicate rather than triplicate. A representative gas chromatogram is provided in Appendix I. The carbon isotopic compositions were corrected for kinetic isotopic effects and added carbon during derivatization following the

Lab ID	Species	Tissue	Ala	Glu	Gly	Hyp	Leu	Phe	Pro	Thr	Val	$\delta^{15}\text{N}_{\text{Bulk}}$
YT1RD	Mammoth	RD	3.6±0.5	7.2±0.1	4.2±0.5	10.2±0.3	ND	11.6±0.7	8.4±0.1	-4.8±1.2	13.5±1.1	9.8
YT2RD	Mammoth	RD	4.6±0.3	11.9±0.5	5.5±0.2	11.4±0.1	ND	16.1±0.9	8.9±0.9	ND	ND	8.7
YT3D	Mammoth	D	6.4±0.9	11.5±0.3	5.8±0.2	13.2±0.2	ND	15.3±0.7	11.9±0.3	-3.5±1.1	14.6±0.7	8.4
YT4B	Mammoth	B	4.3±0.5	10.8±0.2	5.6±0.4	12.9±0.4	ND	14.0±0.7	11.4±0.1	-3.2±0.6	12.2±1.1	9.7
YT5RD	Mammoth	RD	8.3±1.0	10.6±0.4	6.4±0.4	12.3±0.1	ND	13.2±0.9	10.4±0.3	-5.8±1.3	13.4±2.0	9.5
YT6C	Mammoth	C	5.2±0.3	9.6±1.5	6.6±0.1	11.2±0.3	ND	13.8±1.4	10.9±0.2	-13.3±0.3	5.5±1.4	7.7
YT7B	Mammoth	B	4.3±0.2	9.5±0.7	5.2±0.2	11.2±0.0	ND	11.7±0.3	10.8±0.3	-11.4±0.4	6.4±0.4	7.6
YT9C	Mammoth	C	4.6±1.1	9.4±0.5	5.9±0.8	11.6±0.2	ND	11.6±0.8	9.6±0.3	ND	ND	8.2
YT10RD	Mammoth	RD	8.7±0.2	10.6±0.8	11.8±0.2	12.2±1.1	ND	11.2±0.2	11.6±0.2	-10.2±0.1	8.8±0.7	9.8
YT11C	Mammoth	C	5.4±0.2	11.6±0.3	6.8±0.3	13.6±0.7	ND	10.4±0.5	11.6±0.3	-11.8±0.4	7.2±0.8	9.5
YT11RD	Mammoth	RD	9.7±0.8	8.8±3.9	8.4±1.2	13.2±1.1	ND	14.1±1.3	13.1±3.1	-7.5±1.1	8.4±3.1	8.3
YT51T	Mammoth	T	10.1±0.5	12.4±1.0	11.3±0.5	13.8±0.7	ND	12.9±1.3	13.1±0.6	-6.9±0.8	8.9±1.5	11.3
	Mammoths		6.3±2.3	10.3±1.5	7.0±2.4	12.2±1.1		13.0±1.7	11.0±1.5	-7.8±3.6	9.9±3.3	9.0±1.1
AMNH1	Giant beaver	B	3.8±0.5	9.2±0.2	2.8±0.2	10.1±0.6	ND	8.4±0.2	6.9±0.2	ND	4.8±0.4	5.4
YT8D	Mastodon	D	-0.4±0.1	4.2±0.3	5.3±0.9	5.5±0.9	ND	8.9±1.5	5.0±0.2	-15.7±1.1	-1.6±0.4	3.5

Table 4.1 continues on next page.

Lab ID	Species	Tissue	Ala	Glu	Gly	Hyp	Leu	Phe	Pro	Thr	Val	$\delta^{15}\text{N}_{\text{Bulk}}$
YT129	Horse	B	3.5±1.0	8.6±0.8	1.1±0.7	10.6±0.5	ND	11.2±0.5	9.7±0.4	-5.2±1.5	12.7±1.5	7.0
YT130	Horse	B	7.2±1.2	11.1±0.7	1.6±0.3	12.8±	ND	10.6±0.7	12.8±0.8	-5.8±1.1	3.7±1.4	8.1
YT131	Horse	B	10.5±0.4	11.2±0.7	3.9±0.1	13.1±0.8	ND	12.0±0.0	14.7±0.5	-4.3±1.5	7.4±2.2	9.9
YT132	Horse	B	3.4±0.4	6.7±0.8	0.6±0.4	9.1±0.0	ND	7.8±0.7	9.4±0.2	-10.9±0.7	2.0±1.2	4.2
YT133	Horse	B	7.8±0.7	11.0±0.3	4.6±0.8	13.0±0.4	ND	13.6±0.2	13.7±0.5	-3.1±1.2	8.1±1.2	8.7
	Horses		6.5±3.0	9.7±2.0	2.4±1.8	11.7±1.8		11.0±2.1	12.0±2.4	-5.8±3.0	6.8±4.2	7.6±2.2
YT68	Brown bear Short-faced	B	11.7±0.5	13.7±0.6	2.3±0.8	12.2±0.7	ND	9.3±0.7	13.8±1.3	-20.6±0.8	10.2±0.8	8.4
YT81	bear	B	11.8±0.4	16.6±0.4	2.1±0.6	15.9±0.5	ND	10.1±0.4	13.7±0.4	-19.2±0.9	12.4±0.4	9.1
YT82	Scimitar cat	B	13.0±0.5	14.3±0.6	2.1±0.4	17.5±0.2	ND	9.7±0.8	15.7±0.5	-22.0±1.5	11.7±0.8	9.9
YT84	Brown bear	B	10.6±0.8	13.3±0.8	6.8±1.4	16.0±1.9	ND	10.7±0.3	14.6±0.2	-18.1±0.2	10.6±1.5	11.5
AMNH3	Canid	B	9.2±0.3	11.8±0.7	1.8±0.2	11.9±0.2	ND	8.7±0.9	9.7±0.4	-16.8±0.8	12.2±1.5	8.5
	Carnivores		11.3±1.4	14.0±1.7	3.0±2.1	14.7±2.5		9.7±0.7	13.5±2.3	-19.3±2.0	11.4±1.0	9.5±1.3
YT83	Holocene brown bear	B	10.1±0.6	13.0±0.7	-1.0±0.5	12.2±0.3	ND	10.0±1.5	10.9±0.7	-13.2±3.6	14.7±1.7	6.8

Table 4.1 $\delta^{15}\text{N}$ for bulk collagen and individual amino acids. The nitrogen isotopic compositions of the specimens' amino acids (Ala = alanine, Val = valine, Gly = glycine, Leu = leucine, Thr = threonine, Pro = proline, Glu = glutamate, Phe = phenylalanine and Hyp = hydroxyproline) and bulk collagen are listed for all samples, along with the standard deviation (SD) for triplicate measurements of each amino acid. The average $\delta^{15}\text{N}$ (and SD) for each species or group of animals is also provided. Peaks that did not give reliable isotopic compositions are listed as ND (not determined). Except for sample YT83, the phenylalanine, glutamate and bulk collagen isotopic compositions were previously reported (Metcalf, 2011; Metcalf et al., 2010; Schwartz-Narbonne et al., 2015). RD = root dentin, D = crown dentin, B = bone, C = cementum and T = tusk.

methods of Corr et al. (Corr et al., 2007a, 2007b). The measurement error, and the compounding of this error introduced by the measurements used to correct for the carbon added during derivatization, is calculated following the methods of Docherty et al. (Docherty et al., 2001). The SD of duplicate measurements of individual amino acids ranged from ± 0.1 to ± 2.4 ‰, with an average SD of ± 0.6 ‰. The average $\delta^{13}\text{C}$ of the internal standard norleucine over all analytical sessions was -28.2 ± 0.6 ‰ (SD). A value of -27.8 ‰ was obtained for the same standard using a Costech elemental combustion system (ECS 4010) connected to a Thermo-Scientific Delta V IRMS.

The $\delta^{13}\text{C}$ of 9 amino acids are reported in this paper (Ala, Glu, Gly, Hyp, Leu, Phe, Pro, Thr and Val; Table 4.2). The same methods were used as for measurement of the nitrogen isotopic compositions, except that a liquid nitrogen trap was not used to trap the CO_2 , and samples were analyzed in duplicate rather than triplicate. A representative gas chromatogram is provided in Appendix I. The carbon isotopic compositions were corrected for kinetic isotopic effects and added carbon during derivatization following the methods of Corr et al. (Corr et al., 2007a, 2007b). The measurement error, and the compounding of this error introduced by the measurements used to correct for the carbon added during derivatization, is calculated following the methods of Docherty et al. (Docherty et al., 2001). The SD of duplicate measurements of individual amino acids ranged from ± 0.1 to ± 2.4 ‰, with an average SD of ± 0.6 ‰. The average $\delta^{13}\text{C}$ of the internal standard norleucine over all analytical sessions was -28.2 ± 0.6 ‰ (SD). A value of -27.8 ‰ was obtained for the same standard using a Costech elemental combustion system (ECS 4010) connected to a Thermo-Scientific Delta V IRMS.

4.2.4 Amino acid profiles

Amino acid profiles were obtained at the Advanced Protein Technology Centre, located in the Sick Kids Hospital, Toronto, Canada. The collagen samples were hydrolysed using a Waters Pico-Tag Workstation. The amino acids were derivatized, and measured using a Waters Acquity Ultra Performance Liquid Chromatography System.

Lab ID	Species	Ala	Glu	Gly	Hyp	Leu	Phe	Pro	Thr	Val	$\delta^{13}\text{C}_{\text{Bulk}}$
YT 1RD	Mammoth	-25.2±0.8	-18.4±0.2	-15.4±1.1	-21.2±0.4	-26.2±0.6	-28.5±0.3	-22.5±0.4	-15.2±1.1	-28.7±0.4	-21.5
YT 2RD	Mammoth	-25.6±0.7	-17.9±0.2	-14.7±1.0	-22.0±0.3	-27.4±0.4	-28.4±0.4	-23.6±0.3	-16.5±1.1	-29.9±0.2	-21.4
YT 3D	Mammoth	-25.1±1.1	-19.5±0.3	-11.2±1.0	-21.7±0.5	-25.8±1.0	-28.0±0.4	-23.0±0.5	-13.6±1.4	-29.6±0.8	-20.9
YT 4B	Mammoth	-22.6±0.8	-19.3±0.7	-13.1±0.6	-22.0±0.4	-27.8±0.4	-27.6±1.1	-22.8±0.3	-14.5±1.1	-27.9±0.2	-21.8
YT 5RD	Mammoth	-23.9±0.6	-17.9±0.3	-11.3±1.3	-21.3±0.6	-25.7±0.5	-27.8±0.2	-22.0±0.5	-13.8±1.0	-28.2±0.3	-21.4
YT 6C	Mammoth	-22.5±0.7	-19.3±0.5	-12.4±0.6	-21.5±0.3	-29.5±0.5	-27.9±0.5	-22.6±0.3	-14.7±0.9	-28.7±0.1	-21.7
YT 7B	Mammoth	-24.5±0.8	-19.6±0.1	-16.5±0.7	-23.2±0.4	-28.1±0.3	-28.6±0.4	-24.2±0.1	-18.9±1.0	-31.9±0.2	-21.4
YT 9C	Mammoth	-24.9±0.7	-20.5±0.1	-13.5±0.5	-22.4±0.3	-26.5±0.5	-29.4±0.3	-23.4±0.1	-17.8±1.0	-30.1±0.6	-21.5
YT 10RD	Mammoth	-24.9±0.6	-18.5±1.3	-16.2±0.7	-21.9±1.2	-26.7±0.4	-28.2±1.6	-23.0±0.3	-15.1±1.9	-28.1±0.6	-21.5
YT 11C	Mammoth	-24.9±0.6	-20.0±0.4	-16.1±0.9	-22.6±0.4	-27.6±0.7	-28.5±0.3	-23.5±0.3	-17.6±1.0	-30.1±1.3	-21.5
YT 11RD	Mammoth	-26.6±0.6	-20.7±0.2	-16.7±0.7	-23.1±0.3	-28.1±0.4	-29.5±0.3	-24.2±0.4	-19.4±1.2	-31.5±0.7	-21.5
YT 51T	Mammoth	-24.9±0.6	-16.8±0.3	-13.8±1.0	-20.8±0.5	-27.5±0.8	-28.1±0.4	-21.4±0.3	-16.4±1.0	-29.2±0.2	-20.7
	Mammoths	-24.6±1.1	-19.0±1.1	-14.2±2.0	-22.0±0.7	-27.2±1.1	-28.4±0.6	-23.0±0.8	-16.1±2.0	-29.5±1.3	-21.4±0.3
AMNH 1	Giant beaver	-14.6±0.6	-14.0±0.8	-6.0±0.6	-17.0±0.7	-21.8±0.5	-23.0±0.5	-18.6±0.5	-9.0±0.9	-23.0±0.2	-18.8
YT 8D	Mastodon	-24.3±1.1	-18.6±0.3	-13.2±1.0	-22.1±0.5	-27.5±1.0	-27.4±0.4	-22.8±0.5	-12.9±1.4	-29.5±0.8	-20.6

Table 4.2 continues on next page.

Lab ID	Species	Ala	Glu	Gly	Hyp	Leu	Phe	Pro	Thr	Val	$\delta^{13}\text{C}_{\text{Bulk}}$
YT129B	Horse	-19.9±0.6	-17.1±0.1	-9.6±0.8	-17.1±0.9	-22.0±0.6	-27.9±0.3	-21.3±0.1	-11.9±1.4	-24.7±1.5	-20.8
YT130B	Horse	-20.4±0.9	-17.2±1.7	-7.0±1.1	-18.3±1.1	-21.7±1.0	-26.8±1.7	-21.9±1.3	-11.3±1.0	-28.2±0.8	-21.1
YT131B	Horse	-22.1±0.6	-17.3±0.1	-14.6±2.4	-19.6±0.4	-23.8±1.3	-27.0±0.3	-22.4±0.1	-12.9±1.0	-30.7±0.6	-20.7
YT132B	Horse	-22.1±0.6	-18.0±0.3	-12.7±0.8	-19.6±0.3	-24.3±0.2	-26.5±0.2	-22.6±0.2	-13.7±1.1	-32.6±0.8	-21.2
YT133B	Horse	-22.2±0.8	-18.0±0.2	-12.7±1.0	-19.8±0.3	-24.9±0.3	-26.4±0.3	-22.7±0.2	-13.8±1.0	-32.0±0.9	-20.9
	Horses	-21.4±1.1	-17.5±0.4	-11.3±3.0	-18.9±1.2	-23.4±1.4	-26.9±0.6	-22.2±0.6	-12.7±1.1	-29.7±3.2	-20.9±0.2
YT 68B	Brown bear	-20.8±0.8	-18.3±0.2	-6.0±0.6	-17.2±0.3	-24.2±0.2	-25.4±0.6	-19.9±0.6	-10.7±0.9	-23.8±0.2	-18.8
YT 81B	Short-faced bear	-23.9±0.6	-18.8±0.2	-8.7±0.7	-19.3±0.3	-22.8±0.3	-26.8±0.2	-21.3±0.2	-11.4±1.0	-25.4±0.2	-19.7
YT 82B	Homotherium serum	-20.9±0.6	-18.0±0.2	-9.5±0.6	-18.8±0.4	-23.7±0.2	-27.1±0.3	-21.4±0.1	-13.0±1.0	-25.4±0.2	-19.0
YT 84B	Brown bear	-22.4±0.6	-17.1±0.1	-8.7±0.7	-18.6±0.4	-23.9±0.2	-26.4±0.3	-21.5±0.1	-11.9±1.0	-26.2±0.5	-19.8
AMNH 3B	Canid	-21.3±0.7	-19.6±0.6	-10.0±0.7	-19.8±0.4	-25.7±0.2	-27.4±0.3	-22.0±0.3	-11.9±0.9	-25.0±0.5	-19.7
	Carnivores	-21.8±1.3	-18.4±0.9	-8.6±1.6	-18.7±1.0	-24.1±1.1	-26.6±0.8	-21.2±0.8	-11.8±0.8	-25.2±0.9	-19.4±0.4
YT 83B	Holocene brown bear	-17.5±1.0	-17.1±0.1	-4.7±0.6	-17.3±0.3	-22.8±0.5	-25.6±0.4	-19.8±0.2	-12.5±1.0	-24.7±0.4	-18.2

Table 4.2 $\delta^{13}\text{C}$ for bulk collagen and individual amino acids. The carbon isotopic compositions of the specimens' amino acids and bulk collagen are listed for all samples, along with the SD of duplicate measurements for the amino acids. Amino acids and tissues are labelled as in Table 1. The average $\delta^{13}\text{C}$ (and SD) for each species or group of animals is also provided. The bulk collagen isotopic compositions of the mammoths and mastodons were previously reported (Metcalf, 2011; Metcalfe et al., 2010)

4.2.5 Radiocarbon dating

The majority of samples were dated previously (Chapter 3; Metcalfe, 2011; Metcalfe et al., 2010; Schwartz-Narbonne et al., 2015). Radiocarbon dates for the two additional samples included in the present study were obtained following the same procedure at the University of Arizona Accelerator Mass Spectrometry (AMS) Laboratory, and are reported in Appendix H. All dates are reported as uncalibrated radiocarbon years before present (1950).

4.2.6 Mathematical treatment

Previous work has established isotopic “fingerprints” for aquatic plants, bacteria, fungi and terrestrial plants using their carbon isotopic compositions (Larsen et al., 2013, 2012, 2009). As the samples from Larsen et al. (2012, 2009) were collected in 2007, a Suess effect correction of +1.67 ‰ was applied to the 2007 data to correct it to the Pleistocene data using the formula from Long et al. (2005). LDA was then applied to the Larsen et al. dataset to separate the four groups based on the $\delta^{13}\text{C}$ values of 7 amino acids (Ala, Glu, Leu, Phe, Pro, Thr, Val). Samples were included only when all seven amino acid carbon isotopic compositions were measured. Each herbivore and carnivore sample from this study was then classified using LDA to predict its membership in each group. The MASS package (Venables and Ripley, 2002) was used to perform the LDA in R version 3.1.1 (R Core Team, 2014) using the R Studio interface version 0.98.1083.

4.3 Results

4.3.1 Evaluation of collagen extraction and hydrolysis technique

Amino acid profiles were obtained for tissues at a variety of stages of preparation: whole tissue, extracted collagen and hydrolysed collagen (Fig. 4.3; Appendix J). These tissues included a modern cow bone (KFC), an archaeological human bone, (REG97), and mastodon crown dentin, (YT8D). The amino acid profiles for the human bone sample were presented previously by Olsen et al. (2010). The data were compared to previously published amino acid profiles of mammal bone (Szpak, 2011) to assess the integrity of the collagen extraction and hydrolysis technique. The whole bone has substantially

different amino acid profiles than collagen. The extracted and hydrolysed collagen, however, have the expected amino acid profiles. This outcome indicates that the collagen extraction successfully removed the non-collagenous proteins, and that hydrolysis did not cause preferential loss of some amino acids.

4.3.2 Sample preservation

The preservation of the collagen from the two additional samples used in this analysis was considered following the typical criteria. Samples are considered well-preserved if they have a collagen yield >1%, a C/N ratio between 2.9 to 3.6, carbon content ≥ 13 wt.% and nitrogen content ≥ 4.8 wt.% (Ambrose, 1990; DeNiro, 1985; van Klinken, 1999). The brown bear sample met these criteria, but the collagen yield for the giant beaver was too low (Appendix H). An infinite radiocarbon date was obtained for the giant beaver sample. As previously suggested for Old Crow by Harington (2011), such a date could suggest that the giant beaver lived in this area during an interglacial period, as has also been interpreted from infinite radiocarbon dates obtained for Beringian mastodons (Zazula et al., 2014).

4.3.3 Bulk collagen stable isotope compositions

The $\delta^{13}\text{C}_{\text{Bulk}}$ and $\delta^{15}\text{N}_{\text{Bulk}}$ are displayed in Figure 4.4. The general pattern of $\delta^{15}\text{N}_{\text{Bulk}}$ has been described previously (Chapter 3; Schwartz-Narbonne et al., 2015). Mastodon has the lowest $\delta^{15}\text{N}_{\text{Bulk}}$. Beaver and some horse samples also have low $\delta^{15}\text{N}_{\text{Bulk}}$, while other horse samples and all woolly mammoths have high $\delta^{15}\text{N}_{\text{Bulk}}$. Three of five horse specimens were dated. The horse with the lowest $\delta^{15}\text{N}_{\text{Bulk}}$ has an infinite date, whereas the horse dated to 27,180 ^{14}C BP has a $\delta^{15}\text{N}_{\text{Bulk}}$ ~ 3 ‰ higher. The horse with the highest $\delta^{15}\text{N}_{\text{Bulk}}$ was dated to 18,370 ^{14}C BP. The mastodon and woolly mammoth samples have infinite dates, precluding investigation of radiocarbon date-dependent patterns in isotopic composition.

Two of the carnivore specimens, the canid and the scimitar cat, have infinite radiocarbon dates. The short-faced bear specimen was not dated, but this species went extinct by the end of the Pleistocene (Barnes et al., 2002). Brown bears were present in high latitudes

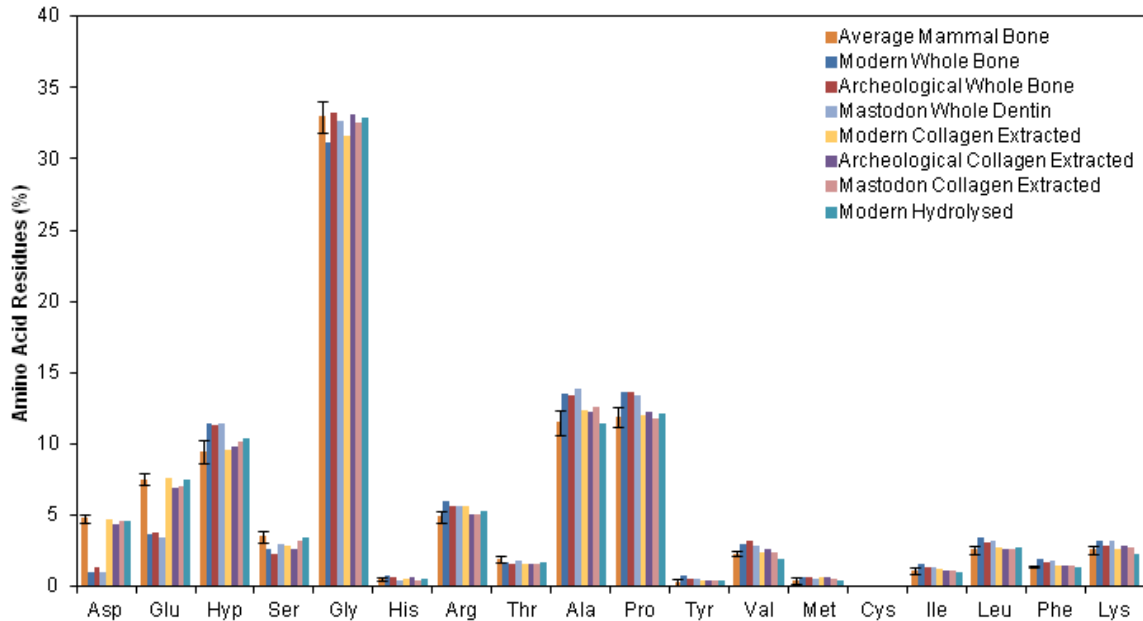


Figure 4.3 Amino acid profiles of samples after a variety of treatments. The modern bone measured was a cow femur. The archeological bone is a human rib bone and its amino acid profile was presented previously by (Olsen et al., 2010). The average mammal bone amino acid profile and SD is taken from (Szpak, 2011). Amino acid profiles are presented as the percentage of the tissue comprising each amino acid.

through the Pleistocene and Holocene (Barnes et al., 2002). A date of 5,941 ^{14}C BP was obtained for one brown bear sample, but radiocarbon dates for the other two samples have not yet been obtained. The undated carnivores and those dated to the Pleistocene have high $\delta^{15}\text{N}_{\text{Bulk}}$, similar to the woolly mammoth. The Holocene brown bear, however, has a lower $\delta^{15}\text{N}_{\text{Bulk}}$ than any other carnivore or woolly mammoth sample described in this paper. The two undated brown bears have the highest and lowest $\delta^{15}\text{N}_{\text{Bulk}}$ of the other carnivores.

The woolly mammoths tend to have the lowest $\delta^{13}\text{C}_{\text{Bulk}}$ of all the species, followed by horse and then mastodon. Of the three dated horses, the horse having an infinite radiocarbon date has the lowest $\delta^{13}\text{C}_{\text{Bulk}}$, while the other two horses have virtually identical carbon isotopic compositions. The giant beaver has a higher $\delta^{13}\text{C}_{\text{Bulk}}$ than any of the other herbivores, and is the only herbivore whose $\delta^{13}\text{C}_{\text{Bulk}}$ overlaps with those of the

carnivores. Of the carnivores, the Holocene brown bear has the highest $\delta^{13}\text{C}_{\text{Bulk}}$, whereas the undated brown bears have the highest and lowest $\delta^{13}\text{C}_{\text{Bulk}}$ of the remaining carnivores.

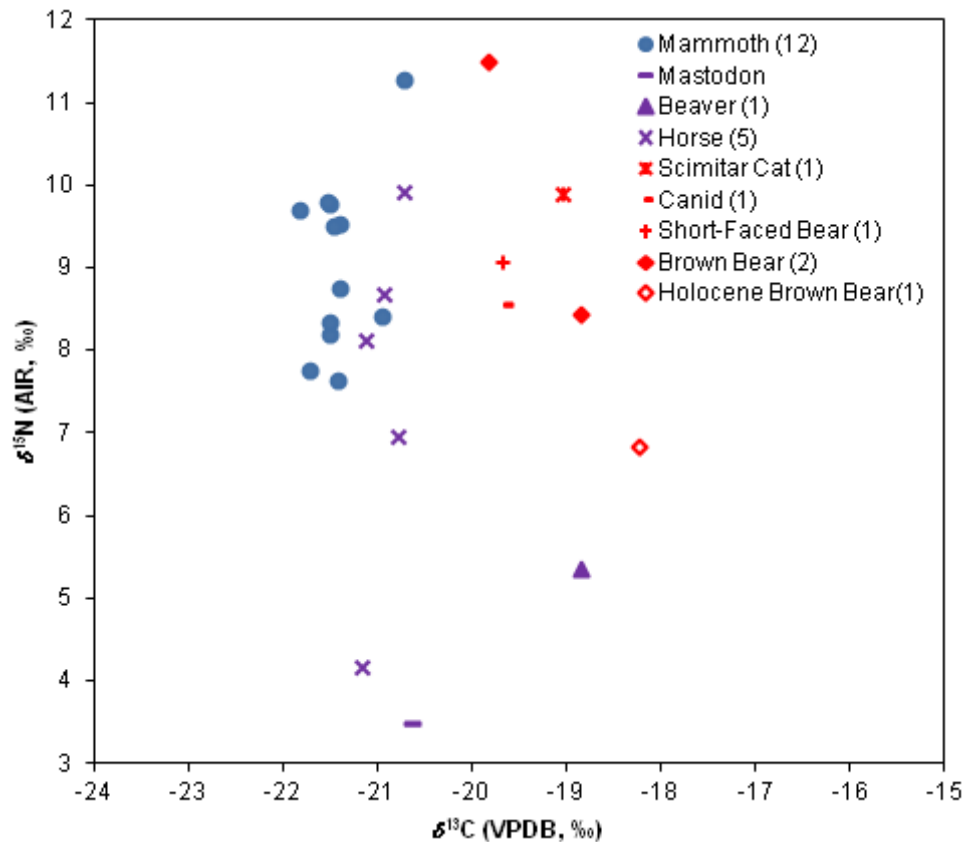


Figure 4.4 $\delta^{13}\text{C}$ and $\delta^{15}\text{N}$ of bulk collagen for all samples. Values in parentheses in the legend indicate the number of specimens.

4.3.4 Inter-tissue differences

For most species, only a single tissue type (bone or crown dentin) was analyzed. Previous work (Metcalf, 2011), however, suggested that there might be differences in isotopic compositions of woolly mammoth collagen from different tissues at some sites.

Therefore, five tissue types were measured for the woolly mammoth (Appendix J), including tusk, root dentin, cementum and bone from adult mammoths. Root dentin from a juvenile mammoth, for which the $\delta^{13}\text{C}_{\text{Bulk}}$ and $\delta^{15}\text{N}_{\text{Bulk}}$ was reported previously by Metcalfe et al. (2010), and dentin from a mastodon were also examined (Appendix J).

The amino acid profiles of these samples were obtained to determine if differences in

$\delta^{13}\text{C}_{\text{Bulk}}$ and $\delta^{15}\text{N}_{\text{Bulk}}$ were related to variation in the amino acid profile of the collagen (Fig. 4.5). There was little variation in the amino acid profile among these tissues, or from average mammalian bone collagen amino acid profiles (Szpak, 2011). Hence, differences in isotopic composition among the collagen from the various tissues do not result from atypical amino acid profiles.

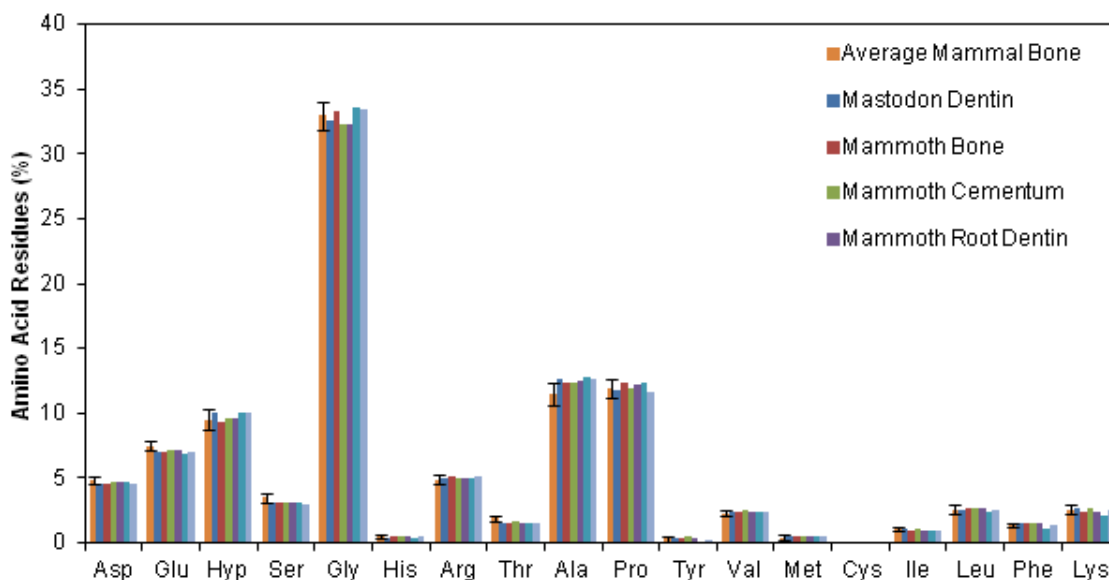


Figure 4.5 Amino acid profiles for various mammalian tissue types from Old Crow samples. Amino acid profiles are presented as the percentage of the tissue comprising each amino acid. The average mammal bone amino acid profile and SD is taken from (Szpak, 2011).

Woolly mammoth tusk has higher $\delta^{15}\text{N}_{\text{Bulk}}$ than the other tissues (Fig. 4.6a; Table 4.1). Crown dentin and root dentin have higher average $\delta^{15}\text{N}_{\text{Bulk}}$ than cementum. Tusk also has the highest average $\delta^{15}\text{N}$ for Ala, Glu, Gly, Hyp and Pro, but it does not have the highest value for Phe, Thr or Val. Crown dentin has higher average $\delta^{15}\text{N}$ than cementum for Ala, Glu, Phe, Pro, Thr and Val, lower average $\delta^{15}\text{N}_{\text{Gly}}$, and overlapping $\delta^{15}\text{N}_{\text{Hyp}}$ (within SD) with cementum $\delta^{15}\text{N}_{\text{Hyp}}$. Root dentin $\delta^{15}\text{N}$ and cementum have the same $\delta^{15}\text{N}$ (within SD) for most amino acids, though the root dentin has higher $\delta^{15}\text{N}$ for Thr and Val.

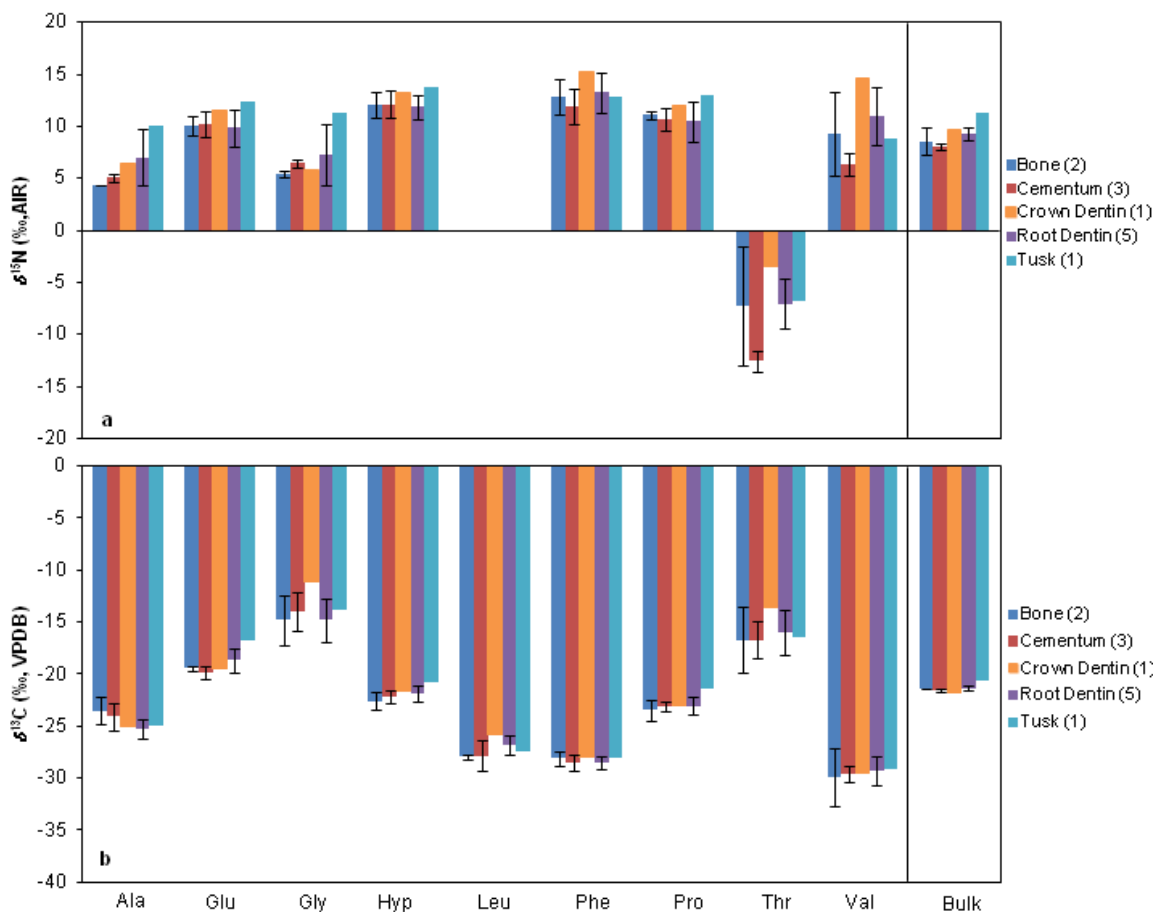


Figure 4.6 Amino acid: a. $\delta^{13}\text{C}$; b. $\delta^{15}\text{N}$ in a variety of woolly mammoth tissues.

Values in parentheses in the legend are the number of tissues measured. Error bars (whiskers) show SD.

There are no large isotopic differences in $\delta^{13}\text{C}_{\text{Bulk}}$ between tissues (Fig. 4.6b; Table 4.2). The tusk has the highest $\delta^{13}\text{C}_{\text{Bulk}}$ and the crown dentin the lowest, with the other three tissues having values that overlap (within SD). In most cases, individual amino acids also have $\delta^{13}\text{C}$ that overlap (within SD) with the same amino acids in the other tissues. The only exceptions are tusk $\delta^{13}\text{C}_{\text{Glu}}$, $\delta^{13}\text{C}_{\text{Hyp}}$, and $\delta^{13}\text{C}_{\text{Pro}}$, which are higher than $\delta^{13}\text{C}_{\text{Glu}}$, $\delta^{13}\text{C}_{\text{Hyp}}$, and $\delta^{13}\text{C}_{\text{Pro}}$ of other tissues, and crown dentin $\delta^{13}\text{C}_{\text{Gly}}$, which is higher than $\delta^{13}\text{C}_{\text{Gly}}$ of other tissues.

4.3.5 Amino acid $\delta^{15}\text{N}$

Three source amino acids were analyzed in this study: Gly, Phe and Thr (Figs. 4.7a-c;

Table 4.1). The results for phenylalanine have been presented previously (Chapter 3; Schwartz-Narbonne et al., 2015). The woolly mammoth generally has higher $\delta^{15}\text{N}_{\text{Bulk}}$ than the other herbivores and carnivores, with some overlap with horse and one carnivore (Fig. 4.7a). The undated brown bear with the highest $\delta^{15}\text{N}_{\text{Bulk}}$ of the carnivores shows overlap in $\delta^{15}\text{N}_{\text{Phe}}$ with the woolly mammoth having the lowest $\delta^{15}\text{N}_{\text{Phe}}$. Four of five horses show overlap in $\delta^{15}\text{N}_{\text{Phe}}$ with woolly mammoths. The horse with the lowest $\delta^{15}\text{N}_{\text{Bulk}}$ and an infinite radiocarbon date also has the lowest $\delta^{15}\text{N}_{\text{Phe}}$.

All Pleistocene and undated carnivore samples have lower $\delta^{15}\text{N}_{\text{Thr}}$ than the Pleistocene herbivores (Fig. 4.7b). The Holocene brown bear is the only carnivore with a higher $\delta^{15}\text{N}_{\text{Thr}}$ than at least one herbivore, being higher than that of the mastodon and one woolly mammoth. There was complete overlap between horse and the woolly mammoth $\delta^{15}\text{N}_{\text{Thr}}$. These two species have the highest $\delta^{15}\text{N}_{\text{Thr}}$ of all species examined in this study.

Woolly mammoths have the highest $\delta^{15}\text{N}_{\text{Gly}}$, with some overlap with mastodon and horse (Fig. 4.7c). The two horse samples (undated, 18,370 ^{14}C BP) with the highest $\delta^{15}\text{N}_{\text{Bulk}}$ also have the highest $\delta^{15}\text{N}_{\text{Gly}}$, overlapping those of mammoth. Carnivore $\delta^{15}\text{N}_{\text{Gly}}$ is generally lower than that of woolly mammoth, mastodon, giant beaver and some horse samples. The only exception is for the brown bear with the highest $\delta^{15}\text{N}_{\text{Bulk}}$; it also has a high $\delta^{15}\text{N}_{\text{Gly}}$, overlapping those of woolly mammoth. The Holocene brown bear had the lowest $\delta^{15}\text{N}_{\text{Gly}}$ of any of the specimens sampled here.

The trophic position of each species was examined by as follows:

$$\delta^{15}\text{N}_{\text{Trophic Amino Acid}} - \delta^{15}\text{N}_{\text{Source Amino Acid}} = \Delta^{15}\text{N}_{\text{Trophic-Source}}$$

Glutamate was always used as the trophic amino acid, and results for the three source amino acids compared. There is a range of several per mil in $\Delta^{15}\text{N}_{\text{Glu-Phe}}$ and $\Delta^{15}\text{N}_{\text{Glu-Thr}}$ of the herbivores and carnivores, but no overlap between them (Figs. 4.7d-e). There is overlap in $\Delta^{15}\text{N}_{\text{Glu-Gly}}$ between herbivores and carnivores (Fig. 4.7f). Woolly mammoth and mastodon have the lowest $\Delta^{15}\text{N}_{\text{Glu-Gly}}$. The woolly mammoth with the largest $\Delta^{15}\text{N}_{\text{Glu-Gly}}$ overlaps with those of the giant beaver and two horse samples, including one horse

with an infinite radiocarbon date, but the rest of the horse samples have higher $\Delta^{15}\text{N}_{\text{Glu-Gly}}$ than the woolly mammoth. Carnivore $\Delta^{15}\text{N}_{\text{Glu-Gly}}$ is generally higher than herbivore, but the brown bear with the highest $\delta^{15}\text{N}_{\text{Bulk}}$ and $\delta^{15}\text{N}_{\text{Gly}}$ has lower $\Delta^{15}\text{N}_{\text{Glu-Gly}}$ than any other carnivore, and overlaps the $\Delta^{15}\text{N}_{\text{Glu-Gly}}$ of some horses.

When considering all the herbivores together, the $\delta^{15}\text{N}_{\text{Bulk}}$ correlates positively with the $\delta^{15}\text{N}$ of phenylalanine, threonine and glycine (Fig. 4.8). These trends are not strong, with $R^2 = 0.4-0.5$. However, they are significant, with p values ≤ 0.01 .

4.3.6 Amino acid $\delta^{13}\text{C}$

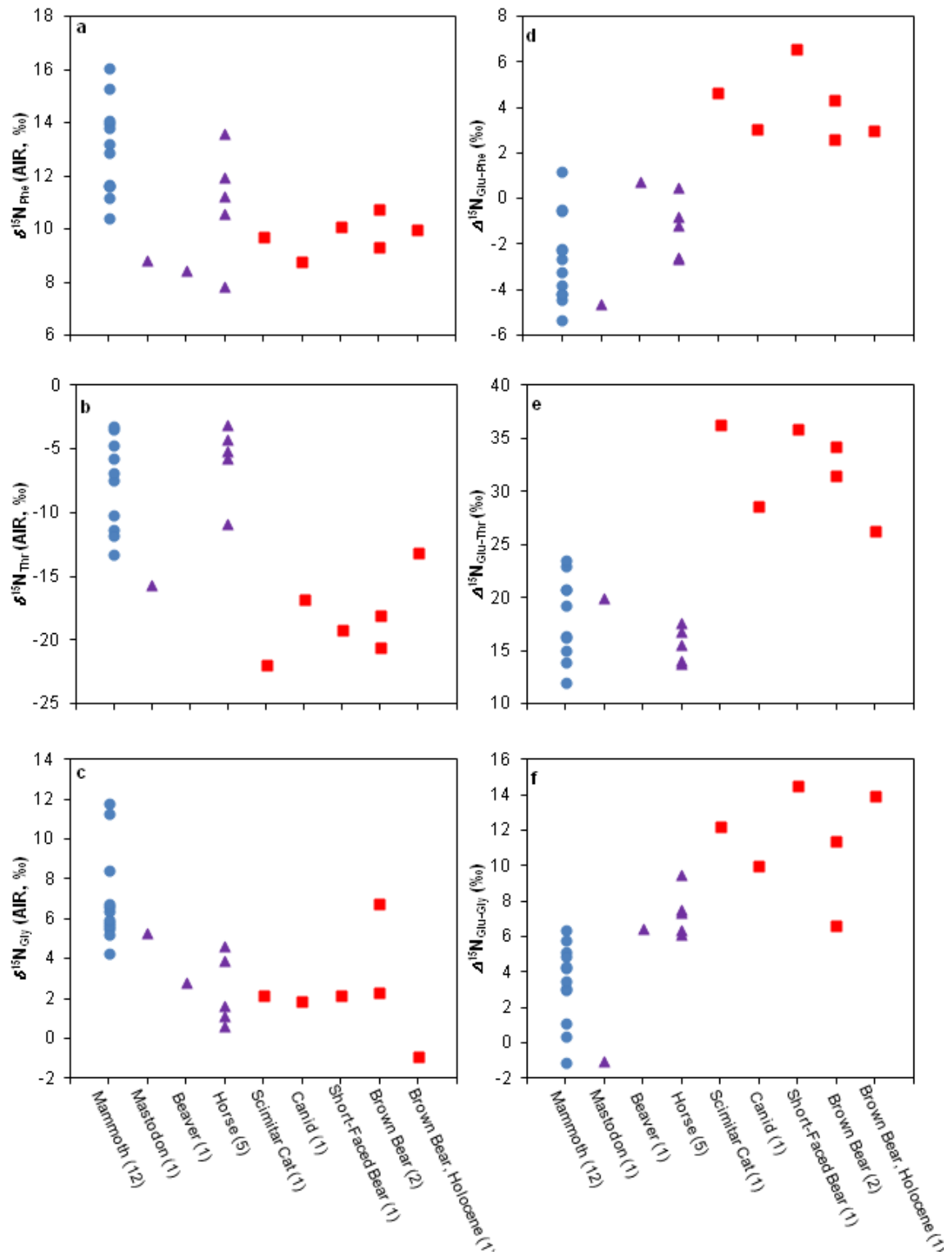
Values of $\delta^{13}\text{C}$ have been measured for four essential amino acids (Leu, Phe, Thr and Val; Table 4.2) and five nonessential amino acids (Ala, Glu, Gly, Hyp and Pro; Table 4.2). Larsen et al. (Larsen et al., 2009) highlighted leucine, isoleucine and lysine as the three most informative essential amino acids for classification of samples such as bacteria, plants or fungi using LDA. Because of analytical limitations, the $\delta^{13}\text{C}$ of isoleucine or lysine were not measured in the present study. To accurately classify groups, however, LDA requires that the amino acid $\delta^{13}\text{C}$ inputs are sufficiently distinct and informative between groups. As two of the most informative essential amino acids could not be included, it was considered beneficial to add nonessential amino acids to the classification. Addition of nonessential amino acids to the LDA analysis, however, requires that those amino acids had been directly routed from the diet and so would have a similar isotopic composition to their $\delta^{13}\text{C}$ in the diet.

Determining which amino acids were most likely directly routed from diet, and which were strongly affected by metabolic processes was accomplished by normalizing all amino acids carbon isotopic compositions in a specimen to its $\delta^{13}\text{C}_{\text{Bulk}}$ (Figs. 4.9a-d; Table 4.3):

$$\delta^{13}\text{C}_{\text{Amino Acid}} - \delta^{13}\text{C}_{\text{Bulk}} = \Delta^{13}\text{C}_{\text{Amino Acid-Bulk}}$$

This approach serves to remove the effects of consumption of plants with varying $\delta^{13}\text{C}$. The amount of variation in $\Delta^{13}\text{C}_{\text{Amino Acid-Bulk}}$ for a given amino acid can then be compared

within and between species (Table 4.3). Since most animals within a species are expected



Caption on facing page.

Figure 4.7 Nitrogen isotopic compositions of amino acids and amino acid pairs. Results for woolly mammoths are displayed as blue circles, other herbivores are displayed as purple triangles, and carnivores are displayed as red squares: a. Phenylalanine (source) amino acid nitrogen isotopic compositions ($\delta^{15}\text{N}_{\text{Phe}}$) of each species. These data have been presented previously (Chapter 3; Schwartz-Narbonne et al., 2015); b. Threonine (source) amino acid nitrogen isotopic compositions ($\delta^{15}\text{N}_{\text{Thr}}$) of each species; c. Glycine (source) amino acid nitrogen isotopic compositions ($\delta^{15}\text{N}_{\text{Gly}}$) of each species; d. Difference between the nitrogen isotopic composition of glutamate and phenylalanine ($\Delta^{15}\text{N}_{\text{Glu-Phe}}$) for each species. These data have been presented previously (Chapter 3; Schwartz-Narbonne et al., 2015); e. Difference between the nitrogen isotopic composition of glutamate and threonine ($\Delta^{15}\text{N}_{\text{Glu-Thr}}$) for each species; f. Difference between the nitrogen isotopic composition of glutamate and glycine ($\Delta^{15}\text{N}_{\text{Glu-Gly}}$) for each species.

to have eaten similar plants, more variation (i.e., larger SD) is predicted for the $\Delta^{13}\text{C}_{\text{Amino Acid-Bulk}}$ affected by metabolic processes than for amino acids that were directly routed from diet. Of the nine amino acids, glycine shows the greatest variation for woolly mammoth, and the second largest variation for horse (after valine), and was tied for alanine for the highest variation within the carnivores. Across all species, $\Delta^{13}\text{C}_{\text{Amino Acid-Bulk}}$ for glycine has second highest variation among the amino acids. Valine and alanine also have high variability of $\Delta^{13}\text{C}_{\text{Amino Acid-Bulk}}$, but not for all groupings of species. Based upon variation in $\Delta^{13}\text{C}_{\text{Amino Acid-Bulk}}$, glycine appears to be the amino acid, overall, that is most affected by metabolic processes. This suggests that glycine should not be used in the LDA. Since $\delta^{13}\text{C}_{\text{Gly}}$ is not considered in the LDA, its isotopic composition is examined individually. Woolly mammoth tends to have lower $\delta^{13}\text{C}_{\text{Gly}}$ than any of the other groups of species, followed by mastodon, which has the next lowest $\delta^{13}\text{C}_{\text{Gly}}$ (Table 4.2).

The $\delta^{13}\text{C}$ values of 8 amino acids other than glycine were measured (Ala, Glu, Hyp, Leu, Phe, Pro, Thr, Val). Of these, only the $\delta^{13}\text{C}$ of hydroxyproline was not measured in plants (Larsen et al., 2012, 2009). As mentioned earlier, only essential amino acids would

normally be used in LDA. The small degree of variability in the $\delta^{13}\text{C}$ of the nonessential amino acids other than glycine, however, suggests retention of isotopic composition from the diet. With this assumption in place, the dietary sources were first classified and defined using the $\delta^{13}\text{C}$ of these 7 amino acids, and then these linear functions were used to classify the diets of the consumers. The LDA classifications for the diet of each

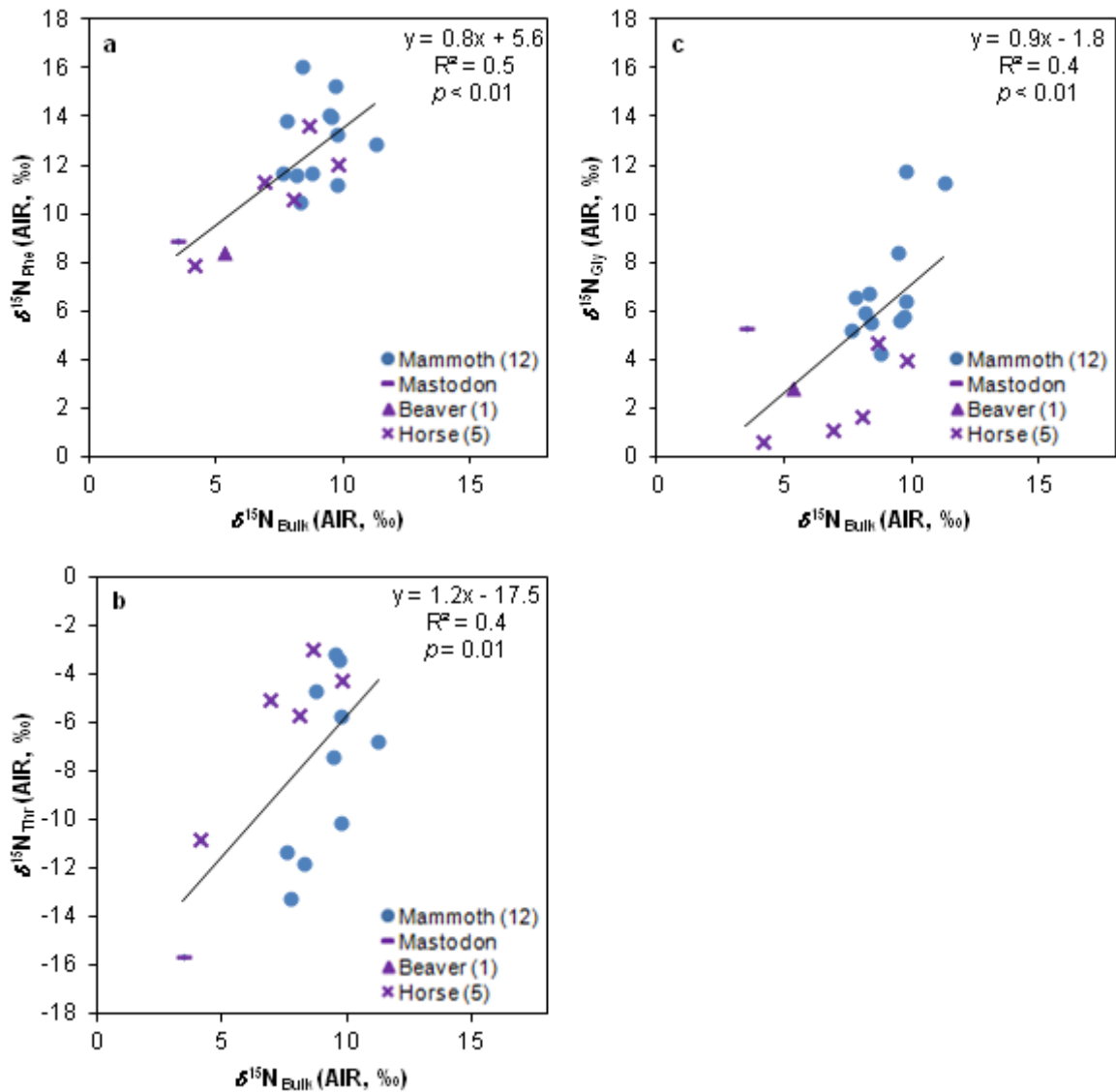


Figure 4.8 $\delta^{15}\text{N}$ of individual amino acids versus $\delta^{15}\text{N}_{\text{Bulk}}$ for all herbivores: a. $\delta^{15}\text{N}_{\text{Phe}}$; b. $\delta^{15}\text{N}_{\text{Thr}}$; c. $\delta^{15}\text{N}_{\text{Gly}}$. Trendline, R^2 and p value include data for all herbivores. Individual herbivores have distinct symbols and colours so that species-specific deviations from linearity can be observed.

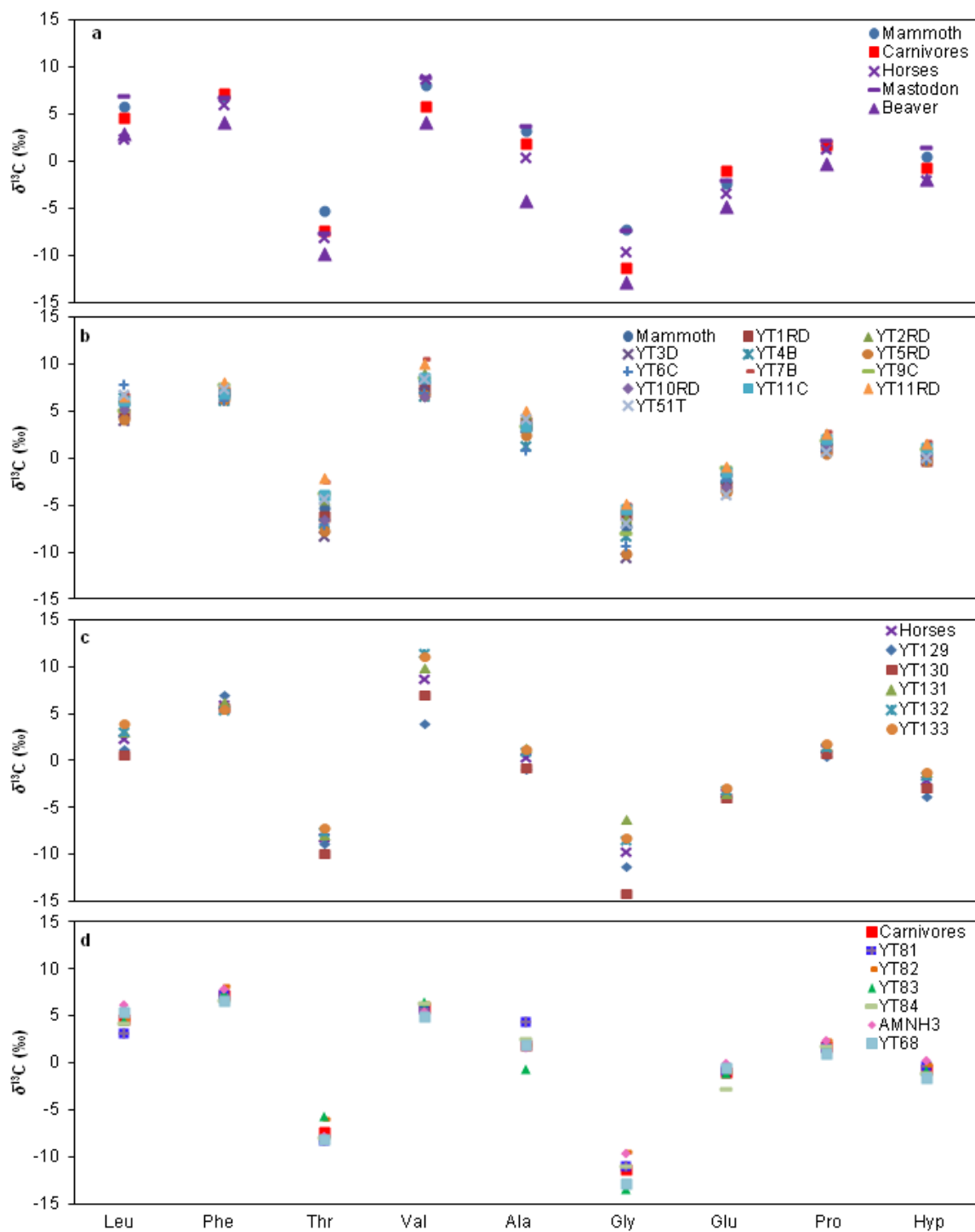


Figure 4.9 Normalized carbon isotopic compositions of amino acids ($\Delta^{13}\text{C}_{\text{Amino acid-Bulk}} = \delta^{13}\text{C}_{\text{Amino acid}} - \delta^{13}\text{C}_{\text{Bulk}}$): **a.** Average for species or groups of species; **b.** woolly mammoth; **c.** horse; **d.** carnivore.

Lab ID	Species	Leu	Phe	Thr	Val	Ala	Gly	Glu	Pro	Hyp
YT1RD	Mammoth	4.8	7.1	-6.2	7.3	3.8	-6.0	-2.9	1.1	-0.2
YT2RD	Mammoth	6.5	7.5	-4.4	9.0	4.7	-6.3	-3.0	2.7	1.1
YT3D	Mammoth	4.0	6.2	-8.2	7.8	3.3	-10.6	-2.3	1.2	-0.1
YT4B	Mammoth	6.4	6.2	-6.9	6.5	1.2	-8.2	-2.1	1.4	0.6
YT5RD	Mammoth	4.2	6.3	-7.7	6.8	2.4	-10.2	-3.5	0.5	-0.2
YT6C	Mammoth	7.8	6.2	-7.0	7.0	0.8	-9.3	-2.4	0.9	-0.2
YT7B	Mammoth	6.7	7.2	-2.5	10.5	3.1	-4.9	-1.8	2.8	1.8
YT9C	Mammoth	5.0	7.9	-3.7	8.6	3.4	-8.0	-1.0	1.9	0.9
YT10RD	Mammoth	5.2	6.7	-6.4	6.6	3.3	-5.3	-3.0	1.5	0.4
YT11C	Mammoth	6.2	7.0	-3.9	8.6	3.4	-5.4	-1.5	2.0	1.1
YT11RD	Mammoth	6.6	8.1	-2.1	10.1	5.1	-4.8	-0.8	2.7	1.6
YT51T	Mammoth	6.8	7.4	-4.3	8.5	4.2	-6.9	-3.9	0.7	0.1
	Average	5.8	7.0	-5.3	8.1	3.2	-7.2	-2.4	1.6	0.6
	SD	1.2	0.7	2.0	1.3	1.3	2.1	1.0	0.8	0.7
AMNH1	Giant beaver	3.0	4.1	-9.8	4.2	-4.2	-12.9	-4.9	-0.2	-1.8
YT8D	Mastodon	6.9	6.8	-7.7	8.9	3.6	-7.4	-2.0	2.1	1.5
YT129	Horse	1.3	7.1	-8.8	4.0	-0.9	-11.2	-3.7	0.5	-3.7
YT130	Horse	0.6	5.7	-9.8	7.1	-0.7	-14.1	-3.9	0.8	-2.8
YT131	Horse	3.0	6.2	-7.9	9.9	1.4	-6.2	-3.5	1.6	-1.2
YT132	Horse	3.2	5.3	-7.5	11.4	1.0	-8.4	-3.2	1.5	-1.6
YT133	Horse	4.0	5.5	-7.1	11.1	1.3	-8.2	-2.9	1.8	-1.1
	Average	2.4	6.0	-8.2	8.7	0.4	-9.6	-3.4	1.2	-2.1
	SD	1.4	0.7	1.1	3.2	1.1	3.1	0.4	0.6	1.1
YT68	Brown bear	5.3	6.6	-8.2	5.0	1.9	-12.9	-0.5	1.0	-1.7
YT81	Short-faced bear	3.1	7.2	-8.3	5.7	4.3	-11.0	-0.9	1.7	-0.4
YT82	Scimitar cat	4.7	8.0	-6.1	6.4	1.8	-9.5	-1.0	2.4	-0.2
YT83	Holocene brown bear	4.5	7.3	-5.7	6.5	-0.7	-13.5	-1.1	1.5	-0.9
YT84	Brown bear	4.1	6.6	-7.9	6.3	2.6	-11.1	-2.8	1.7	-1.2
AMNH3	Canid	6.1	7.8	-7.8	5.4	1.6	-9.7	0.0	2.3	0.2
	Average	4.6	7.3	-7.3	5.9	1.9	-11.3	-1.1	1.8	-0.7
	SD	1.0	0.6	1.1	0.6	1.6	1.6	0.9	0.5	0.7
	Avg. mammoth, avg. horse, avg carnivore, beaver and mastodon									
	SD	1.9	1.3	1.6	2.1	3.2	2.5	1.5	0.9	1.5

Table 4.3 $\Delta^{13}\text{C}$ of individual amino acids normalized to bulk collagen $\delta^{13}\text{C}$.

$\Delta^{13}\text{C}_{\text{Normalized}} = \delta^{13}\text{C}_{\text{Amino Acid}} - \delta^{13}\text{C}_{\text{Bulk}}$. The average $\Delta^{13}\text{C}$ and SD for each species or group of animals is also listed. The average SD of the average $\Delta^{13}\text{C}$ for each species is also listed.

individual animal are presented in Table 4.4, along with the posterior probabilities for

each classification. The posterior probabilities give a measure of how well the specimens fit into the group that they were assigned. With the exception of one brown bear, the various species are all considered to be well-classified, with posterior probabilities of $\geq 78\%$. Ten of the twelve mammoth specimens are classified as bacterial consumers, with the remaining two specimens classified as terrestrial plant consumers. These two mammoths do not have distinct $\delta^{15}\text{N}_{\text{Bulk}}$ from the other woolly mammoths, but they have the two lowest $\delta^{13}\text{C}_{\text{Bulk}}$. The mastodon is classified as a terrestrial-plant consumer. All horses are classified as bacterial consumers. The giant beaver is classified as an aquatic plant consumer.

Since carnivores consume primarily protein, it is assumed that the $\delta^{13}\text{C}$ of their amino acids reflects the amino acids of the herbivores they consumed, and thus the plants consumed by those herbivores. Using LDA, the majority of the carnivores are classified as having consumed animals that had consumed bacterial inputs, while the canid and one brown bear are classified as having consumed herbivores that had consumed terrestrial plants. The $\delta^{13}\text{C}_{\text{Bulk}}$ and $\delta^{15}\text{N}_{\text{Bulk}}$ of the canid are within the range of the other carnivores. However, this brown bear is more distinct. This brown bear has the highest $\delta^{13}\text{C}_{\text{Bulk}}$ and lowest $\delta^{15}\text{N}_{\text{Bulk}}$ of the undated brown bears. As well, its classification as a terrestrial plant consumer is not strong (posterior probability of terrestrial plants was 48%), making LDA a poor method of categorizing its diet.

4.4 Discussion

4.4.1 Inter-tissue variation

Variation in $\delta^{13}\text{C}_{\text{Bulk}}$ and $\delta^{15}\text{N}_{\text{Bulk}}$ of different woolly mammoth tissues almost certainly arises from differences in the isotopic composition of the component amino acids, since all tissues have similar amino acid profiles. The nitrogen isotopic variation observed between bulk collagen of different mammoth tissues is generally small (Fig. 4.6a; Table 4.1). In every case where $\delta^{15}\text{N}_{\text{Bulk}}$ differences are observed among tissues, these effects are also observed for both source and trophic amino acids. This result suggests that a metabolic effect was not the primary cause of these isotopic differences. Differences in growth rates, amino acid routing or other metabolic changes do not seem to be

controlling differences in $\delta^{15}\text{N}_{\text{Bulk}}$ among tissues. Instead, it seems that certain tissues may record $\delta^{15}\text{N}_{\text{Bulk}}$ from different plants or plant parts, or from plants grown in different environments.

There are minimal differences in the bulk collagen or individual amino acid $\delta^{13}\text{C}$ among tissues, and the ranges measured for most $\delta^{13}\text{C}$ of individual amino acids overlap among the tissues (Fig. 4.6b; Table 4.2). There are also no clear tissue-dependent patterns in plant consumption, as identified using LDA (Table 4.4). Tusk has the largest $\delta^{15}\text{N}_{\text{Bulk}}$ difference among these tissues, but only one tusk was sampled. As well, there is only one individual for which more than one tissue was sampled. This dataset is too small to demonstrate whether consistent isotopic differences exist between tissues or to explore the causes of these putative differences. Since the isotopic compositions are similar among tissues, all tissues are considered to be equivalent for the remainder of this discussion.

4.4.2 Dietary patterns suggested by $\delta^{15}\text{N}$

The general dietary patterns suggested by $\delta^{15}\text{N}_{\text{Phe}}$ and $\Delta^{15}\text{N}_{\text{Glu-Phe}}$ (Figs. 4.7a, d) have been discussed previously by (Chapter 3; Schwartz-Narbonne et al., 2015). Woolly mammoth consumed a diet of plants with high $\delta^{15}\text{N}$, which reflected a distinct dietary or habitat niche. Mammoth $\delta^{15}\text{N}_{\text{Phe}}$ is higher than those of mastodon, giant beaver, and most carnivores, and similar to those of horse, suggesting a shared dietary or habitat niche with some horses. Herbivore $\Delta^{15}\text{N}_{\text{Glu-Phe}}$ is lower than measured for carnivores, consistent with a trophic enrichment in ^{15}N of the carnivores. The negative $\Delta^{15}\text{N}_{\text{Glu-Phe}}$ of some herbivores has been reported in previous terrestrial studies (Chikaraishi et al., 2011; Ishikawa et al., 2014).

The low $\delta^{15}\text{N}_{\text{Bulk}}$ and $\delta^{15}\text{N}_{\text{Phe}}$ of the mastodon (Figs. 4.4; 4.7a) are consistent with previous interpretations that it ate mainly browse (Metcalf, 2011; Metcalfe et al., 2013). Its $\delta^{15}\text{N}_{\text{Bulk}}$ and $\delta^{15}\text{N}_{\text{Phe}}$ are lower than those of the giant beaver, which fits the interpretation that the giant beaver consumed aquatic plants with higher $\delta^{15}\text{N}$ than browse (Milligan et al., 2010; Perkins, 2009; Stuart-Williams et al., 1997). These two animals are

species that likely lived in Old Crow during interglacial periods when more browse and more aquatic vegetation would have been available (Harington, 2011; Grant D Zazula et al., 2014).

Lab ID	Species	Class	Aquatic producer	Bacteria	Fungi	Terrestrial plant
YT1RD	Mammoth	Bacteria	0	100	0	0
YT2RD	Mammoth	Bacteria	0	99	1	0
YT3D	Mammoth	Bacteria	0	100	0	0
YT4B	Mammoth	Terrestrial plant	1	0	15	84
YT5RD	Mammoth	Bacteria	0	99	0	0
YT6C	Mammoth	Terrestrial plant	0	0	4	96
YT7B	Mammoth	Bacteria	0	99	1	0
YT9C	Mammoth	Bacteria	0	100	0	0
YT10RD	Mammoth	Bacteria	0	98	1	1
YT11C	Mammoth	Bacteria	0	99	1	0
YT11RD	Mammoth	Bacteria	0	100	0	0
YT51T	Mammoth	Bacteria	0	78	15	8
AMNH1	Giant beaver	Aquatic producer	86	0	6	7
YT8D	Mastodon	Terrestrial plant	1	3	14	83
YT129	Horse	Bacteria	0	100	0	0
YT130	Horse	Bacteria	0	100	0	0
YT131	Horse	Bacteria	0	100	0	0
YT132	Horse	Bacteria	0	100	0	0
YT133	Horse	Bacteria	0	100	0	0
YT68	Brown bear	Terrestrial plant	7	14	31	48
YT81	Short-faced bear	Bacteria	0	100	0	0
YT82	Homotherium serum	Bacteria	0	100	0	0
YT83	Holocene brown bear	Bacteria	2	96	1	1
YT84	Brown bear	Bacteria	0	100	0	0
AMNH3	Canid	Terrestrial plant	2	4	8	86

Table 4.4 Linear discriminant analysis (LDA) classification of herbivore and carnivore diets. The most probable diet of each specimen is indicated, along with the posterior probabilities of these classifications.

Among the source amino acids, the patterns observed for $\delta^{15}\text{N}_{\text{Thr}}$ (Fig. 4.7b) and $\Delta^{15}\text{N}_{\text{Glu-Thr}}$ (Fig. 4.7e) are generally consistent with those suggested by $\delta^{15}\text{N}_{\text{Phe}}$. Overlap between woolly mammoth and horse $\delta^{15}\text{N}_{\text{Thr}}$ further suggest that woolly mammoth and horse shared a dietary or habitat niche that had high plant $\delta^{15}\text{N}$, and the lower values for

mastodon $\delta^{15}\text{N}_{\text{Thr}}$ again suggest that it consumed plant types such as browse that had lower $\delta^{15}\text{N}$. Consistent with the $\Delta^{15}\text{N}_{\text{Glu-Phe}}$ pattern, there is clear differentiation between the $\Delta^{15}\text{N}_{\text{Glu-Thr}}$ of the herbivores and the carnivores, again demonstrating their trophic separation.

The patterns observed using the third source amino acid, glycine (Fig. 4.7c), are generally similar to those obtained using the other two source amino acids. There are several differences, however, that again point to consumption of different plants that have distinct $\delta^{15}\text{N}$ amino acid fingerprints from each other. The mastodon has a higher $\delta^{15}\text{N}_{\text{Gly}}$ than would be expected based on the relative position of its $\delta^{15}\text{N}_{\text{Phe}}$ and $\delta^{15}\text{N}_{\text{Thr}}$ compared to the other animals. The mastodon and woolly mammoth have overlapping $\delta^{15}\text{N}_{\text{Gly}}$. It is possible that browse has a $\delta^{15}\text{N}$ amino acid fingerprint that is distinct from the graminoids and forbs that likely dominated the woolly mammoth diet, though no study of the $\delta^{15}\text{N}$ fingerprint of these plants types has been done so far.

The carnivores with the highest and lowest $\delta^{15}\text{N}_{\text{Bulk}}$ (the undated brown bear and the Holocene brown bear, respectively) also have the highest and lowest $\delta^{15}\text{N}_{\text{Gly}}$ of the carnivores, a pattern not observed for the other source amino acids. Since glycine comprises approximately a third of the amino acids in collagen, the glycine $\delta^{15}\text{N}$ may explain the $\delta^{15}\text{N}_{\text{Bulk}}$ of these carnivores. The fact that this pattern was observed in glycine but not in the other source amino acids again suggests a distinct $\delta^{15}\text{N}$ fingerprint for the plants eaten by the herbivores that the carnivores consumed. It has been suggested that $\delta^{15}\text{N}_{\text{Gly}}$ is a marker of plant decay (Calleja et al., 2013; Fogel and Tuross, 1999; Smallwood et al., 2003). On one hand, the particularly high $\delta^{15}\text{N}_{\text{Gly}}$ for the woolly mammoth, some horse samples and the undated brown bear may suggest the consumption of a large quantity of decayed plant material, which may have comprised winter or year-round fodder (Chapter 3; Schwartz-Narbonne et al., 2015; Tahmasebi, 2015). The much lower $\delta^{15}\text{N}_{\text{Gly}}$ of Holocene brown bear, on the other hand, may point to a shift in plant type or plant part being consumed following the Pleistocene.

The patterns observed for $\Delta^{15}\text{N}_{\text{Glu-Gly}}$ (Fig. 4.7f) further support the idea that some species consumed plants (or animals that consumed plants) that had different $\delta^{15}\text{N}$ fingerprints from each other. Rather than providing a clear separation between the herbivores and carnivores, a range of values is observed, with woolly mammoth $\Delta^{15}\text{N}_{\text{Glu-Gly}}$ overlapping with some but not all of the other herbivores. Using $\Delta^{15}\text{N}_{\text{Trophic amino acid} - \text{Source amino acid}}$ to determine trophic position relies on the assumption that the same processes affect the plants at the base of the food web for all species. This approach may not be valid for all amino acids if some species consume plants with different $\delta^{15}\text{N}$ amino acid fingerprints. This possibility should be considered in future work that applies this approach when comparing the trophic level of species with potentially distinct diets.

In general, herbivores with higher $\delta^{15}\text{N}_{\text{Bulk}}$ have higher $\delta^{15}\text{N}_{\text{Phe}}$, $\delta^{15}\text{N}_{\text{Thr}}$ and $\delta^{15}\text{N}_{\text{Gly}}$ (Fig. 4.8). This trend suggests that similar metabolic effects occurred, and that differences in the $\delta^{15}\text{N}_{\text{Bulk}}$ arise because of differences in the $\delta^{15}\text{N}$ of the plants at the base of the food chain. Deviations from this pattern may arise because of: (i) large analytical errors, (ii) metabolic effects, and (iii) differences in the $\delta^{15}\text{N}$ amino acid fingerprint of the various plant types that different species consumed. Again, this suggests that different plant $\delta^{15}\text{N}$ fingerprints play a role in the observed patterns. Future work should focus on determining $\delta^{15}\text{N}$ fingerprints for different dietary sources.

4.4.3 Dietary patterns suggested by $\delta^{13}\text{C}$

LDA is an emerging technique for identifying consumer diets, and it suffers from a relatively small dataset of dietary sources and little differentiation within the groups of dietary sources (Larsen et al., 2013, 2012, 2009). Here, only four dietary groups were used: aquatic producers, bacteria, fungi, and terrestrial plants. Within the groups, there is no differentiation between the $\delta^{13}\text{C}$ fingerprints of terrestrial graminoids, forbs or browse, or between different types of bacteria (Larsen et al., 2013, 2012, 2009). This means that such dietary classifications should be treated with caution at this stage of their development. Nonetheless, there is still value in applying this technique to assess species' diets, as is considered next.

Using LDA, the majority of woolly mammoth and all horse samples are classified as having consumed primarily bacterial diets (Fig. 4.10; Table 4.4). Since these species are non-ruminants, it is unlikely that the majority of their amino acids were derived from gut microbes. In this case, the bacterial content of their diet could reflect consumption a large quantity of decayed plants and their associated bacteria and microbes (Beare et al., 1990), as may have occurred during winter or year-round (Chapter 3; Putshkov, 2003; Schwartz-Narbonne et al., 2015; Tahmasebi, 2015). Consumption of decayed plants has been hypothesized to be an explanation for the high $\delta^{15}\text{N}$ of woolly mammoth (Chapter 3; Schwartz-Narbonne et al., 2015; Tahmasebi, 2015). Some woolly mammoth samples are classified by LDA as unmodified terrestrial plants consumers, which is also consistent with interpretations of a diet consisting of graminoids and forbs (Guthrie, 2001, 1982; Haynes, 1991). Why the LDA-driven classification of dietary inputs is different among the woolly mammoth samples is unknown, especially as there is no correlation with $\delta^{15}\text{N}_{\text{Bulk}}$ (Figs. 4.10c-d), as might be expected between animals consuming unmodified terrestrial plants and decayed plants. Similarly, the LDA-driven classification of all horse samples indicated primarily bacterial inputs to diet but only some samples have high $\delta^{15}\text{N}_{\text{Bulk}}$ (Figs. 4.10c-d). These discrepancies may suggest that while consumption of decayed plants may part be of the explanation for woolly mammoth high $\delta^{15}\text{N}_{\text{Bulk}}$, other aspects of dietary or habitat selection may also be involved. These discrepancies may also suggest that a larger database of plants and other dietary sources is necessary to provide a more robust classification, and that the currently available $\delta^{13}\text{C}$ fingerprints are insufficient to fully interpret megafaunal diets.

There are modern species that preferentially consume partially decayed plants. The North American pika, *Ochotona princeps*, caches plant material with high toxin levels and consumes it after decomposition has lowered the quantity of toxin in the forage (Dearing, 1997). In feeding trials, several species of freshwater herbivorous invertebrates were found to consume more decomposed plants than fresh plants, likely because of loss of toxins during decomposition, though changes in nutritional content may also have been a factor (Suren and Lake, 1989). Previous work has found that decayed plants have lower C/N ratios (Tahmasebi, 2015), and thus may be more nutritious for herbivores than

unmodified plants. Decayed plants are principally suggested as forage for herbivores in the winter, when minimal forage is not available. It is also possible that some species preferentially selected decomposing forage year-round.

The LDA-driven classification of a diet of aquatic producers for the giant beaver matches other dietary reconstructions for this species (Perkins, 2009; Stuart-Williams et al., 1997). Likewise, the mastodon was found to have consumed unmodified terrestrial plants, consistent with previous reconstructions of a browse diet (Metcalf, 2011; Metcalf et al., 2013). Such diets are also consistent with the hypotheses that giant beaver and mastodon lived during interglacial periods (Harington, 2011; Zazula et al., 2014) when more aquatic habitats might have been available in Old Crow. If animals ate decayed plants to survive winters during glacial periods, there may have been less need to consume decayed plants during interglacial periods.

For the most part, the LDA-driven classification suggests that carnivores consumed herbivores that had consumed bacteria. However, the $\delta^{15}\text{N}$ of carnivore source amino acids are low, which is not consistent with a diet of herbivores that ate decayed plants with high source amino acid $\delta^{15}\text{N}$. An alternative explanation is that these carnivores ate ruminant species and that the gut microbes in the ruminants' digestive tract were the source of the bacterial classification. Gut microbes have been suggested as the source of bacterial classification of diets in previous work, though they have not been studied specifically in ruminants (Arthur et al., 2014; Larsen et al., 2011). Previous work on Alaskan carnivores suggests that ruminant species may have been part of the diet for gray wolves, scimitar cats and some brown bears, and that short-faced bears and other brown bears primarily consumed caribou, a ruminant species (Fox-Dobbs et al., 2008). Using LDA, the canid is classified as a consumer of herbivores that consumed mainly unmodified terrestrial plants, which may indicate that it fed mainly on non-ruminant rather than ruminant species.

One of the undated brown bears is classified as having consumed herbivores that ate unmodified terrestrial plants, with a weak LDA classification (low posterior probabilities for this specimen's LDA classification). It is possible that this bear ate herbivores that

had eaten a mixed diet or ate a variety of herbivores with different diets; the LDA approach is not well suited to classification of mixed diets (Larsen et al., 2012).

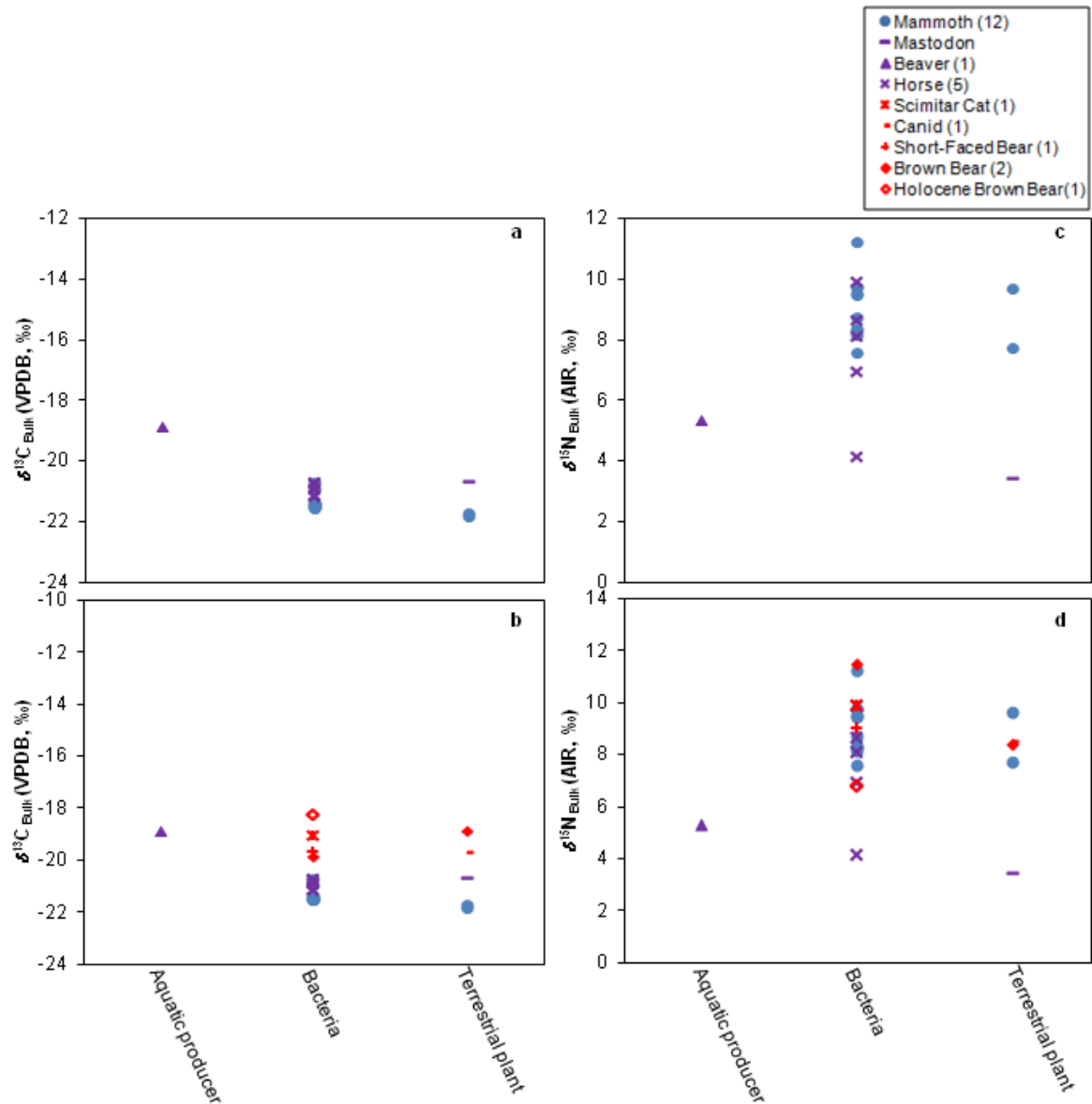


Figure 4.10 LDA Dietary classifications versus: a. $\delta^{13}\text{C}_{\text{Bulk}}$ for each herbivore species; b. $\delta^{13}\text{C}_{\text{Bulk}}$ for all species; c. $\delta^{15}\text{N}_{\text{Bulk}}$ for each herbivore species; d. $\delta^{15}\text{N}_{\text{Bulk}}$ for all species. Values in parentheses in the legend indicate the number of samples analyzed.

A Bayesian analysis could help to elucidate the exact dietary compositions of the species consumed, if a larger baseline database could be assembled (Larsen et al., 2013). It is also

possible that this bear consumed herbivores that ate a dietary input whose $\delta^{13}\text{C}$ amino acid fingerprint has yet to be characterized. For example, there is no distinction between different types of terrestrial plants currently built into the LDA groups of dietary sources.

This study found glycine to be the amino acid having the most variable $\delta^{13}\text{C}$. This variability has been observed in earlier studies, which suggest its relationship to other portions of the diet such as lipids or carbohydrates (Jim et al., 2006). Woolly mammoth has the lowest $\delta^{13}\text{C}_{\text{Gly}}$ of any of the species analyzed here, followed by mastodon (Table 4.2). It is possible that proboscideans had a greater lipid input to the $\delta^{13}\text{C}$ of their glycine, and that this is responsible for their low $\delta^{13}\text{C}_{\text{Bulk}}$.

4.5 Conclusion

A combined interpretation of amino acid $\delta^{15}\text{N}$ and $\delta^{13}\text{C}$ provides valuable insight into the diets of Old Crow herbivores and carnivores. The majority of woolly mammoths analyzed consumed a diet with a strong bacterial amino acid isotopic signal, which may reflect significant consumption of decayed plants. The nitrogen isotopic composition of the source amino acids, particularly the high values for glycine, support the hypothesis that mammoths may have obtained a portion of their protein from bacteria associated consumption of decayed plants. Mastodon and some woolly mammoths consumed a diet of unmodified terrestrial plants. Additional investigation of carbon and nitrogen isotope plant amino acid fingerprints is needed to differentiate whether those terrestrial plants were browse for the mastodon and either graminoids or forbs, or both, for the woolly mammoth. The low $\delta^{13}\text{C}$ of glycine for woolly mammoth and mastodon may suggest derivation of a large portion of their winter diet from stored lipids. Horse consumed a diet having a strong bacterial signal, and source amino acid $\delta^{15}\text{N}$ of horse and woolly mammoth commonly overlapped, which may suggest that they both consumed decayed plants. There is less overlap, however, between horse and woolly mammoth $\delta^{15}\text{N}_{\text{Gly}}$. This amino acid has been suggested to be a strong marker for degraded plants; hence the more limited overlap may suggest that more than one factor is at play in generating the high $\delta^{15}\text{N}$ of woolly mammoth and horse. Analysis of additional horse samples for which radiocarbon dates are available may provide insight into this question; the current small

dataset makes it impossible to determine whether the differences observed in horse $\delta^{15}\text{N}$ resulted from environmental changes over time or different dietary preferences. The giant beaver consumed aquatic plants at Old Crow, consistent with previous dietary reconstructions for this animal.

All species in this study known to be either carnivores or omnivores have been classified as carnivores on the basis of the separation in $\delta^{15}\text{N}$ between their trophic and source amino acids. There are differences, however, in their amino acid isotopic compositions that suggest different diets for the two undated brown bears, and that some carnivores consumed ruminants while others consumed non-ruminants. Future work focused the isotopic compositions of all the herbivore species present at Old Crow could utilize this information, in combination with SIAR analysis of $\delta^{13}\text{C}_{\text{Bulk}}$ and $\delta^{15}\text{N}_{\text{Bulk}}$, to obtain a more accurate understanding of carnivore diet in this portion of the mammoth steppe.

The Holocene brown bear has lower $\delta^{15}\text{N}_{\text{Bulk}}$ and higher $\delta^{13}\text{C}_{\text{Bulk}}$, and a distinct pattern of $\delta^{15}\text{N}$ for its source amino acids, notwithstanding its LDA-derived amino acid signature that suggests consumption of herbivores that primarily ate diets rich in bacteria. The climatic and environmental change during the Pleistocene to Holocene transition caused significant changes in the plant species that occupied the mammoth steppe. Further work on the $\delta^{15}\text{N}$ and $\delta^{13}\text{C}$ amino acid fingerprints this entire range of plant types may allow the diet of the Holocene brown bear (and other megafauna) to be better characterized and distinguished from the diet of the Pleistocene carnivores. Overall, combined analysis of amino acid carbon and nitrogen isotopic compositions of collagen can provide a much greater amount of information about the diets of megafauna species of the mammoth steppe ecosystem than can be obtained from isotopic analysis of bulk collagen.

4.6 References

- Ambrose, S., 1990. Preparation and characterization of bone and tooth collagen for isotopic analysis. *J. Archaeol. Sci.* 17, 431–451.
- Ambrose, S., 1991. Effects of diet, climate and physiology on nitrogen isotope abundances in terrestrial foodwebs. *J. Archaeol. Sci.* 18, 293–317.
- Amundson, R., Austin, A., Schuur, E.A.G., Yoo, K., Matzek, V., Kendall, C., Uebersax,

- A., Brenner, D., Baisden, W.T., 2003. Global patterns of the isotopic composition of soil and plant nitrogen. *Glob. Biogeochemical Cycles* 17. doi:10.1029/2002GB001903
- Arthur, K.E., Kelez, S., Larsen, T., Choy, C.A., Popp, B.N., 2014. Tracing the biosynthetic source of essential amino acids in marine turtles using $\delta^{13}\text{C}$ fingerprints. *Ecology* 95, 1285–1293. doi:10.1890/13-0263.1
- Barnes, I., Matheus, P., Shapiro, B., Jensen, D., Cooper, A., 2002. Dynamics of Pleistocene population extinctions in Beringian brown bears. *Science* 295, 2267–70. doi:10.1126/science.1067814
- Barnett, B., 1994. Carbon and nitrogen isotope ratios of caribou tissues, vascular plants, and lichens from northern Alaska. University of Alaska, Master's Thesis. Fairbanks.
- Beare, M.H., Neely, C.L., Coleman, D.C., Hargrove, W.L., 1990. A substrate-induced respiration (SIR) method for measurement of fungal and bacterial biomass on plant residues. *Soil Biol. Biochem.* 22, 585–594. doi:10.1016/0038-0717(90)90002-H
- Ben-David, M., Shochat, E., Adams, L., 2001. Utility of stable isotope analysis in studying foraging ecology of herbivores: examples from moose and caribou. *Alces* 37, 421–434.
- Bligh, E.G., Dyer, W.J., 1959. A rapid method of total lipid extraction and purification. *Can. J. Biochem. Physiol.* 37, 911–917. doi:10.1139/o59-099
- Bocherens, H., 2003. Isotopic biogeochemistry and the paleoecology of the mammoth steppe fauna. *Deinsea* 9, 57–76.
- Bocherens, H., Drucker, D., 2003. Trophic level isotopic enrichment of carbon and nitrogen in bone collagen: case studies from recent and ancient terrestrial ecosystems. *Int. J. Osteoarchaeol.* 13, 46–53. doi:10.1002/oa.662
- Bocherens, H., Drucker, D.G., Bonjean, D., Bridault, A., Conard, N.J., Cupillard, C., Germonpré, M., Höneisen, M., Münzel, S.C., Napierala, H., Patou-Mathis, M., Stephan, E., Uerpmann, H.-P., Ziegler, R., 2011. Isotopic evidence for dietary ecology of cave lion (*Panthera spelaea*) in North-Western Europe: prey choice, competition and implications for extinction. *Quat. Int.* 245, 249–261. doi:10.1016/j.quaint.2011.02.023
- Bocherens, H., Emslie, S., Billiou, D., Mariotti, A., 1995. Stables isotopes (^{13}C , ^{15}N) and paleodiet of the giant short-faced bear (*Arctodus simus*). *Comptes rendus l'Académie des Sci. Série 2. Sci. la terre des planètes* 320, 779–784.
- Bocherens, H., Pacaud, G., Lazarev, P.A., Mariotti, A., 1996. Stable isotope abundances (^{13}C , ^{15}N) in collagen and soft tissues from Pleistocene mammals from Yakutia: implications for the palaeobiology of the Mammoth Steppe. *Palaeogeogr. Palaeoclimatol. Palaeoecol.* 126, 31–44.

- Bol, R., Ostle, N.J., Petzke, K.J., 2002. Compound specific plant amino acid $\delta^{15}\text{N}$ values differ with functional plant strategies in temperate grassland. *J. Plant Nutr. Soil Sci.* 165, 661–667. doi:10.1002/jpln.200290000
- Burns, J., Young, R., 1994. Pleistocene mammals of the Edmonton area, Alberta. Part I. The carnivores. *Can. J. Earth Sci.* 31, 393–400.
- Calleja, M.L., Batista, F., Peacock, M., Kudela, R., McCarthy, M.D., 2013. Changes in compound specific $\delta^{15}\text{N}$ amino acid signatures and D/L ratios in marine dissolved organic matter induced by heterotrophic bacterial reworking. *Mar. Chem.* 149, 32–44. doi:10.1016/j.marchem.2012.12.001
- Chikaraishi, Y., Kashiyama, Y., Ogawa, N.O., Kitazato, H., Ohkouchi, N., 2007. Metabolic control of nitrogen isotope composition of amino acids in macroalgae and gastropods: implications for aquatic food web studies. *Mar. Ecol. Prog. Ser.* 342, 85–90.
- Chikaraishi, Y., Ogawa, N.O., Doi, H., Ohkouchi, N., 2011. $^{15}\text{N}/^{14}\text{N}$ ratios of amino acids as a tool for studying terrestrial food webs: a case study of terrestrial insects (bees, wasps, and hornets). *Ecol. Res.* 26, 835–844. doi:10.1007/s11284-011-0844-1
- Chikaraishi, Y., Ogawa, N.O., Ohkouchi, N., 2010. Further evaluation of the trophic level estimation based on nitrogen isotopic composition of amino acids, in: Ohkouchi, N., Tayasu, I., Koba, K. (Eds.), *Earth, Life, and Isotopes*. Kyoto University Press, Kyoto, pp. 37–51.
- Chikaraishi, Y., Steffan, S.A., Ogawa, N.O., Ishikawa, N.F., Sasaki, Y., Tsuchiya, M., Ohkouchi, N., 2014. High-resolution food webs based on nitrogen isotopic composition of amino acids. *Ecol. Evol.* 4, 2423–49. doi:10.1002/ece3.1103
- Coltrain, J.B., Harris, J.M., Cerling, T.E., Ehleringer, J.R., Dearing, M.-D., Ward, J., Allen, J., 2004. Rancho La Brea stable isotope biogeochemistry and its implications for the palaeoecology of late Pleistocene, coastal southern California. *Palaeogeogr. Palaeoclimatol. Palaeoecol.* 205, 199–219. doi:10.1016/j.palaeo.2003.12.008
- Coplen, T., Brand, W., Gehre, M., Gröning, M., Meijer, H.A., Toman, B., Verkouteren, R.M., 2006. New guidelines for $\delta^{13}\text{C}$ measurements. *Anal. Chem.* 78, 2439–2441.
- Corr, L., Berstan, R., Evershed, R., 2007a. Optimisation of derivatisation procedures for the determination of $\delta^{13}\text{C}$ values of amino acids by gas chromatography/combustion/isotope ratio mass spectrometry. *Rapid Commun. Mass Spectrom.* 21, 3759–3771.
- Corr, L., Berstan, R., Evershed, R., 2007b. Development of N-acetyl methyl ester derivatives for the determination of $\delta^{13}\text{C}$ values of amino acids using gas chromatography-combustion-isotope ratio mass spectrometry. *Anal. Chem.* 79, 9082–90. doi:10.1021/ac071223b

- Corr, L.T., Richards, M.P., Grier, C., Mackie, A., Beattie, O., Evershed, R.P., 2009. Probing dietary change of the Kwäday Dän Ts'inchí individual, an ancient glacier body from British Columbia: II. Deconvoluting whole skin and bone collagen $\delta^{13}\text{C}$ values via carbon isotope analysis of individual amino acids. *J. Archaeol. Sci.* 36, 12–18. doi:10.1016/j.jas.2008.06.027
- de Bello, F., Buchmann, N., Casals, P., Lepš, J., Sebastià, M.-T., 2009. Relating plant species and functional diversity to community $\delta^{13}\text{C}$ in NE Spain pastures. *Agric. Ecosyst. Environ.* 131, 303–307. doi:10.1016/j.agee.2009.02.002
- Dearing, M.D., 1997. The manipulation of plant toxins by a food-hoarding herbivore, *Ochotona princeps*. *Ecology* 78, 774–781. doi:10.1890/0012-9658(1997)078[0774:TMOPTB]2.0.CO;2
- Delong, M.D., Thorp, J.H., 2006. Significance of instream autotrophs in trophic dynamics of the Upper Mississippi River. *Oecologia* 147, 76–85. doi:10.1007/s00442-005-0241-y
- DeNiro, M., 1985. Postmortem preservation and alteration of in vivo bone collagen isotope ratios in relation to palaeodietary reconstruction. *Nature* 317, 806–809. doi:10.1038/317806a0
- Diefendorf, A., Mueller, K., Wing, S.L., Koch, P.L., Freeman, K.H., 2010. Global patterns in leaf ^{13}C discrimination and implications for studies of past and future climate. *Proc. Natl. Acad. Sci.* 107, 5738–5743.
- Docherty, G., Jones, V., Evershed, R.P., 2001. Practical and theoretical considerations in the gas chromatography/combustion/isotope ratio mass spectrometry $\delta^{13}\text{C}$ analysis of small polyfunctional compounds. *Rapid Commun. Mass Spectrom.* 15, 730–738. doi:10.1002/rcm.270
- Drucker, D.G., Bocherens, H., Billiou, D., 2003. Evidence for shifting environmental conditions in Southwestern France from 33 000 to 15 000 years ago derived from carbon-13 and nitrogen-15 natural abundances in collagen of large herbivores. *Earth Planet. Sci. Lett.* 216, 163–173. doi:10.1016/S0012-821X(03)00514-4
- Drucker, D.G., Bridault, A., Hobson, K.A., Szuma, E., Bocherens, H., 2008. Can carbon-13 in large herbivores reflect the canopy effect in temperate and boreal ecosystems? Evidence from modern and ancient ungulates. *Palaeogeogr. Palaeoclimatol. Palaeoecol.* 266, 69–82. doi:10.1016/j.palaeo.2008.03.020
- Drucker, D.G., Hobson, K.A., Ouellet, J.-P., Courtois, R., 2010. Influence of forage preferences and habitat use on ^{13}C and ^{15}N abundance in wild caribou (*Rangifer tarandus caribou*) and moose (*Alces alces*) from Canada. *Isotopes Environ. Health Stud.* 46, 107–21. doi:10.1080/10256010903388410
- Ehleringer, J., Comstock, J., Cooper, T., 1987. Leaf-twig carbon isotope ratio differences in photosynthetic-twig desert shrubs. *Oecologia* 71, 318–320.

- Ehleringer, J., Cooper, T., 1988. Correlations between carbon isotope ratio and microhabitat in desert plants. *Oecologia* 76, 562–566.
- Ehleringer, J., Phillips, S., Comstock, J., 1992. Seasonal variation in the carbon isotopic composition of desert plants. *Funct. Ecol.* 6, 396–404.
- Evershed, R., Bull, I., Corr, L.T., Crossman, Z.M., Dongen, B.E. van, Evans, C.J., Jim, S., Mottram, H.R., Mukherjee, A.J., Pancost, R.D., 2007. Compound-specific stable isotope analysis in ecology and paleoecology, in: Michener, R., Lajtha, K. (Eds.), *Stable Isotopes in Ecology and Environmental Science*. Blackwell Publishing Ltd, Malden, MA, pp. 480–540.
- Farquhar, G., 1989. Carbon isotope discrimination and photosynthesis. *Annu. Rev. Plant Biol.* 40, 503–537.
- Feranec, R., García, N., Díez, J.C., Arsuaga, J.L., 2010. Understanding the ecology of mammalian carnivores and herbivores from Valdegoba cave (Burgos, northern Spain) through stable isotope analysis. *Palaeogeogr. Palaeoclimatol. Palaeoecol.* 297, 263–272. doi:10.1016/j.palaeo.2010.08.006
- Finlay, J., Kendall, C., 2007. Stable isotope tracing of temporal and spatial variability in organic matter sources to freshwater ecosystems, in: Michener, R., Lajtha, K. (Eds.), *Stable Isotopes in Ecology and Environmental Science*. Blackwell Publishing Ltd, Hong Kong, pp. 283–333.
- Finstad, G.L., Kielland, K., 2011. Landscape variation in the diet and productivity of reindeer in Alaska based on stable isotope analyses. *Arctic, Antarct. Alp. Res.* 43, 543–554. doi:10.1657/1938-4246-43.4.543
- Fizet, M., Mariotti, A., Bocherens, H., Lange-Badré, B., Vandermeersch, B., Borel, J.P., Bellon, G., 1995. Effect of diet, physiology and climate on carbon and nitrogen stable isotopes of collagen in a Late Pleistocene anthropic palaeoecosystem: Marillac, Charente, France. *J. Archaeol. Sci.* 22, 67–79.
- Fogel, M., Tuross, N., 2003. Extending the limits of paleodietary studies of humans with compound specific carbon isotope analysis of amino acids. *J. Archaeol. Sci.* 30, 535–545.
- Fogel, M.L., Tuross, N., 1999. Transformation of plant biochemicals to geological macromolecules during early diagenesis. *Oecologia* 120, 336–346. doi:10.1007/s004420050867
- Fox-Dobbs, K., Leonard, J., Koch, P., 2008. Pleistocene megafauna from eastern Beringia: paleoecological and paleoenvironmental interpretations of stable carbon and nitrogen isotope and radiocarbon records. *Palaeogeogr. Palaeoclimatol. Palaeoecol.* 261, 30–46.
- France, R.L., 1995. Source variability in $\delta^{15}\text{N}$ of autotrophs as a potential aid in

- measuring allochthony in freshwaters. *Ecography*. 18, 318–320. doi:10.1111/j.1600-0587.1995.tb00134.x
- Fry, B., 1991. Stable isotope diagrams of freshwater food webs. *Ecology* 72, 2293–2297.
- Gaglioti, B. V., Barnes, B.M., Zazula, G.D., Beaudoin, A.B., Wooller, M.J., 2011. Late Pleistocene paleoecology of arctic ground squirrel (*Urocitellus parryii*) caches and nests from Interior Alaska's mammoth steppe ecosystem, USA. *Quat. Res.* 76, 373–382. doi:10.1016/j.yqres.2011.08.004
- Gannes, L., del Rio, C., Koch, P., 1998. Natural abundance variations in stable isotopes and their potential uses in animal physiological ecology. *Comp. Biochem. Physiol. Part A Mol. Integr. Physiol.* 119, 725–737.
- Gebauer, G., Schulze, E., 1991. Carbon and nitrogen isotope ratios in different compartments of a healthy and a declining *Picea abies* forest in the Fichtelgebirge, NE Bavaria. *Oecologia* 87, 198–207.
- Guthrie, R.D., 1982. Mammals of the mammoth steppe as paleoenvironmental indicators, in: Hopkins, D.M., Matthews, Jr., J.V., Schweger, C.E., Young, S.B. (Eds.), *Paleoecology of Beringia*. Academic Press, New York, pp. 307–326.
- Guthrie, R.D., 1990. *Frozen fauna of the mammoth steppe: the story of Blue Babe*. The University of Chicago Press, Chicago.
- Guthrie, R.D., 2001. Origin and causes of the mammoth steppe: a story of cloud cover, woolly mammal tooth pits, buckles, and inside-out Beringia. *Quat. Sci. Rev.*
- Hannides, C.C.S., Popp, B.N., Landry, M.R., Graham, B.S., 2009. Quantification of zooplankton trophic position in the North Pacific Subtropical Gyre using stable nitrogen isotopes. *Limnol. Oceanogr.* 54, 50–61. doi:10.4319/lo.2009.54.1.0050
- Hare, P.E., Fogel, M., Edgar Hare, P., Fogel, M.L., Stafford Jr, T.W., Mitchell, A.D., Hoering, T.C., 1991. The isotopic composition of carbon and nitrogen in individual amino acids isolated from modern and fossil proteins. *J. Archaeol. Sci.* 18, 277–292.
- Harrington, C., 2011. Pleistocene vertebrates of the Yukon Territory. *Quat. Sci. Rev.* 30, 2341–2354.
- Haynes, G., 1991. *Mammoths, mastodons, and elephants*. Cambridge University Press, Cambridge.
- Heaton, T.H.E., 1987. The $^{15}\text{N}/^{14}\text{N}$ ratios of plants in South Africa and Namibia: relationship to climate and coastal/saline environments. *Oecologia* 74, 236–246.
- Hobson, K.A., Alisauskas, R.T., Clark, R.G., 1993. Stable-nitrogen isotope enrichment in avian tissues due to fasting and nutritional stress: implications for isotopic analyses of diet. *Condor* 95, 388–394.

- Howland, M.R., Corr, L.T., Young, S.M.M., Jones, V., Jim, S., Van Der Merwe, N.J., Mitchell, A.D., Evershed, R.P., 2003. Expression of the dietary isotope signal in the compound-specific $\delta^{13}\text{C}$ values of pig bone lipids and amino acids. *Int. J. Osteoarchaeol.* 13, 54–65. doi:10.1002/oa.658
- Iacumin, P., Matteo, A. Di, Nikolaev, V., Kuznetsova, T., 2010. Climate information from C, N and O stable isotope analyses of mammoth bones from northern Siberia. *Quat. Int.* 212, 206–212.
- Iacumin, P., Nikolaev, V., Ramigni, M., 2000. C and N stable isotope measurements on Eurasian fossil mammals, 40 000 to 10 000 years BP: herbivore physiologies and palaeoenvironmental reconstruction. *Palaeogeogr. Palaeoclimatol. Palaeoecol.* 163, 33–47.
- Ishikawa, N.F., Kato, Y., Togashi, H., Yoshimura, M., Yoshimizu, C., Okuda, N., Tayasu, I., 2014. Stable nitrogen isotopic composition of amino acids reveals food web structure in stream ecosystems. *Oecologia* 175, 911–22. doi:10.1007/s00442-014-2936-4
- Jim, S., Jones, V., Ambrose, S.H., Evershed, R.P., 2006. Quantifying dietary macronutrient sources of carbon for bone collagen biosynthesis using natural abundance stable carbon isotope analysis. *Br. J. Nutr.* 95, 1055–1062. doi:10.1079/BJN20051685
- Kelly, J., 2000. Stable isotopes of carbon and nitrogen in the study of avian and mammalian trophic ecology. *Can. J. Zool.* 78, 1–27.
- Kielland, K., 2001. Stable isotope signatures of moose in relation to seasonal forage composition: a hypothesis. *Alces* 37, 329–337.
- Koch, P., 2007. Isotopic study of the biology of modern and fossil vertebrates, in: Michener, R., Lajtha, K. (Eds.), *Stable Isotopes in Ecology and Environmental Science*. Blackwell Publishing Ltd, Hong Kong, pp. 99–154.
- Koch, P., Fogel, M., Tuross, N., 1994. Tracing the diets of fossil animals using stable isotopes, in: Lajtha, K., Michener, R. (Eds.), *Stable Isotopes in Ecology and Environmental Science*. Blackwell Scientific Publications, pp. 63–92.
- Kohn, M.J., 2010. Carbon isotope compositions of terrestrial C_3 plants as indicators of (paleo)ecology and (paleo)climate. *Proc. Natl. Acad. Sci. U. S. A.* 107, 19691–5. doi:10.1073/pnas.1004933107
- Kristensen, D.K., Kristensen, E., Forchhammer, M.C., Michelsen, A., Schmidt, N.M., 2011. Arctic herbivore diet can be inferred from stable carbon and nitrogen isotopes in C_3 plants, faeces, and wool. *Can. J. Zool.* 89, 892–899. doi:10.1139/z11-073
- Larsen, T., Taylor, D.L., Leigh, M.B., O'Brien, D.M., 2009. Stable isotope fingerprinting: a novel method for identifying plant, fungal, or bacterial origins of

- amino acids. *Ecology* 90, 3526–35.
- Larsen, T., Ventura, M., Andersen, N., O'Brien, D.M., Piatkowski, U., McCarthy, M.D., 2013. Tracing carbon sources through aquatic and terrestrial food webs using amino acid stable isotope fingerprinting. *PLoS One* 8, e73441. doi:10.1371/journal.pone.0073441
- Larsen, T., Ventura, M., O'Brien, D.M., Magid, J., Lomstein, B.A., Larsen, J., 2011. Contrasting effects of nitrogen limitation and amino acid imbalance on carbon and nitrogen turnover in three species of Collembola. *Soil Biol. Biochem.* 43, 749–759. doi:10.1016/j.soilbio.2010.12.008
- Larsen, T., Wooller, M.J., Fogel, M.L., O'Brien, D.M., 2012. Can amino acid carbon isotope ratios distinguish primary producers in a mangrove ecosystem? *Rapid Commun. Mass Spectrom.* 26, 1541–1548. doi:10.1002/rcm.6259
- Long, E.S., Sweitzer, R.A., Diefenbach, D.R., Ben-David, M., 2005. Controlling for anthropogenically induced atmospheric variation in stable carbon isotope studies. *Oecologia* 146, 148–156. doi:10.1007/s00442-005-0181-6
- Longin, R., 1971. New method of collagen extraction for radiocarbon dating. *Nature* 230, 241–242. doi:10.1038/230241a0
- Lorrain, A., Graham, B., Ménard, F., Popp, B., Bouillon, S., van Breugel, P., Cherel, Y., 2009. Nitrogen and carbon isotope values of individual amino acids: a tool to study foraging ecology of penguins in the Southern Ocean. *Mar. Ecol. Prog. Ser.* 391, 293–306. doi:10.3354/meps08215
- Lynch, A.H., McCullagh, J.S.O., Hedges, R.E.M., 2011. Liquid chromatography/isotope ratio mass spectrometry measurement of $\delta^{13}\text{C}$ of amino acids in plant proteins. *Rapid Commun. Mass Spectrom.* 25, 2981–8. doi:10.1002/rcm.5142
- Mann, D.H., Groves, P., Kunz, M.L., Reanier, R.E., Gaglioti, B. V., 2013. Ice-age megafauna in Arctic Alaska: extinction, invasion, survival. *Quat. Sci. Rev.* 70, 91–108. doi:10.1016/j.quascirev.2013.03.015
- Matheus, P., 1995. Diet and co-ecology of Pleistocene short-faced bears and brown bears in eastern Beringia. *Quat. Res.* 44, 447–453.
- Matheus, P., Guthrie, R., Kunz, M., 2003. Isotope ecology of late Quaternary megafauna in eastern Beringia, in: 3rd International Mammoth Conference. Dawson City, pp. 80–83.
- McCarthy, M.D., Benner, R., Lee, C., Fogel, M.L., 2007. Amino acid nitrogen isotopic fractionation patterns as indicators of heterotrophy in plankton, particulate, and dissolved organic matter. *Geochim. Cosmochim. Acta* 71, 4727–4744. doi:10.1016/j.gca.2007.06.061

- McCarthy, M.D., Lehman, J., Kudela, R., 2013. Compound-specific amino acid $\delta^{15}\text{N}$ patterns in marine algae: Tracer potential for cyanobacterial vs. eukaryotic organic nitrogen sources in the ocean. *Geochim. Cosmochim. Acta* 103, 104–120. doi:10.1016/j.gca.2012.10.037
- McClelland, J., Montoya, J., 2002. Trophic relationships and the nitrogen isotopic composition of amino acids in plankton. *Ecology* 83, 2173–2180.
- McClelland, J.W., Holl, C.M., Montoya, J.P., 2003. Relating low $\delta^{15}\text{N}$ values of zooplankton to N_2 -fixation in the tropical North Atlantic: insights provided by stable isotope ratios of amino acids. *Deep Sea Res. Part I Oceanogr. Res. Pap.* 50, 849–861. doi:10.1016/S0967-0637(03)00073-6
- McMahon, K.W., Fogel, M.L., Elsdon, T.S., Thorrold, S.R., 2010. Carbon isotope fractionation of amino acids in fish muscle reflects biosynthesis and isotopic routing from dietary protein. *J. Anim. Ecol.* 79, 1132–41. doi:10.1111/j.1365-2656.2010.01722.x
- Metcalf, J.Z., 2011. Late Pleistocene climate and proboscidean paleoecology in North America: insights from stable isotope compositions of skeletal remains. University of Western Ontario.
- Metcalf, J.Z., Longstaffe, F.J., Hodgins, G., 2013. Proboscideans and paleoenvironments of the Pleistocene Great Lakes: landscape, vegetation, and stable isotopes. *Quat. Sci. Rev.* 76, 102–113. doi:10.1016/j.quascirev.2013.07.004
- Metcalf, J.Z., Longstaffe, F.J., Zazula, G.D., 2010. Nursing, weaning, and tooth development in woolly mammoths from Old Crow, Yukon, Canada: implications for Pleistocene extinctions. *Palaeogeogr. Palaeoclimatol. Palaeoecol.* 298, 257–270. doi:10.1016/j.palaeo.2010.09.032
- Milligan, H.E., Pretzlaw, T.D., Humphries, M.M., 2010. Stable isotope differentiation of freshwater and terrestrial vascular plants in two subarctic regions. *Ecoscience* 17, 265–275. doi:10.2980/17-3-3282
- Nadelhoffer, K., Shaver, G., Fry, B., Giblin, A., 1996. ^{15}N natural abundances and N use by tundra plants. *Oecologia* 107, 386–394.
- Newsome, S.D., Fogel, M.L., Kelly, L., del Rio, C.M., 2011. Contributions of direct incorporation from diet and microbial amino acids to protein synthesis in Nile tilapia. *Funct. Ecol.* 25, 1051–1062. doi:10.1111/j.1365-2435.2011.01866.x
- Newsome, S.D., Wolf, N., Peters, J., Fogel, M.L., 2014. Amino acid $\delta^{13}\text{C}$ analysis shows flexibility in the routing of dietary protein and lipids to the tissue of an omnivore. *Integr. Comp. Biol.* 54, 890–902. doi:10.1093/icb/icu106
- Ogawa, N.O., Chikaraishi, Y., Ohkouchi, N., 2012. Trophic position estimates of formalin-fixed samples with nitrogen isotopic compositions of amino acids: an

- application to gobiid fish (Isaza) in Lake Biwa, Japan. *Ecol. Res.* 28, 697–702. doi:10.1007/s11284-012-0967-z
- Olsen, K., White, C., Longstaffe, F., von Heyking, K., McGlynn, G., 2010. Bulk and compound-specific isotope analysis of pathological bone collagen: preliminary results, in: 4th International Symposium on Biomolecular Archaeology. Copenhagen, Denmark.
- Pakhomov, E. a., McClelland, J.W., Bernard, K., Kaehler, S., Montoya, J.P., 2004. Spatial and temporal shifts in stable isotope values of the bottom-dwelling shrimp *Nauticaris marionis* at the sub-Antarctic archipelago. *Mar. Biol.* 144, 317–325. doi:10.1007/s00227-003-1196-3
- Parnell, A.C., Inger, R., Bearhop, S., Jackson, A.L., 2010. Source partitioning using stable isotopes: coping with too much variation. *PLoS One* 5, e9672. doi:10.1371/journal.pone.0009672
- Perkins, S., 2009. Earth: Ancient beavers did not eat trees: now-extinct giant creatures had hippopotamus-like diet. *Sci. News* 176, 10–10.
- Polischuk, S., Hobson, K., Ramsay, M., 2011. Use of stable-carbon and -nitrogen isotopes to assess weaning and fasting in female polar bears and their cubs. *Can. J. Zool.* 79, 499–511.
- Popp, B., Graham, B., Olson, R., Hannides, C., Lott, M.J., López-Ibarra, G.A., Galván-Magaña, F., Fry, B., 2007. Insight into the trophic ecology of Yellowfin Tuna, *Thunnus albacares*, from compound-specific nitrogen isotope analysis of proteinaceous amino acids. *Terr. Ecol.* 1, 173–190.
- Putshkov, P., 2003. The impact of mammoths in their biome: clash of two paradigms. *Deinsea* 9, 365–379.
- Qi, H., Coplen, T.B., Geilmann, H., Brand, W., Böhlke, J.K., 2003. Two new organic reference materials for $\delta^{13}\text{C}$ and $\delta^{15}\text{N}$ measurements and a new value for the $\delta^{13}\text{C}$ of NBS 22 oil. *Rapid Commun. Mass Spectrom.* 17, 2483–2487. doi:10.1002/rcm.1219
- R Core Team, 2014. R: A language and environment for statistical computing. R Foundation for Statistical Computing, Vienna, Austria.
- Rivals, F., Solounias, N., 2007. Differences in tooth microwear of populations of caribou (*Rangifer tarandus*, Ruminantia, Mammalia) and implications to ecology, migration, glaciations and dental evolution. *J. Mamm. Evol.* 14, 182–192. doi:10.1007/s10914-007-9044-8
- Rivals, F., Solounias, N., Muhlbachler, M.C., 2007. Evidence for geographic variation in the diets of late Pleistocene and early Holocene bison in North America, and differences from the diets of recent bison. *Quat. Res.* 68, 338–346. doi:10.1016/j.yqres.2007.07.012

- Ruiz-Cooley, R.I., Ballance, L.T., McCarthy, M.D., 2013. Range expansion of the jumbo squid in the NE Pacific: $\delta^{15}\text{N}$ decrypts multiple origins, migration and habitat use. PLoS One 8, e59651. doi:10.1371/journal.pone.0059651
- Schmidt, K., McClelland, J.W., Mente, E., Montoya, J.P., Atkinson, A., Voss, M., 2004. Trophic-level interpretation based on $\delta^{15}\text{N}$ values : implications of tissue-specific fractionation and amino acid composition 266, 43–58.
- Schwartz-Narbonne, R., Longstaffe, F.J., Metcalfe, J.Z., Zazula, G., 2015. Solving the woolly mammoth conundrum: amino acid ^{15}N -enrichment suggests a distinct forage or habitat. Sci. Rep. 5, 9791. doi:10.1038/srep09791
- Sealy, J., van der Merwe, N., Thorp, J.A.L., Lanham, J.L., 1987. Nitrogen isotopic ecology in southern Africa: implications for environmental and dietary tracing. Geochim. Cosmochim. Acta 51, 2707–2717.
- Seminoff, J. a, Benson, S.R., Arthur, K.E., Eguchi, T., Dutton, P.H., Tapilatu, R.F., Popp, B.N., 2012. Stable isotope tracking of endangered sea turtles: validation with satellite telemetry and $\delta^{15}\text{N}$ analysis of amino acids. PLoS One 7, e37403. doi:10.1371/journal.pone.0037403
- Sherwood, O.A., Lehmann, M.F., Schubert, C.J., Scott, D.B., McCarthy, M.D., 2011. Nutrient regime shift in the western North Atlantic indicated by compound-specific $\delta^{15}\text{N}$ of deep-sea gorgonian corals. Proc. Natl. Acad. Sci. U. S. A. 108, 1011–1015. doi:10.1073/pnas.1004904108
- Smallwood, B.J., Wooller, M.J., Jacobson, M.E., Fogel, M.L., 2003. Isotopic and molecular distributions of biochemicals from fresh and buried *Rhizophora mangle* leaves. Geochem. Trans. 4, 38–46. doi:10.1039/b308902a
- Sponheimer, M., Robinson, T., Ayliffe, L., Roeder, B., Hammer, J., Passey, B., West, A., Cerling, T., Dearing, D., Ehleringer, J., 2003. Nitrogen isotopes in mammalian herbivores: hair $\delta^{15}\text{N}$ values from a controlled feeding study. Int. J. Osteoarchaeol. 13, 80–87. doi:10.1002/oa.655
- Stevens, R.E., Hedges, R.E., 2004. Carbon and nitrogen stable isotope analysis of northwest European horse bone and tooth collagen, 40,000 BP – present: palaeoclimatic interpretations. Quat. Sci. Rev. 23, 977–991. doi:10.1016/j.quascirev.2003.06.024
- Stevens, R.E., Jacobi, R., Street, M., Germonpré, M., Conard, N.J., Münzel, S.C., Hedges, R.E.M., 2008. Nitrogen isotope analyses of reindeer (*Rangifer tarandus*), 45,000 BP to 9,000 BP: palaeoenvironmental reconstructions. Palaeogeogr. Palaeoclimatol. Palaeoecol. 262, 32–45. doi:10.1016/j.palaeo.2008.01.019
- Stirton, R., 1965. Cranial morphology of *Castoroides*, in: Dr. D.N. Wadia Commemorative Volume. Mining, Geological and Metallurgical Institute of India, Calcutta, pp. 273–289.

- Stuart-Williams, Q., H. Le, Schwarcz, H.P., 1997. Oxygen isotopic determination of climatic variation using phosphate from beaver bone, tooth enamel, and dentine. *Geochim. Cosmochim. Acta* 61, 2539–2550.
- Styring, A.K., Fraser, R.A., Bogaard, A., Evershed, R.P., 2014. Cereal grain, rachis and pulse seed amino acid $\delta^{15}\text{N}$ values as indicators of plant nitrogen metabolism. *Phytochemistry* 97, 20–9. doi:10.1016/j.phytochem.2013.05.009
- Suren, A.M., Lake, P.S., 1989. Edibility of fresh and decomposing macrophytes to three species of freshwater invertebrate herbivores. *Hydrobiologia* 178, 165–178. doi:10.1007/BF00011667
- Szpak, P., 2011. Fish bone chemistry and ultrastructure: implications for taphonomy and stable isotope analysis. *J. Archaeol. Sci.* 38, 3358–3372. doi:10.1016/j.jas.2011.07.022
- Szpak, P., Gröcke, D.R., Debruyne, R., MacPhee, R.D.E., Guthrie, R.D., Froese, D., Zazula, G.D., Patterson, W.P., Poinar, H.N., 2010. Regional differences in bone collagen $\delta^{13}\text{C}$ and $\delta^{15}\text{N}$ of Pleistocene mammoths: implications for paleoecology of the mammoth steppe. *Palaeogeogr. Palaeoclimatol. Palaeoecol.* 286, 88–96. doi:10.1016/j.palaeo.2009.12.009
- Tahmasebi, F., 2015. Carbon and nitrogen isotopic investigations of the late Pleistocene paleoecology of eastern Beringia, Yukon Territory, using soils, plants and rodent bones. Doctoral Thesis. University of Western Ontario.
- Tieszen, L., 1991. Natural variations in the carbon isotope values of plants: implications for archaeology, ecology, and paleoecology. *J. Archaeol. Sci.* 18, 227–248.
- Tischler, K., 2004. Aquatic plant nutritional quality and contribution to moose diet at Isle Royale National Park. Master's Thesis. Michigan Technological University.
- Ukrainitseva, V. V., 2013. Mammoths and the environment. Cambridge University Press, Cambridge.
- van Klinken, G., 1999. Bone collagen quality indicators for palaeodietary and radiocarbon measurements. *J. Archaeol. Sci.* 26, 687–695.
- Venables, W.N., Ripley, B.D., 2002. Modern applied statistics with S, Fourth Edition. Springer, New York.
- Willerslev, E., Davison, J., Moora, M., Zobel, M., Coissac, E., Edwards, M.E., Lorenzen, E.D., Vestergård, M., Gussarova, G., Haile, J., Craine, J., Gielly, L., Boessenkool, S., Epp, L.S., Pearman, P.B., Cheddadi, R., Murray, D., Bråthen, K.A., Yoccoz, N., Binney, H., Cruaud, C., Wincker, P., Goslar, T., Alsos, I.G., Bellemain, E., Brysting, A.K., Elven, R., Sønstebø, J.H., Murton, J., Sher, A., Rasmussen, M., Rønn, R., Mourier, T., Cooper, A., Austin, J., Möller, P., Froese, D., Zazula, G., Pompanon, F., Rioux, D., Niderkorn, V., Tikhonov, A., Savvinov, G., Roberts, R.G., MacPhee,

- R.D.E., Gilbert, M.T.P., Kjær, K.H., Orlando, L., Brochmann, C., Taberlet, P., 2014. Fifty thousand years of Arctic vegetation and megafaunal diet. *Nature* 506, 47–51. doi:10.1038/nature12921
- Wooller, M., Zazula, G., Edwards, M., Froese, D.G., Boone, R.D., Parker, C., Bennett, B., 2007. Stable carbon isotope compositions of Eastern Beringian grasses and sedges: investigating their potential as paleoenvironmental indicators. *Arctic, Antarct. Alp. Res.* 39, 318–331.
- Yeakel, J.D., Guimarães, P.R., Bocherens, H., Koch, P.L., 2013. The impact of climate change on the structure of Pleistocene food webs across the mammoth steppe. *Proc. R. Soc. B Biol. Sci.* 280, 20130239.
- Zazula, G.D., MacPhee, R.D., Metcalfe, J.Z., Reyes, A. V., Brock, F., Druckenmiller, P.S., Groves, P., Harington, R., Hodgins, G.W.L., Kunz, M.L., Longstaffe, F.J., Mann, D.H., McDonald, H.G., Nalawade-Chavan, S., Southon, J.R., 2014. American mastodon extirpation in the Arctic and Subarctic predates human colonization and terminal Pleistocene climate change. *Proc. Natl. Acad. Sci.* 111, 18460–18465.
- Zazula, G.D., MacPhee, R.D.E., Metcalfe, J.Z., Reyes, A. V, Brock, F., Druckenmiller, P.S., Groves, P., Harington, C.R., Hodgins, G.W.L., Kunz, M.L., Longstaffe, F.J., Mann, D.H., McDonald, H.G., Nalawade-Chavan, S., Southon, J.R., 2014. American mastodon extirpation in the Arctic and Subarctic predates human colonization and terminal Pleistocene climate change. *Proc. Natl. Acad. Sci. U. S. A.* 111, 18460–18465. doi:10.1073/pnas.1416072111

Chapter 5

5 Insights from mathematical analysis of isotopic niche on the mammoth steppe

5.1 Introduction

5.1.1 The Pleistocene mammoth steppe

The Pleistocene mammoth steppe was a megacontinental biome, stretching from north-eastern Canada (the Yukon), across Alaska and northern Asia to western Europe (Fig. 5.1; Bocherens, 2003; Guthrie, 1990, 1984, 1982). This ecosystem disappeared at the end of the Pleistocene, accompanied by the extinction or extirpation of many of the megaherbivore species that lived there (Barnosky et al., 2004; Koch and Barnosky, 2006). Stable carbon and nitrogen isotopic studies of preserved animal tissues can yield a better understanding of the species that lived there, in particular how they coexisted across this vast biome, and how they adapted to climate change during the Pleistocene. This, in turn, can inform our understanding of extant species and the adaptability of species and ecosystems to major climatic changes.

The mammoth steppe biome was defined by the occurrence of the woolly mammoth in the fossil remains and an arid, graminoid- and forb-dominated environment (Bocherens, 2003; Guthrie, 1990, 1984, 1982). This large geographic area was characterized by a diverse set of megafauna, and by a high degree of faunal homogeneity. Faunal ecosystems throughout this area were dominated by mammoth, bison and horse, and shared a number of common species among the less prevalent fauna, such as caribou. The majority of these species (e.g. saiga antelope, woolly mammoth, caballid horse, bison, etc.) migrated across the exposed Bering Strait during glacial periods, and were able to fully disperse across the mammoth steppe (Guthrie, 2001; Shapiro et al., 2004). The flora of the mammoth steppe was also relatively homogeneous, particularly during pre-Last Glacial Maximum (pre-LGM) time periods (Guthrie, 1982; Willerslev et al., 2014). Pollen, plant macrofossil and ancient DNA studies suggest that the mammoth steppe was an herb-steppe-tundra environment, dominated by grasses, sedges, forbs and

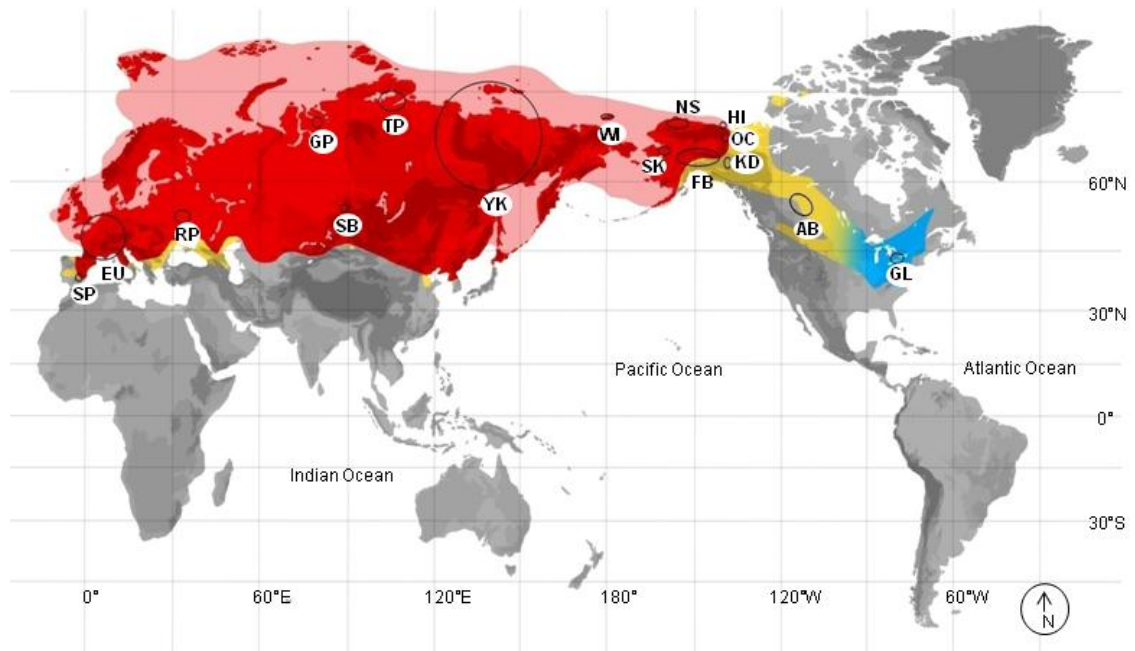


Figure 5.1 Location of sites across the mammoth steppe. ‘Red’ represents the mammoth steppe as defined by Guthrie (1982). ‘Yellow’ represents areas where woolly mammoth, horse and bison remains are present in an environment hypothesized to have had steppe elements. ‘Blue’ represents areas where woolly mammoth, horse and bison remains are present, but in an environment hypothesized to be primarily forested. Darker shades represent higher elevations. Sites are lettered: SP. Spain; EU. NW Europe; RP. Russian Plain; GP. Gydan Peninsula; SB. south central Siberia; TP. Taymyr Peninsula; YK. Yakutia; WI. Wrangel Island, SK. Selawik; NS. North Slope; FB. Fairbanks; HI. Herschel Island; OC. Old Crow; KD. Klondike; AB. Alberta; GL. Great Lakes Area. Artwork by Katherine Allan.

herbaceous species. There is little evidence for tree growth during glacial periods, though some studies suggest that the mammoth steppe contained forests during interglacial periods (Burns, 1991; Guthrie, 1990, 1982; Huntley et al., 2013; Iacumin et al., 2000; Mandryk, 1996; Nogués-Bravo et al., 2008; Rasic and Matheus, 2007; Willerslev et al., 2014; Zazula et al., 2011; Zimov et al., 2012).

Several other areas may have contained the same floral and faunal elements as the traditionally defined mammoth steppe (yellow in Fig. 5.1; Álvarez-Lao et al., 2009; Harington and Ashworth, 1986; Harington, 2003). For example, previous studies suggest that Alberta was cold and arid, with herb-steppe-tundra flora, and contained the same faunal elements, including the woolly mammoth, present in the traditionally defined mammoth steppe regions (Burns, 2010, 1991; Burns and Young, 1994; Jass et al., 2011; Mandryk, 1996). We suggest that these areas fit current definitions of the mammoth steppe. Still further southeast, reaching through Ontario and Quebec are sites (blue in Fig. 5.1) where woolly mammoth, horse and bison bones from the Pleistocene have been found (Harington, 2003). These remains, however, occur in contexts previously reconstructed as mesic, forested areas (Metcalf et al., 2013; Saunders et al., 2010). In the present study, we consider these populations within the context of the other regions examined, while acknowledging this difference in floral elements from those of the traditionally defined mammoth steppe.

The coexistence of various megaherbivores in the mammoth steppe may have been facilitated by niche feeding (Graham and Lundelius, 1984; Guthrie, 1984, 1982), in which each species consumed a narrow portion of available resources, thus limiting competition. Niche feeding could have been accomplished through partitioning of habitats or forage (Britton et al., 2012; Guthrie, 1982). The exact mechanisms of niche separation are not fully understood (Bocherens, 2003; Guthrie, 2001; Schwartz-Narbonne et al., 2015). While there was a high degree of floral and faunal continuity across the mammoth steppe, it was not a uniform environment. While some species migrated across the Bering Land Bridge during glacial periods, others, such as the woolly rhinoceros and the short-faced bear, stayed in the west or the east, respectively (Guthrie, 2001). A range of environmental conditions across the mammoth steppe has also been posited (Strong and Hills, 2005; Szpak et al., 2010; Willerslev et al., 2014), along with significant ecological changes over time that affected temperature, aridity, and floral and faunal compositions (Elias, 2001, 2000; Huntley et al., 2013; Rasic and Matheus, 2007; Strong and Hills, 2005; Willerslev et al., 2014; Zazula et al., 2014).

5.1.2 Stable isotopes

5.1.2.1 Carbon isotopes in plants and collagen

There are three main plant categories of plants with distinct mechanisms of carbon fixation, and thus distinct $\delta^{13}\text{C}$: C_3 (average -27‰), C_4 (average -13‰), and CAM (average -11‰ ; Koch, 2007; Marshall et al., 2007; O’Leary, 1988). As the high latitude environments being considered here are dominated by C_3 plants, and no C_4 vegetation has been found from glacial periods (Gaglioti et al., 2011; Wooller et al., 2007), this paper focuses on the isotopic compositions of C_3 plants. The $\delta^{13}\text{C}$ of a plant growth form or species depends on the $\delta^{13}\text{C}$ of the CO_2 accessible to the plant, the mechanism of CO_2 uptake, and the plant’s access to water and thus water use efficiency. In modern tundra environments, plants have a general pattern of $\delta^{13}\text{C}$: shrubs < forbs < graminoids < fungi < lichens (Fig. 1.2; Barnett, 1994; Ben-David et al., 2001; Drucker et al., 2010; Kristensen et al., 2011). The variation between the average $\delta^{13}\text{C}$ of any two pairs of plant groups is $\geq 1.5\text{‰}$, but the ranges overlap considerably between species (Barnett, 1994). This overlap partially results from environmental differences between habitats and microhabitats of plants, which can have a significant effect on their carbon isotopic composition. Plants in a more arid environment have higher $\delta^{13}\text{C}$ than those in a more mesic environment (de Bello et al., 2009; Diefendorf et al., 2010; Ehleringer and Cooper, 1988; Ehleringer et al., 1987; Farquhar, 1989; Kohn, 2010; Tieszen, 1991; Wooller et al., 2007). Higher elevation, higher mean annual temperature and lower latitudes also correlate with higher plant $\delta^{13}\text{C}$, though only weakly (Kohn, 2010), and the temperature and altitude effects are disputed (Heaton, 1999; Kohn, 2011; Stevens et al., 2006). Some work suggests that temperature is a stronger control on plant $\delta^{13}\text{C}$ than aridity in Arctic environments (Iacumin et al., 2006). Also, plants underneath a dense canopy cover have lower $\delta^{13}\text{C}$ than plants growing in an open environment likely because of recycling of organic matter and/or lower light levels affecting leaf processes in forested environments (Bocherens et al., 2011; Bonafini et al., 2013).

The $\delta^{13}\text{C}$ of a consumer’s collagen is generally higher than that of the plants consumed. For large herbivores, a difference between collagen and diet $\delta^{13}\text{C}$ ($\Delta^{13}\text{C}_{\text{Bulk-Diet}}$) of $+5.1 \pm 0.3\text{‰}$ has been measured in several systems (Drucker et al., 2008). Carbon in herbivore

collagen can be derived from the plants it eats, milk from its mother and its own fat reserves. As adult teeth and bones were selected in this study, nursing was not considered to be a factor. In high latitude environments, however, winter diets are often quite poor, and so animals are expected to rely on their fat reserves to survive. Lipids generally have low $\delta^{13}\text{C}$, and winter reliance on lipids has been suggested to be responsible for the low $\delta^{13}\text{C}$ of Beringian mammoths (Szpak et al., 2010). It has also been suggested that ruminants should have a higher $\delta^{13}\text{C}$ than non-ruminants consuming the same diet, as the former produce more methane, and methane is depleted of ^{13}C relative to the diet (Coltrain et al., 2004).

5.1.2.2 Nitrogen isotopes in plants and collagen

In the tundra, nitrogen availability to plants is usually limited. As a result, plants take up nitrogen in several forms, from varying soil depth, and through mycorrhizal associations (Nadelhoffer et al., 1996). These variations led to a general pattern of nitrogen isotopic compositions among species in tundra ecosystems: shrubs < fungi < forbs < graminoids < lichens (Fig. 1.2; Ben-David et al., 2001; Drucker et al., 2010; Finstad and Kielland, 2011; Kristensen et al., 2011; Nadelhoffer et al., 1996). While baseline isotopic compositions may vary between environments (Richards and Hedges, 2003; Syväranta et al., 2013), the general patterns are hypothesized to be largely consistent (Fox-Dobbs et al., 2008). The $\delta^{15}\text{N}$ of an ecosystem as a whole relates to the degree of nitrogen cycling, and thus the quantity of nitrogen loss, in an ecosystem. A hotter, more arid ecosystem tends to have more nitrogen cycling and greater loss of nitrogen, predominately as ^{14}N . As a result, plants and soil of arid ecosystems typically have lower $\delta^{15}\text{N}$ than cooler, more mesic ecosystems (Ambrose, 1991; Amundson et al., 2003; Drucker et al., 2003a; Heaton, 1987; Stevens and Hedges, 2004; Stevens et al., 2008).

There is an increase in the $\delta^{15}\text{N}$ between an animal's collagen and the diet it consumes. Although various trophic enrichment factors have been measured, they average around +3 ‰, ranging from +2 to +5 ‰ (Gannes et al., 1998; Koch, 2007; Koch et al., 1994). Beyond the trophic enrichment, a number of physiological effects can change the $\delta^{15}\text{N}$ of animal collagen. Several authors have suggested that physiological factors cause the $\delta^{15}\text{N}$

of a consumer's tissues in arid regions to be increased beyond that expected from the increase in plant $\delta^{15}\text{N}$ (Kelly, 2000; Koch et al., 1994; Sealy et al., 1987; Sponheimer et al., 2003). As well, when animals are on below-maintenance diets, they must recycle their body protein to survive. This causes an increase in tissue $\delta^{15}\text{N}$ (Gannes et al., 1998; Hobson et al., 1993; Kelly, 2000; Koch, 2007; Polischuk et al., 2011). While suckling has the same effect on $\delta^{15}\text{N}$ as an increase in trophic level (Metcalf et al., 2010), none of the tissues studied here are expected to be from nursing animals.

5.1.2.3 Isotopic niche

A significant body of previous work has examined the relative carbon and nitrogen isotopic compositions of several megaherbivores at single mammoth steppe sites, or of fewer species at multiple sites (e.g. Bocherens et al., 2011, 1994; Drucker et al., 2003a, b; Fizet et al., 1995; Fox-Dobbs et al., 2008; Iacumin et al., 2010; Mann et al., 2013; Metcalfe, 2011; Metcalfe et al., 2013; Raghavan et al., 2014; Stevens et al., 2009; Szpak et al., 2010), either at for single point in time or over several time periods. The present work expands that approach to a comparison of much of the available $\delta^{13}\text{C}$ and $\delta^{15}\text{N}$ data (and the associated ecological niche) across multiple species, time periods and sites for the entirety of the mammoth steppe, so far as these data have been published.

Previous work has generally focussed on the relative isotopic position in $\delta^{13}\text{C}$ - $\delta^{15}\text{N}$ space of each species, site or time period in order to determine which had a higher average $\delta^{13}\text{C}$ or $\delta^{15}\text{N}$. This is only one of the isotopic approaches that can be used to understand ecological relationships. Also of significance is the area on a plot of $\delta^{15}\text{N}$ versus $\delta^{13}\text{C}$ encompassed by the carbon and nitrogen isotopic compositions of each group, that is, all the individuals of a species measured at a single site and time period. This area provides a representation of their 'isotopic niche'. The isotopic niche encompasses a subset of a group's ecological niche, describing the sum of the dietary, environmental and physiological factors that combine to affect the placement and size of the group's isotopic compositions (Bearhop et al., 2004; Hammerschlag-Peyer et al., 2011; Layman et al., 2012). In the present study, the isotopic niche was assessed using three metrics. First, we examined niche position using the group's average $\delta^{13}\text{C}$ and $\delta^{15}\text{N}$. This approach

provides information about the isotopic composition of the species' main forage, which is influenced by the plant type(s) consumed and environment of plant growth (Hammerschlag-Peyer et al., 2011), and the animals' physiological state. Figure 5.2a illustrates two hypothetical groups with different isotopic niche positions. Second, we examined isotopic niche width, which describes the degree of variety in resources consumed, as illustrated in Figure 5.2b. Third, we examined isotopic niche overlap, which describes the similarity in resource use between groups, as illustrated by Figure 5.2c (Hammerschlag-Peyer et al., 2011).

Assessment of the size of the isotopic niche of an animal can be performed using several mathematical approaches. The convex hull method, otherwise known as total area (TA), describes a polygon encompassing all data points (Layman et al., 2007), as illustrated in Figure 5.3a. A larger TA suggests a dietary generalist or consumption of food from a variety of habitats. A second method uses the small-sample-size corrected standard ellipse area (SEA_c), which includes the core 40% of data (Fig. 5.3b; Jackson et al., 2011). Bayesian statistics (Markov Chain Monte Carlo) provide a third way to estimate most probable niche sizes, after taking into account sample set size (Jackson et al., 2011). In the Bayesian approach, the most probable sizes of the standard ellipse can be estimated in a statistically rigorous fashion (SEA_b). Two sets of estimated niche sizes can be compared in a to establish the proportion of estimated niches of one set that are larger than the second set (SEA_{b-prop}). Again, a larger sample size provides more accurate estimates.

Niche overlap between two sample groups can be assessed using either the TA or the SEA_c . The size of the overlap is calculated, and then divided by the area of the first group. This calculation provides an estimate of the degree to which two groups utilized similar forage, or habitat, or made use of similar physiological adaptations.

There are three main concerns that can decrease the power of these metrics. First, since the TA includes the total area covered within a group, adding additional samples to a group can increase the size of that group, but can never decrease it. This means that the niche for a group containing a large number of analyzed specimens has the potential to

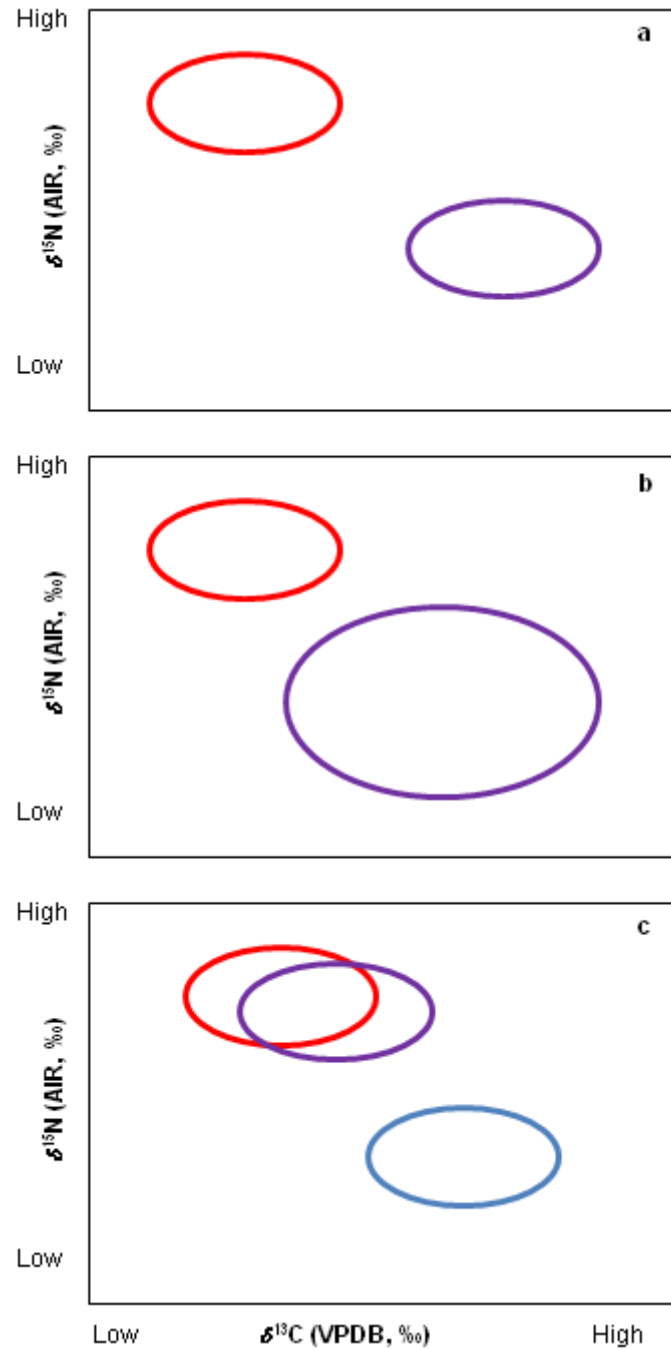


Figure 5.2 Conceptual model of hypothetical niche differences: a. Variation in carbon and nitrogen isotopic position between the isotopic niche of two species; b. Variation in the size of two isotopic niches; c. Variation between isotopic niches with an overlap and without an overlap.

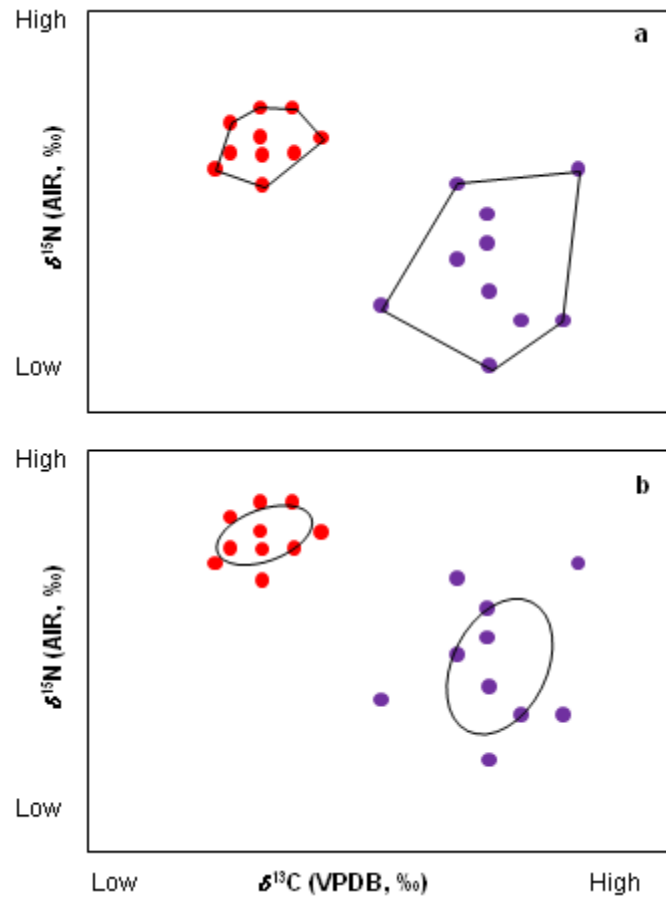


Figure 5.3 Conceptual model of isotopic niche based on hypothetical points and groupings: a. The outer edge, or convex hull, of the group of data points for each species; b. Same data as for (a), but showing a standard ellipse corrected for small sample-size. The ellipses encompass 40% of the dataset for each group.

appear larger than one containing a small number of specimens (Jackson et al., 2011). Such an outcome is a particular worry in palaeoecology, where samples sets are commonly small and of varying sizes. Second, the SEA_c and SEA_b measures of niche size assume that the data are normally distributed (Jackson et al., 2011); the results are less rigorous if the data are nonparametric. Third, these metrics should be viewed with caution when comparing groups containing fewer than 10-30 individuals each (Jackson et al., 2011; Syväranta et al., 2013). Especially for paleontological data, there are commonly severe limits on the sample sizes within a group, especially for rare species. Such cases

remain interpretable, but the test is less powerful than for ecological data meeting these conditions.

5.2 Methods

5.2.1 Sample selection

Specimens were obtained from a variety of institutions and their stable carbon and nitrogen isotopic compositions were measured. Radiocarbon dates were also obtained for a subset of these samples. These new data were integrated with other information on species proportions, radiocarbon dates, and carbon and nitrogen isotopic compositions compiled from the literature (Bellissimo, 2013; Bocherens et al., 2011, 2005, 2001, 1997, 1996, 1995, 1994; Burns, 2010, 1996; Burns and Young, 1994; Debruyne et al., 2008; Druckenmiller, 2008; Drucker and Henry-Gambier, 2005; Drucker et al., 2003a, b, 2011; Fizet et al., 1995; Fox-Dobbs et al., 2008; García-Alix et al., 2012; Guthrie, 2006, 1968; Iacumin et al., 2010, 2000; Jass et al., 2011; Jass and Beaudoin, 2014; Leonard et al., 2007; MacPhee et al., 2002; Mann et al., 2013; McAndrews and Jackson, 1988; Metcalfe, 2011; Metcalfe et al., 2013, 2010; Mol et al., 2006; Raghavan et al., 2014; Shapiro et al., 2004; Stevens and Hedges, 2004; Stevens et al., 2009; Szpak et al., 2010; Zazula et al., 2014; Zimov et al., 2012).

A compilation of the data used is provided in Appendices K-AA. Data were removed from the compilation if the collagen for which they were obtained did not meet preservation criterion (collagen yield $\geq 1\%$, C (wt %) $\geq 13\%$, N (wt %) $\geq 4.8\%$, atomic C/N ratio between 2.9-3.6 (Ambrose, 1990; DeNiro, 1985). Isotopic data for teeth from most species were not included in the compilation, except for adult mammoth teeth (Metcalfe et al., 2010) and bison third molars (Balasse et al., 1999), which are known to reflect adult diets and are devoid of nursing or weaning isotopic signals. Isotopic data for antler were also not utilized, as this tissue reflects seasonal rather than yearly signals (Chapter 2).

The database includes samples from 16 sites (Fig. 5.1): southern Alberta (Alberta), the Fairbanks area (Fairbanks), the Great Lakes area (Great Lakes), Gydan Peninsula, Herschel Island, Klondike area (Klondike), Alaskan North Slope area (North Slope),

north-western Europe (NW Europe), Old Crow area (Old Crow), Russian Plain, Selawik Wildlife Refuge and surrounding areas (Selawik), south central Siberia, Spain, Taymyr Peninsula, Wrangel Island and Yakutia. Species proportions were compiled from the literature, and assigned to the appropriate time period where possible. Stable carbon and nitrogen isotopic data were available for multiple species over multiple time periods for each site evaluated. When multiple radiocarbon dates were available for a given sample, the stable isotopic results associated with the oldest date produced for collagen that had undergone ultrafiltration was used in the mathematical analysis (Zazula et al., 2014).

5.2.2 Sample preparation and analysis

5.2.2.1 Collagen extraction

Collagen extraction was performed at the Laboratory for Stable Isotope Science, University of Western Ontario, London, Canada, following published methods with minor modifications (Metcalf et al., 2010). Samples were extracted using a Dremel[®] cutting wheel, and the exposed surfaces cleaned. Consolidant was removed from sample surfaces using a Dremel[®] equipped with a burr attachment. Previous work has shown that consolidant and its removal does not significantly affect collagen carbon and nitrogen isotopic compositions (France et al., 2011). Samples were then powdered.

A subset of the samples was lipid-extracted using a modified Bligh and Dyer method (Bligh and Dyer, 1959). The powdered samples were treated with a 2:1 chloroform:methanol solution (v:v) for 15 minutes, repeated 3 times, and then dried at room temperature. A comparison of 15 samples analyzed in duplicate both with and without lipid extraction showed a standard deviation between sets for $\delta^{13}\text{C} \leq 0.1 \text{ ‰}$ and for $\delta^{15}\text{N} \leq 0.2 \text{ ‰}$. As this is within the expected error for method duplicates, isotopic results for untreated and lipid-extracted collagen are considered to be equivalent for the purposes of this study. All samples were treated with 0.25 M HCl at room temperature for 24 hours. This was then replaced with 0.5 M HCl at room temperature until the samples were gelatinized. After gelatinization, humic removal was performed at room temperature with a solution of 0.1 M NaOH for 20 minutes, and repeated as necessary. The samples were then rinsed with water at room temperature until NaOH was removed

completely. HCl was then used to adjust the pH to less than 3, and the collagen was solubilised at 90°C.

5.2.2.2 Stable isotope analysis

A Costech elemental combustion system (ECS 4010) attached to a Thermo-Scientific Delta V or to a Thermo-Scientific Delta Plus XL stable isotope ratio mass spectrometer (IRMS) operated in continuous-flow mode was used to measure the carbon and nitrogen isotopic compositions. These data were collected over a total of 13 analytical sessions. Two-point calibrations were used to relate the measured carbon and nitrogen isotopic compositions to internationally accepted standards (VPDB for carbon, AIR for nitrogen). Values of $\delta^{13}\text{C}$ were calibrated to VPDB using NBS-22 (accepted value -30.0‰) and IAEA-CH-6 (accepted value -10.5‰) or USGS-40 (accepted value -26.4‰) and USGS-41 (accepted value $+37.6\text{‰}$). Values of $\delta^{15}\text{N}$ were calibrated to AIR using USGS-40 (accepted value -4.5‰) and either IAEA-N2 (accepted value $+20.3\text{‰}$) or USGS-41 (accepted value $+47.6\text{‰}$). The same standards were used to provide two-point calibration curves for sample carbon and nitrogen contents, using the following accepted values: NBS-22, C = 86.3 %; IAEA-CH-6, C = 42.1 %; USGS-40, C = 40.7%, N = 9.5 %; USGS-41, C = 40.7%, N = 9.5%; IAEA-N2, N = 21.5%.

Accuracy (and precision) was also assessed using an internal laboratory keratin standard (MP Biomedicals Inc., Catalogue No. 90211, Lot No. 9966H), which was included in all analytical sessions. For 92 measurements of this standard, $\delta^{13}\text{C} = -24.1 \pm 0.1\text{‰}$ (mean \pm 1 SD) (accepted value, -24.1‰), $\delta^{15}\text{N} = +6.3 \pm 0.2\text{‰}$ (accepted value, $+6.4\text{‰}$), C content = $48 \pm 1\text{ wt\%}$ (accepted value, 46.8 wt%) N content = $15 \pm 1\text{ wt\%}$ (accepted value, 14.6 wt%), and atomic C/N ratio = 3.7 ± 0.2 (accepted value, 3.7). Reproducibility of the isotopic data was evaluated for 31 samples. The difference between values varied for $\delta^{13}\text{C}$ from 0.0 - 0.5 ‰ (SD), with an average difference of 0.1 ‰, and for $\delta^{15}\text{N}$, from 0.0 - 0.2 ‰ (SD), with an average difference of 0.1 ‰.

5.2.2.3 Radiocarbon dating

Radiocarbon dates were obtained for several samples, as listed in Appendices L, M, Q and V. Collagen extraction, combustion, graphitization and radiocarbon dating were

performed at the University of Arizona Accelerator Mass Spectrometry (AMS) Laboratory. Dates are presented as uncalibrated radiocarbon years before present (1950).

5.2.3 Mathematical treatment

The majority of the isotopic datasets were analyzed using the using SIBER (stable isotope Bayesian ellipses in R) scripts (Jackson et al., 2011) from the SIAR (stable isotope analysis in R) package (Parnell et al., 2010) in R version 3.1.1 (R Core Team, 2014) using the R Studio interface version 0.98.1083. Datasets were only included in the SIBER analysis if there were results for: (i) at least 3 specimens of a species present at a given site and time period, and (ii) at least two sets of the species, site or time, thus providing a basis for comparison. Datasets for groups that did not meet these requirements were interpreted by considering the average (mean) $\delta^{13}\text{C}$ and $\delta^{15}\text{N}$ of the group calculated in Microsoft Excel.

The data were sorted into four time bins for interpretation, pre-LGM, LGM, post-LGM and Holocene, based on their radiocarbon date, physical context (Jass et al., 2011), or prior knowledge of the species at the site (Guthrie, 2006; Zazula et al., 2014). The clear separation in $\delta^{15}\text{N}$ between pre-LGM and post-LGM samples at Alberta was used to help sort horse and caribou samples at this site (Bellissimo, 2013). Multiple definitions of the timing of the LGM are present in the literature. To test for differences that might arise in the statistical modeling from the use of different LGM timings, the data were binned twice and the results compared. The first test (binning approach A) used the timing bins applied in several previous isotopic studies (Fox-Dobbs et al., 2008; Yeakel et al., 2013): pre-LGM, > 23,000 ^{14}C BP; LGM, 23,000-18,000 ^{14}C BP; post-LGM, 18,000-10,000 ^{14}C BP, and Holocene, < 10,000 ^{14}C BP. The second test (binning approach B) used the EPILOG preferred LGM chronozone (Mix et al., 2001): pre-LGM, > 19,500 ^{14}C BP; LGM, 19,500-16,100 ^{14}C BP; post-LGM, 16,100-10,000 ^{14}C , and Holocene < 10,000 ^{14}C BP. All dated Holocene samples used in the quantitative analysis were older than 150 years old, and therefore no corrections were made for the Suess effect.

The database was interrogated to make comparisons for three types of variation: (1) groups of species at a given site and time period; (2) groups of sites at a given time and

for a given species, and (3) time periods at a given site for given species. Examples of the mathematical treatments to the data set of species in Alberta during the pre-LGM period are presented in Figure 5.4. Isotopic niche position, niche size and niche overlap of the groups was evaluated for each comparison. Niche position was determined using the mean $\delta^{13}\text{C}$ and $\delta^{15}\text{N}$ of each group. These two metrics were organized from highest to lowest within a dataset, to help discern larger ecological patterns. Niche size was determined using the TA, SEA_c and $\text{SEA}_{b\text{-prop}}$ of each group; SEA_b was calculated using 10^6 iterations. The relative niche size rankings for two sites, species or time periods were only defined when all three metrics gave the same result. Exceptions were made when one of the three metrics produced a tie, and the other two metrics were in agreement. Niche overlap was determined by calculating the proportion of the TA or SEA_c overlap between two groups, rounded to the nearest 10%. Groups were considered to overlap if either metric showed overlap. The overlap was calculated by dividing the area of overlap by the area of one of the two groups. This created situations where an overlap was obscured because one of the two groups was much larger than the other. To prevent this, the data was processed twice. The area of overlap was divided by the size of the first group the first time, and the second group the second time.

The normality of the data was tested in R version 3.1.1 (R Core Team, 2014) using the R Studio interface version 0.98.1083 using a multivariate Shapiro-Wilk test, using the `mshapiro.test` function in the ‘`mvnormtest`’ package (Royston, 1982). Out of a total of 95 distinct groups of species at a specific site and time period (including all groups from age binning methods one and two), 38 (40%) are non-parametric. Virtually every site, species and time period includes groups for which the data are parametric and groups for which the data are nonparametric (Appendix HH).

5.3 Results

5.3.1 Age binning approaches

As mentioned earlier, two approaches to the age binning were tested in this work. Binning approach A followed Fox Dobbs et al. (Fox-Dobbs et al., 2008), and binning approach B followed the model presented by the EPILOG project (Mix et al., 2001),

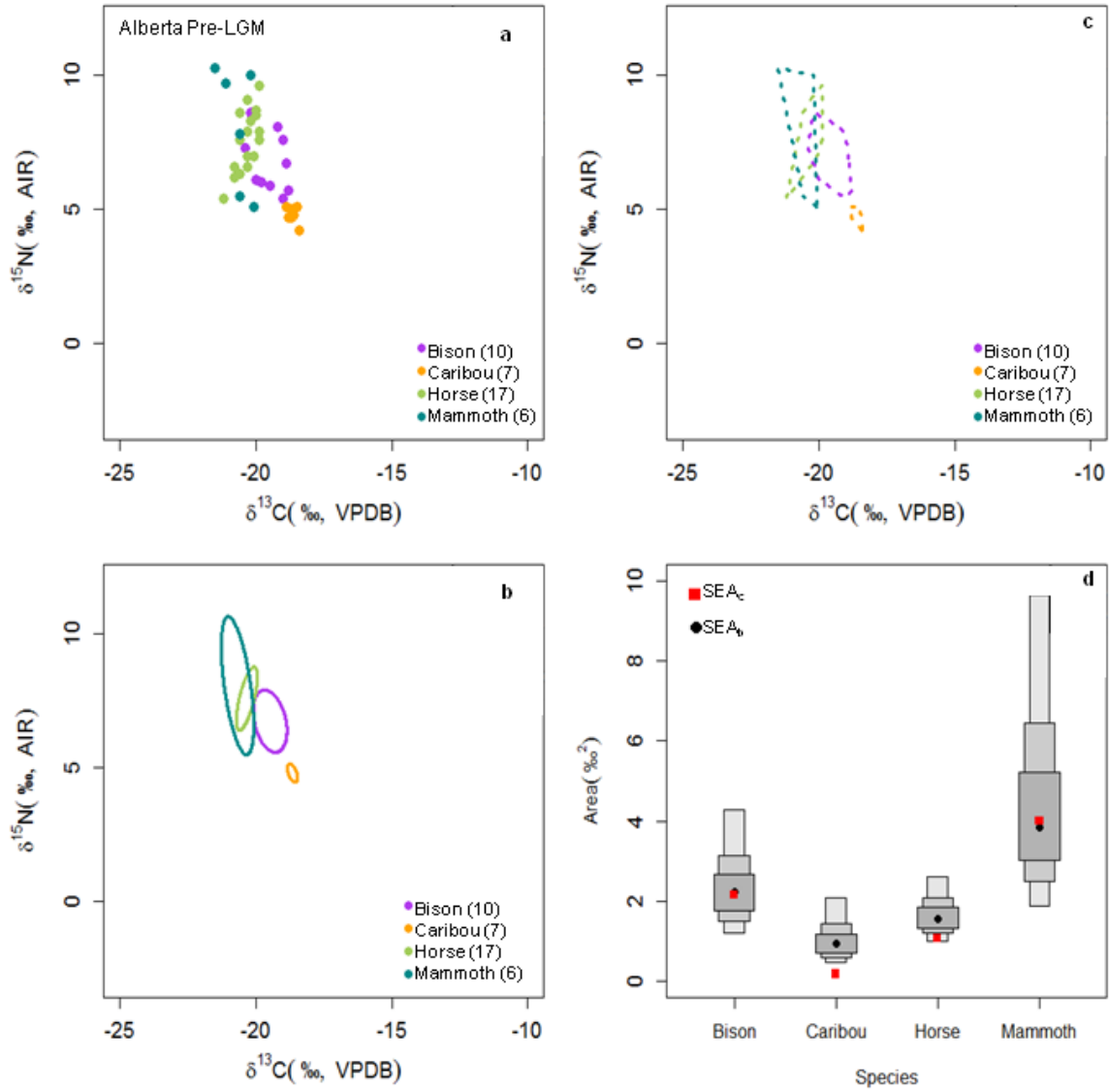


Figure 5.4 Graphs of $\delta^{13}\text{C}$ and $\delta^{15}\text{N}$ of pre-LGM Albertan megafauna produced in SIBER: a. Individual data; b. Small-sample-size corrected ellipses encompassing 40% of the data for each species; c. Convex hulls encompassing the total area of all data for each species; d. Density plots of the most probable sizes of the standard ellipses for each species, based on Bayesian statistical analysis. The most probable size predicted by Bayesian statistical analysis for each species is shown by a black diamond (SEA_b), while the size of the small sample-size corrected ellipse (SEA_c) is shown by a red square.

which was based on a compilation of climatic evidence from a variety of proxies. When the data was subdivided using each of the approaches, and overall isotopic ecological patterns were compared, both models produced the same general results. These patterns, however, held more strongly for data that was subdivided using the Mix et al. (Mix et al., 2001) model, with fewer species, sites or time periods appearing as outliers to the general patterns. The remainder of the paper presents the results obtained solely from the second binning approach (Mix et al., 2001). Results from the first binning approach are listed in Appendices BB, DD and GG.

5.3.2 Species proportions at each site

Data on species proportions were available for: (1) two Russian sites, Taymyr Peninsula and Kolyma River Lowland, Siberia (Mol et al., 2006; Zimov et al., 2012); (2) three Alaskan sites, Fairbanks, the North Slope and Selawik (Druckenmiller, 2008; Guthrie, 1968; Mann et al., 2013), and one Canadian site, Alberta (Appendix K; Jass et al., 2011). These analyses were conducted by counting the number of individual specimens, and generally were not corrected for differences in the number of skeletal elements in different species, or other collection biases, such as the risk of over-representing species with more robust material (Guthrie, 1968; Mann et al., 2013; Zimov et al., 2012). Neither of the two Russian sites has strong associated dating. The Yakutia site is known to contain specimens spanning the range from the pre-LGM to the post-LGM time periods (Zimov et al., 2012). Some samples from Taymyr Peninsula are dated, and the majority of these are from the pre-LGM time period (MacPhee et al., 2002; Mol et al., 2006). Four sites from Fairbanks (Guthrie, 1968) were first considered separately. As the general patterns obtained were similar for each site, an average set of proportions was then calculated; all samples from Guthrie's study are undated. Dates for the North Slope site (Mann et al., 2013) were combined with information from Groves (2015, personal communication) to obtain time-dependent species proportions. Radiocarbon dates were obtained for several Selawik samples in this study and in previous work (Druckenmiller, 2008), the majority of which were pre-LGM. Species abundances and radiocarbon dating are available at the Alberta site (Jass et al., 2011) for both the pre-LGM and post-LGM time periods.

Individual sites across the entire mammoth steppe, or even just within eastern Beringia, show a large difference in relative species abundances, even between sites that are geographically close (Fig. 5.5; Appendix K). For example, Fairbanks is bison-dominated, the North Slope is horse-dominated and the Selawik is mammoth-dominated, despite these all being Alaskan sites. Some weak patterns can be discerned from these data, although out of the six sites, no pattern holds for more than four sites. Generally, horse is most prevalent at a site, followed by bison and then mammoth or muskox, and caribou is less prevalent than mammoth, bison or horse.

The two sites for which the strongest temporal control is available show different patterns in their response to the LGM (Fig. 5.6). Alberta shifts from a horse-dominated assemblage with bison as the secondary species to a bison-dominated assemblage with horse as the secondary species after the LGM. The North Slope remained horse-dominated during the entire late Pleistocene, and there was an increase in the proportion of horse at the site over time. The secondary species at the North Slope shifted from bison during the pre-LGM, to caribou during the LGM, and then back to bison during the post-LGM time period. The modern North Slope is composed almost entirely of caribou.

5.3.3 Variation between species at a given site and time period

The isotopic niche characteristics for each species at a given site and time period are detailed in Appendix CC. Figure 5.7 displays SEA_c for species at two sites (Alberta, North Slope) for two time periods (pre-LGM, post-LGM).

5.3.3.1 Typical pre-LGM patterns and exceptions

The pattern of species' average $\delta^{13}C$ and $\delta^{15}N$ is relatively consistent among the 7 measured mammoth steppe sites for the pre-LGM time period (Fig. 5.8), though there were deviations from typical species $\delta^{13}C$ and $\delta^{15}N$ patterns at one site. Average $\delta^{13}C$ of horse < mastodon at Fairbanks, and average $\delta^{15}N$ of mastodon > caribou and horse at Fairbanks (Fig. 5.9). At the majority of sites (Klondike, NW Europe, North Slope, Fairbanks and Yakutia), mammoth and mastodon isotopic niches were smaller than those

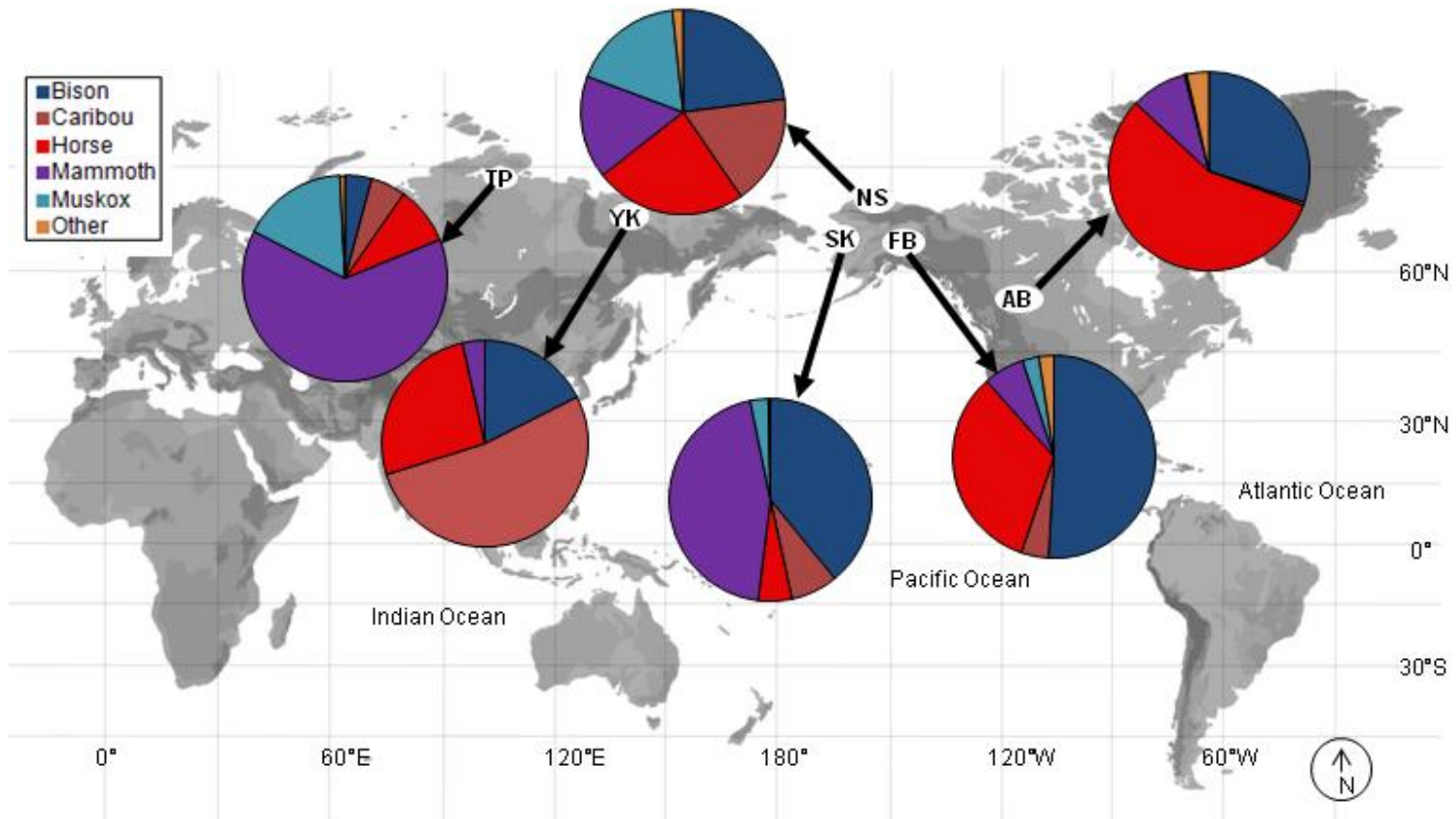


Figure 5.5 Herbivore species proportions at sites across the mammoth steppe. Sites lettered as in Figure 5.1. Proportions are shown for sites known to represent pre-LGM species abundances (Alberta and North Slope), sites that are primarily composed of pre-LGM samples (Selawik and Taymry Peninsula), and sites for which there is no dating control (Fairbanks and Yakutia). Higher altitudes are represented by darker shades of grey. Artwork by Katherine Allan.

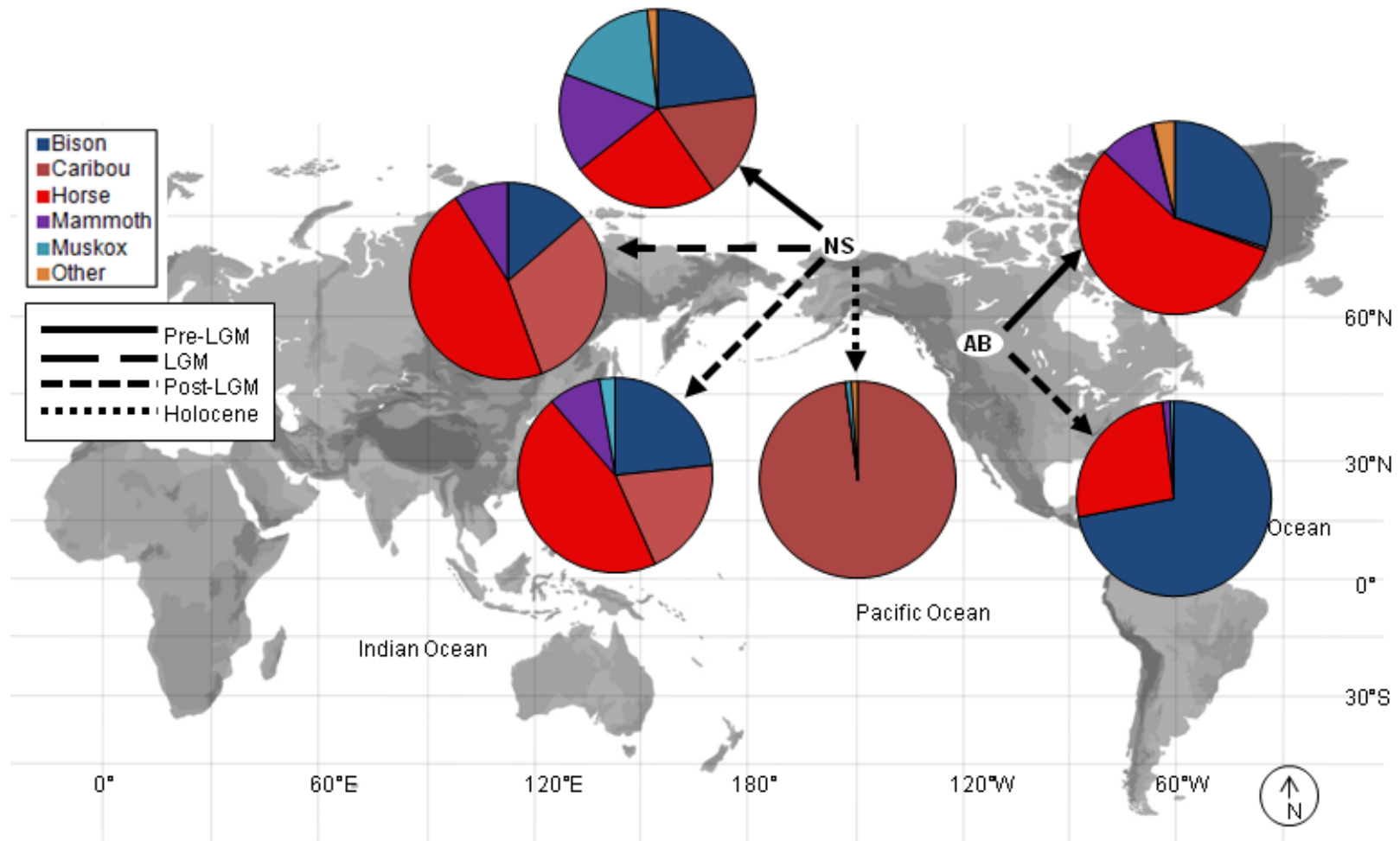


Figure 5.6 Changes in herbivore species proportions over time at Alberta and the North Slope. Sites lettered as in Figure 5.1. Higher altitudes are represented by darker shades of grey. Artwork by Katherine Allan.

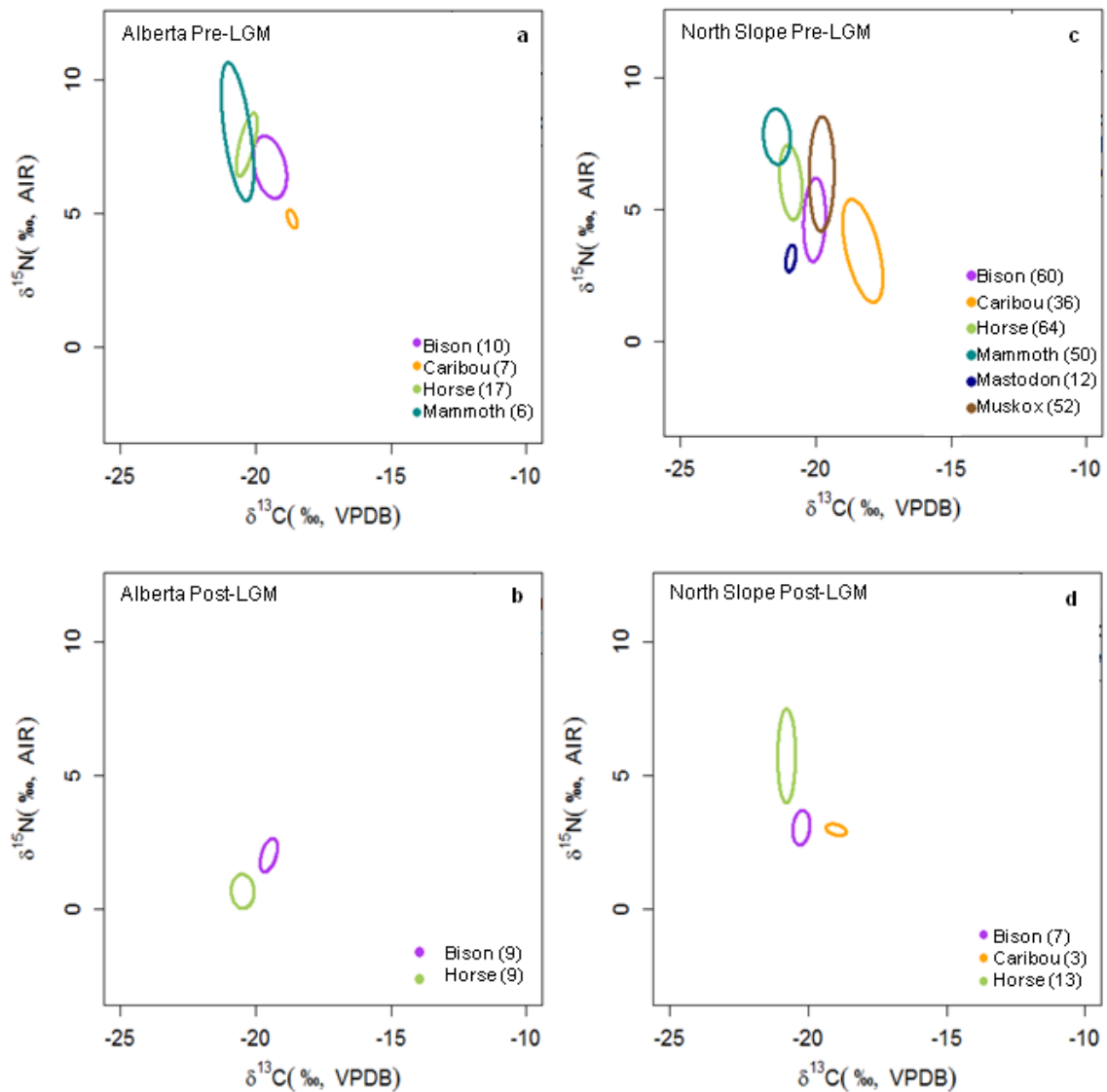


Figure 5.7 Small-sample size corrected ellipses (SEAc) of species at two periods at two sites: **a.** Alberta species during the pre-LGM period; **b.** Alberta species during the post-LGM period; **c.** North Slope species during the pre-LGM period; **d.** North Slope species during the post-LGM period.

for muskox, horse and caribou. Only at Alberta and Taymyr was the mammoth isotopic niche larger than caribou, horse or muskox. The typically smaller isotopic niche of pre-LGM mammoths and mastodons than muskox, horse and caribou can be seen in Figure 5.7c. The larger isotopic niche of mammoth at Alberta is displayed in Figure 5.7a.

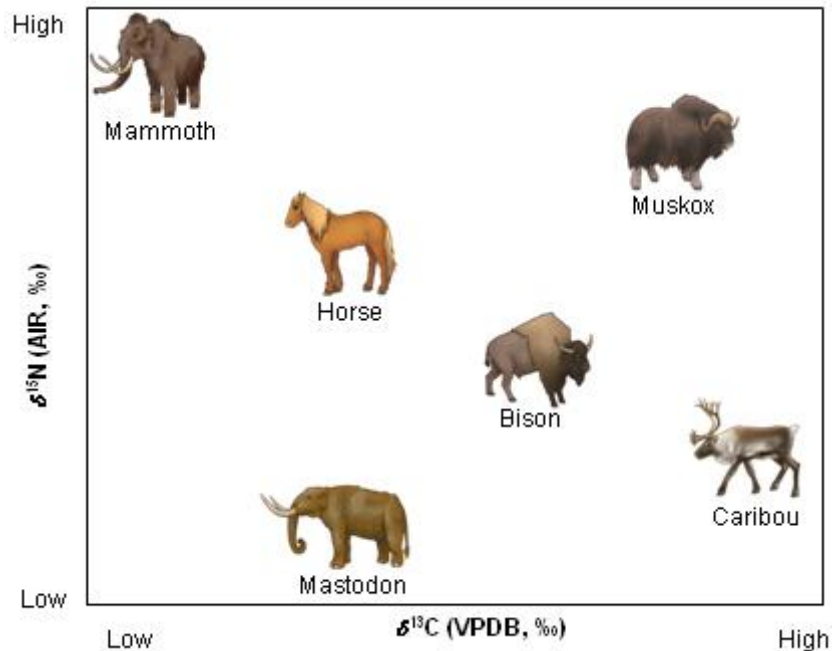


Figure 5.8 Typical carbon and nitrogen isotopic ranking of species at pre-LGM sites. From lowest to highest, average $\delta^{13}\text{C}$ tended to follow the order: mammoth < mastodon = horse < bison < muskox < caribou. From lowest to highest, the average $\delta^{15}\text{N}$ tended to follow the order: mastodon < caribou < bison < horse < muskox < mammoth. Artwork by Katherine Allan. Mammoth drawing from Chapter 3 and Schwartz-Narbonne et al. (2015). Mastodon drawing from Chapter 4.

Species are considered to overlap when there is at least 10% overlap using one of the two metrics. There are five species pairings showing isotopic niche overlap at multiple sites: bison-horse, bison-caribou, bison-muskox, horse-mammoth, and horse-mastodon. These five overlaps are considered ‘typical’ niche overlaps. Figures 5.7a and 5.7c display the horse-mammoth overlap at Alberta and the North Slope and the bison-muskox overlap at the North Slope. The TA isotopic niches overlapped for the bison-horse at Alberta and the North Slope (e.g. Fig. 5.4c), and for bison-caribou at the North Slope, but these overlaps are not visible in the graphs illustrating SEA_c .

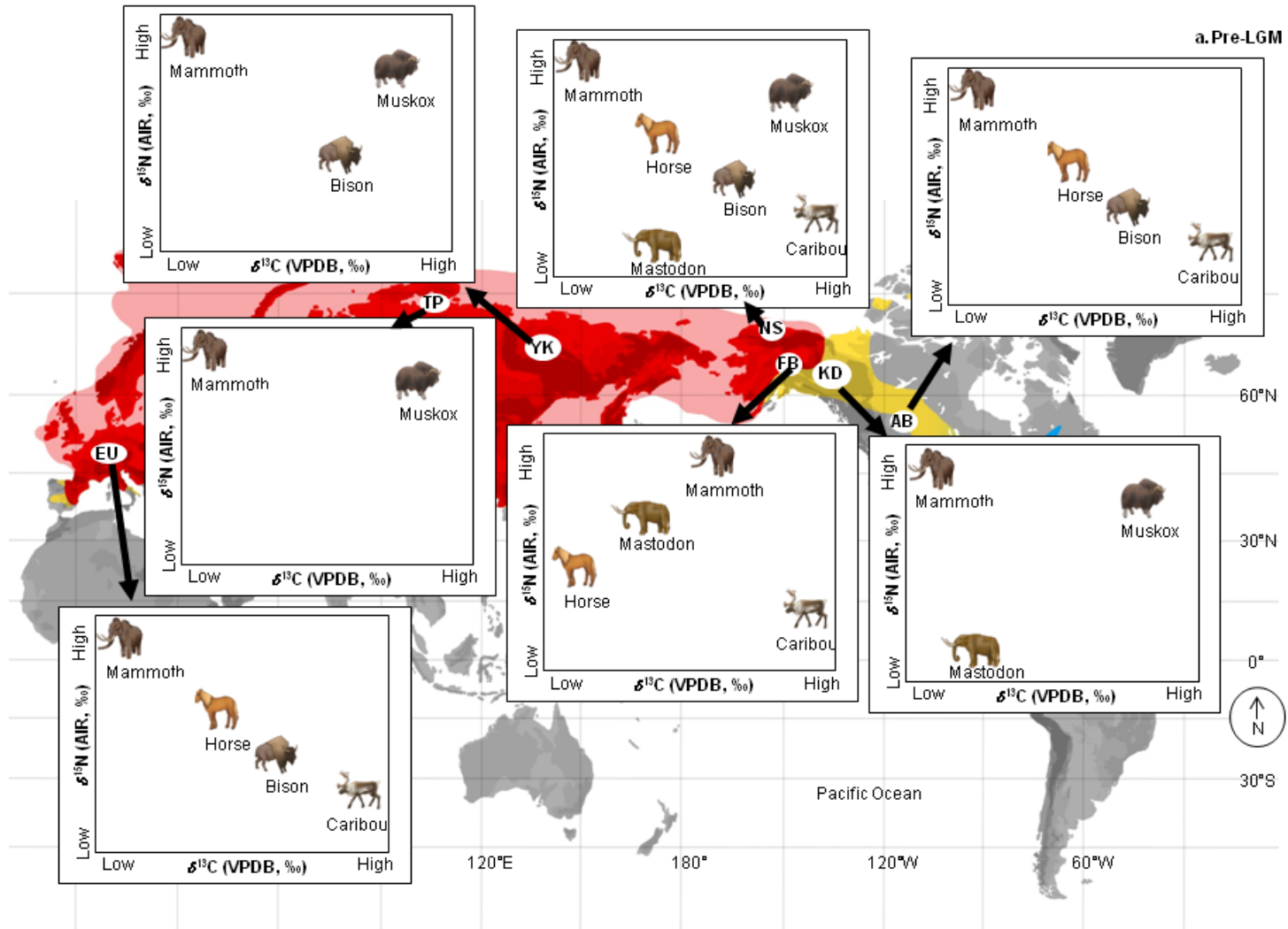


Figure 5.9 continues on next page.

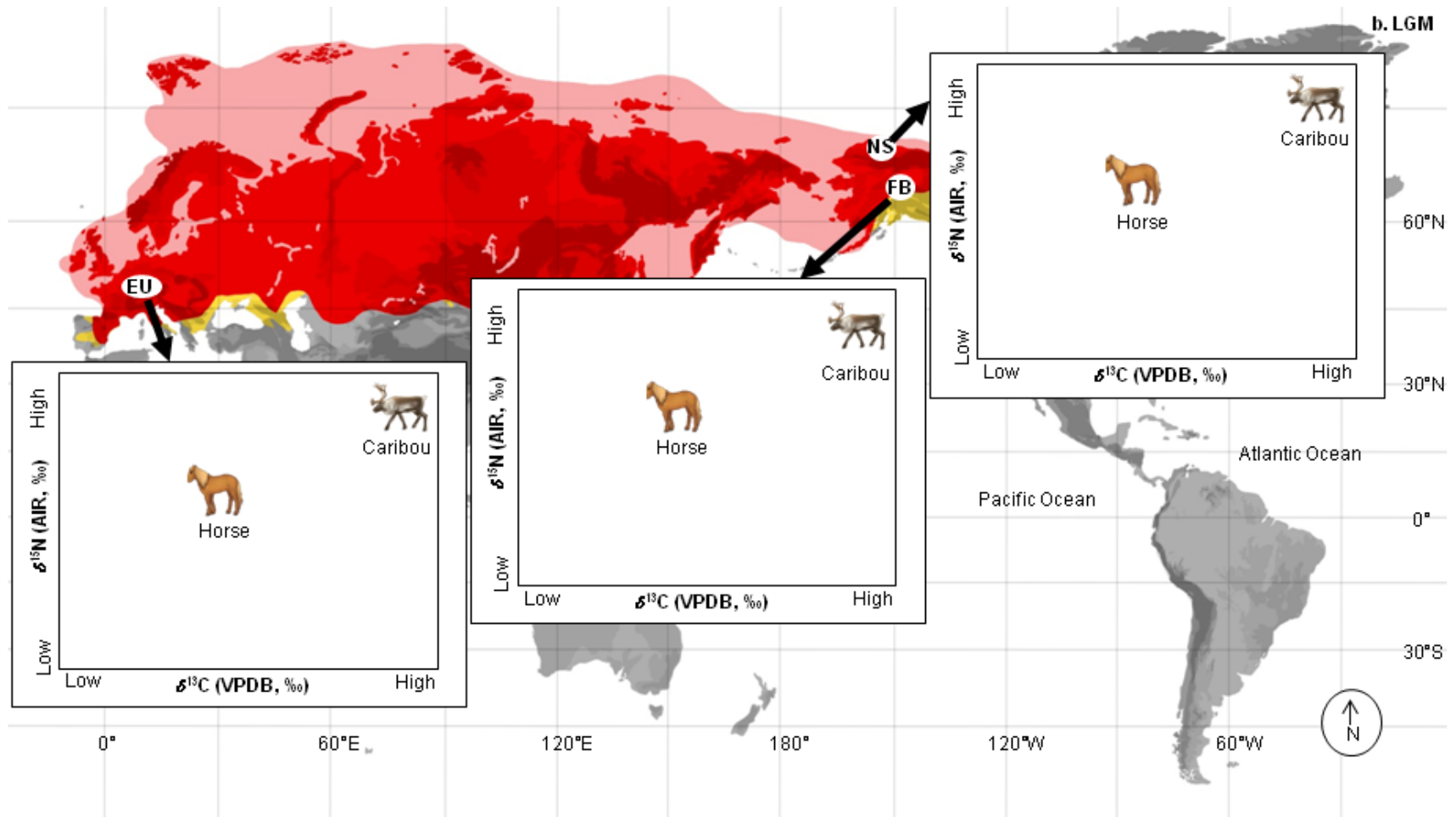


Figure 5.9 continues on next page.

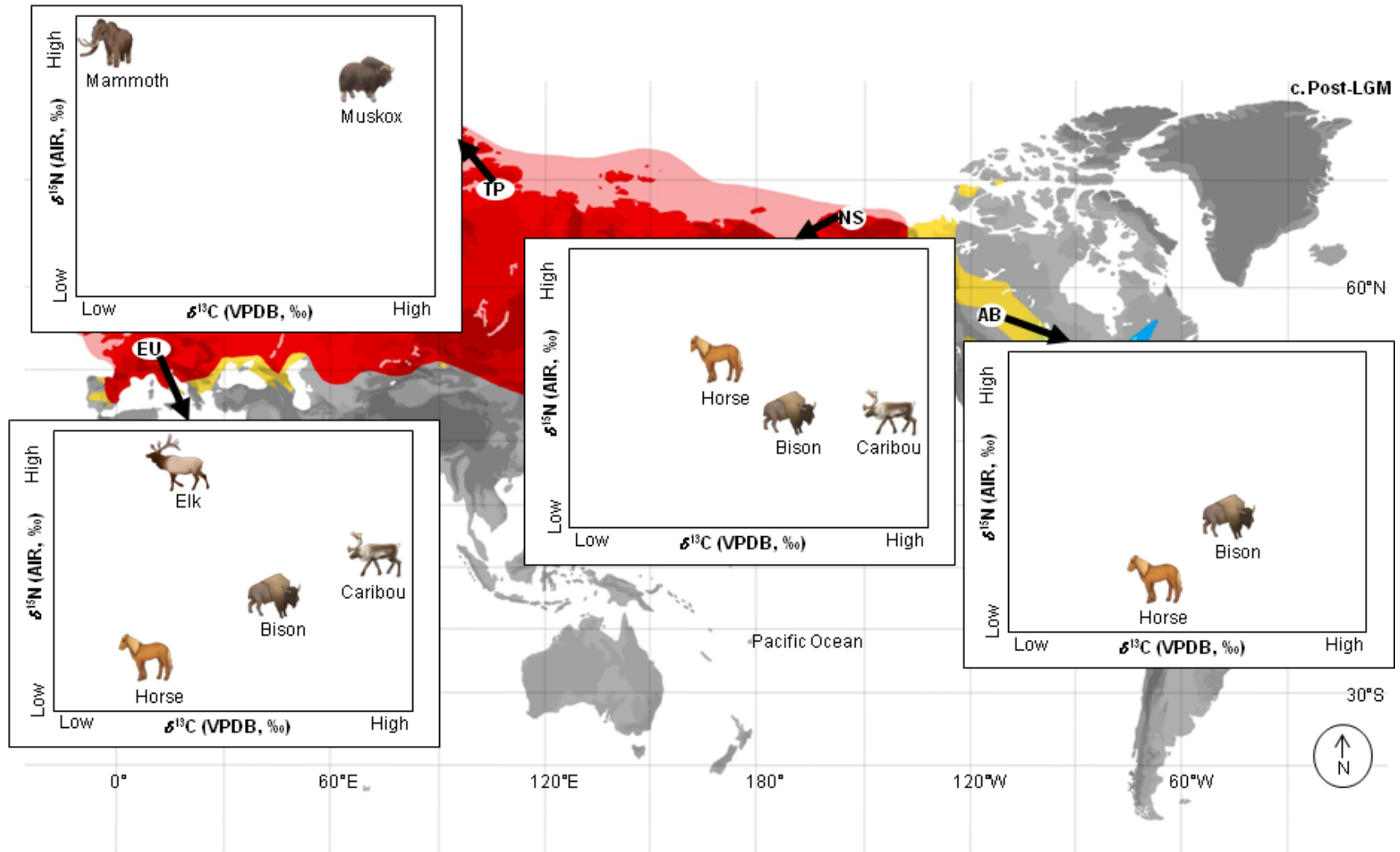


Figure 5.9 continues on next page.

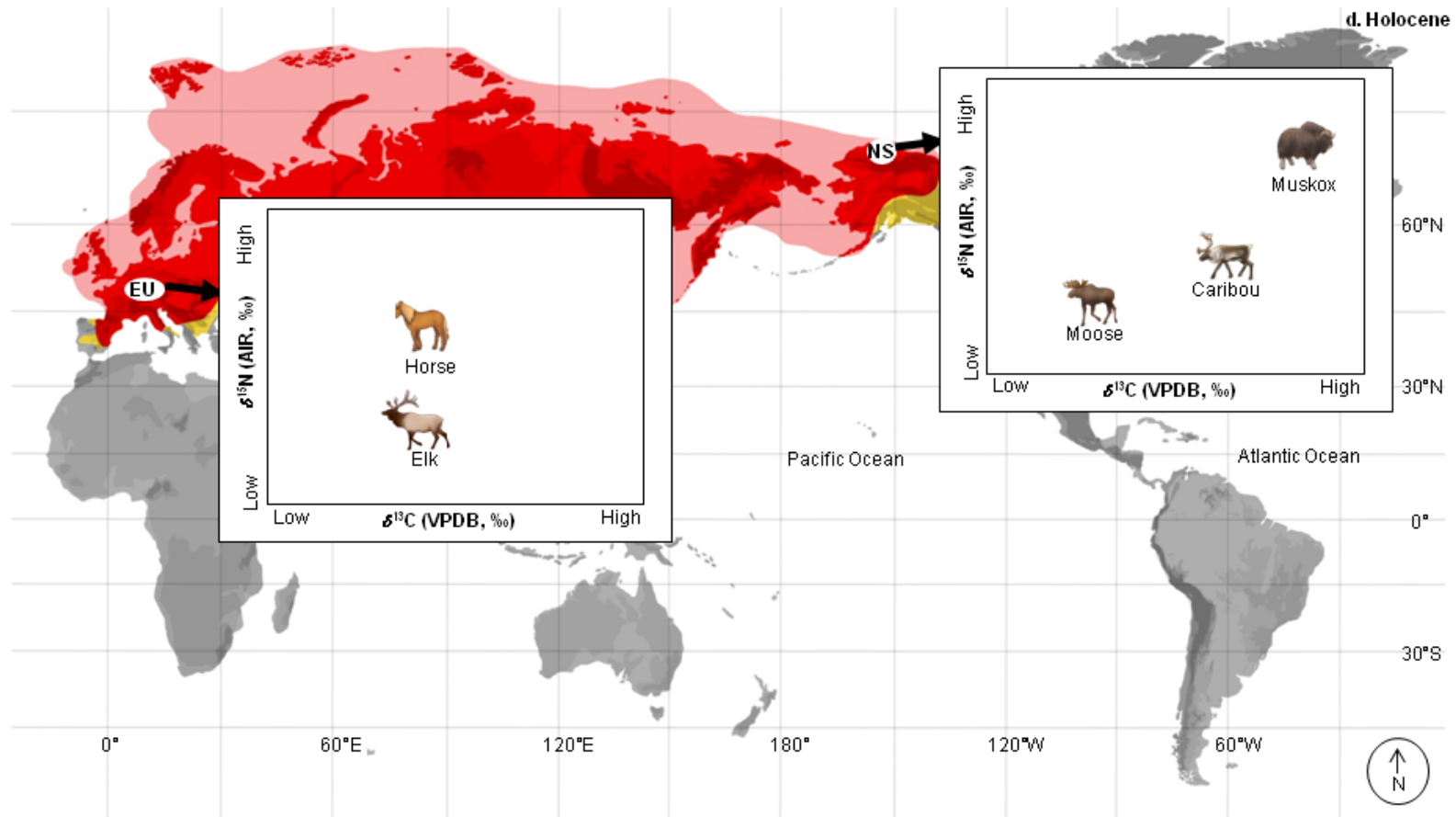


Figure 5.9 Average and nitrogen isotopic rankings of species from at all pre-LGM site having sufficient data for qualitative analysis. Sites lettered as in Figure 5.1. Higher altitudes are represented by darker shades of grey: a. Pre-LGM isotopic rankings; b. LGM isotopic rankings; c. Post-LGM isotopic rankings; d. Holocene isotopic rankings. Artwork by Katherine Allan. Mammoth drawing from Schwartz-Narbonne et al. (2015). Mastodon drawing from Chapter 4.

There are exceptions to the ‘typical’ niche overlaps. Situations where these niche overlaps are missing are mostly related to species occurring in smaller abundances than typical, or niche sizes that are small relative to other species at the site. For example, horse and mammoth did not overlap at Fairbanks or Selawik. At Fairbanks, horse abundance is lower than bison, which is atypical for the mammoth steppe. At Selawik, mammoth abundance is higher than horse. Likewise, bison and caribou did not overlap at Alberta. There, caribou has the smallest isotopic niche and caribou abundance is low compared to other species at this site.

There are also a number of isotopic niche overlaps that occur only at one site, and which can be related to species with the largest niches at that site. Bison and mammoth overlapped at Alberta, where they had the largest niches but abundances lower than horse (Figs. 5.4c; 5.5). Muskox-mastodon and mastodon-mammoth overlap at Klondike, a pattern driven by the large niches of mastodon and muskox. Caribou-horse overlap in NW Europe, where they have the largest niche, as is also the case for the North Slope for muskox-caribou. There is also overlap between horse-muskox at the North Slope.

5.3.3.2 Typical LGM patterns and exceptions

Three sites had sufficient dated samples for analysis of the species patterns for caribou and horse during the LGM (Fairbanks, North Slope and NW Europe). The $\delta^{13}\text{C}$ patterns were the same as for the pre-LGM, but the average $\delta^{15}\text{N}$ of horse was lower than caribou at all three sites (Fig. 5.9b). This shift corresponded to an increase in the relative proportion of caribou at the North Slope (Fig. 5.6). This site shifted from horse- and bison-dominated to horse-dominated, with caribou being the second most prevalent species. There was no overlap between caribou and horse at these three sites, which corresponds to expected pre-LGM conditions.

5.3.3.3 Typical post-LGM patterns and exceptions

Only four sites had sufficient samples for $\delta^{13}\text{C}$ and $\delta^{15}\text{N}$ patterns to be assigned to species (Alberta, NW Europe, North Slope and Taymyr Peninsula; see Fig. 5.9c). Horse, bison, caribou, mammoth and muskox all had the same and expected patterns for average

species $\delta^{13}\text{C}$ observed for the pre-LGM and LGM. There was too much variation among sites to ascribe patterns to the average $\delta^{15}\text{N}$ of the species. The Taymyr Peninsula retained the expected relative $\delta^{15}\text{N}$ rankings of mammoth and muskox from the pre-LGM. No consistent patterns were observed in horse, bison and caribou $\delta^{15}\text{N}$ rankings at Alberta, NW Europe or North Slope. The three sites did not consistently follow patterns expected based on pre-LGM $\delta^{15}\text{N}$ or the post-LGM $\delta^{15}\text{N}$. This variation can be seen in Figures 5.7a-d. In Alberta, the average $\delta^{15}\text{N}$ of pre-LGM horse are higher than bison for the pre-LGM, but lower for the post-LGM (Figs. 5.7a, b). In contrast, in the North Slope, the horse consistently has higher average $\delta^{15}\text{N}$ than bison for both pre-LGM and post-LGM (Figs. 5.7c, d). Alberta shifted from horse-dominated during the pre-LGM to bison-dominated during the post-LGM (Fig. 5.6). In contrast the North Slope remained horse-dominated throughout the late Pleistocene. At both Alberta and the North Slope, the bison isotopic niche was larger than the horse niche during the pre-LGM, and was smaller during the post-LGM (Fig. 5.7). At both sites, there was a shift from pre-LGM overlap between the species to no overlap during the post-LGM. NW Europe was distinct in its complete overlap among the four species measured at the site (bison, elk, caribou and horse). A shift also occurs in the position of caribou, which moves from generally having the lowest $\delta^{15}\text{N}$ during the pre-LGM to commonly having the same or higher average higher $\delta^{15}\text{N}$ than bison and horse at North Slope and NW Europe (Fig. 5.9c). This change in position comes without a change in caribou relative abundance at the North Slope, where it remains less abundant than horse or bison (Fig. 5.6). During the post-LGM, the caribou overlaps with horse and bison at NW Europe but not at the North Slope, and caribou has a smaller isotopic niche than horse at both sites.

5.3.3.4 Typical Holocene patterns and exceptions

Holocene samples were only measured for the North Slope and NW Europe (Fig. 5.9d). There were no common species between the two sites. Both sites contained species that were present at those sites during earlier time periods. In NW Europe, elk and horse were both present and exhibited niche overlap during the post-LGM time period and the Holocene. The average $\delta^{13}\text{C}$ and $\delta^{15}\text{N}$ rankings, however, changed between these time periods. During the post-LGM period, horse had lower average $\delta^{13}\text{C}$ and $\delta^{15}\text{N}$ than elk,

while in the Holocene horse and elk had the same average $\delta^{13}\text{C}$ and horse had higher average $\delta^{15}\text{N}$ than elk. The horse and elk isotopic niches overlapped.

Muskox and caribou were both present at the North Slope during the pre-LGM and the Holocene. The $\delta^{13}\text{C}$ and $\delta^{15}\text{N}$ rankings remained consistent between these species, but niche overlap disappeared in the Holocene. The species proportions of muskox also decreased considerably, and caribou became dominant species at the North Slope in the Holocene.

5.3.3.5 Qualitative interpretations

In some cases where there are insufficient numbers of dated specimens to make quantitative comparisons of the isotopic data, there remains value in comparing the average $\delta^{13}\text{C}$ and $\delta^{15}\text{N}$ of a species to their expected patterns in isotopic space. The ranking of $\delta^{13}\text{C}$ for mastodon and horse was not well-established in the quantitative results, since these two species only coexisted in time at two sites, and one of those sites was Fairbanks which did not follow typical isotopic patterns for the majority of species at the site. For this reason, the “typical” pattern of mastodon and horse having the same average $\delta^{13}\text{C}$ is not observed in the qualitative analysis of other sites. At Alberta, the Klondike and Old Crow, the $\delta^{13}\text{C}$ pattern was horse < mastodon. This was consistent with the pattern observed at Fairbanks.

When considering patterns other than the mastodon versus the horse, of the ten sites where qualitative observations were available, six sites for $\delta^{13}\text{C}$ and three sites for $\delta^{15}\text{N}$ did not match the expected pattern for at least one species. At Fairbanks, the bison average $\delta^{15}\text{N}$ fits the expected pre-LGM pattern for the most part; mastodon, however, is not in its typical place in the pattern, as was previously observed when comparing other species at this site to mastodon. At Yakutia, the pre-LGM material follows the expected patterns, whereas undated material does not. This may suggest that the majority of the undated material is not from the pre-LGM, and that the pattern of average $\delta^{15}\text{N}$ of species at the site changed over time. Post-LGM elk and caribou in south central Siberia do not match the pattern observed in NW Europe. Similarly, Holocene moose and caribou at Selawik do not match the North Slope pattern when only dated caribou specimens are

considered, though they match when both dated and undated material are included in comparisons. Pre-LGM bison, caribou, horse and muskox do not follow the expected patterns at Selawik; horse and bison do not follow expected patterns in later time periods at this site.

There were three species for which the isotopic data could only be examined qualitatively: sheep, woolly rhinoceros, and muskox. At Fairbanks, the muskox species *Symbos cavifrons* (helmeted muskox) was sampled rather than *Ovibos* sp. *S. cavifrons* had the same pattern of average $\delta^{13}\text{C}$ as the other species of muskox, but had the lowest $\delta^{15}\text{N}$ of any species at the site for any time period. Data for woolly rhinoceros was available in NW Europe for both pre- and post-LGM time periods. In both cases, it had the second highest $\delta^{15}\text{N}$, following mammoth. Its $\delta^{13}\text{C}$ ranking varied between time periods, but was generally similar to bison. Data for Dall sheep were examined both for Fairbanks and Klondike, though for different time periods. Their average $\delta^{13}\text{C}$ tended to be high, similar to caribou and higher than muskox. The average $\delta^{15}\text{N}$ of Dall sheep were always lower than woolly mammoth. At Fairbanks, Dall sheep had a higher average $\delta^{15}\text{N}$ than horse, and at Klondike average $\delta^{15}\text{N}$ was lower than muskox.

5.3.4 Variation between sites for a given species and time period

The isotopic niche characteristics of a species at a given time period between varied sites are detailed in Appendix EE. The SEA_c for two species (bison and horse) during two time periods (pre-LGM and post-LGM) are illustrated in Figure 5.10. The overall patterns based on the quantitative results are displayed in Figure 5.11, and the patterns based on both quantitative and qualitative results are displayed in Figure 5.12.

5.3.4.1 Typical pre-LGM patterns and exceptions

General patterns of site differentiation are displayed in Figures 5.11a and b, where sites are listed from west to east. As seen in Figure 5.11a, $\delta^{13}\text{C}$ tended to be lowest for animals from sites between Taymyr Peninsula and Fairbanks, with higher average $\delta^{13}\text{C}$ associated with animals of the same species that lived to the west in NW Europe and to the east in Klondike or Alberta. A similar pattern is visible in the average $\delta^{15}\text{N}$ of sites (Fig. 5.11b).

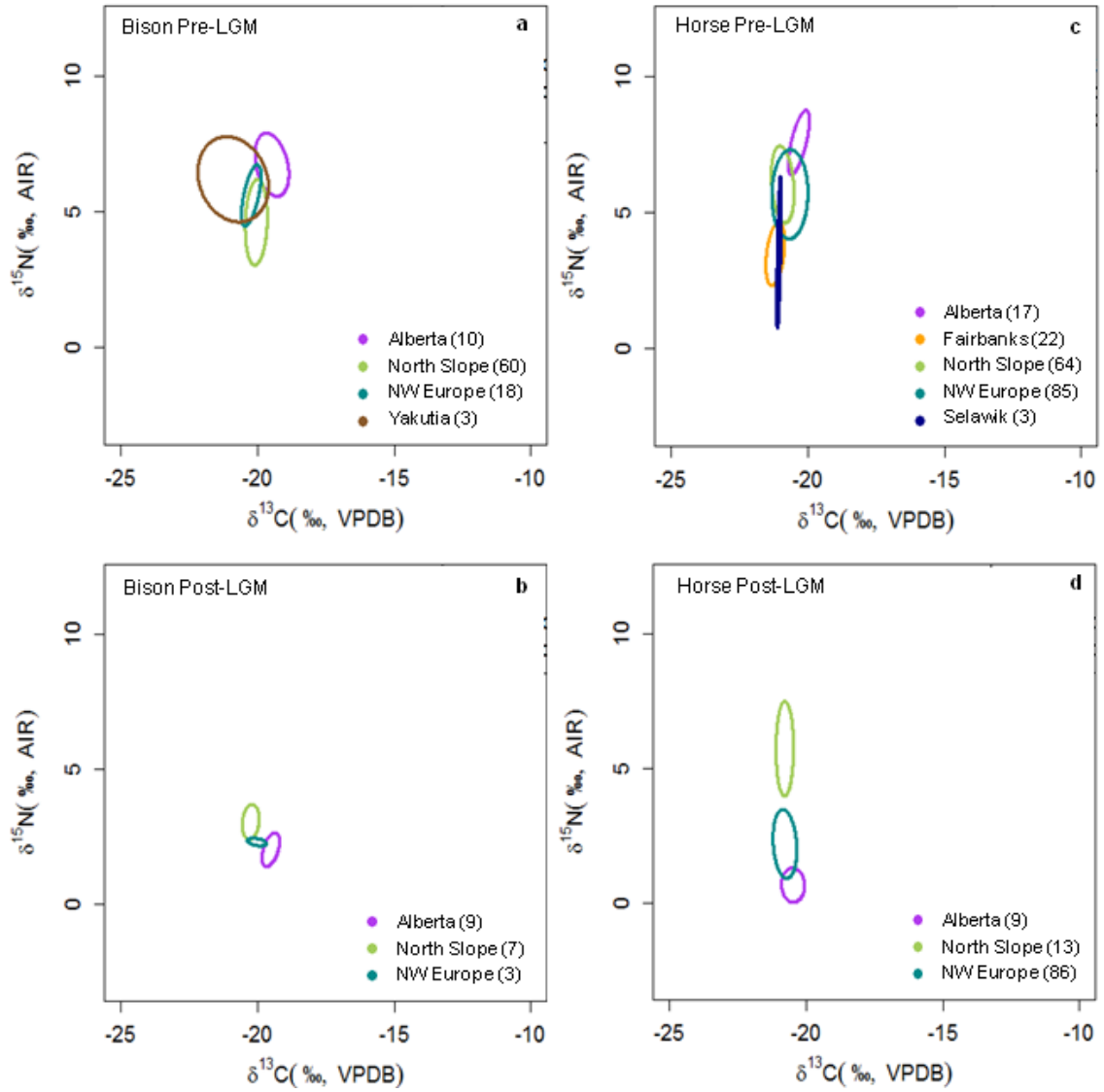


Figure 5.10 Small-sample size corrected ellipses (SEAc) of sites at two periods for two species: **a. Bison during the pre-LGM period; b. Bison during the post-LGM period; c. Horse during the pre-LGM period; d. Horse during the post-LGM period.**

Species who lived in the west (NW Europe and Yakutia) or east (Alberta) had higher average $\delta^{15}\text{N}$ than species who lived in the middle region from Selawik to Klondike.

In several cases, unambiguous distinction between sites was not possible using the available data, in which case those sites were assigned the same relative position in $\delta^{13}\text{C}$ - $\delta^{15}\text{N}$ isotopic space. Sites were not ranked if data were available for only one species or if data were available for only two species and gave conflicting rankings. Nonetheless,

using the ranking associated with each bin, the same sites – Fairbanks or North Slope – always fell outside of expected patterns. These deviations can be seen in four cases: (i) the average $\delta^{13}\text{C}$ of Fairbanks was higher than NW Europe or North Slope for mammoth, (ii) the average $\delta^{13}\text{C}$ of Alberta was higher than North Slope for caribou, (iii) the average $\delta^{15}\text{N}$ of North Slope was higher than NW Europe for horse (see Fig. 5.10c), and (iv) average $\delta^{15}\text{N}$ of North Slope was lower than Fairbanks and Klondike for mastodon. In all other cases, the species fit the expected patterns (see Figs. 5.10a, c)

No consistent pattern of niche size ranking could be discerned among sites for the pre-LGM samples. The isotopic niches for the majority of sites (~two-thirds) overlapped for the species analyzed (e.g. Figs. 5.10a, c). Three sets of sites, however, did not show isotopic niche overlap for multiple species: (i) Alberta-Fairbanks for caribou or horse (Fig. 5.10c) (though there was overlap for mammoth); (ii) Alberta-Selawik for horse or mammoth (Fig. 5.10c); and (iii) Fairbanks-Old Crow for mammoth or mastodon. The isotopic niches for ~one-third of the sites did not overlap for mammoth and mastodon. These were the only two species that showed no isotopic niche overlap for multiple site pairs where those site pairs had overlap for other species.

5.3.4.2 Typical LGM patterns and exceptions

The $\delta^{13}\text{C}$ pattern of Fairbanks, NW Europe and North Slope for horse and caribou are similar to the pre-LGM (Figs. 5.11a, c). The only difference is that the average $\delta^{13}\text{C}$ of species at the North Slope is higher than those in NW Europe during the LGM (Fig. 5.11c). The $\delta^{15}\text{N}$ pattern of the pre-LGM is not retained in the LGM for horse or caribou. As well, unlike the pre-LGM, Fairbanks-North Slope and North Slope-NW Europe isotopic niches no longer overlap, though Fairbanks-NW Europe isotopic niches continue to overlap.

5.3.4.3 Typical post-LGM patterns and exceptions

The general site patterns for the post-LGM time period based on $\delta^{13}\text{C}$ are similar to the pre-LGM (Figs. 5.11a, e). In contrast, the patterns based on $\delta^{15}\text{N}$ are largely reversed compared to the pre-LGM, though they are somewhat similar to the LGM (Figs. 5.11b, d,

f). A clear pattern of isotopic niches sizes for species at individual sites is difficult to discern, as there were too few species that were found at multiple sites. Similarly to the LGM, there were a greater proportion of sites without isotopic niche overlap than there was during the pre-LGM. Approximately two-thirds of sites did not have isotopic overlap during the post-LGM period. This greater degree of separation between sites is illustrated in Figure 5.10, where the isotopic niches of horse and bison from different sites are shown to be less likely to overlap during the post-LGM period than the pre-LGM period.

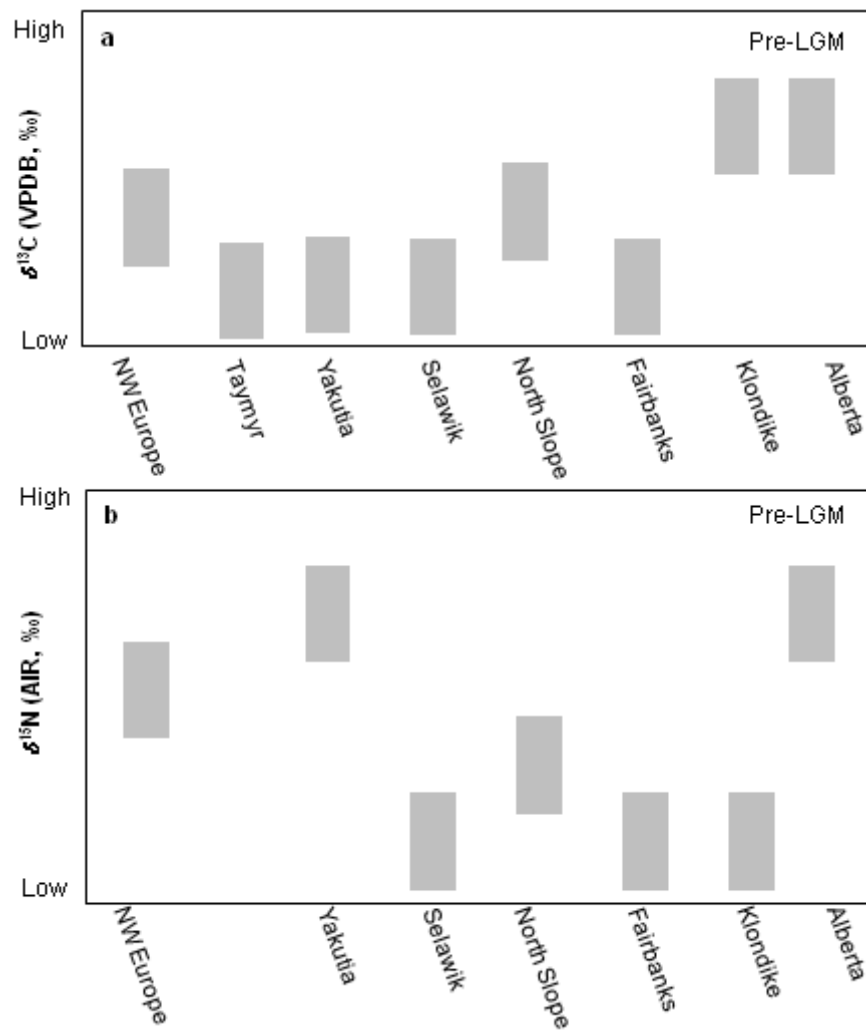


Figure 5.11 continues on next page.

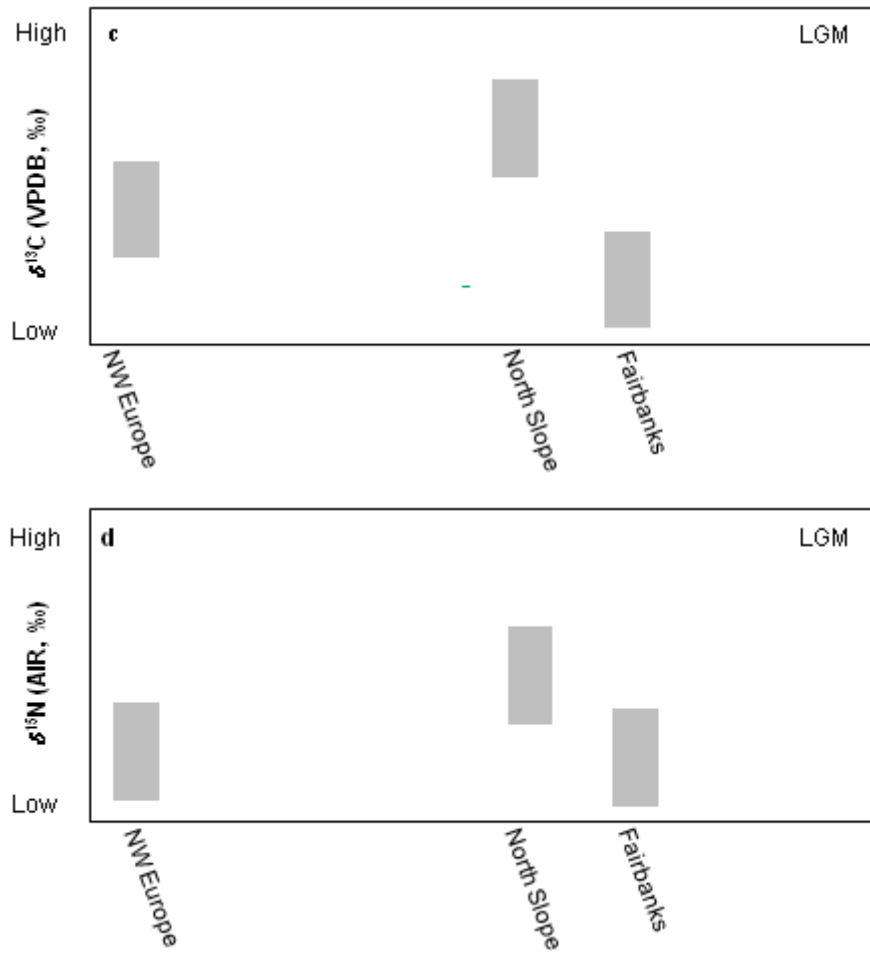


Figure 5.11 continues on next page.

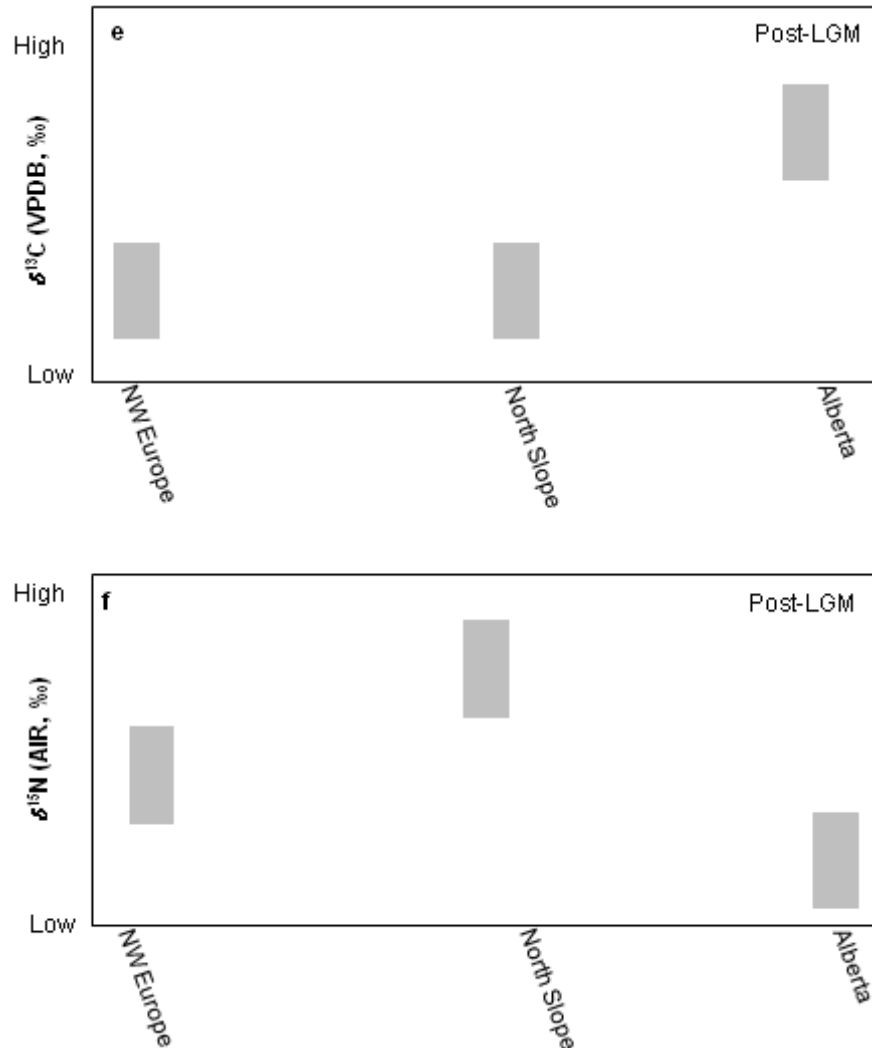


Figure 5.11 Typical isotopic ranking of sites across the mammoth steppe based on the δ -values of multiple species, incorporating results from quantitative analysis. Sites are presented from west to east; note x-axis spacing is not proportional to geographic separation: a. Average pre-LGM $\delta^{13}\text{C}$: Fairbanks = Yakutia = Selawik = Taymyr Peninsula (Taymyr) < NW Europe = North Slope < Alberta = Klondike; b. Average pre-LGM $\delta^{15}\text{N}$: Fairbanks = Klondike = Selawik < North Slope < NW Europe < Yakutia = Alberta; c. Average post-LGM $\delta^{13}\text{C}$: North Slope = NW Europe < Alberta. d. Average post-LGM $\delta^{15}\text{N}$: Alberta < NW Europe < North Slope.

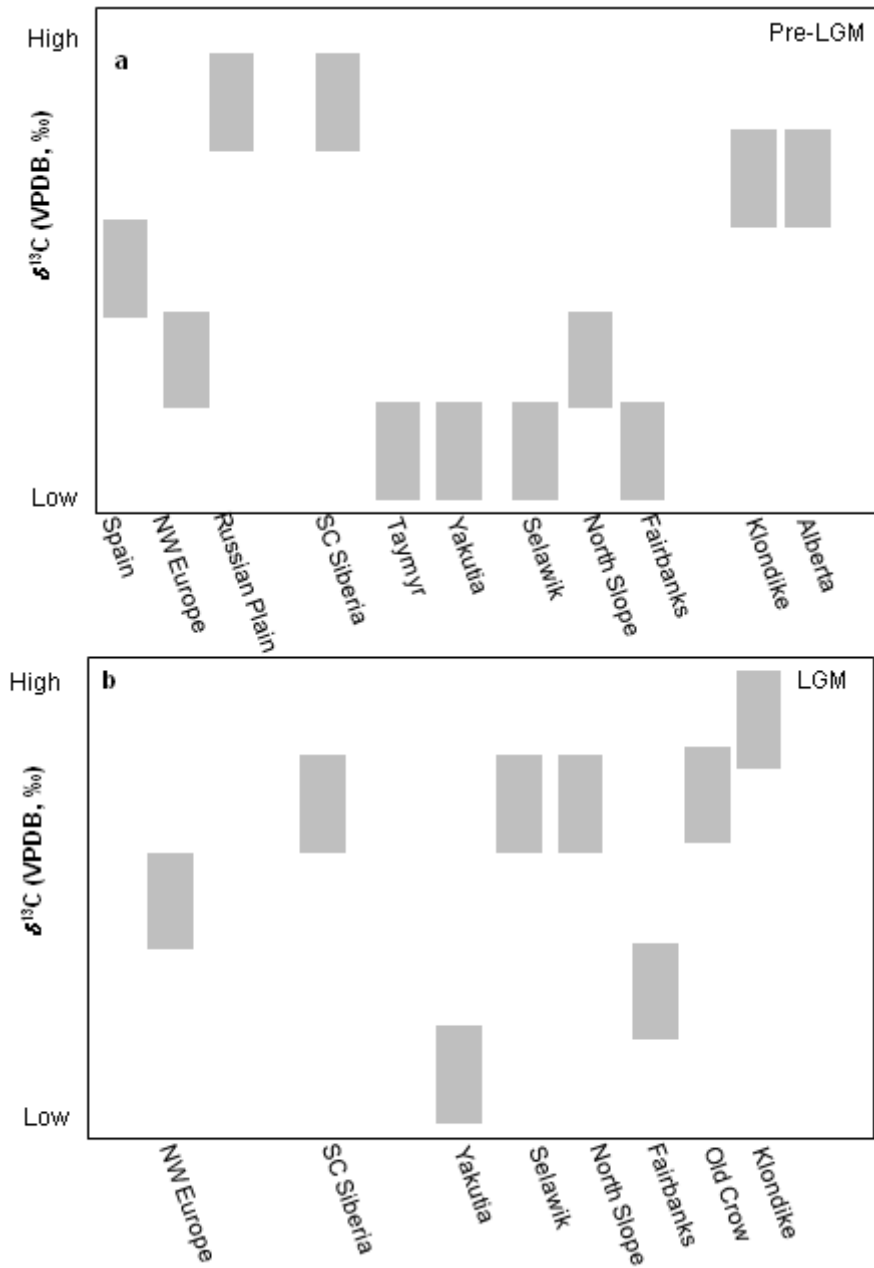


Figure 5.12 continues on next page.

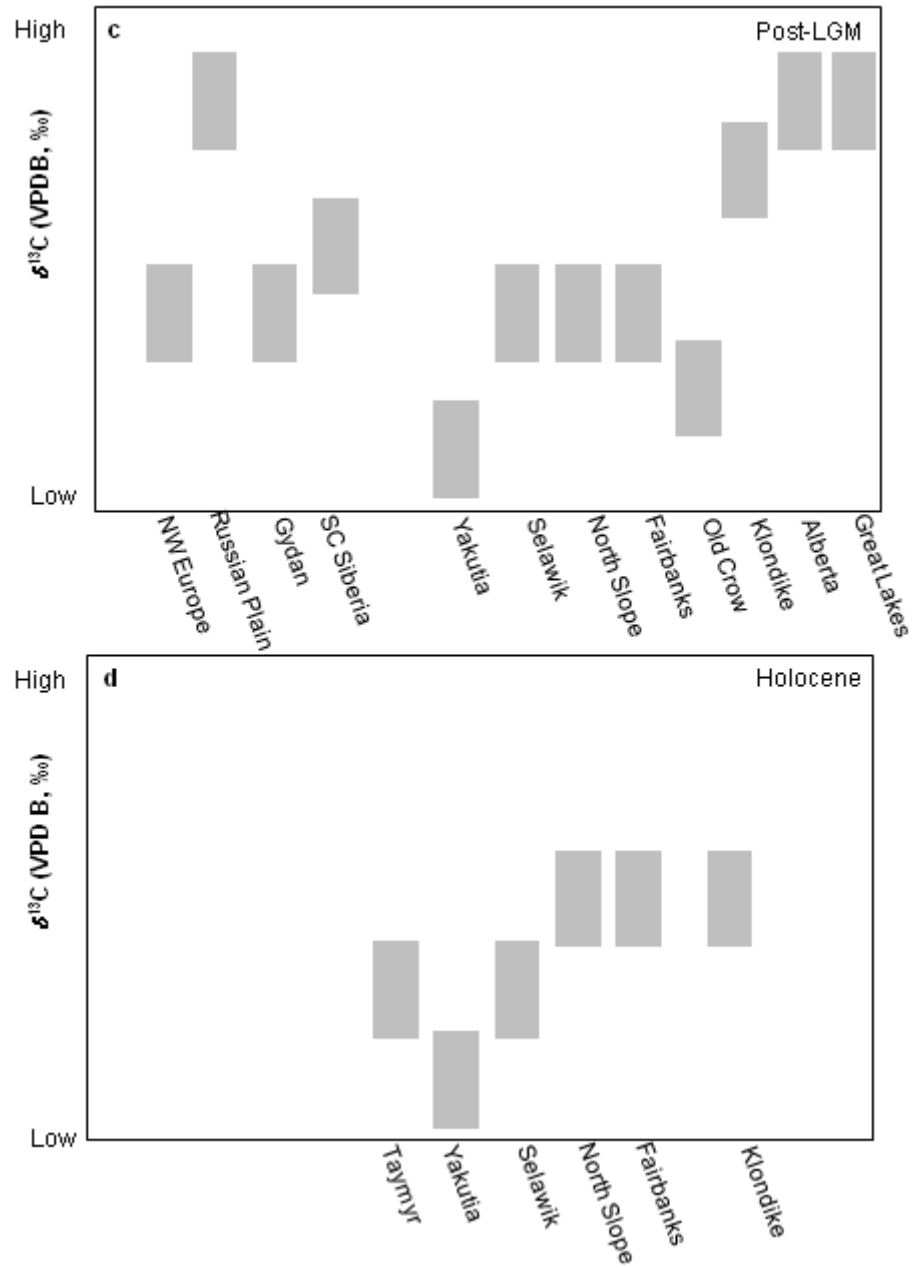


Figure 5.12 continues on next page.

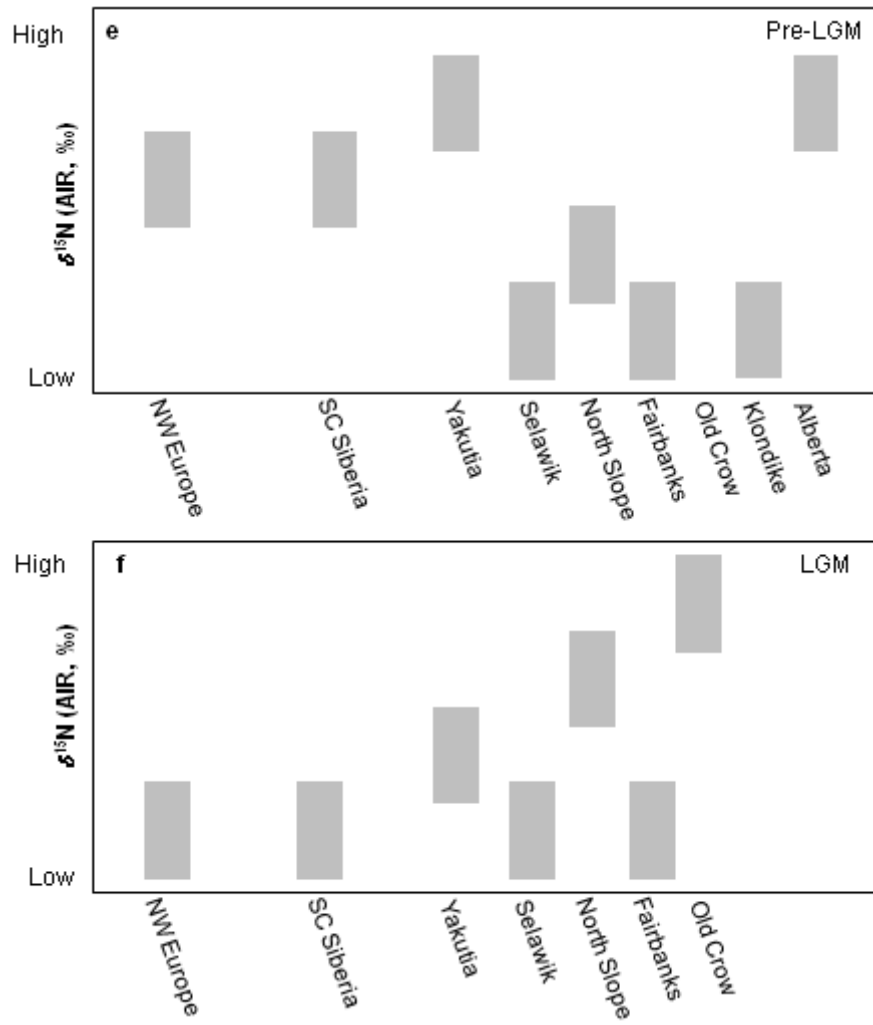
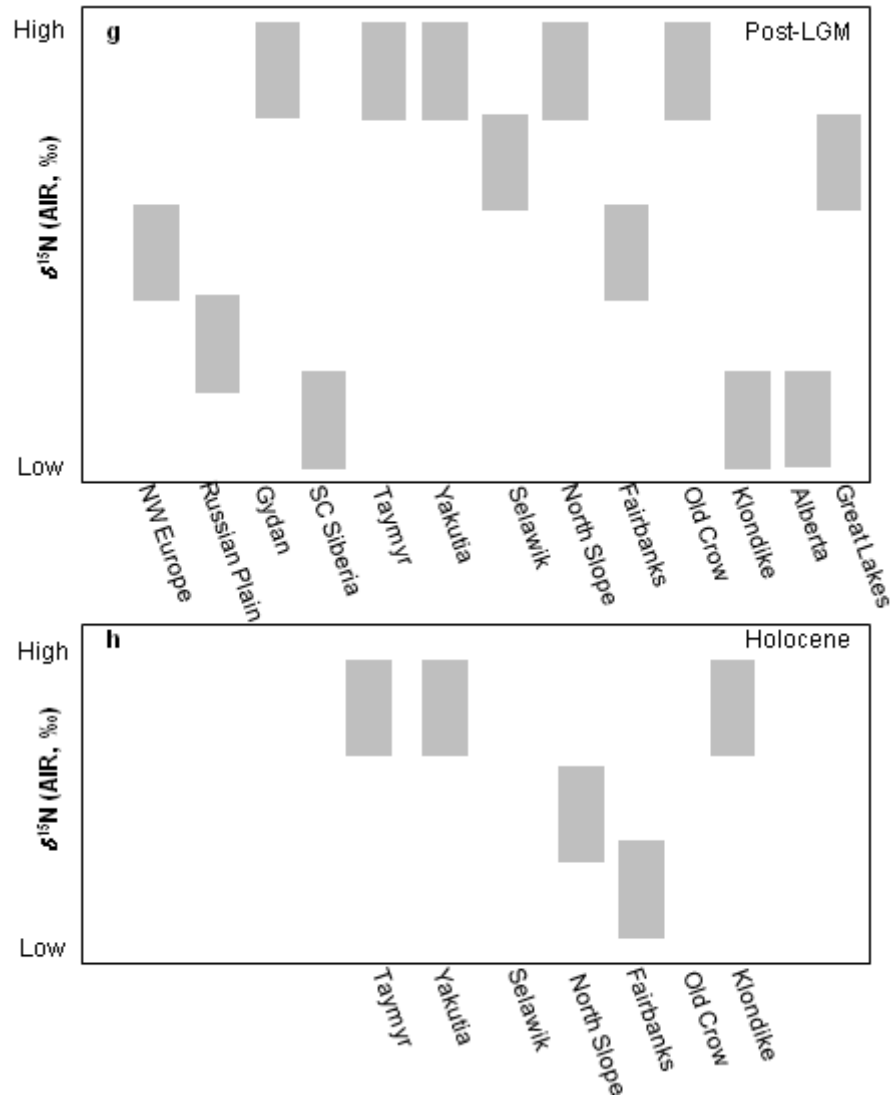


Figure 5.12 continues on next page.



Caption on facing page.

Figure 5.12 Typical isotopic ranking of sites across the mammoth steppe based on the δ -values of multiple species, incorporating results from both qualitative and quantitative analysis. Sites are presented from west to east; note x-axis spacing is not proportional to geographic separation: a. Average pre-LGM $\delta^{13}\text{C}$: Fairbanks = Yakutia = Selawik = Taymyr Peninsula (Taymyr) < NW Europe = North Slope < Spain < Alberta = Klondike < Russian Plain = south central Siberia (SC Siberia); b. Average LGM $\delta^{13}\text{C}$: Yakutia < Fairbanks < NW Europe < SC Siberia = Selawik = North Slope = Old Crow < Klondike; c. Average post-LGM $\delta^{13}\text{C}$: Yakutia < Old Crow < Selawik = Fairbanks = North Slope = NW Europe = Gydan Peninsula (Gydan) < SC Siberia < Klondike < Russian Plain = Great Lakes = Alberta; d. Average Holocene $\delta^{13}\text{C}$: Yakutia < Taymyr = Selawik < North Slope = Klondike = Fairbanks; e. Average pre-LGM $\delta^{15}\text{N}$: Fairbanks = Klondike = Selawik < North Slope < SC Siberia = NW Europe < Yakutia = Alberta < Russian Plain < Spain; f. Average LGM $\delta^{15}\text{N}$: SC Siberia = Selawik = NW Europe = Fairbanks < Yakutia < North Slope < Old Crow; g. Average post-LGM $\delta^{15}\text{N}$: Alberta = SC Siberia = Klondike < Russian Plain < NW Europe = Fairbanks < Great Lakes = Selawik < Yakutia = North Slope = Old Crow = Taymyr = Gydan; h. Average Holocene $\delta^{15}\text{N}$: Fairbanks < North Slope < Klondike = Taymyr = Yakutia.

5.3.4.4 Typical Holocene patterns and exceptions

There are only two Holocene species, muskox and caribou, where samples were analyzed from more than one site. Since the two species were not found at the same two sites, analysis of ‘typical’ Holocene patterns is not possible. The rankings of the two species can be compared to the typical patterns during the pre-LGM, as presented in Figures 5.11a, b. The $\delta^{13}\text{C}$ pattern for Taymyr Peninsula and North Slope based on the muskox average $\delta^{13}\text{C}$ is the same as the typical pattern during the pre-LGM, but this pattern is reversed from the typical pre-LGM pattern for $\delta^{15}\text{N}$. For caribou, the $\delta^{13}\text{C}$ and $\delta^{15}\text{N}$ pattern for Klondike and North Slope are not the same as the typical patterns during the pre-LGM.

5.3.4.5 Qualitative interpretations

Based on the qualitative observations, additional sites were added to the quantitative patterns, as depicted in Figures 5.12a-h. Generally, similar trends were observed from east to west as were observed using the quantitative analysis. During the pre-LGM, the lowest average $\delta^{13}\text{C}$ was generally observed for species living between Taymyr Peninsula and Fairbanks (Fig. 5.12a). This general trend of the highest average $\delta^{13}\text{C}$ occurring in species that lived in the east or west regions of the mammoth steppe held throughout the Pleistocene and Holocene, though there was considerable variability between specific sites (Figs. 5.12b-d). Similarly, the quantitative pre-LGM $\delta^{15}\text{N}$ patterns were also present in the qualitative results, with species living in sites between Selawik and Klondike having lower average $\delta^{15}\text{N}$ than those to the east and to the west (Fig. 5.12e). This pattern shifted over time such that sites on the east and west of the mammoth steppe tended to have the lowest, rather than the highest, average $\delta^{15}\text{N}$ for the species that lived there during the LGM, post-LGM and Holocene (Figs. 5.12 f-h). Again, this matched the changes in the $\delta^{15}\text{N}$ pattern over time detected using the quantitative approach (Figs. 5.11b, d, f).

5.3.5 Variation between time periods for a given species and site

The isotopic niche characteristics of a species at a site over varying time periods are detailed in Appendix GG. The SEA_c for two species (bison and horse) for two sites (Alberta and North Slope) are illustrated in Figure 5.13. The overall patterns are shown in Figure 5.14.

5.3.5.1 Typical patterns and exceptions

The typical $\delta^{13}\text{C}$ and $\delta^{15}\text{N}$ patterns for the time periods (Fig. 5.14a) are highly generalized. While a comparison of any two time periods for either isotope retained these patterns in most cases, results for almost half of the species analyzed at specific sites do not match the general pattern for at least one isotope during at least one time period. For example, bison and horse from Alberta and North Slope follow the expected pattern for average $\delta^{15}\text{N}$ but Alberta bison and North Slope horse do not follow the expected pattern

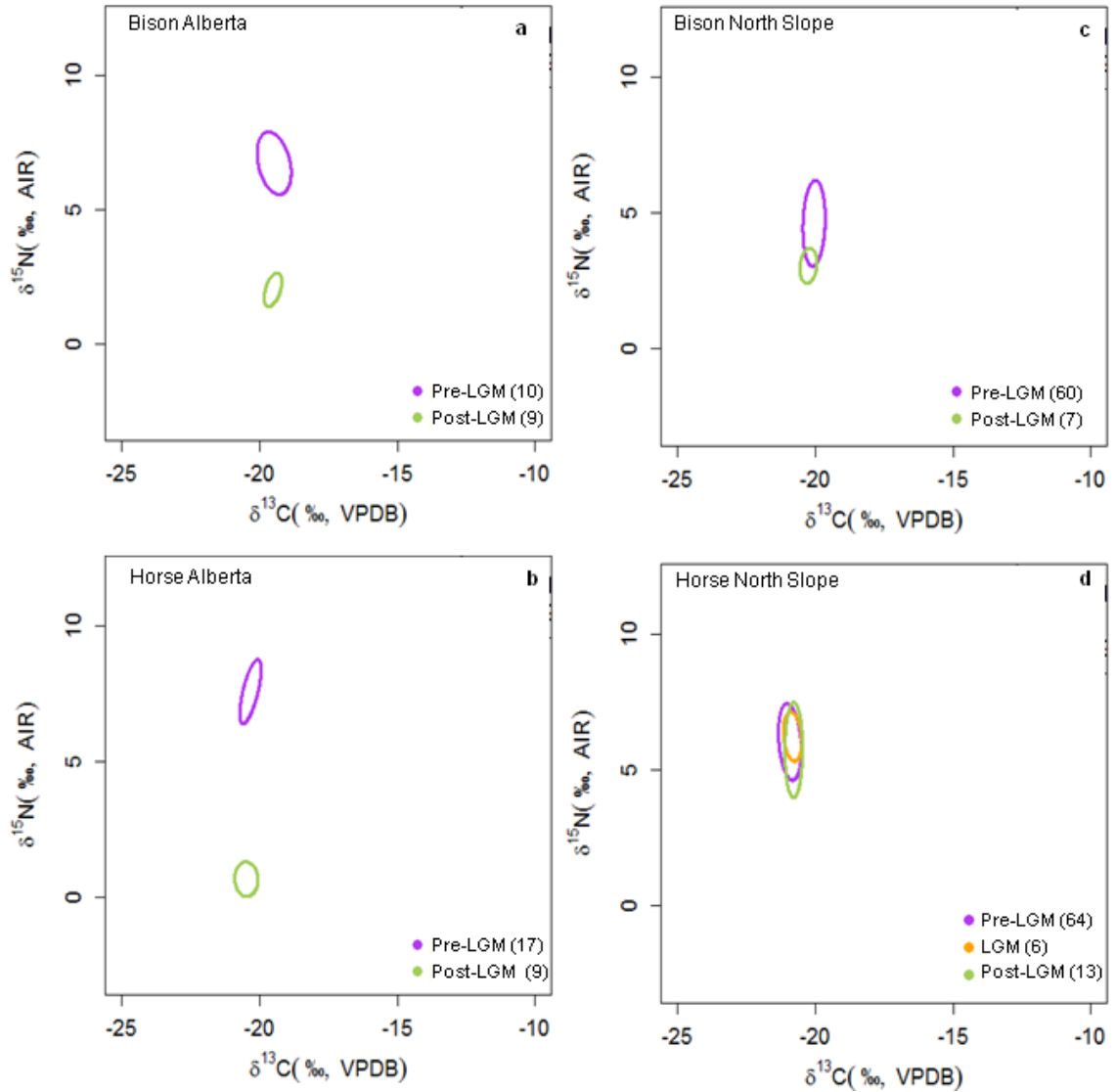


Figure 5.13 Small-sample size corrected ellipses (SEAc) of multiple time periods for two species at two sites: **a. Bison in Alberta; b. Horse in Alberta; c. Bison in the North Slope; d. Horse in the North Slope.**

for average $\delta^{13}\text{C}$ (Figs. 5.13a, d). As well, the extent of the isotopic shift over time varies between species at a site. For example, the change of $\delta^{15}\text{N}$ for bison in Alberta from the pre-LGM to the post-LGM is less than the change observed for horse (Figs. 5.13a, b).

The relative sizes of isotopic niche for species at a specific site changed between time periods. At most sites, the largest number of species have the smallest isotopic niches during the LGM, larger niches during the post-LGM, and the largest niches during the

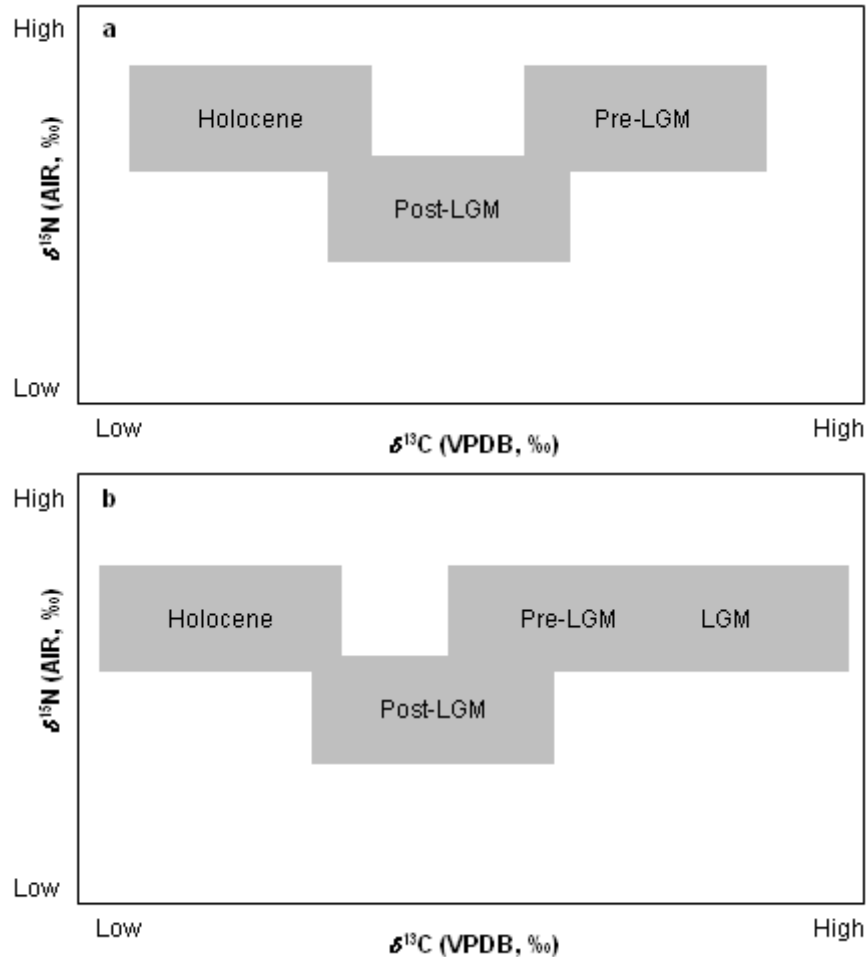


Figure 5.14 Typical isotopic ranking of time periods in the mammoth steppe: a. Rankings based on quantitative observations. Average $\delta^{13}\text{C}$: Holocene < post-LGM < pre-LGM; average $\delta^{15}\text{N}$: post-LGM < pre-LGM = Holocene; b. Rankings based both on qualitative and quantitative observations. Average $\delta^{13}\text{C}$: Holocene < post-LGM < pre-LGM < LGM. Average $\delta^{15}\text{N}$: post-LGM < Holocene = pre-LGM = LGM.

pre-LGM. A comparison of the size of the isotopic niches for bison and horse from Alberta and North Slope provides a good example (Fig. 5.13). For bison at both site, and for Albertan horse, the niches were larger for pre-LGM than they were for post-LGM. At the North Slope, horse and bison had overlapping isotopic niches between time periods (Figs. 13c, d). This pattern of overlap was observed for most species at most sites. Bison

and horse in Alberta were some of the exceptions to the general pattern, as their isotopic niches did not overlap between the pre-LGM and post-LGM periods (Figs. 5.13a, b).

5.3.5.2 Qualitative results

Patterns observed for groups of individuals of the same species at the same site, but having only limited numbers of radiocarbon dates, are similar to those arising from the datasets for which quantitative analysis was possible. The isotopic characteristics of the various time periods are better resolved when information from the qualitative inspection of the dataset is combined with that of the quantitative analysis and the isotopic ranking of the LGM can be added to the general patterns. As seen in Figure 5.14b, when the qualitative data is added to the quantitative data, the $\delta^{13}\text{C}$ and $\delta^{15}\text{N}$ isotopic ranking of the LGM can be added to the observed patterns.

5.4 Discussion

5.4.1 Pre-LGM mammoth steppe

5.4.1.1 Species

The statistical and qualitative examinations of the isotopic data suggest that the mammoth steppe was a relatively homogeneous ecosystem during the pre-LGM. There is remarkable consistency in the patterns of average carbon and nitrogen isotopic compositions among species at various sites (Fig. 5.8). This consistency suggests that the herbivores' main dietary and environmental niches were conserved across the mammoth steppe. This general pre-LGM pattern has been suggested previously (Bocherens, 2015) and its causes are discussed below.

Horses, bison and mammoth were the grazers of the mammoth steppe (Bocherens, 2015, 2003; Guthrie, 2001, 1990). While all three species primarily ate grasses, there is some isotopic evidence that horse and bison diets included sedges and herbaceous plant species (Fox-Dobbs et al., 2008), and some authors have suggested that bison diets included a minor browse component (Rivals et al., 2007). Other forms of plant or habitat differentiation have also been suggested among grazers. Modern European horses are known to consume shorter herbaceous forage (monocots) than ruminants such as bison,

which tend to consume more dicots (Britton et al., 2012). These factors could have contributed to the generally lower $\delta^{13}\text{C}$ and $\delta^{15}\text{N}$ of bison than horse. Mammoths have been shown to consume an isotopically distinct food source with higher $\delta^{15}\text{N}$, likely because they ate in arid regions, fertilized plants with dung, selected specific plants or plant parts and/or ate decayed plants (Chapter 3, 4; Schwartz-Narbonne et al., 2015; Tahmasebi, 2015).

Mixed-feeding or browse dietary niches have been suggested for mastodon, caribou and muskox. The browse component of mastodon diet could be responsible for their low $\delta^{15}\text{N}$ (Coltrain et al., 2004; Koch et al., 1998; Metcalfe et al., 2013; Zazula et al., 2014). Evidence from plant material preserved in caribou teeth suggests winter feeding on lichens, and an otherwise mixed-feeding diet (Guthrie, 2001), potentially containing a large quantity of moss and fungi. Such a diet has been hypothesized to be responsible for the generally low $\delta^{15}\text{N}$ and generally high $\delta^{13}\text{C}$ of Pleistocene caribou (Bocherens, 2015, 2003; Bocherens et al., 1996; Fizet et al., 1995; Fox-Dobbs et al., 2008; Iacumin et al., 2000). Reconstructed diets of Pleistocene muskox have included varying proportions of graze (graminoids, forbs, sedges) and browse (Guthrie, 2001; Mann et al., 2013; Raghavan et al., 2014), and/or large quantities of lichen (Fox-Dobbs et al., 2008). The fact that muskox generally had higher $\delta^{15}\text{N}$ than the grazing horse and bison, and much higher $\delta^{15}\text{N}$ than the browsing mastodon suggests that it did not consume much browse in the mammoth steppe. Perhaps it was a grazer that ate from more arid environments than horse or bison. More studies are necessary to further characterize the isotopic compositions of plant families (e.g. graminoids, forbs and shrubs) and plant parts at high latitude environments, including amino-acid-specific stable isotopic studies, which might help to better understand plant isotopic responses to environmental stressors.

Some of the isotopic differences among species have been attributed to physiological differences, rather than environmental or dietary origins. The non-ruminant species (mammoth, mastodon and horse) have lower average $\delta^{13}\text{C}$ than the ruminant species (caribou, bison, muskox), perhaps because the latter release a larger quantity of methane, which has low $\delta^{13}\text{C}$, than the former (France et al., 2007). While this physiological explanation may be part of the answer, it does not explain the variation in average $\delta^{13}\text{C}$

within ruminant and non-ruminant species, or the fact that the differences in average $\delta^{13}\text{C}$ are not consistent between sites, which might be expected if the cause was purely physiological (Britton et al., 2012).

Animals living in high latitude environments rely on their fat reserves for nourishment in winter; this fat is depleted of ^{13}C relative to the whole body, which likely contributes to a lower $\delta^{13}\text{C}$ in all species than would otherwise occur (Szpak et al., 2010). The impact, however, was likely larger for some species than others. For example, mastodons are suggested to have lived on the mammoth steppe only during interglacial periods (Zazula et al., 2014), which would have had milder winters than during glacial periods. By comparison, mammoths, whose fossils include individuals present during interglacial and glacial periods, would have been present during harsher winters and relied more on their fat reserves, thus leading to their lower $\delta^{13}\text{C}$ than mastodons. This is consistent with mastodons generally having higher $\delta^{13}\text{C}$ than horses, which were also present during glacial and interglacial periods (Fig. 5.4). More detailed feeding studies of megaherbivores are necessary to better discriminate among the physiological, habitat and dietary components contributing to the $\delta^{13}\text{C}$ of herbivore collagen.

Some studies have suggested that the $\delta^{15}\text{N}$ of ruminant and non-ruminant species is also affected by gut physiology and digestive capacity (Britton et al., 2012; Coltrain et al., 2004; Fizet et al., 1995). However, there is no clear separation in the $\delta^{15}\text{N}$ of ruminant versus non-ruminant species considered in this study, or in previous work (Britton et al., 2012).

Mammoth and mastodon isotopic niches were generally smaller than muskox, horse and caribou niches, suggesting that mammoth and mastodon were more specialized to their distinct niche. This conclusion supports previous hypothesis regarding the woolly mammoth (Chapter 3; Schwartz-Narbonne et al., 2015) and mastodon (Zazula et al., 2014). In the present study, mammoth and mastodon were two of the species that occasionally did not fit the typical pattern of species isotopic compositions. This outcome may relate to their tracking a specialized diet or habitat niche that did not shift in isotopic tandem with the rest of the forage. For example, an increase in aridity could have caused

higher $\delta^{13}\text{C}$ and $\delta^{15}\text{N}$ for the majority of the plants in an ecosystem. However, it is possible that the browse species preferred by the mastodon were unable to grow in more arid environments. If so, the mastodon would have eaten from more mesic microhabitats or only lived in the region during more mesic time periods, and its forage – and thus its collagen isotopic composition – would not have shown the same increase in $\delta^{13}\text{C}$ and $\delta^{15}\text{N}$ as the rest of the plants and animals in the ecosystem.

Horse typically overlapped their isotopic niche with bison, mammoth and mastodon, suggesting that it consumed a mix of food from different niches, rather than eating from a separate, distinct niche. As well, when the relative isotopic ranking of two species changed from the expected pattern, horse was commonly one of the two species whose ranking changed. This supports the hypothesis that horse ate from a mix of niches rather than being confined to one specific niche. Bison also typically overlapped their isotopic niche with three herbivore species: caribou, muskox and horse. Again, this suggests that bison were more generalized foragers. It has been suggested that horse and bison had flexible feeding niches during the Pleistocene and Holocene (Britton et al., 2012). This more generalist strategy seems to correspond to a higher relative abundance of horse or bison than mammoth, muskox or caribou at a majority of sites. Interestingly, species identified as generalists (horse and bison) typically had smaller isotopic niches than the species with which they were sharing an isotopic niche (bison and mammoth for horse; muskox and caribou for bison). This may indicate that, by their very numbers, horse and bison monopolized the most favourable forage or habitat at these sites, forcing other species to expand beyond their ideal isotopic and ecological niche.

Situations where an atypical overlap between two isotopic niches was present, or a typical overlap between two isotopic niches was absent, corresponded to larger or smaller niches sizes for one of the two species involved. Commonly, this increase or decrease in isotopic niche size can be correlated to smaller relative abundances of that species at the site. Niche contraction may arise from an external cause, such as predation, which causes a species' relative abundance to decline while a large quantity of ideal forage remained, or it may indicate a species that was not able to adapt to changing conditions such as the loss of habitat or forage. Predation is known to play a role in determining the ecological

niche width, with species that are under less predation pressure able to expand their niches (Hammerschlag-Peyer et al., 2011).

Only qualitative assessments were possible for three species. The extinct muskox species *Symbos cavifrons*, the helmeted muskox, was examined at Fairbanks, while every other site contained *Ovibos* sp. *S. cavifrons* had unusually low $\delta^{15}\text{N}$ and did not fit the expected $\delta^{15}\text{N}$ pattern for muskox, suggesting that it had an entirely distinct diet, possibly containing a larger browse element. The woolly rhinoceros had a high average $\delta^{15}\text{N}$, second only to the woolly mammoth, and a similar average $\delta^{13}\text{C}$ to bison, consistent with its currently accepted status as a grazer (Bocherens, 2003). Based on the $\delta^{13}\text{C}$ and $\delta^{15}\text{N}$ of Dall sheep they seem to have occupied a similar isotopic niche to muskox (*Ovibos* sp.). The Dall sheep and the muskox (*Ovibos* sp.) both escaped terminal Pleistocene extinction. Dall sheep currently occupy alpine habitats (Guthrie, 1982), while the muskox inhabit in some North American sites (Koch and Barnosky, 2006). If the extinctions occurred because species experienced a loss of their habitat or dietary niche (Barnosky et al., 2004; Koch and Barnosky, 2006; Shapiro et al., 2004), it appears that these sheep and muskox were able to find places where their niche persisted, and to live in these habitats.

5.4.1.2 Sites

This study examines isotopic differences in megafauna collagen that occur in tandem for multiple species at each site. These differences result from environmental shifts that either caused (i) changes in the isotopic compositions of the plants at the base of the food web, or (ii) physiological responses that provoked the same isotopic changes in all the species. Since the observed changes affect multiple species at the same time, despite the varied diets of these species, it is unlikely to have resulted from a dietary shift. As shown by Figure 5.11a, the lowest pre-LGM $\delta^{13}\text{C}$ for the majority of the species occur in Yakutia. Values of $\delta^{13}\text{C}$ increase moving both eastward through North America, and, to a lesser extent, westward through Europe. The qualitative data (Fig. 5.12a.) support these patterns, with increasing average $\delta^{13}\text{C}$ observed moving south and westward into Europe. These isotopic patterns generally correspond to those observed using only data for woolly mammoth (Iacumin et al., 2000; Szpak et al., 2010). These results were interpreted as

reflecting an increase in fat use, resulting from colder conditions and harsher winters (Szpak et al., 2010).

As seen in Figure 5.11b, the highest pre-LGM $\delta^{15}\text{N}$ for the majority of species occurred in Yakutia. The values generally decrease to the east and west, opposite to that observed for $\delta^{13}\text{C}$. There are exceptions; for example, the lowest $\delta^{13}\text{C}$ occurs in North America, while the average $\delta^{15}\text{N}$ is higher in NW Europe than in North America (Fig. 5.6e). Average $\delta^{15}\text{N}$ is similar in Yakutia and in Alberta, which follows the general pattern observed in previous work (Bocherens et al., 1994; Szpak et al., 2010). Greater aridity in Eurasia than much of North America is the most likely explanation for the higher $\delta^{15}\text{N}$. The results, however, also suggest that Alberta was atypically arid relative to the other North America sites, perhaps because it was located within the rain shadow of the Rocky Mountains. Other explanations are possible. For example, if colder winters led to increased nutritional stress as well as increased fat use, it would explain the inverse correlation between $\delta^{13}\text{C}$ and $\delta^{15}\text{N}$. However, that would not explain why Alberta was an exceptions to these patterns. Amino acid analyses would allow the baseline shifts in the plants' $\delta^{15}\text{N}$ arising from aridity to be distinguished from increases in animal protein recycling, and is recommended for future work (Chapter 3; Schwartz-Narbonne et al., 2015; Styring et al., 2010).

The overlap among sites in isotopic niches occupied by each species suggests a level of similarity that surpasses differences in foodweb baseline isotopic compositions among sites. Mammoth and mastodon are the most likely not to show overlap, which likely relates to their generally smaller isotopic niches (i.e., specialist status) than other species. Fairbanks and Alberta are the only sites that did not show isotopic overlap with multiple sites for multiple species. Alberta's climate seems to have been strongly influenced by local topography of the Rocky Mountains. Fairbanks provides an exception to many of the typical isotopic patterns across the mammoth steppe, being bison-dominated, and having multiple species showing atypical patterns of average $\delta^{13}\text{C}$ or $\delta^{15}\text{N}$ (Fig. 9a). Based on species proportions and qualitative inspection of species isotopic ranking, Selawik also may be an exception to many of the typical mammoth steppe isotopic

patterns. More dating and stable isotopic analyses are needed to determine whether and why these sites differ from the majority of other sites examined.

The average isotopic niche pattern of species and sites, and species proportions, are relatively consistent for the pre-LGM mammoth steppe, but exceptions exist for virtually every pattern. This suggests that generalized observations for the entire landscape are not sufficient to describe and understand variability across the mammoth steppe. Smaller scale, site-specific environmental or vegetation differences likely play a significant role. This is consistent with earlier reconstructions of the mammoth steppe that describe it a mosaic of smaller floral units (Guthrie, 1982). It is also clear, however, that the pre-LGM had a strong level of connectivity and similarity across the entirety of the biome.

5.4.2 Response of the mammoth steppe to environmental changes over time

The response of the mammoth steppe as a whole to the climatic change that occurred from the pre-LGM to the Holocene can be examined using the shifts in typical $\delta^{13}\text{C}$, $\delta^{15}\text{N}$ and niche size of each species at each site with time (Fig. 5.14a). In general, pre-LGM groups have higher $\delta^{13}\text{C}$ and $\delta^{15}\text{N}$ than post-LGM groups, and larger isotopic niche sizes.

Several previous studies have observed decreases in the $\delta^{13}\text{C}$ of plant and animal specimens over the Pleistocene and into the pre-industrial Holocene, although it has not been observed in every study, and the cause of this shift is disputed. Changes in the atmospheric $p\text{CO}_2$ during these time periods could have affected the isotopic composition of the plants, and thus the animals that consumed them (Bocherens, 2003; Richards and Hedges, 2003; Schubert and Jahren, 2015; Stevens and Hedges, 2004). The decrease in $\delta^{13}\text{C}$ at some sites has also be attributed to changes in degree of canopy cover (Drucker et al., 2008; Iacumin et al., 1997). Previous work did not identify temporal changes in the $\delta^{13}\text{C}$ of herbivores at Fairbanks, and suggested that such changes were either site-specific and local, or affected plants or habitats not used by most of the herbivores (Fox-Dobbs et al., 2008). The $\delta^{13}\text{C}$ shift is not observed in all species at all sites examined in this study, suggesting that it is a weaker trend that can be overprinted by other site- or species-specific variables, such as local changes in aridity or canopy cover. The trend to lower

$\delta^{15}\text{N}$ in the post-LGM relative to the pre-LGM has been observed at multiple sites, though its timing and magnitude varied among sites and species (Bocherens et al., 2011; Drucker et al., 2003a; Fox-Dobbs et al., 2008; Mann et al., 2013; Stevens and Hedges, 2004; Stevens et al., 2008). The lowering of $\delta^{15}\text{N}$ in the post-LGM has been attributed to increased moisture from permafrost melting and to shifts in the floral species (Stevens and Hedges, 2004; Stevens et al., 2008). The large variability in isotopic patterns of time periods for varying species at varying sites may relate to differences in the extent to which a species' diet or microhabitat was affected by climate change, or other factors, such as distance from the ice front (Drucker et al., 2003b).

Many of the species at many of the sites here do not follow the general pattern of $\delta^{13}\text{C}$ or $\delta^{15}\text{N}$ rankings of time periods shown in Figure 5.14a. When they do follow a pattern, the extent of changes of $\delta^{13}\text{C}$ and $\delta^{15}\text{N}$ varies between species within a site, and between sites. This outcome suggests that the interplay of global factors and site- or species-specific factors is more complex than previously documented. The addition of qualitative data to the quantitative data set gave better resolution in the isotopic patterns of different time periods (Fig. 5.14b), suggesting more isotopic data may help to resolve the isotopic changes over time. As well, more detailed mathematical tools could be used. Principal component analysis of these plus additional data may be invaluable. Similarly, time series analysis of each species at each could fully elucidate the shifts in patterns over time, though this method will require much better dating control than is currently available.

Isotopic niche size changes substantially between time bins, with LGM and post-LGM species generally having smaller niches than pre-LGM species (e.g. Fig. 5.13). The LGM was a disruption to the ecological equilibrium that characterized pre-LGM time, and after the change, almost every species measured at every site had a more specialized isotopic niche (Alberta bison, North Slope bison, North Slope caribou, south central Siberia caribou, NW Europe caribou, Alberta horse, NW Europe horse and Hershel Island muskox). This may have been caused by reduced availability of different floral species after the LGM (Willerslev et al., 2014).

These changing niches can also be explored by comparing the shifts in the $\delta^{13}\text{C}$ and $\delta^{15}\text{N}$ patterns of species at a site over the different time periods (Fig. 5.9). The average $\delta^{13}\text{C}$ patterns of species are relatively constant through time when only the quantitative results are considered, suggesting that this was heavily controlled by a species' physiology. There are some differences in the $\delta^{13}\text{C}$ patterns of species using the qualitative results, which admittedly have weaker temporal control. This suggests that the changes in the $\delta^{13}\text{C}$ of a species at a site over time may make ranking the species without strong temporal control impossible, as the isotopic differences between species are overprinted by the isotopic differences over time. The average $\delta^{15}\text{N}$ patterns of species at a site are not constant over time in either the quantitative or qualitative results. Similarly, there are differences in which species had overlap, and some expected overlaps, such as between the horse and the bison, were not seen post-LGM (e.g. Fig. 5.7). These differences suggest that some species were not able to return to their previously occupied niche in post-LGM time; instead they were forced to specialize in different dietary or habitat niches, where they may have had reduced fitness, as was previously noted for European bison (Bocherens et al., 2015). In Alberta, between the pre-LGM and post-LGM, the relative niche ranking of horse and bison became reversed, as was their relative isotopic niche sizes and relative abundances. This site was glaciated and repopulated post-LGM (Burns, 2010; Jass et al., 2011). There appears to have been a complete shift in the ecosystem resulting from this change. Even at sites that were not glaciated during the LGM, (e.g. North Slope), the ecosystem clearly changed over time. Species proportions, isotopic patterns of species, species isotopic niche size, and isotopic niche overlaps among species all changed at the North Slope after the pre-LGM (Figs. 5.6; 5.7; 5.9; 5.13).

The $\delta^{13}\text{C}$ patterns of sites are relatively stable, but there are changes in $\delta^{15}\text{N}$ patterns of the sites during the LGM, post-LGM and Holocene (Figs. 5.11, 5.12). This likely reflects a fundamental shift in the ecosystems of the mammoth steppe over time. The pre-LGM pattern has been interpreted as suggesting that sites in the east (Alberta) and west (Yakutia and NW Europe) were more arid. However, during and after the LGM, the reverse situation may have occurred. There is a large increase in the number of species

where their isotopic niches at different sites that do not overlap post-LGM, likely because of the general decrease in isotopic niche sizes that occurred post-LGM.

It is intriguing that there is no return to pre-LGM isotopic niche sizes, niche patterns or niche overlaps of species at any site after the LGM (Fig. 5.9). The ranking of post-LGM average $\delta^{15}\text{N}$ of sites is also distinct from the pre-LGM (Fig. 5.11). Clearly, the mammoth steppe did not return to its previous state of equilibrium after the LGM, and instead became a more heterogeneous, and likely more fragmented ecosystem. This pattern echoes the floral pattern observed in the Arctic, where post-LGM flora had more geographic diversity than pre-LGM flora, and different plant species were present post-LGM (Willerslev et al., 2014), and the general patterns observed in the Americas that Pleistocene ecosystems were more sensitive to perturbations than Holocene ecosystems (Pires et al., 2015). Ecological changes during the LGM may have permanently destabilized the mammoth steppe. Changes in the physical geography may also have played a role, such as the opening and closing of the Bering land bridge over time. It is possible that the ecosystem shifted during each previous glaciation event (Stevens and Hedges, 2004), or that the LGM was a particularly severe glaciation event. It is also possible, however, that restoration of mammoth steppe equilibrium required more than the few thousand years before the Holocene climate changes and/or human impacts perturbed the system to the point that there was a major state change that led to the loss of the entire biome.

5.5 Conclusion

By the start of the Holocene, a permanent change had affected the mammoth steppe ecosystem, including extinction or extirpation of many of its megafauna species. It has been suggested that megafaunal herbivores had previously maintained this ecosystem through mechanisms such as trampling and selective consumption of flora (Willerslev et al., 2014). The isotopic changes in the ecosystem over time, however, even at sites having the typical mammoth steppe herbivore species, suggest that this was not necessarily the case. The Great Lakes area during the post-LGM period particularly demonstrates that mammoth steppe herbivores were not always able to maintain their

ideal forage and habitat. Yet, the species examined at this site retained the expected isotopic pattern, notwithstanding that the habitat was primarily forested rather than steppe-like (Metcalf et al., 2013; Saunders et al., 2010). Rather than the loss of the species contributing to the changing of the ecosystem, the reverse may have occurred. The fragmentation of the mammoth steppe into heterogeneous ecosystems may have contributed to some extirpations, as this loss of connectivity may have prevented species from locating ideal habitat and forage. As such, these species may have been restricted to narrow ranges with reduced migration range or sub-ideal habitat and forage. In short, although many megafaunal species survived the climate changes of the LGM, significant changes to the overall ecosystem impacted their ability to survive into the Holocene.

5.6 References

- Álvarez-Lao, D.J., Kahlke, R.-D., García, N., Mol, D., 2009. The Padul mammoth finds — On the southernmost record of *Mammuthus primigenius* in Europe and its southern spread during the Late Pleistocene. *Palaeogeogr. Palaeoclimatol. Palaeoecol.* 278, 57–70. doi:10.1016/j.palaeo.2009.04.011
- Ambrose, S., 1990. Preparation and characterization of bone and tooth collagen for isotopic analysis. *J. Archaeol. Sci.* 17, 431–451.
- Ambrose, S., 1991. Effects of diet, climate and physiology on nitrogen isotope abundances in terrestrial foodwebs. *J. Archaeol. Sci.* 18, 293–317.
- Amundson, R., Austin, A., Schuur, E.A.G., Yoo, K., Matzek, V., Kendall, C., Uebersax, A., Brenner, D., Baisden, W.T., 2003. Global patterns of the isotopic composition of soil and plant nitrogen. *Glob. Biogeochemical Cycles* 17. doi:10.1029/2002GB001903
- Balasse, M., Bocherens, H., Mariotti, A., 1999. Intra-bone variability of collagen and apatite isotopic composition used as evidence of a change of diet. *J. Archaeol. Sci.* 26, 593–598.
- Barnett, B., 1994. Carbon and nitrogen isotope ratios of caribou tissues, vascular plants, and lichens from northern Alaska. Master's Thesis. University of Alaska, Fairbanks.
- Barnosky, A.D., Koch, P.L., Feranec, R.S., Wing, S.L., Shabel, A.B., 2004. Assessing the causes of late Pleistocene extinctions on the continents. *Science* 306, 70–75. doi:10.1126/science.1101476
- Bearhop, S., Adams, C.E., Waldron, S., Fuller, R.A., Macleod, H., 2004. Determining trophic niche width: a novel approach using stable isotope analysis. *J. Anim. Ecol.*

73, 1007–1012.

- Bellissimo, N.S., 2013. Origins of stable isotopic variations in late Pleistocene horse enamel and bone from Alberta. Master's Thesis. University of Western Ontario.
- Ben-David, M., Shochat, E., Adams, L., 2001. Utility of stable isotope analysis in studying foraging ecology of herbivores: examples from moose and caribou. *Alces* 37, 421–434.
- Bligh, E.G., Dyer, W.J., 1959. A rapid method of total lipid extraction and purification. *Can. J. Biochem. Physiol.* 37, 911–917. doi:10.1139/o59-099
- Bocherens, H., 2003. Isotopic biogeochemistry and the paleoecology of the mammoth steppe fauna. *Deinsea* 9, 57–76.
- Bocherens, H., 2015. Isotopic tracking of large carnivore palaeoecology in the mammoth steppe. *Quat. Sci. Rev.* 117, 42–71. doi:10.1016/j.quascirev.2015.03.018
- Bocherens, H., Billiou, D., Mariotti, A., Toussaint, M., Patou-Mathis, M., Bonjean, D., Otte, M., 2001. New isotopic evidence for dietary habits of Neandertals from Belgium. *J. Hum. Evol.* 40, 497–505. doi:10.1006/jhev.2000.0452
- Bocherens, H., Billiou, D., Patou-Mathis, M., Bonjean, D., Otte, M., Mariotti, A., 1997. Paleobiological implications of the isotopic Signatures (^{13}C , ^{15}N) of fossil mammal collagen in Scladina Cave (Sclayn, Belgium). *Quat. Res.* 48, 370–380. doi:10.1006/qres.1997.1927
- Bocherens, H., Drucker, D.G., Billiou, D., Patou-Mathis, M., Vandermeersch, B., 2005. Isotopic evidence for diet and subsistence pattern of the Saint-Césaire I Neanderthal: review and use of a multi-source mixing model. *J. Hum. Evol.* 49, 71–87. doi:10.1016/j.jhevol.2005.03.003
- Bocherens, H., Drucker, D.G., Bonjean, D., Bridault, A., Conard, N.J., Cupillard, C., Germonpré, M., Höneisen, M., Münzel, S.C., Napierala, H., Patou-Mathis, M., Stephan, E., Uerpmann, H.-P., Ziegler, R., 2011. Isotopic evidence for dietary ecology of cave lion (*Panthera spelaea*) in North-Western Europe: prey choice, competition and implications for extinction. *Quat. Int.* 245, 249–261. doi:10.1016/j.quaint.2011.02.023
- Bocherens, H., Fizet, M., Mariotti, A., Gangloff, R., Burns, J., 1994. Contribution of isotopic biogeochemistry (^{13}C , ^{15}N , ^{18}O) to the paleoecology of mammoths (*Mammuthus primigenius*). *Hist. Biol.* 7, 187–202.
- Bocherens, H., Emslie, S., Billiou, D., Mariotti, A., 1995. Stables isotopes (^{13}C , ^{15}N) and paleodiet of the giant short-faced bear (*Arctodus simus*). *Comptes rendus l'Académie des Sci. Série 2. Sci. la terre des planètes* 320, 779–784.
- Bocherens, H., Hofman-Kamińska, E., Drucker, D.G., Schmölcke, U., Kowalczyk, R.,

2015. European bison as a refugee species? Evidence from isotopic data on Early Holocene bison and other large herbivores in northern Europe. *PLoS One* 10, e0115090. doi:10.1371/journal.pone.0115090
- Bocherens, H., Pacaud, G., Lazarev, P.A., Mariotti, A., 1996. Stable isotope abundances (^{13}C , ^{15}N) in collagen and soft tissues from Pleistocene mammals from Yakutia: implications for the palaeobiology of the Mammoth Steppe. *Palaeogeogr. Palaeoclimatol. Palaeoecol.* 126, 31–44.
- Bonafini, M., Pellegrini, M., Ditchfield, P., Pollard, A.M., 2013. Investigation of the “canopy effect” in the isotope ecology of temperate woodlands. *J. Archaeol. Sci.* 40, 3926–3935. doi:10.1016/j.jas.2013.03.028
- Britton, K., Gaudzinski-Windheuser, S., Roebroeks, W., Kindler, L., Richards, M.P., 2012. Stable isotope analysis of well-preserved 120,000-year-old herbivore bone collagen from the Middle Palaeolithic site of Neumark-Nord 2, Germany reveals niche separation between bovids and equids. *Palaeogeogr. Palaeoclimatol. Palaeoecol.* 333–334, 168–177. doi:10.1016/j.palaeo.2012.03.028
- Burns, J. a., 2010. Mammalian faunal dynamics in Late Pleistocene Alberta, Canada. *Quat. Int.* 217, 37–42. doi:10.1016/j.quaint.2009.08.003
- Burns, J., Young, R., 1994. Pleistocene mammals of the Edmonton area, Alberta. Part I. The carnivores. *Can. J. Earth Sci.* 31, 393–400.
- Burns, J.A., 1991. Mid-Wisconsinan vertebrates and their environment from January Cave, Alberta, Canada. *Quat. Res.* 35, 130–143. doi:10.1016/0033-5894(91)90100-J
- Burns, J.A., 1996. Vertebrate paleontology and the alleged ice-free corridor: the meat of the matter. *Quat. Int.* 32, 107–112.
- Coltrain, J.B., Harris, J.M., Cerling, T.E., Ehleringer, J.R., Dearing, M.-D., Ward, J., Allen, J., 2004. Rancho La Brea stable isotope biogeochemistry and its implications for the palaeoecology of late Pleistocene, coastal southern California. *Palaeogeogr. Palaeoclimatol. Palaeoecol.* 205, 199–219. doi:10.1016/j.palaeo.2003.12.008
- de Bello, F., Buchmann, N., Casals, P., Lepš, J., Sebastià, M.-T., 2009. Relating plant species and functional diversity to community $\delta^{13}\text{C}$ in NE Spain pastures. *Agric. Ecosyst. Environ.* 131, 303–307. doi:10.1016/j.agee.2009.02.002
- Debruyne, R., Chu, G., King, C.E., Bos, K., Kuch, M., Schwarz, C., Szpak, P., Gröcke, D.R., Matheus, P., Zazula, G., Guthrie, D., Froese, D., Buigues, B., de Marliave, C., Flemming, C., Poinar, D., Fisher, D., Southon, J., Tikhonov, A.N., MacPhee, R.D.E., Poinar, H.N., 2008. Out of America: ancient DNA evidence for a new world origin of late Quaternary woolly mammoths. *Curr. Biol.* 18, 1320–6. doi:10.1016/j.cub.2008.07.061
- DeNiro, M., 1985. Postmortem preservation and alteration of in vivo bone collagen

- isotope ratios in relation to palaeodietary reconstruction. *Nature* 317, 806–809. doi:10.1038/317806a0
- Diefendorf, A., Mueller, K., Wing, S.L., Koch, P.L., Freeman, K.H., 2010. Global patterns in leaf ^{13}C discrimination and implications for studies of past and future climate. *Proc. Natl. Acad. Sci.* 107, 5738–5743.
- Druckenmiller, P.S., 2008. Survey of Pleistocene (Ice Age) vertebrates from the Selawik and Kobuk River areas of Northwestern Alaska. *Intern. Rep. U.S. Fish Wildl. Serv.* 1–56.
- Drucker, D.G., Bocherens, H., Bridault, A., Billiou, D., 2003a. Carbon and nitrogen isotopic composition of red deer (*Cervus elaphus*) collagen as a tool for tracking palaeoenvironmental change during the Late-Glacial and Early Holocene in the northern Jura (France). *Palaeogeogr. Palaeoclimatol. Palaeoecol.* 195, 375–388. doi:10.1016/S0031-0182(03)00366-3
- Drucker, D.G., Bocherens, H., Billiou, D., 2003b. Evidence for shifting environmental conditions in Southwestern France from 33 000 to 15 000 years ago derived from carbon-13 and nitrogen-15 natural abundances in collagen of large herbivores. *Earth Planet. Sci. Lett.* 216, 163–173. doi:10.1016/S0012-821X(03)00514-4
- Drucker, D.G., Bridault, A., Cupillard, C., Hujic, A., Bocherens, H., 2011. Evolution of habitat and environment of red deer (*Cervus elaphus*) during the Late-glacial and early Holocene in eastern France (French Jura and the western Alps) using multi-isotope analysis ($\delta^{13}\text{C}$, $\delta^{15}\text{N}$, $\delta^{18}\text{O}$, $\delta^{34}\text{S}$) of archaeological remains. *Quat. Int.* 245, 268–278. doi:10.1016/j.quaint.2011.07.019
- Drucker, D.G., Bridault, A., Hobson, K.A., Szuma, E., Bocherens, H., 2008. Can carbon-13 in large herbivores reflect the canopy effect in temperate and boreal ecosystems? Evidence from modern and ancient ungulates. *Palaeogeogr. Palaeoclimatol. Palaeoecol.* 266, 69–82. doi:10.1016/j.palaeo.2008.03.020
- Drucker, D.G., Henry-Gambier, D., 2005. Determination of the dietary habits of a Magdalenian woman from Saint-Germain-la-Rivière in southwestern France using stable isotopes. *J. Hum. Evol.* 49, 19–35. doi:10.1016/j.jhevol.2005.02.007
- Drucker, D.G., Hobson, K.A., Ouellet, J.-P., Courtois, R., 2010. Influence of forage preferences and habitat use on ^{13}C and ^{15}N abundance in wild caribou (*Rangifer tarandus caribou*) and moose (*Alces alces*) from Canada. *Isotopes Environ. Health Stud.* 46, 107–21. doi:10.1080/10256010903388410
- Ehleringer, J., Comstock, J., Cooper, T., 1987. Leaf-twig carbon isotope ratio differences in photosynthetic-twig desert shrubs. *Oecologia* 71, 318–320.
- Ehleringer, J., Cooper, T., 1988. Correlations between carbon isotope ratio and microhabitat in desert plants. *Oecologia* 76, 562–566.

- Elias, S. a, 2001. Mutual climatic range reconstructions of seasonal temperatures based on Late-Pleistocene fossil beetle assemblages in Eastern Beringia. *Quat. Sci. Rev.* 20, 77–91. doi:10.1016/S0277-3791(00)00130-X
- Elias, S. a., 2000. Late Pleistocene climates of Beringia, based on analysis of fossil beetles. *Quat. Res.* 53, 229–235. doi:10.1006/qres.1999.2093
- Farquhar, G., 1989. Carbon isotope discrimination and photosynthesis. *Annu. Rev. Plant Biol.* 40, 503–537.
- Finstad, G.L., Kielland, K., 2011. Landscape variation in the diet and productivity of reindeer in Alaska based on stable isotope analyses. *Arctic, Antarct. Alp. Res.* 43, 543–554. doi:10.1657/1938-4246-43.4.543
- Fizet, M., Mariotti, A., Bocherens, H., Lange-Badré, B., Vandermeersch, B., Borel, J.P., Bellon, G., 1995. Effect of diet, physiology and climate on carbon and nitrogen stable isotopes of collagen in a Late Pleistocene anthropic palaeoecosystem: Marillac, Charente, France. *J. Archaeol. Sci.* 22, 67–79.
- Fox-Dobbs, K., Leonard, J., Koch, P., 2008. Pleistocene megafauna from eastern Beringia: paleoecological and paleoenvironmental interpretations of stable carbon and nitrogen isotope and radiocarbon records. *Palaeogeogr. Palaeoclimatol. Palaeoecol.* 261, 30–46.
- France, C., Giaccari, J., Cano, N., 2011. The effects of PVAc treatment and organic solvent removal on $\delta^{13}\text{C}$, $\delta^{15}\text{N}$, and $\delta^{18}\text{O}$ values of collagen and hydroxyapatite in a modern bone. *J. Archaeol. Sci.* 38, 3387–3393.
- France, C.A.M., Zelanko, P.M., Kaufman, A.J., Holtz, T.R., 2007. Carbon and nitrogen isotopic analysis of Pleistocene mammals from the Saltville Quarry (Virginia, USA): implications for trophic relationships. *Palaeogeogr. Palaeoclimatol. Palaeoecol.* 249, 271–282. doi:10.1016/j.palaeo.2007.02.002
- García-Alix, A., Delgado Huertas, A., Martín Suárez, E., 2012. Unravelling the Late Pleistocene habitat of the southernmost woolly mammoths in Europe. *Quat. Sci. Rev.* 32, 75–85. doi:10.1016/j.quascirev.2011.11.007
- Gaglioti, B. V., Barnes, B.M., Zazula, G.D., Beaudoin, A.B., Wooller, M.J., 2011. Late Pleistocene paleoecology of arctic ground squirrel (*Urocitellus parryii*) caches and nests from Interior Alaska's mammoth steppe ecosystem, USA. *Quat. Res.* 76, 373–382. doi:10.1016/j.yqres.2011.08.004
- Gannes, L., del Rio, C., Koch, P., 1998. Natural abundance variations in stable isotopes and their potential uses in animal physiological ecology. *Comp. Biochem. Physiol. Part A Mol. Integr. Physiol.* 119, 725–737.
- Graham, R., Lundelius, E.J., 1984. Coevolutionary disequilibrium and Pleistocene extinctions., in: Martin, P.S., Klein, R.G. (Eds.), *Quaternary Extinctions: A*

- Prehistoric Revolution. The University of Arizona Press, Tucson, pp. 223–249.
- Groves, Personal communication (e-mail), 2015
- Guthrie, R.D., 1968. Paleoecology of the large-mammal community in interior Alaska during the late Pleistocene. *Am. Midl. Nat.* 79, 346–363.
- Guthrie, R.D., 1982. Mammals of the mammoth steppe as paleoenvironmental indicators, in: Hopkins, D.M., Matthews, Jr., J.V., Schweger, C.E., Young, S.B. (Eds.), *Paleoecology of Beringia*. Academic Press, New York, pp. 307–326.
- Guthrie, R.D., 1984. Mosaics, allelochemicals and nutrients: an ecological theory of late Pleistocene megafaunal extinctions, in: *Quaternary Extinctions: A Prehistoric Revolution*. pp. 259–298.
- Guthrie, R.D., 1990. *Frozen fauna of the mammoth steppe: the story of Blue Babe*. The University of Chicago Press, Chicago.
- Guthrie, R.D., 2001. Origin and causes of the mammoth steppe: a story of cloud cover, woolly mammal tooth pits, buckles, and inside-out Beringia. *Quat. Sci. Rev.*
- Guthrie, R.D., 2006. New carbon dates link climatic change with human colonization and Pleistocene extinctions. *Nature* 441, 207–209. doi:10.1038/nature04604
- Hammerschlag-Peyer, C.M., Yeager, L.A., Araújo, M.S., Layman, C.A., 2011. A hypothesis-testing framework for studies investigating ontogenetic niche shifts using stable isotope ratios. *PLoS One* 6, e27104. doi:10.1371/journal.pone.0027104
- Harington, C., Ashworth, A., 1986. A mammoth (*Mammuthus primigenius*) tooth from late Wisconsin deposits near Embden, North Dakota, and comments on the distribution of woolly mammoths south of the Wisconsin ice sheets. *Can. J. Earth Sci.* 23, 909–918.
- Harington, C.R., 2003. *Annotated bibliography of Quaternary vertebrates of northern North America: with radiocarbon dates*. University of Toronto Press.
- Heaton, T.H.E., 1987. The $^{15}\text{N}/^{14}\text{N}$ ratios of plants in South Africa and Namibia: relationship to climate and coastal/saline environments. *Oecologia* 74, 236–246.
- Heaton, T.H.E., 1999. Spatial, species, and temporal variations in the $^{13}\text{C}/^{12}\text{C}$ ratios of C_3 plants: implications for palaeodiet studies. *J. Archaeol. Sci.* 26, 637–649.
- Hobson, K.A., Alisauskas, R.T., Clark, R.G., 1993. Stable-nitrogen isotope enrichment in avian tissues due to fasting and nutritional stress: implications for isotopic analyses of diet. *Condor* 95, 388–394.
- Huntley, B., Allen, J.R.M., Collingham, Y.C., Hickler, T., Lister, A.M., Singarayer, J., Stuart, A.J., Sykes, M.T., Valdes, P.J., 2013. Millennial climatic fluctuations are key

- to the structure of last glacial ecosystems. *PLoS One* 8, e61963.
doi:10.1371/journal.pone.0061963
- Iacumin, P., Bocherens, H., Delgado Huertas, A., Mariotti, A., Longinelli, A., 1997. A stable isotope study of fossil mammal remains from the Paglicci cave, Southern Italy. N and C as palaeoenvironmental indicators. *Earth Planet. Sci. Lett.* 148, 349–357. doi:10.1016/S0012-821X(97)00015-0
- Iacumin, P., Davanzo, S., Nikolaev, V., 2006. Spatial and temporal variations in the $^{13}\text{C}/^{12}\text{C}$ and $^{15}\text{N}/^{14}\text{N}$ ratios of mammoth hairs: palaeodiet and palaeoclimatic implications. *Chem. Geol.* 231, 16–25. doi:10.1016/j.chemgeo.2005.12.007
- Iacumin, P., Matteo, A. Di, Nikolaev, V., Kuznetsova, T., 2010. Climate information from C, N and O stable isotope analyses of mammoth bones from northern Siberia. *Quat. Int.* 212, 206–212.
- Iacumin, P., Nikolaev, V., Ramigni, M., 2000. C and N stable isotope measurements on Eurasian fossil mammals, 40 000 to 10 000 years BP: herbivore physiologies and palaeoenvironmental reconstruction. *Palaeogeogr. Palaeoclimatol. Palaeoecol.* 163, 33–47.
- Jackson, A.L., Inger, R., Parnell, A.C., Bearhop, S., 2011. Comparing isotopic niche widths among and within communities: SIBER - Stable Isotope Bayesian Ellipses in R. *J. Anim. Ecol.* 80, 595–602. doi:10.1111/j.1365-2656.2011.01806.x
- Jass, C., Burns, J., Milot, P.J., 2011. Description of fossil muskoxen and relative abundance of Pleistocene megafauna in central Alberta. *Can. J. Earth* 48, 793–800.
- Jass, C.N., Beaudoin, A.B., 2014. Radiocarbon dates of Late Quaternary megafauna and botanical remains from central Alberta, Canada. *Radiocarbon* 56, 1215–1222. doi:10.2458/56.17922
- Kelly, J., 2000. Stable isotopes of carbon and nitrogen in the study of avian and mammalian trophic ecology. *Can. J. Zool.* 78, 1–27.
- Koch, P., 2007. Isotopic study of the biology of modern and fossil vertebrates, in: Michener, R., Lajtha, K. (Eds.), *Stable Isotopes in Ecology and Environmental Science*. Blackwell Publishing Ltd, Hong Kong, pp. 99–154.
- Koch, P., Fogel, M., Tuross, N., 1994. Tracing the diets of fossil animals using stable isotopes, in: Lajtha, K., Michener, R. (Eds.), *Stable Isotopes in Ecology and Environmental Science*. Blackwell Scientific Publications, pp. 63–92.
- Koch, P., Hoppe, K., Webb, S., 1998. The isotopic ecology of late Pleistocene mammals in North America: Part 1. Florida. *Chem. Geol.* 152, 119–138.
- Koch, P.L., Barnosky, A.D., 2006. Late Quaternary extinctions: state of the debate. *Annu. Rev. Ecol. Evol. Syst.* 37, 215–250.

doi:10.1146/annurev.ecolsys.34.011802.132415

- Kohn, M.J., 2010. Carbon isotope compositions of terrestrial C₃ plants as indicators of (paleo)ecology and (paleo)climate. *Proc. Natl. Acad. Sci. U. S. A.* 107, 19691–5. doi:10.1073/pnas.1004933107
- Kohn, M.J., 2011. Reply to Freeman et al.: Carbon isotope discrimination by C₃ plants. *Proc. Natl. Acad. Sci.* 108, E61–E61. doi:10.1073/pnas.1103222108
- Kristensen, D.K., Kristensen, E., Forchhammer, M.C., Michelsen, A., Schmidt, N.M., 2011. Arctic herbivore diet can be inferred from stable carbon and nitrogen isotopes in C₃ plants, faeces, and wool. *Can. J. Zool.* 89, 892–899. doi:10.1139/z11-073
- Layman, C., Arrington, D., Montaña, C., Post, D., 2007. Can stable isotope ratios provide for community-wide measures of trophic structure? *Ecology* 88, 42–48.
- Layman, C.A., Araujo, M.S., Boucek, R., Hammerschlag-Peyer, C.M., Harrison, E., Jud, Z.R., Matich, P., Rosenblatt, A.E., Vaudo, J.J., Yeager, L.A., Post, D.M., Bearhop, S., 2012. Applying stable isotopes to examine food-web structure: an overview of analytical tools. *Biol. Rev. Camb. Philos. Soc.* 87, 545–62. doi:10.1111/j.1469-185X.2011.00208.x
- Leonard, J.A., Vilà, C., Fox-Dobbs, K., Koch, P.L., Wayne, R.K., Van Valkenburgh, B., 2007. Megafaunal extinctions and the disappearance of a specialized wolf ecomorph. *Curr. Biol.* 17, 1146–50. doi:10.1016/j.cub.2007.05.072
- MacPhee, R.D.E., Tikhonov, A.N., Mol, D., de Marliave, C., van der Plicht, H., Greenwood, A.D., Flemming, C., Agenbroad, L., 2002. Radiocarbon chronologies and extinction dynamics of the late Quaternary mammalian megafauna of the Taimyr Peninsula, Russian Federation. *J. Archaeol. Sci.* 29, 1017–1042. doi:10.1006/jasc.2001.0802
- Mandryk, C.S., 1996. Late-glacial vegetation and environment on the eastern slope foothills of the Rocky Mountains, Alberta, Canada. *J. Paleolimnol.* 16, 37–57. doi:10.1007/BF00173270
- Mann, D.H., Groves, P., Kunz, M.L., Reanier, R.E., Gaglioti, B. V., 2013. Ice-age megafauna in Arctic Alaska: extinction, invasion, survival. *Quat. Sci. Rev.* 70, 91–108. doi:10.1016/j.quascirev.2013.03.015
- Marshall, J.D., Brooks, J.R., Lajtha, K., 2007. Sources of variation in the stable isotopic composition of plants, in: Michener, R., Lajtha, K. (Eds.), *Stable Isotopes in Ecology and Environmental Science*. Blackwell Publishing Ltd, Hong Kong, pp. 22–60.
- McAndrews, J., Jackson, L., 1988. Age and environment of late Pleistocene mastodont and mammoth in southern Ontario. *Bull. Buffalo Soc. Nat. Sci.* 33, 161–172.

- Metcalfe, J.Z., 2011. Late Pleistocene climate and proboscidean paleoecology in North America: insights from stable isotope compositions of skeletal remains. Doctoral Thesis. University of Western Ontario.
- Metcalfe, J.Z., Longstaffe, F.J., Hodgins, G., 2013. Proboscideans and paleoenvironments of the Pleistocene Great Lakes: landscape, vegetation, and stable isotopes. *Quat. Sci. Rev.* 76, 102–113. doi:10.1016/j.quascirev.2013.07.004
- Metcalfe, J.Z., Longstaffe, F.J., Zazula, G.D., 2010. Nursing, weaning, and tooth development in woolly mammoths from Old Crow, Yukon, Canada: implications for Pleistocene extinctions. *Palaeogeogr. Palaeoclimatol. Palaeoecol.* 298, 257–270. doi:10.1016/j.palaeo.2010.09.032
- Mix, A., Bard, E., Schneider, R., 2001. Environmental processes of the ice age: land, oceans, glaciers (EPILOG). *Quat. Sci. Rev.* 20, 627–657.
- Mol, D., Tikhonov, A., van der Plicht, J., Kahlke, R.-D., Debruyne, R., van Geel, B., van Reenen, G., Pals, J.P., de Marliave, C., Reumer, J.W.F., 2006. Results of the CERPOLEX/Mammuthus Expeditions on the Taimyr Peninsula, Arctic Siberia, Russian Federation. *Quat. Int.* 142-143, 186–202. doi:10.1016/j.quaint.2005.03.016
- Nadelhoffer, K., Shaver, G., Fry, B., Giblin, A., 1996. ^{15}N natural abundances and N use by tundra plants. *Oecologia* 107, 386–394.
- Nogués-Bravo, D., Rodríguez, J., Hortal, J., Batra, P., Araújo, M.B., 2008. Climate change, humans, and the extinction of the woolly mammoth. *PLoS Biol.* 6, e79.
- O’Leary, M., 1988. Carbon isotopes in photosynthesis. *Bioscience* 38, 328–336.
- Parnell, A.C., Inger, R., Bearhop, S., Jackson, A.L., 2010. Source partitioning using stable isotopes: coping with too much variation. *PLoS One* 5, e9672. doi:10.1371/journal.pone.0009672
- Pires, M.M., Koch, P.L., Farina, R.A., de Aguiar, M.A.M., dos Reis, S.F., Guimaraes, Paulo R., J., 2015. Pleistocene megafaunal interaction networks became more vulnerable after human arrival. *Proc R Soc B* 282, 20151367. doi:10.1098/rspb.2015.1367
- Polischuk, S., Hobson, K., Ramsay, M., 2011. Use of stable-carbon and -nitrogen isotopes to assess weaning and fasting in female polar bears and their cubs. *Can. J. Zool.* 79, 499–511.
- R Core Team, 2014. R: A language and environment for statistical computing. R Foundation for Statistical Computing, Vienna, Austria.
- Raghavan, M., Espregueira Themudo, G., Smith, C.I., Zazula, G., Campos, P.F., 2014. Musk ox (*Ovibos moschatus*) of the mammoth steppe: tracing palaeodietary and palaeoenvironmental changes over the last 50,000 years using carbon and nitrogen

- isotopic analysis. *Quat. Sci. Rev.* 102, 192–201.
doi:10.1016/j.quascirev.2014.08.001
- Rasic, J., Matheus, P., 2007. A reconsideration of purported Holocene bison bones from northern Alaska. *Arctic* 60, 381–388.
- Richards, M.P., Hedges, R.E.M., 2003. Variations in bone collagen $\delta^{13}\text{C}$ and $\delta^{15}\text{N}$ values of fauna from Northwest Europe over the last 40 000 years. *Palaeogeogr. Palaeoclimatol. Palaeoecol.* 193, 261–267. doi:10.1016/S0031-0182(03)00229-3
- Rivals, F., Solounias, N., Mithlbackler, M.C., 2007. Evidence for geographic variation in the diets of late Pleistocene and early Holocene bison in North America, and differences from the diets of recent bison. *Quat. Res.* 68, 338–346.
doi:10.1016/j.yqres.2007.07.012
- Royston, J., 1982. Algorithm AS 181: the W test for normality. *Appl. Stat.* 31, 176–180.
- Saunders, J.J., Grimm, E.C., Widga, C.C., Campbell, G.D., Curry, B.B., Grimley, D.A., Hanson, P.R., McCullum, J.P., Oliver, J.S., Treworgy, J.D., 2010. Paradigms and proboscideans in the southern Great Lakes region, USA. *Quat. Int.* 217, 175–187.
doi:10.1016/j.quaint.2009.07.031
- Schubert, B.A., Jahren, A.H., 2015. Global increase in plant carbon isotope fractionation following the Last Glacial Maximum caused by increase in atmospheric $p\text{CO}_2$. *Geology* 43, 435–438. doi:10.1130/G36467.1
- Schwartz-Narbonne, R., Longstaffe, F.J., Metcalfe, J.Z., Zazula, G., 2015. Solving the woolly mammoth conundrum: amino acid ^{15}N -enrichment suggests a distinct forage or habitat. *Sci. Rep.* 5, 9791. doi:10.1038/srep09791
- Sealy, J., van der Merwe, N., Thorp, J.A.L., Lanham, J.L., 1987. Nitrogen isotopic ecology in southern Africa: implications for environmental and dietary tracing. *Geochim. Cosmochim. Acta* 51, 2707–2717.
- Shapiro, B., Drummond, A.J., Rambaut, A., Wilson, M.C., Matheus, P.E., Sher, A. V., Pybus, O.G., Gilbert, M.T.P., Barnes, I., Binladen, J., Willerslev, E., Hansen, A.J., Baryshnikov, G.F., Burns, J. a, Davydov, S., Driver, J.C., Froese, D.G., Harington, C.R., Keddie, G., Kosintsev, P., Kunz, M.L., Martin, L.D., Stephenson, R.O., Storer, J., Tedford, R., Zimov, S., Cooper, A., 2004. Rise and fall of the Beringian steppe bison. *Science* 306, 1561–5. doi:10.1126/science.1101074
- Sponheimer, M., Robinson, T., Ayliffe, L., Roeder, B., Hammer, J., Passey, B., West, A., Cerling, T., Dearing, D., Ehleringer, J., 2003. Nitrogen isotopes in mammalian herbivores: hair $\delta^{15}\text{N}$ values from a controlled feeding study. *Int. J. Osteoarchaeol.* 13, 80–87. doi:10.1002/oa.655
- Stevens, R.E., Germonpré, M., Petrie, C.A., O’Connell, T.C., 2009. Palaeoenvironmental and chronological investigations of the Magdalenian sites of Goyet Cave and Trou

- de Chaleux (Belgium), via stable isotope and radiocarbon analyses of horse skeletal remains. *J. Archaeol. Sci.* 36, 653–662. doi:10.1016/j.jas.2008.10.008
- Stevens, R.E., Hedges, R.E., 2004. Carbon and nitrogen stable isotope analysis of northwest European horse bone and tooth collagen, 40,000 BP – present: palaeoclimatic interpretations. *Quat. Sci. Rev.* 23, 977–991. doi:10.1016/j.quascirev.2003.06.024
- Stevens, R.E., Jacobi, R., Street, M., Germonpré, M., Conard, N.J., Münzel, S.C., Hedges, R.E.M., 2008. Nitrogen isotope analyses of reindeer (*Rangifer tarandus*), 45,000 BP to 9,000 BP: palaeoenvironmental reconstructions. *Palaeogeogr. Palaeoclimatol. Palaeoecol.* 262, 32–45. doi:10.1016/j.palaeo.2008.01.019
- Stevens, R.E., Lister, A., Hedges, R., 2006. Predicting diet, trophic level and palaeoecology from bone stable isotope analysis: a comparative study of five red deer populations. *Oecologia* 149, 12–21.
- Strong, W.L., Hills, L. V., 2005. Late-glacial and Holocene palaeovegetation zonal reconstruction for central and north-central North America. *J. Biogeogr.* 32, 1043–1062. doi:10.1111/j.1365-2699.2004.01223.x
- Styring, A.K., Sealy, J.C., Evershed, R.P., 2010. Resolving the bulk $\delta^{15}\text{N}$ values of ancient human and animal bone collagen via compound-specific nitrogen isotope analysis of constituent amino acids. *Geochim. Cosmochim. Acta* 74, 241–251. doi:10.1016/j.gca.2009.09.022
- Syväranta, J., Lensu, A., Marjomäki, T.J., Oksanen, S., Jones, R.I., 2013. An empirical evaluation of the utility of convex hull and standard ellipse areas for assessing population niche widths from stable isotope data. *PLoS One* 8, e56094. doi:10.1371/journal.pone.0056094
- Szpak, P., Gröcke, D.R., Debruyne, R., MacPhee, R.D.E., Guthrie, R.D., Froese, D., Zazula, G.D., Patterson, W.P., Poinar, H.N., 2010. Regional differences in bone collagen $\delta^{13}\text{C}$ and $\delta^{15}\text{N}$ of Pleistocene mammoths: implications for paleoecology of the mammoth steppe. *Palaeogeogr. Palaeoclimatol. Palaeoecol.* 286, 88–96. doi:10.1016/j.palaeo.2009.12.009
- Tahmasebi, F., 2015. Carbon and nitrogen isotopic investigations of the late Pleistocene paleoecology of eastern Beringia, Yukon Territory, using soils, plants and rodent bones. Doctoral Thesis. University of Western Ontario.
- Tieszen, L., 1991. Natural variations in the carbon isotope values of plants: implications for archaeology, ecology, and paleoecology. *J. Archaeol. Sci.* 18, 227–248.
- Willerslev, E., Davison, J., Moora, M., Zobel, M., Coissac, E., Edwards, M.E., Lorenzen, E.D., Vestergård, M., Gussarova, G., Haile, J., Craine, J., Gielly, L., Boessenkool, S., Epp, L.S., Pearman, P.B., Cheddadi, R., Murray, D., Bråthen, K.A., Yoccoz, N., Binney, H., Cruaud, C., Wincker, P., Goslar, T., Alsos, I.G., Bellemain, E., Brysting,

- A.K., Elven, R., Sønstebo, J.H., Murton, J., Sher, A., Rasmussen, M., Rønn, R., Mourier, T., Cooper, A., Austin, J., Möller, P., Froese, D., Zazula, G., Pompanon, F., Rioux, D., Niderkorn, V., Tikhonov, A., Savvinov, G., Roberts, R.G., MacPhee, R.D.E., Gilbert, M.T.P., Kjær, K.H., Orlando, L., Brochmann, C., Taberlet, P., 2014. Fifty thousand years of Arctic vegetation and megafaunal diet. *Nature* 506, 47–51. doi:10.1038/nature12921
- Wooller, M., Zazula, G., Edwards, M., Froese, D.G., Boone, R.D., Parker, C., Bennett, B., 2007. Stable carbon isotope compositions of Eastern Beringian grasses and sedges: investigating their potential as paleoenvironmental indicators. *Arctic, Antarct. Alp. Res.* 39, 318–331.
- Yeakel, J.D., Guimarães, P.R., Bocherens, H., Koch, P.L., 2013. The impact of climate change on the structure of Pleistocene food webs across the mammoth steppe. *Proc. R. Soc. B Biol. Sci.* 280, 20130239.
- Zazula, G.D., Froese, D.G., Elias, S.A., Kuzmina, S., Mathewes, R.W., 2011. Early Wisconsinan (MIS 4) Arctic ground squirrel middens and a squirrel-eye-view of the mammoth-steppe. *Quat. Sci. Rev.* 30, 2220–2237. doi:10.1016/j.quascirev.2010.04.019
- Zazula, G.D., MacPhee, R.D., Metcalfe, J.Z., Reyes, A. V., Brock, F., Druckenmiller, P.S., Groves, P., Harington, R., Hodgins, G.W.L., Kunz, M.L., Longstaffe, F.J., Mann, D.H., McDonald, H.G., Nalawade-Chavan, S., Southon, J.R., 2014. American mastodon extirpation in the Arctic and Subarctic predates human colonization and terminal Pleistocene climate change. *Proc. Natl. Acad. Sci.* 111, 18460–18465.
- Zimov, S.A., Zimov, N.S., Tikhonov, A.N., Chapin, F.S., 2012. Mammoth steppe: a high-productivity phenomenon. *Quat. Sci. Rev.* 57, 26–45. doi:10.1016/j.quascirev.2012.10.005

Chapter 6

6 Conclusions

This thesis explores the ecology of megaherbivore species across the mammoth steppe. The use of several techniques that had not been previously applied to the mammoth steppe research has allowed a deeper understanding of the diets and habitat preferences of these animals. This chapter summarizes those techniques, the conclusions drawn from them regarding the ecology of mammoth steppe megafauna, and the implications for mammoth steppe ecology and extinction as a whole.

6.1 Summary of the thesis

To fully understand mammoth steppe ecology, a better understanding of the diet and habitats of individual mammoth steppe species was necessary. In Chapter 2, the seasonal diets of species with antlers (moose, elk and caribou) were investigated through isotopic analysis of serially sampled antler collagen, and comparison of the isotopic composition of antler to that of bone collagen. Moose consumed aquatic plants in the summer, and browse during the rest of the year. Elk consumed graminoids and forbs during the fall and winter, and browse during the spring and summer. Caribou consumed primarily lichen in the winter. Caribou ate some ground shrubs during the late spring, and concentrated their diet on graminoids and forbs during the rest of the year. In Chapters 3 and 4, the diet and habitat preferences of a number of non-ruminant herbivores (woolly mammoth, mastodon, beaver, horse) were assessed through carbon and nitrogen isotopic analysis of bone, tooth and tusk collagen amino acids and comparisons with carnivore bone collagen and plant tissue amino acid isotopic compositions. Woolly mammoth consumed a distinct diet or food from a distinct habitat. This could reflect forage from extremely arid areas, plants fertilized by dung, and/or selection for specific plants. I suggest that woolly mammoths selected for decayed plants, primarily during the winter. Horse also ate decayed plants, though they consumed plants with a wider variety of isotopic compositions than woolly mammoths; this additional forage likely included fresh

graminoids and forbs. Mastodon focused their diet on terrestrial plants, mostly browse. Giant beaver consumed primarily aquatic plants.

The review in Chapter 5 of the carbon and nitrogen isotopic patterns exhibited by megaherbivores at 16 sites across the mammoth steppe provided context for these dietary patterns. The isotopic patterns exhibited by a variety of species from the mammoth steppe during various time slices of the Pleistocene and Holocene were considered using the mathematical tool SIBER in R (Jackson et al., 2011; Parnell et al., 2010; R Core Team, 2014). The general isotopic pattern (relative position of $\delta^{13}\text{C}$ and $\delta^{15}\text{N}$ in isotopic space) of species during the pre-LGM (Last Glacial Maximum) was found to be consistent among most sites, which suggests that the dietary and habitat patterns reported in Chapters 2-4 were typical of each species during this time period across the entirety of the mammoth steppe. Figure 6.1 presents the typical carbon and nitrogen isotopic pattern of pre-LGM mammoth steppe species, as well as the diets suggested by the carbon and nitrogen isotopic analyses of antler and bone collagen and amino acids from bone, tooth and tusk collagen. It also details which species had larger isotopic niches (larger standard ellipses or convex hulls in carbon and nitrogen isotopic space as measured in per mil), suggesting that they were generalists (caribou and horse) and which had smaller isotopic niches, suggesting that they were specialists (mammoth and mastodon).

The changes in species' carbon and nitrogen isotopic patterns and in species' relative niche that occurred in the mammoth steppe during the Pleistocene and Holocene are also described in Chapter 5. The size of a species' isotopic niche tended to be smaller in the post-LGM than the pre-LGM. The relative positions of species isotopic niches in nitrogen-carbon isotopic space (e.g., Fig. 6.1) also changed from the LGM to the post-LGM to the Holocene. These changes suggest that the ecological equilibrium that allowed megaherbivores to coexist during the pre-LGM period was not re-established in later times.

6.2 Mammoth steppe ecology and extinction

It is important to consider both how the mammoth steppe biome was maintained as well as the causes for its disappearance. Guthrie (2001, 1982) suggested that mammoth steppe

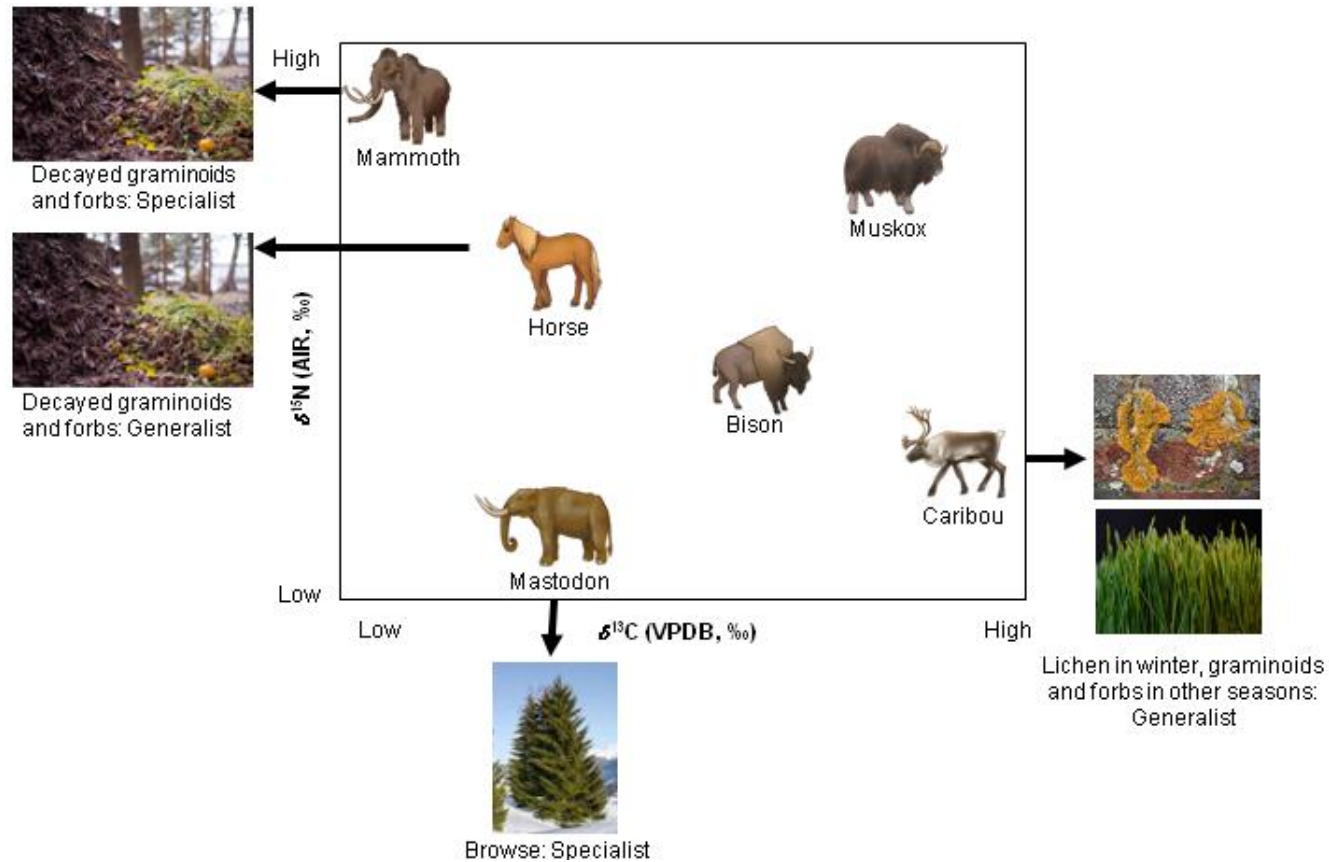


Figure 6.1 Typical carbon and nitrogen isotopic pattern observed for collagen of pre-LGM mammoth steppe megaherbivores, as well as the hypothesized diets of these animals. Megaherbivores images drawn by Kate Allan. Spruce from <https://en.wikipedia.org/wiki/Spruce>. Lichen from <https://en.wikipedia.org/wiki/Lichen>. Grass from <https://en.wikipedia.org/wiki/Grass>. Decayed plants from <http://biogrounds.org/category/life-in-soils/>.

herbivores coexisted by minimizing competition through ecological niche partitioning. The consistency of the isotopic niches (Fig. 6.1), as described in Chapter 5 and in previous work (Bocherens, 2015, 2003) supports this hypothesis for the pre-LGM mammoth steppe. However, the isotopic niches of several species invariably overlap (bison-horse, bison-caribou, bison-muskox, horse-mammoth, and horse-mastodon). These species may have used other mechanisms to avoid competition that are not visible isotopically, or there may have been some ecological overlap, particularly among species with more generalist feeding strategies.

At the end of the Pleistocene, several mammoth steppe species were extirpated or went extinct, and the ecological relationships characteristic of the ecosystem were lost. This thesis demonstrates that the mammoth steppe underwent ecological shifts in response to the climatic changes of the LGM. An evaluation of the North American Pleistocene megafaunal networks by Pires et al. (2015) found that they were more vulnerable to perturbations than the megafaunal networks of Africa (Pires et al., 2015). This thesis suggests that the LGM caused a major ecological perturbation that resulted in changed species associations. This change might have been sufficient to destabilize the biome. It is also possible, however, that the ecosystem would have returned to its previous equilibrium, or developed a new one, given time, and that it was the combination of ecosystem instability caused by climatic changes and hunting pressure from anatomically modern humans that caused the extinctions to occur.

6.3 Future work

There are a number of additional groundwork-level isotopic studies that could aid the interpretation of the data presented in this thesis, and are recommended for future studies. In Chapter 2, serial sampling of antler was performed at 10 cm intervals. Antlers, however, do not grow at a constant rate (Chapman, 1975), and so the distance between measurements did not represent a constant interval of time. Future work should determine a generalized sampling strategy for antlers through a histological analysis of the antler tissue, including thin sectioning and observations of antler cross-sections. As well, more isotopic analysis of bone and antler from populations with known or controlled diets is

needed to establish if there are any physiological differences between the two tissues, or if differences in their isotopic compositions are based purely on dietary and habitat differences.

More groundwork is necessary to more firmly establish and distinguish the carbon and nitrogen amino acid isotopic compositions of dietary sources (plants, fungi and bacteria). Previous work has established that several forage types (terrestrial plants, aquatic plants, fungi and bacteria) have a $\delta^{13}\text{C}$ fingerprint that is distinct to that dietary source (Arthur et al., 2014; Larsen et al., 2013, 2012, 2009). Previous investigations of the amino acid isotopic compositions of plants suggests that there might be distinct patterns visible in both the $\delta^{13}\text{C}$ and $\delta^{15}\text{N}$ of different plant types, different plant parts, plants grown in different environments, and decayed plants (Bol et al., 2002; Calleja et al., 2013; Chikaraishi et al., 2010; Fogel and Tuross, 2003, 1999; Larsen et al., 2013, 2012, 2011, 2009; Lynch et al., 2011; Smallwood et al., 2003; Styring et al., 2014). Elucidating these patterns would allow a more comprehensive analysis of the amino acid isotopic compositions of the mammoth steppe fauna that consumed them.

There are a number of further analyses that could be performed on the samples and data presented in Chapter 5. This thesis performed amino acid analysis solely on species from Old Crow, Yukon Territory, and the majority of the samples were dated to the pre-LGM. Amino acid analyses of species from different time periods and sites could provide insights into the sources of variability. As well, more comprehensive mathematical modeling of the bulk collagen isotopic compositions would be valuable in helping to explain why certain species and sites were outliers from the general observed patterns. Time-series analysis, for example, would allow species isotopic compositions to be compared without the potential bias introduced by selection of one particular method for binning samples into time periods. A substantial investment in the dating of many more samples, however, would be prerequisite to such an effort.

6.4 Concluding remarks

Understanding the ecology of mammoth steppe megaherbivores is necessary to understand how this biome was maintained during the Pleistocene, and what factors may

have been involved in its disappearance. This study has provided an in-depth analysis of the diet and habitat preferences of several species, as well as providing insight into their interactions. It also considered how those interactions shifted over time, which was likely a response to climatic changes and possibly also anthropogenic influences. In short, the results of this thesis improve our understanding of the Pleistocene ecology of the mammoth steppe, and of how its species and ecosystems responded to environmental changes.

6.5 References

- Arthur, K.E., Kelez, S., Larsen, T., Choy, C.A., Popp, B.N., 2014. Tracing the biosynthetic source of essential amino acids in marine turtles using $\delta^{13}\text{C}$ fingerprints. *Ecology* 95, 1285–1293. doi:10.1890/13-0263.1
- Bocherens, H., 2003. Isotopic biogeochemistry and the paleoecology of the mammoth steppe fauna. *Deinsea* 9, 57–76.
- Bocherens, H., 2015. Isotopic tracking of large carnivore palaeoecology in the mammoth steppe. *Quat. Sci. Rev.* 117, 42–71. doi:10.1016/j.quascirev.2015.03.018
- Bol, R., Ostle, N.J., Petzke, K.J., 2002. Compound specific plant amino acid $\delta^{15}\text{N}$ values differ with functional plant strategies in temperate grassland. *J. Plant Nutr. Soil Sci.* 165, 661–667. doi:10.1002/jpln.200290000
- Calleja, M.L., Batista, F., Peacock, M., Kudela, R., McCarthy, M.D., 2013. Changes in compound specific $\delta^{15}\text{N}$ amino acid signatures and D/L ratios in marine dissolved organic matter induced by heterotrophic bacterial reworking. *Mar. Chem.* 149, 32–44. doi:10.1016/j.marchem.2012.12.001
- Chapman, D., 1975. Antlers – bones of contention. *Mamm. Rev.* 5, 121–172.
- Chikaraishi, Y., Ogawa, N.O., Ohkouchi, N., 2010. Further evaluation of the trophic level estimation based on nitrogen isotopic composition of amino acids, in: Ohkouchi, N., Tayasu, I., Koba, K. (Eds.), *Earth, Life, and Isotopes*. Kyoto University Press, Kyoto, pp. 37–51.
- Fogel, M., Tuross, N., 2003. Extending the limits of paleodietary studies of humans with compound specific carbon isotope analysis of amino acids. *J. Archaeol. Sci.* 30, 535–545.
- Fogel, M.L., Tuross, N., 1999. Transformation of plant biochemicals to geological macromolecules during early diagenesis. *Oecologia* 120, 336–346. doi:10.1007/s004420050867

- Guthrie, R.D., 1982. Mammals of the mammoth steppe as paleoenvironmental indicators, in: Hopkins, D.M., Matthews, Jr., J.V., Schweger, C.E., Young, S.B. (Eds.), *Paleoecology of Beringia*. Academic Press, New York, pp. 307–326.
- Guthrie, R.D., 2001. Origin and causes of the mammoth steppe: a story of cloud cover, woolly mammal tooth pits, buckles, and inside-out Beringia. *Quat. Sci. Rev.*
- Jackson, A.L., Inger, R., Parnell, A.C., Bearhop, S., 2011. Comparing isotopic niche widths among and within communities: SIBER - Stable Isotope Bayesian Ellipses in R. *J. Anim. Ecol.* 80, 595–602. doi:10.1111/j.1365-2656.2011.01806.x
- Larsen, T., Taylor, D.L., Leigh, M.B., O'Brien, D.M., 2009. Stable isotope fingerprinting: a novel method for identifying plant, fungal, or bacterial origins of amino acids. *Ecology* 90, 3526–35.
- Larsen, T., Ventura, M., Andersen, N., O'Brien, D.M., Piatkowski, U., McCarthy, M.D., 2013. Tracing carbon sources through aquatic and terrestrial food webs using amino acid stable isotope fingerprinting. *PLoS One* 8, e73441. doi:10.1371/journal.pone.0073441
- Larsen, T., Ventura, M., O'Brien, D.M., Magid, J., Lomstein, B.A., Larsen, J., 2011. Contrasting effects of nitrogen limitation and amino acid imbalance on carbon and nitrogen turnover in three species of Collembola. *Soil Biol. Biochem.* 43, 749–759. doi:10.1016/j.soilbio.2010.12.008
- Larsen, T., Wooller, M.J., Fogel, M.L., O'Brien, D.M., 2012. Can amino acid carbon isotope ratios distinguish primary producers in a mangrove ecosystem? *Rapid Commun. Mass Spectrom.* 26, 1541–1548. doi:10.1002/rcm.6259
- Lynch, A.H., McCullagh, J.S.O., Hedges, R.E.M., 2011. Liquid chromatography/isotope ratio mass spectrometry measurement of $\delta^{13}\text{C}$ of amino acids in plant proteins. *Rapid Commun. Mass Spectrom.* 25, 2981–8. doi:10.1002/rcm.5142
- Parnell, A.C., Inger, R., Bearhop, S., Jackson, A.L., 2010. Source partitioning using stable isotopes: coping with too much variation. *PLoS One* 5, e9672. doi:10.1371/journal.pone.0009672
- Pires, M.M., Koch, P.L., Farina, R.A., de Aguiar, M.A.M., dos Reis, S.F., Guimaraes, Paulo R., J., 2015. Pleistocene megafaunal interaction networks became more vulnerable after human arrival. *Proc R Soc B* 282, 20151367. doi:10.1098/rspb.2015.1367
- R Core Team, 2014. R: A language and environment for statistical computing. R Foundation for Statistical Computing, Vienna, Austria.
- Smallwood, B.J., Wooller, M.J., Jacobson, M.E., Fogel, M.L., 2003. Isotopic and molecular distributions of biochemicals from fresh and buried *Rhizophora* mangle leaves. *Geochem. Trans.* 4, 38–46. doi:10.1039/b308902a

Styring, A.K., Fraser, R.A., Bogaard, A., Evershed, R.P., 2014. Cereal grain, rachis and pulse seed amino acid $\delta^{15}\text{N}$ values as indicators of plant nitrogen metabolism. *Phytochemistry* 97, 20–9. doi:10.1016/j.phytochem.2013.05.009

Appendices

Appendix A: Sample information for specimens whose isotopic compositions were included in this study. Previously reported radiocarbon dates are taken from literature sources (Druckenmiller, 2008; Mann et al., 2013; Meiri et al., 2014, Zazula, pers. comm., 2015).

Lab ID	Common Name	Species	Area	Collection Site	Lat.	Long.	Source	Sample Number
AB14	Caribou	<i>Rangifer tarandus</i>	Edmonton	Consolidated Concrete Pit 48			RAM	P89.13.160
AB23	Caribou	<i>Rangifer tarandus</i>	Edmonton	Consolidated Concrete Pit 48			RAM	P94.1.438
AB31	Caribou	<i>Rangifer tarandus</i>	Edmonton	Consolidated Concrete Pit 48			RAM	P95.6.29
AB34	Caribou	<i>Rangifer tarandus</i>	Edmonton	Consolidated Concrete Pit 48			RAM	P98.5.35
AB35	Caribou	<i>Rangifer tarandus</i>	Edmonton	Consolidated Concrete Pit 48			RAM	P98.5.185
AB36	Caribou	<i>Rangifer tarandus</i>	Edmonton	Consolidated Concrete Pit 48			RAM	P98.5.328
AB37	Caribou	<i>Rangifer tarandus</i>	Edmonton	Consolidated Concrete Pit 48			RAM	P98.5.347
AB42	Caribou	<i>Rangifer tarandus</i>	Edmonton	Consolidated Concrete Pit 48			RAM	P02.10.3
AB16	Caribou	<i>Rangifer tarandus</i>	Edmonton	Consolidated Concrete Pit 48			RAM	P89.13.316
AB24	Caribou	<i>Rangifer tarandus</i>	Edmonton	Consolidated Concrete Pit 48			RAM	P94.1.459
YT126	Caribou	<i>Rangifer tarandus</i>	Herschel Island		69.6	-139.0	YG	381.52
YT126	Caribou	<i>Rangifer tarandus</i>	Herschel Island		69.6	-139.0	YG	381.52
YT135	Caribou	<i>Rangifer tarandus</i>	Klondike	Irish Gulch			YG	126.6
YT136	Caribou	<i>Rangifer tarandus</i>	Klondike	Irish Gulch			YG	126.13

YT137	Caribou	<i>Rangifer tarandus</i>	Klondike	Irish Gulch			YG	126.31
YT138	Caribou	<i>Rangifer tarandus</i>	Klondike				YG	306.194
YT139	Caribou	<i>Rangifer tarandus</i>	Klondike				YG	376.47
YT140	Caribou	<i>Rangifer tarandus</i>	Klondike				YG	378.48
YT141	Caribou	<i>Rangifer tarandus</i>	Klondike				YG	404.321
YT142	Caribou	<i>Rangifer tarandus</i>	Klondike				YG	406.665
YT143	Caribou	<i>Rangifer tarandus</i>	Klondike				YG	407.304
YT144	Caribou	<i>Rangifer tarandus</i>	Klondike				YG	421.163
YT145	Caribou	<i>Rangifer tarandus</i>	Klondike				YG	435.103
YT95	Caribou	<i>Rangifer tarandus</i>	Klondike	Paradise Hill	64.0	-139.0	YG	5.77
YT125	Caribou	<i>Rangifer tarandus</i>	Klondike	Quartz Creek	63.8	-139.0	YG	109.9
YT127	Caribou	<i>Rangifer tarandus</i>	Klondike	Hunker Creek	64.0	-139.2	YG	404.657
YT128	Caribou	<i>Rangifer tarandus</i>	Klondike	Last Chance Creek	64.0	-139.2	YG	306.468
UAK6	Caribou	<i>Rangifer tarandus</i>	Selawik	Elephant Point			UAMES	UAMES 1122
UAK12	Caribou	<i>Rangifer tarandus</i>	Selawik	Koyukuk River			UAMES	UAMES 2214
UAK8	Caribou	<i>Rangifer tarandus</i>	Selawik	Elephant Point			UAMES	UAMES 1151
UAK9	Caribou	<i>Rangifer tarandus</i>	Selawik	Elephant Point			UAMES	UAMES 1180
UAK7	Caribou	<i>Rangifer tarandus</i>	Selawik	Elephant Point			UAMES	UAMES 1123
UAK11	Caribou	<i>Rangifer tarandus</i>	Selawik	Kateel River			UAMES	UAMES 2114
UAK1	Caribou	<i>Rangifer tarandus</i>	Selawik	Inglutalik River			UAMES	UAMES1033
UAK2	Caribou	<i>Rangifer tarandus</i>	Selawik	Inglutalik River			UAMES	UAMES1035
UAK3	Caribou	<i>Rangifer tarandus</i>	Selawik	Inglutalik River			UAMES	UAMES 1036
UAK4	Caribou	<i>Rangifer tarandus</i>	Selawik	Elephant Point			UAMES	UAMES 1080
UAK5	Caribou	<i>Rangifer tarandus</i>	Selawik	Elephant Point			UAMES	UAMES 1081

UAK10	Caribou	<i>Rangifer tarandus</i>	Selawik	Mud Creek			UAMES	UAMES 1900
UAK13	Caribou	<i>Rangifer tarandus</i>	Selawik	Kateel River			UAMES	UAMES 7716
YT87	Elk	<i>Cervus elaphus</i>	Klondike	Goldbottom Creek	64.0	-139.0	YG	192.1
YT92	Elk	<i>Cervus elaphus</i>	Klondike	No Bottom Gulch	63.9	-138.9	YG	377.43
YT94	Elk	<i>Cervus elaphus</i>	Klondike	Little John Site	62.6	-140.9	YG	Fa06-141
YT85/123	Elk	<i>Cervus elaphus</i>	Klondike	Last Chance Creek	64.0	-139.2	YG	104.04
YT88	Elk	<i>Cervus elaphus</i>	Klondike	Meadow Creek	63.8	-138.9	YG	208.1
YT89	Elk	<i>Cervus elaphus</i>	Klondike	Homestake Gulch	63.9	-139.2	YG	301.17
YT90	Elk	<i>Cervus elaphus</i>	Klondike	Eldorado Creek	63.9	-139.3	YG	303.168
YT91	Elk	<i>Cervus elaphus</i>	Klondike	Last Chance Creek	64.0	-139.2	YG	306.449
YT93	Elk	<i>Cervus elaphus</i>	Klondike	Little Blanche Creek	63.8	-139.1	YG	378.53
YT124	Elk	<i>Cervus elaphus</i>	Klondike	Dawson City	64.1	-139.4	YG	420.1
YT96	Moose	<i>Alces alces</i>	Klondike				YG	29.69
YT99	Moose	<i>Alces alces</i>	Klondike				YG	134.1
YT100	Moose	<i>Alces alces</i>	Klondike				YG	136.1
YT101B	Moose	<i>Alces alces</i>	Klondike				YG	193.1
YT102	Moose	<i>Alces alces</i>	Klondike	Quartz Creek			YG	269.1
YT103	Moose	<i>Alces alces</i>	Klondike				YG	300.2
YT105	Moose	<i>Alces alces</i>	Klondike	Lindow Creek			YG	300.96
YT106	Moose	<i>Alces alces</i>	Klondike				YG	308.21
YT107	Moose	<i>Alces alces</i>	Klondike				YG	354.3
YT108	Moose	<i>Alces alces</i>	Klondike	Green Gulch			YG	355.113
YT110	Moose	<i>Alces alces</i>	Klondike				YG	376.56
YT86	Moose	<i>Alces alces</i>	Klondike	Sulphur Creek	63.7	-138.8	YG	136.8
YT98	Moose	<i>Alces alces</i>	Klondike	Hester Creek	64.0	-139.1	YG	129.2

YT101A	Moose	<i>Alces alces</i>	Klondike	Lucky Lady Sulphur Creek	63.7	-138.9	YG	193.1
YT104	Moose	<i>Alces alces</i>	Klondike	Lindow Creek	64.0	-139.2	YG	300.226
YT109	Moose	<i>Alces alces</i>	Klondike	Green Gulch	63.8	-138.9	YG	355.99
YT121	Moose	<i>Alces alces</i>	Klondike	Laskey Creek	63.7	-138.7	YG	190.1
YT122	Moose	<i>Alces alces</i>	Klondike	Thistle Creek	63.1	-139.3	YG	162.46
IK02-210	Moose	<i>Alces alces</i>	North Slope	Ikpikpuk R.			UAMES	UAMES 10355
IK01-404	Moose	<i>Alces alces</i>	North Slope	Ikpikpuk R.			UAMES	UAMES 11844
IK12-077	Moose	<i>Alces alces</i>	North Slope	Ikpikpuk R.			UAMES	UAMES 30183
IK99-229	Moose	<i>Alces alces</i>	North Slope	Ikpikpuk R.			UAMES	UAMES 10691
IK08-016	Moose	<i>Alces alces</i>	North Slope	Ikpikpuk R.			UAMES	UAMES 30180
IK99-776	Moose	<i>Alces alces</i>	North Slope	Ikpikpuk R.			UAMES	UAMES 11066
IK99-556	Moose	<i>Alces alces</i>	North Slope	Ikpikpuk R.			UAMES	UAMES 10996
IK01-023	Moose	<i>Alces alces</i>	North Slope	Ikpikpuk R.			UAMES	UAMES 12022
KIG05-4.1	Moose	<i>Alces alces</i>	North Slope	Kigalik R.			UAMES	UAMES 30186
MAY12-64	Moose	<i>Alces alces</i>	North Slope	Maybe Cr.			UAMES	UAMES 30187
IK08-129	Moose	<i>Alces alces</i>	North Slope	Ikpikpuk R.			UAMES	UAMES 30181
TIT10-58	Moose	<i>Alces alces</i>	North Slope	Titaluk R.			UAMES	UAMES 30188
IK12-094	Moose	<i>Alces alces</i>	North Slope	Maybe Cr.			UAMES	UAMES 30184
IK12-096	Moose	<i>Alces alces</i>	North Slope	Ikpikpuk R.			UAMES	UAMES 30185
TIT12-35	Moose	<i>Alces alces</i>	North Slope	Titaluk R.			UAMES	UAMES 30191
IK09-70	Moose	<i>Alces alces</i>	North Slope	Ikpikpuk R.			UAMES	UAMES 30182
	Moose	<i>Alces alces</i>	Selawik	Elephant Point			UAMES	UAMES 29656
	Moose	<i>Alces alces</i>	Selawik	Koyukuk River			UAMES	UAMES 29692

Moose	<i>Alces alces</i>	Selawik	Mud Creek	UAMES	UAMES 29663
-------	------------------------	---------	-----------	-------	----------------

Appendix A continues below.

Lab ID	Common Name	Classification	¹⁴ C Date	¹⁴ C Lab No.	¹⁴ C Date Reference	Tissue	Bone Type
AB14	Caribou		29600±970	AA97953	Chapter 2	Bone	
AB23	Caribou		27,250±420	AA103879	Chapter 2	Bone	
AB31	Caribou					Bone	
AB34	Caribou		26,450±390	AA103880	Chapter 2	Bone	
AB35	Caribou					Bone	
AB36	Caribou					Bone	
AB37	Caribou					Bone	
AB42	Caribou		11,360±120	AA103826	Chapter 2	Bone	
AB16	Caribou					Antler	
AB24	Caribou					Antler	
YT126	Caribou	Female or juvenile male	post-bomb	AA103889	Chapter 2	Bone	Right occipital condyle
YT126	Caribou	Female or juvenile male	post-bomb	AA103889	Chapter 2	Antler	
YT135	Caribou					Bone	tibia
YT136	Caribou					Bone	metatarsal
YT137	Caribou					Bone	cranium
YT138	Caribou					Bone	
YT139	Caribou					Bone	
YT140	Caribou					Bone	
YT141	Caribou					Bone	

YT142	Caribou					Bone	
YT143	Caribou					Bone	
YT144	Caribou					Bone	
YT145	Caribou					Bone	
YT95	Caribou					Antler	
YT125	Caribou	Female or juvenile male				Antler	
YT127	Caribou	Adult male	>41,100	AA103824	Chapter 2	Antler	
YT128	Caribou	Adult male	29,570±970	AA103825	Chapter 2	Antler	
UAK6	Caribou		26,360±650	AA103840	Chapter 2	Bone	tibia
UAK12	Caribou		29,020±910	AA103841	Chapter 2	Bone	humerus
UAK8	Caribou					Bone	innominate
UAK9	Caribou					Bone	scapula
UAK7	Caribou					Bone	humerus
UAK11	Caribou					Bone	mantible
UAK1	Caribou		201±33	AA103881	Chapter 2	Bone	metatarsal
UAK2	Caribou					Bone	humerus
UAK3	Caribou					Bone	radius
UAK4	Caribou					Antler	
UAK5	Caribou					Antler	
UAK10	Caribou					Antler	
UAK13	Caribou					Antler	
YT87	Elk		10,825±50	OxA20920	Meiri et al., 2014	Bone	metacarpal
YT92	Elk					Bone	

YT94	Elk		10960 ±30	UCIAMS 88769	Zazula, 2015	Bone	innominate fragment
YT85/123	Elk	Male	11,675±45; 11,785±50	OxA20918; OxA20919	Meiri et al., 2014	Antler	
YT88	Elk	Male				Antler	
YT89	Elk	Male	12,100±120	AA103823	Chapter 2	Antler	
YT90	Elk	Male				Antler	
YT91	Elk	Male				Antler	
YT93	Elk	Male				Antler	
YT124	Elk	Male	9,064±41	WK-32828	Kristensen and Heffner, 2011	Antler	
YT96	Moose					Bone	
YT99	Moose					Bone	
YT100	Moose					Bone	
YT101B	Moose					Bone	
YT102	Moose		2,700±29	OxA22266	Meiri et al., 2014	Bone	Humerus
YT103	Moose					Bone	
YT105	Moose		4,916±33	OxA22265	Meiri et al., 2014	Bone	Metatarsal
YT106	Moose					Bone	
YT107	Moose					Bone	
YT108	Moose		152±26	OxA22264	Meiri, 2010	Bone	
YT110	Moose					Bone	
YT86	Moose	Male	10,790±110	AA103822	Chapter 2	Antler	
YT98	Moose	Male				Antler	
YT101A	Moose	Male				Antler	
YT104	Moose	Male				Antler	
YT109	Moose	Male				Antler	
YT121	Moose	Male				Antler	
YT122	Moose	Male	1,363±35; 1,197±27	AA103820; OxA22267	Chapter 2; Meiri et al., 2014	Antler	
IK02-210	Moose		320±35	CAMS- 91966	Mann et al., 2013	Bone	mandible

IK01-404	Moose	665±35	CAMS-92094	Mann et al., 2013	Bone	mandible
IK12-077	Moose	950±30	Beta-339274	Mann et al., 2013	Bone	cranium
IK99-229	Moose	980±40	CAMS-64459	Mann et al., 2013	Bone	mandible
IK08-016	Moose	1,180±30	Beta-339268	Mann et al., 2013	Bone	mandible
IK99-776	Moose	1,370±40	CAMS-64474	Mann et al., 2013	Bone	mandible
IK99-556	Moose	1,760±40	CAMS-64467	Mann et al., 2013	Bone	mandible
IK01-023	Moose	2,450±35	CAMS-92076	Mann et al., 2013	Bone	mandible
KIG05-4.1	Moose	107±0.3	Beta-339266	Mann et al., 2013	Antler	
MAY12-64	Moose	116±0.3	Beta-339275	Mann et al., 2013	Antler	
IK08-129	Moose	210±30	Beta-339280	Mann et al., 2013	Antler	
TIT10-58	Moose	290±30	Beta-339271	Mann et al., 2013	Antler	
IK12-094	Moose	310±30	Beta-339281	Mann et al., 2013	Antler	
IK12-096	Moose	2,790±30	Beta-339282	Mann et al., 2013	Antler	
TIT12-35	Moose	9,310±40	Beta-339283	Mann et al., 2013	Antler	
IK09-70	Moose	9,610±40	Beta-339270	Mann et al., 2013	Antler	
	Moose	80±40		Drukenmiller, 2008	Bone	innominate
	Moose	7,870±50		Drukenmiller, 2008	Bone	jaw
	Moose	7,470±40		Drukenmiller, 2008	Antler	

RAM = Royal Alberta Museum
 UAMES = University of Alaska Museum Earth Sciences
 YG = Yukon Government

References:

Druckenmiller, P.S., 2008. Survey of Pleistocene (Ice Age) vertebrates from the Selawik and Kobuk River areas of Northwestern Alaska. Intern. Rep. U.S. Fish Wildl. Serv. 1–56.

- Kristensen, T., Heffner, T., 2011. Heritage resources impact assessment of the Yukon Hospital Corporation proposed Dawson City multi-level care facility conducted under Permit 10-02ASR. Whitehorse, YT.
- Mann, D.H., Groves, P., Kunz, M.L., Reanier, R.E., Gaglioti, B. V., 2013. Ice-age megafauna in Arctic Alaska: extinction, invasion, survival. *Quat. Sci. Rev.* 70, 91–108. doi:10.1016/j.quascirev.2013.03.015
- Meiri, M., 2010. The role of environmental change in species range shifts – analysis of Quaternary deer using ancient DNA. Doctoral Thesis. University of London.
- Meiri, M., Lister, A.M., Collins, M.J., Tuross, N., Goebel, T., Blockley, S., Zazula, G.D., van Doorn, N., Guthrie, R.D., Boeskorov, G.G., Baryshnikov, G.F., Sher, A., Barnes, I., 2014. Faunal record identifies Bering isthmus conditions as constraint to end-Pleistocene migration to the New World. *Proc. Biol. Sci.* 281, 20132167. doi:10.1098/rspb.2013.2167
- Zazula, G.D., Personal communication (e-mail), 2015

Appendix B: Carbon and nitrogen isotopic compositions of serially sampled antlers, as well as information about sample size and antler beam completeness.

Sample Information	Antler Information		Sampling Location (base as 0 cm)	$\delta^{13}\text{C}$	$\delta^{15}\text{N}$	%C	%N	C/N	% Yield
Species: Caribou	Base circumference (cm)	9	0 cm	-22.3	0.9	40.8	14.4	3.3	26.3
Sample Number: 381.52	Length of sample edge (cm)	39	10 cm	-22.5	1.1	40.7	14.5	3.3	29.6
Site: Herschel Island	Complete Antler?	Yes	20 cm	-22.4	1.5	39.6	14.2	3.3	31.9
^{14}C Date: post bomb			30 cm	-22.3	1.7	41.5	14.8	3.3	27.8
			Mean	-22.4	1.3	40.7	14.5	3.3	28.9
			SD	0.1	0.4				
			Max.	-22.3	1.7				
			Min.	-22.5	0.9				
			Shift (Tip-Base)	-0.1	0.8				
			Difference (Max-Min)	0.2	0.8				
Species: Caribou	Base circumference (cm)	7	0 cm	-18.0	3.7	38.7	13.6	3.3	7.2
Sample Number: 109.9	Length of sample edge (cm)	34	10 cm	-18.6	3.7	34.5	12.0	3.3	4.5
Site: Klondike	Complete Antler?	Mostly	20 cm	-18.5	3.6	38.3	13.5	3.3	21.6
			Mean	-18.4	3.7	37.2	13.0	3.3	11.1
			SD	0.3	0.1				
			Max.	-18.0	3.7				
			Min.	-18.6	3.6				
			Shift (Tip-Base)	-0.5	-0.1				

			Difference (Max-Min)	0.6	0.1				
Species: Caribou	Base circumference (cm)	12	0 cm	-18.5	1.8	39.1	13.8	3.3	20.6
Sample Number: 404.657	Length of sample edge (cm)	70	10 cm	-18.7	1.8	36.3	12.7	3.3	15.2
Site: Klondike	Complete Antler?	Mostly	20 cm	-18.9	1.8	38.1	13.3	3.3	19.2
¹⁴ C Date: >41,100			30 cm	-19.1	1.8	36.4	12.7	3.3	15.1
			40 cm	-19.2	1.8	37.0	12.9	3.3	13.2
			50 cm	-19.0	1.9	38.3	13.5	3.3	22.1
			60 cm	-19.2	1.8	37.6	13.2	3.3	17.1
			70 cm	-19.5	1.9	37.8	13.4	3.3	22.8
			Mean	-19.0	1.8	37.6	13.2	3.3	18.2
			SD	0.3	0.0				
			Max.	-18.5	1.9				
			Min.	-19.5	1.8				
			Shift (Tip-Base)	-1.1	0.0				
			Difference (Max-Min)	1.1	0.1				
Species: Caribou	Base circumference (cm)	13	0 cm	-18.4	4.5	36.6	13.0	3.3	44.2
Sample Number: 306.468	Length of sample edge (cm)	53	10 cm	-18.7	4.2	39.4	13.9	3.3	12.0
Site: Klondike	Complete Antler?	No	20 cm	-18.9	4.2	35.7	12.3	3.4	5.4
¹⁴ C Date: 29,570± 970			30 cm	-18.8	4.1	42.3	15.0	3.3	17.8
			40 cm	-18.8	4.0	37.6	13.2	3.3	10.6
			50 cm	-18.8	4.1	39.4	13.9	3.3	15.8
			Mean	-18.7	4.2	38.5	13.5	3.3	17.7
			SD	0.2	0.2				

			Max.	-18.4	4.5				
			Min.	-18.9	4.0				
			Shift (Tip-Base)	-0.4	-0.4				
			Difference (Max-Min)	0.4	0.5				
Species: Elk	Base circumference (cm)	22	0 cm	-19.2	2.6	37.2	13.4	3.2	15.7
Sample Number: 104.4	Length of sample edge (cm)	71	10 cm	-19.1	2.4	37.3	13.3	3.3	9.1
Site: Klondike	Complete Antler?	No	20 cm	-19.2	2.5	37.2	13.5	3.2	17.1
¹⁴ C Date: 11,675±45; 11,785±50			30 cm	-19.2	2.5	38.7	14.0	3.2	15.9
			40 cm	-19.1	2.5	37.9	13.8	3.2	13.4
			50 cm	-19.1	2.6	37.3	13.6	3.2	14.1
			60 cm	-19.1	2.8	37.7	13.7	3.2	15.6
			Mean	-19.2	2.6	37.6	13.6	3.2	14.4
			SD	0.1	0.1				
			Max.	-19.1	2.8				
			Min.	-19.2	2.4				
			Shift (Tip-Base)	0.1	0.2				
			Difference (Max-Min)	0.2	0.4				
Species: Elk	Base circumference (cm)	22	0 cm	-21.1	2.4	40.1	14.2	3.3	25.3
Sample Number: 420.1	Length of sample edge (cm)	43	10 cm	-21.0	2.2	39.6	13.8	3.3	12.9
Site: Klondike	Complete Antler?	No	20 cm	-21.1	2.1	40.3	14.1	3.3	12.3
¹⁴ C Date: 9,064±41			30 cm	-21.2	2.0	38.7	13.5	3.3	13.4

			Mean	-21.1	2.2	39.7	13.9	3.3	16.0
			SD	0.1	0.2				
			Max.	-21.0	2.4				
			Min.	-21.2	2.0				
			Shift (Tip-Base)	-0.1	-0.4				
			Difference (Max-Min)	0.2	0.4				
Species: Moose	Base circumference (cm)	18	0 cm	-19.9	1.8	34.8	12.1	3.3	3.9
Sample Number: 190.1	Length of sample edge (cm)	60	10 cm	-19.8	2.1	39.9	14.0	3.3	17.5
Site: Klondike	Complete Antler?	Yes	20 cm	-19.9	1.5	40.3	14.0	3.3	13.5
			30 cm	-20.2	1.9	37.0	12.9	3.3	10.8
			40 cm	-20.4	2.3	36.5	12.7	3.3	7.4
			50 cm	-20.4	2.5	34.4	11.8	3.4	7.7
			Mean	-20.1	2.0	37.2	12.9	3.4	10.1
			SD	0.2	0.4				
			Max.	-19.8	2.5				
			Min.	-20.4	1.5				
			Shift (Tip-Base)	-0.5	0.8				
			Difference (Max-Min)	0.6	1.0				
Species: Moose	Base circumference (cm)	20	0 cm	-20.5	2.4	36.1	12.5	3.4	3.2
Sample Number: 162.46	Length of sample edge (cm)	44	10 cm	-20.7	2.2	34.6	12.0	3.4	1.4
Site: Klondike	Complete Antler?	Mostly	20 cm	-20.5	2.2	36.8	12.9	3.3	10.6
¹⁴ C Date: 1,363±35; 1,197±27			30 cm	-20.6	2.2	38.6	13.5	3.3	15.2

40 cm	-20.8	2.4	39.5	13.9	3.3	15.5
Mean	-20.6	2.3	37.1	13.0	3.3	9.2
SD	0.1	0.1				
Max.	-20.5	2.4				
Min.	-20.8	2.2				
Shift (Tip-Base)	-0.2	0.0				
Difference (Max-Min)	0.3	0.3				

Samples analyzed multiple times in this work are in bold and the average value is given.

Specimens are classified by how complete they are along the beam that was sampled. They range from fully complete, to a small section broken off, to a large portion of the antler missing.

Appendix C: Carbon and nitrogen isotopic data for collagen from specimens described in this study.

Common Name	Sample Number	Stable Isotope Reference	¹⁴ C Date	Area	Tissue	Sampling Method	δ ¹³ C _{Coll}	δ ¹⁵ N	% Yield	%C	%N	C/N
Caribou	P89.13.160	Chapter 2	29600±970	Edmonton	B	Single	-18.7	5.0	7.9	36.9	13.9	3.1
Caribou	P94.1.438	Chapter 2	27,250±420	Edmonton	B	Single	-18.4	4.2	12.0	39.2	14.7	3.1
Caribou	P95.6.29	Chapter 2		Edmonton	B	Single	-18.8	4.7	10.7	45.7	17.0	3.1
Caribou	P98.5.35	Chapter 2	26,450±390	Edmonton	B	Single	-18.5	5.1	8.5	36.0	13.5	3.1
Caribou	P98.5.185	Chapter 2		Edmonton	B	Single	-18.9	5.1	10.4	38.1	14.3	3.1
Caribou	P98.5.328	Chapter 2		Edmonton	B	Single	-18.6	4.8	10.0	38.1	14.5	3.1
Caribou	P98.5.347	Chapter 2		Edmonton	B	Single	-18.7	4.7	8.1	38.7	14.3	3.2
Caribou	P02.10.3	Chapter 2	11,360±120	Edmonton	B	Single	-18.7	2.9	12.6	38.6	14.6	3.1
						Mean	-18.7	4.6				
						SD	0.2	0.7				
Caribou	P89.13.316	Chapter 2		Edmonton	A	Single	-18.3	4.9	23.2	41.4	15.7	3.1
Caribou	P94.1.459	Chapter 2		Edmonton	A	Single	-19.4	2.2	19.1	40.8	15.5	3.1
						Mean	-18.9	3.6				
						SD	0.8	1.9				
Caribou	381.52	Chapter 2	post bomb	Herschel Island Suess effect corrected to 1987	B	Single	-21.0	2.6	18.0	34.6	11.9	3.4
							-20.2					
Caribou	381.52	Chapter 2	post bomb	Herschel Island Suess effect corrected to	A	Serial	-22.4	1.3	28.9	40.7	14.5	3.3
							-21.6					

1987

Caribou	126.6	Chapter 2		Klondike	B	Single	-18.1	4.0	13.6	38.0	13.7	3.2
Caribou	126.13	Chapter 2		Klondike	B	Single	-18.5	3.1	17.0	39.3	14.3	3.2
Caribou	126.31	Chapter 2		Klondike	B	Single	-18.7	6.8	16.7	41.7	15.2	3.2
Caribou	306.194	Chapter 2		Klondike	B	Single	-19.6	6.0	9.6	36.7	13.2	3.3
Caribou	376.47	Chapter 2		Klondike	B	Single	-18.5	4.1	7.6	33.4	12.8	3.3
Caribou	378.48	Chapter 2		Klondike	B	Single	-17.7	6.1	9.6	37.2	13.4	3.2
Caribou	404.321	Chapter 2		Klondike	B	Single	-19.0	5.4	10.6	38.3	13.9	3.2
Caribou	406.665	Chapter 2		Klondike	B	Single	-18.1	3.1	5.7	38.6	14.1	3.2
Caribou	407.304	Chapter 2		Klondike	B	Single	-18.5	7.3	12.4	33.6	12.3	3.2
Caribou	421.163	Chapter 2		Klondike	B	Single	-18.2	8.7	7.0	36.7	13.2	3.2
Caribou	435.103	Chapter 2		Klondike	B	Single	-18.9	4.8	7.4	37.4	13.5	3.2
						Mean	-18.5	5.4				
						SD	0.5	1.8				
Caribou	5.77	Chapter 2		Klondike	A	Single	-20.2	1.0	14.0	39.4	14.9	3.1
Caribou	109.9	Chapter 2		Klondike	A	Serial	-18.4	3.7	11.1	37.2	13.0	3.3
Caribou	404.657	Chapter 2	>41,100	Klondike	A	Serial	-19.0	1.8	18.2	37.6	13.2	3.3
Caribou	306.468	Chapter 2	29,570±970	Klondike	A	Serial	-18.7	4.2	17.7	38.5	13.5	3.3
							-19.1	2.7				
							0.8	1.5				
Caribou	UAMES 1122	Chapter 2	26,360±650	Selawik	B	Single	-19.7	4.6	7.2	37.9	13.2	3.4
Caribou	UAMES 2214	Chapter 2	29,020±910	Selawik	B	Single	-18.5	4.1	5.5	38.9	13.7	3.3
Caribou	UAMES 1151	Chapter 2		Selawik	B	Single	-18.6	3.5	19.4	33.5	12.0	3.2
Caribou	UAMES 1180	Chapter 2		Selawik	B	Single	-18.7	1.9	16.7	36.8	13.3	3.2
Caribou	UAMES 1123	Chapter 2		Selawik	B	Single	-19.0	4.1	11.9	41.2	14.7	3.3

Caribou	UAMES 2114	Chapter 2		Selawik	B	Single	-19.7	4.8	4.2	37.6	13.3	3.3
Caribou	UAMES1033	Chapter 2	201±33	Selawik	B	Single	-19.3	2.1	13.7	40.0	13.9	3.3
Caribou	UAMES1035	Chapter 2		Selawik	B	Single	-19.2	3.4	14.6	42.2	14.9	3.3
Caribou	UAMES 1036	Chapter 2		Selawik	B	Single	-19.2	2.7	12.8	41.3	14.4	3.3
							Mean	-19.1	3.5			
							SD	0.4	1.0			
Caribou	UAMES 1080	Chapter 2		Selawik	A	Single	-19.6	4.2	19.3	43.7	15.4	3.3
Caribou	UAMES 1081	Chapter 2		Selawik	A	Single	-20.0	4.2	17.7	42.9	15.2	3.3
Caribou	UAMES 1900	Chapter 2		Selawik	A	Single	-19.4	2.8	14.6	41.6	14.6	3.3
Caribou	UAMES 7716	Chapter 2		Selawik	A	Single	-19.7	4.5	18.9	40.2	14.2	3.3
							Mean	-19.7	3.9			
							SD	0.3	0.7			
Elk	192.1	Chapter 2	10,825±50	Klondike	B	Single	-19.8	1.6	9.5	38.6	14.6	3.1
Elk	377.43	Chapter 2		Klondike	B	Single	-20.0	1.9	11.1	39.0	14.8	3.1
Elk	Fa06-141	Chapter 2	10960 ±30	Klondike	B	Single	-19.7	1.6	12.3	39.6	14.9	3.1
							Mean	-19.8	1.7			
							SD	0.1	0.2			
Elk	104.04	Chapter 2	11,675±45, 11,785±50	Klondike	A	Serial	-19.2	2.6	14.4	37.6	13.6	3.2
Elk	208.1	Chapter 2		Klondike	A	Single	-19.0	2.1	14.8	39.5	14.9	3.1

Elk	301.17	Chapter 2	12,100±120	Klondike	A	Single	-18.6	2.1	15.0	38.4	14.5	3.1
Elk	303.168	Chapter 2		Klondike	A	Single	-18.7	1.9	14.9	40.4	15.2	3.1
Elk	306.449	Chapter 2		Klondike	A	Single	-18.5	1.3	16.5	37.0	13.9	3.1
Elk	378.53	Chapter 2		Klondike	A	Single	-18.8	2.7	18.2	37.8	14.3	3.1
Elk	420.1	Chapter 2	9,064±41	Klondike	A	Serial	-21.1	2.2	16.0	39.7	13.9	3.3
						Mean	-19.1	2.1				
						SD	0.9	0.5				
Moose	29.69	Chapter 2		Klondike	B	Single	-21.1	1.2	9.9	36.8	13.9	3.1
Moose	134.1	Chapter 2		Klondike	B	Single	-20.0	1.6	7.4	37.2	14.2	3.0
Moose	136.1	Chapter 2		Klondike	B	Single	-20.6	1.9	9.6	38.9	14.6	3.1
Moose	193.1	Chapter 2		Klondike	B	Single	-20.0	3.0	18.4	39.9	15.3	3.0
Moose	269.1	Chapter 2	2,700±29	Klondike	B	Single	-20.6	2.2	7.5	38.0	14.4	3.1
Moose	300.2	Chapter 2		Klondike	B	Single	-20.0	2.7	9.9	40.0	15.1	3.1
Moose	300.96	Chapter 2	4,916±33	Klondike	B	Single	-20.6	2.5	8.4	37.3	14.2	3.1
Moose	308.21	Chapter 2		Klondike	B	Single	-21.0	1.5	19.2	40.4	15.6	3.0
Moose	354.3	Chapter 2		Klondike	B	Single	-20.7	2.3	12.5	38.6	14.8	3.0
Moose	355.113	Chapter 2	152±26	Klondike	B	Single	-21.0	3.2	14.7	39.6	14.8	3.1
Moose	376.56	Chapter 2		Klondike	B	Single	-20.2	2.1	17.8	37.8	14.6	3.0
						Mean	-20.5	2.2				
						SD	0.4	0.6				
Moose	136.8	Chapter 2	10,790±110	Klondike	A	Single	-19.6	-0.9	15.7	40.2	14.7	3.2
Moose	129.2	Chapter 2		Klondike	A	Single	-20.2	1.4	29.4	41.4	15.7	3.1
Moose	193.1	Chapter 2		Klondike	A	Single	-19.9	2.1	17.1	39.4	14.9	3.1
Moose	300.226	Chapter 2		Klondike	A	Single	-20.6	1.4	18.3	43.0	16.0	3.1
Moose	355.99	Chapter 2		Klondike	A	Single	-20.6	0.9	20.9	41.3	15.1	3.2
Moose	190.1	Chapter 2		Klondike	A	Serial	-20.1	2.0	10.1	37.2	12.9	3.4
Moose	162.46	Chapter 2	1,363±35; 1,197±27	Klondike	A	Serial	-20.6	2.3	9.2	37.1	13.0	3.3
						Mean	-20.2	1.3				

							SD	0.4	1.1
Moose	UAMES 10355	Mann et al., 2013	320±35	North Slope	B	Single	-20.3	0.3	
Moose	UAMES 11844	Mann et al., 2013	665±35	North Slope	B	Single	-20.9	-0.6	
Moose	UAMES 30183	Mann et al., 2013	950±30	North Slope	B	Single	-20.7	1.0	
Moose	UAMES 10691	Mann et al., 2013	980±40	North Slope	B	Single	-20.0	8.6	
Moose	UAMES 30180	Mann et al., 2013	1,180±30	North Slope	B	Single	-21.3	1.8	
Moose	UAMES 11066	Mann et al., 2013	1,370±40	North Slope	B	Single	-20.4	1.3	
Moose	UAMES 10996	Mann et al., 2013	1,760±40	North Slope	B	Single	-19.9	0.7	
Moose	UAMES 12022	Mann et al., 2013	2,450±35	North Slope	B	Single	-20.8	1.0	
							Mean	-20.5	1.8
							SD	0.5	2.8
Moose	UAMES 30186	Mann et al., 2013	107±0.3	North Slope	A	Single	-23.4	0.5	
Moose	UAMES 30187	Mann et al., 2013	116±0.3	North Slope	A	Single	-21.3	0.6	
Moose	UAMES 30181	Mann et al., 2013	210±30	North Slope	A	Single	-20.8	0.7	
Moose	UAMES 30188	Mann et al., 2013	290±30	North Slope	A	Single	-20.7	0.9	
Moose	UAMES 30184	Mann et al., 2013	310±30	North Slope	A	Single	-21.1	-0.4	
Moose	UAMES 30185	Mann et al., 2013	2,790±30	North Slope	A	Single	-21.3	-0.6	

Moose	UAMES 30191	Mann et al., 2013	9,310±40	North Slope	A	Single	-20.3	-1.2	
Moose	UAMES 30182	Mann et al., 2013	9,610±40	North Slope	A	Single	-21	0.9	
							Mean	-21.2	0.2
							SD	0.9	0.8
Moose	UAMES 29656	Drukenmiller, 2008	80±40	Selawik	B	Single	-21.0	2.1	
Moose	UAMES 29692	Drukenmiller, 2008	7,870±50	Selawik	B	Single	-20.9	3.9	
							Mean	-20.9	3.0
							SD	0.1	1.2
Moose	UAMES 29663	Drukenmiller, 2008	7,470±40	Selawik	A	Single	-21.0	0.8	

Samples analyzed multiple times in Chapter 2 are in bold and the average value is given.

Single refers to specimens where a single sample was taken.

Serial refers to specimens which were serially sampled, and the average value is given.

A = Antler

B = Bone

References:

Drukenmiller, P.S., 2008. Survey of Pleistocene (Ice Age) vertebrates from the Selawik and Kobuk River areas of Northwestern Alaska. Intern. Rep. U.S. Fish Wildl. Serv. 1–56.

Mann, D.H., Groves, P., Kunz, M.L., Reanier, R.E., Gaglioti, B. V., 2013. Ice-age megafauna in Arctic Alaska: extinction, invasion, survival. *Quat. Sci. Rev.* 70, 91–108. doi:10.1016/j.quascirev.2013.03.015

Appendix D: Comparison of the $\delta^{13}\text{C}$ and $\delta^{15}\text{N}$ of lipid-extracted versus unextracted tissues.

Lab ID	Pre-collagen extraction treatment	d13C	d15N	%C	%N	C/N Ratio	Yield
YT101B	None	-20.01	2.95	40.15	15.42	3.02	23.8
YT101B	Lipids extracted	-20.02	2.96	39.65	15.11	3.04	13.0
Mean		-20.0	3.0	39.9	15.3	3.0	18.4
SD		0.01	0.00	0.35	0.22	0.02	7.64
YT87	None	-19.87	1.58	39.02	14.64	3.09	9.6
YT87	None	-19.82	1.65	39.08	14.77	3.06	
YT87	Lipids extracted	-19.83	1.62	37.81	14.31	3.06	9.4
Mean		-19.8	1.6	38.6	14.6	3.1	9.5
SD		0.03	0.04	0.72	0.24	0.01	0.08
YT85	None	-19.04	2.38	38.22	14.44	3.07	16.3
YT85	Lipids extracted	-18.96	2.43	37.26	14.02	3.08	11.5
Mean		-19.0	2.4	37.7	14.2	3.1	13.9
SD		0.06	0.03	0.67	0.30	0.01	3.39
YT108	None	-20.89	3.31	37.24	13.66	3.18	11.7
YT108	Lipids extracted	-21.06	3.12	42.00	15.89	3.08	17.7
Mean		-21.0	3.2	39.6	14.8	3.1	14.7
SD		0.12	0.14	3.37	1.58	0.07	4.28
YT95	None	-20.20	0.99	38.88	14.78	3.05	12.7
YT95	Lipids extracted	-20.27	0.93	39.90	15.04	3.10	15.3
Mean		-20.2	1.0	39.4	14.9	3.1	14.0
SD		0.05	0.04	0.72	0.19	0.04	1.83
UAK10	None	-19.42	2.84	42.32	14.94	3.30	15.37
UAK10	None	-19.41	2.81	42.29	14.82	3.33	
UAK10	Lipids extracted	-19.37	2.86	40.08	14.02	3.33	13.79
Mean		-19.4	2.8	41.6	14.6	3.3	14.6
Std. Dev.		0.03	0.02	1.29	0.50	0.02	1.12
AB16	None	-18.34	5.00	41.74	15.87	3.07	22.99
AB16	None	-18.35	4.89	40.62	15.44	3.07	
AB16	Lipids extracted	-18.31	4.87	41.72	15.87	3.07	23.37
Mean		-18.3	4.9	41.4	15.7	3.1	23.2
SD		0.02	0.07	0.64	0.25	0.00	0.27
	Maximum SD	0.1	0.1	3.4	1.6	0.1	7.6
	Mean SD	0.0	0.0	1.1	0.5	0.0	2.7

Appendix E Sample Information for Old Crow megafauna analyzed in Chapter 3.

Lab ID	Common Name	Sample Number	¹⁴ C Date	Lat.	Long.	Collection Site	Tissue	Tissue Type	¹⁴ C Lab Number	Source
YT1RD	Mammoth	291.1	>41,100	68.0	-139.6	Old Crow River	Root dentin	LRM6	AA84987*	YG
YT2RD	Mammoth	122.2	>41,100	68.1	-139.8	CRH 94 Old Crow River	Root dentin	ULM6	AA84992*	YG
YT3D	Mammoth	173.5		67.5	-139.9	Ch'ijee's Bluff, Porcupine River	Crown dentin	U M6		YG
YT4B	Mammoth	285.1	>39,100	67.9	-139.7	OCR, REM 78-1	Bone		AA85002*	YG
YT5RD	Mammoth	60.2		68.1	-140.0	OCR, Bluffs-R bank	Root dentin	LRM5/M6		YG
YT6C	Mammoth	57.1		68.2	-140.5	OCR, Bluffs-R bank	Cementum	LRM6		YG
YT7B	Mammoth	325.22	>40,100	67.9	-139.8	HH-68-10 Old Crow River	Bone		AA84984*	YG
YT9C	Mammoth	284.4		67.8	-139.8	CRH 11 Old Crow River	Cementum	ULM6		YG
YT10 RD	Mammoth	252.2	>40,000	68.0	-139.6	CRH 20 Old Crow River	Root dentin	LLM6	AA85001*	YG
YT11C	Mammoth	173.1		67.6	-139.9	Ch'ijee's Bluff, Porcupine River	Cementum	U M6		YG
YT11 RD							Root dentin	U M6		
YT51T	Mammoth	317.51	MIS5, ~140,000			CRH 11 Old Crow River	Tusk dentin	Tusk	†	YG
YT68	Brown Bear	282.38		68.0	-139.6	Old Crow River	Bone			YG
YT81	Short-Faced Bear	177.49		67.8	-139.9	CRH 11A Old Crow River	Bone	Innominate		YG
YT82	Scimitar Cat	236.133	>37,200	68.0	-139.6	CRH 67 Old Crow River	Bone		Beta 227532	YG
YT84	Brown Bear	236.16		68.0	-139.6	CRH 67 Old Crow River	Bone			YG
AMNH3	Canid	F:AM 97114	40,800 ± 3,900			Old Crow River	Bone		AA97954	AMNH
YT129	Horse	178.9	27,180 ± 420	67.5	-140.0	Porcupine River, downstream from Ch'ijee's Bluff	Bone		AA103890	YG
YT130	Horse	179.14		68.3	-140.4	CRH 47 Old Crow River	Bone			YG
YT131	Horse	236.24	18,370 ± 260	68.0	-139.6	CRH 67 Old Crow River	Bone		AA103835	YG
YT132	Horse	295.2	> 41,100	67.5	-139.7	HH-68-21 Old Crow River	Bone		AA103836	YG

YT133	Horse	315.1		68.2	-140.0	CRH 44 Old Crow River	Bone			YG
AMNH1	Giant Beaver	F:AM 65186				Old Crow River	Bone			AMNH
YT8D	Mastodon	357.1	>41,100			Old Crow River	Crown dentin	M5/M6	AA84995*	YG

YG = Yukon Government

AMNH = American Museum of Natural History.

Radiocarbon dates shown in bold were measured as part of this study.

*Radiocarbon date previously reported (Metcalf et al., 2010).

† Date previously reported (Metcalf, 2011).

References:

Metcalf, J.Z., 2011. Late Pleistocene climate and proboscidean paleoecology in North America: insights from stable isotope compositions of skeletal remains. University of Western Ontario.

Metcalf, J.Z., Longstaffe, F.J., Zazula, G.D., 2010. Nursing, weaning, and tooth development in woolly mammoths from Old Crow, Yukon, Canada: implications for Pleistocene extinctions. *Palaeogeogr. Palaeoclimatol. Palaeoecol.* 298, 257–270. doi:10.1016/j.palaeo.2010.09.032

Appendix F Nitrogen isotopic data and preservation information.

Lab ID	Source	Species	$\delta^{15}\text{N}_{\text{Bulk}}$	% Yield	%C	%N	C/N	$\delta^{15}\text{N}_{\text{Phe}}$	$\delta^{15}\text{N}_{\text{Glu}}$	$\Delta^{15}\text{N}_{\text{Glu-Phe}}$
YT1RD	YG	Mammoth*	+8.7	14.4	41.6	15.6	3.1	+11.6 ± 0.7	+7.2 ± 0.1	-4.4 ± 0.9
YT2RD	YG	Mammoth*	+8.4	11.0	39.2	14.6	3.1	+16.1 ± 0.9	+11.9 ± 0.5	-4.2 ± 1.4
YT3D	YG	Mammoth*	+9.7	>6.7	44.0	16.4	3.1	+15.3 ± 0.7	+11.5 ± 0.3	-3.8 ± 1.0
YT4B	YG	Mammoth*	+9.5	13.1	41.1	15.2	3.1	+14.0 ± 0.7	+10.8 ± 0.2	-3.2 ± 0.9
YT5RD	YG	Mammoth*	+9.8	11.2	42.9	15.5	3.2	+13.2 ± 0.9	+10.6 ± 0.4	-2.6 ± 1.4
YT6C	YG	Mammoth*	+7.7	10.1	42.5	15.2	3.3	+13.8 ± 1.4	+9.6 ± 1.5	-4.2 ± 2.9
YT7B	YG	Mammoth*	+7.6	15.7	42.3	15.8	3.1	+11.7 ± 0.3	+9.5 ± 0.7	-2.2 ± 1.0
YT9C	YG	Mammoth*	+8.2	7.1	41.4	15.0	3.2	+11.6 ± 0.8	+9.4 ± 0.5	-2.2 ± 1.4
YT10RD	YG	Mammoth*	+9.8	11.4	38.9	14.4	3.2	+11.2 ± 0.2	+10.6 ± 0.8	-0.6 ± 0.9
YT11C	YG	Mammoth*	+8.3	18.2	44.1	15.9	3.2	+10.4 ± 0.5	+11.6 ± 0.3	+1.2 ± 0.7
YT11RD	YG	Mammoth†	+9.5	14.3	47.2	17.6	3.1	+14.1 ± 1.3	+8.8 ± 3.9	-5.3 ± 5.2
YT51T	YG	Mammoth*	+11.3	18.6	37.9	13.9	3.2	+12.9 ± 1.3	+12.4 ± 1.0	-0.5 ± 2.2
YT68	YG	Brown Bear	+8.4	9.7	45.4	16.8	3.1	+9.3 ± 0.7	+13.7 ± 0.6	+4.4 ± 1.3
YT81	YG	Short-Faced Bear	+9.1	7.6	45.0	16.7	3.2	+10.1 ± 0.4	+16.6 ± 0.4	+6.5 ± 0.7
YT82	YG	Scimitar Cat	+9.9	8.0	46.0	17.2	3.1	+9.7 ± 0.8	+14.3 ± 0.6	+4.6 ± 1.4
YT84	YG	Brown Bear	+11.5	6.2	43.6	16.1	3.2	+10.7 ± 0.3	+13.3 ± 0.8	+2.6 ± 1.1
AMNH3	AMNH	Canid	+8.5	8.5	42.0	15.1	3.2	+8.7 ± 0.9	+11.8 ± 0.7	+3.1 ± 1.6
YT129	YG	Horse	+7.0	10.2	39.7	15.5	3.3	+11.2 ± 0.5	+8.6 ± 0.8	-2.6 ± 1.3
YT130	YG	Horse	+8.1	11.2	40.3	15.6	3.2	+10.6 ± 0.7	+11.1 ± 0.7	+0.5 ± 1.3
YT131	YG	Horse	+9.9	5.4	36.1	14.0	3.4	+12.0 ± 0.0	+11.2 ± 0.7	-0.8 ± 0.7
YT132	YG	Horse	+4.2	8.2	38.5	14.8	3.1	+7.8 ± 0.7	+6.7 ± 0.8	-1.1 ± 1.6

YT133	YG	Horse	+8.7	10.9	42.0	16.2	3.2	+13.6 ± 0.2	+11.0 ± 0.3	-2.6 ± 0.6
AMNH1	AMNH	Giant Beaver	+5.4	5.1	37.5	13.5	3.2	+8.4 ± 0.2	+9.2 ± 0.2	+0.8 ± 0.4
YT8D	YG	Mastodon†	+3.5	17.8	42.3	16.0	3.1	+8.9 ± 1.5	+4.2 ± 0.1	-4.7 ± 1.6

Tissue: RD = root dentin, D = crown dentin, T = tusk dentin, B = bone, C = cementum, E = enamel.

The average results of duplicate measurements for bulk collagen are shown in bold-faced font.

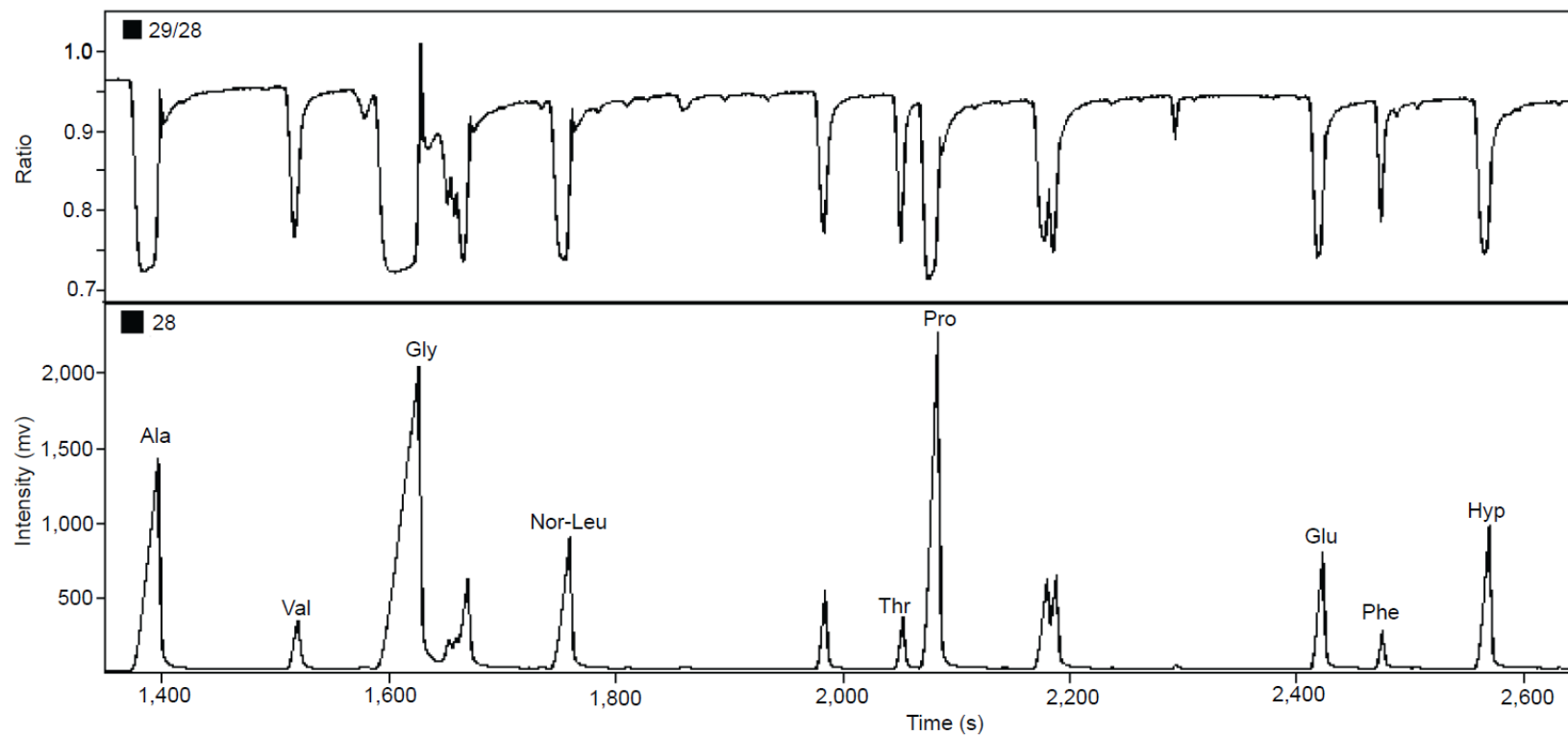
*Data for bulk collagen previously reported (Metcalf et al., 2010).

†Data for bulk collagen previously reported (Metcalf, 2011).

Amino acid $\delta^{15}\text{N}$ values represent the average (± 1 SD) of triplicate analyses.

References:

- Metcalf, J.Z., 2011. Late Pleistocene climate and proboscidean paleoecology in North America: insights from stable isotope compositions of skeletal remains. University of Western Ontario.
- Metcalf, J.Z., Longstaffe, F.J., Zazula, G.D., 2010. Nursing, weaning, and tooth development in woolly mammoths from Old Crow, Yukon, Canada: implications for Pleistocene extinctions. *Palaeogeogr. Palaeoclimatol. Palaeoecol.* 298, 257–270. doi:10.1016/j.palaeo.2010.09.032

Appendix G Typical gas chromatogram (sample YT51T) of N-acetyl-methyl ester derivatized amino acids from collagen.

Ala = alanine, Val = valine, Gly = glycine, Leu = leucine, Thr = threonine, Pro = proline, Asp = aspartate, Ser = serine, Glu = glutamate, Phe = phenylalanine and Hyp = hydroxyproline.

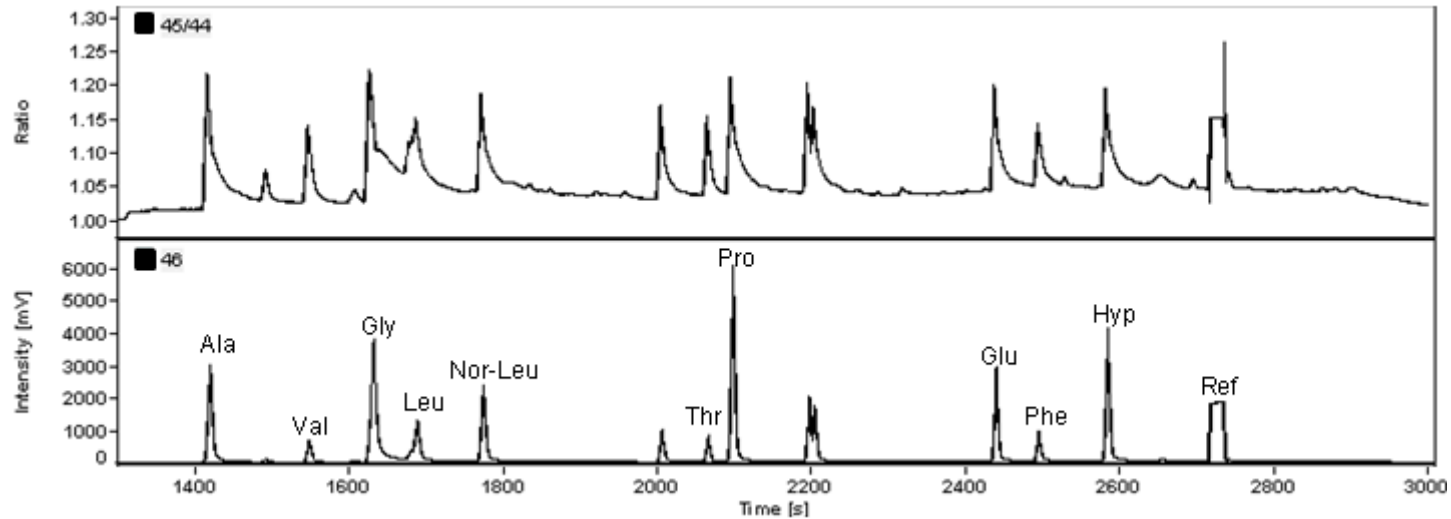
The top scan is the ratio of mass 29/28, and the bottom scan is the amplitude of mass 28.

Appendix H Sample information for additional specimens used in this study.

Lab ID	Common Name	Species Name	Sample Number	¹⁴ C Date	Latitude	Longitude	Collection Site	Tissue	Tissue Type	¹⁴ C Lab No.	Source	% Yield	%C	%N	C/N
YT83	Brown Bear	<i>Ursus arctos</i>	236.157	5,941±66	68.0	-139.6	CRH 67 Old Crow River	Bone		AA103837	YG	9.2	44.1	16.5	3.1
AMNH2	Giant Beaver	<i>Castoroides ohioensis</i>	F:AM 65187	>41,100			Old Crow River	Bone	Right femur	AA97952	AMNH	0.3	18.0	5.5	3.8

**YG = Yukon Government, AMNH = American Museum of Natural History.
Results shown in bold-faced font are the average of replicate measurements.**

Appendix I Gas chromatogram arising from compound-specific carbon isotopic measurements of amino acids from collagen extracted from sample YT51T following derivatization to their N-acetyl-methyl ester.



Ala = alanine, Val = valine, Gly = glycine, Leu = leucine, Thr = threonine, Pro = proline, Glu = glutamate, Phe = phenylalanine, Hyp = hydroxyproline and Ref = reference gas.

The scans show different masses.

The upper graph shows the ratio of CO₂ mass 45/44 peak for each amino acid on the y-axis and the retention time of that compound on the x-axis.

The lower graph shows the relative amplitude of the CO₂ mass 46 peak for each amino acid on the y-axis and the retention time of that compound on the x-axis.

Appendix J Amino acid profiles of collagenous tissues determined in this study and previous work.

Lab ID	Sample Type	Treatment	Ala	Arg	Asp	Cys	Glu	Gly	His	Hyp	Ile	Leu	Lys	Met	Phe	Pro	Ser	Thr	Tyr	Val
YT7B	Mammoth Bone	Collagen Extrated	12.3	5.1	4.5	0.0	7.0	33.3	0.5	9.3	1.0	2.6	2.4	0.6	1.5	12.4	3.1	1.6	0.3	2.4
YT11C	Mammoth Cementum	Collagen Extrated	12.4	5.1	4.6	0.0	7.1	32.4	0.5	9.7	1.1	2.7	2.7	0.6	1.5	12.0	3.2	1.6	0.5	2.5
YT11RD	Mammoth Root Dentin	Collagen Extrated	12.5	5.1	4.8	0.0	7.2	32.3	0.5	9.6	1.0	2.6	2.5	0.6	1.5	12.2	3.2	1.6	0.4	2.4
YT12RD	Juvenile Mammoth Root Dentin	Collagen Extrated	12.6	5.1	4.5	0.0	7.0	33.5	0.4	10.0	1.0	2.5	2.6	0.5	1.4	11.7	3.0	1.6	0.2	2.4
YT51T	Mammoth Tusk	Collagen Extrated	12.9	4.9	4.7	0.0	6.9	33.5	0.4	10.0	1.0	2.4	2.2	0.5	1.1	12.3	3.1	1.6	0.1	2.4
YT8D	Mastodon Crown Dentin	Collagen Extrated	12.6	5.0	4.6	0.0	7.1	32.6	0.4	10.1	1.1	2.6	2.7	0.5	1.5	11.8	3.2	1.6	0.4	2.4
YT8D	Mastodon Crown Dentin	Whole	13.9	5.7	1.0	0.0	3.4	32.6	0.5	11.4	1.3	3.2	3.2	0.5	1.8	13.4	2.9	1.7	0.5	2.8
REG97	Archeological Human Rib Bone	Collagen Extrated	12.2	5.0	4.4	0.0	6.9	33.1	0.6	9.8	1.1	2.6	2.9	0.6	1.4	12.2	2.7	1.5	0.4	2.6
REG97	Archeological Human Rib Bone	Whole	13.4	5.6	1.3	0.0	3.7	33.3	0.6	11.4	1.3	3.1	2.8	0.6	1.7	13.7	2.3	1.5	0.5	3.2
KFC	Modern Cow Femur Bone	Collagen Extrated	12.4	5.6	4.7	0.0	7.6	31.6	0.6	9.5	1.2	2.7	2.7	0.6	1.4	12.0	2.9	1.6	0.5	2.4
KFC	Modern Cow Femur Bone	Collagen Extrated and Hydrolyzed	11.4	5.3	4.5	0.0	7.5	32.9	0.5	10.4	1.1	2.7	2.3	0.4	1.4	12.1	3.5	1.6	0.4	1.9
KFC	Modern Cow Femur Bone	Whole	13.5	6.0	1.0	0.0	3.7	31.1	0.7	11.5	1.6	3.5	3.2	0.7	1.9	13.7	2.6	1.7	0.8	2.9

Ala = alanine, Val = valine, Gly = glycine, Leu = leucine, Thr = threonine, Pro = proline, Glu = glutamate, Phe = phenylalanine and Hyp = hydroxyproline. Amino acid profiles are presented as the percentage of the tissue comprising each amino acid.

The amino acid profile for REG97 has been presented previously by Olsen et al. (2010).

References:

Olsen, K., White, C., Longstaffe, F., von Heyking, K., McGlynn, G., 2010. Bulk and compound-specific isotope analysis of pathological bone collagen: preliminary results, in: 4th International Symposium on Biomolecular Archaeology. Copenhagen, Denmark.

**Appendix K Relative abundances of megafaunal herbivores from various sites
across the mammoth steppe.**

Taymyr Peninsula

Dates range from ~9000 14C yr BP to
infinite.

Reference: MacPhee et al., 2002; Mol et al.,
2006

Species (Common Name)	Species (Scientific Name)	Percent abundance
Steppe Bison	<i>Bison priscus</i>	4.2
Caribou*	<i>Rangifer tarandus</i>	5.5
Horse	<i>Equus cf. caballus</i>	9.2
Woolly Mammoth	<i>Mammuthus primigenius</i>	63.4
Moose	<i>Alces alces</i>	0.8
Muskox	<i>Ovibos moschatus</i>	16.5
Wolf	<i>Canis lupus</i>	0.5

**Duvanniy Yar, Kolyma River Lowland,
Siberia**

Pleistocene material (42,000 to 13,000 year
BP)

Reference: Zimov et al., 2012

Species (Common Name)	Species (Scientific Name)	Percent abundance
Bison	<i>Bison priscus</i>	17.5
Caribou*	<i>Rangifer tarandus</i>	52.6
Horse	<i>Equus cf. caballus</i>	26.3
Mammoth	<i>Mammuthus primigenius</i>	3.5

Edmonton Area, Alberta, Canada

Pre-LGM

Reference: Jass et al., 2011

Species (Common Name)	Species (Scientific Name)	Percent abundance
Bison	<i>Bison</i>	30.1
Camel*	<i>Camelops</i>	0.5
Caribou	<i>Rangifer</i>	0.5
Elk	<i>Cervus</i>	1.8
Horse	<i>Equus</i>	56.4
Mammoth	<i>Mammuthus</i>	9.1
Mastodon	<i>Mammut</i>	0.9
Sheep	<i>Ovis</i>	0.2
Ground Sloth+	<i>Megalonyx</i>	0.2
Helmeted Muskox	<i>Bootherium</i>	0.4

Edmonton Area, Alberta, Canada

Post-LGM

Reference: Jass et al., 2011

Species (Common Name)	Species (Scientific Name)	Percent abundance
Bison	<i>Bison</i>	72.0
Horse	<i>Equus</i>	26.1
Mammoth	<i>Mammuthus</i>	1.3
Helmeted Muskox	<i>Bootherium</i>	0.6

Fairbanks

No associated dates**Reference: Guthrie, 1968**

Species (Common Name)	Species (Scientific Name)	Percent abundance
Brown bear+	<i>Ursus arctos</i>	0.1
Steppe bison	<i>Bison priscus</i>	50.1
Camel+	<i>Camelops</i> sp.	0.1
Caribou	<i>Rangifer tarandus</i>	4.3
Coyote+	<i>Canis latrans</i>	0.0
Wapiti/ elk	<i>Cervus elaphus</i>	0.5
Horse	<i>Equus caballus</i>	32.6
Lion+	<i>Felis</i> sp.	0.4
Woolly mammoth	<i>Mammuthus primigenius</i>	6.4
Moose	<i>Alces alces</i>	1.5
Moose stag+	<i>Cervalces</i> sp.	0.2
Muskox	<i>Ovibos moschatus</i>	2.3
Woodland muskox	<i>Symbos</i> sp.: <i>Bootherium</i> sp.	0.3
Dall sheep	<i>Ovis dalli</i>	0.0
Wolf+	<i>Canis lupus</i>	0.8
Yak+	<i>Bos</i> sp.	0.1

Selawik and Kobuk River Areas, Alaska, USA**No associated dates, presumed mainly pre-LGM****Reference: Chapter 5; Druckenmiller, 2008**

Megaherbivore Species (Common Name)	Species (Scientific Name)	Percent abundance
Steppe bison	<i>Bison priscus</i>	39.1
Caribou	<i>Rangifer tarandus</i>	7.5
Horse	<i>Equus</i> sp.	5.4
Woolly Mammoth	<i>Mammuthus primigenius</i>	44.8
Moose	<i>Alces alces</i>	0.4
Muskox	<i>Ovibos moschatus</i>	2.9

North Slope, Alaska, USA**Pleistocene (43,500 - 10,000 ¹⁴C BP)****Reference: Mann et al., 2013**

Species (Common Name)	Species (Scientific Name)	Percent abundance
Bison	<i>Bison priscus</i>	23
Caribou	<i>Rangifer tarandus</i>	16
Horse	<i>Equus</i> sp.	41
Mammoth	<i>Mammuthus primigenius</i>	9
Moose	<i>Alces alces</i>	<1
Muskox	<i>Ovibos moschatus</i>	9
Saiga antelope+	<i>Saiga</i> sp.	<1
Predator		2

North Slope, Alaska, USA**Modern****Reference: Mann et al., 2013**

Species (Common Name)	Species (Scientific Name)	Percent abundance
Caribou	<i>Bison priscus</i>	97
Moose	<i>Alces alces</i>	<1
Muskox	<i>Ovibos moschatus</i>	<1

Predator+~

3

North Slope, Alaska, USA**Infinite to 19,500 ¹⁴C BP****Reference: Groves, 2015; Mann et al., 2013**

Species (Common Name)	Species (Scientific Name)	Percent abundance
Antelope+	<i>Saiga</i> sp.	1.7
Bison	<i>Bison priscus</i>	22.7
Caribou	<i>Rangifer tarandus</i>	17.2
Horse	<i>Equus</i> sp.	23.7
Mammoth	<i>Mammuthus primigenius</i>	16.1
Muskox	<i>Ovibos moschatus</i>	17.4
Predator+		1.2

North Slope, Alaska, USA**19,500 to 16,100 ¹⁴C BP****Groves, 2015; Mann et al., 2013**

Species (Common Name)	Species (Scientific Name)	Percent abundance
Bison	<i>Bison priscus</i>	13.7
Caribou	<i>Rangifer tarandus</i>	30.8
Horse	<i>Equus</i> sp.	46.6
Mammoth	<i>Mammuthus primigenius</i>	8.9

North Slope, Alaska, USA**16,100 to 10,000 ¹⁴C BP****Groves, 2015; Mann et al., 2013**

Species (Common Name)	Species (Scientific Name)	Percent abundance
Bison	<i>Bison priscus</i>	21.8
Caribou	<i>Rangifer tarandus</i>	18.7
Horse	<i>Equus</i> sp.	42.4
Mammoth	<i>Mammuthus primigenius</i>	8.1
Moose	<i>Alces alces</i>	2.1
Muskox	<i>Ovibos moschatus</i>	2.5
Predator+		4.5

*In Western Beringia, this would have been a reindeer, rather than a caribou.

+ Not included in this study

For the Edmonton samples, the numbers of specimens from each site were combined, and this was used to calculate abundance

For the Fairbanks samples, the sites were combined and averaged

For the North Slope samples, abundances were calculated based on the data in Mann et al., 2013 and information from Groves (2015)

References:

Druckenmiller, P.S., 2008. Survey of Pleistocene (Ice Age) vertebrates from the Selawik and Kobuk River areas of Northwestern Alaska. Intern. Rep. U.S. Fish Wildl. Serv. 1–56.

Groves, P., Personal communication (e-mail), 2015

Guthrie, R.D., 1968. Paleocology of the large-mammal community in interior Alaska during the late Pleistocene. Am. Midl. Nat. 79, 346–363.

- Jass, C., Burns, J., Milot, P.J., 2011. Description of fossil muskoxen and relative abundance of Pleistocene megafauna in central Alberta. *Can. J. Earth* 48, 793–800.
- MacPhee, R.D.E., Tikhonov, A.N., Mol, D., de Marliave, C., van der Plicht, H., Greenwood, A.D., Flemming, C., Agenbroad, L., 2002. Radiocarbon chronologies and extinction dynamics of the late Quaternary mammalian megafauna of the Taimyr Peninsula, Russian Federation. *J. Archaeol. Sci.* 29, 1017–1042. doi:10.1006/jasc.2001.0802
- Mann, D.H., Groves, P., Kunz, M.L., Reanier, R.E., Gaglioti, B. V., 2013. Ice-age megafauna in Arctic Alaska: extinction, invasion, survival. *Quat. Sci. Rev.* 70, 91–108. doi:10.1016/j.quascirev.2013.03.015
- Mol, D., Tikhonov, A., van der Plicht, J., Kahlke, R.-D., Debruyne, R., van Geel, B., van Reenen, G., Pals, J.P., de Marliave, C., Reumer, J.W.F., 2006. Results of the CERPOLEX/Mammuthus Expeditions on the Taimyr Peninsula, Arctic Siberia, Russian Federation. *Quat. Int.* 142-143, 186–202. doi:10.1016/j.quaint.2005.03.016
- Zimov, S.A., Zimov, N.S., Tikhonov, A.N., Chapin, F.S., 2012. Mammoth steppe: a high-productivity phenomenon. *Quat. Sci. Rev.* 57, 26–45. doi:10.1016/j.quascirev.2012.10.005

Appendix L Sample information for megafaunal herbivores from Alberta.

Lab ID	Common Name	Scientific Name	Sample Number	Stable Isotope Reference	¹⁴ C Date	Date Lab #	Date reference	Site
AB21	Bison	<i>Bison priscus</i>	P89.14.16	Chapter 5	>41,800	AECV: 1862c	Jass, 2015	CloverBar Sand and Gravel Consolidated Concrete Pit 48
AB15	Bison	<i>Bison sp. indet</i>	P89.13.255	Chapter 5	40,000±3,070	AECV: 1864c	Shapiro et al. 2004	Consolidated Concrete Pit 48
AB17	Bison	<i>Bison sp. indet</i>	P89.13.500	Chapter 5	>41,850	AECV:1865c	Jass, 2015	Consolidated Concrete Pit 48
AB18	Bison	<i>Bison sp. indet</i>	P89.13.692	Chapter 5	60,400±2,900	OxA-12086	Shapiro et al., 2004	Consolidated Concrete Pit 48
AB19	Bison	<i>Bison sp. indet</i>	P89.13.693	Chapter 5	>55,200	OxA-11611	Shapiro et al., 2004	Consolidated Concrete Pit 48
AB20	Bison	<i>Bison sp. indet</i>	P89.14.8	Chapter 5	>41,700	AECV:1861c	Jass, 2015	CloverBar Sand and Gravel Consolidated Concrete Pit 48
AB22	Bison	<i>Bison sp. indet</i>	P94.1.201	Chapter 5	53,800±2,200	OxA-11620	Shapiro et al., 2004	Riverview Pit
AB27	Bison	<i>Bison sp. indet</i>	P94.8.55	Chapter 5	>58,500	OxA-11619	Shapiro et al., 2004	Apex Evergreen Pit
AB30	Bison	<i>Bison sp. indet</i>	P95.2.87	Chapter 5	>59,400	OxA-11616	Shapiro et al., 2004	Consolidated Concrete Pit 48
AB41	Bison	<i>Bison sp. indet</i>	P99.3.44	Chapter 5	>52,600	OxA-1609	Shapiro et al., 2004	Byrtus Bison Site
AB46	Bison	<i>Bison sp. indet</i>	P00.1.1	Chapter 5	10,335±90	BGS 2225	Jass, 2015	Byrtus Bison Site
AB50	Bison	<i>Bison sp. indet</i>	P00.1.11	Chapter 5	10,425±50	OxA-11592	Shapiro et al., 2004	Byrtus Bison Site
AB47	Bison	<i>Bison sp. indet</i>	P00.1.13	Chapter 5	10,275±90	BGS 2226	Jass, 2015	Byrtus Bison Site
AB49	Bison	<i>Bison sp. indet</i>	P00.1.4	Chapter 5	10,450±55	OxA-11584	Shapiro et al., 2004	Byrtus Bison Site
AB48	Bison	<i>Bison sp. indet</i>	P01.1.1	Chapter 5	10,270±90	BGS 2310	Jass, 2015	Hall Site
AB51	Bison	<i>Bison sp. indet</i>	P10.12.2	Chapter 5	10,320±40	Beta-316503	Jass and Beaudoin, 2014	Henkel Farm
AB43	Bison	<i>Bison sp. indet</i>	P88.26.1	Chapter 5	10,320±200	AECV:851c	Jass, 2015	Twin Bridges Gravel Pit 80
AB44	Bison	<i>Bison sp. indet</i>	P90.4.1	Chapter 5	10,730±160	AECV: 1111c	Burns et al., 1996	Twin Bridges Gravel Pit 80
AB45	Bison	<i>Bison sp. indet</i>	P94.6.1	Chapter 5	10,410±70	AECV: 1973c	Jass, 2015	Smokey River T2
AB14	Caribou	<i>Rangifer tarandus</i>	P89.13.160	Chapter 2	29600±970	AA97953	Chapter 2	Consolidated Concrete Pit 48
AB23	Caribou	<i>Rangifer tarandus</i>	P94.1.438	Chapter 2	27,250±420	AA103879	Chapter 2	Consolidated Concrete Pit 48
AB31	Caribou	<i>Rangifer tarandus</i>	P95.6.29	Chapter 2				Consolidated Concrete Pit 48
AB34	Caribou	<i>Rangifer</i>	P98.5.35	Chapter 2	26,450±390	AA103880	Chapter 2	Consolidated Concrete Pit

		<i>tarandus</i>							48
AB35	Caribou	<i>Rangifer tarandus</i>	P98.5.185	Chapter 2					Consolidated Concrete Pit 48
AB36	Caribou	<i>Rangifer tarandus</i>	P98.5.328	Chapter 2					Consolidated Concrete Pit 48
AB37	Caribou	<i>Rangifer tarandus</i>	P98.5.347	Chapter 2					Consolidated Concrete Pit 48
AB42	Caribou	<i>Rangifer tarandus</i>	P02.10.3	Chapter 2	11,360±120	AA103826	Chapter 2		Consolidated Concrete Pit 48
AB13	Horse	<i>Equus sp.indet.</i>	P88.19.3	Chapter 5	>59,900	OxA-14269	Jass et al., 2011		Apex Evergreen Pit
AB25	Horse	<i>Equus sp.indet.</i>	P94.1.463	Chapter 5	>61,700	OxA-14272	Jass, 2015		Consolidated Concrete Pit 48
AB26	Horse	<i>Equus sp.indet.</i>	P94.1.693	Chapter 5	56,800 ±2,800	Unknown	Jass, 2015		Consolidated Concrete Pit 48
AB28	Horse	<i>Equus sp.indet.</i>	P95.1.12	Chapter 5	>56,300	Unknown	Jass, 2015		CloverBar Sand and Gravel
AB29	Horse	<i>Equus sp.indet.</i>	P95.2.29	Chapter 5	>61,300	OxA-14277	Jass, 2015		Apex Evergreen Pit
AB32	Horse	<i>Equus sp.indet.</i>	P96.2.33	Chapter 5	>62,200	OxA-14275	Jass et al., 2011		Consolidated Concrete Pit 48
AB33	Horse	<i>Equus sp.indet.</i>	P97.12.9	Chapter 5	>60,800	OxA-14278	Jass, 2015		CloverBar Sand and Gravel
AB38	Horse	<i>Equus sp.indet.</i>	P98.6.8	Chapter 5	>59,900	OxA-14271	Jass, 2015		CloverBar Sand and Gravel
AB39	Horse	<i>Equus sp.indet.</i>	P99.2.1	Chapter 5	>62,300	OxA-14576	Jass, 2015		CloverBar Sand and Gravel
AB40	Horse	<i>Equus sp.indet.</i>	P99.2.2	Chapter 5	>63,100	OxA-14274	Jass et al., 2011		CloverBar Sand and Gravel
AB56	Horse	<i>Equus sp.indet.</i>	P01.3.25	Chapter 5	11,090±55	OxA-14578	Jass et al., 2011		CloverBar Sand and Gravel
AB57	Horse	<i>Equus sp.indet.</i>	P02.10.87	Chapter 5	11,065±55	OxA-14579	Jass et al., 2011		Inland Aggregates Pit 48
AB52	Horse	<i>Equus sp.indet.</i>	P89.21.1	Chapter 5	11,200±90	AECV:1940c	Jass, 2015		Lingrell Pit
AB54	Horse	<i>Equus sp.indet.</i>	P96.9.16	Chapter 5	11,285±55	OxA-14573	Jass et al., 2011		Twin Bridges Gravel Pit 80
AB55	Horse	<i>Equus sp.indet.</i>	P98.8.86	Chapter 5	11,520±55	OxA-14574	Jass, 2015		Gertzen Pit
AB53	Horse	<i>Equus sp.indet.</i>	P98.8.90	Chapter 5	11,620±150	OxA-14273	Burns (2010)		Gertzen Pit
RAM 1B	Horse	<i>Equus sp.indet.</i>	P97.11.2A	Bellissimo, 2013	11 240±110	AA97948	Bellissimo, 2013		Riverview Pit
RAM2B	Horse	<i>Equus sp.indet.</i>	P96.3.13	Bellissimo, 2013	11 260±110	AA97949	Bellissimo, 2013		CloverBar Sand and Gravel
RAM4B	Horse	<i>Equus sp.indet.</i>	P02.10.4	Bellissimo, 2013					Pit 48
RAM5B	Horse	<i>Equus sp.indet.</i>	P99.3.163	Bellissimo, 2013	>38,900	AA97950	Bellissimo, 2013		Pit 48
RAM6B	Horse	<i>Equus sp.indet.</i>	P05.10.103	Bellissimo, 2013					Pit 48
RAM7B	Horse	<i>Equus sp.indet.</i>	P94.8.79	Bellissimo,					Riverview Pit

				2013				
RAM8B	Horse	<i>Equus sp.indet.</i>	P94.1.380	Bellissimo, 2013	>46 700	AA97951	Bellissimo, 2013	Pit 48
RAM9B	Horse	<i>Equus sp.indet.</i>	P04.3.33B	Bellissimo, 2013				Pit 48
RAM10B	Horse	<i>Equus sp.indet.</i>	P94.2.33	Bellissimo, 2013				Pit 80
	Horse	<i>Equus sp.</i>	P89.13.681	Bocherens et al., 1994				Pit 48
	Mammoth	<i>Mammuthus sp.</i>	P89.13.532	Bocherens et al., 1994				Pit 48
AB1	Mammoth	<i>Mammuthus</i>	P97.11.1B	Metcalf, 2011	43,300±3,000		Burns and Young, 1994	Riverview Pit
AB2	Mammoth	<i>Mammuthus</i>	P94.1.698	Metcalf, 2011	>37,700	AA84996	Metcalf, 2011	Consolidated Concrete Pit 48
AB5	Mammoth	<i>Mammuthus</i>	P90.7.1	Metcalf, 2011				Alberta Concrete Products Ltd.
AB11	Mammoth	<i>Mammuthus</i>	P00.2.1	Metcalf, 2011	40,000±3,500	AA84979	Metcalf, 2011	Smoky River
AB6	Mammoth	<i>Mammuthus</i>	P94.4.3	Metcalf, 2011	Pre-LGM		Dated by context	Consolidated Concrete Pit 46
AB4	Mastodon	<i>Mammut</i>	P94.16.1B	Metcalf, 2011	Pre-LGM		Dated by context	Apex Galloway Pit
AB10	Mastodon	<i>Mammut</i>	P97.7.1	Metcalf, 2011	>41,100	AA84997	Metcalf, 2011	Consolidated Concrete Pit 46

Appendix L continues below.

Lab ID	Common Name	Tissue	Stable Isotope Reference	Source	$\delta^{13}\text{C}_{\text{Bulk}}$	$\delta^{15}\text{N}_{\text{Bulk}}$	% Yield	%C	%N	C/N
AB21	Bison	B	Chapter 5	RAM	-18.9	6.7	15.4	38.8	14.7	3.1
AB15	Bison	B	Chapter 5	RAM	-19.0	5.4	13.6	37.9	14.4	3.1
AB17	Bison	B	Chapter 5	RAM	-19.2	8.1	12.5	38.8	14.7	3.1
AB18	Bison	B	Chapter 5	RAM	-19.8	6.0	7.5	43.9	16.4	3.1
AB19	Bison	B	Chapter 5	RAM	-20.0	6.1	10.0	39.5	15.0	3.1
AB20	Bison	B	Chapter 5	RAM	-19.0	7.6	22.8	41.2	15.6	3.1
AB22	Bison	B	Chapter 5	RAM	-18.8	5.7	14.2	38.6	14.6	3.1
AB27	Bison	B	Chapter 5	RAM	-20.2	8.6	9.5	37.6	14.4	3.0
AB30	Bison	B	Chapter 5	RAM	-19.5	5.9	14.3	38.4	14.6	3.1
AB41	Bison	B	Chapter 5	RAM	-20.4	7.3	12.6	37.8	14.3	3.1
AB46	Bison	B	Chapter 5	RAM	-19.7	1.4	13.5	31.2	10.6	3.4
AB50	Bison	B	Chapter 5	RAM	-19.5	2.2	7.4	33.4	11.6	3.4
AB47	Bison	B	Chapter 5	RAM	-19.7	1.2	13.0	33.2	11.5	3.4
AB49	Bison	B	Chapter 5	RAM	-19.7	1.7	13.9	31.1	10.8	3.4
AB48	Bison	B	Chapter 5	RAM	-18.8	2.3	8.8	29.9	10.3	3.4
AB51	Bison	B	Chapter 5	RAM	-19.8	2.2	13.5	34.6	12.2	3.3
AB43	Bison	B	Chapter 5	RAM	-19.4	3.1	12.5	33.3	11.6	3.3
AB44	Bison	B	Chapter 5	RAM	-19.6	1.6	12.3	36.1	12.5	3.4
AB45	Bison	B	Chapter 5	RAM	-19.5	2.4	9.0	32.6	11.4	3.4
AB14	Caribou	B	Chapter 2	RAM	-18.7	5.0	7.9	36.9	13.9	3.1
AB23	Caribou	B	Chapter 2	RAM	-18.4	4.2	12.0	39.2	14.7	3.1
AB31	Caribou	B	Chapter 2	RAM	-18.8	4.7	10.7	45.7	17.0	3.1
AB34	Caribou	B	Chapter 2	RAM	-18.5	5.1	8.5	36.0	13.5	3.1
AB35	Caribou	B	Chapter 2	RAM	-18.9	5.1	10.4	38.1	14.3	3.1
AB36	Caribou	B	Chapter 2	RAM	-18.6	4.8	10.0	38.1	14.5	3.1
AB37	Caribou	B	Chapter 2	RAM	-18.7	4.7	8.1	38.7	14.3	3.2

AB42	Caribou	B	Chapter 2	RAM	-18.7	2.9	12.6	38.6	14.6	3.1
AB13	Horse	B	Chapter 5	RAM	-20.1	7.0	12.4	42.1	15.5	3.2
AB25	Horse	B	Chapter 5	RAM	-20.0	8.5	12.9	37.6	14.3	3.1
AB26	Horse	B	Chapter 5	RAM	-19.9	7.6	10.5	37.3	14.2	3.1
AB28	Horse	B	Chapter 5	RAM	-20.0	8.7	12.0	37.4	14.1	3.1
AB29	Horse	B	Chapter 5	RAM	-19.9	9.6	10.5	34.1	12.9	3.1
AB32	Horse	B	Chapter 5	RAM	-20.3	7.9	9.5	36.4	13.8	3.1
AB33	Horse	B	Chapter 5	RAM	-20.6	8.6	9.2	45.0	15.7	3.3
AB38	Horse	B	Chapter 5	RAM	-20.2	8.3	14.6	39.2	14.9	3.1
AB39	Horse	B	Chapter 5	RAM	-20.3	9.1	15.3	41.2	15.4	3.1
AB40	Horse	B	Chapter 5	RAM	-20.6	7.6	12.8	39.4	14.7	3.1
AB56	Horse	B	Chapter 5	RAM	-20.8	0.3	14.9	35.4	12.3	3.3
AB57	Horse	B	Chapter 5	RAM	-20.7	1.8	6.4	32.7	11.2	3.4
AB52	Horse	B	Chapter 5	RAM	-19.7	0.9	7.5	41.1	14.4	3.3
AB54	Horse	B	Chapter 5	RAM	-20.1	0.3	5.0	34.3	11.8	3.4
AB55	Horse	B	Chapter 5	RAM	-20.7	0.5	7.6	32.0	11.1	3.4
AB53	Horse	B	Chapter 5	RAM	-20.6	1.4	8.1	28.0	9.6	3.4
RAM 1B	Horse	B	Bellissimo, 2013	RAM	-20.2	0.0	5.6	36.7	12.9	3.3
RAM2B	Horse	B	Bellissimo, 2013	RAM	-20.9	0.2	6.2	38.7	13.5	3.3
RAM4B	Horse	B	Bellissimo, 2013	RAM	-20.7	0.5	15.0	39.4	14.0	3.3
RAM5B	Horse	B	Bellissimo, 2013	RAM	-20.3	6.6	6.8	37.5	13.3	3.3
RAM6B	Horse	B	Bellissimo, 2013	RAM	-20.6	6.3	7.8	39.1	13.8	3.3
RAM7B	Horse	B	Bellissimo, 2013	RAM	-20.8	6.6	8.2	38.9	13.7	3.3
RAM8B	Horse	B	Bellissimo, 2013	RAM	-21.2	5.4	8.1	36.7	12.9	3.3
RAM9B	Horse	B	Bellissimo, 2013	RAM	-20.8	6.2	4.2	37.5	13.2	3.3
RAM10B	Horse	B	Bellissimo, 2013	RAM	-20.3	7.0	8.3	37.7	13.4	3.3
	Horse	B	Bocherens et al., 1994		-19.9	7.9				
	Mammoth	B	Bocherens et al., 1994		-20.2	10.0				

AB1	Mammoth	<u>B/C/D:</u> <u>mandibular</u> <u>symphysis</u> <u>/LLM6</u>	Metcalfé, 2011	RAM	<u>-20.6</u>	<u>7.8</u>	<u>16.0</u>	<u>40.9</u>	<u>15.6</u>	<u>3.1</u>
AB2	Mammoth	<u>C/D:</u> URM5	Metcalfé, 2011	RAM	<u>-21.1</u>	<u>9.7</u>	<u>14.4</u>	<u>36.1</u>	<u>13.3</u>	<u>3.2</u>
AB5	Mammoth	<u>C/D:</u> ULM6	Metcalfé, 2011	RAM	<u>-21.5</u>	<u>10.3</u>	<u>6.1</u>	<u>35.6</u>	<u>12.9</u>	<u>3.2</u>
AB11	Mammoth	<u>C/D:</u> LRM4/M5	Metcalfé, 2011	RAM	<u>-20.6</u>	<u>5.5</u>	<u>16.1</u>	<u>34.9</u>	<u>13.0</u>	<u>3.1</u>
AB6	Mammoth	D: LLM6	Metcalfé, 2011	RAM	-20.1	5.1	>14.7	28.0	10.2	3.2
AB4	Mastodon	<u>B/D:</u> <u>mandible</u> <u>(ascending</u> <u>ramus)</u> <u>/LLM5</u>	Metcalfé, 2011	RAM	<u>-20.8</u>	<u>4.5</u>	<u>13.6</u>	<u>40.3</u>	<u>15.0</u>	<u>3.1</u>
AB10	Mastodon	D: LLM6	Metcalfé, 2011	RAM	-19.5	5.0	12.4	41.1	15.4	3.1

Samples analyzed multiple times (duplicate/triplicate) in Chapter 5 are in bold

Dates obtained in Chapter 5 are in bold

Average of repeat measurements on different tissues from the same specimen are underlined

RAM = Royal Alberta Museum

Tissue: B = Bone; RD = Root dentin; C = Cementum; D = Crown dentin; T= Tusk dentin

References:

- Bellissimo, N.S., 2013. Origins of stable isotopic variations in late Pleistocene horse enamel and bone from Alberta. Master's Thesis. University of Western Ontario.
- Burns, J., Young, R., 1994. Pleistocene mammals of the Edmonton area, Alberta. Part I. The carnivores. *Can. J. Earth Sci.* 31, 393–400.
- Burns, J.A., 1996. Vertebrate paleontology and the alleged ice-free corridor: the meat of the matter. *Quat. Int.* 32, 107–112.
- Burns, J. a., 2010. Mammalian faunal dynamics in Late Pleistocene Alberta, Canada. *Quat. Int.* 217, 37–42. doi:10.1016/j.quaint.2009.08.003
- Bocherens, H., Fizet, M., Mariotti, A., Gangloff, R., Burns, J., 1994. Contribution of isotopic biogeochemistry (^{13}C , ^{15}N , ^{18}O) to the paleoecology of mammoths (*Mammuthus primigenius*). *Hist. Biol.* 7, 187–202.
- Jass, C., Personal communication (e-mail), 2015
- Jass, C.N., Beaudoin, A.B., 2014. Radiocarbon dates of Late Quaternary megafauna and botanical remains from central Alberta, Canada. *Radiocarbon* 56, 1215–1222. doi:10.2458/56.17922
- Jass, C., Burns, J., Milot, P.J., 2011. Description of fossil muskoxen and relative abundance of Pleistocene megafauna in central Alberta. *Can. J. Earth* 48, 793–800.
- Metcalfé, J.Z., 2011. Late Pleistocene climate and proboscidean paleoecology in North

America: insights from stable isotope compositions of skeletal remains. Doctoral Thesis. University of Western Ontario.

Shapiro, B., Drummond, A.J., Rambaut, A., Wilson, M.C., Matheus, P.E., Sher, A. V, Pybus, O.G., Gilbert, M.T.P., Barnes, I., Binladen, J., Willerslev, E., Hansen, A.J., Baryshnikov, G.F., Burns, J. a, Davydov, S., Driver, J.C., Froese, D.G., Harington, C.R., Keddie, G., Kosintsev, P., Kunz, M.L., Martin, L.D., Stephenson, R.O., Storer, J., Tedford, R., Zimov, S., Cooper, A., 2004. Rise and fall of the Beringian steppe bison. *Science* 306, 1561–5. doi:10.1126/science.1101074

Appendix M Sample information for megafaunal herbivores from Fairbanks.

Lab ID	Common Name	Scientific Name	Sample Number	Stable Isotope Reference	¹⁴ C Date	Date Lab #	Date reference
	Bison	<i>Bison bison</i>	F:AM 5092	Leonard et al., 2007			
	Bison	<i>Bison bison</i>	F:AM 46555	Leonard et al., 2007			
	Bison	<i>Bison bison</i>	F:AM 46858	Leonard et al., 2007			
	Bison	<i>Bison bison</i>	F:AM 46856	Leonard et al., 2007			
	Bison	<i>Bison bison</i>	F:AM 3135	Leonard et al., 2007			
	Bison	<i>Bison bison</i>	F:AM 1636	Leonard et al., 2007			
	Caribou	<i>Rangifer tarandus</i>	F:AM 142443	Leonard et al., 2007	16,000± 190	AA48686	Leonard et al., 2007
	Caribou	<i>Rangifer tarandus</i>	F:AM 142444	Leonard et al., 2007	16,400± 202	AA48687	Leonard et al., 2007
	Caribou	<i>Rangifer tarandus</i>	F:AM 142440	Leonard et al., 2007	16,700± 207	AA48682	Leonard et al., 2007
	Caribou	<i>Rangifer tarandus</i>	F:AM 142441	Leonard et al., 2007	17,300± 222	AA48683	Leonard et al., 2007
	Caribou	<i>Rangifer tarandus</i>	F:AM 142438	Leonard et al., 2007	21,000± 361	AA48680	Leonard et al., 2007
	Caribou	<i>Rangifer tarandus</i>	F:AM 142446	Leonard et al., 2007	29,640± 370	CAMS120070	Leonard et al., 2007
	Caribou	<i>Rangifer tarandus</i>	F:AM 142439	Leonard et al., 2007	>40,700	AA48681	Leonard et al., 2007
	Caribou	<i>Rangifer tarandus</i>	F:AM 142442	Leonard et al., 2007	>40,700	AA48685	Leonard et al., 2007
	Caribou	<i>Rangifer tarandus</i>	F:AM 142445	Leonard et al., 2007	>41,100	AA48688	Leonard et al., 2007
	Caribou	<i>Rangifer tarandus</i>	F:AM 142447	Leonard et al., 2007	>45,200	CAMS120071	Leonard et al., 2007
	Caribou	<i>Rangifer tarandus</i>	AMNH A-121-3512	Bocherens et al., 1995			
	Horse	<i>Equus lambei</i>	F:AM 142429	Leonard et al., 2007	12,310± 45	CAMS119982	Leonard et al., 2007
	Horse	<i>Equus lambei</i>	F:AM 142423	Leonard et al., 2007	12,560± 50	CAMS119976	Leonard et al., 2007
	Horse	<i>Equus lambei</i>	F:AM 60025	Leonard et al., 2007	13,710± 60	CAMS120061	Leonard et al., 2007
	Horse	<i>Equus lambei</i>	F:AM 60005	Leonard et al., 2007	14,630± 60	CAMS119969	Leonard et al., 2007
	Horse	<i>Equus lambei</i>	F:AM 142421	Leonard et al., 2007	14,860± 60	CAMS119974	Leonard et al., 2007
	Horse	<i>Equus lambei</i>	F:AM 142424	Leonard et al., 2007	15,460± 70	CAMS119977	Leonard et al., 2007
	Horse	<i>Equus lambei</i>	F:AM 60032	Leonard et al., 2007	15,850± 70	CAMS120068	Leonard et al., 2007
	Horse	<i>Equus lambei</i>	F:AM 60004	Leonard et al., 2007	16,370± 80	CAMS119968	Leonard et al., 2007
	Horse	<i>Equus lambei</i>	F:AM 60044	Leonard et al., 2007	18,630± 100	CAMS119970	Leonard et al., 2007
	Horse	<i>Equus lambei</i>	F:AM 60023	Leonard et al., 2007	19,000± 100	CAMS120058	Leonard et al., 2007
	Horse	<i>Equus lambei</i>	F:AM 60027	Leonard et al., 2007	19,590± 110	CAMS120059	Leonard et al., 2007
	Horse	<i>Equus lambei</i>	F:AM 142420	Leonard et al., 2007	19,870± 110	CAMS119973	Leonard et al., 2007
	Horse	<i>Equus lambei</i>	F:AM 142430	Leonard et al., 2007	19,950± 110	CAMS119983	Leonard et al., 2007

Horse	<i>Equus lambei</i>	F:AM 60020	Leonard et al., 2007	19,950± 120	CAMS120062	Leonard et al., 2007
Horse	<i>Equus lambei</i>	F:AM 142427	Leonard et al., 2007	19,960± 110	CAMS119980	Leonard et al., 2007
Horse	<i>Equus lambei</i>	F:AM 142426	Leonard et al., 2007	20,300± 120	CAMS119979	Leonard et al., 2007
Horse	<i>Equus lambei</i>	F:AM 142425	Leonard et al., 2007	20,440± 120	CAMS119978	Leonard et al., 2007
Horse	<i>Equus lambei</i>	F:AM 142419	Leonard et al., 2007	20,520± 120	CAMS119971	Leonard et al., 2007
Horse	<i>Equus lambei</i>	F:AM 142428	Leonard et al., 2007	21,280± 130	CAMS119981	Leonard et al., 2007
Horse	<i>Equus lambei</i>	F:AM 60026	Leonard et al., 2007	21,310± 140	CAMS120060	Leonard et al., 2007
Horse	<i>Equus lambei</i>	F:AM 142435	Leonard et al., 2007	21,840± 140	CAMS119989	Leonard et al., 2007
Horse	<i>Equus lambei</i>	F:AM 142434	Leonard et al., 2007	22,610± 150	CAMS119988	Leonard et al., 2007
Horse	<i>Equus lambei</i>	F:AM 60003	Leonard et al., 2007	24,260± 200	CAMS120077	Leonard et al., 2007
Horse	<i>Equus lambei</i>	F:AM 142431	Leonard et al., 2007	25,710± 230	CAMS119985	Leonard et al., 2007
Horse	<i>Equus lambei</i>	F:AM 142433	Leonard et al., 2007	25,960± 240	CAMS119987	Leonard et al., 2007
Horse	<i>Equus lambei</i>	F:AM 60033	Leonard et al., 2007	39,910± 1330	CAMS120069	Leonard et al., 2007
Horse	<i>Equus lambei</i>	F:AM 60017	Leonard et al., 2007	41,000± 1500	CAMS119972	Leonard et al., 2007
Horse	<i>Equus lambei</i>	F:AM 60221	Leonard et al., 2007	43,700± 2000	CAMS120067	Leonard et al., 2007
Horse	<i>Equus lambei</i>	F:AM 60028	Leonard et al., 2007	>48,400	CAMS120064	Leonard et al., 2007
Horse	<i>Equus lambei</i>	F:AM 142422	Leonard et al., 2007	>48,500	CAMS119975	Leonard et al., 2007
Horse	<i>Equus lambei</i>	F:AM 60019	Leonard et al., 2007	>48,500	CAMS119984	Leonard et al., 2007
Horse	<i>Equus lambei</i>	F:AM 142432	Leonard et al., 2007	>48,500	CAMS119986	Leonard et al., 2007
Mammoth	<i>Mammuthus</i>	V-54-1 367	Bocherens et al., 1994			
Mammoth	<i>Mammuthus</i>	V-74-2	Bocherens et al., 1994			
Mammoth	<i>Mammuthus</i>	V-78-1	Bocherens et al., 1994			
Mammoth	<i>Mammuthus</i>	AK-171-V-1	Bocherens et al., 1994			
Mammoth	<i>Mammuthus primigenius</i>	AM 1114	Szpak et al., 2010	46,391± 2,699	AA14939	Debruyne et al., 2008
Mammoth	<i>Mammuthus primigenius</i>	AM 1208	Szpak et al., 2010	12,677± 142	AA14888	Debruyne et al., 2008
Mammoth	<i>Mammuthus primigenius</i>	AM 2446	Szpak et al., 2010	26,022± 640	AA14855	Debruyne et al., 2008
Mammoth	<i>Mammuthus primigenius</i>	AM 523	Szpak et al., 2010	43,239± 2,219	AA14904	Debruyne et al., 2008
Mammoth	<i>Mammuthus primigenius</i>	AM 8052	Szpak et al., 2010	18,379± 124	AA14935	Debruyne et al., 2008
Mammoth	<i>Mammuthus primigenius</i>	NMC 42135	Szpak et al., 2010	30,000± 1,000	AA17538	Debruyne et al., 2008
Mammoth	<i>Mammuthus primigenius</i>	NMC 6746	Szpak et al., 2010	23,150± 460	AA17574	Debruyne et al., 2008
Mastodon	<i>Mammuthus americanum</i>	F:AM: 103281	Zazula et al., 2014	>50,800	UCIAMS 88775	Zazula et al., 2014
Mastodon	<i>Mammuthus americanum</i>	F:AM: 103292	Zazula et al., 2014	46,100± 2,100	UCIAMS 88771	Zazula et al., 2014
Mastodon	<i>Mammuthus americanum</i>	F:AM: 103295	Zazula et al., 2014	>46,900	UCIAMS 88774	Zazula et al., 2014

	Mastodon	<i>Mammut americanum</i>	UAMES 7666	Zazula et al., 2014	>50,800	UCIAMS 88767	Zazula et al., 2014
	Mastodon	<i>Mammut americanum</i>	UAMES 7667	Zazula et al., 2014	51,300± 4,000	UCIAMS 88766	Zazula et al., 2014
	Moose		AMNH 1367	Bocherens et al., 1995			
	Moose		AMNH 4324	Bocherens et al., 1995			
	Muskox	<i>Symbos cavifrons</i>	F:AM 142452	Fox-Dobbs et al., 2008			
	Muskox	<i>Symbos cavifrons</i>	F:AM 142453	Fox-Dobbs et al., 2008			
	Muskox	<i>Symbos cavifrons</i>	F:AM 142454	Fox-Dobbs et al., 2008			
	Muskox	<i>Symbos cavifrons</i>	F:AM 142455	Fox-Dobbs et al., 2008			
	Muskox	<i>Symbos cavifrons</i>	F:AM 142456	Fox-Dobbs et al., 2008			
	Muskox	<i>Symbos cavifrons</i>	F:AM 142457	Fox-Dobbs et al., 2008			
	Muskox	<i>Symbos cavifrons</i>	F:AM 142458	Fox-Dobbs et al., 2008	41,200± 1500	CAMS120072	Fox-Dobbs et al., 2008
	Muskox	<i>Symbos cavifrons</i>	F:AM 142459	Fox-Dobbs et al., 2008	>48,800	CAMS120073	Fox-Dobbs et al., 2008
	Muskox	<i>Symbos cavifrons</i>	F:AM 142460	Fox-Dobbs et al., 2008			
	Muskox	<i>Symbos cavifrons</i>	F:AM 142461	Fox-Dobbs et al., 2008			
AMNH 4	Sheep	<i>Ovis dalli</i>	F:AM 143759	Chapter 5			
AMNH 5	Sheep	<i>Ovis dalli kaiseni</i>	F:AM 34647	Chapter 5			
AMNH 6	Sheep	<i>Ovis dalli</i>	F:AM 143760	Chapter 5	21,660±380	AA103842	Chapter 5
AMNH 7	Sheep	<i>Ovis dalli kaiseni</i>	F:AM 34659	Chapter 5			
AMNH 8	Sheep	<i>Ovis dalli</i>	F:AM 143761	Chapter 5			
AMNH 9	Sheep	<i>Ovis dalli</i>	F:AM 143762	Chapter 5			
AMNH 10	Sheep	<i>Ovis dalli kaiseni</i>	F:AM 34650	Chapter 5			
AMNH 11	Sheep	<i>Ovis dalli kaiseni</i>	F:AM 34648	Chapter 5	>41,100	AA103843	Chapter 5
AMNH 12	Sheep	<i>Ovis dalli</i>	F:AM 143763	Chapter 5			
AMNH 13	Sheep	<i>Ovis dalli kaiseni</i>	F:AM 34646	Chapter 5			

Appendix M continues below

Lab ID	Latitude	Longitude	Site	Tissue	Tissue Type	Source	$\delta^{13}_{\text{Bulk}}$	$\delta^{15}_{\text{N}_{\text{Bulk}}}$	% Yield	%C	%N	C/N
				B		AMNH	-20.1	4.4				
				B		AMNH	-20.1	5.2				
				B		AMNH	-20.9	3.7				

	B	AMNH	-19.8	2.9				
	B	AMNH	-20.5	5.2				
	B	AMNH	-21.3	4.4				
	B	AMNH	-19.2	3.3				
	B	AMNH	-19.0	3.1				
	B	AMNH	-19.5	2.0				
	B	AMNH	-20.1	5.4				
	B	AMNH	-20.1	3.6				
	B	AMNH	-19.3	3.1				
	B	AMNH	-19.4	4.7				
	B	AMNH	-19.3	2.1				
	B	AMNH	-19.7	3.7				
	B	AMNH	-19.2	1.7				
Upper Cleary	B	humerus	-18.4	2.7	7.2	41.3	14.8	3.3
	B	AMNH	-21.3	4.3				
	B	AMNH	-20.9	3.9				
	B	AMNH	-21.2	4.7				
	B	AMNH	-21.3	1.6				
	B	AMNH	-21.0	4.8				
	B	AMNH	-20.7	2.9				
	B	AMNH	-20.9	2.5				
	B	AMNH	-20.9	3.1				
	B	AMNH	-20.9	3.5				
	B	AMNH	-21.5	2.5				
	B	AMNH	-20.8	3.6				
	B	AMNH	-21.2	5.0				
	B	AMNH	-21.4	3.2				
	B	AMNH	-21.3	4.0				
	B	AMNH	-21.1	4.7				
	B	AMNH	-21.2	5.1				
	B	AMNH	-20.8	4.2				
	B	AMNH	-21.1	4.5				
	B	AMNH	-21.0	3.7				
	B	AMNH	-21.3	4.0				
	B	AMNH	-21.9	3.8				
	B	AMNH	-21.0	3.8				

			B		AMNH	-21.3	1.4				
			B		AMNH	-21.1	3.9				
			B		AMNH	-20.7	2.9				
			B		AMNH	-20.9	2.6				
			B		AMNH	-21.6	3.6				
			B		AMNH	-21.7	0.7				
			B		AMNH	-20.6	4.4				
			B		AMNH	-21.5	3.0				
			B		AMNH	-21.5	1.7				
			B		AMNH	-21.5	2.5				
		Lost Chicken Creek, Alaska	D			-20.8	6.8				
		Chatanika, Alaska	D			-21.0	6.4				
		Fairbanks, Alaska	T	averaged base to tip		-21.3	6.9				
		Eilson AFB, Alaska	D			-21.1	8.3				
64°50N	148°00W	Ester Creek	D/RD/C			-20.5	5.0	13.2	40.5	14.9	3.2
65°10N	151°W	Sullivan Creek	D/RD/C			-20.8	5.9	11.4	34.7	12.2	3.3
64°60N	148°W	Cripple Creek	D/RD/C			-20.8	6.4	3.0	38.5	13.0	3.5
65°10N	147°30W	Cleary Creek	D/RD/C			-20.8	4.4	2.9	25.8	8.7	3.5
65°10N	147°30W	Cleary Creek	D/RD/C			-21.0	7.0	19.8	36.9	13.6	3.2
64°50N	147°40W	Eldorado Creek	D/RD/C			-20.7	7.8	13.4	37.9	14.0	3.2
65°18N	151°54W	Tanana	D/RD/C			-21.0	9.7	14.5	35.8	13.4	3.1
		Engineer Creek			AMNH	-21.0	4.6	6.7	43.4	15.7	3.2
		Livengood			AMNH	-20.9	4.9	4.8	42.6	15.4	3.2
		Engineer Creek			AMNH	-21.0	4.5	5.4	40.9	14.7	3.3
		Fairbanks Creek			UAMES	-21.0	4.3	8.6	40.9	14.9	3.2
		Fairbanks Creek			UAMES	-20.9	3.6	4.2	42.2	15.2	3.2
		Ester Creek	B	mandible	AMNH	-21.0	1.9	11.8	42.2	15.2	3.2
		Cripple Creek	B	mandible	AMNH	-19.9	0.8	9.0	33.0	11.7	3.3
						-20.3	0.8				
						-20.2	0.0				
						-20.0	-0.4				
						-19.7	-0.2				
						-20.9	1.2				
						-19.9	-0.3				
						-19.9	0.1				
						-20.4	3.3				

					-20.7	3.2					
					-17.5	4.0					
AMNH 4	Fairbanks Creek Alaska	B	Long bone	AMNH	-18.4	4.5	3.8	32.0	11.0	3.4	
AMNH 5	10 min W of Fairbanks	B	Skull and horncone	AMNH	-20.1	3.4	13.0	30.3	10.4	3.4	
AMNH 6	Chicken Creek	B	Skull and horncone	AMNH	-19.5	7.6	4.3	32.0	10.9	3.4	
AMNH 7		B	Long bone	AMNH	-19.3	4.0	5.1	34.0	11.6	3.4	
AMNH 8	Mastodon Creek Circle Area	B	Skull and horncone	AMNH	-19.2	5.2	10.0	34.7	12.0	3.4	
AMNH 9	Jackovich-Hunter Creek Rampart	B	Skull and horncone	AMNH	-19.5	4.4	12.9	32.8	11.4	3.4	
AMNH 10	Cleary Alaska	B	Long bone	AMNH	-19.2	4.2	7.5	30.9	10.6	3.4	
AMNH 11		B	Skull and horncone	AMNH	-19.6	2.1	10.6	34.3	11.9	3.4	
AMNH 12	Woodchopper Creek	B	Skull and horncone	AMNH	-19.8	3.2	6.8	34.7	11.9	3.4	
AMNH 13	Banner Creek near Richardson Road House	B	Skull and horncone	AMNH	-19.4	4.2	9.8	33.0	11.4	3.4	

Samples analyzed multiple times (duplicate/triplicate) in Chapter 5 are in bold

Dates obtained in Chapter 5 are in bold

AMNH = American Museum of Natural History; UAMES = University of Alaska Museum Earth Science

Tissue: B = Bone; RD = Root dentin; C = Cementum; D = Crown dentin; T = Tusk dentin

References:

- Bocherens, H., Fizet, M., Mariotti, A., Gangloff, R., Burns, J., 1994. Contribution of isotopic biogeochemistry (^{13}C , ^{15}N , ^{18}O) to the paleoecology of mammoths (*Mammuthus primigenius*). *Hist. Biol.* 7, 187–202.
- Bocherens, H., Emslie, S., Billiou, D., Mariotti, A., 1995. Stables isotopes (^{13}C , ^{15}N) and paleodiet of the giant short-faced bear (*Arctodus simus*). *Comptes rendus l'Académie des Sci. Série 2. Sci. la terre des planètes* 320, 779–784.
- Debruyne, R., Chu, G., King, C.E., Bos, K., Kuch, M., Schwarz, C., Szpak, P., Gröcke, D.R., Matheus, P., Zazula, G., Guthrie, D., Froese, D., Buigues, B., de Marliave, C., Flemming, C., Poinar, D., Fisher, D., Southon, J., Tikhonov, A.N., MacPhee, R.D.E., Poinar, H.N., 2008. Out of America: ancient DNA evidence for a new world origin of late Quaternary woolly mammoths. *Curr. Biol.* 18, 1320–6. doi:10.1016/j.cub.2008.07.061
- Fox-Dobbs, K., Leonard, J., Koch, P., 2008. Pleistocene megafauna from eastern Beringia: paleoecological and paleoenvironmental interpretations of stable carbon and nitrogen isotope and radiocarbon records. *Palaeogeogr. Palaeoclimatol. Palaeoecol.* 261, 30–

46.

- Leonard, J.A., Vilà, C., Fox-Dobbs, K., Koch, P.L., Wayne, R.K., Van Valkenburgh, B., 2007. Megafaunal extinctions and the disappearance of a specialized wolf ecomorph. *Curr. Biol.* 17, 1146–50. doi:10.1016/j.cub.2007.05.072
- Szpak, P., Gröcke, D.R., Debruyne, R., MacPhee, R.D.E., Guthrie, R.D., Froese, D., Zazula, G.D., Patterson, W.P., Poinar, H.N., 2010. Regional differences in bone collagen $\delta^{13}\text{C}$ and $\delta^{15}\text{N}$ of Pleistocene mammoths: implications for paleoecology of the mammoth steppe. *Palaeogeogr. Palaeoclimatol. Palaeoecol.* 286, 88–96. doi:10.1016/j.palaeo.2009.12.009
- Zazula, G.D., MacPhee, R.D., Metcalfe, J.Z., Reyes, A. V., Brock, F., Druckenmiller, P.S., Groves, P., Harington, R., Hodgins, G.W.L., Kunz, M.L., Longstaffe, F.J., Mann, D.H., McDonald, H.G., Nalawade-Chavan, S., Southon, J.R., 2014. American mastodon extirpation in the Arctic and Subarctic predates human colonization and terminal Pleistocene climate change. *Proc. Natl. Acad. Sci.* 111, 18460–18465.

Appendix N Sample information for megafaunal herbivores from the Great Lakes Area.

Lab ID	Common Name	Scientific Name	Stable Isotope Reference	¹⁴ C Date	Date Lab #	Date reference
ON17	Mammoth	<i>Mammuthus</i> sp.	Metcalfe et al., 2013			
ON18	Mammoth	<i>Mammuthus</i> sp.	Metcalfe et al., 2013	post-12,800, pre-11,100		Metcalfe et al., 2013
ON19	Mammoth	<i>Mammuthus</i> sp.	Metcalfe et al., 2013			
ON12	Mammoth	<i>Mammuthus primigenius</i>	Metcalfe et al., 2013	10,790 ± 150	WAT-999	Metcalfe et al., 2013
ON3	Mastodon	<i>Mammuth americanum</i>	Metcalfe et al., 2013	11,820 ± 120	AA84989	Metcalfe et al., 2013
ON4	Mastodon	<i>Mammuth americanum</i>	Metcalfe et al., 2013			
ON7	Mastodon	<i>Mammuth americanum</i>	Metcalfe et al., 2013	11,120 ± 110	AA84980	Metcalfe et al., 2013
ON9	Mastodon	<i>Mammuth americanum</i>	Metcalfe et al., 2013	12,360 ± 120	AA84998	Metcalfe et al., 2013
NY3	Mastodon	<i>Mammuth americanum</i>	Metcalfe et al., 2013	11,033 ± 40 to 10,430 ± 60 °		Metcalfe et al., 2013
NY4	Mastodon	<i>Mammuth americanum</i>	Metcalfe et al., 2013	11,033 ± 40 to 10,430 ± 60 °		Metcalfe et al., 2013
<u>ON10X/x/1/2</u>	Mastodon	<i>Mammuth americanum</i>	Metcalfe et al., 2013	11,380 ± 170 ^b	GSC-611	Metcalfe et al., 2013
ON14	Mastodon	<i>Mammuth americanum</i>	Metcalfe et al., 2013	11,400 ± 450, 12,000 ± 500 (muck)		McAndrews & Jackson (1988)
ON20	Mastodon	<i>Mammuth americanum</i>	Metcalfe et al., 2013	spruce pollen zone		McAndrews & Jackson (1988)
ON7	Mastodon	<i>Mammuth americanum</i>	Metcalfe et al., 2013	11,120 ± 110 (bone collagen)	AA84980	Metcalfe et al., 2013
ON9	Mastodon	<i>Mammuth americanum</i>	Metcalfe et al., 2013	12,360 ± 120 (dentin collagen)	AA84998	Metcalfe et al., 2013
ON13	Mastodon	<i>Mammuth americanum</i>	Metcalfe et al., 2013	spruce pollen zone		McAndrews & Jackson (1988)
ON15	Mastodon	<i>Mammuth americanum</i>	Metcalfe et al., 2013			
NY1	Mastodon	<i>Mammuth americanum</i>	Metcalfe et al., 2013	11,033 ± 40 to 10,430 ± 60 °		Metcalfe et al., 2013
NY2	Mastodon	<i>Mammuth americanum</i>	Metcalfe et al., 2013	11,033 ± 40 to 10,430 ± 60 °		Metcalfe et al., 2013
NY6	Mastodon	<i>Mammuth americanum</i>	Metcalfe et al., 2013	11,033 ± 40 to 10,430 ± 60 °		Metcalfe et al., 2013
NY7	Mastodon	<i>Mammuth americanum</i>	Metcalfe et al., 2013	11,033 ± 40 to 10,430 ± 60 °		Metcalfe et al., 2013
NY8	Mastodon	<i>Mammuth americanum</i>	Metcalfe et al., 2013	11,033 ± 40 to 10,430 ± 60 °		Metcalfe et al., 2013

NY9	Mastodon	<i>Mammut americanum</i>	Metcalfe et al., 2013	11,033 ± 40 to 10,430 ± 60 °	Metcalfe et al., 2013
NY10	Mastodon	<i>Mammut americanum</i>	Metcalfe et al., 2013	11,033 ± 40 to 10,430 ± 60 °	Metcalfe et al., 2013
NY11	Mastodon	<i>Mammut americanum</i>	Metcalfe et al., 2013	11,033 ± 40 to 10,430 ± 60 °	Metcalfe et al., 2013
NY12	Mastodon	<i>Mammut americanum</i>	Metcalfe et al., 2013	11,033 ± 40 to 10,430 ± 60 °	Metcalfe et al., 2013

Appendix N continues below.

Lab ID	Sample Number	Site	Tissue	Tissue Type	$\delta^{13}\text{C}_{\text{Bulk}}$	$\delta^{15}\text{N}_{\text{Bulk}}$	% Yield	%C	%N	C/N
ON17	01195	Toronto	RD		-20.5	8.0	17.8	46.6	17.2	3.2
ON18	1973	West Hill	RD	URM6	-21.2	8.5	9.3	45.8	16.9	3.2
ON19	3118	St. Catherine's	D	ULM5/M6	-20.7	7.3	5.2	45.4	16.6	3.2
ON12	29,753	Rostock	T		-19.8	7.5	21.2	46.6	17.0	3.2
ON3		Norfolk Port	D	M5/M6	-20.7	4.6	13.3	43.7	16.3	3.1
ON4		Burwell	D	M4/M5	-19.5	3.1	13.8	44.1	16.5	3.1
ON7		Caradoc	D	M6	-19.9	3.6	17.7	46.2	17.4	3.1
ON9		Delaware?	D	M6	-20.1	2.2	14.7	41.9	15.7	3.1
NY3	TailingI	Hiscock	D	URM5	-21.0	3.5	11.0 ^a	36.1	13.5	3.1
NY4	TailingI	Hiscock	D	ULM6	-20.9	3.5	6.9 ^a	33.1	12.4	3.1
<u>ON10X/x/1/2</u>	52,589	Thamesville	<u>RD/T/B</u>	<u>M5?/two ribs</u>	<u>-20.1</u>	<u>2.4</u>	<u>11.6</u>	<u>45.0</u>	<u>16.8</u>	<u>3.1</u>
ON14	1792c	Rodney	RD	LLM6	-20.2	3.1	11.0	45.1	16.4	3.2
ON20	65?	Welland?	T		-20.7	2.2	3.8	44.9	16.3	3.2
ON7		Caradoc	B	bone & dentin (crown)	-20.1	2.6	13.2	43.3	16.2	3.1
ON9		Delaware?	B	bone & dentin (crown)	-20.9	2.0	1.5	19.5	6.7	3.4
ON13	4184	Wellandport	B	bone (frags)	-20.0	1.8	7.8 ^a	46.4	17.3	3.1
ON15	03232	Tupperville	B	bone	-20.6	2.0	4.6	45.2	15.9	3.3
NY1	J2NE-85	Hiscock	B	bone (rib)	-21.2	2.3	14.6	44.0	16.6	3.1
	I2SE(S1/2)-									
NY2	61	Hiscock	B	bone (rib)	-21.1	2.5	7.2	42.3	16.1	3.1
NY6	G7SW-156	Hiscock	B	bone (R scapula)	-21.3	2.5	8.7 ^a	41.2	15.4	3.1
NY7	I3NW-107	Hiscock	B	bone (R scapula)	-21.0	2.7	6.6 ^a	42.6	16.0	3.1
NY8	F5NW-27	Hiscock	B	bone (R scapula)	-21.5	2.3	15.3 ^a	41.5	15.7	3.1
NY9	I4SE-46	Hiscock	B	bone (R scapula)	-21.4	2.3	13.2 ^a	42.5	16.0	3.1

NY10	I2NE-173	Hiscock	B	bone (R scapula)	-21.4	2.4	9.9 ^a	43.7	16.5	3.1
NY11	G6SW-118	Hiscock	B	bone (L scapula)	-21.6	2.5	10.3 ^a	43.5	16.3	3.1
NY12	G6SW-125	Hiscock	B	bone (L scapula)	-20.8	2.7	14.1 ^a	42.5	16.0	3.1

Average of repeat measurements on different tissues from the same specimen are underlined

^a Yield may be artificially low

^b This radiocarbon date may correspond to a different individual

^c Range for the Hiscock mastodon bone collagen which had been radiocarbon dated (Laub, 2010, 2003).

Tissue: B = Bone; RD = Root dentin; C = Cementum; D = Crown dentin; T= Tusk dentin

References:

McAndrews, J., Jackson, L., 1988. Age and environment of late Pleistocene mastodont and mammoth in southern Ontario. Bull. Buffalo Soc. Nat. Sci. 33, 161–172.

Metcalfe, J.Z., Longstaffe, F.J., Hodgins, G., 2013. Proboscideans and paleoenvironments of the Pleistocene Great Lakes: landscape, vegetation, and stable isotopes. Quat. Sci. Rev. 76, 102–113. doi:10.1016/j.quascirev.2013.07.004

Appendix O Sample information for megafaunal herbivores from the Gydan Peninsula.

Common Name	Scientific Name	Sample Number	Stable Isotope Reference	¹⁴ C Date	Date reference
Mammoth	<i>Mammuthus primigenius</i>	GDY1	Szpak et al., 2010	15,160±60	Debruyne et al., 2008

Appendix O continues below.

Sample Number	Latitude	Longitude	Site	$\delta^{13}\text{C}_{\text{Bulk}}$	$\delta^{15}\text{N}_{\text{Bulk}}$	% Yield	%C	%N	C/N
GDY1	71°N	79°E	Gydan Peninsula	-21.1	9.8	18.9	44	15	3.3

References:

- Debruyne, R., Chu, G., King, C.E., Bos, K., Kuch, M., Schwarz, C., Szpak, P., Gröcke, D.R., Matheus, P., Zazula, G., Guthrie, D., Froese, D., Buigues, B., de Marliave, C., Flemming, C., Poinar, D., Fisher, D., Southon, J., Tikhonov, A.N., MacPhee, R.D.E., Poinar, H.N., 2008. Out of America: ancient DNA evidence for a new world origin of late Quaternary woolly mammoths. *Curr. Biol.* 18, 1320–6. doi:10.1016/j.cub.2008.07.061
- Szpak, P., Gröcke, D.R., Debruyne, R., MacPhee, R.D.E., Guthrie, R.D., Froese, D., Zazula, G.D., Patterson, W.P., Poinar, H.N., 2010. Regional differences in bone collagen $\delta^{13}\text{C}$ and $\delta^{15}\text{N}$ of Pleistocene mammoths: implications for paleoecology of the mammoth steppe. *Palaeogeogr. Palaeoclimatol. Palaeoecol.* 286, 88–96. doi:10.1016/j.palaeo.2009.12.009

Appendix P Sample information for megafaunal herbivores from Herschel Island.

Lab ID	Common Name	Scientific Name	Sample Number	Stable Isotope Reference	¹⁴ C Date	Date Lab #	Date reference
YT126	Caribou	<i>Rangifer tarandus</i>	381.52	Chapter 2 Metcalfe, 2011	post-bomb	AA103889	Chapter 2
YT46	Mammoth	<i>Mammuthus</i>	271.93	Metcalfe, 2011			
YT40	Mammoth	<i>Mammuthus</i>	68.4	Metcalfe, 2011	>35,900	AA84988	Metcalfe, 2011
YT39	Mammoth	<i>Mammuthus</i>	68.2	Metcalfe, 2011			
YT38	Mastodon	<i>Mammut</i>	33.3	Metcalfe, 2011	>45 130	Beta 189291	Zazula et al., 2009
	Muskox	<i>Ovibos</i>	CMNFV 17678	Raghavan et al., 2014	1100 ± 40		Raghavan et al., 2014
	Muskox	<i>Ovibos</i>	YHR 155.7	Raghavan et al., 2014	17265 ± 65		Raghavan et al., 2014
	Muskox	<i>Ovibos</i>	YHR 206.48	Raghavan et al., 2014	20080 ± 150		Raghavan et al., 2014
	Muskox	<i>Ovibos</i>	YHR271.128	Raghavan et al., 2014	45700 ± 2600		Raghavan et al., 2014
	Muskox	<i>Ovibos</i>	YHR 206.42	Raghavan et al., 2014	46700 ± 2300		Raghavan et al., 2014
	Muskox	<i>Ovibos</i>	YHR 12.26	Raghavan et al., 2014	49200 ± 3500		Raghavan et al., 2014
	Muskox	<i>Ovibos</i>	YHR 151.1	Raghavan et al., 2014	51700 ± 1100		Raghavan et al., 2014
	Muskox	<i>Ovibos</i>	YHR 271.35	Raghavan et al., 2014	12590 ± 75		Raghavan et al., 2014
	Muskox	<i>Ovibos</i>	YHR 271.129	Raghavan et al., 2014	12600 ± 100		Raghavan et al., 2014
	Muskox	<i>Ovibos</i>	YHR 12.42	Raghavan et al., 2014	14770 ± 120		Raghavan et al., 2014
	Muskox	<i>Ovibos</i>	YHR 271.12	Raghavan et al., 2014	24160 ± 210		Raghavan et al., 2014

Appendix P continues below.

Lab ID	Site	Tissue	Tissue Type	Source	$\delta^{13}\text{C}_{\text{Bulk}}$	$\delta^{15}\text{N}_{\text{Bulk}}$	% Yield	%C	%N	C/N
YT126		B	Right occipital condyle	YG	-21.0	2.6	18.0	34.6	11.9	3.4
YT46	Simpson Point	B	thoracic vertebra	YG	-21.6	5.5	14.8	41.7	15.5	3.1
YT40	Simpson Point	C		YG	-21.5	6.8	14.1	42.4	15.9	3.1
YT39	Simpson Point	D		YG	-21.7	9.7	9.0	44.4	16.2	3.2
YT38	Simpson Point	B	cubeoid	YG	-21.8	5.8	13.9	41.8	15.1	3.2
	Herschel Island	B			-20.5	4.3	6.7	43.6	16.1	3.2
	Herschel Island	B			-19.1	8.0	12.9	44.8		3.1

Herschel Island	B	-19.3	7.4	5.0	44.1	16.2	3.2
Herschel Island	B	-19.3	8.0	7.6	44.8	16.5	3.2
Herschel Island	B	-19.9	4.7	9.0	44.7	16.3	3.2
Herschel Island	B	-19.1	7.4	12.5	44.4	16.4	3.2
Herschel Island	B	-19.3	6.4	14.4	43.4		3.1
Herschel Island	B	-20.3	8.5	11.6	44.2	16.4	3.2
Herschel Island	B	-20.0	8.9	12.3	43.9	16.3	3.2
Herschel Island	B	-19.5	8.7	4.1	43.8	16.2	3.2
Herschel Island	B	-18.6	7.9	3.8	43.8	16.2	3.2

YG = Yukon Government Paleontology Program

Tissue: B = Bone; RD = Root dentin; C = Cementum; D = Crown dentin; T= Tusk dentin

References:

Metcalfe, J.Z., 2011. Late Pleistocene climate and proboscidean paleoecology in North America: insights from stable isotope compositions of skeletal remains. Doctoral Thesis. University of Western Ontario.

Raghavan, M., Espregueira Themudo, G., Smith, C.I., Zazula, G., Campos, P.F., 2014. Musk ox (*Ovibos moschatus*) of the mammoth steppe: tracing palaeodietary and palaeoenvironmental changes over the last 50,000 years using carbon and nitrogen isotopic analysis. *Quat. Sci. Rev.* 102, 192–201.
doi:10.1016/j.quascirev.2014.08.001

Zazula, G., Hare, P., Storer, J., 2009. New radiocarbon-dated vertebrate fossils from Herschel Island: implications for the palaeoenvironments and glacial chronology of the Beaufort Sea coastlands. *Arctic* 273–280.

Appendix Q Sample information for megafaunal herbivores from the Klondike area.

Lab ID	Common Name	Scientific Name	Sample Number	Stable Isotope Reference	¹⁴ C Date	Date Lab #	Date reference
YT135	Caribou	<i>Rangifer tarandus</i>	126.6	Chapter 2			
YT136	Caribou	<i>Rangifer tarandus</i>	126.13	Chapter 2			
YT137	Caribou	<i>Rangifer tarandus</i>	126.31	Chapter 2			
YT138	Caribou	<i>Rangifer tarandus</i>	306.194	Chapter 2			
YT139	Caribou	<i>Rangifer tarandus</i>	376.47	Chapter 2			
YT140	Caribou	<i>Rangifer tarandus</i>	378.48	Chapter 2			
YT141	Caribou	<i>Rangifer tarandus</i>	404.321	Chapter 2			
YT142	Caribou	<i>Rangifer tarandus</i>	406.665	Chapter 2			
YT143	Caribou	<i>Rangifer tarandus</i>	407.304	Chapter 2			
YT144	Caribou	<i>Rangifer tarandus</i>	421.163	Chapter 2			
YT145	Caribou	<i>Rangifer tarandus</i>	435.103	Chapter 2			
YT87	Elk	<i>Cervus elaphus</i>	192.1	Chapter 2	10,825±50	OxA20920	Meiri et al., 2014
YT92	Elk	<i>Cervus elaphus</i>	377.43	Chapter 2			
						UCIAMS	
YT94	Elk	<i>Cervus elaphus</i>	Fa06-141	Chapter 2	10960 ±30	88769	Zazula, 2015
YT97	Horse	<i>Equus sp.</i>	126.26	Chapter 5	35,800	AA103821	Chapter 5
YT30	Mammoth	<i>Mammuthus</i>	302.26	Mecalfe, 2011	>39,200	AA84983	Mecalfe, 2011
YT31	Mammoth	<i>Mammuthus</i>	2.4	Mecalfe, 2011	27380±730	AA85000	Mecalfe, 2011
		<i>Mammuthus primigenius</i>					
YT27	Mammoth	<i>Mammuthus primigenius</i>	29.248	Mecalfe, 2011	43500±1900	UCIAMS41493	Debruyne et al., 2008
YT29	Mammoth	<i>Mammuthus</i>	358.1	Mecalfe, 2011			
		<i>Mammuthus sp.</i>					
YT49	Mammoth	<i>Mammuthus sp.</i>	5.46	Mecalfe, 2011	22430±140	UCIAMS41487	Debruyne et al., 2008
YT28a	Mammoth	<i>Mammuthus</i>	6.51, 6.49	Mecalfe, 2011	17950±120	Beta 70099	Mecalfe, 2011
		<i>Mammuthus primigenius</i>				UCIAMS	
YT47	Mammoth	<i>Mammuthus primigenius</i>	2.7	Mecalfe, 2011	27540±270	41488	Debruyne et al., 2008
		<i>Mammuthus sp.</i>					
YT48	Mammoth	<i>Mammuthus sp.</i>	133.21	Mecalfe, 2011	34180±590	UCIAMS41489	Debruyne et al., 2008
		<i>Mammuthus primigenius</i>					
YT26	Mammoth	<i>Mammuthus primigenius</i>	2.14	Mecalfe, 2011	35500±2000	AA84986	Mecalfe, 2011
YT25	Mammoth	<i>Mammuthus</i>	2.16	Mecalfe, 2011			

YT32	Mammoth	<i>Mammuthus</i>	84.1	Mecalfe, 2011			
YT24	Mammoth	<i>Mammuthus primigenius</i>	78.1	Mecalfe, 2011	>48,800	UCIAMS41491	Debruyne et al., 2008
	Mammoth	<i>Mammuthus primigenius</i>	NMC 42292	Szpak et al., 2010	37,920±2,700	AA17535	Debruyne et al., 2008
	Mammoth	<i>Mammuthus primigenius</i>	NMC 49927	Szpak et al., 2010	46,600±200	UCIAMS39883	Debruyne et al., 2008
	Mammoth	<i>Mammuthus primigenius</i>	NMC 49928	Szpak et al., 2010	>46,200	UCIAMS39884	Debruyne et al., 2008
	Mammoth	<i>Mammuthus sp.</i>	YU 130.2	Szpak et al., 2010	36,690±810	UCIAMS39891	Debruyne et al., 2008
	Mammoth	<i>Mammuthus sp.</i>	YU 133.18	Szpak et al., 2010	32,140±370	UCIAMS38675	Debruyne et al., 2008
	Mammoth	<i>Mammuthus primigenius</i>	YU 136.9	Szpak et al., 2010	45,900±2,600	UCIAMS39116	Debruyne et al., 2008
	Mammoth	<i>Mammuthus primigenius</i>	YU 137.3	Szpak et al., 2010	39,800±1,200	UCIAMS39892	Debruyne et al., 2008
	Mammoth	<i>Mammuthus primigenius</i>	YU 3.133	Szpak et al., 2010	29,030+310	UCIAMS39112	Debruyne et al., 2008
	Mammoth	<i>Mammuthus primigenius</i>	YU 3.135	Szpak et al., 2010	45,700±2,500	UCIAMS39113	Debruyne et al., 2008
	Mammoth	<i>Mammuthus primigenius</i>	YU 3.136	Szpak et al., 2010	29,170±320	UCIAMS39114	Debruyne et al., 2008
	Mammoth	<i>Mammuthus primigenius</i>	YU 3.19	Szpak et al., 2010	44,700±2,200	UCIAMS39887	Debruyne et al., 2008
	Mammoth	<i>Mammuthus primigenius</i>	YU 3.229	Szpak et al., 2010			
	Mammoth	<i>Mammuthus primigenius</i>	YU 3.256	Szpak et al., 2010	28,960±310	UCIAMS39115	Debruyne et al., 2008
	Mammoth	<i>Mammuthus primigenius</i>	YU 5.13	Szpak et al., 2010	32,470±480	UCIAMS39889	Debruyne et al., 2008
	Mammoth	<i>Mammuthus primigenius</i>	YU 5.46	Szpak et al., 2010	22,430±140	UCIAMS41487	Debruyne et al., 2008
	Mammoth	<i>Mammuthus primigenius</i>	YU 5.69	Szpak et al., 2010	>47,500	UCIAMS39888	Debruyne et al., 2008

	Mammoth	<i>Mammuthus primigenius</i>	YU 52.36	Szpak et al., 2010	30,630±870	UCIAMS39890	Debruyne et al., 2008
YT35	Mastodon	<i>Mammut</i>	26.1	Zazula et al., 2014	>51,700	UCIAMS78704	Zazula et al., 2014
YT36	Mastodon	<i>Mammut</i>	50.1	Mecalfe, 2011	>41,100	AA84994	Metcalf (2011)
YT37	Mastodon	<i>Mammut</i>	139.5	Mecalfe, 2011	>41,100	AA84985	Metcalf (2011)
YT33	Mastodon	<i>Mammut</i>	159.83	Mecalfe, 2011			
YT34	Mastodon	<i>Mammut</i>	43.2	Zazula et al., 2014	>49,200	UCIAMS75320	Zazula et al., 2014
K-33897	Mastodon	<i>Mammut</i>		Zazula et al., 2014	>51700	UCIAMS78694	Zazula et al., 2014
	Mastodon	<i>Mammut</i>		Zazula et al., 2014	>51700	UCIAMS78698	Zazula et al., 2014
	Mastodon	<i>Mammut</i>		Zazula et al., 2014	>51700	UCIAMS78699	Zazula et al., 2014
	Mastodon	<i>Mammut</i>		Zazula et al., 2014	>51700	UCIAMS78700	Zazula et al., 2014
	Mastodon	<i>Mammut</i>	CMN 333	Zazula et al., 2014	>47,800	UCIAMS83803	Zazula et al., 2014
	Mastodon	<i>Mammut</i>	F:AM: 103842	Zazula et al., 2014	42,100±1,300	UCIAMS 88773	Zazula et al., 2014
	Mastodon	<i>Mammut</i>	YG 361.9	Zazula et al., 2014	>49,900	UCIAMS72419	Zazula et al., 2014
YT96	Moose	<i>Alces alces</i>	29.69	Chapter 2			
YT99	Moose	<i>Alces alces</i>	134.1	Chapter 2			
YT100	Moose	<i>Alces alces</i>	136.1	Chapter 2			
YT101B	Moose	<i>Alces alces</i>	193.1	Chapter 2			
YT102	Moose	<i>Alces alces</i>	269.1	Chapter 2	2,700±29	OxA22266	Meiri et al., 2014
YT103	Moose	<i>Alces alces</i>	300.2	Chapter 2			
YT105	Moose	<i>Alces alces</i>	300.96	Chapter 2	4,916±33	OxA22265	Meiri et al., 2014
YT106	Moose	<i>Alces alces</i>	308.21	Chapter 2			
YT107	Moose	<i>Alces alces</i>	354.3	Chapter 2			
YT108	Moose	<i>Alces alces</i>	355.113	Chapter 2	152±26	OxA22264	Meiri, 2010
YT110	Moose	<i>Alces alces</i>	376.56	Chapter 2			
	Muskox	<i>Obivos</i>	YHR 276.1	Raghavan et al., 2014	9280 ± 60		Raghavan et al., 2014
	Muskox	<i>Obivos</i>	YHR157.24	Raghavan et al., 2014	38350 ± 900		Raghavan et al., 2014

	Muskox	<i>Ovibos moschatus</i>	CMNFV 44525	Raghavan et al., 2014	> 46400		Raghavan et al., 2014
	Muskox	<i>Ovibos moschatus</i>	CMNFV 42049	Raghavan et al., 2014	> 49000		Raghavan et al., 2014
	Muskox	<i>Ovibos moschatus</i>	CMNFV 47248	Raghavan et al., 2014	> 49400		Raghavan et al., 2014
	Muskox	<i>Ovibos moschatus</i>	CMNFV 46449	Raghavan et al., 2014	> 49436		Raghavan et al., 2014
	Muskox	<i>Ovibos moschatus</i>	CMNFV 46689	Raghavan et al., 2014	> 49634		Raghavan et al., 2014
	Muskox	<i>Ovibos moschatus</i>	CMNFV 46438	Raghavan et al., 2014	> 49662		Raghavan et al., 2014
	Muskox	<i>Ovibos moschatus</i>	CMNFV 46657	Raghavan et al., 2014	> 49724		Raghavan et al., 2014
	Muskox	<i>Ovibos moschatus</i>	CMNFV 46637	Raghavan et al., 2014	> 49738		Raghavan et al., 2014
YT111	Sheep	<i>Ovis dalli</i>	312.1	Chapter 5	18,120±240	AA103830	Chapter 5
YT112	Sheep	<i>Ovis dalli</i>	328.141	Chapter 5	13,850±150	AA103831	Chapter 5
YT113	Sheep	<i>Ovis dalli</i>	328.158	Chapter 5			
YT114	Sheep	<i>Ovis dalli</i>	328.16	Chapter 5			
YT115	Sheep	<i>Ovis dalli</i>	328.17	Chapter 5			
YT116	Sheep	<i>Ovis dalli</i>	328.211	Chapter 5			
YT117	Sheep	<i>Ovis dalli</i>	328.278	Chapter 5			
YT118	Sheep	<i>Ovis dalli</i>	328.279	Chapter 5			
YT119	Sheep	<i>Ovis dalli</i>	328.99	Chapter 5			
YT120	Sheep	<i>Ovis dalli</i>	376.31	Chapter 5			
YT134	Sheep	<i>Ovis dalli</i>	3.216	Chapter 5			

Appendix Q continues below.

Lab ID	Latitude	Longitude	Site	Source	Tissue	Tissue Type	$\delta^{13}\text{C}_{\text{Bulk}}$	$\delta^{15}\text{N}_{\text{Bulk}}$	% Yield	%C	%N	C/N
YT135			Irish Gulch	YG	B	tibia	-18.1	4.0	13.6	38.0	13.7	3.2
YT136			Irish Gulch	YG	B	metatarsal	-18.5	3.1	17.0	39.3	14.3	3.2
YT137			Irish Gulch	YG	B	cranium	-18.7	6.8	16.7	41.7	15.2	3.2
YT138				YG	B		-19.6	6.0	9.6	36.7	13.2	3.3
YT139				YG	B		-18.5	4.1	7.6	33.4	12.8	3.3
YT140				YG	B		-17.7	6.1	9.6	37.2	13.4	3.2
YT141				YG	B		-19.0	5.4	10.6	38.3	13.9	3.2
YT142				YG	B		-18.1	3.1	5.7	38.6	14.1	3.2
YT143				YG	B		-18.5	7.3	12.4	33.6	12.3	3.2
YT144				YG	B		-18.2	8.7	7.0	36.7	13.2	3.2
YT145				YG	B		-18.9	4.8	7.4	37.4	13.5	3.2
YT87	63°57N	138°57W	Goldbottom Creek	YG	B	metacarpal	-19.8	1.6	9.5	38.6	14.6	3.1

YT92	63°53N	138°54W	No Bottom Gulch	YG	B		-20.0	1.9	11.1	39.0	14.8	3.1
YT94	62°36N	140°56W	Little John Site	YG	B	innominate fragment	-19.7	1.6	12.3	39.6	14.9	3.1
YT97					B		-20.8	4.9	11.4	40.0	14.6	3.2
YT30			Skookum Gulch		B		-20.3	5.8	18.0	41.5	15.6	3.1
YT31			Hester Creek		B		-20.5	7.0	13.0	37.8	14.1	3.1
YT27	63°59N	139°02W	Hunker Creek		B		-21.1	7.0	13.5	44.4	16.3	3.2
YT29					B		-20.6	7.2	12.7	42.0	15.2	3.2
YT49	63°59N	139°02W	Hunker Creek		B		-21.3	8.7	20.6	45.0	16.3	3.2
YT28a			Gold Run Creek		B		-20.7	10.5	19.1	47.5	18.0	3.1
YT47	63°58N	139°03W	Hester Creek		B		-20.6	6.5	16.8	46.8	17.6	3.1
YT48	64°43N	138°38W	Whitman Gulch		B		-20.7	6.8	21.0	46.6	17.3	3.1
YT26			Hester Creek		C		-20.5	7.4	15.3	43.3	16.0	3.2
YT25			Hester Creek		C		-21.2	8.0	7.3	42.0	15.5	3.2
YT32			Hunker Creek		C		-20.7	7.7	12.4	45.9	16.9	3.2
YT24	63°59N	139°06W	Last Chance Creek		RD	M6	-20.8	8.2	20.2	45.7	16.9	3.2
	64°03N	139°25W	Dawson area		C/D/RD		-20.6	7.9	13.7	39.4	13.5	3.4
	64°03N	139°25N	Dawson area		C/D/RD		-20.4	8.7	19.9	37.8	13.3	3.3
	64°03N	139°25W	Dawson area		C/D/RD		-20.3	6.9	19.7	37.3	13.0	3.3
	63°49N	139°02W	Quartz Creek		B		-20.5	6.6	13.3	35.0	12.4	3.3
	63°43N	138°38W	Whitman Gulch		B		-20.7	8.1	17.8	39.5	14.8	3.1
	63°44N	138°50W			B		-20.8	7.5	12.9	41.1	14.5	3.3
	63°43N	138°38W	Whitman Gulch		B		-20.5	7.3	13.0	31.0	11.0	3.3
	63°50N	138°15W	Finning		B		-20.5	7.2	22.8	38.5	13.6	3.3
	63°50N	138°15W	Finning		B		-20.6	6.4	16.5	39.7	13.8	3.4
	63°50N	138°15W	Finning		B		-20.9	7.1	18.6	30.3	10.8	3.3
	63°50N	138°15W	Finning		B		-20.6	5.7	19.5	38.3	13.5	3.3
	63°50N	138°15W	Finning		B		-20.5	7.1	22.9	37.4	13.3	3.3
	63°50N	138°15W	Finning		B		-20.6	6.8	10.4	39.7	14.0	3.3

	63°59N	139°02W	Hunker Creek		B		-20.6	6.9	14.5	33.5	12.5	3.1
	63°59N	139°02W	Hunker Creek		B		-21.0	9.4	11.4	37.7	13.3	3.3
	63°59N	139°02W	Hunker Creek		B		-20.7	9.0	13.2	36.7	13.0	3.3
	63°46N	139°19W	Indian River		B		-20.9	6.4	12.0	36.8	13.3	3.2
YT35			Gold Run Creek	YG	RD	M6	-20.3	4.8	19.9	41.8	15.2	3.2
YT36			Thistle Creek	YG	RD	M5?	-21.2	4.3	12.6	41.7	15.6	3.1
YT37			Unknown?	YG	B	mandible	-20.6	3.5	14.5	42.0	15.0	3.3
YT33			Quartz Creek	YG	B	fibula	-20.9	6.9	18.5	43.2	15.8	3.2
YT34			Upper Gold Run	YG	RD	M6	-19.9	5.3	10.0	44.2	16.2	3.2
K-33897			Sixtymile Loc. 5	CMN			-19.9	4.9	7.6	42.7	15.7	3.2
			Dawson Loc. 19	CMN			-20.5	4.6	8.5	42.2	15.4	3.2
			Sixtymile Loc. 3	CMN			-20.1	3.0	4.0	42.2	15.1	3.3
			Dawson	CMN			-20.8	4.3	8.4	42.9	15.6	3.2
			McQuesten Creek	CMN			-20.3	4.1	7.6	43.4	15.8	3.2
			Hunker Creek	AMNH			-21.4	3.6	4.1	43.5	15.3	3.3
			Bonanza Creek	YG			-20.7	3.2	8.9	41.0	14.5	3.3
YT96				YG	B		-21.1	1.2	9.9	36.8	13.9	3.1
YT99				YG	B		-20.0	1.6	7.4	37.2	14.2	3.0
YT100				YG	B		-20.6	1.9	9.6	38.9	14.6	3.1
YT101B				YG	B		-20.0	3.0	18.4	39.9	15.3	3.0
YT102			Quartz Creek	YG	B	humerus	-20.6	2.2	7.5	38.0	14.4	3.1
YT103				YG	B		-20.0	2.7	9.9	40.0	15.1	3.1
YT105			Lindow Creek	YG	B	metatarsal	-20.6	2.5	8.4	37.3	14.2	3.1
YT106				YG	B		-21.0	1.5	19.2	40.4	15.6	3.0
YT107				YG	B		-20.7	2.3	12.5	38.6	14.8	3.0
YT108			Green Gulch	YG	B		-21.0	3.2	14.7	39.6	14.8	3.1
YT110				YG	B		-20.2	2.1	17.8	37.8	14.6	3.0
			Klondike	YG	B		-18.8	3.2	77.0	44.8	16.5	3.2

			Klondike	YG	B		-19.7	6.8	4.6	44.1	16.1	3.2
			Dawson Area	CMN	B		-18.9	7.7	7.6	43.0	15.7	3.2
			Sixtymile Area	CMN	B		-20.2	4.2	4.7	42.4	15.5	3.2
			Sixtymile Area	CMN	B		-19.3	2.4	7.5	44.7	16.2	3.2
			Sixtymile Area	CMN	B		-19.7	6.2	7.7	44.0	16.1	3.2
			Sixtymile Area	CMN	B		-19.8	7.5	7.2	44.3	16.2	3.2
			Sixtymile Area	CMN	B		-19.8	6.4	6.9	41.2	15.0	3.2
			Sixtymile Area	CMN	B		-19.4	4.1	7.0	42.6	15.5	3.2
			Sixtymile Area	CMN	B		-19.4	6.8	11.9	43.2	15.9	3.2
YT111	64°N	139°0W	Hunker Creek	YG	B	metatarsal	-19.0	7.5	11.3	35.9	13.9	3.0
YT112	64°N	139°9W	Hunker Creek	YG	B	tibia	-19.6	3.9	10.0	34.9	12.7	3.2
YT113	64°N	139°9W	Hunker Creek	YG	B	humerus	-18.7	7.5	6.9	37.2	14.1	3.1
YT114	64°N	139°9W	Hunker Creek	YG	B	tibia	-18.6	6.8	18.0	41.5	16.1	3.0
YT115	64°N	139°9W	Hunker Creek	YG	B	radio-ulna	-19.8	7.3	15.3	39.7	15.1	3.1
YT116	64°N	139°9W	Hunker Creek	YG	B	tibia	-18.8	4.2	9.8	37.6	14.3	3.1
YT117	64°N	139°9W	Hunker Creek	YG	B	humerus	-19.3	4.4	12.0	40.5	14.8	3.2
YT118	64°N	139°9W	Hunker Creek	YG	B	metatarsal	-19.3	7.7	8.3	35.9	13.1	3.2
YT119	64°N	139°9W	Hunker Creek	YG	B	radius	-18.9	5.2	16.2	37.7	14.3	3.1
YT120	64°N	139°9W	Hunker Creek	YG	B	metacarpal	-19.1	4.7	18.3	41.4	15.6	3.1
YT134				YG	B		-18.4	3.2	8.7	33.4	11.8	3.3

Samples analyzed multiple times (duplicate/triplicate) in Chapter 5 are in bold

Dates obtained in Chapter 5 are in bold

YG = Yukon Government Paleontology Program; CMN = Canadian Museum of Nature; AMNH = American Museum of Natural History

Tissue: B = Bone; RD = Root dentin; C = Cementum; D = Crown dentin; T= Tusk dentin

References:

Debruyne, R., Chu, G., King, C.E., Bos, K., Kuch, M., Schwarz, C., Szpak, P., Gröcke, D.R., Matheus, P., Zazula, G., Guthrie, D., Froese, D., Buigues, B., de Marliave, C., Flemming, C., Poinar, D., Fisher, D., Southon, J., Tikhonov, A.N., MacPhee, R.D.E.,

- Poinar, H.N., 2008. Out of America: ancient DNA evidence for a new world origin of late Quaternary woolly mammoths. *Curr. Biol.* 18, 1320–6. doi:10.1016/j.cub.2008.07.061
- Metcalf, J.Z., 2011. Late Pleistocene climate and proboscidean paleoecology in North America: insights from stable isotope compositions of skeletal remains. Doctoral Thesis. University of Western Ontario.
- Meiri, M., 2010. The role of environmental change in species range shifts – analysis of Quaternary deer using ancient DNA. Doctoral Thesis. University of London.
- Meiri, M., Lister, A.M., Collins, M.J., Tuross, N., Goebel, T., Blockley, S., Zazula, G.D., van Doorn, N., Guthrie, R.D., Boeskorov, G.G., Baryshnikov, G.F., Sher, A., Barnes, I., 2014. Faunal record identifies Bering isthmus conditions as constraint to end-Pleistocene migration to the New World. *Proc. Biol. Sci.* 281, 20132167. doi:10.1098/rspb.2013.2167
- Raghavan, M., Espregueira Themudo, G., Smith, C.I., Zazula, G., Campos, P.F., 2014. Musk ox (*Ovibos moschatus*) of the mammoth steppe: tracing palaeodietary and palaeoenvironmental changes over the last 50,000 years using carbon and nitrogen isotopic analysis. *Quat. Sci. Rev.* 102, 192–201. doi:10.1016/j.quascirev.2014.08.001
- Szpak, P., Gröcke, D.R., Debruyne, R., MacPhee, R.D.E., Guthrie, R.D., Froese, D., Zazula, G.D., Patterson, W.P., Poinar, H.N., 2010. Regional differences in bone collagen $\delta^{13}\text{C}$ and $\delta^{15}\text{N}$ of Pleistocene mammoths: implications for paleoecology of the mammoth steppe. *Palaeogeogr. Palaeoclimatol. Palaeoecol.* 286, 88–96. doi:10.1016/j.palaeo.2009.12.009
- Zazula, G.D., MacPhee, R.D., Metcalfe, J.Z., Reyes, A. V., Brock, F., Druckenmiller, P.S., Groves, P., Harington, R., Hodgins, G.W.L., Kunz, M.L., Longstaffe, F.J., Mann, D.H., McDonald, H.G., Nalawade-Chavan, S., Southon, J.R., 2014. American mastodon extirpation in the Arctic and Subarctic predates human colonization and terminal Pleistocene climate change. *Proc. Natl. Acad. Sci.* 111, 18460–18465.
- Zazula, G., Personal communication (e-mail), 2015

Appendix R Sample information for megafaunal herbivores from the North Slope.

Lab ID/Fie Id ID	Common Name	Scientific Name	Sample Number	Stable Isotope Reference	¹⁴ C Date	Date Lab #	Date reference	Site	Tissue	Tissue Type	Source	$\delta^{13}\text{C}_{\text{Bulk}}$	$\delta^{15}\text{N}_{\text{Bulk}}$
IK98-0343	Bison	<i>Bison priscus</i>	UAMES 9079	Mann et al., 2013	10,510 ±50	CAMS-53767	Mann et al., 2013	Ikpikpuk R.	B	humerus	UAMES	-20.6	2.8
IK98-1114	Bison	<i>Bison priscus</i>	UAMES 9896	Mann et al., 2013	10,990 ±50	CAMS-53891	Mann et al., 2013	Ikpikpuk R.	B	astragalus	UAMES	-20.1	2.7
IK98-0027	Bison	<i>Bison priscus</i>	UAMES 8847	Mann et al., 2013	11,810 ±50	CAMS-53756	Mann et al., 2013	Ikpikpuk R.	B	astragalus	UAMES	-20.7	2.6
IK98-0528	Bison	<i>Bison priscus</i>	UAMES 9577	Mann et al., 2013	12,270 ±50	CAMS-53774	Mann et al., 2013	Ikpikpuk R.	B	humerus	UAMES	-20.2	4.1
IK98-0303	Bison	<i>Bison priscus</i>		Mann et al., 2013	12,320 ±60	CAMS-58091	Mann et al., 2013	Ikpikpuk R.	B	vertebra	UAMES	-20.2	3.7
IK98-0142	Bison	<i>Bison priscus</i>	UAMES 8801	Mann et al., 2013	12,410 ±50	CAMS-53760	Mann et al., 2013	Ikpikpuk R.	B	metatarsal	UAMES	-20.0	2.7
IK01-428	Bison	<i>Bison priscus</i>	UAMES 11664	Mann et al., 2013	12,560 ±130	AA-48281	Mann et al., 2013	Ikpikpuk R.	B	astragalus	UAMES	-20.0	2.7
IK98-0661	Bison	<i>Bison priscus</i>	UAMES 9464	Mann et al., 2013	17,160 ±80	CAMS-53777	Mann et al., 2013	Ikpikpuk R.	B	metapodial	UAMES	-20.2	2.8
IK98-0504	Bison	<i>Bison priscus</i>	UAMES 9238	Mann et al., 2013	19,420 ±100	CAMS-53772	Mann et al., 2013	Ikpikpuk R.	B	femur	UAMES	-20.0	3.8
IK98-1090	Bison	<i>Bison priscus</i>	UAMES 9804	Mann et al., 2013	21,040 ±120	CAMS-53890	Mann et al., 2013	Ikpikpuk R.	B	astragalus	UAMES	-20.0	6.5
IK98-0401	Bison	<i>Bison priscus</i>	UAMES 8842	Mann et al., 2013	21,530 ±130	CAMS-53770	Mann et al., 2013	Ikpikpuk R.	B	metatarsal	UAMES	-20.4	4.4
IK98-1254	Bison	<i>Bison priscus</i>	UAMES 9967	Mann et al., 2013	23,680 ±170	CAMS-53901	Mann et al., 2013	Ikpikpuk R.	B	humerus	UAMES	-19.9	5.5
IK98-0302	Bison	<i>Bison priscus</i>	UAMES 8998	Mann et al., 2013	24,500 ±180	CAMS-53764	Mann et al., 2013	Ikpikpuk R.	B	metatarsal	UAMES	-20.2	4.3
IK98-1184	Bison	<i>Bison priscus</i>	UAMES 10031	Mann et al., 2013	25,980 ±230	CAMS-53899	Mann et al., 2013	Ikpikpuk R.	B	horn core	UAMES	-19.7	4.2
IK98-1043	Bison	<i>Bison priscus</i>	UAMES 10043	Mann et al., 2013	26,550 ±230	CAMS-53888	Mann et al., 2013	Ikpikpuk R.	B	astragalus	UAMES	-19.5	5.7

IK98-0095	Bison	<i>Bison priscus</i>	UAMES 9206	Mann et al., 2013	27,400 ±260	CAMS-53758	Mann et al., 2013	Ikpikpuk R.	B	tibia	UAMES	-20.6	4.6
IK98-0374	Bison	<i>Bison priscus</i>		Mann et al., 2013	27,590 ±280	CAMS-53768	Mann et al., 2013	Ikpikpuk R.	B	metatarsal	UAMES	-20.5	2.7
IK98-1115	Bison	<i>Bison priscus</i>	UAMES 9897	Mann et al., 2013	28,120 ±290	CAMS-53892	Mann et al., 2013	Ikpikpuk R.	B	astragalus	UAMES	-19.3	4.8
IK98-0616	Bison	<i>Bison priscus</i>	UAMES 9648	Mann et al., 2013	29,040 ±340	CAMS-53775	Mann et al., 2013	Ikpikpuk R.	B	metacarpal	UAMES	-20.2	5.2
IK98-1164	Bison	<i>Bison priscus</i>	UAMES 10073	Mann et al., 2013	29,570 ±340	CAMS-53897	Mann et al., 2013	Ikpikpuk R.	B	metacarpal	UAMES	-20.0	5.0
IK98-0256	Bison	<i>Bison priscus</i>	UAMES 9156	Mann et al., 2013	31,410 ±420	CAMS-53763	Mann et al., 2013	Ikpikpuk R.	B	metatarsal	UAMES	-20.4	4.2
IK98-0096	Bison	<i>Bison priscus</i>	UAMES 9207	Mann et al., 2013	31,630 ±440	CAMS-53759	Mann et al., 2013	Ikpikpuk R.	B	tibia	UAMES	-19.9	4.9
IK98-1035	Bison	<i>Bison priscus</i>	UAMES 9988	Mann et al., 2013	32,270 ±470	CAMS-53885	Mann et al., 2013	Ikpikpuk R.	B	humerus	UAMES	-19.6	5.3
IK01-215	Bison	<i>Bison priscus</i>	UAMES 11742	Mann et al., 2013	32,300 ±1,500	AA-48772	Mann et al., 2013	Ikpikpuk R.	B	metatarsal	UAMES	-20.2	4.4
IK01-433	Bison	<i>Bison priscus</i>	UAMES 11669	Mann et al., 2013	33,000 ±1,500	AA-48282	Mann et al., 2013	Ikpikpuk R.	B	radius	UAMES	-19.9	3.5
IK98-0012	Bison	<i>Bison priscus</i>	UAMES 9172	Mann et al., 2013	33,280 ±530	CAMS-53755	Mann et al., 2013	Ikpikpuk R.	B	femur	UAMES	-19.4	3.5
IK98-1323	Bison	<i>Bison priscus</i>	UAMES 9877	Mann et al., 2013	33,320 ±540	CAMS-53903	Mann et al., 2013	Ikpikpuk R.	B	femur	UAMES	-20.2	4.4
IK01-460	Bison	<i>Bison priscus</i>	UAMES 11934	Mann et al., 2013	33,520 ±940	AA-48775	Mann et al., 2013	Ikpikpuk R.	B	astragalus	UAMES	-19.9	5.1
IK98-1121	Bison	<i>Bison priscus</i>	UAMES 11159	Mann et al., 2013	33,580 ±550	CAMS-53894	Mann et al., 2013	Ikpikpuk R.	B	metacarpal	UAMES	-19.6	3.8
IK01-234	Bison	<i>Bison priscus</i>	UAMES 11947	Mann et al., 2013	34,100 ±1,000	AA-48773	Mann et al., 2013	Ikpikpuk R.	B	astragalus	UAMES	-20.0	5.9
IK98-0659	Bison	<i>Bison priscus</i>	UAMES 9462	Mann et al., 2013	35,580 ±720	CAMS-53776	Mann et al., 2013	Ikpikpuk R.	B	mandible	UAMES	-20.0	4.6
IK98-0916	Bison	<i>Bison priscus</i>	UAMES 9348	Mann et al., 2013	35,710 ±730	CAMS-53782	Mann et al., 2013	Ikpikpuk R.	B	astragalus	UAMES	-20.3	4.2
IK98-1222	Bison	<i>Bison priscus</i>	UAMES 9899	Mann et al., 2013	36,320 ±780	CAMS-53900	Mann et al., 2013	Ikpikpuk R.	B	metatarsal	UAMES	-20.8	5.7

IK01-373	Bison	<i>Bison priscus</i>	UAMES 11981	Mann et al., 2013	36,500 ±2,300	AA-48278	Mann et al., 2013	Ikpikpuk R.	B	astragalus	UAMES	-20.0	6.4
IK98-0863	Bison	<i>Bison priscus</i>	UAMES 9327	Mann et al., 2013	36,520 ±800	CAMS-53914	Mann et al., 2013	Ikpikpuk R.	B	astragalus	UAMES	-20.6	4.5
IK98-1120	Bison	<i>Bison priscus</i>	UAMES 9906	Mann et al., 2013	37,460 ±890	CAMS-53893	Mann et al., 2013	Ikpikpuk R.	B	metatarsal	UAMES	-20.7	6.7
IK98-0377	Bison	<i>Bison priscus</i>	UAMES 8811	Mann et al., 2013	38,700 ±1,000	CAMS-53769	Mann et al., 2013	Ikpikpuk R.	B	radius	UAMES	-19.9	4.5
IK98-0889	Bison	<i>Bison priscus</i>	UAMES 9343	Mann et al., 2013	38,800 ±1,100	CAMS-53779	Mann et al., 2013	Ikpikpuk R.	B	astragalus	UAMES	-20.3	3.7
IK98-0890	Bison	<i>Bison priscus</i>	UAMES 9532	Mann et al., 2013	38,800 ±1,100	CAMS-53780	Mann et al., 2013	Ikpikpuk R.	B	astragalus	UAMES	-20.4	5.3
IK98-0915	Bison	<i>Bison priscus</i>	UAMES 9347	Mann et al., 2013	39,800 ±1,200	CAMS-53781	Mann et al., 2013	Ikpikpuk R.	B	astragalus	UAMES	-20.3	4.5
IK98-0174	Bison	<i>Bison priscus</i>	UAMES 8931	Mann et al., 2013	39,850 ±1,200	CAMS-53761	Mann et al., 2013	Ikpikpuk R.	B	astragalus	UAMES	-20.4	4.5
IK98-1122	Bison	<i>Bison priscus</i>	UAMES 9919	Mann et al., 2013	40,700 ±1,300	CAMS-53895	Mann et al., 2013	Ikpikpuk R.	B	metacarpal	UAMES	-20.0	4.3
IK98-1045	Bison	<i>Bison priscus</i>	UAMES 10045	Mann et al., 2013	43,000 ±1,800	CAMS-53889	Mann et al., 2013	Ikpikpuk R.	B	mandible	UAMES	-20.2	4.2
IK98-1042	Bison	<i>Bison priscus</i>		Mann et al., 2013	44,800 ±2,200	CAMS-53887	Mann et al., 2013	Ikpikpuk R.	B	radius	UAMES	-19.6	3.5
IK98-1125	Bison	<i>Bison priscus</i>	UAMES 9923	Mann et al., 2013	45,300 ±2,400	CAMS-53896	Mann et al., 2013	Ikpikpuk R.	B	astragalus	UAMES	-20.0	4.5
IK98-0032	Bison	<i>Bison priscus</i>	UAMES 9090	Mann et al., 2013	46,100 ±2,200	CAMS-53757	Mann et al., 2013	Ikpikpuk R.	B	metacarpal	UAMES	-20.6	3.3
IK98-0305	Bison	<i>Bison priscus</i>	UAMES 8917	Mann et al., 2013	46,100 ±2,600	CAMS-53766	Mann et al., 2013	Ikpikpuk R.	B	radius	UAMES	-20.1	5.7
IK98-0671	Bison	<i>Bison priscus</i>	UAMES 9303	Mann et al., 2013	47,000 ±2,900	CAMS-53778	Mann et al., 2013	Ikpikpuk R.	B	metatarsal	UAMES	-20.5	6.2
IK98-0928	Bison	<i>Bison priscus</i>	UAMES 9506	Mann et al., 2013	49,600 ±4,000	CAMS-53783	Mann et al., 2013	Ikpikpuk R.	B	astragalus	UAMES	-20.3	-3.3
IK98-0527	Bison	<i>Bison priscus</i>	UAMES 9567	Mann et al., 2013	50,000 ±4,200	CAMS-53773	Mann et al., 2013	Ikpikpuk R.	B	vertebra	UAMES	-20.7	2.7
IK01-074	Bison	<i>Bison priscus</i>	UAMES 11863	Mann et al., 2013	>38,000	AA-48770	Mann et al., 2013	Ikpikpuk R.	B	metatarsal	UAMES	-20.0	5.8

IK99-501	Bison	<i>Bison priscus</i>	UAMES 10881	Mann et al., 2013	>39,000	AA-48766	Mann et al., 2013	Ikpikpuk R.	B	metatarsal	UAMES	-20.4	4.0
IK99-145	Bison	<i>Bison priscus</i>	UAMES 10738	Mann et al., 2013	>39,400	AA-48262	Mann et al., 2013	Ikpikpuk R.	B	cranium	UAMES	-19.1	4.0
IK01-315	Bison	<i>Bison priscus</i>	UAMES 11687	Mann et al., 2013	>40,000	AA-48774	Mann et al., 2013	Ikpikpuk R.	B	metacarpal	UAMES	-19.5	7.6
IK01-098	Bison	<i>Bison priscus</i>	UAMES 11770	Mann et al., 2013	>40,700	AA-48270	Mann et al., 2013	Ikpikpuk R.	B	metatarsal	UAMES	-19.7	5.9
IK01-143	Bison	<i>Bison priscus</i>	UAMES 11943	Mann et al., 2013	>40,900	AA-48248	Mann et al., 2013	Ikpikpuk R.	B	metatarsal	UAMES	-20.0	6.6
IK01-095	Bison	<i>Bison priscus</i>	UAMES 11701	Mann et al., 2013	>41,000	AA-48269	Mann et al., 2013	Ikpikpuk R.	B	metacarpal	UAMES	-19.2	4.9
IK01-260	Bison	<i>Bison priscus</i>	UAMES 12012	Mann et al., 2013	>41,000	AA-48274	Mann et al., 2013	Ikpikpuk R.	B	radius	UAMES	-19.8	6.5
IK99-141	Bison	<i>Bison priscus</i>	UAMES 11142	Mann et al., 2013	>41,100	AA-48243	Mann et al., 2013	Ikpikpuk R.	B	astragalus	UAMES	-19.2	2.8
IK01-065	Bison	<i>Bison priscus</i>	UAMES 11855	Mann et al., 2013	>41,100	AA-48266	Mann et al., 2013	Ikpikpuk R.	B	astragalus	UAMES	-20.4	4.3
IK01-088	Bison	<i>Bison priscus</i>	UAMES 11676	Mann et al., 2013	>41,100	AA-48268	Mann et al., 2013	Ikpikpuk R.	B	metatarsal	UAMES	-20.2	6.5
IK99-530	Bison	<i>Bison priscus</i>	UAMES 10858	Mann et al., 2013	>41,100	AA-48767	Mann et al., 2013	Ikpikpuk R.	B	metacarpal	UAMES	-19.8	6.9
IK99-567	Bison	<i>Bison priscus</i>	UAMES 11233	Mann et al., 2013	>41,500	AA-48246	Mann et al., 2013	Ikpikpuk R.	B	astragalus	UAMES	-20.3	6.2
IK12-001	Bison	<i>Bison priscus</i>	UAMES 29458	Mann et al., 2013	>43,500	Beta-324600	Mann et al., 2013	Ikpikpuk R.	B	entire skeleton	UAMES	-20.0	4.2
IK98-0218	Bison	<i>Bison priscus</i>	UAMES 8851	Mann et al., 2013	>46,600	CAMS-53762	Mann et al., 2013	Ikpikpuk R.	B	astragalus	UAMES	-20.4	2.7
IK98-1041	Bison	<i>Bison priscus</i>	UAMES 10041	Mann et al., 2013	>48,500	CAMS-53886	Mann et al., 2013	Ikpikpuk R.	B	radius	UAMES	-19.5	4.0
IK98-1299	Bison	<i>Bison priscus</i>	UAMES 9819	Mann et al., 2013	>49,500	CAMS-53902	Mann et al., 2013	Ikpikpuk R.	B	ulna	UAMES	-20.1	3.3
IK98-1015	Bison	<i>Bison priscus</i>	UAMES 9912	Mann et al., 2013	>49,900	CAMS-53784	Mann et al., 2013	Ikpikpuk R.	B	horn core	UAMES	-20.4	2.0
IK98-1167	Bison	<i>Bison priscus</i>	UAMES 10090	Mann et al., 2013	>49,900	CAMS-53898	Mann et al., 2013	Ikpikpuk R.	B	astragalus	UAMES	-20.2	4.9

IK98-0804	Caribou	<i>Rangifer tarandus</i>	UAMES 9426	Mann et al., 2013	160 ±40	CAMS-64413	Mann et al., 2013	Ikpikpuk R.	B	mandible	UAMES	-19.2	3.8
IK98-0589	Caribou	<i>Rangifer tarandus</i>	UAMES 9283	Mann et al., 2013	200 ±50	CAMS-64409	Mann et al., 2013	Ikpikpuk R.	B	humerus	UAMES	-18.3	2.1
IK98-0875	Caribou	<i>Rangifer tarandus</i>	UAMES 9496	Mann et al., 2013	220 ±40	CAMS-64416	Mann et al., 2013	Ikpikpuk R.	B	mandible	UAMES	-18.7	2.9
IK99-421	Caribou	<i>Rangifer tarandus</i>	UAMES 10579	Mann et al., 2013	350 ±30	CAMS-64465	Mann et al., 2013	Ikpikpuk R.	B	humerus	UAMES	-18.7	2.3
IK98-0385	Caribou	<i>Rangifer tarandus</i>	UAMES 8784	Mann et al., 2013	390 ±40	CAMS-64403	Mann et al., 2013	Ikpikpuk R.	B	humerus	UAMES	-18.2	2.7
IK98-0155	Caribou	<i>Rangifer tarandus</i>		Mann et al., 2013	1120 ±40	CAMS-64397	Mann et al., 2013	Ikpikpuk R.	B	metapodial	UAMES	-18.1	2.5
IK99-314	Caribou	<i>Rangifer tarandus</i>	UAMES 10766	Mann et al., 2013	1,190 ±30	CAMS-64462	Mann et al., 2013	Ikpikpuk R.	B	mandible	UAMES	-18.2	2.3
IK98-1284	Caribou	<i>Rangifer tarandus</i>	UAMES 10013	Mann et al., 2013	2,140 ±40	CAMS-64453	Mann et al., 2013	Ikpikpuk R.	B	humerus	UAMES	-18.5	2.7
IK98-888	Caribou	<i>Rangifer tarandus</i>		Mann et al., 2013	2,540 ±50	CAMS-64418	Mann et al., 2013	Ikpikpuk R.		unknown	UAMES	-20.6	-0.5
IK98-1038	Caribou	<i>Rangifer tarandus</i>	UAMES 9983	Mann et al., 2013	2,600 ±40	CAMS-64420	Mann et al., 2013	Ikpikpuk R.	B	metatarsal	UAMES	-17.6	2.4
IK98-0083	Caribou	<i>Rangifer tarandus</i>	UAMES 8988	Mann et al., 2013	7,830 ±40	CAMS-64395	Mann et al., 2013	Ikpikpuk R.	B	mandible	UAMES	-19.1	2.4
IK99-397	Caribou	<i>Rangifer tarandus</i>	UAMES 10740	Mann et al., 2013	8,830 ±40	CAMS-64463	Mann et al., 2013	Ikpikpuk R.	B	humerus	UAMES	-18.1	1.7
IK99-044	Caribou	<i>Rangifer tarandus</i>	UAMES 10571	Mann et al., 2013	8,890 ±50	CAMS-64454	Mann et al., 2013	Ikpikpuk R.	B	metatarsal	UAMES	-17.8	1.4
IK98-0627	Caribou	<i>Rangifer tarandus</i>	UAMES 9601	Mann et al., 2013	12,370 ±50	CAMS-64410	Mann et al., 2013	Ikpikpuk R.	B	metapodial	UAMES	-18.8	2.8
IK99-594	Caribou	<i>Rangifer tarandus</i>	UAMES 11000	Mann et al., 2013	13,250 ±50	CAMS-64470	Mann et al., 2013	Ikpikpuk R.	B	metacarpal	UAMES	-18.9	3.1
IK98-0585	Caribou	<i>Rangifer tarandus</i>	UAMES 9704	Mann et al., 2013	14,380 ±50	CAMS-64408	Mann et al., 2013	Ikpikpuk R.	B	metacarpal	UAMES	-19.3	3.0
IK98-0879	Caribou	<i>Rangifer tarandus</i>	UAMES 3296	Mann et al., 2013	16,950 ±50	CAMS-64417	Mann et al., 2013	Ikpikpuk R.	B	metacarpal	UAMES	-18.9	9.2
IK98-0846	Caribou	<i>Rangifer tarandus</i>	UAMES 9325	Mann et al., 2013	17,610 ±60	CAMS-64415	Mann et al., 2013	Ikpikpuk R.	B	humerus	UAMES	-19.2	7.6

IK99-089	Caribou	<i>Rangifer tarandus</i>	UAMES 10654	Mann et al., 2013	18,410 ±60	CAMS-64456	Mann et al., 2013	Ikpikpuk R.	B	metatarsal	UAMES	-18.9	5.9
IK98-0265	Caribou	<i>Rangifer tarandus</i>	UAMES 9186	Mann et al., 2013	20,480 ±80	CAMS-64398	Mann et al., 2013	Ikpikpuk R.	B	humerus	UAMES	-19.0	7.2
IK98-0031	Caribou	<i>Rangifer tarandus</i>	UAMES 9089	Mann et al., 2013	24,750 ±110	CAMS-64392	Mann et al., 2013	Ikpikpuk R.	B	metacarpal	UAMES	-19.9	8.7
M-98-064	Caribou	<i>Rangifer tarandus</i>	UAMES 9110	Mann et al., 2013	24,940 ±110	CAMS-64475	Mann et al., 2013	Meade R.	B	mandible	UAMES	-19.2	6.2
IK98-0690	Caribou	<i>Rangifer tarandus</i>	UAMES 9598	Mann et al., 2013	27,420 ±190	CAMS-64412	Mann et al., 2013	Ikpikpuk R.	B	humerus	UAMES	-17.9	6.3
IK98-0311	Caribou	<i>Rangifer tarandus</i>	UAMES 8944	Mann et al., 2013	28,760 ±160	CAMS-64400	Mann et al., 2013	Ikpikpuk R.	B	humerus	UAMES	-18.4	3.7
IK98-0833	Caribou	<i>Rangifer tarandus</i>	UAMES 9300	Mann et al., 2013	28,930 ±170	CAMS-64414	Mann et al., 2013	Ikpikpuk R.	B	humerus	UAMES	-18.5	7.0
IK98-0079	Caribou	<i>Rangifer tarandus</i>	UAMES 8900	Mann et al., 2013	30,050 ±210	CAMS-64394	Mann et al., 2013	Ikpikpuk R.	B	metacarpal	UAMES	-18.3	3.3
IK98-1207	Caribou	<i>Rangifer tarandus</i>	UAMES 9831	Mann et al., 2013	30,270 ±200	CAMS-64471	Mann et al., 2013	Ikpikpuk R.	B	mandible	UAMES	-18.2	3.8
IK99-171	Caribou	<i>Rangifer tarandus</i>	UAMES 10994	Mann et al., 2013	30,820 ±200	CAMS-64457	Mann et al., 2013	Ikpikpuk R.	B	metacarpal	UAMES	-19.0	3.9
IK99-570	Caribou	<i>Rangifer tarandus</i>	UAMES 10847	Mann et al., 2013	31,830 ±330	CAMS-64468	Mann et al., 2013	Ikpikpuk R.	B	cranium	UAMES	-17.7	2.3
IK99-409	Caribou	<i>Rangifer tarandus</i>	UAMES 3281	Mann et al., 2013	31,920 ±240	CAMS-64464	Mann et al., 2013	Ikpikpuk R.	B	humerus	UAMES	-18.2	4.0
IK98-0983	Caribou	<i>Rangifer tarandus</i>	UAMES 9743	Mann et al., 2013	32,570 ±250	CAMS-64419	Mann et al., 2013	Ikpikpuk R.	B	humerus	UAMES	-18.6	2.6
IK98-0479	Caribou	<i>Rangifer tarandus</i>	UAMES 9270	Mann et al., 2013	37,570 ±580	CAMS-64406	Mann et al., 2013	Ikpikpuk R.	B	metapodial	UAMES	-17.7	1.6
IK99-543	Caribou	<i>Rangifer tarandus</i>	UAMES 10919	Mann et al., 2013	38,830 ±540	CAMS-64466	Mann et al., 2013	Ikpikpuk R.	B	metacarpal	UAMES	-18.1	3.8
IK99-066	Caribou	<i>Rangifer tarandus</i>	UAMES 10547	Mann et al., 2013	40,840 ±950	CAMS-64455	Mann et al., 2013	Ikpikpuk R.	B	humerus	UAMES	-18.1	5.4
IK98-0350	Caribou	<i>Rangifer tarandus</i>	UAMES 9107	Mann et al., 2013	41,100 ±1,100	CAMS-64401	Mann et al., 2013	Ikpikpuk R.	B	metatarsal	UAMES	-18.0	1.0
IK98-0450	Caribou	<i>Rangifer tarandus</i>	UAMES 9032	Mann et al., 2013	42,040 ±800	CAMS-64404	Mann et al., 2013	Ikpikpuk R.	B	metatarsal	UAMES	-19.4	2.4

IK99-764	Caribou	<i>Rangifer tarandus</i>	UAMES 11016	Mann et al., 2013	42,500 ±1,200	CAMS-64473	Mann et al., 2013	Ikpikpuk R.	B	humerus	UAMES	-18.5	1.8
IK98-0478	Caribou	<i>Rangifer tarandus</i>	UAMES 9269	Mann et al., 2013	44,200 ±1,000	CAMS-64405	Mann et al., 2013	Ikpikpuk R.	B	metapodial	UAMES	-17.3	3.0
IK98-0041	Caribou	<i>Rangifer tarandus</i>	UAMES 9204	Mann et al., 2013	44,300 ±1,100	CAMS-64393	Mann et al., 2013	Ikpikpuk R.	B	metacarpal	UAMES	-17.8	1.2
IK98-0687	Caribou	<i>Rangifer tarandus</i>	UAMES 9596	Mann et al., 2013	45,500 ±1,200	CAMS-64411	Mann et al., 2013	Ikpikpuk R.	B	metapodial	UAMES	-17.2	1.9
IK98-1051	Caribou	<i>Rangifer tarandus</i>	UAMES 10065	Mann et al., 2013	46,300 ±1,400	CAMS-64421	Mann et al., 2013	Ikpikpuk R.	B	metatarsal	UAMES	-18.7	3.9
IK98-1108	Caribou	<i>Rangifer tarandus</i>	UAMES 9867	Mann et al., 2013	46,500 ±1,600	CAMS-64422	Mann et al., 2013	Ikpikpuk R.	B	metapodial	UAMES	-18.1	3.3
IK98-0153	Caribou	<i>Rangifer tarandus</i>	UAMES 9045	Mann et al., 2013	48,300 ±1,700	CAMS-64396	Mann et al., 2013	Ikpikpuk R.	B	humerus	UAMES	-18.1	1.7
IK98-0351	Caribou	<i>Rangifer tarandus</i>	UAMES 9108	Mann et al., 2013	48,000 ±2,600	CAMS-64402	Mann et al., 2013	Ikpikpuk R.	B	metatarsal	UAMES	-18.9	4.3
IK99-247	Caribou	<i>Rangifer tarandus</i>	UAMES 10566	Mann et al., 2013	52,000 ±2,700	CAMS-64460	Mann et al., 2013	Ikpikpuk R.	B	humerus	UAMES	-18.5	4.6
IK99-199	Caribou	<i>Rangifer tarandus</i>	UAMES 12288	Mann et al., 2013	52,600 ±3,500	CAMS-64458	Mann et al., 2013	Ikpikpuk R.	B	metapodial	UAMES	-17.6	1.8
IK99-740	Caribou	<i>Rangifer tarandus</i>	UAMES 10876	Mann et al., 2013	53,300 ±3,800	CAMS-64472	Mann et al., 2013	Ikpikpuk R.	B	humerus	UAMES	-17.0	2.9
IK98-0310	Caribou	<i>Rangifer tarandus</i>	UAMES 8943	Mann et al., 2013	>46,900	CAMS-64399	Mann et al., 2013	Ikpikpuk R.	B	humerus	UAMES	-19.7	5.0
IK98-1227	Caribou	<i>Rangifer tarandus</i>	UAMES 9903	Mann et al., 2013	>47,200	CAMS-64424	Mann et al., 2013	Ikpikpuk R.	B	humerus	UAMES	-18.5	1.7
IK98-1228	Caribou	<i>Rangifer tarandus</i>	UAMES 9876	Mann et al., 2013	>49,900	CAMS-64425	Mann et al., 2013	Ikpikpuk R.	B	humerus	UAMES	-18.0	4.3
IK99-286	Caribou	<i>Rangifer tarandus</i>	UAMES 10726	Mann et al., 2013	>49,900	CAMS-64461	Mann et al., 2013	Ikpikpuk R.	B	humerus	UAMES	-17.5	2.0
IK98-1158	Caribou	<i>Rangifer tarandus</i>	UAMES 10053	Mann et al., 2013	>51,200	CAMS-64423	Mann et al., 2013	Ikpikpuk R.	B	tibia	UAMES	-17.5	0.1
IK99-585	Caribou	<i>Rangifer tarandus</i>	UAMES 10938	Mann et al., 2013	>51,700	CAMS-64469	Mann et al., 2013	Ikpikpuk R.	B	mandible	UAMES	-17.2	2.3
IK98-0573	Caribou	<i>Rangifer tarandus</i>	UAMES 9457	Mann et al., 2013	>52,800	CAMS-64407	Mann et al., 2013	Ikpikpuk R.	B	mandible	UAMES	-19.7	3.1

IK98-1230	Caribou	<i>Rangifer tarandus</i>	UAMES 9921	Mann et al., 2013	>54,000	CAMS-64426	Mann et al., 2013	Ikpikpuk R.	B	metatarsal	UAMES	-17.8	1.5
Tes57-02	Horse	<i>Equus sp.</i>	UAMES 30196	Mann et al., 2013	10,570 ±40	Beta-339279	Mann et al., 2013	Tesh 57	B	phalange	UAMES	-21.2	2.5
JDL12-1	Horse	<i>Equus sp.</i>	UAMES 29462	Mann et al., 2013	11,710 ±50	Beta-331878	Mann et al., 2013	Judy Cr.	B	cranium	UAMES	-20.7	4.5
IK01-353	Horse	<i>Equus sp.</i>	UAMES 11953	Mann et al., 2013	12,465 ±40	CAMS-92091	Mann et al., 2013	Ikpikpuk R.	B	mandible	UAMES	-20.6	2.9
IK02-109	Horse	<i>Equus sp.</i>	UAMES 3294	Mann et al., 2013	12,480 ±35; 12,490 ±45	CAMS-120651; CAMS-121738	Mann et al., 2013	Ikpikpuk R.	B	metacarpal	UAMES	-20.4	5.5
IK99-033	Horse	<i>Equus sp.</i>	UAMES 3300	Mann et al., 2013	12,780 ±35	CAMS-120673	Mann et al., 2013	Ikpikpuk R.	D/C/RD	tooth	UAMES	-20.7	5.4
IK07-08	Horse	<i>Equus sp.</i>	UAMES 29463	Mann et al., 2013	12,980 ±50	Beta-331866	Mann et al., 2013	Ikpikpuk R.	B	metacarpal	UAMES	-20.8	6.4
TIT05-07.1	Horse	<i>Equus sp.</i>	UAMES 29464	Mann et al., 2013	13,010 ±60	Beta-331882	Mann et al., 2013	Titaluk R.	B	metacarpal	UAMES	-20.7	7.1
TIT10-35	Horse	<i>Equus sp.</i>	UAMES 29465	Mann et al., 2013	13,400 ±50	Beta-331883	Mann et al., 2013	Titaluk R.	B	metacarpal	UAMES	-20.9	8.4
IK98-0537	Horse	<i>Equus sp.</i>	UAMES 3283	Mann et al., 2013	13,685 ±40	CAMS-91792	Mann et al., 2013	Ikpikpuk R.	B	metatarsal	UAMES	-20.8	6.6
IK98-0111	Horse	<i>Equus sp.</i>	UAMES 3284	Mann et al., 2013	13,925 ±40	CAMS-120655	Mann et al., 2013	Ikpikpuk R.	B	metatarsal	UAMES	-20.6	7.0
TIT11-069	Horse	<i>Equus sp.</i>	UAMES 29467	Mann et al., 2013	14,360 ±60	Beta-331887	Mann et al., 2013	Titaluk R.	B	mandible	UAMES	-20.4	6.3
T04-001	Horse	<i>Equus sp.</i>	UAMES 3289	Mann et al., 2013	14,540 ±45	CAMS-120711	Mann et al., 2013	Titaluk R.	B	tibia	UAMES	-21.0	5.0
IK99-335	Horse	<i>Equus sp.</i>	UAMES 3295	Mann et al., 2013	15,095 ±40	CAMS-120676	Mann et al., 2013	Ikpikpuk R.	B	metatarsal	UAMES	-21.5	7.0
WC11-09	Horse	<i>Equus sp.</i>	UAMES 29469	Mann et al., 2013	16,170 ±60	Beta-331891	Mann et al., 2013	Wolf Cr.	B	phalange	UAMES	-20.4	6.4
IK99-461	Horse	<i>Equus sp.</i>	UAMES 3299	Mann et al., 2013	16,885 ±45	CAMS-120683	Mann et al., 2013	Ikpikpuk R.	B	metatarsal	UAMES	-20.8	6.4
IK99-514	Horse	<i>Equus sp.</i>	UAMES 3290	Mann et al., 2013	16,925 ±45	CAMS-120685	Mann et al., 2013	Ikpikpuk R.	B	metacarpal	UAMES	-21.0	7.6

IK99-774	Horse	<i>Equus sp.</i>	UAMES 3297	Mann et al., 2013	17,290 ±60	CAMS-92073	Mann et al., 2013	Ikpikpuk R.	B	metacarpal	UAMES	-20.7	5.4
IK99-562	Horse	<i>Equus sp.</i>	UAMES 3286	Mann et al., 2013	17,300 ±60	CAMS-120700	Mann et al., 2013	Ikpikpuk R.	B	metatarsal	UAMES	-21.3	6.2
BR12-01	Horse	<i>Equus sp.</i>	UAMES 29471	Mann et al., 2013	17,720 ±70	Beta-331862	Mann et al., 2013	Bronx Cr.	B	astragulus	UAMES	-20.8	5.4
IK98-0246	Horse	<i>Equus sp.</i>	UAMES 3280	Mann et al., 2013	19,880 ±70; 19,900 ±60	CAMS-120656; CAMS-121741	Mann et al., 2013	Ikpikpuk R.	B	metatarsal	UAMES	-20.7	6.2
IK02-191	Horse	<i>Equus sp.</i>	UAMES 3298	Mann et al., 2013	20,050 ±70	CAMS-91964	Mann et al., 2013	Ikpikpuk R.	B	metacarpal	UAMES	-20.5	6.3
T02-016	Horse	<i>Equus sp.</i>	UAMES 3292	Mann et al., 2013	20,190 ±70	CAMS-120703	Mann et al., 2013	Titaluk R.	B	metatarsal	UAMES	-20.5	6.9
IK01-342	Horse	<i>Equus sp.</i>	UAMES 3285	Mann et al., 2013	20,640 ±80; 20,720 ±90	CAMS-120647; CAMS-121734	Mann et al., 2013	Ikpikpuk R.	B	metacarpal	UAMES	-20.4	6.6
IK99-207	Horse	<i>Equus sp.</i>	UAMES 3293	Mann et al., 2013	20,850 ±80	CAMS-91802	Mann et al., 2013	Ikpikpuk R.	B	metacarpal	UAMES	-20.5	5.9
IK99-442	Horse	<i>Equus sp.</i>	UAMES 3282	Mann et al., 2013	21,560 ±80	CAMS-91809	Mann et al., 2013	Ikpikpuk R.	B	metacarpal	UAMES	-20.9	5.9
IK99-789	Horse	<i>Equus sp.</i>	UAMES 3291	Mann et al., 2013	21,750 ±80	CAMS-120702	Mann et al., 2013	Ikpikpuk R.	B	cranium	UAMES	-21.0	5.6
IK99-577	Horse	<i>Equus sp.</i>	UAMES 10890	Mann et al., 2013	22,110 ±90	CAMS-91983	Mann et al., 2013	Ikpikpuk R.	B	metacarpal	UAMES	-20.8	5.4
IK10-073	Horse	<i>Equus sp.</i>	UAMES 29473	Mann et al., 2013	22,170 ±90	Beta-331872	Mann et al., 2013	Ikpikpuk R.	B	metacarpal	UAMES	-20.9	4.7
IK02-200	Horse	<i>Equus sp.</i>	UAMES 10354	Mann et al., 2013	22,330 ±90	CAMS-91965	Mann et al., 2013	Ikpikpuk R.	B	mandible	UAMES	-20.0	4.8
IK99-711	Horse	<i>Equus sp.</i>	UAMES 10885	Mann et al., 2013	22,450 ±90	CAMS-120701	Mann et al., 2013	Ikpikpuk R.	B	metatarsal	UAMES	-20.7	6.2
IK07-02	Horse	<i>Equus sp.</i>	UAMES 29474	Mann et al., 2013	22,860 ±90	Beta-331864	Mann et al., 2013	Ikpikpuk R.	B	metacarpal	UAMES	-20.3	5.1
IK06-23	Horse	<i>Equus sp.</i>	UAMES 30194	Mann et al., 2013	23,230 ±90	Beta-339267	Mann et al., 2013	Ikpikpuk R.	B	cranium	UAMES	-19.7	5.5

IK01-320	Horse	<i>Equus sp.</i>	UAMES 11735	Mann et al., 2013	23,790 ±110; 24,070 ±100	CAMS-120646; CAMS-121733	Mann et al., 2013	Ikpikpuk R.	B	metatarsal	UAMES	-20.9	5.6
IK08-080	Horse	<i>Equus sp.</i>	UAMES 29484	Mann et al., 2013	24,690 ±110	Beta-331870	Mann et al., 2013	Ikpikpuk R.	B	metacarpal	UAMES	-21.1	4.8
IK99-129	Horse	<i>Equus sp.</i>	UAMES 10814	Mann et al., 2013	24,900 ±100	CAMS-91801	Mann et al., 2013	Ikpikpuk R.	B	mandible	UAMES	-20.3	4.9
T02-001	Horse	<i>Equus sp.</i>	UAMES 8607	Mann et al., 2013	25,680 ±140	CAMS-91958	Mann et al., 2013	Titaluk R.	B	mandible	UAMES	-20.8	3.7
IK01-218	Horse	<i>Equus sp.</i>	UAMES 11745	Mann et al., 2013	26,210 ±130; 26,130 ±120	CAMS-120717; CAMS-121731	Mann et al., 2013	Ikpikpuk R.	B	metatarsal	UAMES	-20.9	6.0
IK12-063	Horse	<i>Equus sp.</i>	UAMES 30195	Mann et al., 2013	26,190 ±120	Beta-339273	Mann et al., 2013	Ikpikpuk R.	B	mandible	UAMES	-20.5	7.7
IK99-367	Horse	<i>Equus sp.</i>	UAMES 10548	Mann et al., 2013	26,020 ±120; 26,460 ±130	CAMS-120679; CAMS-121752	Mann et al., 2013	Ikpikpuk R.	B	metatarsal	UAMES	-20.6	5.3
KIK08-01	Horse	<i>Equus sp.</i>	UAMES 29475	Mann et al., 2013	26,770 ±140	Beta-331879	Mann et al., 2013	Kikiakrorak R.	B	metacarpal	UAMES	-21.6	4.6
IK11-001	Horse	<i>Equus sp.</i>	UAMES 29476	Mann et al., 2013	26,890 ±150	Beta-331874	Mann et al., 2013	Ikpikpuk R.	B	metacarpal	UAMES	-20.8	4.5
TIT11-070	Horse	<i>Equus sp.</i>	UAMES 29477	Mann et al., 2013	27,060 ±140	Beta-331888	Mann et al., 2013	Titaluk R.	B	mandible	UAMES	-20.6	7.4
IK12-015	Horse	<i>Equus sp.</i>	UAMES 29478	Mann et al., 2013	27,930 ±150	Beta-331877	Mann et al., 2013	Ikpikpuk R.	B	metacarpal	UAMES	-20.7	6.4
IK01-080	Horse	<i>Equus sp.</i>	UAMES 11647	Mann et al., 2013	27,810 ±210; 28,600 ±200	CAMS-92078; CAMS-91781	Mann et al., 2013	Ikpikpuk R.	B	mandible	UAMES	-21.1	5.4
IK01-459	Horse	<i>Equus sp.</i>	UAMES 11933	Mann et al., 2013	28,260 ±210	CAMS-91957	Mann et al., 2013	Ikpikpuk R.	B	metapodial	UAMES	-20.9	7.6
IK10-074	Horse	<i>Equus sp.</i>	UAMES 29479	Mann et al., 2013	28,330 ±150	Beta-331873	Mann et al., 2013	Ikpikpuk R.	B	metacarpal	UAMES	-20.6	5.0

IK99-244	Horse	<i>Equus sp.</i>	UAMES 10834	Mann et al., 2013	28,500 ±160	CAMS-120675	Mann et al., 2013	Ikpikpuk R.	B	metacarpal	UAMES	-20.6	8.2
IK98-1176	Horse	<i>Equus sp.</i>	UAMES 10009	Mann et al., 2013	28,500 ±200	CAMS-91797	Mann et al., 2013	Ikpikpuk R.	B	metacarpal	UAMES	-20.9	5.1
T04-004	Horse	<i>Equus sp.</i>	UAMES 11353	Mann et al., 2013	28,540 ±170	CAMS-120712	Mann et al., 2013	Titaluk R.	B	radius	UAMES	-21.3	6.1
IK01-368	Horse	<i>Equus sp.</i>	UAMES 12011	Mann et al., 2013	28,690 ±160	CAMS-121736	Mann et al., 2013	Ikpikpuk R.	B	metatarsal	UAMES	-21.2	7.6
IK06-17	Horse	<i>Equus sp.</i>	UAMES 29480	Mann et al., 2013	29,560 ±150	Beta-331863	Mann et al., 2013	Ikpikpuk R.	B	metacarpal	UAMES	-20.9	6.5
IK99-254	Horse	<i>Equus sp.</i>	UAMES 10644	Mann et al., 2013	29,700 ±200	CAMS-91806	Mann et al., 2013	Ikpikpuk R.	B	metacarpal	UAMES	-21.2	9.8
IK99-383	Horse	<i>Equus sp.</i>	UAMES 11205	Mann et al., 2013	29,830 ±190; 30,560 ±200	CAMS-120680; CAMS-121753	Mann et al., 2013	Ikpikpuk R.	B	metatarsal	UAMES	-21.3	6.4
TIT11-071	Horse	<i>Equus sp.</i>	UAMES 29481	Mann et al., 2013	30,260 ±190	Beta-331889	Mann et al., 2013	Titaluk R.	B	mandible	UAMES	-20.9	6.8
IK07-06	Horse	<i>Equus sp.</i>	UAMES 29495	Mann et al., 2013	30,560 ±160	Beta-331865	Mann et al., 2013	Ikpikpuk R.	B	metacarpal	UAMES	-21.1	5.8
TIT11-072	Horse	<i>Equus sp.</i>	UAMES 29482	Mann et al., 2013	30,610 ±200	Beta-331890	Mann et al., 2013	Titaluk R.	B	mandible	UAMES	-21.7	8.1
IK98-0539	Horse	<i>Equus sp.</i>	UAMES 9548	Mann et al., 2013	30,900 ±300	CAMS-91793	Mann et al., 2013	Ikpikpuk R.	B	mandible	UAMES	-21.2	7.9
IK01-183	Horse	<i>Equus sp.</i>	UAMES 11878	Mann et al., 2013	31,230 ±270	CAMS-92083	Mann et al., 2013	Ikpikpuk R.	B	metatarsal	UAMES	-21.7	5.3
IK08-082	Horse	<i>Equus sp.</i>	UAMES 29483	Mann et al., 2013	31,680 ±190	Beta-331869	Mann et al., 2013	Ikpikpuk R.	B	metacarpal	UAMES	-21.0	7.4
TIT10-38	Horse	<i>Equus sp.</i>	UAMES 29485	Mann et al., 2013	32,250 ±220	Beta-331886	Mann et al., 2013	Titaluk R.	B	metacarpal	UAMES	-21.3	5.1
IK98-1142	Horse	<i>Equus sp.</i>	UAMES 9972	Mann et al., 2013	32,600 ±300	CAMS-91796	Mann et al., 2013	Ikpikpuk R.	B	mandible	UAMES	-21.1	5.1
IK01-282	Horse	<i>Equus sp.</i>	UAMES 11794	Mann et al., 2013	32,700 ±300	CAMS-92089	Mann et al., 2013	Ikpikpuk R.	B	metacarpal	UAMES	-20.9	4.5
IK09-51	Horse	<i>Equus sp.</i>	UAMES 29486	Mann et al., 2013	33,150 ±200	Beta-331871	Mann et al., 2013	Ikpikpuk R.	B	metacarpal	UAMES	-21.6	5.5

TIT10-36	Horse	<i>Equus sp.</i>	UAMES 29487	Mann et al., 2013	33,200 ±240	Beta-331884	Mann et al., 2013	Titaluk R.	B	metacarpal	UAMES	-21.4	6.2
IK98-0288	Horse	<i>Equus sp.</i>	UAMES 8859	Mann et al., 2013	33,420 ±340; 33,820 ±290	CAMS-120721; CAMS-121742	Mann et al., 2013	Ikpikpuk R.	B	metatarsal	UAMES	-21.5	6.8
IK98-0112	Horse	<i>Equus sp.</i>	UAMES 9021	Mann et al., 2013	33,800 ±400	CAMS-91790	Mann et al., 2013	Ikpikpuk R.	B	metacarpal	UAMES	-21.1	7.9
IK99-790	Horse	<i>Equus sp.</i>	UAMES 10910	Mann et al., 2013	33,870 ±350	CAMS-92074	Mann et al., 2013	Ikpikpuk R.	B	mandible	UAMES	-20.7	5.9
IK01-369	Horse	<i>Equus sp.</i>	UAMES 11973	Mann et al., 2013	33,900 ±400; 34,200 ±400	CAMS-92093; CAMS-91782	Mann et al., 2013	Ikpikpuk R.	B	metacarpal	UAMES	-21.2	5.9
IK01-150	Horse	<i>Equus sp.</i>	UAMES 12014	Mann et al., 2013	34,210 ±370	CAMS-92081	Mann et al., 2013	Ikpikpuk R.	B	mandible	UAMES	-21.2	7.2
TIT10-37	Horse	<i>Equus sp.</i>	UAMES 29488	Mann et al., 2013	34,320 ±270	Beta-331885	Mann et al., 2013	Titaluk R.	B	metacarpal	UAMES	-20.9	9.1
IK99-404	Horse	<i>Equus sp.</i>	UAMES 11122	Mann et al., 2013	34,690 ±340; 35,380 ±360	CAMS-120681; CAMS-121754	Mann et al., 2013	Ikpikpuk R.	B	metacarpal	UAMES	-22.1	8.3
IK98-0009	Horse	<i>Equus sp.</i>	UAMES 9169	Mann et al., 2013	35,500 ±400	CAMS-91789	Mann et al., 2013	Ikpikpuk R.	B	mandible	UAMES	-21.0	5.9
IK98-0394	Horse	<i>Equus sp.</i>	UAMES 8814	Mann et al., 2013	36,500 ±500	CAMS-91791	Mann et al., 2013	Ikpikpuk R.	B	metacarpal	UAMES	-21.4	6.0
IK01-121	Horse	<i>Equus sp.</i>	UAMES 11782	Mann et al., 2013	37,400 ±540	CAMS-92079	Mann et al., 2013	Ikpikpuk R.	B	metacarpal	UAMES	-21.2	6.8
IK99-806	Horse	<i>Equus sp.</i>	UAMES 11068	Mann et al., 2013	38,090 ±590	CAMS-92075	Mann et al., 2013	Ikpikpuk R.	B	metacarpal	UAMES	-20.8	5.8
IK08-079	Horse	<i>Equus sp.</i>	UAMES 29489	Mann et al., 2013	40,880 ±400	Beta-331868	Mann et al., 2013	Ikpikpuk R.	B	metacarpal	UAMES	-21.2	5.7
IK08-078	Horse	<i>Equus sp.</i>	UAMES 29490	Mann et al., 2013	40,960 ±370	Beta-331867	Mann et al., 2013	Ikpikpuk R.	B	metacarpal	UAMES	-20.6	7.0
IK99-111	Horse	<i>Equus sp.</i>	UAMES 10544	Mann et al., 2013	41,000 ±800	CAMS-91799	Mann et al., 2013	Ikpikpuk R.	B	metacarpal	UAMES	-20.8	3.1

IK12-011	Horse	<i>Equus sp.</i>	UAMES 29491	Mann et al., 2013	41,410 ±570	Beta-331876	Mann et al., 2013	Ikpikpuk R.	B	metacarpal	UAMES	-20.9	4.2
IK12-010	Horse	<i>Equus sp.</i>	UAMES 29492	Mann et al., 2013	41,840 ±410	Beta-331875	Mann et al., 2013	Ikpikpuk R.	B	metacarpal	UAMES	-20.4	4.3
IK02-072	Horse	<i>Equus sp.</i>	UAMES 10534	Mann et al., 2013	±1,000; 43,700 ±1,000	CAMS-120650; CAMS-121737	Mann et al., 2013	Ikpikpuk R.	B	metatarsal	UAMES	-21.3	7.7
IK02-026	Horse	<i>Equus sp.</i>	UAMES 10434	Mann et al., 2013	46,770 ±1,710	CAMS-91959	Mann et al., 2013	Ikpikpuk R.	B	mandible	UAMES	-20.7	1.7
KIK12-02	Horse	<i>Equus sp.</i>	UAMES 29494	Mann et al., 2013	>43,500	Beta-331880	Mann et al., 2013	Kikiakrorak R.	B	phalange	UAMES	-21.0	5.7
IK02-181	Mammoth	<i>Mammuthus primigenius</i>	UAMES 10522	Mann et al., 2013	17,870 ±60; 17,965 ±50	CAMS-120653; CAMS-121739	Mann et al., 2013	Ikpikpuk R.	B	fibula	UAMES	-20.9	7.6
IK01-257	Mammoth	<i>Mammuthus primigenius</i>	UAMES 12016	Mann et al., 2013	19,530 ±80	CAMS-92087	Mann et al., 2013	Ikpikpuk R.	D/RD/C	molar	UAMES	-21.3	10.1
IK98-0339	Mammoth	<i>Mammuthus primigenius</i>	UAMES 9053	Mann et al., 2013	24,460 ±130; 24,850 ±110	CAMS-120677; CAMS-121751	Mann et al., 2013	Ikpikpuk R.	B	scapula	UAMES	-21.5	7.6
T02-110	Mammoth	<i>Mammuthus primigenius</i>		Mann et al., 2013	26,410 ±150	CAMS-91967	Mann et al., 2013	Titaluk R.		unknown	UAMES	-20.5	8.0
IK99-120b	Mammoth	<i>Mammuthus primigenius</i>	UAMES 10688	Mann et al., 2013	28,200 ±200	CAMS-91800	Mann et al., 2013	Ikpikpuk R.	B	mandible	UAMES	-21.2	7.9
IK01-040	Mammoth	<i>Mammuthus primigenius</i>	UAMES 11998	Mann et al., 2013	28,220 ±210; 29,100 ±200	CAMS-92077; CAMS-91783	Mann et al., 2013	Ikpikpuk R.	B	radius	UAMES	-21.2	7.6
IK99-495	Mammoth	<i>Mammuthus primigenius</i>	UAMES 10851	Mann et al., 2013	29,740 ±190	CAMS-120684	Mann et al., 2013	Ikpikpuk R.	B	mandible	UAMES	-21.2	8.0
IK98-0063	Mammoth	<i>Mammuthus primigenius</i>	UAMES 9096	Mann et al., 2013	30,730 ±200; 29,250 ±200	CAMS-121740; CAMS-120654	Mann et al., 2013	Ikpikpuk R.	B	tibia	UAMES	-21.1	8.3
IK99-745	Mammoth	<i>Mammuthus primigenius</i>	UAMES 10905	Mann et al., 2013	30,990 ±250	CAMS-92072	Mann et al., 2013	Ikpikpuk R.	D/RD/C	molar	UAMES	-20.6	9.0

IK99-5001	Mammoth	<i>Mammuthus primigenius</i>	UAMES 8632	Mann et al., 2013	33,000 ±300; 33,530 ±340 33,400	CAMS-91779; CAMS-91968	Mann et al., 2013	Ikpikpuk R.	T	tusk	UAMES	-20.8	7.2
IK99-575	Mammoth	<i>Mammuthus primigenius</i>	UAMES 11028	Mann et al., 2013	±300; 33,600 ±400 33,880	CAMS-91812; CAMS-91780	Mann et al., 2013	Ikpikpuk R.	D/RD/C	molar	UAMES	-20.8	9.1
T02-033	Mammoth	<i>Mammuthus primigenius</i>		Mann et al., 2013	±300; 33,920 ±310	CAMS-120706; CAMS-121757	Mann et al., 2013	Titaluk R.		unknown	UAMES	-21.4	7.0
IK98-1275	Mammoth	<i>Mammuthus primigenius</i>	UAMES 10080	Mann et al., 2013	40,760± 830	CAMS-120670	Mann et al., 2013	Ikpikpuk R.	B	humerus	UAMES	-21.8	7.1
IK99-235	Mammoth	<i>Mammuthus primigenius</i>	UAMES 10752	Mann et al., 2013	40,870± 820	CAMS-91803	Mann et al., 2013	Ikpikpuk R.	D/RD/C	molar	UAMES	-21.5	8.4
IK98-1102	Mammoth	<i>Mammuthus primigenius</i>	UAMES 9823	Mann et al., 2013	45,100 ±1,400; 46,900 ±1400 47,300	CAMS-120666; CAMS-121748	Mann et al., 2013	Ikpikpuk R.	B	vertebra	UAMES	-21.4	7.8
IK01-250	Mammoth	<i>Mammuthus primigenius</i>	UAMES 11964	Mann et al., 2013	±1,500; 48,760 ±2,200	CAMS-120643; CAMS-120718	Mann et al., 2013	Ikpikpuk R.	B	tibia	UAMES	-21.5	6.7
IK01-201	Mammoth	<i>Mammuthus primigenius</i>	UAMES 11715	Mann et al., 2013	48,040± 2,000	CAMS-92085	Mann et al., 2013	Ikpikpuk R.	D/RD/C	molar	UAMES	-21.4	8.2
IK01-166	Mammoth	<i>Mammuthus primigenius</i>	UAMES 11821	Mann et al., 2013	49,310± 1,950	CAMS-120716	Mann et al., 2013	Ikpikpuk R.	B	ulna	UAMES	-20.9	6.6
IK98-1033	Mammoth	<i>Mammuthus primigenius</i>	UAMES 9970	Mann et al., 2013	49,700± 2,500	CAMS-120665	Mann et al., 2013	Ikpikpuk R.	B	scapula	UAMES	-21.4	7.4
IK01-291	Mammoth	<i>Mammuthus primigenius</i>		Mann et al., 2013	48,900 ±1,900; 51,000 ±2,400	CAMS-120645; CAMS-121732	Mann et al., 2013	Ikpikpuk R.	T	tusk	UAMES	-21.2	8.2
IK99-070	Mammoth	<i>Mammuthus primigenius</i>	UAMES 10694	Mann et al., 2013	>49,000 ; 51,900 ±3,200	CAMS-91798; CAMS-91778	Mann et al., 2013	Ikpikpuk R.	B	mandible	UAMES	-22.3	9.5

IK98-1012	Mammoth	<i>Mammuthus primigenius</i>	UAMES 9933	Mann et al., 2013	50,800±2,400	CAMS-120664	Mann et al., 2013	Ikpikpuk R.	B	cranium	UAMES	-21.4	7.1
IK99-524	Mammoth	<i>Mammuthus primigenius</i>	UAMES 11007	Mann et al., 2013	51,000±2,900	CAMS-91811	Mann et al., 2013	Ikpikpuk R.	D/RD/C	molar	UAMES	-21.8	9.7
IK98-1013	Mammoth	<i>Mammuthus primigenius</i>	UAMES 9934	Mann et al., 2013	±1,800; 55,700±4,300	CAMS-120722; CAMS-121747	Mann et al., 2013	Ikpikpuk R.	B	scapula	UAMES	-21.8	7.4
IK02-173	Mammoth	<i>Mammuthus primigenius</i>	UAMES 10458	Mann et al., 2013	51,900±3,200	CAMS-91963	Mann et al., 2013	Ikpikpuk R.	B	fibula	UAMES	-21.3	6.4
IK98-1243	Mammoth	<i>Mammuthus primigenius</i>	UAMES 9945	Mann et al., 2013	±2,700; 53,400±3,900	CAMS-121750; CAMS-120668	Mann et al., 2013	Ikpikpuk R.	B	radius	UAMES	-21.7	6.8
IK98-1195	Mammoth	<i>Mammuthus primigenius</i>	UAMES 9811	Mann et al., 2013	50,400±2,700; >55,500	CAMS-120667; CAMS-121749	Mann et al., 2013	Ikpikpuk R.	B	radius	UAMES	-21.1	6.1
IK01-274	Mammoth	<i>Mammuthus primigenius</i>		Mann et al., 2013	53,000±3,700	CAMS-92088	Mann et al., 2013	Ikpikpuk R.	B	femur	UAMES	-21.4	9.8
IK98-0957	Mammoth	<i>Mammuthus primigenius</i>		Mann et al., 2013	>48,900	CAMS-120662	Mann et al., 2013	Ikpikpuk R.	B	long bone	UAMES	-20.7	8.1
IK99-236	Mammoth	<i>Mammuthus primigenius</i>	UAMES 11111	Mann et al., 2013	>49,000	CAMS-91804	Mann et al., 2013	Ikpikpuk R.	D/RD/C	molar	UAMES	-21.8	8.1
T02-038	Mammoth	<i>Mammuthus primigenius</i>	UAMES 8617	Mann et al., 2013	>49,200	CAMS-91960	Mann et al., 2013	Titaluk R.	B	scapula	UAMES	-22.4	6.6
IK01-256	Mammoth	<i>Mammuthus primigenius</i>	UAMES 11972	Mann et al., 2013	>49,200	CAMS-92086	Mann et al., 2013	Ikpikpuk R.	D/RD/C	molar	UAMES	-21.4	8.2
IK98-1312	Mammoth	<i>Mammuthus primigenius</i>	UAMES 9853	Mann et al., 2013	>50,100	CAMS-120672	Mann et al., 2013	Ikpikpuk R.	B	femur	UAMES	-22.0	6.9
IK01-079	Mammoth	<i>Mammuthus primigenius</i>	UAMES 11646	Mann et al., 2013	>49,100 ; >52,000	CAMS-120638; CAMS-120713	Mann et al., 2013	Ikpikpuk R.	B	rib	UAMES	-23.2	8.4
IK98-0298	Mammoth	<i>Mammuthus primigenius</i>	UAMES 8889	Mann et al., 2013	>50,600	CAMS-120657	Mann et al., 2013	Ikpikpuk R.	B	radius	UAMES	-22.1	7.8

IK99-366	Mammoth	<i>Mammuthus primigenius</i>	UAMES 11180	Mann et al., 2013	>51,000	CAMS-120678	Mann et al., 2013	Ikpikpuk R.	T	tusk	UAMES	-21.6	8.5
IK01-255	Mammoth	<i>Mammuthus primigenius</i>	UAMES 11971	Mann et al., 2013	>50,000 ; >52,100	CAMS-120644; CAMS-120719	Mann et al., 2013	Ikpikpuk R.	B	femur	UAMES	-22.0	7.7
IK98-1281	Mammoth	<i>Mammuthus primigenius</i>	UAMES 9996	Mann et al., 2013	>51,100	CAMS-120671	Mann et al., 2013	Ikpikpuk R.	B	tibia	UAMES	-21.4	7.2
IK98-1000	Mammoth	<i>Mammuthus primigenius</i>	UAMES 9773	Mann et al., 2013	>51,300	CAMS-120663	Mann et al., 2013	Ikpikpuk R.	T	tusk	UAMES	-21.6	7.6
IK98-1274	Mammoth	<i>Mammuthus primigenius</i>	UAMES 10079	Mann et al., 2013	>51,300	CAMS-120669	Mann et al., 2013	Ikpikpuk R.	B	radius	UAMES	-21.7	7.2
IK99-130	Mammoth	<i>Mammuthus primigenius</i>	UAMES 11120	Mann et al., 2013	>51,500	CAMS-120674	Mann et al., 2013	Ikpikpuk R.	B	femur	UAMES	-21.4	6.8
IK01-132	Mammoth	<i>Mammuthus primigenius</i>	UAMES 12035	Mann et al., 2013	>49,100 ; >54,500	CAMS-120640; CAMS-120715	Mann et al., 2013	Ikpikpuk R.	B	radius	UAMES	-21.5	6.6
IK99-322	Mammoth	<i>Mammuthus primigenius</i>	UAMES 10561	Mann et al., 2013	>52,000	CAMS-91807	Mann et al., 2013	Ikpikpuk R.	D/RD/C	molar	UAMES	-21.9	9.4
IK98-0759	Mammoth	<i>Mammuthus primigenius</i>	UAMES 9541	Mann et al., 2013	>52,200	CAMS-121743	Mann et al., 2013	Ikpikpuk R.	B	scapula	UAMES	-21.2	9.3
IK99-5000b	Mammoth	<i>Mammuthus primigenius</i>	UAMES 7954	Mann et al., 2013	>52,500	CAMS-92095	Mann et al., 2013	Ikpikpuk R.	T	tusk	UAMES	-21.6	7.4
IK01-082	Mammoth	<i>Mammuthus primigenius</i>		Mann et al., 2013	>51,000 ; >55,100	CAMS-120639; CAMS-120714	Mann et al., 2013	Ikpikpuk R.	B	leg bone	UAMES	-20.8	5.1
IK98-0761	Mammoth	<i>Mammuthus primigenius</i>	UAMES 9543	Mann et al., 2013	>53,400	CAMS-121744	Mann et al., 2013	Ikpikpuk R.	B	ulna	UAMES	-20.8	7.7
IK98-1087	Mammoth	<i>Mammuthus primigenius</i>	UAMES 9813	Mann et al., 2013	>54,000	CAMS-91795	Mann et al., 2013	Ikpikpuk R.	D/RD/C	molar	UAMES	-21.8	8.7
IK02-042	Mammoth	<i>Mammuthus primigenius</i>		Mann et al., 2013	>54,000	CAMS-91961	Mann et al., 2013	Ikpikpuk R.	B	pelvis	UAMES	-21.4	6.4
IK01-359	Mammoth	<i>Mammuthus primigenius</i>	UAMES 12008	Mann et al., 2013	>54,000	CAMS-92092	Mann et al., 2013	Ikpikpuk R.	D/RD/C	molar	UAMES	-21.7	8.4

IK98-0801	Mammoth	<i>Mammuthus primigenius</i>	UAMES 9424	Mann et al., 2013	>55,500	CAMS-121746	Mann et al., 2013	Ikpikpuk R.	B	metapodial	UAMES	-20.8	7.9
MAY 12-69	Mastodon	<i>Mammut americanum</i>		Mann et al., 2013	31,780 +360; Infinite	UCIAMS-117238	Mann et al., 2013	Maybe Cr.	D/RD/C	molar	UAMES	-21.0	2.1
MAY 12-45	Mastodon	<i>Mammut americanum</i>	UAMES 30200	Mann et al., 2013; Zazula et al., 2014	47,000±2,300	UCIAMS-117241	Zazula et al., 2014	Maybe Cr.	D/RD/C	molar	UAMES	-20.9	3.5
IK01-277	Mastodon	<i>Mammut americanum</i>	UAMES 12060	Mann et al., 2013; Zazula et al., 2014	49,800 ±3,300	UCIAMS-117236	Zazula et al., 2014	Ikpikpuk R.	D/RD/C	molar	UAMES	-20.9	3.1
MAY 12-70	Mastodon	<i>Mammut americanum</i>	UAMES 34126	Mann et al., 2013; Zazula et al., 2014	>46,100	UCIAMS-117237	Zazula et al., 2014	Maybe Cr.	D/RD/C	molar	UAMES	-21.1	3.5
KIG12-15	Mastodon	<i>Mammut americanum</i>	UAMES 30199	Mann et al., 2013; Zazula et al., 2014	>46,400	UCIAMS-117235	Zazula et al., 2014	Kigalik R.	D/RD/C	molar	UAMES	-20.9	3.2
IK10-106	Mastodon	<i>Mammut americanum</i>	UAMES 30201	Mann et al., 2013; Zazula et al., 2014	>47,500	UCIAMS-117232	Zazula et al., 2014	Ikpikpuk R.	D/RD/C	molar	UAMES	-20.8	3.0
IK99-237	Mastodon	<i>Mammut americanum</i>	UAMES 2414	Mann et al., 2013; Zazula et al., 2014	>48,100	UCIAMS-117234	Zazula et al., 2014	Ikpikpuk R.	D/RD/C	molar	UAMES	-20.8	4.1
IK01-321	Mastodon	<i>Mammut americanum</i>	UAMES 12047	Mann et al., 2013; Zazula et al., 2014	>48,800	UCIAMS-117240	Zazula et al., 2014	Ikpikpuk R.	D/RD/C	molar	UAMES	-20.7	3.5
IK08-127	Mastodon	<i>Mammut americanum</i>	UAMES 30198	Mann et al., 2013; Zazula et al., 2014	>51,200	UCIAMS-117243	Zazula et al., 2014	Ikpikpuk R.	D/RD/C	molar	UAMES	-20.7	3.0
IK99-328	Mastodon	<i>Mammut americanum</i>	UAMES 11095	Mann et al., 2013; Zazula et al., 2014	>51,200	UCIAMS-117233	Zazula et al., 2014	Ikpikpuk R.	D/RD/C	molar	UAMES	-21.2	3.1

IK05-3.5	Mastodon	<i>Mammut americanum</i>	UAMES 30197	Mann et al., 2013; Zazula et al., 2014	>51,700	UCIAMS-117242	Zazula et al., 2014	Ikpikpuk R.	D/RD/C	molar	UAMES	-21.2	2.8
IK98-963	Mastodon	<i>Mammut americanum</i>	UAMES 9705	Mann et al., 2013; Zazula et al., 2014	>51,700	UCIAMS-117239	Zazula et al., 2014	Ikpikpuk R.	D/RD/C	molar	UAMES	-21.0	2.8
IK02-210	Moose	<i>Alces alces</i>	UAMES 10355	Mann et al., 2013	320±35	CAMS-91966	Mann et al., 2013	Ikpikpuk R.	B	mandible	UAMES	-20.3	0.3
IK01-404	Moose	<i>Alces alces</i>	UAMES 11844	Mann et al., 2013	665±35	CAMS-92094	Mann et al., 2013	Ikpikpuk R.	B	mandible	UAMES	-20.9	-0.6
IK12-077	Moose	<i>Alces alces</i>	UAMES 30183	Mann et al., 2013	950±30	Beta-339274	Mann et al., 2013	Ikpikpuk R.	B	cranium	UAMES	-20.7	1.0
IK99-229	Moose	<i>Alces alces</i>	UAMES 10691	Mann et al., 2013	980±40	CAMS-64459	Mann et al., 2013	Ikpikpuk R.	B	mandible	UAMES	-20.0	8.6
IK08-016	Moose	<i>Alces alces</i>	UAMES 30180	Mann et al., 2013	1,180±30	Beta-339268	Mann et al., 2013	Ikpikpuk R.	B	mandible	UAMES	-21.3	1.8
IK99-776	Moose	<i>Alces alces</i>	UAMES 11066	Mann et al., 2013	1,370±40	CAMS-64474	Mann et al., 2013	Ikpikpuk R.	B	mandible	UAMES	-20.4	1.3
IK99-556	Moose	<i>Alces alces</i>	UAMES 10996	Mann et al., 2013	1,760±40	CAMS-64467	Mann et al., 2013	Ikpikpuk R.	B	mandible	UAMES	-19.9	0.7
IK01-023	Moose	<i>Alces alces</i>	UAMES 12022	Mann et al., 2013	2,450±35	CAMS-92076	Mann et al., 2013	Ikpikpuk R.	B	mandible	UAMES	-20.8	1.0
ING-99-1001	Muskox	<i>Ovibos moschatus</i>	UAMES 8638	Mann et al., 2013	226±59	AA-48776	Mann et al., 2013	NPRA	B	cranium	UAMES	-19.8	3.8
Sing1 2-2	Muskox	<i>Ovibos moschatus</i>	UAMES 30202	Mann et al., 2013	250±30	Beta-339445	Mann et al., 2013	tundra	B	cranium	UAMES	-20.0	3.6
TUN1 2-1	Muskox	<i>Ovibos moschatus</i>	UAMES 30203	Mann et al., 2013	340±30	Beta-339278	Mann et al., 2013	tundra	B	cranium	UAMES	-18.5	4.8
ING-99-1002	Muskox	<i>Ovibos moschatus</i>	UAMES 8639	Mann et al., 2013	1,148±42	AA-48283	Mann et al., 2013	NPRA	B	cranium	UAMES	-20.0	5.6
IK99-353	Muskox	<i>Ovibos moschatus</i>	UAMES 29501	Mann et al., 2013	7,127±59	AA-48263	Mann et al., 2013	Ikpikpuk R.	B	cranium	UAMES	-19.6	6.8

IK98-1032	Muskox	<i>Ovibos moschatus</i>	UAMES 10098	Mann et al., 2013	10,180±110	AA-48757	Mann et al., 2013	Ikpikpuk R.	B	cranium	UAMES	-19.8	3.7
IK98-0819	Muskox	<i>Ovibos moschatus</i>	UAMES 9673	Mann et al., 2013	21,670±370	AA-48753	Mann et al., 2013	Ikpikpuk R.	B	metatarsal	UAMES	-19.4	9.3
IK98-0871	Muskox	<i>Ovibos moschatus</i>	UAMES 9753	Mann et al., 2013	27,580±750	AA-48239	Mann et al., 2013	Ikpikpuk R.	B	metatarsal	UAMES	-19.6	9.3
IK01-159	Muskox	<i>Ovibos moschatus</i>	UAMES 11886	Mann et al., 2013	34,570±250	Beta-286418	Mann et al., 2013	Ikpikpuk R.	B	metatarsal	UAMES	-20.2	8.6
IK01-313	Muskox	<i>Ovibos moschatus</i>	UAMES 11685	Mann et al., 2013	35,920±930	AA-48277	Mann et al., 2013	Ikpikpuk R.	B	metatarsal	UAMES	-19.6	7.4
IK01-294	Muskox	<i>Ovibos moschatus</i>	UAMES 11628	Mann et al., 2013	36,400±770	AA-48276	Mann et al., 2013	Ikpikpuk R.	B	metatarsal	UAMES	-20.0	7.3
IK98-1173	Muskox	<i>Ovibos moschatus</i>		Mann et al., 2013	43,000±1,800	CAMS-53908	Mann et al., 2013	Ikpikpuk R.	B	axis	UAMES	-19.9	4.3
IK98-0393	Muskox	<i>Ovibos moschatus</i>	UAMES 8813	Mann et al., 2013	>35,500	AA-48748	Mann et al., 2013	Ikpikpuk R.	B	metacarpal	UAMES	-19.1	8.2
IK98-0673	Muskox	<i>Ovibos moschatus</i>	UAMES 9641	Mann et al., 2013	>36,200	Beta-286422	Mann et al., 2013	Ikpikpuk R.	B	metatarsal	UAMES	-20.7	5.3
IK98-0654	Muskox	<i>Ovibos moschatus</i>	UAMES 9439	Mann et al., 2013	>37,100	AA-48750	Mann et al., 2013	Ikpikpuk R.	B	metacarpal	UAMES	-18.7	2.4
IK98-0469	Muskox	<i>Ovibos moschatus</i>	UAMES 9259	Mann et al., 2013	>37,300	Beta-286421	Mann et al., 2013	Ikpikpuk R.	B	metacarpal	UAMES	-20.2	7.3
IK98-0387	Muskox	<i>Ovibos moschatus</i>	UAMES 8786	Mann et al., 2013	>39,500	Beta-286420	Mann et al., 2013	Ikpikpuk R.	B	cranium	UAMES	-20.5	7.2
IK98-1221	Muskox	<i>Ovibos moschatus</i>	UAMES 9875	Mann et al., 2013	>39,800	AA-48258	Mann et al., 2013	Ikpikpuk R.	B	metacarpal	UAMES	-20.1	5.3
IK98-1324	Muskox	<i>Ovibos moschatus</i>	UAMES 9890	Mann et al., 2013	>39,900	AA-48260	Mann et al., 2013	Ikpikpuk R.	B	horn core	UAMES	-19.2	2.7
IK01-086	Muskox	<i>Ovibos moschatus</i>	UAMES 11674	Mann et al., 2013	>40,000	AA-48771	Mann et al., 2013	Ikpikpuk R.	B	metatarsal	UAMES	-20.4	3.2
IK98-1028	Muskox	<i>Ovibos moschatus</i>	UAMES 9959	Mann et al., 2013	>40,000	AA-48756	Mann et al., 2013	Ikpikpuk R.	B	cranium	UAMES	-19.9	8.8
IK98-1309	Muskox	<i>Ovibos moschatus</i>	UAMES 9834	Mann et al., 2013	>40,000	AA-48761	Mann et al., 2013	Ikpikpuk R.	B	metacarpal	UAMES	-19.2	8.4
IK99-142	Muskox	<i>Ovibos moschatus</i>	UAMES 10682	Mann et al., 2013	>40,000	AA-48764	Mann et al., 2013	Ikpikpuk R.	B	cranium	UAMES	-19.4	3.5

IK99-731	Muskox	<i>Ovibos moschatus</i>	UAMES 10845	Mann et al., 2013	>40,000	AA-48768	Mann et al., 2013	Ikpikpuk R.	B	metatarsal	UAMES	-19.6	9.2
IK99-754	Muskox	<i>Ovibos moschatus</i>	UAMES 10936	Mann et al., 2013	>40,000	AA-48769	Mann et al., 2013	Ikpikpuk R.	B	metatarsal	UAMES	-18.9	8.8
IK98-0028	Muskox	<i>Ovibos moschatus</i>	UAMES 9068	Mann et al., 2013	>40,100	AA-48252	Mann et al., 2013	Ikpikpuk R.	B	metacarpal	UAMES	-19.3	4.2
IK98-0818	Muskox	<i>Ovibos moschatus</i>	UAMES 9677	Mann et al., 2013	>40,100	AA-48238	Mann et al., 2013	Ikpikpuk R.	B	metatarsal	UAMES	-19.7	8.0
IK98-1288	Muskox	<i>Ovibos moschatus</i>	UAMES 10017	Mann et al., 2013	>40,200	AA-48259	Mann et al., 2013	Ikpikpuk R.	B	metacarpal	UAMES	-19.4	6.9
IK98-0441	Muskox	<i>Ovibos moschatus</i>	UAMES 8926	Mann et al., 2013	>40,300	AA-48254	Mann et al., 2013	Ikpikpuk R.	B	metacarpal	UAMES	-19.9	5.5
IK01-311	Muskox	<i>Ovibos moschatus</i>	UAMES 11662	Mann et al., 2013	>40,700	AA-48250	Mann et al., 2013	Ikpikpuk R.	B	metacarpal	UAMES	-20.0	7.0
IK01-398	Muskox	<i>Ovibos moschatus</i>	UAMES 11840	Mann et al., 2013	>40,900	AA-48279	Mann et al., 2013	Ikpikpuk R.	B	metacarpal	UAMES	-20.2	5.8
IK01-136	Muskox	<i>Ovibos moschatus</i>	UAMES 11888	Mann et al., 2013	>41,000	AA-48272	Mann et al., 2013	Ikpikpuk R.	B	metatarsal	UAMES	-19.9	5.5
IK01-160	Muskox	<i>Ovibos moschatus</i>	UAMES 11887	Mann et al., 2013	>41,000	AA-48249	Mann et al., 2013	Ikpikpuk R.	B	metatarsal	UAMES	-20.0	7.1
IK98-0849	Muskox	<i>Ovibos moschatus</i>	UAMES 9336	Mann et al., 2013	>41,000	AA-48257	Mann et al., 2013	Ikpikpuk R.	B	metacarpal	UAMES	-19.6	5.5
IK99-729	Muskox	<i>Ovibos moschatus</i>	UAMES 10843	Mann et al., 2013	>41,000	AA-48265	Mann et al., 2013	Ikpikpuk R.	B	metacarpal	UAMES	-19.7	9.2
IK01-073	Muskox	<i>Ovibos moschatus</i>	UAMES 11862	Mann et al., 2013	>41,100	AA-48267	Mann et al., 2013	Ikpikpuk R.	B	cranium	UAMES	-19.8	5.6
IK98-0029	Muskox	<i>Ovibos moschatus</i>	UAMES 9069	Mann et al., 2013	>41,100	AA-48744	Mann et al., 2013	Ikpikpuk R.	B	metacarpal	UAMES	-19.3	3.4
IK98-0049	Muskox	<i>Ovibos moschatus</i>	UAMES 8911	Mann et al., 2013	>41,100	AA-48745	Mann et al., 2013	Ikpikpuk R.	B	metacarpal	UAMES	-19.2	10.7
IK98-0089	Muskox	<i>Ovibos moschatus</i>	UAMES 9095	Mann et al., 2013	>41,100	AA-48746	Mann et al., 2013	Ikpikpuk R.	B	metacarpal	UAMES	-19.7	8.9
IK98-0133	Muskox	<i>Ovibos moschatus</i>	UAMES 9122	Mann et al., 2013	>41,100	AA-48747	Mann et al., 2013	Ikpikpuk R.	B	metacarpal	UAMES	-20.2	7.7
IK98-0286	Muskox	<i>Ovibos moschatus</i>	UAMES 8836	Mann et al., 2013	>41,100	AA-48236	Mann et al., 2013	Ikpikpuk R.	B	metacarpal	UAMES	-19.8	2.3

IK98-0461	Muskox	<i>Ovibos moschatus</i>	UAMES 9251	Mann et al., 2013	>41,100	AA-48237	Mann et al., 2013	Ikpikpuk R.	B	metacarpal	UAMES	-19.9	6.0
IK98-0513	Muskox	<i>Ovibos moschatus</i>	UAMES 9610	Mann et al., 2013	>41,100	AA-48255	Mann et al., 2013	Ikpikpuk R.	B	metatarsal	UAMES	-20.1	6.6
IK98-0653	Muskox	<i>Ovibos moschatus</i>	UAMES 9438	Mann et al., 2013	>41,100	AA-48256	Mann et al., 2013	Ikpikpuk R.	B	metacarpal	UAMES	-19.6	6.0
IK98-0742	Muskox	<i>Ovibos moschatus</i>	UAMES 9471	Mann et al., 2013	>41,100	AA-48752	Mann et al., 2013	Ikpikpuk R.	B	metatarsal	UAMES	-19.7	2.6
IK98-0930	Muskox	<i>Ovibos moschatus</i>	UAMES 9504	Mann et al., 2013	>41,100	AA-48754	Mann et al., 2013	Ikpikpuk R.	B	metacarpal	UAMES	-20.1	6.6
IK98-1027	Muskox	<i>Ovibos moschatus</i>	UAMES 9958	Mann et al., 2013	>41,100	AA-48240	Mann et al., 2013	Ikpikpuk R.	B	cranium	UAMES	-19.6	3.1
IK98-1044	Muskox	<i>Ovibos moschatus</i>	UAMES 10044	Mann et al., 2013	>41,100	AA-48241	Mann et al., 2013	Ikpikpuk R.	B	metacarpal	UAMES	-19.0	7.4
IK98-1124	Muskox	<i>Ovibos moschatus</i>	UAMES 9918	Mann et al., 2013	>41,100	AA-48242	Mann et al., 2013	Ikpikpuk R.	B	metacarpal	UAMES	-19.4	6.1
IK99-143	Muskox	<i>Ovibos moschatus</i>	UAMES 10683	Mann et al., 2013	>41,100	AA-48244	Mann et al., 2013	Ikpikpuk R.	B	cranium	UAMES	-20.4	4.7
IK99-320	Muskox	<i>Ovibos moschatus</i>	UAMES 10559	Mann et al., 2013	>41,100	AA-48245	Mann et al., 2013	Ikpikpuk R.	B	metacarpal	UAMES	-20.1	3.8
IK99-504	Muskox	<i>Ovibos moschatus</i>	UAMES 10883	Mann et al., 2013	>41,100	AA-48264	Mann et al., 2013	Ikpikpuk R.	B	metatarsal	UAMES	-20.0	8.8
IK98-1123	Muskox	<i>Ovibos moschatus</i>	UAMES 9922	Mann et al., 2013	>41,100	AA-48758	Mann et al., 2013	Ikpikpuk R.	B	metacarpal	UAMES	-19.9	6.5
IK98-1289	Muskox	<i>Ovibos moschatus</i>	UAMES 10018	Mann et al., 2013	>41,100	AA-48760	Mann et al., 2013	Ikpikpuk R.	B	metacarpal	UAMES	-20.6	7.3
IK98-1267	Muskox	<i>Ovibos moschatus</i>	UAMES 10058	Mann et al., 2013	>41,100	AA-48759	Mann et al., 2013	Ikpikpuk R.	B	cranium	UAMES	-20.5	6.4
IK99-255	Muskox	<i>Ovibos moschatus</i>	UAMES 10645	Mann et al., 2013	>41,100	AA-48765	Mann et al., 2013	Ikpikpuk R.	B	metacarpal	UAMES	-19.5	9.1
IK98-1220	Muskox	<i>Ovibos moschatus</i>	UAMES 9874	Mann et al., 2013	>45,720	Beta-175459	Mann et al., 2013	Ikpikpuk R.	B	phalange	UAMES	-20.5	6.4
IK99-142	Muskox	<i>Ovibos moschatus</i>	UAMES 10682	Mann et al., 2013	>48,420	Beta-175460	Mann et al., 2013	Ikpikpuk R.	B	cranium	UAMES	-19.9	3.5

Appendix R continues below. A limited number of specimens had additional information (i.e. % yield, %C, %N and C/N).

Lab ID/Field ID	% Yield	%C	%N	C/N
MAY12-45	10.6	43.8	15.9	3.2
IK01-277	11.9	43.0	15.7	3.2
MAY12-70	13.7	41.7	15.3	3.2
KIG12-15	9.8	44.8	16.4	3.2
IK10-106	8.8	44.2	16.3	3.2
IK99-237	13.3	44.4	16.3	3.2
IK01-321	10.2	44.1	16.0	3.2
IK08-127	9.9	43.8	15.9	3.2

UAMES = University of Alaska Museum Earth Sciences

Tissue: B = Bone; RD = Root dentin; C = Cementum; D = Crown dentin; T= Tusk dentin

References:

- Mann, D.H., Groves, P., Kunz, M.L., Reanier, R.E., Gaglioti, B. V., 2013. Ice-age megafauna in Arctic Alaska: extinction, invasion, survival. *Quat. Sci. Rev.* 70, 91–108. doi:10.1016/j.quascirev.2013.03.015
- Zazula, G.D., MacPhee, R.D., Metcalfe, J.Z., Reyes, A. V., Brock, F., Druckenmiller, P.S., Groves, P., Harington, R., Hodgins, G.W.L., Kunz, M.L., Longstaffe, F.J., Mann, D.H., McDonald, H.G., Nalawade-Chavan, S., Southon, J.R., 2014. American mastodon extirpation in the Arctic and Subarctic predates human colonization and terminal Pleistocene climate change. *Proc. Natl. Acad. Sci.* 111, 18460–18465.

Appendix S Sample information for megafaunal herbivores from NW Europe.

Lab ID	Common Name	Scientific Name	Sample Number	Stable Isotope Reference	¹⁴ C Date	Date Lab #	Calibrated Date	Date reference
KSL-10	Bison	<i>Bison</i> sp.	M001:144	Bocherens et al., 2011	~14~12,000			Bocherens et al., 2011
KSL-11	Bison	<i>Bison</i> sp.	M001:152	Bocherens et al., 2011	~14~12,000			Bocherens et al., 2011
KSL-12	Bison	<i>Bison</i> sp.	HE30:8	Bocherens et al., 2011	~14~12,000			Bocherens et al., 2011
Goyet-A3-13	Bison	<i>Bison priscus</i>	2230-1	Bocherens et al., 2011	~24~40,000			Bocherens et al., 2011
Goyet-A3-14	Bison	<i>Bison priscus</i>	2230-2	Bocherens et al., 2011	~24~40,000			Bocherens et al., 2011
Goyet-B4-5	Bison	<i>Bison priscus</i>	2737-1	Bocherens et al., 2011	~24~40,000			Bocherens et al., 2011
Goyet-B4-7	Bison	<i>Bison priscus</i>	2737-3	Bocherens et al., 2011	~24~40,000			Bocherens et al., 2011
SC29000	Bison	<i>Bison priscus</i>	SC91 213 H30 (4)	Bocherens et al., 2011	~24~40,000			Bocherens et al., 2011
LBR100	Bison	<i>Bison priscus</i>		Bocherens et al., 2005			~35,000	Bocherens et al., 2005
LBR200	Bison	<i>Bison priscus</i>		Bocherens et al., 2005			~35,000	Bocherens et al., 2005
LBR300	Bison	<i>Bison priscus</i>		Bocherens et al., 2005			~35,000	Bocherens et al., 2005
LBR400	Bison	<i>Bison priscus</i>		Bocherens et al., 2005			~35,000	Bocherens et al., 2005
LBR500	Bison	<i>Bison priscus</i>		Bocherens et al., 2005			~35,000	Bocherens et al., 2005
LBR600	Bison	<i>Bison priscus</i>		Bocherens et al., 2005			~35,000	Bocherens et al., 2005
LBR700	Bison	<i>Bison priscus</i>		Bocherens et al., 2005			~35,000	Bocherens et al., 2005
LBR3100	Bison	<i>Bison priscus</i>		Bocherens et al., 2005			~35,000	Bocherens et al., 2005
	Bison	<i>Bison priscus</i>		Fizet et al., 1995			~40- 45,000	Fizet et al., 1995
	Bison	<i>Bison priscus</i>		Fizet et al., 1995			~40- 45,000	Fizet et al., 1995
	Bison	<i>Bison priscus</i>		Fizet et al., 1995			~40- 45,000	Fizet et al., 1995
	Bison	<i>Bison priscus</i>		Fizet et al., 1995			~40- 45,000	Fizet et al., 1995
	Bison	<i>Bison priscus</i>		Fizet et al., 1995			~40- 45,000	Fizet et al., 1995
RA-KSL-620	Caribou*	<i>Rangifer tarandus</i>		Drucker et al., 2011 as referenced in Bocherens et al., 2011	~14~12,000			Bocherens et al., 2011

RA-KSL-628	Caribou*	<i>Rangifer tarandus</i>	Drucker et al., 2011 as referenced in Bocherens et al., 2011	~14~12,000	Bocherens et al., 2011
RA-KSL-632	Caribou*	<i>Rangifer tarandus</i>	Drucker et al., 2011 as referenced in Bocherens et al., 2011	~14~12,000	Bocherens et al., 2011
RA-KSL-633	Caribou*	<i>Rangifer tarandus</i>	Drucker et al., 2011 as referenced in Bocherens et al., 2011	~14~12,000	Bocherens et al., 2011
RA-KSL-635	Caribou*	<i>Rangifer tarandus</i>	Drucker et al., 2011 as referenced in Bocherens et al., 2011	~14~12,000	Bocherens et al., 2011
RA-PTF 363	Caribou*	<i>Rangifer tarandus</i>	Drucker et al., 2011 as referenced in Bocherens et al., 2011	~14~12,000	Bocherens et al., 2011
RA-PTF 364	Caribou*	<i>Rangifer tarandus</i>	Drucker et al., 2011 as referenced in Bocherens et al., 2011	~14~12,000	Bocherens et al., 2011
RA-PTF 365	Caribou*	<i>Rangifer tarandus</i>	Drucker et al., 2011 as referenced in Bocherens et al., 2011	~14~12,000	Bocherens et al., 2011
RA-PTF 366	Caribou*	<i>Rangifer tarandus</i>	Drucker et al., 2011 as referenced in Bocherens et al., 2011	~14~12,000	Bocherens et al., 2011
RA-PTF 367	Caribou*	<i>Rangifer tarandus</i>	Drucker et al., 2011 as referenced in Bocherens et al., 2011	~14~12,000	Bocherens et al., 2011
RA-PTF 368	Caribou*	<i>Rangifer tarandus</i>	Drucker et al., 2011 as referenced in Bocherens et al., 2011	~14~12,000	Bocherens et al., 2011
RA-PTF 369	Caribou*	<i>Rangifer tarandus</i>	Drucker et al., 2011 as referenced in Bocherens et al., 2011	~14~12,000	Bocherens et al., 2011
RA-PTF 370	Caribou*	<i>Rangifer tarandus</i>	Drucker et al., 2011 as referenced in Bocherens et al., 2011	~14~12,000	Bocherens et al., 2011

RA-PTF 371	Caribou*	<i>Rangifer tarandus</i>	Drucker et al., 2011 as referenced in Bocherens et al., 2011	~14~12,000	Bocherens et al., 2011
RA-PTF 373	Caribou*	<i>Rangifer tarandus</i>	Drucker et al., 2011 as referenced in Bocherens et al., 2011	~14~12,000	Bocherens et al., 2011
RA-PTF 374	Caribou*	<i>Rangifer tarandus</i>	Drucker et al., 2011 as referenced in Bocherens et al., 2011	~14~12,000	Bocherens et al., 2011
RA-PTF 375	Caribou*	<i>Rangifer tarandus</i>	Drucker et al., 2011 as referenced in Bocherens et al., 2011	~14~12,000	Bocherens et al., 2011
RA-PTF 376	Caribou*	<i>Rangifer tarandus</i>	Drucker et al., 2011 as referenced in Bocherens et al., 2011	~14~12,000	Bocherens et al., 2011
RA-PTF 377	Caribou*	<i>Rangifer tarandus</i>	Drucker et al., 2011 as referenced in Bocherens et al., 2011	~14~12,000	Bocherens et al., 2011
RA-PTF 379	Caribou*	<i>Rangifer tarandus</i>	Drucker et al., 2011 as referenced in Bocherens et al., 2011	~14~12,000	Bocherens et al., 2011
RA-PTF 380	Caribou*	<i>Rangifer tarandus</i>	Drucker et al., 2011 as referenced in Bocherens et al., 2011	~14~12,000	Bocherens et al., 2011
RA-PTF 381	Caribou*	<i>Rangifer tarandus</i>	Drucker et al., 2011 as referenced in Bocherens et al., 2011	~14~12,000	Bocherens et al., 2011
RA-PTF 382	Caribou*	<i>Rangifer tarandus</i>	Drucker et al., 2011 as referenced in Bocherens et al., 2011	~14~12,000	Bocherens et al., 2011
RA-PTF 383	Caribou*	<i>Rangifer tarandus</i>	Drucker et al., 2011 as referenced in Bocherens et al., 2011	~14~12,000	Bocherens et al., 2011
SCH-1	Caribou*	<i>Rangifer tarandus</i>	Drucker et al., 2011 as referenced in Bocherens et al., 2011	~14~12,000	Bocherens et al., 2011

SCH-2	Caribou*	<i>Rangifer tarandus</i>		Drucker et al., 2011 as referenced in Bocherens et al., 2011	~14~12,000		Bocherens et al., 2011
SCH-3	Caribou*	<i>Rangifer tarandus</i>		Drucker et al., 2011 as referenced in Bocherens et al., 2011	~14~12,000		Bocherens et al., 2011
SCH-4	Caribou*	<i>Rangifer tarandus</i>		Drucker et al., 2011 as referenced in Bocherens et al., 2011	~14~12,000		Bocherens et al., 2011
SCH-5	Caribou*	<i>Rangifer tarandus</i>		Drucker et al., 2011 as referenced in Bocherens et al., 2011	~14~12,000		Bocherens et al., 2011
FLS-7	Caribou*	<i>Rangifer tarandus</i>	Q8 Nr1515	Drucker et al., 2011 as referenced in Bocherens et al., 2011	~14~12,000		Bocherens et al., 2011
FLS-8	Caribou*	<i>Rangifer tarandus</i>	Q304 Nr59 Nr54+43	Drucker et al., 2011 as referenced in Bocherens et al., 2011	~14~12,000		Bocherens et al., 2011
FLS-9	Caribou*	<i>Rangifer tarandus</i>	Q300 Nr352+365	Drucker et al., 2011 as referenced in Bocherens et al., 2011	~14~12,000		Bocherens et al., 2011
HFL-1	Caribou*	<i>Rangifer tarandus</i>	99 178	Bocherens et al., 2011	~14~12,000		Bocherens et al., 2011
GSK-1	Caribou*	<i>Rangifer tarandus</i>	78 22	Bocherens et al., 2011	~14~12,000		Bocherens et al., 2011
OxA-6254	Caribou*	<i>Rangifer tarandus</i>		Bocherens et al., 2011	13,130±100	OxA-6254	Stevens & Hedges, 2004 as referenced in Bocherens et al., 2011
TUB-57	Caribou*	<i>Rangifer tarandus</i>		Bocherens et al., 2011	13,020±130	OxA-4602	Bocherens et al., 2011
RAN-10	Caribou*	<i>Rangifer tarandus</i>	Ran 88 F12 lim 260- 270	Bocherens et al., 2011	13,965±101	Erl-9392	Bocherens et al., 2011
RCD100	Caribou*	<i>Rangifer tarandus</i>	C8 Lg D1 - 235 -240	Bocherens et al., 2011	~14~12,000		Bocherens et al., 2011
RCD200	Caribou*	<i>Rangifer tarandus</i>	A9 -205 -230	Bocherens et al., 2011	~14~12,000		Bocherens et al., 2011
RCD400	Caribou*	<i>Rangifer</i>	A8 -210	Bocherens et al., 2011	~14~12,000		Bocherens et al., 2011

RCD10800	Caribou*	<i>tarandus</i> <i>Rangifer tarandus</i>	Ro70 220 47 28	Bocherens et al., 2011	12,420±75	OxA-8030	Bocherens et al., 2011
BLS 1	Caribou*	<i>Rangifer tarandus</i>	31-11-A	Bocherens et al., 2011	12,530±120	Ly-3280(Poz)	Bocherens et al., 2011
FRT 1	Caribou*	<i>Rangifer tarandus</i>	Fr-87-17-M3- 297	Bocherens et al., 2011	13,045±75	Ly-3292(Poz)	Bocherens et al., 2011
ARL 6	Caribou*	<i>Rangifer tarandus</i>	44J- sect1/1998-3- 384	Bocherens et al., 2011	13,640±60	Ly-3878(GrA)	Bocherens et al., 2011
TDG500	Caribou*	<i>Rangifer tarandus</i>	MAR97 TDG	Bocherens et al., 2011	13,000- 12,000		Drucker et al., 2011 as referenced in Bocherens et al., 2011
TDG600	Caribou*	<i>Rangifer tarandus</i>	MAR97 TDG	Bocherens et al., 2011	13,000- 12,000		Drucker et al., 2011 as referenced in Bocherens et al., 2011
TDG700	Caribou*	<i>Rangifer tarandus</i>	MAR97 TDG	Bocherens et al., 2011	13,000- 12,000		Drucker et al., 2011 as referenced in Bocherens et al., 2011
TDG1400	Caribou*	<i>Rangifer tarandus</i>	sondage 1	Bocherens et al., 2011	13,000- 12,000		Drucker et al., 2011 as referenced in Bocherens et al., 2011
TDG1500	Caribou*	<i>Rangifer tarandus</i>	sondage 1	Bocherens et al., 2011	13,000- 12,000		Drucker et al., 2011 as referenced in Bocherens et al., 2011
TDG1600	Caribou*	<i>Rangifer tarandus</i>	sondage 1	Bocherens et al., 2011	13,000- 12,000		Drucker et al., 2011 as referenced in Bocherens et al., 2011
PCV-7	Caribou*	<i>Rangifer tarandus</i>	Pinc99 IV0 S°34 Y124b n°382	Bocherens et al., 2011	13,000- 12,000		Drucker et al., 2011 as referenced in Bocherens et al., 2011
PCV-14	Caribou*	<i>Rangifer tarandus</i>	Pinc98 IV0 S°43 T128 n°11	Bocherens et al., 2011	13,000- 12,000		Drucker et al., 2011 as referenced in Bocherens et al., 2011

PCV-22	Caribou*	<i>Rangifer tarandus</i>	Pinc69 IV20 S°36 U106 595	Bocherens et al., 2011	13,000- 12,000		Drucker et al., 2011 as referenced in Bocherens et al., 2011
ETL-3	Caribou*	<i>Rangifer tarandus</i>	G68 n°124	Bocherens et al., 2011	13,000- 12,000		Drucker et al., 2011 as referenced in Bocherens et al., 2011
ETL-4	Caribou*	<i>Rangifer tarandus</i>	A66 n°18	Bocherens et al., 2011	13,000- 12,000		Drucker et al., 2011 as referenced in Bocherens et al., 2011
ETL-9	Caribou*	<i>Rangifer tarandus</i>	n°20	Bocherens et al., 2011	12315±75	(OxA-8757)	Drucker et al., 2011 as referenced in Bocherens et al., 2011
ETL-6	Caribou*	<i>Rangifer tarandus</i>	N16 n°15	Bocherens et al., 2011	13,000- 12,000		Drucker et al., 2011 as referenced in Bocherens et al., 2011
VRB-4	Caribou*	<i>Rangifer tarandus</i>	VBC79 201 C18 55 et 56	Bocherens et al., 2011	13,000- 12,000		Drucker et al., 2011 as referenced in Bocherens et al., 2011
VRB-5	Caribou*	<i>Rangifer tarandus</i>	VBC79-201 G18-137	Bocherens et al., 2011	13,000- 12,000		Drucker et al., 2011 as referenced in Bocherens et al., 2011
VRB-6	Caribou*	<i>Rangifer tarandus</i>	VBC79.201 B17-89	Bocherens et al., 2011	13,000- 12,000		Drucker et al., 2011 as referenced in Bocherens et al., 2011
MN700	Caribou*	<i>Rangifer tarandus</i>	MN c2b foyer	Drucker et al., 2003b	~13,000- ~15,300 BP	Based on layer date	Drucker et al., 2003b
MN800	Caribou*	<i>Rangifer tarandus</i>	MNJ28 311 c2b	Drucker et al., 2003b	~13,000- ~15,300 BP	Based on layer date	Drucker et al., 2003b
MN900	Caribou*	<i>Rangifer tarandus</i>	MNJ28 428 c2b	Drucker et al., 2003b	~13,000- ~15,300 BP	Based on layer date	Drucker et al., 2003b
MN1100	Caribou*	<i>Rangifer tarandus</i>	MN H28 c2c	Drucker et al., 2003b	~13,000- ~15,300 BP	Based on layer date	Drucker et al., 2003b
FLG200	Caribou*	<i>Rangifer tarandus</i>	FLAGII phi5'cIX309	Drucker et al., 2003b	~13,000- ~15,300 BP	Based on layer date	Drucker et al., 2003b
FLG300	Caribou*	<i>Rangifer tarandus</i>	FLAGII phi5'cIX300	Drucker et al., 2003b	~13,000- ~15,300 BP	Based on layer date	Drucker et al., 2003b

FLG400	Caribou*	<i>Rangifer tarandus</i>	FLAGII phi5'cIX338	Drucker et al., 2003b	~13,000- ~15,300 BP	Based on layer date	Drucker et al., 2003b
FLG500	Caribou*	<i>Rangifer tarandus</i>	FLAG4/5K5'c IX	Drucker et al., 2003b	~13,000- ~15,300 BP	Based on layer date	Drucker et al., 2003b
FLG600	Caribou*	<i>Rangifer tarandus</i>	FLAG4/5K5'c IX114	Drucker et al., 2003b	~13,000- ~15,300 BP	Based on layer date	Drucker et al., 2003b
SGR200	Caribou*	<i>Rangifer tarandus</i>	St Gr R t.s.	Drucker et al., 2003b	~13,000- ~15,300 BP	Based on layer date	Drucker et al., 2003b
SGR2700	Caribou*	<i>Rangifer tarandus</i>	L22c#168	Drucker et al., 2003b	~13,000- ~15,300 BP	Based on layer date	Drucker et al., 2003b
LGH1400	Caribou*	<i>Rangifer tarandus</i>	LHE Magd.III2	Drucker et al., 2003b	~13,000- ~15,300 BP	Based on layer date	Drucker et al., 2003b
LGH1500	Caribou*	<i>Rangifer tarandus</i>	LHE Magd.III	Drucker et al., 2003b	~13,000- ~15,300 BP	Based on layer date	Drucker et al., 2003b
PRG200	Caribou*	<i>Rangifer tarandus</i>	46PRG 18E.3	Drucker et al., 2003b	~13,000- ~15,300 BP	Based on layer date	Drucker et al., 2003b
PRG300	Caribou*	<i>Rangifer tarandus</i>	46PRG 12B.3b 261	Drucker et al., 2003b	~13,000- ~15,300 BP	Based on layer date	Drucker et al., 2003b
PRG400	Caribou*	<i>Rangifer tarandus</i>	46PRG 19C.3 T.515	Drucker et al., 2003b	~13,000- ~15,300 BP	Based on layer date	Drucker et al., 2003b
PRG500	Caribou*	<i>Rangifer tarandus</i>	46PRG 16C.3 T.439	Drucker et al., 2003b	~13,000- ~15,300 BP	Based on layer date	Drucker et al., 2003b
JBL1300	Caribou*	<i>Rangifer tarandus</i>	JBL 90AFEQ2c.1	Drucker et al., 2003b	14,850±130 (Gif8667)	Based on layer date	Drucker et al., 2003b
JBL1400	Caribou*	<i>Rangifer tarandus</i>	JBL 90AFEQ2c.1	Drucker et al., 2003b	14,850±130 (Gif8667)	Based on layer date	Drucker et al., 2003b
JBL1500	Caribou*	<i>Rangifer tarandus</i>	JBL 90AFEQ2c.1	Drucker et al., 2003b	14,850±130 (Gif8667)	Based on layer date	Drucker et al., 2003b
JBL900	Caribou*	<i>Rangifer tarandus</i>	JBL 89AFWD3c.2 #205	Drucker et al., 2003b	16,490±130 (Gif8668)	Based on layer date	Drucker et al., 2003b
JBL1000	Caribou*	<i>Rangifer tarandus</i>	JBL 89AFWD2c.2 #393	Drucker et al., 2003b	17,490±130 (Gif8668)	Based on layer date	Drucker et al., 2003b

JBL1100	Caribou*	<i>Rangifer tarandus</i>	JBL 89AFWD3c.2 #324	Drucker et al., 2003b	18,490±130 (Gif8668)	Based on layer date	Drucker et al., 2003b
JBL1700	Caribou*	<i>Rangifer tarandus</i>	JBL 86CL9c.2	Drucker et al., 2003b	17,770±260 (Ly4589)	Based on layer date	Drucker et al., 2003b
JBL1800	Caribou*	<i>Rangifer tarandus</i>	JBL 86CL9c.2	Drucker et al., 2003b	17,770±260 (Ly4589)	Based on layer date	Drucker et al., 2003b
JBL1900	Caribou*	<i>Rangifer tarandus</i>	JBL 81CL5c.2	Drucker et al., 2003b	17,770±260 (Ly4589)	Based on layer date	Drucker et al., 2003b
PRG1000	Caribou*	<i>Rangifer tarandus</i>	46PRG 10E.5b 190	Drucker et al., 2003b	16,140±150 (GifA95446)	Based on layer date	Drucker et al., 2003b
PRG1200	Caribou*	<i>Rangifer tarandus</i>	46PRG 12H.5x 13	Drucker et al., 2003b	16,960±190 (GifA93085)	Based on layer date	Drucker et al., 2003b
PRG1300	Caribou*	<i>Rangifer tarandus</i>	46PRG 10G.7 259	Drucker et al., 2003b	17,560±160 (GifA96227)	Based on layer date	Drucker et al., 2003b
PRG1400	Caribou*	<i>Rangifer tarandus</i>	46PRG 12F.7	Drucker et al., 2003b	17,560±160 (GifA96227)	Based on layer date	Drucker et al., 2003b
PRG1500	Caribou*	<i>Rangifer tarandus</i>	46PRG 8D.7 103	Drucker et al., 2003b	17,560±160 (GifA96227)	Based on layer date	Drucker et al., 2003b
PRG1600	Caribou*	<i>Rangifer tarandus</i>	46PRG 7G.7 13	Drucker et al., 2003b	17,560±160 (GifA96227)	Based on layer date	Drucker et al., 2003b
PRG1700	Caribou*	<i>Rangifer tarandus</i>	46PRG 11A.7	Drucker et al., 2003b	17,560±160 (GifA96227)	Based on layer date	Drucker et al., 2003b
PRG1800	Caribou*	<i>Rangifer tarandus</i>	46PRG 7A.7	Drucker et al., 2003b	17,560±160 (GifA96227)	Based on layer date	Drucker et al., 2003b
PRG2200	Caribou*	<i>Rangifer tarandus</i>	46PRG 9G.9b T.750	Drucker et al., 2003b	18,600±140 (GifA96228)	Based on layer date	Drucker et al., 2003b
PRG2300	Caribou*	<i>Rangifer tarandus</i>	46PRG 9E.9b 232	Drucker et al., 2003b	18,600±140 (GifA96228)	Based on layer date	Drucker et al., 2003b
JBL3100	Caribou*	<i>Rangifer tarandus</i>	JBL 81SCL2bc.3	Drucker et al., 2003b	19,010±310 (Ly4588)	Based on layer date	Drucker et al., 2003b
JBL3200	Caribou*	<i>Rangifer tarandus</i>	JBL 85CL7.8c.3	Drucker et al., 2003b	19,010±310 (Ly4588)	Based on layer date	Drucker et al., 2003b
JBL3300	Caribou*	<i>Rangifer tarandus</i>	JBL 86CL7c.3	Drucker et al., 2003b	19,010±310 (Ly4588)	Based on layer date	Drucker et al., 2003b

JBL3400	Caribou*	<i>Rangifer tarandus</i>	JBL 86CL7c.3	Drucker et al., 2003b	19,010±310 (Ly4588)	Based on layer date	Drucker et al., 2003b
JBL3500	Caribou*	<i>Rangifer tarandus</i>	JBL P87CL2c.3	Drucker et al., 2003b	19,010±310 (Ly4588)	Based on layer date	Drucker et al., 2003b
PRG3100	Caribou*	<i>Rangifer tarandus</i>	46PRG 9E 12 307	Drucker et al., 2003b	19,310±210 (GifA92166)	Based on layer date	Drucker et al., 2003b
PRG3200	Caribou*	<i>Rangifer tarandus</i>	46PRG 8E 12 158	Drucker et al., 2003b	19,310±210 (GifA92166)	Based on layer date	Drucker et al., 2003b
PRG3300	Caribou*	<i>Rangifer tarandus</i>	46PRG 9F 12 307	Drucker et al., 2003b	19,310±210 (GifA92166)	Based on layer date	Drucker et al., 2003b
PRG3400	Caribou*	<i>Rangifer tarandus</i>	46PRG 11A 12 171	Drucker et al., 2003b	19,310±210 (GifA92166)	Based on layer date	Drucker et al., 2003b
PRG3500	Caribou*	<i>Rangifer tarandus</i>	46PRG 8A 12 113	Drucker et al., 2003b	19,310±210 (GifA92166)	Based on layer date	Drucker et al., 2003b
PRG3600	Caribou*	<i>Rangifer tarandus</i>	46PRG 10B 12 414	Drucker et al., 2003b	19,310±210 (GifA92166)	Based on layer date	Drucker et al., 2003b
CS2600	Caribou*	<i>Rangifer tarandus</i>	H20D 120(5)	Drucker et al., 2003b	18,350±160 (Oxa6870), 19,760±160 (Oxa6518)	Based on layer date	Drucker et al., 2003b
CS2700	Caribou*	<i>Rangifer tarandus</i>	H21B 100(4)	Drucker et al., 2003b	18,350±160 (Oxa6870), 19,760±160 (Oxa6518)	Based on layer date	Drucker et al., 2003b
CS3100	Caribou*	<i>Rangifer tarandus</i>	J15D 154(10)	Drucker et al., 2003b	18,350±160 (Oxa6870), 19,760±160 (Oxa6518)	Based on layer date	Drucker et al., 2003b
PRG4200	Caribou*	<i>Rangifer tarandus</i>	46PRG 9E 18 T763	Drucker et al., 2003b	22,400±280 (GifA92169), 22,750±250 (GifA96224)	Based on layer date	Drucker et al., 2003b
PRG4300	Caribou*	<i>Rangifer tarandus</i>	46PRG 8C 18 377	Drucker et al., 2003b	22,400±280 (GifA92169), 22,750±250 (GifA96224)	Based on layer date	Drucker et al., 2003b

PRG4400	Caribou*	<i>Rangifer tarandus</i>	46PRG 6C 18 77	Drucker et al., 2003b	22,400±280 (GifA92169), 22,750±250 (GifA96224)	Based on layer date	Drucker et al., 2003b
PRG4500	Caribou*	<i>Rangifer tarandus</i>	46PRG 9B 18 323	Drucker et al., 2003b	22,400±280 (GifA92169), 22,750±250 (GifA96224)	Based on layer date	Drucker et al., 2003b
PRG4600	Caribou*	<i>Rangifer tarandus</i>	46PRG 7C 18 205	Drucker et al., 2003b	22,400±280 (GifA92169), 22,750±250 (GifA96224)	Based on layer date	Drucker et al., 2003b
PRG4700	Caribou*	<i>Rangifer tarandus</i>	46PRG 12C 18 464	Drucker et al., 2003b	22,400±280 (GifA92169), 22,750±250 (GifA96224)	Based on layer date	Drucker et al., 2003b
PRG5300	Caribou*	<i>Rangifer tarandus</i>	46PRG 9D 22 969	Drucker et al., 2003b	24,800±500 (Gif7998)	Based on layer date	Drucker et al., 2003b
PRG5400	Caribou*	<i>Rangifer tarandus</i>	46PRG 9D 22 246	Drucker et al., 2003b	24,800±500 (Gif7998)	Based on layer date	Drucker et al., 2003b
PRG5500	Caribou*	<i>Rangifer tarandus</i>	46PRG 9D 22 348	Drucker et al., 2003b	24,800±500 (Gif7998)	Based on layer date	Drucker et al., 2003b
PRG5600	Caribou*	<i>Rangifer tarandus</i>	46PRG 9D 22 347	Drucker et al., 2003b	24,800±500 (Gif7998)	Based on layer date	Drucker et al., 2003b
PRG5700	Caribou*	<i>Rangifer tarandus</i>	46PRG 9C 22 T270	Drucker et al., 2003b	24,800±500 (Gif7998)	Based on layer date	Drucker et al., 2003b
PRG5800	Caribou*	<i>Rangifer tarandus</i>	46PRG 9C 22 348	Drucker et al., 2003b	24,800±500 (Gif7998)	Based on layer date	Drucker et al., 2003b
CS1000	Caribou*	<i>Rangifer tarandus</i>	G22D 14	Drucker et al., 2003b	26,620±340 (Oxa6876), 27,880±440 (Oxa6514)	Based on layer date	Drucker et al., 2003b
Goyet-A3-15	Caribou*	<i>Rangifer tarandus</i>	2791-1	Bocherens et al., 2011	~24-~40,000		Bocherens et al., 2011
Goyet-A3-16	Caribou*	<i>Rangifer tarandus</i>	2791-2	Bocherens et al., 2011	~24-~40,000		Bocherens et al., 2011

Goyet-A3-17	Caribou*	<i>Rangifer tarandus</i>	2791-3	Bocherens et al., 2011	~24~40,000	Bocherens et al., 2011
Goyet-A3-18	Caribou*	<i>Rangifer tarandus</i>	2791-4	Bocherens et al., 2011	~24~40,000	Bocherens et al., 2011
Goyet-A3-19	Caribou*	<i>Rangifer tarandus</i>	2791-5	Bocherens et al., 2011	~24~40,000	Bocherens et al., 2011
Goyet-B4-8	Caribou*	<i>Rangifer tarandus</i>	2737	Bocherens et al., 2011	~24~40,000	Bocherens et al., 2011
RA-GK 294	Caribou*	<i>Rangifer tarandus</i>		Bocherens et al., 2011	~26~40,000	Bocherens et al., 2011
RA-GK 295	Caribou*	<i>Rangifer tarandus</i>		Bocherens et al., 2011	~26~40,000	Bocherens et al., 2011
RA-GK 296	Caribou*	<i>Rangifer tarandus</i>		Bocherens et al., 2011	~26~40,000	Bocherens et al., 2011
RA-GK 298	Caribou*	<i>Rangifer tarandus</i>		Bocherens et al., 2011	~26~40,000	Bocherens et al., 2011
RA-GK 299	Caribou*	<i>Rangifer tarandus</i>		Bocherens et al., 2011	~26~40,000	Bocherens et al., 2011
RA-GK 300	Caribou*	<i>Rangifer tarandus</i>		Bocherens et al., 2011	~26~40,000	Bocherens et al., 2011
RA-GK 302	Caribou*	<i>Rangifer tarandus</i>		Bocherens et al., 2011	~26~40,000	Bocherens et al., 2011
RA-GK 304	Caribou*	<i>Rangifer tarandus</i>		Bocherens et al., 2011	~26~40,000	Bocherens et al., 2011
RA-GK 306	Caribou*	<i>Rangifer tarandus</i>		Bocherens et al., 2011	~26~40,000	Bocherens et al., 2011
OxA-6256	Caribou*	<i>Rangifer tarandus</i>		Bocherens et al., 2011	30100±550	Stevens & Hedges, 2004 as referenced in Bocherens et al., 2011
RA-GK 303	Caribou*	<i>Rangifer tarandus</i>		Bocherens et al., 2011	~26~40,000	Bocherens et al., 2011
RA-GK 308	Caribou*	<i>Rangifer tarandus</i>		Bocherens et al., 2011	~26~40,000	Bocherens et al., 2011
RA-GK 309	Caribou*	<i>Rangifer tarandus</i>		Bocherens et al., 2011	~26~40,000	Bocherens et al., 2011
RA-GK 311	Caribou*	<i>Rangifer tarandus</i>		Bocherens et al., 2011	~26~40,000	Bocherens et al., 2011
RA-GK 312	Caribou*	<i>Rangifer tarandus</i>		Bocherens et al., 2011	~26~40,000	Bocherens et al., 2011

SC22400	Caribou*	<i>Rangifer tarandus</i>	SC95 475 F39	Bocherens et al., 2001	Based on estimated age of layer	~40,000	Bocherens et al., 1997
RPB7200	Caribou*	<i>Rangifer tarandus</i>		Bocherens et al., 2005		~35,000	Bocherens et al., 2005
LBR900	Caribou*	<i>Rangifer tarandus</i>		Bocherens et al., 2005		~35,000	Bocherens et al., 2005
LBR1000	Caribou*	<i>Rangifer tarandus</i>		Bocherens et al., 2005		~35,000	Bocherens et al., 2005
LBR1100	Caribou*	<i>Rangifer tarandus</i>		Bocherens et al., 2005		~35,000	Bocherens et al., 2005
LBR3400	Caribou*	<i>Rangifer tarandus</i>		Bocherens et al., 2005		~35,000	Bocherens et al., 2005
	Caribou*	<i>Rangifer tarandus</i>		Fizet et al., 1995		~40-45,000	Fizet et al., 1995
	Caribou*	<i>Rangifer tarandus</i>		Fizet et al., 1995		~40-45,000	Fizet et al., 1995
	Caribou*	<i>Rangifer tarandus</i>		Fizet et al., 1995		~40-45,000	Fizet et al., 1995
	Caribou*	<i>Rangifer tarandus</i>		Fizet et al., 1995		~40-45,000	Fizet et al., 1995
	Caribou*	<i>Rangifer tarandus</i>		Fizet et al., 1995		~40-45,000	Fizet et al., 1995
	Caribou*	<i>Rangifer tarandus</i>		Fizet et al., 1995		~40-45,000	Fizet et al., 1995
	Caribou*	<i>Rangifer tarandus</i>		Fizet et al., 1995		~40-45,000	Fizet et al., 1995
	Caribou*	<i>Rangifer tarandus</i>		Fizet et al., 1995		~40-45,000	Fizet et al., 1995
	Caribou*	<i>Rangifer tarandus</i>		Fizet et al., 1995		~40-45,000	Fizet et al., 1995
	Elk**	<i>Cervus elaphus</i>	PAM200	Drucker et al., 2003a		~10,000-8,000	Drucker et al., 2003a
	Elk**	<i>Cervus elaphus</i>	PAM300	Drucker et al., 2003a		~10,000-8,000	Drucker et al., 2003a
	Elk**	<i>Cervus elaphus</i>	PAM400	Drucker et al., 2003a		~10,000-8,000	Drucker et al., 2003a

	Elk**	<i>Cervus elaphus</i>	PAM500	Drucker et al., 2003a	~10,000-8,000		Drucker et al., 2003a
	Elk**	<i>Cervus elaphus</i>	RCD6200	Drucker et al., 2003a	~10,000-8,000		Drucker et al., 2003a
	Elk**	<i>Cervus elaphus</i>	RCD6300	Drucker et al., 2003a	~10,000-8,000		Drucker et al., 2003a
	Elk**	<i>Cervus elaphus</i>	RCD6400	Drucker et al., 2003a	~10,000-8,000		Drucker et al., 2003a
	Elk**	<i>Cervus elaphus</i>	RCD6500	Drucker et al., 2003a	~10,000-8,000		Drucker et al., 2003a
	Elk**	<i>Cervus elaphus</i>	RCD10100	Drucker et al., 2003a	~10,000-8,000		Drucker et al., 2003a
	Elk**	<i>Cervus elaphus</i>	RCD10200	Drucker et al., 2003a	~10,000-8,000		Drucker et al., 2003a
	Elk**	<i>Cervus elaphus</i>	RCD10300	Drucker et al., 2003a	~10,000-8,000		Drucker et al., 2003a
	Elk**	<i>Cervus elaphus</i>	RCD10400	Drucker et al., 2003a	~10,000-8,000		Drucker et al., 2003a
BVN-9(2)	Elk**	<i>Cervus elaphus</i>	Y8 -156-160 n°5	Bocherens et al., 2011	12,170±60	GrA-23129	Drucker et al., 2011 as referenced in Bocherens et al., 2011
KSL-45	Elk**	<i>Cervus elaphus</i>	M001:271	Bocherens et al., 2011	12,335±45	KIA-33351	Bocherens et al., 2011
RCD11000	Elk**	<i>Cervus elaphus</i>	A3	Bocherens et al., 2011	12,230±50	GrA-45781	Bocherens et al., 2011
RCD10900	Elk**	<i>Cervus elaphus</i>	A3	Bocherens et al., 2011	~14~12,000		Bocherens et al., 2011
RCD500	Elk**	<i>Cervus elaphus</i>	D6 Roch70 n°19	Bocherens et al., 2011	12,250±70	GrA-21512	Bocherens et al., 2011
CLS1000	Elk**	<i>Cervus elaphus</i>	LC97IFP3S6 L46 E268 139	Bocherens et al., 2011	13,000-12,000		Bocherens et al., 2011
CLS1100	Elk**	<i>Cervus elaphus</i>	LC97IFP3S6 L46 E270 67	Bocherens et al., 2011	13,000-12,000		Bocherens et al., 2011
CLS1200-3	Elk**	<i>Cervus elaphus</i>	LC97IFP3S6 L46 D268 280	Bocherens et al., 2011	13,000-12,000		Bocherens et al., 2011
CLS1300	Elk**	<i>Cervus elaphus</i>	LC97IFP3S6 L46 E267 13	Bocherens et al., 2011	13,000-12,000		Bocherens et al., 2011
CLS1400-1	Elk**	<i>Cervus elaphus</i>	LC97IFP3S6 L46 D267 82	Bocherens et al., 2011	13,000-12,000		Bocherens et al., 2011

CLS1500	Elk**	<i>Cervus elaphus</i>	LC97IFP3S6 L46 Z266 15	Bocherens et al., 2011	13,000- 12,000		Bocherens et al., 2011
LGH3300	Elk**	<i>Cervus elaphus</i>	LHE coupe II fn	Drucker and Gamvier (2004)	~13,500- 15,800	Based on context	Drucker and Gamvier (2004)
LGH1100	Elk**	<i>Cervus elaphus</i>	LHE Magd.III	Drucker and Gamvier (2004)	~13,500- 15,800	Based on context	Drucker and Gamvier (2004)
	Elk**	<i>Cervus elaphus</i>	PAM2800	Drucker et al., 2003a	~12,500- 10,000		Drucker et al., 2003a
	Elk**	<i>Cervus elaphus</i>	PAM2900	Drucker et al., 2003a	~12,500- 10,000		Drucker et al., 2003a
	Elk**	<i>Cervus elaphus</i>	PAM3000	Drucker et al., 2003a	~12,500- 10,000		Drucker et al., 2003a
	Elk**	<i>Cervus elaphus</i>	PAM3300	Drucker et al., 2003a	~12,500- 10,000		Drucker et al., 2003a
	Elk**	<i>Cervus elaphus</i>	PAM3400	Drucker et al., 2003a	~12,500- 10,000		Drucker et al., 2003a
	Elk**	<i>Cervus elaphus</i>	PAM3500	Drucker et al., 2003a	~12,500- 10,000		Drucker et al., 2003a
	Elk**	<i>Cervus elaphus</i>	RCD500	Drucker et al., 2003a	~12,500- 10,000		Drucker et al., 2003a
	Elk**	<i>Cervus elaphus</i>	RCD900	Drucker et al., 2003a	~12,500- 10,000		Drucker et al., 2003a
	Elk**	<i>Cervus elaphus</i>	RCD1000	Drucker et al., 2003a	~12,500- 10,000		Drucker et al., 2003a
	Elk**	<i>Cervus elaphus</i>	RCD1100	Drucker et al., 2003a	~12,500- 10,000		Drucker et al., 2003a
	Elk**	<i>Cervus elaphus</i>	RCD1200	Drucker et al., 2003a	~12,500- 10,000		Drucker et al., 2003a
	Elk**	<i>Cervus elaphus</i>	RCD1300	Drucker et al., 2003a	~12,500- 10,000		Drucker et al., 2003a
	Elk**	<i>Cervus elaphus</i>	RCD1400	Drucker et al., 2003a	~12,500- 10,000		Drucker et al., 2003a
	Elk**	<i>Cervus elaphus</i>	RCD2300	Drucker et al., 2003a	~12,500- 10,000		Drucker et al., 2003a
	Elk**	<i>Cervus elaphus</i>	RCD2400	Drucker et al., 2003a	~12,500- 10,000		Drucker et al., 2003a

	Elk**	<i>Cervus elaphus</i>	RCD2500	Drucker et al., 2003a	~12,500-10,000		Drucker et al., 2003a
	Elk**	<i>Cervus elaphus</i>	RCD2600	Drucker et al., 2003a	~12,500-10,000		Drucker et al., 2003a
	Elk**	<i>Cervus elaphus</i>	RCD2700	Drucker et al., 2003a	~12,500-10,000		Drucker et al., 2003a
	Elk**	<i>Cervus elaphus</i>	RCD2800	Drucker et al., 2003a	~12,500-10,000		Drucker et al., 2003a
SC29200	Elk**	<i>Cervus elaphus</i>	SC91 319 C32	Bocherens et al., 2011	~24-~40,000		Bocherens et al., 2011
CAM1100	Elk**	<i>Cervus elaphus</i>		Bocherens et al., 2005		~35,000	Bocherens et al., 2005
A/GOY/B/2	Horse	<i>Equus</i> sp.	DP2832 MG3	Stevens et al., 2009	12775 ±55	OxA-V-2223-48	Stevens et al., 2009
A/CX/B/27	Horse	<i>Equus</i> sp.	DP2297	Stevens et al., 2009	Post-LGM	Based on context	Stevens et al., 2009
A/CX/B/29	Horse	<i>Equus</i> sp.	DP2298	Stevens et al., 2009	Post-LGM	Based on context	Stevens et al., 2009
A/CX/B/30	Horse	<i>Equus</i> sp.	DP2297	Stevens et al., 2009	Post-LGM	Based on context	Stevens et al., 2009
A/CX/B/31	Horse	<i>Equus</i> sp.	DP2298	Stevens et al., 2009	Post-LGM	Based on context	Stevens et al., 2009
A/CX/B/32	Horse	<i>Equus</i> sp.	DP2298	Stevens et al., 2009	12375 ±50	OxA-V-2216-44	Stevens et al., 2009
A/CX/B/33	Horse	<i>Equus</i> sp.	DP2298	Stevens et al., 2009	Post-LGM	Based on context	Stevens et al., 2009
A/CX/B/34	Horse	<i>Equus</i> sp.	DP2298	Stevens et al., 2009	Post-LGM	Based on context	Stevens et al., 2009
A/CX/B/35	Horse	<i>Equus</i> sp.	DP2298	Stevens et al., 2009	Post-LGM	Based on context	Stevens et al., 2009
A/CX/B/36	Horse	<i>Equus</i> sp.	DP2298	Stevens et al., 2009	Post-LGM	Based on context	Stevens et al., 2009
A/CX/B/37	Horse	<i>Equus</i> sp.	DP2298	Stevens et al., 2009	Post-LGM	Based on context	Stevens et al., 2009
A/CX/B/40	Horse	<i>Equus</i> sp.	DP2298	Stevens et al., 2009	12630 ±55	OxA-V-2216-45	Stevens et al., 2009

A/CX/B/42	Horse	<i>Equus</i> sp.	DP2298	Stevens et al., 2009	Post-LGM	Based on context	Stevens et al., 2009
A/CX/B/43	Horse	<i>Equus</i> sp.	DP2298	Stevens et al., 2009	Post-LGM	Based on context	Stevens et al., 2009
A/CX/B/45	Horse	<i>Equus</i> sp.	DP2342	Stevens et al., 2009	12800 ±100	OxA- 3633	Stevens et al., 2009
A/CX/B/46	Horse	<i>Equus</i> sp.	DP2342	Stevens et al., 2009	12790 ±100	OxA- 3632	Stevens et al., 2009
SHN11	Horse	<i>Equus</i> sp.	2272 MG1	Stevens et al., 2009	Post-LGM	Based on context	Stevens et al., 2009
SHN12	Horse	<i>Equus</i> sp.	2272 MG5	Stevens et al., 2009	Post-LGM	Based on context	Stevens et al., 2009
SHN13	Horse	<i>Equus</i> sp.	2272 MG2	Stevens et al., 2009	Post-LGM	Based on context	Stevens et al., 2009
SHN14	Horse	<i>Equus</i> sp.	2272	Stevens et al., 2009	Post-LGM	Based on context	Stevens et al., 2009
SHN15	Horse	<i>Equus</i> sp.	2272	Stevens et al., 2009	Post-LGM	Based on context	Stevens et al., 2009
SHN16	Horse	<i>Equus</i> sp.	2272	Stevens et al., 2009	Post-LGM	Based on context	Stevens et al., 2009
SHN18	Horse	<i>Equus</i> sp.	2266 MG2	Stevens et al., 2009	Post-LGM	Based on context	Stevens et al., 2009
SHN19	Horse	<i>Equus</i> sp.	2266 MG1	Stevens et al., 2009	Post-LGM	Based on context	Stevens et al., 2009
SHN20	Horse	<i>Equus</i> sp.	2266 MG3	Stevens et al., 2009	Post-LGM	Based on context	Stevens et al., 2009
SHN21	Horse	<i>Equus</i> sp.	2265 MG21	Stevens et al., 2009	Post-LGM	Based on context	Stevens et al., 2009
SHN22	Horse	<i>Equus</i> sp.	2266 MG7	Stevens et al., 2009	Post-LGM	Based on context	Stevens et al., 2009
SHN23	Horse	<i>Equus</i> sp.	2266 MG4	Stevens et al., 2009	Post-LGM	Based on context	Stevens et al., 2009
SHN24	Horse	<i>Equus</i> sp.	2266 MG5	Stevens et al., 2009	Post-LGM	Based on context	Stevens et al., 2009
SHN25	Horse	<i>Equus</i> sp.	2266 MG6	Stevens et al., 2009	Post-LGM	Based on context	Stevens et al., 2009
SHN26	Horse	<i>Equus</i> sp.	2266	Stevens et al., 2009	Post-LGM	Based on context	Stevens et al., 2009

SHN27	Horse	<i>Equus</i> sp.	2266 MG8	Stevens et al., 2009	Post-LGM	Based on context	Stevens et al., 2009
KSL-1	Horse	<i>Equus ferus</i>	NESH:232	Bocherens et al., 2011	12,774±54	KIA-11825	Bocherens et al., 2011
KSL-2	Horse	<i>Equus ferus</i>	MEQ1:253	Bocherens et al., 2011	12,502±52	KIA-11826	Bocherens et al., 2011
KSL-3	Horse	<i>Equus ferus</i>	HE12/10	Bocherens et al., 2011	13,052±53	KIA-11827	Bocherens et al., 2011
KSL-4	Horse	<i>Equus ferus</i>	HE21:13	Bocherens et al., 2011	13,858±55	KIA-11828	Bocherens et al., 2011
KSL-5	Horse	<i>Equus ferus</i>	HE33:24	Bocherens et al., 2011	12,897±53	KIA-11829	Bocherens et al., 2011
CHM-2	Horse	<i>Equus ferus</i>	HrCh85 O21 #12	Bocherens et al., 2011	12,815±65	OxA-20700	Bocherens et al., 2011
MRZ-2	Horse	<i>Equus ferus</i>	NE-MZ92 O47 #142	Bocherens et al., 2011	13,055±60	OxA-20699	Bocherens et al., 2011
SCH-10	Horse	<i>Equus ferus</i>	Nr.4816.14	Bocherens et al., 2011	~14-~12,000		Bocherens et al., 2011
CLS100-2	Horse	<i>Equus</i> sp.	LC97IFP3S6 L46 D267 73	Bocherens et al., 2011	13,000- 12,000		Bocherens et al., 2011
CLS200	Horse	<i>Equus</i> sp.	LC97IFP3S6 L46 E268 575	Bocherens et al., 2011	12350±60	(GrA-11664)	Bocherens et al., 2011
CLS300	Horse	<i>Equus</i> sp.	LC97IFP3S6 L46 E268 281	Bocherens et al., 2011	13,000- 12,000		Bocherens et al., 2011
CLS400	Horse	<i>Equus</i> sp.	LC97IFP3S6 L46 K273 10	Bocherens et al., 2011	13,000- 12,000		Bocherens et al., 2011
CLS500	Horse	<i>Equus</i> sp.	LC97IFP3S6 L46 P271 14	Bocherens et al., 2011	13,000- 12,000		Bocherens et al., 2011
TDG100	Horse	<i>Equus</i> sp.	MAR97 TDG	Bocherens et al., 2011	13,000- 12,000		Bocherens et al., 2011
TDG1700	Horse	<i>Equus</i> sp.	sondage	Bocherens et al., 2011	13,000- 12,000		Bocherens et al., 2011
TDG1800	Horse	<i>Equus</i> sp.	sondage	Bocherens et al., 2011	13,000- 12,000		Bocherens et al., 2011
TDG1900	Horse	<i>Equus</i> sp.	sondage	Bocherens et al., 2011	13,000- 12,000		Bocherens et al., 2011
TDG2000	Horse	<i>Equus</i> sp.	MAR93 TDG	Bocherens et al., 2011	13,000- 12,000		Bocherens et al., 2011
TDG2100	Horse	<i>Equus</i> sp.	MAR93 TDG	Bocherens et al., 2011	13,000- 12,000		Bocherens et al., 2011
TDG2500	Horse	<i>Equus</i> sp.	-	Bocherens et al., 2011	13,000- 12,000		Bocherens et al., 2011

PCV-2	Horse	<i>Equus</i> sp.	Pinc98 IV0 S°43 T129 n°87	Bocherens et al., 2011	13,000- 12,000		Bocherens et al., 2011
PCV-3	Horse	<i>Equus</i> sp.	Pinc90 IV0 S°44 X136 n°1	Bocherens et al., 2011	13,000- 12,000		Bocherens et al., 2011
PCV-17	Horse	<i>Equus</i> sp.	Pinc67 IV20 S°36 T111 327	Bocherens et al., 2011	13,000- 12,000		Bocherens et al., 2011
PCV-21	Horse	<i>Equus</i> sp.	Pinc81 IV21.3 S°27 J85 11	Bocherens et al., 2011	13,000- 12,000		Bocherens et al., 2011
MN200	Horse	<i>Equus</i> sp.	MN H25 193	Drucker et al., 2003b	~13,000- ~15,300 BP	Based on layer date	Drucker et al., 2003b
MN300	Horse	<i>Equus</i> sp.	MN J28 577	Drucker et al., 2003b	~13,000- ~15,300 BP	Based on layer date	Drucker et al., 2003b
MN400	Horse	<i>Equus</i> sp.	MN J24 22	Drucker et al., 2003b	~13,000- ~15,300 BP	Based on layer date	Drucker et al., 2003b
MN500	Horse	<i>Equus</i> sp.	MN H25 c2	Drucker et al., 2003b	~13,000- ~15,300 BP	Based on layer date	Drucker et al., 2003b
MN600	Horse	<i>Equus</i> sp.	MN J25 152	Drucker et al., 2003b	~13,000- ~15,300 BP	Based on layer date	Drucker et al., 2003b
FLG100	Horse	<i>Equus</i> sp.	FLAG4/5N5'c IX100 ss dal.	Drucker et al., 2003b	~13,000- ~15,300 BP	Based on layer date	Drucker et al., 2003b
SGR2800	Horse	<i>Equus</i> sp.	L21c#172	Drucker et al., 2003b	~13,000- ~15,300 BP	Based on layer date	Drucker et al., 2003b
SGR2900	Horse	<i>Equus</i> sp.	121c1 18439	Drucker et al., 2003b	~13,000- ~15,300 BP	Based on layer date	Drucker et al., 2003b
JBL1200	Horse	<i>Equus</i> sp.	JBL 90AFEQ2c.1	Drucker et al., 2003b	14,850±130 (Gif8667)	Based on layer date	Drucker et al., 2003b
JBL1600	Horse	<i>Equus</i> sp.	JBL 90AFEQ2c.1	Drucker et al., 2003b	14,850±130 (Gif8667)	Based on layer date	Drucker et al., 2003b
JBL2000	Horse	<i>Equus</i> sp.	JBL P.86CL9c.2	Drucker et al., 2003b	17,770±260 (Ly4589)	Based on layer date	Drucker et al., 2003b
JBL2100	Horse	<i>Equus</i> sp.	JBL 88CL10c.2	Drucker et al., 2003b	17,770±260 (Ly4589)	Based on layer date	Drucker et al., 2003b
JBL2300	Horse	<i>Equus</i> sp.	JBL 85CL7c.3	Drucker et al., 2003b	19,010±310 (Ly4588)	Based on layer date	Drucker et al., 2003b

JBL2500	Horse	<i>Equus</i> sp.	JBL 88CL5Ec.3	Drucker et al., 2003b	19,010±310 (Ly4588)	Based on layer date	Drucker et al., 2003b
JBL2800	Horse	<i>Equus</i> sp.	JBL 85CL8.9c.3	Drucker et al., 2003b	19,010±310 (Ly4588)	Based on layer date	Drucker et al., 2003b
JBL2900	Horse	<i>Equus</i> sp.	JBL P86CL8c.3	Drucker et al., 2003b	19,010±310 (Ly4588)	Based on layer date	Drucker et al., 2003b
CS3500	Horse	<i>Equus</i> sp.	J15D 428	Drucker et al., 2003b	18,350±160 (Oxa6870), 19,760±160 (Oxa6518)	Based on layer date	Drucker et al., 2003b
CS3600	Horse	<i>Equus</i> sp.	K17A 70	Drucker et al., 2003b	18,350±160 (Oxa6870), 19,760±160 (Oxa6518)	Based on layer date	Drucker et al., 2003b
CS3700	Horse	<i>Equus</i> sp.	I16D 28(5)	Drucker et al., 2003b	18,350±160 (Oxa6870), 19,760±160 (Oxa6518)	Based on layer date	Drucker et al., 2003b
CS300	Horse	<i>Equus</i> sp.	G21C 0	Drucker et al., 2003b	26,620±340 (Oxa6876), 27,880±440 (Oxa6514)	Based on layer date	Drucker et al., 2003b
CS400	Horse	<i>Equus</i> sp.	H21C 27	Drucker et al., 2003b	26,620±340 (Oxa6876), 27,880±440 (Oxa6514)	Based on layer date	Drucker et al., 2003b
CS600	Horse	<i>Equus</i> sp.	G22C 11	Drucker et al., 2003b	26,620±340 (Oxa6876), 27,880±440 (Oxa6514)	Based on layer date	Drucker et al., 2003b
CS700	Horse	<i>Equus</i> sp.	G22C 9	Drucker et al., 2003b	26,620±340 (Oxa6876), 27,880±440 (Oxa6514)	Based on layer date	Drucker et al., 2003b

CS800	Horse	<i>Equus</i> sp.	H22C 27	Drucker et al., 2003b	26,620±340 (Oxa6876), 27,880±440 (Oxa6514)	Based on layer date	Drucker et al., 2003b
	Horse	<i>Equus</i> sp.		Stevens & Hedges, 2004	12,970±70	OxA-10494	Stevens & Hedges, 2004
	Horse	<i>Equus</i> sp.		Stevens & Hedges, 2004	13,105±70	OxA-10470	Stevens & Hedges, 2004
	Horse	<i>Equus</i> sp.		Stevens & Hedges, 2004	12,040±120	OxA-4981	Stevens & Hedges, 2004
	Horse	<i>Equus</i> sp.		Stevens & Hedges, 2004	12,450±120	OxA-5158	Stevens & Hedges, 2004
	Horse	<i>Equus</i> sp.		Stevens & Hedges, 2004	13,130±100	OxA-6254	Stevens & Hedges, 2004
	Horse	<i>Equus</i> sp.		Stevens & Hedges, 2004	13,150±130	OxA-4848	Stevens & Hedges, 2004
	Horse	<i>Equus</i> sp.		Stevens & Hedges, 2004	13,190±130	OxA-4846	Stevens & Hedges, 2004
	Horse	<i>Equus</i> sp.		Stevens & Hedges, 2004	13,520±130	OxA-4852	Stevens & Hedges, 2004
	Horse	<i>Equus</i> sp.		Stevens & Hedges, 2004	13,185±80	OxA-10493	Stevens & Hedges, 2004
	Horse	<i>Equus</i> sp.		Stevens & Hedges, 2004	13,270±180	OxA-10651	Stevens & Hedges, 2004
	Horse	<i>Equus</i> sp.		Stevens & Hedges, 2004	13,500±90	OxA-10492	Stevens & Hedges, 2004
	Horse	<i>Equus</i> sp.		Stevens & Hedges, 2004	10,380±140	OxA-78	Stevens & Hedges, 2004
	Horse	<i>Equus</i> sp.		Stevens & Hedges, 2004	12,630±75	OxA-8076	Stevens & Hedges, 2004
	Horse	<i>Equus</i> sp.		Stevens & Hedges, 2004	12,660±80	OxA-8075	Stevens & Hedges, 2004
	Horse	<i>Equus</i> sp.		Stevens & Hedges, 2004	10,040±120	OxA-5727	Stevens & Hedges, 2004
	Horse	<i>Equus</i> sp.		Stevens & Hedges, 2004	12,090±90	OxA-5680	Stevens & Hedges, 2004
	Horse	<i>Equus</i> sp.		Stevens & Hedges, 2004	12,790±100	OxA-3632	Stevens & Hedges, 2004
	Horse	<i>Equus</i> sp.		Stevens & Hedges, 2004	12,800±100	OxA-3633	Stevens & Hedges, 2004
	Horse	<i>Equus</i> sp.		Stevens & Hedges, 2004	12,800±130	OxA-4197	Stevens & Hedges, 2004
	Horse	<i>Equus</i> sp.		Stevens & Hedges, 2004	12,630±140	Date based on associated material	Stevens & Hedges, 2004
	Horse	<i>Equus</i> sp.		Stevens & Hedges, 2004	27,480±340	OxA-8511	Stevens & Hedges, 2004
	Horse	<i>Equus</i> sp.		Stevens & Hedges, 2004	28,050±550	OxA-5227	Stevens & Hedges, 2004
	Horse	<i>Equus</i> sp.		Stevens & Hedges, 2004	30,100±50	OxA-6256	Stevens & Hedges, 2004
	Horse	<i>Equus</i> sp.		Stevens & Hedges, 2004	33,200±800	OxA-5707	Stevens & Hedges, 2004
	Horse	<i>Equus</i> sp.		Stevens & Hedges, 2004	27,500±550	OxA-4857	Stevens & Hedges, 2004
	Horse	<i>Equus</i> sp.		Stevens & Hedges, 2004	30,950±800	OxA-4856	Stevens & Hedges, 2004
	Horse	<i>Equus</i> sp.		Stevens & Hedges, 2004	31,750±650	OxA-6369	Stevens & Hedges, 2004
	Horse	<i>Equus</i> sp.		Stevens & Hedges, 2004	32,900±850	OxA-6255	Stevens & Hedges, 2004
	Horse	<i>Equus</i> sp.		Stevens & Hedges, 2004	27,150±600	OxA-4978	Stevens & Hedges, 2004
	Horse	<i>Equus</i> sp.		Stevens & Hedges, 2004	19,320±240	OxA-7502	Stevens & Hedges, 2004

	Horse	<i>Equus</i> sp.		Stevens & Hedges, 2004	9,815±60	OxA-7653		Stevens & Hedges, 2004
	Horse	<i>Equus</i> sp.		Stevens & Hedges, 2004	38,400±1,600	OxA-10017		Stevens & Hedges, 2004
	Horse	<i>Equus</i> sp.		Stevens & Hedges, 2004	33,400±600	OxA-8122		Stevens & Hedges, 2004
	Horse	<i>Equus</i> sp.		Stevens & Hedges, 2004	34,450±750	OxA-8452		Stevens & Hedges, 2004
	Horse	<i>Equus</i> sp.		Stevens & Hedges, 2004	38,300±1,300	OxA-8451		Stevens & Hedges, 2004
	Horse	<i>Equus</i> sp.		Stevens & Hedges, 2004	27,740±340	OxA-8370		Stevens & Hedges, 2004
	Horse	<i>Equus</i> sp.		Stevens & Hedges, 2004	6,360±55	OxA-8942		Stevens & Hedges, 2004
	Horse	<i>Equus</i> sp.		Stevens & Hedges, 2004	7,970±80	OxA-8996		Stevens & Hedges, 2004
	Horse	<i>Equus</i> sp.		Stevens & Hedges, 2004	36,650±1,000	OxA-8369		Stevens & Hedges, 2004
	Horse	<i>Equus</i> sp.		Stevens & Hedges, 2004	22,160±360	OxA-7428		Stevens & Hedges, 2004
Goyet-A3-10	Horse	<i>Equus ferus</i>	2224-1	Bocherens et al., 2011	~24~40,000			Bocherens et al., 2011
Goyet-A3-11	Horse	<i>Equus ferus</i>	2224-2	Bocherens et al., 2011	~24~40,000			Bocherens et al., 2011
Goyet-A3-12	Horse	<i>Equus ferus</i>	2224-3	Bocherens et al., 2011	~24~40,000			Bocherens et al., 2011
Goyet-B4-4	Horse	<i>Equus ferus</i>	2737	Bocherens et al., 2011	~24~40,000			Bocherens et al., 2011
SC28400	Horse	<i>Equus ferus</i>	SC95 524 E41	Bocherens et al., 2011	~24~40,000			Bocherens et al., 2011
SC3900	Horse	<i>Equus ferus</i>	SC87 140 (I27)	Bocherens et al., 1997; 2011		Based on estimated age of layer	~40,000	Bocherens et al., 1997
SC4100	Horse	<i>Equus ferus</i>	SC89 135 (G29)	Bocherens et al., 1997; 2011		Based on estimated age of layer	~40,000	Bocherens et al., 1997
SC4200	Horse	<i>Equus ferus</i>	SC87 126 (F25)	Bocherens et al., 1997; 2011		Based on estimated age of layer	~40,000	Bocherens et al., 1997
SC4300	Horse	<i>Equus ferus</i>	SC85 121	Bocherens et al., 1997; 2011		Based on estimated age of layer	~40,000	Bocherens et al., 1997
SC4400	Horse	<i>Equus ferus</i>	SC85 141	Bocherens et al., 1997; 2011		Based on estimated age of layer	~40,000	Bocherens et al., 1997
	Horse			Stevens & Hedges, 2004	27,740±340	OxA-8370		Stevens & Hedges, 2004
	Horse			Stevens & Hedges, 2004	36,650±1,000	OxA-8369		Stevens & Hedges, 2004
A/GOY/B/1	Horse		DP2832 MG2	Stevens et al., 2009	31,750 ±200	OxA-V-2223-44		Stevens et al., 2009
A/GOY/B/32	Horse		DP2809	Stevens et al., 2009	29,420 ±170	OxA-V-2223-49		Stevens et al., 2009

EQ-GK 313	Horse	<i>Equus sp.</i>	Bocherens et al., 2011	~26~40,000		Bocherens et al., 2011
EQ-GK 314	Horse	<i>Equus sp.</i>	Bocherens et al., 2011	~26~40,000		Bocherens et al., 2011
EQ-GK 316	Horse	<i>Equus sp.</i>	Bocherens et al., 2011	~26~40,000		Bocherens et al., 2011
EQ-GK 317	Horse	<i>Equus sp.</i>	Bocherens et al., 2011	~26~40,000		Bocherens et al., 2011
EQ-GK 318	Horse	<i>Equus sp.</i>	Bocherens et al., 2011	~26~40,000		Bocherens et al., 2011
EQ-GK 319	Horse	<i>Equus sp.</i>	Bocherens et al., 2011	~26~40,000		Bocherens et al., 2011
EQ-GK 321	Horse	<i>Equus sp.</i>	Bocherens et al., 2011	~26~40,000		Bocherens et al., 2011
EQ-GK 322	Horse	<i>Equus sp.</i>	Bocherens et al., 2011	~26~40,000		Bocherens et al., 2011
EQ-GK 323	Horse	<i>Equus sp.</i>	Bocherens et al., 2011	~26~40,000		Bocherens et al., 2011
EQ-GK 325	Horse	<i>Equus sp.</i>	Bocherens et al., 2011	~26~40,000		Bocherens et al., 2011
EQ-GK 326	Horse	<i>Equus sp.</i>	Bocherens et al., 2011	~26~40,000		Bocherens et al., 2011
EQ-GK 327	Horse	<i>Equus sp.</i>	Bocherens et al., 2011	~26~40,000		Bocherens et al., 2011
EQ-GK 329	Horse	<i>Equus sp.</i>	Bocherens et al., 2011	~26~40,000		Bocherens et al., 2011
EQ-GK 330	Horse	<i>Equus sp.</i>	Bocherens et al., 2011	~26~40,000		Bocherens et al., 2011
EQ-GK 331	Horse	<i>Equus sp.</i>	Bocherens et al., 2011	~26~40,000		Bocherens et al., 2011
OxA-4857	Horse	<i>Equus sp.</i>	Bocherens et al., 2011	27500±550	OxA-4857	Stevens & Hedges, 2004 as referenced in Bocherens et al., 2011
OxA-5227	Horse	<i>Equus sp.</i>	Bocherens et al., 2011	28050±550	OxA-5227	Stevens & Hedges, 2004 as referenced in Bocherens et al., 2011
OxA-5707	Horse	<i>Equus sp.</i>	Bocherens et al., 2011	33200±800	OxA-5707	Stevens & Hedges, 2004 as referenced in Bocherens et al., 2011
OxA-4856	Horse	<i>Equus sp.</i>	Bocherens et al., 2011	30950±800	OxA-4856	Stevens & Hedges, 2004 as referenced in Bocherens et al., 2011
TUB-77	Horse	<i>Equus sp.</i>	Bocherens et al., 2011	36490+350/- 340	KIA-17303	Bocherens (2011)
TUB-78	Horse	<i>Equus sp.</i>	Bocherens et al., 2011	31870 +260/- 250	KIA-8958	Bocherens (2011)
TUB-79	Horse	<i>Equus sp.</i>	Bocherens et al., 2011	36700+450/- 430	KIA-17299	Bocherens (2011)
OxA-4978	Horse	<i>Equus sp.</i>	Bocherens et al., 2011	27150±600	OxA-4978	Stevens & Hedges, 2004 as referenced in Bocherens et al., 2011

	Horse	<i>Equus sp.</i>		Fizet et al., 1995		45,000 ~40- 45,000	Fizet et al., 1995
	Horse	<i>Equus sp.</i>		Fizet et al., 1995		~40- 45,000	Fizet et al., 1995
	Horse	<i>Equus sp.</i>		Fizet et al., 1995		~40- 45,000	Fizet et al., 1995
	Horse	<i>Equus sp.</i>		Fizet et al., 1995		~40- 45,000	Fizet et al., 1995
KSL-47	Mammoth	<i>Mammuthus primigenius</i>	8740	Bocherens et al., 2011	13,980±110	OxA-10237	Napierala (2008) as referenced in Bocherens et al., 2011
Goyet-A2-1	Mammoth	<i>Mammuthus primigenius</i>	2827	Bocherens et al., 2011	Pre-LGM		Bocherens et al., 2011
Goyet-A3-9	Mammoth	<i>Mammuthus primigenius</i>	2216-1	Bocherens et al., 2011	Pre-LGM		Bocherens et al., 2011
Goyet-B4-2	Mammoth	<i>Mammuthus primigenius</i>	2737-1	Bocherens et al., 2011	Pre-LGM		Bocherens et al., 2011
SC600	Mammoth	<i>Mammuthus primigenius</i>	SC83 285	Bocherens et al., 1997; 2011		Based on estimated age of layer	~40,000 Bocherens et al., 1997
SC700	Mammoth	<i>Mammuthus primigenius</i>	SC85 121	Bocherens et al., 1997; 2011		Based on estimated age of layer	~40,000 Bocherens et al., 1997
SC800	Mammoth	<i>Mammuthus primigenius</i>	SC87 31 (I26)	Bocherens et al., 1997; 2011		Based on estimated age of layer	~40,000 Bocherens et al., 1997
HST-9	Mammoth	<i>Mammuthus primigenius</i>		Bocherens et al., 2011	~26~40,000		Bocherens et al., 2011
LBR1900	Mammoth	<i>Mammuthus primigenius</i>		Bocherens et al., 2005		~35,000	Bocherens et al., 2005
CAM700	Mammoth	<i>Mammuthus primigenius</i>		Bocherens et al., 2005		~35,000	Bocherens et al., 2005
CAM800	Mammoth	<i>Mammuthus primigenius</i>		Bocherens et al., 2005		~35,000	Bocherens et al., 2005
SCH-6	Moose	<i>Alces alces</i>	Nr.33714.3	Bocherens et al., 2011	12,355±45	GrA-39505	Bocherens et al., 2011
SCH-7	Moose	<i>Alces alces</i>	Nr.33714.5	Bocherens et al., 2011	~14~12,000		Bocherens et al., 2011

KSL-7	Woolly Rhinoceros	<i>Coelodonta antiquitatis</i>	M001:307	Bocherens et al., 2011	14,330±110		OxA-10238	Bocherens et al., 2011
ARL-1	Woolly Rhinoceros	<i>Coelodonta antiquitatis</i>	no ref.	Bocherens et al., 2011	13,890±80		Ly-3291(Poz)	Bocherens et al., 2011
Goyet-A2-2	Woolly Rhinoceros	<i>Coelodonta antiquitatis</i>	2755	Bocherens et al., 1997; 2011		Based on estimated age of layer	~40,000	Bocherens et al., 1997
Goyet-A3-2	Woolly Rhinoceros	<i>Coelodonta antiquitatis</i>	2792	Bocherens et al., 2011	~24-~40,000			Bocherens et al., 2011
Goyet-B4-3	Woolly Rhinoceros	<i>Coelodonta antiquitatis</i>	2235-1	Bocherens et al., 2011	~24-~40,000			Bocherens et al., 2011
SC30100	Woolly Rhinoceros	<i>Coelodonta antiquitatis</i>	SC95 521 E41	Bocherens et al., 2011	~24-~40,000			Bocherens et al., 2011
OxA-6255	Woolly Rhinoceros	<i>Cœlodonta antiquitatis</i>		Stevens & Hedges, 2004 as referenced in Bocherens et al., 2011	32900±850	OxA-6255		Stevens & Hedges, 2004 as referenced in Bocherens et al., 2011
LBR2200	Woolly Rhinoceros	<i>Cœlodonta antiquitatis</i>		Bocherens et al., 2005			~35,000	Bocherens et al., 2005
CAM1300	Woolly Rhinoceros	<i>Cœlodonta antiquitatis</i>		Bocherens et al., 2005			~35,000	Bocherens et al., 2005
CAM1400	Woolly Rhinoceros	<i>Cœlodonta antiquitatis</i>		Bocherens et al., 2005			~35,000	Bocherens et al., 2005
CAM1500	Woolly Rhinoceros	<i>Cœlodonta antiquitatis</i>		Bocherens et al., 2005			~35,000	Bocherens et al., 2005

Appendix S continues below.

Lab ID	Area	Site	Tissue	Tissue Type	$\delta^{13}\text{C}_{\text{Bulk}}$	$\delta^{15}\text{N}_{\text{Bulk}}$	% Yield	%C	%N	C/N
KSL-10	France/ Switzerland/ Germany Jura	Kesslerloch	B	metacarpus R	-19.8	2.2	2.4	41.6	14.4	3.4
KSL-11	France/ Switzerland/ Germany Jura	Kesslerloch	B	carpus L	-20.0	2.4	5.7	37.9	13.3	3.3
KSL-12	France/ Switzerland/ Germany Jura	Kesslerloch	B	talus L	-20.3	2.3	1.0	24.0	8.9	3.2
Goyet-A3-13	Ardennes, Belgium	Goyet - Level A3	B	tibia	-20.0	4.1	10.6	40.9	14.6	3.3
Goyet-A3-14	Ardennes, Belgium	Goyet - Level A3	B	tibia	-20.4	4.8	10.4	41.4	14.6	3.3
Goyet-B4-5	Ardennes, Belgium	Goyet - Level B4	B	centrotarsus	-20.0	5.7	10.3	40.9	14.7	3.2

Goyet-B4-7	Ardennes, Belgium	Goyet - Level B4	B	centrotarsus	-20.4	3.9	6.5	38.8	14.1	3.2
SC29000	Ardennes, Belgium	Scladina - Level 1A	D/RD/C	lower M3 (R)	-20.8	4.4	2.4	32.6	11.5	3.3
LBR100	France	La Berbie	B	metatarsus	-20.3	6.1	3.2	39.5	14.5	3.2
LBR200	France	La Berbie	B	metatarsus	-20.1	5.6	1.5	37.8	14.0	3.2
LBR300	France	La Berbie	B	metatarsus	-20.8	4.7	2.8	35.3	13.1	3.1
LBR400	France	La Berbie	B	metatarsus	-20.3	5.6	1.3	36.9	13.7	3.1
LBR500	France	La Berbie	B	metatarsus	-20.2	6.1	2.6	40.3	14.8	3.2
LBR600	France	La Berbie	B	metatarsus	-20.2	6.0	1.8	29.0	11.1	3.0
LBR700	France	La Berbie	B	metatarsus	-20.9	4.6	4.1	38.4	14.3	3.1
LBR3100	France	La Berbie	B	radius	-20.5	5.3	3.6	39.0	14.9	3.0
	France	Marillac - Layer 4	B		-20.1	6.3				
	France	Marillac - Layer 7	B		-19.9	8.1				
	France	Marillac - Layer 7	B		-19.9	7.5				
	France	Marillac - Layer 10	B		-19.7	6.3				
	France	Marillac - Layer 10	B		-19.8	5.9				
RA-KSL-620	France/ Switzerland/ Germany Jura	Kesslerloch	B	metacarpus	-19.1	2.4	2.9	34.4	12.1	3.3
RA-KSL-628	France/ Switzerland/ Germany Jura	Kesslerloch (KSLH Is)	B	tibia R	-19.9	2.6	4.9	43.7	15.0	3.4
RA-KSL-632	France/ Switzerland/ Germany Jura	Kesslerloch (KSLH IIs)	B	humerus R	-19.8	2.7	4.4	39.0	13.4	3.4
RA-KSL-633	France/ Switzerland/ Germany Jura	Kesslerloch (KSLH IIs)	B	humerus R	-20.3	2.9	1.9	36.8	13.1	3.3
RA-KSL-635	France/ Switzerland/ Germany Jura	Kesslerloch (KSLH IIIIn)	B	humerus L	-19.9	2.8	2.3	34.5	12.2	3.3
RA-PTF 363	France/ Switzerland/ Germany Jura	Petersfels (P1 AH2)	B	metapodium L distal	-19.8	2.4	5.5	45.2	15.3	3.4
RA-PTF 364	France/ Switzerland/ Germany Jura	Petersfels (P1 AH2)	B	metapodium R distal	-19.6	2.1	10.5	45.6	15.6	3.4
RA-PTF 365	France/ Switzerland/ Germany Jura	Petersfels (P1 AH2)	B	calcaneus R	-19.9	2.3	2.6	42.5	14.4	3.4
RA-PTF 366	France/ Switzerland/ Germany Jura	Petersfels (P1 AH2)	B	talus R	-20.0	1.2	5.5	34.6	12.5	3.2
RA-PTF 367	France/ Switzerland/ Germany Jura	Petersfels (P1 AH2)	B	tibia R distal	-19.9	1.2	1.8	31.8	11.6	3.2
RA-PTF 368	France/ Switzerland/ Germany Jura	Petersfels (P1 AH3)	B	calcaneus L	-19.4	2.4	4.2	43.5	15.3	3.3
RA-PTF 369	France/ Switzerland/ Germany Jura	Petersfels (P1 AH3)	B	talus L	-20.2	2.6	5.5	39.4	13.8	3.3

RA-PTF 370	France/ Switzerland/ Germany Jura	Petersfels (P1 AH3)	B	tibia L distal	-19.1	2.3	3.1	40.6	13.9	3.4
RA-PTF 371	France/ Switzerland/ Germany Jura	Petersfels (P1 AH3)	B	calcaneus L	-19.7	2.1	14.7	45.9	15.5	3.5
RA-PTF 373	France/ Switzerland/ Germany Jura	Petersfels (P1 AH3)	B	tibia L	-19.7	2.5	4.2	43.7	14.9	3.4
RA-PTF 374	France/ Switzerland/ Germany Jura	Petersfels (P1 AH3)	B	tibia L	-19.7	1.4	3.1	41.5	14.2	3.4
RA-PTF 375	France/ Switzerland/ Germany Jura	Petersfels (P1 AH3)	B	tibia L	-20.0	3.3	3.0	42.1	14.4	3.4
RA-PTF 376	France/ Switzerland/ Germany Jura	Petersfels (P1 AH3)	B	tibia L	-19.7	2.4	4.8	44.1	15.1	3.4
RA-PTF 377	France/ Switzerland/ Germany Jura	Petersfels (P1 AH3)	B	tibia L	-19.9	2.0	5.1	42.8	14.8	3.4
RA-PTF 379	France/ Switzerland/ Germany Jura	Petersfels (P1 AH3)	B	tibia L	-19.5	2.6	4.4	41.8	14.1	3.5
RA-PTF 380	France/ Switzerland/ Germany Jura	Petersfels (P1 AH4)	B	metapodium R distal	-19.6	2.4	14.1	44.6	14.3	3.6
RA-PTF 381	France/ Switzerland/ Germany Jura	Petersfels (P1 AH4)	B	metapodium R	-19.3	2.3	13.4	44.4	14.5	3.6
RA-PTF 382	France/ Switzerland/ Germany Jura	Petersfels (P1 AH4)	B	metapodium R distal	-19.1	1.9	6.4	43.6	15.0	3.4
RA-PTF 383	France/ Switzerland/ Germany Jura	Petersfels (P1 AH4)	B	tibia R	-19.4	2.9	10.4	44.3	14.5	3.6
SCH-1	France/ Switzerland/ Germany Jura	Schussenquelle	B	femur R	-19.8	2.5	10.1	44.7	15.5	3.4
SCH-2	France/ Switzerland/ Germany Jura	Schussenquelle	B	femur R	-19.7	2.8	12.5	44.5	15.9	3.3
SCH-3	France/ Switzerland/ Germany Jura	Schussenquelle	B	femur R	-20.1	1.8	13.5	45.1	15.5	3.4
SCH-4	France/ Switzerland/ Germany Jura	Schussenquelle	B	femur R	-19.4	1.9	13.0	44.0	15.7	3.3
SCH-5	France/ Switzerland/ Germany Jura	Schussenquelle	B	femur R	-19.5	2.2	13.7	45.8	15.4	3.5
FLS-7	France/ Switzerland/ Germany Jura	Fellställe (AH3)	B	mandible	-19.8	2.1	1.5	35.4	12.4	3.3
FLS-8	France/ Switzerland/ Germany Jura	Fellställe (AH3a)	B	mandible	-19.3	2.2	1.4	34.5	12.3	3.3
FLS-9	France/ Switzerland/ Germany Jura	Fellställe (AH3b)	B	mandible	-20.2	2.1	1.7	33.4	11.7	3.3
HFL-1	France/ Switzerland/ Germany Jura	Hohlefels (2b)	B	mandible	-19.4	1.0	14.3	41.8	15.0	3.2

	Germany Jura									
GSK-1	France/ Switzerland/ Germany Jura	Geißenklösterle (Io)	B	talus	-19.6	2.0	7.1	42.7	15.5	3.2
OxA-6254	France/ Switzerland/ Germany Jura	Geißenklösterle	B	bone	-19.4	0.1				3.0
TUB-57	France/ Switzerland/ Germany Jura	Buttentalhöhle	B	bone	-19.7	1.7	9.5	41.1	14.5	3.3
RAN-10	France/ Switzerland/ Germany Jura	Ranchot	B	pelvis	-19.1	3.9	1.5	28.1	11.3	3.0
RCD100	France/ Switzerland/ Germany Jura	Rochedane (D1)	B	astragalus	-19.3	1.7	3.3	42.2	15.4	3.2
RCD200	France/ Switzerland/ Germany Jura	Rochedane (D1)	B	phalanx	-19.7	2.7	8.7	43.1	15.6	3.2
RCD400	France/ Switzerland/ Germany Jura	Rochedane (D1)	B	tibia	-19.5	1.3	2.7	41.0	15.0	3.2
RCD10800	France/ Switzerland/ Germany Jura	Rochedane (D1)	B	metapodial	-20.3	2.1	4.5	37.2	13.7	3.2
BLS 1	France/ Switzerland/ Germany Jura	Grotte du Chaumois- Boivin	B	phalanx	-19.5	2.4	11.1	41.6	14.7	3.3
FRT 1	France/ Switzerland/ Germany Jura	Grotte de la Baume Noire	B	metacarpal	-19.5	3.7	4.6	39.6	14.0	3.3
ARL 6	France/ Switzerland/ Germany Jura	Grotte Grappin	B	astragalus	-19.1	2.8	4.4	42.2	15.7	3.1
TDG500	Paris Basin	Tureau-des-Gardes	B	astragalus	-20.0	2.4	3.1	39.7	14.4	3.2
TDG600	Paris Basin	Tureau-des-Gardes	B	metapodium	-19.9	1.6	4.5	40.3	14.6	3.2
TDG700	Paris Basin	Tureau-des-Gardes	B	metapodium	-19.4	2.3	3.4	41.3	15.0	3.2
TDG1400	Paris Basin	Tureau-des-Gardes	B	femur	-19.9	2.3	1.7	38.5	14.1	3.2
TDG1500	Paris Basin	Tureau-des-Gardes	B	femur	-19.6	2.4	1.6	36.4	13.2	3.2
TDG1600	Paris Basin	Tureau-des-Gardes	B	femur	-19.9	2.7	2.1	37.4	13.6	3.2
PCV-7	Paris Basin	Pincevent	B	radius L	-19.7	3.0	1.4	31.1	11.4	3.2
PCV-14	Paris Basin	Pincevent	B	radius R	-20.1	2.8	1.0	31.7	11.7	3.2
PCV-22	Paris Basin	Pincevent	B	humerus	-19.4	3.1	4.1	35.4	13.5	3.1
ETL-3	Paris Basin	Etiolles	B	phalanx	-19.4	3.9	4.5	37.1	13.5	3.2
ETL-4	Paris Basin	Etiolles	B	phalanx	-19.8	3.6	1.7	29.6	10.0	3.4
ETL-9	Paris Basin	Etiolles	B	metapodium	-20.2	3.1	7.1	33.8	12.7	3.1
ETL-6	Paris Basin	Etiolles	B	humerus	-19.5	3.2	5.3	38.5	14.0	3.2
VRB-4	Paris Basin	Verberie	B	mesial R	-20.3	2.3	2.3	38.0	13.3	3.3
VRB-5	Paris Basin	Verberie	B	metapodium	-19.7	2.9	1.5	38.7	14.3	3.2

VRB-6	Paris Basin	Verberie	B	metapodium	-19.7	3.1	1.3	36.9	13.7	3.1
MN700	SW France	Aquitine Basin	B	metatarsal	-19.9	2.4	4.6	41.5	15.3	3.2
MN800	SW France	Aquitine Basin	B	metatarsal	-19.7	3.6	10.0	41.7	15.0	3.3
MN900	SW France	Aquitine Basin	B	metatarsal	-19.6	3.8	2.2	41.3	14.9	3.2
MN1100	SW France	Aquitine Basin	B	metatarsal	-19.6	4.6	4.6	41.7	15.1	3.2
FLG200	SW France	Aquitine Basin	B	metacarpal	-19.6	3.3	2.9	41.7	15.1	3.2
FLG300	SW France	Aquitine Basin	B	metatarsal	-19.2	4.2	4.6	42.1	15.4	3.2
FLG400	SW France	Aquitine Basin	B	metatarsal	-19.4	3.1	2.9	38.7	14.2	3.2
FLG500	SW France	Aquitine Basin	B	metacarpal	-19.6	2.5	5.6	42.1	15.3	3.2
FLG600	SW France	Aquitine Basin	B	metatarsal	-19.3	3.6	4.0	42.7	15.4	3.2
SGR200	SW France	Aquitine Basin	B	jawbone	-19.2	3.5	2.8	42.4	15.6	3.2
SGR2700	SW France	Aquitine Basin	B	metapodial	-19.1	3.8	2.4	30.4	11.4	3.1
LGH1400	SW France	Aquitine Basin	B	astragalum	-19.1	3.8	3.4	41.7	15.2	3.2
LGH1500	SW France	Aquitine Basin	B	femur	-18.9	2.5	1.1	29.0	11.0	3.1
PRG200	SW France	Aquitine Basin	B	jawbone	-19.3	3.3	1.3	40.5	14.8	3.2
PRG300	SW France	Aquitine Basin	B	jawbone	-18.9	3.5	1.4	38.7	13.9	3.2
PRG400	SW France	Aquitine Basin	B	radius	-19.8	3.2	1.1	41.8	15.1	3.2
PRG500	SW France	Aquitine Basin	B	femur	-19.8	3.0	3.2	37.9	13.8	3.2
JBL1300	SW France	Les Jamblancs		coxal	-19.3	2.7	2.2	40.8	14.9	3.2
JBL1400	SW France	Les Jamblancs		radius	-18.7	3.2	3.8	42.4	15.4	3.2
JBL1500	SW France	Les Jamblancs		humerus	-18.9	3.3	5.9	41.6	15.0	3.2
JBL900	SW France	Les Jamblancs		metatarsal	-18.9	3.1	1.1	37.9	14.7	3.0
JBL1000	SW France	Les Jamblancs		humérus	-18.6	3.2	2.3	42.2	15.4	3.2
JBL1100	SW France	Les Jamblancs		metatarsal	-18.7	2.6	3.5	40.3	14.5	3.3
JBL1700	SW France	Les Jamblancs		astragalum	-19.4	3.0	2.4	42.0	15.2	3.2
JBL1800	SW France	Les Jamblancs		scapula	-19.3	2.9	2.8	39.4	14.3	3.2
JBL1900	SW France	Les Jamblancs		humerus	-19.4	3.6	2.5	42.5	15.5	3.2
PRG1000	SW France	Les Peyrugues		tibia	-19.2	3.5	7.0	42.3	15.5	3.2
PRG1200	SW France	Les Peyrugues		metatarsal	-19.7	3.2	3.0	37.4	13.7	3.2
PRG1300	SW France	Les Peyrugues		metatarsal	-19.7	3.6	2.2	42.7	15.7	3.2
PRG1400	SW France	Les Peyrugues		long bone	-19.4	3.7	2.1	42.8	15.6	3.2
PRG1500	SW France	Les Peyrugues		long bone	-19.4	3.2	7.2	42.9	15.4	3.2
PRG1600	SW France	Les Peyrugues		long bone	-19.0	3.6	7.6	41.7	14.7	3.3
PRG1700	SW France	Les Peyrugues		long bone	-19.1	3.0	4.3	43.4	15.5	3.3
PRG1800	SW France	Les Peyrugues		long bone	-19.4	3.7	2.4	41.1	15.0	3.2
PRG2200	SW France	Les Peyrugues		tibia	-19.3	3.9	9.9	42.9	15.4	3.3

PRG2300	SW France	Les Peyrugues		metatarsal	-19.4	3.4	2.1	41.9	15.2	3.2
JBL3100	SW France	Les Jamblancs		astragalum	-19.8	4.8	1.8	40.0	15.0	3.1
JBL3200	SW France	Les Jamblancs		astragalum	-19.7	2.2	2.4	41.8	15.7	3.1
JBL3300	SW France	Les Jamblancs		astragalum	-19.6	3.6	1.2	38.9	14.4	3.2
JBL3400	SW France	Les Jamblancs		astragalum	-19.5	5.2	3.2	23.6	8.5	3.3
JBL3500	SW France	Les Jamblancs		astragalum	-19.4	3.6	1.6	40.5	14.6	3.2
PRG3100	SW France	Les Peyrugues		rib	-19.7	2.9	8.1	43.5	15.7	3.2
PRG3200	SW France	Les Peyrugues		tibia	-19.3	4.3	3.4	42.3	15.3	3.2
PRG3300	SW France	Les Peyrugues		tibia	-19.2	4.3	9.4	43.1	15.6	3.2
PRG3400	SW France	Les Peyrugues		femur	-19.4	4.4	6.4	42.6	15.4	3.2
PRG3500	SW France	Les Peyrugues		côte	-19.9	2.6	4.3	42.8	15.3	3.3
PRG3600	SW France	Les Peyrugues		tibia	-18.8	4.9	2.5	42.4	15.4	3.2
CS2600	SW France	Combe-Sauniere		tibia	-19.1	4.1	4.7	41.6	14.7	3.3
CS2700	SW France	Combe-Sauniere		tibia	-19.2	2.9	1.1	41.3	14.7	3.3
CS3100	SW France	Combe-Sauniere		antler	-19.3	3.6	9.6	42.5	15.6	3.2
PRG4200	SW France	Les Peyrugues		antler	-19.5	3.8	2.0	40.0	14.6	3.2
PRG4300	SW France	Les Peyrugues		skull	-19.5	5.6	2.2	41.9	15.1	3.3
PRG4400	SW France	Les Peyrugues		femur	-19.2	5.4	5.0	42.6	15.3	3.2
PRG4500	SW France	Les Peyrugues		femur	-19.1	4.8	3.8	42.2	14.9	3.3
PRG4600	SW France	Les Peyrugues		tibia	-18.7	3.8	4.1	42.5	15.4	3.2
PRG4700	SW France	Les Peyrugues		metacarpal	-19.2	3.3	1.2	40.8	14.8	3.2
PRG5300	SW France	Les Peyrugues		radius	-19.8	5.0	5.1	40.5	14.6	3.2
PRG5400	SW France	Les Peyrugues		radius	-19.4	6.0	2.8	36.0	13.5	3.1
PRG5500	SW France	Les Peyrugues		long bone	-19.0	6.1	5.6	40.7	14.6	3.3
PRG5600	SW France	Les Peyrugues		metatarsal	-19.7	6.0	1.9	37.4	13.5	3.2
PRG5700	SW France	Les Peyrugues		radius	-19.3	5.7	2.6	37.7	13.7	3.2
PRG5800	SW France	Les Peyrugues		radius	-19.2	6.1	4.0	40.4	14.5	3.2
CS1000	SW France	Combe-Sauniere		long bone	-19.0	4.4	3.0	40.4	14.9	3.2
Goyet-A3-15	Ardennes, Belgium	Goyet - Level A3	B	astragalus	-18.5	2.6	12.3	42.3	15.5	3.2
Goyet-A3-16	Ardennes, Belgium	Goyet - Level A3	B	astragalus	-18.5	3.3	9.5	43.0	15.1	3.3
Goyet-A3-17	Ardennes, Belgium	Goyet - Level A3	B	astragalus	-18.6	3.4	14.2	43.4	15.3	3.3
Goyet-A3-18	Ardennes, Belgium	Goyet - Level A3	B	astragalus	-18.3	3.1	16.7	43.9	15.4	3.3
Goyet-A3-19	Ardennes, Belgium	Goyet - Level A3	B	astragalus	-19.6	4.5	11.5	44.1	15.2	3.4
Goyet-B4-8	Ardennes, Belgium	Goyet - Level B4	B	centrotarsus	-18.6	3.9	9.6	41.1	14.9	3.2
RA-GK 294	Swabian Jura	Geissenklösterle	B	metatarsus	-18.9	4.3		43.4	15.5	3.2
RA-GK 295	Swabian Jura	Geissenklösterle	B	tibia	-19.3	3.7		43.6	16.0	3.2

RA-GK 296	Swabian Jura	Geissenklösterle	B	tibia	-19.0	4.2		44.0	15.5	3.3
RA-GK 298	Swabian Jura	Geissenklösterle	B	tibia	-19.3	1.0		42.0	14.6	3.3
RA-GK 299	Swabian Jura	Geissenklösterle	B	talus	-19.2	3.8		41.7	14.5	3.3
RA-GK 300	Swabian Jura	Geissenklösterle	B	humerus	-18.6	3.8		40.6	14.3	3.3
RA-GK 302	Swabian Jura	Geissenklösterle	B	metatarsus	-19.1	4.6		39.6	14.8	3.1
RA-GK 304	Swabian Jura	Geissenklösterle	B	humerus	-19.5	4.4		36.2	12.9	3.2
RA-GK 306	Swabian Jura	Geissenklösterle	B	talus	-19.4	4.7		43.1	14.9	3.3
OxA-6256	Swabian Jura	Geissenklösterle	B	bone	-19.0	4.5				3.3
RA-GK 303	Swabian Jura	Geissenklösterle	B	tibia	-18.9	2.4		41.9	15.3	3.2
RA-GK 308	Swabian Jura	Geissenklösterle	B	tibia	-18.7	3.4		41.7	14.4	3.3
RA-GK 309	Swabian Jura	Geissenklösterle	B	tibia	-19.1	3.9		35.7	13.2	3.1
RA-GK 311	Swabian Jura	Geissenklösterle	B	tibia	-18.6	3.4		43.2	14.5	3.4
RA-GK 312	Swabian Jura	Geissenklösterle	B	tibia	-19.0	2.6		41.8	15.3	3.2
SC22400	Ardennes, Belgium	Scladina - Level 1A	B	mandible	-18.7	3.1	1.0	35.6	12.9	3.2
RPB7200	France	Saint Cesaire	B	metapodium	-18.3	7.3	3.2	41.5	15.0	3.2
LBR900	France	La Berbie	B	humerus	-19.2	3.7	1.9	40.4	14.7	3.2
LBR1000	France	La Berbie	B	humerus	-19.4	3.9	2.0	38.3	14.0	3.2
LBR1100	France	La Berbie	B	jawbone	-19.1	7.6	1.5	39.9	14.4	3.2
LBR3400	France	La Berbie	B	femur	-19.4	5.8	1.7	39.4	13.9	3.3
	France	Marillac - Layer 3	B		-19.5	2.6				
	France	Marillac - Layer 4	B		-19.7	3.1				
	France	Marillac - Layer 4	B		-19.9	3.3				
	France	Marillac - Layer 5	B		-20.4	4.4				
	France	Marillac - Layer 6	B		-20.2	4.2				
	France	Marillac - Layer 7	B		-19.7	5.5				
	France	Marillac - Layer 8	B		-19.2	3.8				
	France	Marillac - Layer 9	B		-19.5	3.9				
	France	Marillac - Layer 10	B		-19.6	4.6				
	France	Marillac - Layer 11	B		-19.6	4.4				
	France	Pont d'Ambon			-20.3	3.9				
	France	Pont d'Ambon			-23.4	4.0				
	France	Pont d'Ambon			-20.2	3.1				
	France	Pont d'Ambon			-20.5	4.5				
	Rochedane	France	B	left metatarsal	-22.5	3.5	14.7	38.8	14.2	3.2
	Rochedane	France	B	left metatarsal	-23.4	4.7	22.8	39.1	14.3	3.2
	Rochedane	France	B	left metatarsal	-21.5	3.8	9.6	36.8	13.4	3.2

	Rochedane	France	B	left metatarsal	-23.0	5.2	29.4	40.5	14.6	3.2
	Rochedane	France	B	right metatarsal	-22.8	5.8	26.6	37.4	13.5	3.2
	Rochedane	France	B	right metatarsal	-22.7	4.3	16.2	38.2	14.2	3.1
	Rochedane	France	B	right metatarsal	-22.9	6.4	15.9	38.1	14.0	3.2
	Rochedane	France	B	right metatarsal	-22.6	4.2	12.4	37.7	13.7	3.2
BVN-9(2)	France/ Switzerland/ Germany Jura	Bavans	B	mandible	-20.8	2.1	1.4	28.1	10.3	3.2
KSL-45	France/ Switzerland/ Germany Jura	Kesslerloch	B	calcaneus R	-20.2	2.0	14.2	44.4	15.4	3.4
RCD11000	France/ Switzerland/ Germany Jura	Rochedane	B	metacarpus	-20.6	2.4	5.0	44.0	16.1	3.2
RCD10900	France/ Switzerland/ Germany Jura	Rochedane	B	metacarpus	-20.4	2.0	6.2	41.7	16.0	3.0
RCD500	France/ Switzerland/ Germany Jura	Rochedane	B	radius L	-19.9	0.8	3.0	42.3	15.5	3.2
CLS1000	Paris Basin	Le Closeau	B	tibia L	-20.1	3.4	2.6	38.0	13.8	3.2
CLS1100	Paris Basin	Le Closeau	B	tibia L	-20.2	3.7	1.5	35.4	12.8	3.2
CLS1200-3	Paris Basin	Le Closeau	B	tibia L	-20.4	3.6	1.6	40.5	14.7	3.2
CLS1300	Paris Basin	Le Closeau	B	tibia R	-20.5	4.0	2.2	38.1	13.9	3.2
CLS1400-1	Paris Basin	Le Closeau	B	tibia R	-20.2	3.0	2.9	39.1	14.3	3.2
CLS1500	Paris Basin	Le Closeau	B	tibia R	-20.5	2.8	1.2	39.1	14.2	3.2
LGH3300	SW France		B	metatarsal	-20.0	5.0	1.2	39.3	14.2	3.2
LGH1100	SW France		B	phalanx	-20.2	3.8	3.0	43.4	15.8	3.2
	France	Pont d'Ambon			-20.7	4.4				
	France	Pont d'Ambon			-19.9	4.0				
	France	Pont d'Ambon			-20.6	3.5				
	France	Pont d'Ambon			-20.8	3.6				
	France	Pont d'Ambon			-20.2	2.9				
	France	Pont d'Ambon			-20.3	3.6				
	Rochedane	France	B	left radius	-19.9	0.8	30.0	42.3	15.5	3.2
	Rochedane	France	B	left metatarsal	-20.1	1.8	18.8	40.3	14.6	3.2
	Rochedane	France	B	left metatarsal	-20.7	2.5	29.0	42.5	15.4	3.2
	Rochedane	France	B	left metatarsal	-21.9	3.0	19.2	42.0	15.3	3.2
	Rochedane	France	B	left metatarsal	-19.9	1.3	6.2	38.9	14.4	3.1
	Rochedane	France	B	left metatarsal	-20.6	2.0	10.2	37.8	13.9	3.2
	Rochedane	France	B	left metatarsal	-20.7	0.4	9.4	41.0	15.0	3.2
	Rochedane	France	B	left metatarsal	-20.8	1.6	10.2	38.5	14.2	3.2

	Rochedane	France	B	left metatarsal	-20.6	3.1	8.6	38.9	13.3	3.2
	Rochedane	France	B	left metatarsal	-21.2	2.6	16.5	40.0	14.6	3.2
	Rochedane	France	B	left metatarsal	-20.0	2.3	33.2	38.8	14.0	3.2
	Rochedane	France	B	left metatarsal	-20.9	1.6	12.2	38.2	14.2	3.2
	Rochedane	France	B	left metatarsal	-20.5	1.3	25.9	40.3	14.7	3.2
SC29200	Ardennes, Belgium	Scladina - Level 1A	B	phalanx I	-19.9	2.3	7.1	42.8	15.1	3.3
CAM1100	France	Camiac	B	long bone	-20.0	6.9	2.4	37.5	13.4	3.3
A/GOY/B/2	Belgium	Goyet Horizon 1	B	Canon post.	-20.2	4.1				3.2
A/CX/B/27	Belgium	Trou de Chaleux	B	Scapula	-20.3	0.4				3.1
A/CX/B/29	Belgium	Trou de Chaleux	B	Scapula	-20.9	1.4				3.3
A/CX/B/30	Belgium	Trou de Chaleux	B	Scapula	-20.7	2.2				3.3
A/CX/B/31	Belgium	Trou de Chaleux	B	Scapula	-20.8	2.3				3.4
A/CX/B/32	Belgium	Trou de Chaleux	B	Scapula	-20.9	3.3				3.3
A/CX/B/33	Belgium	Trou de Chaleux	B	Scapula	-20.6	1.9				3.3
A/CX/B/34	Belgium	Trou de Chaleux	B	Scapula	-20.8	1.9				3.2
A/CX/B/35	Belgium	Trou de Chaleux	B	Scapula	-21.0	1.6				3.3
A/CX/B/36	Belgium	Trou de Chaleux	B	Scapula	-21.1	2.1				3.2
A/CX/B/37	Belgium	Trou de Chaleux	B	Scapula	-20.9	1.9				3.3
A/CX/B/40	Belgium	Trou de Chaleux	B	Scapula	-20.9	1.3				3.2
A/CX/B/42	Belgium	Trou de Chaleux	B	Scapula	-21.0	0.6				3.2
A/CX/B/43	Belgium	Trou de Chaleux	B	Scapula	-21.1	2.3				3.3
A/CX/B/45	Belgium	Trou de Chaleux	B	3. Cunief	-20.7	1.3				3.2
A/CX/B/46	Belgium	Trou de Chaleux	B	3. Cunief	-21.1	2.1				3.3
SHN11	Belgium	Trou de Chaleux	B	Maxilla	-20.6	1.8				3.2
SHN12	Belgium	Trou de Chaleux	B	Maxilla	-21.4	1.8				3.3
SHN13	Belgium	Trou de Chaleux	B	Maxilla	-20.9	1.8				3.4
SHN14	Belgium	Trou de Chaleux	B	Maxilla	-21.3	1.0				3.3
SHN15	Belgium	Trou de Chaleux	B	Maxilla	-21.2	1.9				3.3
SHN16	Belgium	Trou de Chaleux	B	Maxilla	-20.7	1.1				3.3
SHN18	Belgium	Trou de Chaleux	B	Maxilla	-21.2	1.9				3.3
SHN19	Belgium	Trou de Chaleux	B	Maxilla	-21.2	2.4				3.4
SHN20	Belgium	Trou de Chaleux	B	Maxilla	-21.0	2.0				3.4
SHN21	Belgium	Trou de Chaleux	B	Maxilla	-21.0	0.6				3.4
SHN22	Belgium	Trou de Chaleux	B	Maxilla	-21.7	1.8				3.4
SHN23	Belgium	Trou de Chaleux	B	Maxilla	-21.2	1.7				3.3
SHN24	Belgium	Trou de Chaleux	B	Maxilla	-20.8	1.9				3.4

SHN25	Belgium	Trou de Chaleux	B	Maxilla	-20.9	1.4					3.4
SHN26	Belgium	Trou de Chaleux	B	Maxilla	-21.1	1.2					3.5
SHN27	Belgium	Trou de Chaleux	B	Maxilla	-21.1	1.0					3.5
KSL-1	France/ Switzerland/ Germany Jura	Kesslerloch	B	phalanx 1 ant	-20.6	1.3	3.7	45.3	15.5		3.4
KSL-2	France/ Switzerland/ Germany Jura	Kesslerloch	B	metacarpus L	-20.4	1.6	3.5	45.3	15.5		3.4
KSL-3	France/ Switzerland/ Germany Jura	Kesslerloch	B	metacarpus R	-20.2	2.3	3.4	43.7	15.0		3.4
KSL-4	France/ Switzerland/ Germany Jura	Kesslerloch	B	radius R	-20.3	0.6	18.1	46.3	15.7		3.4
KSL-5	France/ Switzerland/ Germany Jura	Kesslerloch	B	metacarpus L	-20.0	1.7	2.8	43.0	14.9		3.4
CHM-2	France/ Switzerland/ Germany Jura	Champréveyres	B	astragalus R	-19.8	1.6	1.4	35.7	13.9		3.0
MRZ-2	France/ Switzerland/ Germany Jura	Monruz	B	femur	-20.6	2.1	1.2	39.2	14.3		3.2
SCH-10	France/ Switzerland/ Germany Jura	Schussenquelle	B	metatarsus distal L	-21.2	4.5	20.7	40.1	15.4		3.0
CLS100-2	Paris Basin	Le Closeau	B	tibia R	-20.7	2.9	31.2	40.4	14.8		3.2
CLS200	Paris Basin	Le Closeau	B	tibia R	-21.3	2.0	23.5	39.4	14.7		3.1
CLS300	Paris Basin	Le Closeau	B	tibia R	-20.6	4.2	19.9	36.8	13.6		3.2
CLS400	Paris Basin	Le Closeau	B	tibia R	-20.8	5.4	32.4	36.4	13.4		3.2
CLS500	Paris Basin	Le Closeau	B	tibia R	-20.6	3.6	15.6	37.6	14.1		3.1
TDG100	Paris Basin	Tureau-des-Gardes	B	metapodium	-21.1	3.7	30.8	40.2	14.6		3.2
TDG1700	Paris Basin	Tureau-des-Gardes	B	tibia	-21.3	1.8	19.7	36.8	14.0		3.1
TDG1800	Paris Basin	Tureau-des-Gardes	B	tibia	-20.5	2.9	24.0	39.5	14.4		3.2
TDG1900	Paris Basin	Tureau-des-Gardes	B	tibia	-20.8	2.7	39.5	40.2	14.7		3.2
TDG2000	Paris Basin	Tureau-des-Gardes	B	scapula	-20.9	2.4	16.7	37.4	13.7		3.2
TDG2100	Paris Basin	Tureau-des-Gardes	B	scapula	-20.3	2.3	5.2	31.1	11.6		3.1
TDG2500	Paris Basin	Tureau-des-Gardes	B	lower premolar	-20.7	1.9	26.2	37.9	13.8		3.2
PCV-2	Paris Basin	Pincevent	B	metatarsus	-20.8	3.4	7.8	36.4	14.2		3.0
PCV-3	Paris Basin	Pincevent	B	metacarpum	-20.7	3.2	7.7	26.5	9.9		3.1
PCV-17	Paris Basin	Pincevent	B	femur L	-20.5	2.1	5.8	30.5	11.6		3.1
PCV-21	Paris Basin	Pincevent	B	phalanx	-21.2	4.0	55.0	37.5	13.7		3.2
MN200	SW France	Aquitine Basin	B	metatarsal	-21.0	4.2	2.6	41.7	15.0		3.2
MN300	SW France	Aquitine Basin	B	metatarsal	-20.9	4.8	4.1	41.4	14.9		3.2
MN400	SW France	Aquitine Basin	B	metatarsal	-21.0	4.2	1.2	37.1	13.5		3.2

MN500	SW France	Aquitine Basin	B	metatarsal	-20.9	4.4	3.7	41.7	15.1	3.2
MN600	SW France	Aquitine Basin	B	metatarsal	-20.9	3.4	1.8	40.7	14.5	3.3
FLG100	SW France	Aquitine Basin	B	humerus	-20.7	3.7	5.4	42.0	15.2	3.2
SGR2800	SW France	Aquitine Basin	B	radius	-21.1	4.2	1.8	13.2	5.0	3.1
SGR2900	SW France	Aquitine Basin	B	long bone	-21.1	4.4	1.5	33.6	12.7	3.1
JBL1200	SW France	Les Jamblancs	B	phalanx	-21.1	2.7	2.8	43.2	15.6	3.2
JBL1600	SW France	Les Jamblancs	B	tibia	-20.5	4.0	5.6	43.1	15.8	3.2
JBL2000	SW France	Les Jamblancs	B	humerus	-21.0	2.9	1.5	41.0	14.9	3.2
JBL2100	SW France	Les Jamblancs	B	scapula	-20.7	2.1	2.7	36.6	13.2	3.2
JBL2300	SW France	Les Jamblancs	B	coxal	-20.9	3.0	3.3	42.4	15.4	3.2
JBL2500	SW France	Les Jamblancs	B	radius	-21.3	2.3	3.0	31.0	11.5	3.1
JBL2800	SW France	Les Jamblancs	B	metapodial	-20.9	3.2	3.5	37.5	13.4	3.3
JBL2900	SW France	Les Jamblancs	B	phalanx	-21.3	1.0	4.8	28.3	10.7	3.1
CS3500	SW France	Combe-Sauniere	B	tibia	-21.3	3.3	4.3	41.9	15.4	3.2
CS3600	SW France	Combe-Sauniere	B	tibia	-21.0	2.8	6.2	43.2	15.8	3.2
CS3700	SW France	Combe-Sauniere	B	tibia	-21.0	3.3	1.1	37.6	13.8	3.2
CS300	SW France	Combe-Sauniere	B	phalanx	-20.0	5.5	8.1	43.8	16.0	3.2
CS400	SW France	Combe-Sauniere	B	radius	-21.0	5.1	5.1	42.2	15.4	3.2
CS600	SW France	Combe-Sauniere	B	metapodial	-20.4	3.7	1.7	41.6	15.3	3.2
CS700	SW France	Combe-Sauniere	B	femur	-20.5	4.5	2.9	41.7	15.3	3.2
CS800	SW France	Combe-Sauniere	B	radius	-20.1	4.7	1.4	40.4	15.1	3.1
	Germany	Abri Stendel	B		-20.9	0.2				3.1
	Germany	Abri Stendel	B		-20.6	1.4				3.2
	Germany	Buttentalhole	B		-20.3	-0.2				3.1
	Germany	Geissenklosterle Cave	B		-20.9	2.2				3.2
	Germany	Geissenklosterle Cave	B		-19.4	0.1				3.0
	Germany	Kniegrotte	B		-19.5	2.7				3.0
	Germany	Kniegrotte	B		-19.9	1.7				3.0
	Germany	Kniegrotte	B		-19.7	0.6				3.1
	Germany	Koblenz-Metternich	B		-21.3	0.7				3.1
	Germany	Koblenz-Metternich	B		-21.0	1.9				3.4
	Germany	Koblenz-Metternich	B		-21.3	-0.9				3.2
	Germany	Koslar	B		-21.4	3.3				3.2
	Germany	Oelknitz, Thuringia	B		-20.3	0.7				3.4
	Germany	Oelknitz, Thuringia	B		-20.6	0.2				3.3
	Germany	Teufelsbrücke	B		-21.6	3.7				3.1

	France	Le Closeau	B		-20.8	3.8				3.3
	Belgium	Trou de Chaleux	B		-21.1	1.6				3.2
	Belgium	Trou de Chaleux	B		-20.7	1.3				3.2
	Belgium	Trou de Frontal	B		-20.3	2.1				3.2
	Belgium	Trou de Nutons	B		-20.7	1.0				3.3
	Germany	Breitenbach	B		-20.1	5.2				3.3
	Germany	Geissenklosterle Cave	B		-20.7	9.3				3.2
	Germany	Geissenklosterle Cave	B		-19.0	4.5				3.3
	Germany	Geissenklosterle Cave	B		-20.6	7.5				3.1
	Germany	Geissenklosterle Cave	B		-20.0	9.2				3.0
	Germany	Geissenklosterle Cave	B		-20.6	5.1				3.2
	Germany	Geissenklosterle Cave	B		-19.3	6.8				2.9
	Germany	Geissenklosterle Cave	B		-19.3	6.8				2.9
	Germany	Hohlefels	B		-21.5	4.5				3.2
	Germany	Wiesbaden Igstadt	B		-20.6	5.4				2.9
	France	Conty	B		-20.8	3.8				2.9
	France	Grotte du Bison	B		-20.3	6.2				3.3
	France	Grotte du Renne	B		-18.8	4.6				3.2
	France	Grotte du Renne	B		-19.7	4.2				3.5
	France	Grotte du Renne	B		-19.5	5.4				3.6
	Belgium	Grotte du Docteur	B		-20.5	6.5				3.3
	Belgium	Place Saint-Lambert (Liege)	B		-23.3	5.9				3.3
	Belgium	Place Saint-Lambert (Liege)	B		-22.4	7.7				3.3
	Belgium	Grotte du Docteur	B		-20.9	4.0				3.4
	Belgium	Mengarnie	B		-21.3	1.0				3.2
Goyet-A3-10	Ardennes, Belgium	Goyet - Level A3	B	ectocuneiform	-21.0	5.1	16.5	44.9	15.9	3.3
Goyet-A3-11	Ardennes, Belgium	Goyet - Level A3	B	ectocuneiform	-20.7	6.4	15.4	41.9	15.4	3.2
Goyet-A3-12	Ardennes, Belgium	Goyet - Level A3	B	ectocuneiform	-20.8	5.9	12.7	43.9	15.4	3.3
Goyet-B4-4	Ardennes, Belgium	Goyet - Level B4	B	tibia	-20.5	6.6	7.5	41.0	14.8	3.2
SC28400	Ardennes, Belgium	Scladina - Level 40	D/RD/C	upper P2 (L)	-21.1	6.5	1.1	33.6	12.9	3.0
SC3900	Ardennes, Belgium	Scladina - Level 1A	D	upper tooth (R)	-21.7	5.2	1.9	42.5	15.6	3.2
SC4100	Ardennes, Belgium	Scladina - Level 1A	D	upper tooth (R)	-21.7	5.1	5.2	42.6	15.8	3.1
SC4200	Ardennes, Belgium	Scladina - Level 1A	D	upper tooth (R)	-21.9	5.0	4.4	42.8	15.8	3.2
SC4300	Ardennes, Belgium	Scladina - Level 1A	D	upper tooth (R)	-21.5	4.8	5.4	39.9	14.5	3.2

SC4400	Ardennes, Belgium	Scladina - Level 1A	D	upper tooth (R)	-21.6	7.0	6.0	40.9	15.0	3.2
	Belgium	Grotte du Docteur	B		-20.5	6.5				3.3
	Belgium	Grotte du Docteur	B		-20.9	4.0				3.4
A/GOY/B/1	Ardennes, Belgium	Goyet - Horizen 1	B	Canon post.	-20.4	7.3				3.2
A/GOY/B/32	Ardennes, Belgium	Goyet - Horizen 2	B	Femur	-21.0	6.0				3.2
EQ-GK 313	Swabian Jura	Geissenklösterle	B	radius	-19.8	4.1		39.2	14.1	3.2
EQ-GK 314	Swabian Jura	Geissenklösterle	B	tibia	-20.7	8.7		43.2	15.7	3.2
EQ-GK 316	Swabian Jura	Geissenklösterle	B	humerus	-20.6	7.3		41.5	14.6	3.3
EQ-GK 317	Swabian Jura	Geissenklösterle	B	Femur	-20.7	5.5		36.3	13.5	3.1
EQ-GK 318	Swabian Jura	Geissenklösterle	B	tibia	-21.8	3.4		42.8	14.3	3.5
EQ-GK 319	Swabian Jura	Geissenklösterle	B	tibia	-21.4	4.2		42.2	14.8	3.3
EQ-GK 321	Swabian Jura	Geissenklösterle	B	tibia	-20.1	8.5		37.8	13.9	3.1
EQ-GK 322	Swabian Jura	Geissenklösterle	B	tibia	-20.8	6.3		36.3	13.7	3.1
EQ-GK 323	Swabian Jura	Geissenklösterle	B	tibia	-20.7	6.1		36.1	13.6	3.1
EQ-GK 325	Swabian Jura	Geissenklösterle	B	tibia	-20.8	7.1		41.6	14.4	3.3
EQ-GK 326	Swabian Jura	Geissenklösterle	B	humerus	-21.0	6.1		42.9	15.3	3.2
EQ-GK 327	Swabian Jura	Geissenklösterle	B	tibia	-20.9	5.9		41.6	15.0	3.2
EQ-GK 329	Swabian Jura	Geissenklösterle	B	tibia	-20.8	6.9		40.7	15.5	3.0
EQ-GK 330	Swabian Jura	Geissenklösterle	B	tibia	-21.6	6.9		28.6	10.9	3.0
EQ-GK 331	Swabian Jura	Geissenklösterle	B	tibia	-20.6	6.1		43.8	16.2	3.1
OxA-4857	Swabian Jura	Geissenklösterle			-20.0	9.2				3.0
OxA-5227	Swabian Jura	Geissenklösterle			-20.7	9.3				3.2
OxA-5707	Swabian Jura	Geissenklösterle			-20.6	7.5				3.1
OxA-4856	Swabian Jura	Geissenklösterle			-20.6	5.1				3.2
TUB-77	Swabian Jura	Geißenklösterle	B	Femur	-21.1	3.2	4.7	39.3	14.6	3.1
TUB-78	Swabian Jura	Geißenklösterle	B	Humerus	-21.2	8.5	4.1	39.7	14.2	3.3
TUB-79	Swabian Jura	Geißenklösterle	B	radius	-21.8	4.7	4.0	41.4	14.9	3.2
OxA-4978	Swabian Jura	Hohle Fels	B		-21.5	4.5				3.2
TUB-80	Swabian Jura	Hohle Fels		"retouchoir"	-20.6	6.2	4.9	37.7	13.7	3.2
RPB2300	France	Saint Cesaire	T	upper 2nd premolar	-20.5	7.3	1.4	17.7	6.5	3.1
LBR1600	France	La Berbie	B	metacarpus	-20.4	7.5	2.2	40.3	14.7	3.2
LBR1700	France	La Berbie	B	femur	-20.9	3.5	3.7	41.9	15.3	3.2
CAM1600	France	Camiac	B	tibia	-20.7	5.2	5.6	41.9	14.7	3.2
CAM1700	France	Camiac	B	tibia	-20.5	5.2	3.5	40.6	14.6	3.2
	France	Marillac - Layer 3	B		-20.1	4.9				

	France	Marillac - Layer 3	B		-20.7	4.8				
	France	Marillac - Layer 3	T		-20.8	3.0				
	France	Marillac - Layer 3	T		-20.5	3.0				
	France	Marillac - Layer 4	B		-20.5	5.0				
	France	Marillac - Layer 4	B		-21.0	5.1				
	France	Marillac - Layer 5	B		-20.5	4.8				
	France	Marillac - Layer 6	B		-20.8	4.8				
	France	Marillac - Layer 6	B		-20.3	3.6				
	France	Marillac - Layer 7	B		-21.9	7.9				
	France	Marillac - Layer 7	B		-20.7	6.8				
	France	Marillac - Layer 7	B		-20.4	5.5				
	France	Marillac - Layer 7	B		-20.7	5.9				
	France	Marillac - Layer 7	B		-22.2	6.4				
	France	Marillac - Layer 7	B		-20.4	7.4				
	France	Marillac - Layer 8	B		-19.2	3.9				
	France	Marillac - Layer 8	T		-20.6	5.3				
	France	Marillac - Layer 9	B		-21.4	6.3				
	France	Marillac - Layer 10	B		-20.4	2.3				
	France	Marillac - Layer 10	B		-20.6	5.5				
	France	Marillac - Layer 11	T		-20.1	4.2				
KSL-47	France/ Switzerland/ Germany Jura	Kesslerloch	B	molar	-20.5	6.4	9.5	43.5	15.6	3.2
Goyet-A2-1	Ardennes, Belgium	Goyet - Level A2	B	long bone	-20.7	8.1	6.3	41.0	15.0	3.2
Goyet-A3-9	Ardennes, Belgium	Goyet - Level A3	B	long bone	-21.5	7.0	7.5	43.9	15.6	3.3
Goyet-B4-2	Ardennes, Belgium	Goyet - Level B4	B	skull	-21.6	6.7	14.2	41.0	14.6	3.3
SC600	Ardennes, Belgium	Scladina - Level 1A	D	tooth fragment	-20.9	8.4	4.5	42.6	15.5	3.2
SC700	Ardennes, Belgium	Scladina - Level 1A	D	tooth fragment	-21.5	9.4	3.2	41.5	15.2	3.2
SC800	Ardennes, Belgium	Scladina - Level 1A	D	tooth fragment	-21.6	8.3	2.6	41.3	15.1	3.2
HST-9	Swabian Jura	Hohlenstein-Stadel	D/RD/C	tusk ivory	-21.4	7.4	2.1	40.5	14.5	3.3
LBR1900	France	La Berbie	B	femur	-21.8	8.5	1.2	37.2	13.4	3.2
CAM700	France	Camiac	B	femur	-21.2	8.7	5.7	39.1	14.1	3.2
CAM800	France	Camiac	B	femur	-21.8	7.7	3.2	40.6	14.7	3.2
SCH-6	France/ Switzerland/ Germany Jura	Schussenquelle	B	tibia distal	-20.2	3.0	14.5	45.5	15.6	3.4
SCH-7	France/ Switzerland/ Germany Jura	Schussenquelle	B	metatarsus distal	-19.8	2.9	23.5	45.9	15.6	3.4

KSL-7	France/ Switzerland/ Germany Jura	Kesslerloch	B	phalanx 2 ant	-19.9	2.1	7.9	45.3	16.1	3.3
ARL-1	France/ Switzerland/ Germany Jura	Grotte de Chaze II	B	half-mandible L	-20.3	5.3	2.0	38.4	14.6	3.1
Goyet-A2-2	Ardennes, Belgium	Goyet - Level A2	B	unciforme	-20.0	4.3	13.1	43.8	16.2	3.2
Goyet-A3-2	Ardennes, Belgium	Goyet - Level A3	B	scaphoide	-20.4	5.7	16.9	43.8	15.2	3.4
Goyet-B4-3	Ardennes, Belgium	Goyet - Level B4	B	1st metacarpum	-20.8	5.9	8.7	40.0	14.6	3.2
SC30100	Ardennes, Belgium	Scladina - Level 40	B	metatarsal II R	-21.1	5.5	8.0	44.4	15.7	3.3
OxA-6255	Swabian Jura	Geissenklösterle	B		-19.3	6.8				2.9
LBR2200	France	La Berbie	B	skull	-19.6	7.2	2.8	39.1	14.4	3.2
CAM1300	France	Camiac	B	humerus	-19.9	8.4	2.3	38.1	13.7	3.2
CAM1400	France	Camiac	B	humerus	-20.1	7.1	2.7	39.3	14.3	3.2
CAM1500	France	Camiac	B	humerus	-20.6	7.1	7.8	40.3	14.7	3.2

*In Western Beringia, this would have been a reindeer, rather than a caribou. However, consistent naming of species is used in the thesis.

**In Western Beringia, this would have been a red deer or a wapiti rather than an elk. However, consistent naming of species is used in the thesis.

Tissue: B = Bone; RD = Root dentin; C = Cementum; D = Crown dentin; T= Tusk dentin

References:

- Bocherens, H., Billiou, D., Patou-Mathis, M., Bonjean, D., Otte, M., Mariotti, A., 1997. Paleobiological implications of the isotopic Signatures (^{13}C , ^{15}N) of fossil mammal collagen in Scladina Cave (Sclayn, Belgium). *Quat. Res.* 48, 370–380. doi:10.1006/qres.1997.1927
- Bocherens, H., Billiou, D., Mariotti, A., Toussaint, M., Patou-Mathis, M., Bonjean, D., Otte, M., 2001. New isotopic evidence for dietary habits of Neandertals from Belgium. *J. Hum. Evol.* 40, 497–505. doi:10.1006/jhev.2000.0452
- Bocherens, H., Drucker, D.G., Billiou, D., Patou-Mathis, M., Vandermeersch, B., 2005. Isotopic evidence for diet and subsistence pattern of the Saint-Césaire I Neanderthal: review and use of a multi-source mixing model. *J. Hum. Evol.* 49, 71–87. doi:10.1016/j.jhevol.2005.03.003
- Bocherens, H., Drucker, D.G., Bonjean, D., Bridault, A., Conard, N.J., Cupillard, C., Germonpré, M., Höneisen, M., Münzel, S.C., Napierala, H., Patou-Mathis, M., Stephan, E., Uerpmann, H.-P., Ziegler, R., 2011. Isotopic evidence for dietary ecology of cave lion (*Panthera spelaea*) in North-Western Europe: prey choice, competition and implications for extinction. *Quat. Int.* 245, 249–

261. doi:10.1016/j.quaint.2011.02.023

- Drucker, D.G., Bocherens, H., Bridault, A., Billiou, D., 2003a. Carbon and nitrogen isotopic composition of red deer (*Cervus elaphus*) collagen as a tool for tracking palaeoenvironmental change during the Late-Glacial and Early Holocene in the northern Jura (France). *Palaeogeogr. Palaeoclimatol. Palaeoecol.* 195, 375–388. doi:10.1016/S0031-0182(03)00366-3
- Drucker, D.G., Bocherens, H., Billiou, D., 2003b. Evidence for shifting environmental conditions in Southwestern France from 33 000 to 15 000 years ago derived from carbon-13 and nitrogen-15 natural abundances in collagen of large herbivores. *Earth Planet. Sci. Lett.* 216, 163–173. doi:10.1016/S0012-821X(03)00514-4
- Drucker, D.G., Bridault, A., Cupillard, C., Hujic, A., Bocherens, H., 2011. Evolution of habitat and environment of red deer (*Cervus elaphus*) during the Late-glacial and early Holocene in eastern France (French Jura and the western Alps) using multi-isotope analysis ($\delta^{13}\text{C}$, $\delta^{15}\text{N}$, $\delta^{18}\text{O}$, $\delta^{34}\text{S}$) of archaeological remains. *Quat. Int.* 245, 268–278. doi:10.1016/j.quaint.2011.07.019
- Fizet, M., Mariotti, A., Bocherens, H., Lange-Badré, B., Vandermeersch, B., Borel, J.P., Bellon, G., 1995. Effect of diet, physiology and climate on carbon and nitrogen stable isotopes of collagen in a Late Pleistocene anthropic palaeoecosystem: Marillac, Charente, France. *J. Archaeol. Sci.* 22, 67–79.
- Stevens, R.E., Germonpré, M., Petrie, C.A., O'Connell, T.C., 2009. Palaeoenvironmental and chronological investigations of the Magdalenian sites of Goyet Cave and Trou de Chaleux (Belgium), via stable isotope and radiocarbon analyses of horse skeletal remains. *J. Archaeol. Sci.* 36, 653–662. doi:10.1016/j.jas.2008.10.008
- Stevens, R.E., Hedges, R.E., 2004. Carbon and nitrogen stable isotope analysis of northwest European horse bone and tooth collagen, 40,000 BP – present: palaeoclimatic interpretations. *Quat. Sci. Rev.* 23, 977–991. doi:10.1016/j.quascirev.2003.06.024

Appendix T Sample information for megafaunal herbivores from Old Crow.

Lab ID	Common Name	Scientific Name	Sample Number	Stable Isotope Reference	¹⁴ C Date	Date Lab #	Date reference	Source
YT129	Horse	<i>Equus</i> sp.	178.9	Chapter 3; Schwartz-Narbonne et al., 2015	27,189 ±420	AA103890	Schwartz-Narbonne et al., 2015	YG
YT130	Horse	<i>Equus</i> sp.	179.14	Chapter 3; Schwartz-Narbonne et al., 2015				YG
YT131	Horse	<i>Equus</i> sp.	236.235	Chapter 3; Schwartz-Narbonne et al., 2015	18,370 ±260	AA103835	Schwartz-Narbonne et al., 2015	YG
YT132	Horse	<i>Equus</i> sp.	295.2	Chapter 2; Schwartz-Narbonne et al., 2015	>41,100	AA103836	Schwartz-Narbonne et al., 2015	YG
YT133	Horse	<i>Equus</i> sp.	315.1	Chapter 2; Schwartz-Narbonne et al., 2015				YG
YT1RD	Mammoth	<i>Mammuthus</i>	291.1	Metcalfe et al., 2010	>41,100	AA84987	Metcalfe et al., 2010	YG
YT2RD	Mammoth	<i>Mammuthus</i>	122.2	Metcalfe et al., 2010	>41,100	AA84992	Metcalfe et al., 2010	YG
YT3D	Mammoth	<i>Mammuthus</i>	173.5	Metcalfe et al., 2010				YG
YT4B	Mammoth	<i>Mammuthus</i>	285.1	Metcalfe et al., 2010	>39,100	AA85002	Metcalfe et al., 2010	YG
YT5RD	Mammoth	<i>Mammuthus</i>	60.2	Metcalfe et al., 2010				YG
YT6C	Mammoth	<i>Mammuthus</i>	57.1	Metcalfe et al., 2010				YG
YT7B	Mammoth	<i>Mammuthus</i>	325.22	Metcalfe et al., 2010	>40,100	AA84984	Metcalfe et al., 2010	YG
YT9C	Mammoth	<i>Mammuthus</i>	284.4	Metcalfe et al., 2010				YG
YT10RD	Mammoth	<i>Mammuthus</i>	252.2	Metcalfe et al., 2010	>40,000	AA85001	Metcalfe et al., 2010	YG
YT11C	Mammoth	<i>Mammuthus</i>	173.1	Metcalfe et al., 2010				YG
YT11RD	Mammoth	<i>Mammuthus</i>	173.1	Metcalfe et al., 2010				YG
YT51T	Mammoth	<i>Mammuthus</i>	317.51	Metcalfe et al., 2010	MIS5, ~140,000		Metcalfe (2011)	YG
YT8D	Mastodon	<i>Mammut</i>	357.1	Metcalfe (2011)	>41,100	AA84995	Metcalfe (2011)	YG
K-15352	Mastodon	<i>Mammut</i>	CMN 15352	Zazula et al., 2014	45700 ± 2500	UCIAMS78695	Zazula et al., 2014	
K-31898	Mastodon	<i>Mammut</i>	CMN 31898	Zazula et al., 2014	50300±3500	UCIAMS78696	Zazula et al., 2014	
K-33066	Mastodon	<i>Mammut</i>	CMN 33066	Zazula et al., 2014	>49900	UCIAMS78697	Zazula et al., 2014	

Appendix T continues below.

Lab ID	Latitude	Longitude	Site	Tissue	Tissue Type	$\delta^{13}\text{C}_{\text{Bulk}}$	$\delta^{15}\text{N}_{\text{Bulk}}$	% Yield	%C	%N	C/N
YT129	67°30'00" N	139°57'26" W	Porcupine River, downstream from Ch'ijee's Bluff	B		-20.8	7.0	10.2	39.7	15.5	3.3
YT130	68°15'49" N	140°22'25" W	CRH 47 Old Crow River	B		-21.1	8.1	11.2	40.3	15.6	3.2
YT131	68°02'12" N	139°34'40" W	CRH 67 Old Crow River	B		-20.7	9.9	5.4	36.1	14.0	3.4
YT132	67°54'25" N	139°40'57" W	HH-68-21 Old Crow River	B		-21.2	4.2	8.2	38.5	14.8	3.1
YT133	68°12'48" N	140°00'41" W	CRH 44 Old Crow River	B		-20.9	8.7	10.9	42.0	16.2	3.2
YT1RD	67°58.166' N	139°33.689' W	Old Crow River	RD	LRM6	-21.5	9.8	11.2	42.9	15.5	3.2
YT2RD	68°03'33" N	139°46'07" W	CRH 94 Old Crow River	RD	ULM6	-21.4	8.7	14.4	41.6	15.6	3.1
YT3D	67°29'00" N	139°55'00" W	Ch'ijee's Bluff, Porcupine River	D	U M6	-20.9	8.4	11.0	39.2	14.6	3.1
YT4B	67°55.1' N	139°40.7' W	OCR, REM 78-1	B		-21.8	9.7	>6.7	44.0	16.4	3.1
YT5RD	68°08'44" N	139°58'12" W	OCR, Bluffs-R bank	B	LRM5/M6	-21.4	9.5	13.1	41.1	15.2	3.1
YT6C	68°11'19" N	140°32'04" W	OCR, Bluffs-R bank	C	LRM6	-21.7	7.7	10.1	42.5	15.2	3.3
YT7B	67°51.892' N	139°48.075' W	HH-68-10 Old Crow River	B		-21.4	7.6	15.7	42.3	15.8	3.1
YT9C	67°49'29" N	139°50'11" W	CRH 11 Old Crow River	C	ULM6	-21.5	8.2	7.1	41.4	15.0	3.2
YT10RD	68°01'46" N	139°34'15" W	CRH 20 Old Crow River	RD	LLM6	-21.5	9.8	11.4	38.9	14.4	3.2
YT11C	67°29'00" N	139°55'00" W	Ch'ijee's Bluff, Porcupine River	C	U M6	-21.5	9.5	14.3	47.2	17.6	3.1
YT11RD				RD	U M6	-21.5	8.3	18.2	44.1	15.9	3.2
YT51T			CRH 11 Old Crow River	T	Tusk	-20.7	11.3	18.6	37.9	13.9	3.2
YT8D			Old Crow River	D	M5/M6	-20.6	3.5	17.8	42.3	16.0	3.1
K-15352			Loc. 14N	RD/D		-19.6	4.1	>1.3	43.4	14.8	3.4
K-31898			Loc. 74	RD/D		-19.9	2.4	>2.1	42.6	15.2	3.3
K-33066			Loc. 46	RD/D		-20.1	2.5	>3.9	43.3	15.3	3.3

Samples analyzed multiple times (duplicate/triplicate) in Chapter 5 are in bold

Dates obtained in Chapter 5 are in bold

Tissue: B = Bone; RD = Root dentin; C = Cementum; D = Crown dentin; T= Tusk dentin

References:

Metcalfe, J.Z., Longstaffe, F.J., Zazula, G.D., 2010. Nursing, weaning, and tooth development in woolly mammoths from Old Crow, Yukon, Canada: implications for Pleistocene extinctions. *Palaeogeogr. Palaeoclimatol. Palaeoecol.* 298, 257–270.

doi:10.1016/j.palaeo.2010.09.032

Metcalf, J.Z., 2011. Late Pleistocene climate and proboscidean paleoecology in North America: insights from stable isotope compositions of skeletal remains. Doctoral Thesis. University of Western Ontario.

Schwartz-Narbonne, R., Longstaffe, F.J., Metcalfe, J.Z., Zazula, G., 2015. Solving the woolly mammoth conundrum: amino acid ¹⁵N-enrichment suggests a distinct forage or habitat. *Sci. Rep.* 5, 9791. doi:10.1038/srep09791

Zazula, G.D., MacPhee, R.D., Metcalfe, J.Z., Reyes, A. V., Brock, F., Druckenmiller, P.S., Groves, P., Harington, R., Hodgins, G.W.L., Kunz, M.L., Longstaffe, F.J., Mann, D.H., McDonald, H.G., Nalawade-Chavan, S., Southon, J.R., 2014. American mastodon extirpation in the Arctic and Subarctic predates human colonization and terminal Pleistocene climate change. *Proc. Natl. Acad. Sci.* 111, 18460–18465.

Appendix U Sample information for megafaunal herbivores from the Russian Plain.

Common Name	Sample Number	¹⁴ C Date	Date Lab #	Date reference
Mammoth	1/1	14,100±100 to 14,470±400	Dating based on upper and lower ages of layer	Iacumin et al., 2000
Mammoth	1/2	14,100±100 to 14,470±400	Dating based on upper and lower ages of layer	Iacumin et al., 2000
Mammoth	1/3	14,100±100 to 14,470±400	Dating based on upper and lower ages of layer	Iacumin et al., 2000
Mammoth	1/4	14,100±100 to 14,470±400	Dating based on upper and lower ages of layer	Iacumin et al., 2000
Mammoth	1/5	14,100±100 to 14,470±400	Dating based on upper and lower ages of layer	Iacumin et al., 2000
Mammoth	3/1	23,660±270 to 24,960±400	Dating based on upper and lower ages of layer	Iacumin et al., 2000
Mammoth	3/2	23,660±270 to 24,960±400	Dating based on upper and lower ages of layer	Iacumin et al., 2000
Mammoth	3/3	23,660±270 to 24,960±400	Dating based on upper and lower ages of layer	Iacumin et al., 2000
Mammoth	3/4	23,660±270 to 24,960±400	Dating based on upper and lower ages of layer	Iacumin et al., 2000
Mammoth	3/5	23,660±270 to 24,960±400	Dating based on upper and lower ages of layer	Iacumin et al., 2000
Mammoth	4/1	13,650±200 to 15,790±320	Dating based on upper and lower ages of layer	Iacumin et al., 2000
Mammoth	4/2	13,650±200 to 15,790±320	Dating based on upper and lower ages of layer	Iacumin et al., 2000
Mammoth	4/3	13,650±200 to 15,790±320	Dating based on upper and lower ages of layer	Iacumin et al., 2000
Mammoth	5/1	14,320±270 to 14,400±250	Dating based on upper and lower ages of layer	Iacumin et al., 2000
Mammoth	5/2	14,320±270 to 14,400±250	Dating based on upper and lower ages of layer	Iacumin et al., 2000
Mammoth	5/3	14,320±270 to 14,400±250	Dating based on upper and lower ages of layer	Iacumin et al., 2000
Mammoth				

Appendix U continues below.

Sample Number	Site	Stable Isotope Reference	Scientific Name	Tissue	$\delta^{13}\text{C}_{\text{Bulk}}$	$\delta^{15}\text{N}_{\text{Bulk}}$	% Yield	%C	%N	C/N
1/1	Eliscevichi	Iacumin et al., 2000	<i>Mammuthus primigenius</i>	D/RD/C	-20.2	5.2	2.0	44.2	15.2	3.4
1/2	Eliscevichi	Iacumin et al., 2000	<i>Mammuthus primigenius</i>	B	-20.1	6.1	10.0	43.8	14.6	3.5
1/3	Eliscevichi	Iacumin et al., 2000	<i>Mammuthus primigenius</i>	B	-20.6	6.7	5.0	39.7	13.7	3.4
1/4	Eliscevichi	Iacumin et al., 2000	<i>Mammuthus primigenius</i>	B	-20.6	4.8	15.2	42.1	14.3	3.4
1/5	Eliscevichi	Iacumin et al., 2000	<i>Mammuthus primigenius</i>	B	-20.6	5.3	14.4	42.7	14.4	3.5
3/1	Khotylevo	Iacumin et al., 2000	<i>Mammuthus primigenius</i>	D/RD/C	-19.9	9.0	12.9	40.2	15.1	3.1
3/2	Khotylevo	Iacumin et al., 2000	<i>Mammuthus primigenius</i>	D/RD/C	-19.6	10.1	10.1	41.7	15.2	3.2
3/3	Khotylevo	Iacumin et al., 2000	<i>Mammuthus primigenius</i>	D/RD/C	-20.1	9.4	8.3	42.6	15.1	3.3
3/4	Khotylevo	Iacumin et al., 2000	<i>Mammuthus primigenius</i>	B	-20.3	9.5	5.1	39.5	15.4	3.0
3/5	Khotylevo	Iacumin et al., 2000	<i>Mammuthus primigenius</i>	B	-20.0	9.4	11.8	41.7	15.2	3.2

4/1	Yudinovo	Iacumin et al., 2000	<i>Mammuthus primigenius</i>	B	-19.7	7.4	10.2	44.8	15.4	3.4
4/2	Yudinovo	Iacumin et al., 2000	<i>Mammuthus primigenius</i>	B	-19.5	7.4	4.3	43.1	15.2	3.3
4/3	Yudinovo	Iacumin et al., 2000	<i>Mammuthus primigenius</i>	B	-19.6	7.7	9.0	44.0	14.9	3.4
5/1	Mezhirich	Iacumin et al., 2000	<i>Mammuthus primigenius</i>	T	-19.7	5.3	11.4	44.1	15.6	3.3
5/2	Mezhirich	Iacumin et al., 2000	<i>Mammuthus primigenius</i>	B	-20.1	4.6	3.1	41.9	14.4	3.4
5/3	Mezhirich	Iacumin et al., 2000	<i>Mammuthus primigenius</i>	B	-20.1	4.7	2.1	43.7	15.0	3.4
	Brianskaya oblast	Bocherens et al., 1994		T	-20.7	7.7				

Tissue: B = Bone; RD = Root dentin; C = Cementum; D = Crown dentin; T= Tusk dentin

References:

- Bocherens, H., Fizet, M., Mariotti, A., Gangloff, R., Burns, J., 1994. Contribution of isotopic biogeochemistry (^{13}C , ^{15}N , ^{18}O) to the paleoecology of mammoths (*Mammuthus primigenius*). *Hist. Biol.* 7, 187–202.
- Iacumin, P., Nikolaev, V., Ramigni, M., 2000. C and N stable isotope measurements on Eurasian fossil mammals, 40 000 to 10 000 years BP: herbivore physiologies and palaeoenvironmental reconstruction. *Palaeogeogr. Palaeoclimatol. Palaeoecol.* 163, 33–47.

Appendix V Sample information for megafaunal herbivores from the Selawik area.

Lab ID	Common Name	Sample Number	Stable Isotope Reference	¹⁴ C Date	Date Lab #	Date reference
UAK38	Bison	UAMES 2206	Chapter 5	16,220±190	AA103839	Chapter 5
UAK31	Bison	UAMES 1106	Chapter 5	37,700±2,600	AA103838	Chapter 5
UAK25	Bison	UAMES 991	Chapter 5			
UAK26	Bison	UAMES 1014	Chapter 5			
UAK27	Bison	UAMES 1088	Chapter 5			
UAK28	Bison	UAMES 1095	Chapter 5	>40,300	AA103884	
UAK29	Bison	UAMES 1096	Chapter 5			
UAK30	Bison	UAMES 1097	Chapter 5			
UAK32	Bison	UAMES 1107	Chapter 5			
UAK33	Bison	UAMES 1119	Chapter 5			
UAK34	Bison	UAMES 1121	Chapter 5			
UAK35	Bison	UAMES 1125	Chapter 5			
UAK36	Bison	UAMES 1172	Chapter 5			
UAK37	Bison	UAMES 2096	Chapter 5			
UAK6	Caribou	UAMES 1122	Chapter 2	26,360±650	AA103840	Chapter 2
UAK12	Caribou	UAMES 2214	Chapter 2	29,020±910	AA103841	Chapter 2
UAK8	Caribou	UAMES 1151	Chapter 2			
UAK9	Caribou	UAMES 1180	Chapter 2			
UAK7	Caribou	UAMES 1123	Chapter 2			
UAK11	Caribou	UAMES 2114	Chapter 2			
UAK1	Caribou	UAMES1033	Chapter 2	201±33	AA103881	Chapter 2
UAK2	Caribou	UAMES1035	Chapter 2			
UAK3	Caribou	UAMES 1036	Chapter 2			
UAK14	Horse	UAMES 1024	Chapter 5			
UAK15	Horse	UAMES 1063	Chapter 5			
UAK16	Horse	UAMES 1152	Chapter 5			
UAK17	Horse	UAMES 1153	Chapter 5			
UAK18	Horse	UAMES 1154	Chapter 5			
UAK19	Horse	UAMES 1155	Chapter 5	>40,300	AA103882	Chapter 5
UAK20	Horse	UAMES 1156	Chapter 5			
UAK21	Horse	UAMES 1159	Chapter 5	14,790±100	AA103883	Chapter 5
UAK22	Horse	UAMES 1178	Chapter 5			
UAK23	Horse	UAMES 1179	Chapter 5	30,400±1,100	AA103829	Chapter 5
UAK24	Horse	UAMES 2170	Chapter 5			
	Horse	UAMES 29664	Drukenmiller, 2008	27,980±180		Drukenmiller, 2008
	Horse	UAMES 1064	Drukenmiller, 2008	17,130±80		Drukenmiller, 2008
UAK41	Mammoth	UAMES 2073	Chapter 5	>41,100	AA103828	Chapter 5
UAK42	Mammoth	UAMES 2100	Chapter 5			
UAK43	Mammoth	UAMES 2115	Chapter 5			
UAK44	Mammoth	UAMES 2117	Chapter 5			
UAK45	Mammoth	UAMES 2129	Chapter 5	26,230±380	AA103885	Chapter 5
UAK46	Mammoth	UAMES 2153	Chapter 5			
UAK47	Mammoth	UAMES 2156	Chapter 5			
UAK48	Mammoth	UAMES 2160	Chapter 5	25,070±570	AA103827	Chapter 5
UAK49	Mammoth	UAMES 2180	Chapter 5			
UAK50	Mammoth	UAMES 2209	Chapter 5			
UAK51	Mammoth	UAMES 2217	Chapter 5			

UAK52	Mammoth	UAMES 3869	Chapter 5			
UAK39	Mammoth	UAMES 2066	Chapter 5			
UAK40	Mammoth	UAMES 2071	Chapter 5			
	Mammoth	AK-170-V-1	Bocherens et al., 1994			
	Moose	UAMES 29656	Drukenmiller, 2008	80±40		Drukenmiller, 2008
	Moose	AK-V-60	Drukenmiller, 2008	7870±50		Drukenmiller, 2008
	Muskox	UAMES 29657	Drukenmiller, 2008	44,300±1,900		Drukenmiller, 2008

Appendix V continues below.

Lab ID	Tissue	Tissue Type	Source	$\delta^{13}\text{C}_{\text{Bulk}}$	$\delta^{15}\text{N}_{\text{Bulk}}$	% Yield	%C	%N	C/N
UAK38	B	radius	UAMES	-20.0	2.9	11.4	40.0	14.3	3.3
UAK31	B	calcaneum	UAMES	-20.4	5.7	10.1	40.3	14.3	3.3
UAK25	B	radius	UAMES	-20.2	4.3	15.4	43.0	15.4	3.3
UAK26	B	calcaneum	UAMES	-19.8	3.4	12.7	40.2	14.2	3.3
UAK27	B	humerus	UAMES	-20.1	5.5	14.0	37.2	13.0	3.3
UAK28	B	humerus	UAMES	-20.8	4.0	12.4	44.3	15.6	3.3
UAK29	B	humerus	UAMES	-19.8	3.5	13.9	42.7	15.1	3.3
UAK30	B	radius	UAMES	-20.4	4.7	9.3	38.8	13.7	3.3
UAK32	B	calcaneum	UAMES	-20.3	4.5	7.3	39.3	14.0	3.3
UAK33	B	metacarpal	UAMES	-19.9	3.5	12.5	38.8	14.4	3.1
UAK34	B	radius	UAMES	-20.4	5.3	2.2	38.5	13.5	3.3
UAK35	B	innominate	UAMES	-20.0	2.4	10.4	40.6	14.3	3.3
UAK36	B		UAMES	-20.2	5.2	8.4	38.7	13.7	3.3
UAK37	B	radius	UAMES	-20.0	4.7	11.8	41.6	14.9	3.3
UAK6	B	tibia	UAMES	-19.7	4.6	7.2	37.9	13.2	3.4
UAK12	B	humerus	UAMES	-18.5	4.1	5.5	38.9	13.7	3.3
UAK8	B	innominate	UAMES	-18.6	3.5	19.4	33.5	12.0	3.2
UAK9	B	scapula	UAMES	-18.7	1.9	16.7	36.8	13.3	3.2
UAK7	B	humerus	UAMES	-19.0	4.1	11.9	41.2	14.7	3.3
UAK11	B	mantible	UAMES	-19.7	4.8	4.2	37.6	13.3	3.3
UAK1	B	metatarsal	UAMES	-19.3	2.1	13.7	40.0	13.9	3.3
UAK2	B	humerus	UAMES	-19.2	3.4	14.6	42.2	14.9	3.3
UAK3	B	radius	UAMES	-19.2	2.7	12.8	41.3	14.4	3.3
UAK14	B	metapodial	UAMES	-20.8	3.2	9.6	37.1	13.7	3.2
UAK15	B	tibia	UAMES	-21.0	4.9	4.1	43.0	15.1	3.3
UAK16	B	innominate	UAMES	-21.0	3.0	12.5	38.9	14.2	3.2
UAK17	B	innominate	UAMES	-21.1	5.7	16.3	40.2	14.7	3.2
UAK18	B	innominate	UAMES	-20.4	1.4	12.1	41.0	15.2	3.2
UAK19	B	humerus	UAMES	-21.1	1.3	9.3	39.1	14.6	3.1
UAK20	B	humerus	UAMES	-21.2	4.8	10.6	37.2	13.8	3.1
UAK21	B	scapula	UAMES	-20.9	3.4	14.6	41.1	15.2	3.1
UAK22	B	tibia	UAMES	-20.8	3.9	10.6	40.0	15.1	3.1
UAK23	B	tibia	UAMES	-21.0	5.1	17.4	38.8	14.4	3.2
UAK24	B	innominate	UAMES	-20.8	3.2	10.2	37.1	13.7	3.2
	B	scapula	UAMES	-21.1	4.2				
	B	tibia	UAMES	-21.0	2.0				
UAK41	B	rib	UAMES	-22.0	6.5	14.3	42.5	16.1	3.1
UAK42	B	carpal	UAMES	-22.0	7.7	6.5	33.6	12.5	3.1
UAK43	B	fibula	UAMES	-21.9	7.9	7.3	38.6	14.6	3.1

UAK44	B	fibula	UAMES	-21.5	6.4	13.0	41.1	15.4	3.1
UAK45	B	rib	UAMES	-21.4	7.4	13.5	41.1	15.1	3.2
UAK46	B	radius	UAMES	-21.8	7.3	12.3	41.1	15.1	3.2
UAK47	B	rib	UAMES	-22.4	7.9	14.7	41.8	15.2	3.2
UAK48	B	rib	UAMES	-22.1	8.2	15.4	42.9	15.8	3.2
UAK49	B	rib	UAMES	-21.6	7.5	13.3	41.6	15.3	3.2
UAK50	B	thoracic vertebra	UAMES	-21.6	7.0	14.9	42.6	15.6	3.2
UAK51	B	carpal	UAMES	-21.9	8.1	15.1	41.5	15.2	3.2
UAK52	B	radius	UAMES	-21.8	7.5	10.6	39.0	14.7	3.1
UAK39	B	rib	UAMES	-21.6	8.8	16.1	42.3	16.2	3.0
UAK40	B	carpal	UAMES	-21.0	6.7	13.5	40.9	15.5	3.1
	D			-21.2	8.5				
	B	innominate	UAMES	-21.0	2.1				
	B	jaw	UAMES	-20.9	3.9				
	B	metapodial	UAMES	-20.0	4.2				

Samples analyzed multiple times (duplicate/triplicate) in Chapter 5 are in bold

Dates obtained in Chapter 5 are in bold

UAMES = University of Alaska Museum Earth Science

Tissue: B = Bone; RD = Root dentin; C = Cementum; D = Crown dentin; T= Tusk dentin

References:

Bocherens, H., Fizet, M., Mariotti, A., Gangloff, R., Burns, J., 1994. Contribution of isotopic biogeochemistry (^{13}C , ^{15}N , ^{18}O) to the paleoecology of mammoths (*Mammuthus primigenius*). *Hist. Biol.* 7, 187–202.

Druckenmiller, P.S., 2008. Survey of Pleistocene (Ice Age) vertebrates from the Selawik and Kobuk River areas of Northwestern Alaska. Intern. Rep. U.S. Fish Wildl. Serv. 1–56.

Appendix W Sample information for megafaunal herbivores from south central Siberia.

Sample Number	Stable Isotope Reference	¹⁴ C Date	Date Lab #	Date reference
11/1	Iacumin et al. (2000)	~13,000	dating based on cultural layer	Iacumin et al. (2000)
11/2	Iacumin et al. (2000)	~13,000	dating based on cultural layer	Iacumin et al. (2000)
11/5	Iacumin et al. (2000)	~13,000	dating based on cultural layer	Iacumin et al. (2000)
11/8	Iacumin et al. (2000)	~13,000	dating based on cultural layer	Iacumin et al. (2000)
11/12	Iacumin et al. (2000)	~13,000	dating based on cultural layer	Iacumin et al. (2000)
11/13	Iacumin et al. (2000)	~13,000	dating based on cultural layer	Iacumin et al. (2000)
11/17	Iacumin et al. (2000)	~13,000	dating based on cultural layer	Iacumin et al. (2000)
11/19	Iacumin et al. (2000)	~13,000	dating based on cultural layer	Iacumin et al. (2000)
11/22	Iacumin et al. (2000)	~13,000	dating based on cultural layer	Iacumin et al. (2000)
11/23	Iacumin et al. (2000)	~14,000	dating based on cultural layer	Iacumin et al. (2000)
11/27	Iacumin et al. (2000)	~14,000	dating based on cultural layer	Iacumin et al. (2000)
11/29	Iacumin et al. (2000)	~14,000	dating based on cultural layer	Iacumin et al. (2000)
11/31	Iacumin et al. (2000)	~14,000	dating based on cultural layer	Iacumin et al. (2000)
11/34	Iacumin et al. (2000)	~15,000	dating based on cultural layer	Iacumin et al. (2000)
14/1	Iacumin et al. (2000)	~13,500 to ~20,000	dating based on cultural layer	Iacumin et al. (2000)
15/1	Iacumin et al. (2000)	21000		Iacumin et al. (2000)
15/2	Iacumin et al. (2000)	21000		Iacumin et al. (2000)
15/3	Iacumin et al. (2000)	21000		Iacumin et al. (2000)
15/4	Iacumin et al. (2000)	21000		Iacumin et al. (2000)
15/5	Iacumin et al. (2000)	21000		Iacumin et al. (2000)
15/7	Iacumin et al. (2000)	21000		Iacumin et al. (2000)
15/9	Iacumin et al. (2000)	21000		Iacumin et al. (2000)
12/1	Iacumin et al. (2000)			
12/2	Iacumin et al. (2000)			
12/3	Iacumin et al. (2000)			
11/18	Iacumin et al. (2000)	~13,000	dating based on cultural layer	Iacumin et al. (2000)

Appendix W continues below.

Sample Number	Site	Tissue	$\delta^{13}\text{C}_{\text{Bulk}}$	$\delta^{15}\text{N}_{\text{Bulk}}$	% Yield	%C	%N	C/N
11/1	Afontova Gora II	B	-18.3	2.2	10.6	39.7	14.5	3.2
11/2	Afontova Gora II	B	-19.0	2.3	17.7	40.6	15.3	3.1
11/5	Afontova Gora II	B	-18.5	1.5	19.5	33.5	13.0	3.0
11/8	Afontova Gora II	B	-19.0	1.7	14.0	31.9	11.7	3.2
11/12	Afontova Gora II	B	-18.8	1.5	20.8	38.1	13.9	3.2
11/13	Afontova Gora II	B	-18.4	1.8	16.8	40.9	14.5	3.3
11/17	Afontova Gora II	B	-18.6	1.4	16.5	33.2	12.1	3.2
11/19	Afontova Gora II	B	-18.7	1.3	19.4	43.5	16.4	3.1
11/22	Afontova Gora II	B	-19.0	1.7	17.7	44.2	17.2	3.0
11/23	Afontova Gora II	B	-18.0	2.0	11.9	37.9	13.8	3.2
11/27	Afontova Gora II	B	-18.7	1.3	16.8	39.9	14.5	3.2
11/29	Afontova Gora II	B	-18.3	2.3	20.4	34.2	12.9	3.1
11/31	Afontova Gora II	B	-18.6	1.9	15.5	40.9	14.9	3.2
11/34	Afontova Gora II	B	-18.4	1.9	14.3	44.3	15.7	3.3
14/1	Listvenka	B	-18.5	1.5	13.4	42.9	15.6	3.2
15/1	Kashtanka	B	-18.4	4.2	15.2	41.8	14.8	3.3
15/2	Kashtanka	B	-17.7	4.1	10.9	39.7	14.5	3.2
15/3	Kashtanka	B	-18.6	3.8	9.5	43.3	15.8	3.2
15/4	Kashtanka	B	-18.5	3.2	12.3	43.2	15.8	3.2
15/5	Kashtanka	B	-18.6	3.9	14.2	43.8	14.7	3.5
15/7	Kashtanka	B	-17.6	3.8	12.8	42.8	14.3	3.5
15/9	Kashtanka	B	-18.9	3.6	11.7	43.9	15.1	3.4
12/1	Bolshaya Slezneva	B	-19.7	1.6	8.4	42.4	15.0	3.3
12/2	Bolshaya Slezneva	B	-20.2	1.4	2.4	14.4	5.0	3.4
12/3	Bolshaya Slezneva	B	-19.5	2.0	10.0	25.3	8.2	3.6
11/18	Afontova Gora II	B	-20.8	4.6	10.9	31.9	11.7	3.2

*In Western Beringia, this would have been a reindeer, rather than a caribou. However, consistent naming of species is used in the thesis.

**In Western Beringia, this would have been a red deer or a wapiti rather than an elk. However, consistent naming of species is used in the thesis.

Tissue: B = Bone; RD = Root dentin; C = Cementum; D = Crown dentin; T= Tusk dentin

References:

Iacumin, P., Nikolaev, V., Ramigni, M., 2000. C and N stable isotope measurements on Eurasian fossil mammals, 40 000 to 10 000 years BP: herbivore physiologies and palaeoenvironmental reconstruction. *Palaeogeogr. Palaeoclimatol. Palaeoecol.* 163, 33–47.

Appendix X Sample information for megafaunal herbivores from Spain.

Lab ID	Common Name	Scientific Name	Stable Isotope Reference	¹⁴ C Date	Date reference
DEB2	Mammoth	<i>Mammuthus primigenius</i>	Garcia-Alix et al., 2012	25,700-35,800	Alvarez-Lao et al., 2009
Carpal	Mammoth	<i>Mammuthus primigenius</i>	Garcia-Alix et al., 2012	25,700-35,800	Alvarez-Lao et al., 2009

Appendix X continues below.

Lab ID	Area	Site	Tissue	Tissue Type	$\delta^{13}\text{C}_{\text{Coll}}$	$\delta^{15}\text{N}_{\text{Coll}}$	%C	%N	C/N
DEB2	Granada Basin, southern Spain	El Padul' peat bog	dentin-enamel boundary	adult M3	-20.7	13.2	36	13	3.3
Carpal	Granada Basin, southern Spain	El Padul' peat bog	B	carpal bone	-21.8	10.1	36	12	3.4

Tissue: B = Bone; RD = Root dentin; C = Cementum; D = Crown dentin; T= Tusk dentin

References:

- Álvarez-Lao, D.J., Kahlke, R.-D., García, N., Mol, D., 2009. The Padul mammoth finds — On the southernmost record of *Mammuthus primigenius* in Europe and its southern spread during the Late Pleistocene. *Palaeogeogr. Palaeoclimatol. Palaeoecol.* 278, 57–70. doi:10.1016/j.palaeo.2009.04.011
- García-Alix, a., Delgado Huertas, a., Martín Suárez, E., 2012. Unravelling the Late Pleistocene habitat of the southernmost woolly mammoths in Europe. *Quat. Sci. Rev.* 32, 75–85. doi:10.1016/j.quascirev.2011.11.00

Appendix Y Sample information for megafaunal herbivores from the Taymyr Peninsula.

Common Name	Scientific Name	Sample Number	Stable Isotope Reference	¹⁴ C Date	Date reference	Tissue
Mammoth	<i>Mammuthus primigenius</i>	20/411	Iacumin et al., 2000	11,140±180	Iacumin et al., 2000	B
Mammoth	<i>Mammuthus primigenius</i>	20/407	Iacumin et al., 2000	39,800±600	Iacumin et al., 2000	B
Mammoth	<i>Mammuthus primigenius</i>	20/412	Iacumin et al., 2000	39,800±500	Iacumin et al., 2000	B
Mammoth	<i>Mammuthus primigenius</i>	20/A-50	Iacumin et al., 2000			B
Mammoth	<i>Mammuthus primigenius</i>	20/415	Iacumin et al., 2000	40,800±200	Iacumin et al., 2000	B
Mammoth	<i>Mammuthus primigenius</i>	20/408	Iacumin et al., 2000			B
Mammoth	<i>Mammuthus primigenius</i>	20/8833	Iacumin et al., 2000			B
Mammoth	<i>Mammuthus primigenius</i>	2000/173	Szpak et al., 2010	11,900±40	Debruyne et al., 2008	
Mammoth	<i>Mammuthus primigenius</i>	2000/174	Szpak et al., 2010	28,210±210	Debruyne et al., 2008	
Mammoth	<i>Mammuthus primigenius</i>	2000/183	Szpak et al., 2010	28,260±170	Debruyne et al., 2008	
Mammoth	<i>Mammuthus primigenius</i>	2000/198	Szpak et al., 2010	15,390±50	Debruyne et al., 2008	
Mammoth	<i>Mammuthus primigenius</i>	2001/412	Szpak et al., 2010	>44,400	Debruyne et al., 2008	
Mammoth	<i>Mammuthus primigenius</i>	2002/472	Szpak et al., 2010	>48,800	Debruyne et al., 2008	
Mammoth	<i>Mammuthus primigenius</i>	2002/473	Szpak et al., 2010	46,700±2,800	Debruyne et al., 2008	
Mammoth	<i>Mammuthus primigenius</i>	2002/594	Szpak et al., 2010			
Mammoth	<i>Mammuthus primigenius</i>	2005/897	Szpak et al., 2010	40,150±990	Debruyne et al., 2008	
Mammoth	<i>Mammuthus primigenius</i>	2005/900	Szpak et al., 2010	28,700±310	Debruyne et al., 2008	
Mammoth	<i>Mammuthus primigenius</i>	2005/901	Szpak et al., 2010	17,300±60	Debruyne et al., 2008	
Mammoth	<i>Mammuthus primigenius</i>	2005/907	Szpak et al., 2010	41,000±1,400	Debruyne et al., 2008	
Mammoth	<i>Mammuthus primigenius</i>	2005/915	Szpak et al., 2010	27,740±220	Debruyne et al., 2008	
Mammoth	<i>Mammuthus primigenius</i>	2005/916	Szpak et al., 2010			
Mammoth	<i>Mammuthus primigenius</i>	2005/917	Szpak et al., 2010	35,380±550	Debruyne et al., 2008	
Mammoth	<i>Mammuthus primigenius</i>	2005/928	Szpak et al., 2010			
Mammoth	<i>Mammuthus primigenius</i>	2005/945	Szpak et al., 2010	28,260±170	Debruyne et al., 2008	
Mammoth	<i>Mammuthus primigenius</i>	2005/988	Szpak et al., 2010			
Mammoth	<i>Mammuthus primigenius</i>	2005/999	Szpak et al., 2010	>49,900	Debruyne et al., 2008	
Muskox	<i>Ovibos</i>	KIC 2002/537	Raghavan et al., 2014	2756 ± 27	Raghavan et al., 2014	B
Muskox	<i>Ovibos</i>	KIC 2003/756	Raghavan et al., 2014	2918 ± 28	Raghavan et al., 2014	B
Muskox	<i>Ovibos</i>	KIC 2003/757	Raghavan et al., 2014	3372 ± 43	Raghavan et al., 2014	B
Muskox	<i>Ovibos</i>	KIC 2003/764	Raghavan et al., 2014	4082 ± 30	Raghavan et al., 2014	B
Muskox	<i>Ovibos</i>	KIC 2003/763	Raghavan et al., 2014	5364 ± 49	Raghavan et al., 2014	B
Muskox	<i>Ovibos</i>	PIN 3913-13	Raghavan et al., 2014	12830 ± 80	Raghavan et al., 2014	B

Muskox	<i>Ovibos</i>	KIC 2004/876	Raghavan et al., 2014	12965 ± 80	Raghavan et al., 2014	B
Muskox	<i>Ovibos</i>	KIC 2001/431	Raghavan et al., 2014	13125 ± 80	Raghavan et al., 2014	B
Muskox	<i>Ovibos</i>	KIC 2003/648	Raghavan et al., 2014	14270 ± 90	Raghavan et al., 2014	B
Muskox	<i>Ovibos</i>	KIC 2000/127	Raghavan et al., 2014	15020 ± 90	Raghavan et al., 2014	B
Muskox	<i>Ovibos</i>	KIC 2003/663	Raghavan et al., 2014	15100 ± 100	Raghavan et al., 2014	B
Muskox	<i>Ovibos</i>	KIC 2003/662	Raghavan et al., 2014	15300 ± 90	Raghavan et al., 2014	B
Muskox	<i>Ovibos</i>	KIC 2003/645	Raghavan et al., 2014	15380 ± 100	Raghavan et al., 2014	B
Muskox	<i>Ovibos</i>	KIC 2000/101	Raghavan et al., 2014	15770 ± 55	Raghavan et al., 2014	B
Muskox	<i>Ovibos</i>	KIC 2003/771	Raghavan et al., 2014	15875 ± 60	Raghavan et al., 2014	B
Muskox	<i>Ovibos</i>	KIC 2000/69	Raghavan et al., 2014	16010 ± 100	Raghavan et al., 2014	B
Muskox	<i>Ovibos</i>	KIC 2003/760	Raghavan et al., 2014	16295 ± 60	Raghavan et al., 2014	B
Muskox	<i>Ovibos</i>	KIC 2003/761	Raghavan et al., 2014	16810 ± 150	Raghavan et al., 2014	B
Muskox	<i>Ovibos</i>	KIC 2003/765	Raghavan et al., 2014	17690 ± 120	Raghavan et al., 2014	B
Muskox	<i>Ovibos moschatus</i>	KIC 2002/510	Raghavan et al., 2014	17900 ± 65	Raghavan et al., 2014	B
Muskox	<i>Ovibos</i>	KIC 2003/605	Raghavan et al., 2014	18100 ± 110	Raghavan et al., 2014	B
Muskox	<i>Ovibos</i>	KIC 2001/430-R	Raghavan et al., 2014	18600 ± 140	Raghavan et al., 2014	B
Muskox	<i>Ovibos</i>	KIC 2000/100	Raghavan et al., 2014	18750 ± 120	Raghavan et al., 2014	B
Muskox	<i>Ovibos</i>	KIC 2003/607	Raghavan et al., 2014	18830 ± 170	Raghavan et al., 2014	B
Muskox	<i>Ovibos</i>	KIC 2002/509	Raghavan et al., 2014	19310 ± 140	Raghavan et al., 2014	B
Muskox	<i>Ovibos</i>	KIC 2000/432	Raghavan et al., 2014	19570 ± 130	Raghavan et al., 2014	B
Muskox	<i>Ovibos</i>	KIC 2003/758	Raghavan et al., 2014	19790 ± 160	Raghavan et al., 2014	B
Muskox	<i>Ovibos</i>	KIC 2002/504	Raghavan et al., 2014	19840 ± 140	Raghavan et al., 2014	B
Muskox	<i>Ovibos</i>	KIC 2003/650	Raghavan et al., 2014	19860 ± 130	Raghavan et al., 2014	B
Muskox	<i>Ovibos</i>	KIC 2003/608	Raghavan et al., 2014	19925 ± 80	Raghavan et al., 2014	B
Muskox	<i>Ovibos</i>	KIC 2002/507	Raghavan et al., 2014	20230 ± 160	Raghavan et al., 2014	B
Muskox	<i>Ovibos</i>	KIC 2003/755	Raghavan et al., 2014	20850 ± 150	Raghavan et al., 2014	B
Muskox	<i>Ovibos</i>	KIC 2005/926	Raghavan et al., 2014	21050 ± 160	Raghavan et al., 2014	B
Muskox	<i>Ovibos</i>	KIC 2003/767	Raghavan et al., 2014	21060 ± 90	Raghavan et al., 2014	B
Muskox	<i>Ovibos</i>	KIC 2001/434	Raghavan et al., 2014	21140 ± 160	Raghavan et al., 2014	B
Muskox	<i>Ovibos</i>	KIC 2003/768	Raghavan et al., 2014	21210 ± 150	Raghavan et al., 2014	B
Muskox	<i>Ovibos</i>	KIC 2002/505	Raghavan et al., 2014	21840 ± 210	Raghavan et al., 2014	B
Muskox	<i>Ovibos</i>	KIC 2003/766	Raghavan et al., 2014	22630 ± 180	Raghavan et al., 2014	B
Muskox	<i>Ovibos</i>	KIC 2001/433	Raghavan et al., 2014	23220 ± 180	Raghavan et al., 2014	B
Muskox	<i>Ovibos</i>	KIC 2003/759	Raghavan et al., 2014	24000 ± 210	Raghavan et al., 2014	B
Muskox	<i>Ovibos</i>	KIC 2003/606	Raghavan et al., 2014	24270 ± 160	Raghavan et al., 2014	B
Muskox	<i>Ovibos</i>	KIC 2003/603	Raghavan et al., 2014	24940 ± 230	Raghavan et al., 2014	B

Muskox	<i>Ovibos</i>	KIC 2000/57	Raghavan et al., 2014	25310 ± 240	Raghavan et al., 2014	B
Muskox	<i>Ovibos</i>	KIC 2003/649	Raghavan et al., 2014	25490 ± 230	Raghavan et al., 2014	B
Muskox	<i>Ovibos</i>	KIC 2000/66	Raghavan et al., 2014	33850 ± 600	Raghavan et al., 2014	B
Muskox	<i>Ovibos</i>	KIC 2000/103	Raghavan et al., 2014	34150 ± 600	Raghavan et al., 2014	B
Muskox	<i>Ovibos</i>	KIC 2003/667	Raghavan et al., 2014	35830 ± 240	Raghavan et al., 2014	B
Muskox	<i>Ovibos</i>	KIC 2002/511	Raghavan et al., 2014	45900 ± 2300	Raghavan et al., 2014	B
Muskox	<i>Ovibos</i>	PIN 3913-55	Raghavan et al., 2014	48100	Raghavan et al., 2014	B
Muskox	<i>Ovibos</i>	KIC 2003/668	Raghavan et al., 2014	> 46400	Raghavan et al., 2014	B
Muskox	<i>Ovibos</i>	PIN 3913-65	Raghavan et al., 2014	> 48400	Raghavan et al., 2014	B
Muskox	<i>Ovibos</i>	PIN 3913-60	Raghavan et al., 2014	> 49819	Raghavan et al., 2014	B

Appendix Y continues below.

Sample Number	Latitude	Longitude	Site	$\delta^{13}\text{C}_{\text{Bulk}}$	$\delta^{15}\text{N}_{\text{Bulk}}$	% Yield	%C	%N	C/N
20/411			Taymyr Peninsula	-22.4	8.1	18.7	46.0	15.4	3.5
20/407			Taymyr Peninsula	-21.4	8.2	23.1	42.6	14.6	3.4
20/412			Taymyr Peninsula	-21.4	8.4	20.4	42.2	14.2	3.5
20/A-50			Taymyr Peninsula	-22.4	9.6	18.1	42.9	14.3	3.5
20/415			Taymyr Peninsula	-22.2	6.5	16.7	40.6	13.7	3.5
20/408			Taymyr Peninsula	-21.6	8.6	19.2	44.5	14.8	3.5
20/8833			Taymyr Peninsula	-21.8	8.5	14.4	43.1	14.8	3.4
2000/173	74° 25'N	107° 45'E	Arilakh	-22.5	9.1	10.7	38.2	14.2	3.1
2000/174	74° 25'N	107° 45'E	Arilakh	-21.7	10.7	14.7	39.1	14.5	3.1
2000/183	74° 30'N	100° 30'E	Lake Taymyr	-21.4	9.4	12.2	40.5	15.0	3.2
2000/198	74° 35'N	100° 30'E	Cape Sablera	-21.0	10.6	16.3	37.1	13.7	3.2
2001/412	72°	101°	Ari Mas	-21.8	10.5	7.6	41.1	15.2	3.2
2002/472	74° 25'N	107° 45'E	Arilakh	-22.0	10.0	22.4	38.2	13.4	3.3
2002/473	74° 25'N	107° 45'E	Arilakh	-22.0	11.4	24.0	38.8	14.5	3.1
2002/594	74° 25'N	107° 45'E	Arilakh	-23.2	7.8	15.2	39.8	12.8	3.6
2005/897	74° 15'N	107° 20'E	Baikura-Turku	-21.7	8.9	20.1	38.4	13.6	3.3
2005/900			Lake Taymyr	-21.9	9.7	17.2	36.6	12.9	3.3
2005/901			Lake Taymyr	-21.0	10.7	20.0	39.9	14.2	3.3
2005/907			Taymyr Peninsula	-22.1	8.1	22.3	35.0	12.2	3.3
2005/915	73° 45'N	102° 00'E	Baikura-Turku	-21.9	10.0	26.2	36.7	13.6	3.1
2005/916	73° 45'N	102° 00'E	Baikura-Turku	-21.7	8.9	17.9	38.2	13.5	3.3
2005/917	73° 45'N	102° 00'E	Baikura-Turku	-21.4	8.7	14.7	35.4	12.5	3.3

2005/928	73° 30'N	108° 00'E	Soposhnaya	-22.4	8.0	20.9	36.4	11.9	3.6
2005/945	73° 24'N	101° 39'E	Cape Sablera	-20.8	9.1	25.2	37.3	13.1	3.3
2005/988	72° 38'N	106° 40'E	Popigay	-21.6	8.4	23.8	36.8	13.2	3.3
2005/999	72° 38'N	106° 40'E	Popigay	-22.0	7.5	23.4	32.0	11.1	3.4
KIC 2002/537			Taymyr	-20.3	7.5	21.6	43.2		3.3
KIC 2003/756			Taymyr	-20.4	5.8	17.7	42.5		3.3
KIC 2003/757			Taymyr	-20.9	6.0	7.1	44.2	16.4	3.1
KIC 2003/764			Taymyr	-20.3	6.1	17.7	42.1		3.2
KIC 2003/763			Taymyr	-20.9	4.6	8.8	43.9	16.4	3.1
PIN 3913-13			Taymyr	-20.7	2.1	5.1	44.4	16.3	3.2
KIC 2004/876			Taymyr	-21.3	5.4	5.1	43.7	16.2	3.2
KIC 2001/431			Taymyr	-21.2	2.9	4.3	44.2	16.4	3.1
KIC 2003/648			Taymyr	-20.4	5.7	6.9	43.6	16.1	3.2
KIC 2000/127			Taymyr	-19.6	7.2	6.2	43.9	16.2	3.2
KIC 2003/663			Taymyr	-19.6	7.3	5.7	43.7	16.0	3.2
KIC 2003/662			Taymyr	-19.9	6.2	7.0	45.2	16.6	3.2
KIC 2003/645			Taymyr	-20.6	4.7	5.4	44.6	16.4	3.2
KIC 2000/101			Taymyr	-19.6	5.6	16.3	41.7		3.2
KIC 2003/771			Taymyr	-20.2	6.5	8.4	44.2		3.1
KIC 2000/69			Taymyr	-19.8	4.8	2.6	43.1	15.9	3.2
KIC 2003/760			Taymyr	-19.7	6.0	16.1	44.6		3.1
KIC 2003/761			Taymyr	-20.5	6.7	7.5	43.6	16.1	3.2
KIC 2003/765			Taymyr	-20.4	5.7	6.9	43.8	16.2	3.2
KIC 2002/510			Taymyr	-20.1	5.2	17.7	43.9		3.1
KIC 2003/605			Taymyr	-20.3	5.9	4.0	43.7	16.2	3.2
KIC 2001/430-R			Taymyr	-20.2	7.5	6.7	44.1	16.2	3.2
KIC 2000/100			Taymyr	-20.0	6.9	3.4	44.7	16.1	3.2
KIC 2003/607			Taymyr	-20.6	4.9	4.4	42.4	15.7	3.2
KIC 2002/509			Taymyr	-20.6	5.6	3.3	43.9	16.1	3.2
KIC 2000/432			Taymyr	-20.7	5.3	8.9	45.0	16.5	3.2
KIC 2003/758			Taymyr	-20.6	6.9	6.3	42.6	15.7	3.2
KIC 2002/504			Taymyr	-20.2	5.6	3.5	42.9	16.0	3.1
KIC 2003/650			Taymyr	-20.3	6.1	5.6	44.4	16.5	3.2
KIC 2003/608			Taymyr	-19.6	5.7	11.6	43.8		3.2
KIC 2002/507			Taymyr	-20.3	5.3	5.9	43.8	16.1	3.2
KIC 2003/755			Taymyr	-20.4	6.0	3.7	39.7	14.7	3.2

KIC 2005/926	Taymyr	-20.5	6.2	4.4	44.4	16.3	3.2
KIC 2003/767	Taymyr	-20.8	5.4	17.7	47.3		3.1
KIC 2001/434	Taymyr	-20.3	6.4	7.2	42.8	15.9	3.1
KIC 2003/768	Taymyr	-21.1	5.4	11.8	44.2	16.5	3.2
KIC 2002/505	Taymyr	-21.0	5.9	6.6	43.0	15.9	3.2
KIC 2003/766	Taymyr	-20.3	4.8	3.9	42.9	15.9	3.2
KIC 2001/433	Taymyr	-20.0	5.6	2.9	42.0	15.5	3.2
KIC 2003/759	Taymyr	-20.5	6.4	6.7	44.8	16.5	3.2
KIC 2003/606	Taymyr	-21.1	6.1	8.1	43.9	16.2	3.2
KIC 2003/603	Taymyr	-21.0	4.7	6.4	44.2	16.4	3.2
KIC 2000/57	Taymyr	-20.7	7.6	5.4	44.2	16.4	3.1
KIC 2003/649	Taymyr	-20.9	6.3	5.6	44.8	16.6	3.2
KIC 2000/66	Taymyr	-21.1	5.6	3.7	42.6	15.5	3.2
KIC 2000/103	Taymyr	-21.1	5.4	5.7	44.1	16.4	3.1
KIC 2003/667	Taymyr	-20.6	4.7	10.4	42.7		3.2
KIC 2002/511	Taymyr	-20.8	5.2	5.1	47.4	17.7	3.2
PIN 3913-55	Taymyr	-20.0	4.9	10.1	44.0		3.1
KIC 2003/668	Taymyr	-20.7	3.0	4.2	43.3	16.0	3.2
PIN 3913-65	Taymyr	-20.6	5.1	7.6	44.6	16.4	3.2
PIN 3913-60	Taymyr	-21.0	5.9	5.2	43.7	16.0	3.2

Tissue: **B** = Bone; **RD** = Root dentin; **C** = Cementum; **D** = Crown dentin; **T** = Tusk dentin

References:

- Debruyne, R., Chu, G., King, C.E., Bos, K., Kuch, M., Schwarz, C., Szpak, P., Gröcke, D.R., Matheus, P., Zazula, G., Guthrie, D., Froese, D., Buigues, B., de Marliave, C., Flemming, C., Poinar, D., Fisher, D., Southon, J., Tikhonov, A.N., MacPhee, R.D.E., Poinar, H.N., 2008. Out of America: ancient DNA evidence for a new world origin of late Quaternary woolly mammoths. *Curr. Biol.* 18, 1320–6. doi:10.1016/j.cub.2008.07.061
- Iacumin, P., Nikolaev, V., Ramigni, M., 2000. C and N stable isotope measurements on Eurasian fossil mammals, 40 000 to 10 000 years BP: herbivore physiologies and palaeoenvironmental reconstruction. *Palaeogeogr. Palaeoclimatol. Palaeoecol.* 163, 33–47.
- Raghavan, M., Espregueira Themudo, G., Smith, C.I., Zazula, G., Campos, P.F., 2014. Musk ox (*Ovibos moschatus*) of the mammoth steppe: tracing palaeodietary and palaeoenvironmental changes over the last 50,000 years using carbon and nitrogen isotopic

analysis. *Quat. Sci. Rev.* 102, 192–201. doi:10.1016/j.quascirev.2014.08.001

Szpak, P., Gröcke, D.R., Debruyne, R., MacPhee, R.D.E., Guthrie, R.D., Froese, D., Zazula, G.D., Patterson, W.P., Poinar, H.N., 2010. Regional differences in bone collagen $\delta^{13}\text{C}$ and $\delta^{15}\text{N}$ of Pleistocene mammoths: implications for paleoecology of the mammoth steppe. *Palaeogeogr. Palaeoclimatol. Palaeoecol.* 286, 88–96. doi:10.1016/j.palaeo.2009.12.009

Appendix Z Sample information for megafaunal herbivores from Wrangel Island.

Common Name	Scientific Name	Sample Number	Stable Isotope Reference	¹⁴ C Date	Date reference	Latitude	Longitude
Mammoth	<i>Mammuthus primigenius</i>	WR2	Szpak et al., 2010	4,420±15	Debruyne et al., 2008; Guthrie, 2006	71°N	179°W

Appendix Z continues below.

Sample Number	$\delta^{13}\text{C}_{\text{Bulk}}$	$\delta^{15}\text{N}_{\text{Bulk}}$	% Yield	%C	%N	C/N
WR2	-22.2	8.6	15.5	37.9	13.6	3.3

References:

- Debruyne, R., Chu, G., King, C.E., Bos, K., Kuch, M., Schwarz, C., Szpak, P., Gröcke, D.R., Matheus, P., Zazula, G., Guthrie, D., Froese, D., Buigues, B., de Marliave, C., Flemming, C., Poinar, D., Fisher, D., Southon, J., Tikhonov, A.N., MacPhee, R.D.E., Poinar, H.N., 2008. Out of America: ancient DNA evidence for a new world origin of late Quaternary woolly mammoths. *Curr. Biol.* 18, 1320–6. doi:10.1016/j.cub.2008.07.061
- Guthrie, R.D., 2006. New carbon dates link climatic change with human colonization and Pleistocene extinctions. *Nature* 441, 207–209. doi:10.1038/nature04604
- Szpak, P., Gröcke, D.R., Debruyne, R., MacPhee, R.D.E., Guthrie, R.D., Froese, D., Zazula, G.D., Patterson, W.P., Poinar, H.N., 2010. Regional differences in bone collagen $\delta^{13}\text{C}$ and $\delta^{15}\text{N}$ of Pleistocene mammoths: implications for paleoecology of the mammoth steppe. *Palaeogeogr. Palaeoclimatol. Palaeoecol.* 286, 88–96. doi:10.1016/j.palaeo.2009.12.009

Appendix AA Sample information for megafaunal herbivores from Yakutia.

Common Name	Scientific Name	Sample Number	Stable Isotope Reference	¹⁴ C Date	Calibrated Date	Date reference
Bison	<i>Bison priscus</i>	17/1	Iacumin et al., 2000	~40,000 BP**		Iacumin et al., 2000
Bison	<i>Bison priscus</i>	25	Iacumin et al., 2010	38,200±700		Iacumin et al., 2010
Bison	<i>Bison priscus</i>	26	Iacumin et al., 2010	41,500±1,100		Iacumin et al., 2010
Bison	<i>Bison priscus</i>	101900	Bocherens et al., 1996			
Caribou*		18/1	Iacumin et al., 2000			
Horse	<i>Equus caballus</i>	22	Iacumin et al., 2010	16,380±120		Iacumin et al., 2010
Horse	<i>Equus caballus</i>	24	Iacumin et al., 2010	35,900±600		Iacumin et al., 2010
Horse	<i>Equus caballus</i>	96300	Bocherens et al., 1996		~25,000	Bocherens et al., 1996
Horse	<i>Equus caballus</i>	10200	Bocherens et al., 1996			
Mammoth	<i>Mammuthus primigenius</i>	8/1	Iacumin et al., 2000	~10,000 BP**		Iacumin et al., 2000
Mammoth	<i>Mammuthus primigenius</i>	8/2	Iacumin et al., 2000	~10,000 BP**		Iacumin et al., 2000
Mammoth	<i>Mammuthus primigenius</i>	16/1	Iacumin et al., 2000	~40,000 BP**		Iacumin et al., 2000
Mammoth	<i>Mammuthus primigenius</i>	16/2	Iacumin et al., 2000	~40,000 BP**		Iacumin et al., 2000
Mammoth	<i>Mammuthus primigenius</i>	17/2	Iacumin et al., 2000			
Mammoth	<i>Mammuthus primigenius</i>	19/20	Iacumin et al., 2000			
Mammoth	<i>Mammuthus primigenius</i>	19/35	Iacumin et al., 2000			
Mammoth	<i>Mammuthus primigenius</i>	19/37	Iacumin et al., 2000			
Mammoth	<i>Mammuthus primigenius</i>	19/42	Iacumin et al., 2000			
Mammoth	<i>Mammuthus primigenius</i>	19/52	Iacumin et al., 2000	30,100±550		Iacumin et al., 2000
Mammoth	<i>Mammuthus primigenius</i>	19/58	Iacumin et al., 2000	40,200±1,800		Iacumin et al., 2000
Mammoth	<i>Mammuthus primigenius</i>	19/59	Iacumin et al., 2000			
Mammoth	<i>Mammuthus primigenius</i>	19/75	Iacumin et al., 2000			
Mammoth	<i>Mammuthus primigenius</i>	19/92	Iacumin et al., 2000			
Mammoth	<i>Mammuthus primigenius</i>	21	Iacumin et al., 2000			

Mammoth	<i>Mammuthus primigenius</i>	22	Iacumin et al., 2000		
Mammoth	<i>Mammuthus primigenius</i>	1	Iacumin et al., 2010	12,030±60	Iacumin et al., 2010
Mammoth	<i>Mammuthus primigenius</i>	8	Iacumin et al., 2010	22,100±1,000	Iacumin et al., 2010
Mammoth	<i>Mammuthus primigenius</i>	12	Iacumin et al., 2010	28,000±180	Iacumin et al., 2010
Mammoth	<i>Mammuthus primigenius</i>	A	Iacumin et al., 2010	32,500±500	Iacumin et al., 2010
Mammoth	<i>Mammuthus primigenius</i>	16	Iacumin et al., 2010	37,800±900	Iacumin et al., 2010
Mammoth	<i>Mammuthus primigenius</i>	17	Iacumin et al., 2010	39,600±1,000	Iacumin et al., 2010
Mammoth	<i>Mammuthus primigenius</i>	18	Iacumin et al., 2010	40,200±900	Iacumin et al., 2010
Mammoth	<i>Mammuthus primigenius</i>	19	Iacumin et al., 2010	43,600±1,000	Iacumin et al., 2010
Mammoth	<i>Mammuthus primigenius</i>	20	Iacumin et al., 2010	48,000±2,000	Iacumin et al., 2010
Mammoth	<i>Mammuthus primigenius</i>	21	Iacumin et al., 2010	50,650±1,820	Iacumin et al., 2010
Mammoth	<i>Mammuthus primigenius</i>	3	Iacumin et al., 2010	13,100±500	Iacumin et al., 2010
Mammoth	<i>Mammuthus primigenius</i>	7	Iacumin et al., 2010	20,800±600	Iacumin et al., 2010
Mammoth	<i>Mammuthus primigenius</i>	9	Iacumin et al., 2010	24,300±200	Iacumin et al., 2010
Mammoth	<i>Mammuthus primigenius</i>	10	Iacumin et al., 2010	25,900±600	Iacumin et al., 2010
Mammoth	<i>Mammuthus primigenius</i>	11	Iacumin et al., 2010	27,400±800	Iacumin et al., 2010
Mammoth	<i>Mammuthus primigenius</i>	13	Iacumin et al., 2010	30,200±400	Iacumin et al., 2010
Mammoth	<i>Mammuthus primigenius</i>	14	Iacumin et al., 2010	31,500±650	Iacumin et al., 2010
Mammoth	<i>Mammuthus primigenius</i>	15	Iacumin et al., 2010	34,000±500	Iacumin et al., 2010
Mammoth	<i>Mammuthus primigenius</i>	23	Iacumin et al., 2010	>34,600	Iacumin et al., 2010
Mammoth	<i>Mammuthus primigenius</i>	2006/001	Szpak et al., 2010	41,300+900/-650	Debruyne et al., 2008
Mammoth	<i>Mammuthus primigenius</i>	BER11	Szpak et al., 2010		Debruyne et al., 2008
Mammoth	<i>Mammuthus primigenius</i>	BER12	Szpak et al., 2010	12,350±35	Debruyne et al., 2008
Mammoth	<i>Mammuthus primigenius</i>	BER13	Szpak et al., 2010		Debruyne et al., 2008
Mammoth	<i>Mammuthus primigenius</i>	BER16	Szpak et al., 2010	12,295±40	Debruyne et al., 2008
Mammoth	<i>Mammuthus primigenius</i>	BER20	Szpak et al., 2010		Debruyne et al., 2008
Mammoth	<i>Mammuthus primigenius</i>	BER28	Szpak et al., 2010	12,125±30	Debruyne et al., 2008
Mammoth	<i>Mammuthus primigenius</i>	BER5	Szpak et al., 2010		Debruyne et al., 2008
Mammoth	<i>Mammuthus primigenius</i>	BER7	Szpak et al., 2010		Debruyne et al., 2008
Mammoth	<i>Mammuthus primigenius</i>	BER9	Szpak et al., 2010		Debruyne et al., 2008
Mammoth	<i>Mammuthus primigenius</i>	SYU3	Szpak et al., 2010	>47,800	Debruyne et al., 2008

Mammoth	<i>Mammuthus primigenius</i>	<u>94200/94400</u>	Bocherens et al., 1996		~30,000	Bocherens et al., 1996
Mammoth	<i>Mammuthus primigenius</i>	94800	Bocherens et al., 1996		~15,000	Bocherens et al., 1996
Mammoth	<i>Mammuthus primigenius</i>	95000	Bocherens et al., 1996			
Mammoth	<i>Mammuthus primigenius</i>	95100	Bocherens et al., 1996			
Mammoth	<i>Mammuthus primigenius</i>	95300	Bocherens et al., 1996			
Mammoth	<i>Mammuthus primigenius</i>	<u>95500/95600</u>	Bocherens et al., 1996		~50,000	Bocherens et al., 1996
Mammoth	<i>Mammuthus primigenius</i>	102100	Bocherens et al., 1996			
Mammoth	<i>Mammuthus primigenius</i>	95800	Bocherens et al., 1996			
Muskox	<i>Ovibos moschatus</i>	102200	Bocherens et al., 1996			
Muskox	<i>Ovibos</i> sp.	PIN 3751-152	Raghavan et al., 2014	13270 ± 80		Raghavan et al., 2014
Muskox	<i>Ovibos moschatus</i>	ZIN 34770	Raghavan et al., 2014	24150 ± 110		Raghavan et al., 2014
Muskox	<i>Ovibos</i> cf. <i>pallantis</i>	PIN 3751-007	Raghavan et al., 2014	39000 ± 950		Raghavan et al., 2014
Muskox	<i>Ovibos</i> sp.	GIN 367/117	Raghavan et al., 2014	43400 ± 1700		Raghavan et al., 2014
Muskox	<i>Praeovibos</i> cf. <i>priscus</i>	PIN 3491-1	Raghavan et al., 2014	44500 ± 2100		Raghavan et al., 2014
Muskox	<i>Ovibos pallantis</i>	GIN 772-123	Raghavan et al., 2014	46400 ± 2700		Raghavan et al., 2014
Muskox	<i>Ovibos</i> sp.	PIN 3492-067	Raghavan et al., 2014	46700 ± 2500		Raghavan et al., 2014
Muskox	<i>Praeovibos</i> sp.	PIN 161-000	Raghavan et al., 2014	47000 ± 2600		Raghavan et al., 2014
Muskox	<i>Ovibos</i> sp.	GIN 367/105	Raghavan et al., 2014	47900 ± 3000		Raghavan et al., 2014
Muskox	<i>Ovibos moschatus</i>	ZIN 4546	Raghavan et al., 2014	48000 ± 3100		Raghavan et al., 2014
Muskox	<i>Praeovibos</i> cf. <i>recticornis</i>	PIN 199	Raghavan et al., 2014	48900 ± 3600		Raghavan et al., 2014
Muskox	<i>Ovibos moschatus</i>	ZIN 4565	Raghavan et al., 2014	49700 ± 3400		Raghavan et al., 2014
Muskox	<i>Ovibos moschatus</i>	ZIN 31264	Raghavan et al., 2014	51500 ± 1200		Raghavan et al., 2014
Muskox	<i>Ovibos moschatus</i>	ZIN 4563	Raghavan et al., 2014	56900 ± 0		Raghavan et al., 2014
Muskox	<i>Ovibos moschatus</i>	ZIN 4544	Raghavan et al., 2014	> 44700		Raghavan et al., 2014
Muskox	<i>Ovibos moschatus</i>	ZIN 5050	Raghavan et al., 2014	> 45400		Raghavan et al., 2014
Muskox	<i>Praeovibos</i> sp.	GIN 835-045	Raghavan et al., 2014	> 46000		Raghavan et al., 2014
Muskox	<i>Ovibos moschatus</i>	ZIN 4562	Raghavan et al., 2014	> 46000		Raghavan et al., 2014
Muskox	<i>Ovibos moschatus</i>	ZIN 35434	Raghavan et al., 2014	> 46600		Raghavan et al., 2014
		(6)				

Muskox	<i>Ovibos moschatus</i>	ZIN 64F-35434 (7)	Raghavan et al., 2014	> 47100	Raghavan et al., 2014
Muskox	<i>Ovibos moschatus</i>	ZIN 4227	Raghavan et al., 2014	> 48200	Raghavan et al., 2014
Muskox	<i>Praeovibos</i> sp.	PIN 2998-261	Raghavan et al., 2014	> 48300	Raghavan et al., 2014
Muskox	<i>Ovibos pallantis</i>	PIN 3491-892	Raghavan et al., 2014	> 48900	Raghavan et al., 2014
Muskox	<i>Ovibos moschatus</i>	ZIN 4226	Raghavan et al., 2014	> 49410	Raghavan et al., 2014
Muskox	<i>Ovibos</i> sp.	PIN 3915-34	Raghavan et al., 2014	> 49816	Raghavan et al., 2014
Muskox	<i>Ovibos</i> sp.	PIN 3915-144	Raghavan et al., 2014	> 49821	Raghavan et al., 2014
Muskox	<i>Ovibos</i> sp.	PIN 3915-233	Raghavan et al., 2014	> 49821	Raghavan et al., 2014
Muskox	<i>Ovibos moschatus</i>	ZIN 35434 (10)	Raghavan et al., 2014	> 49886	Raghavan et al., 2014
Muskox	<i>Ovibos moschatus</i>	ZIN 35434 (13)	Raghavan et al., 2014	> 50130	Raghavan et al., 2014
Muskox	<i>Ovibos moschatus</i>	ZIN 35434 (4)	Raghavan et al., 2014	> 50220	Raghavan et al., 2014
Muskox	<i>Ovibos moschatus</i>	ZIN 4557	Raghavan et al., 2014	> 50478	Raghavan et al., 2014
Woolly Rhinoceros	<i>Coelodonta antiquitatis</i>	96000	Bocherens et al., 1996		~20,000 Bocherens et al., 1996

Appendix AA continues below.

Sample Number	Latitude	Longitude	Site	Tissue	Tissue Type	$\delta^{13}\text{C}_{\text{Coll}}$	$\delta^{15}\text{N}_{\text{Coll}}$	% Yield	%C	%N	C/N
17/1			Rebrovo	B		-21.9	6.0	21.4	45.4	15.4	3.4
25	71.79°N	129.40°E	mouth of the delta of the Lena River	B	radius	-20.7	7.4	16.5	42.2	15.8	3.1
26	71.79°N	129.40°E	mouth of the delta of the Lena River	B		-20.1	5.2	17.7	41.3	15.7	3.1
101900				B		-19.3	6.3	18.5	41.9	15.5	3.2
18/1			Kondrat'evo	B		-20.4	6.7	18.9	41.8	13.9	3.5
22	73.32°N	141.39°E	Bol'shoy Lyakhovshy Island	B	radius	-21.6	4.2	18.1	43.7	15.2	3.3
24	73.32°N	141.39°E	Bol'shoy Lyakhovshy Island	B	femur	-20.8	4.4	18.2	42.4	16.2	3.0
96300			Maksounuocha river (northern Yakutia)	B	mandible	-21.1	4.3	16.9	38.5	14.3	3.1
10200				B		-22.7	6.8	30.4	42.3	15.2	3.2

8/1			Yakutia	T		-21.4	10.1	22.5	42.0	15.3	3.2
8/2			Yakutia	T		-21.5	10.5	20.3	44.9	15.0	3.5
16/1			Bolshoy Lyahovsky Is.	T		-22.4	10.3	27.5	46.2	15.5	3.5
16/2			Bolshoy Lyahovsky Is.	B		-21.6	9.8	17.6	43.5	15.4	3.3
17/2			Rebrovo	B		-21.4	9.3	6.2	40.2	14.7	3.2
19/20			Sviatoy site 1	B		-20.9	10.0	9.5	40.1	14.2	3.3
19/35			Sviatoy site 1	B		-21.3	11.1	4.6	41.3	15.1	3.2
19/37			Sviatoy site 1	B		-21.0	11.7	11.1	42.1	15.3	3.2
19/42			Sviatoy site 1	B		-21.2	10.6	9.0	41.6	14.7	3.3
19/52			Sviatoy site 1	B		-22.1	9.1	18.8	41.8	14.8	3.3
19/58			Sviatoy site 1	B		-21.6	11.2	19.2	44.2	15.6	3.3
19/59			Sviatoy site 1	B		-21.6	10.2	14.8	41.9	15.3	3.2
19/75			Sviatoy site 1	B		-21.0	12.3	11.4	42.8	15.6	3.2
19/92			Sviatoy site 1	B		-21.5	12.7	13.3	43.6	15.9	3.2
21			Mamontova Gora	B		-20.1	10.2	17.3	42.1	14.9	3.3
22			Turanha R.	B		-21.1	10.4	19.1	43.5	15.4	3.3
1	71.79°N	129.40°E	mouth of the delta of the Lena River	B	ulna	-21.6	5.7	22.4	41.3	16.1	3.0
8	71.79°N	129.40°E	mouth of the delta of the Lena River	B	pelvis	-21.3	8.3	19.8	41.8	14.8	3.3
12	71.79°N	129.40°E	mouth of the delta of the Lena River	B	ulna	-21.6	9.0	14.4	40.7	15.7	3.0
A	71.79°N	129.40°E	mouth of the delta of the Lena River			-22.6	9.2	17.7	39.2	15.9	2.9
16	71.79°N	129.40°E	mouth of the delta of the Lena River	B	vertebra	-21.9	8.8	16.8	42.7	15.5	3.2
17	71.79°N	129.40°E	mouth of the delta of the Lena River	B	femur	-22.5	9.4	10.2	41.6	15.8	3.1
18	71.79°N	129.40°E	mouth of the delta of the Lena River	B	humerus	-22.3	9.6	16.8	42.2	16.0	3.1
19	71.79°N	129.40°E	mouth of the delta of the Lena River	B	scapula	-23.2	8.7	15.4	40.7	14.6	3.2
20	71.79°N	129.40°E	mouth of the delta of the Lena River	T	tusk	-21.7	7.6	14.1	40.0	15.6	3.0
21	71.79°N	129.40°E	mouth of the delta of the Lena River	D/RD/C	molar	-22.3	9.3	16.1	42.6	16.0	3.1
3	73.32°N	141.39°E	Bol'shoy Lyakhovshy Island	B	pelvis	-22.7	5.6	22.2	39.9	15.4	3.0
7	73.32°N	141.39°E	Bol'shoy Lyakhovshy Island	B	metacarpal	-21.7	8.3	20.7	40.7	15.2	3.1

9	73.32°N	141.39°E	Bol'shoy Lyakhovshy Island	B	vertebra	-22.3	7.3	21.8	42.6	16.1	3.1
10	73.32°N	141.39°E	Bol'shoy Lyakhovshy Island			-22.5	8.9	16.1	39.0	14.8	3.1
11	73.32°N	141.39°E	Bol'shoy Lyakhovshy Island	B	limb bone	-21.9	9.1	14.5	38.6	15.8	2.8
13	73.32°N	141.39°E	Bol'shoy Lyakhovshy Island	B	cranium	-22.1	9.1	5.8	41.8	15.3	3.2
14	73.32°N	141.39°E	Bol'shoy Lyakhovshy Island	B	metatarsal	-21.7	8.9	13.8	38.3	14.9	3.0
15	73.32°N	141.39°E	Bol'shoy Lyakhovshy Island	B	limb bone	-22.0	8.6	16.1	39.6	15.2	3.0
23	73.32°N	141.39°E	Bol'shoy Lyakhovshy Island			-22.2	9.1	10.7	42.1	15.6	3.1
2006/001	63°30'N	142°45'E	Oymyakon	B		-21.7	8.1	23.9	36.7	13.6	3.1
BER11	70°33'N	149°03'E	Berelekh	B		-21.9	9.5	20.4	39.8	14.6	3.2
BER12	70°33'N	149°03'E	Berelekh	B		-22.2	9.4	18.2	37.8	13.5	3.3
BER13	70°33'N	149°03'E	Berelekh	B		-22.0	9.9	26.4	38.1	13.6	3.3
BER16	70°33'N	149°03'E	Berelekh	B		-22.0	9.4	23.4	37.8	13.2	3.3
BER20	70°33'N	149°03'E	Berelekh	B		-22.1	9.1	23.0	36.4	12.9	3.3
BER28	70°33'N	149°03'E	Berelekh	B		-21.5	9.2	11.9	43.7	15.0	3.4
BER5	70°33'N	149°03'E	Berelekh	B		-21.9	8.9	24.4	40.5	14.8	3.2
BER7	70°33'N	149°03'E	Berelekh	B		-22.4	8.9	16.2	38.5	13.4	3.4
BER9	70°33'N	149°03'E	Berelekh	B		-22.2	9.0	19.0	33.9	12.0	3.3
SYU3	71°20'N	151°E	Sanga-Yuriakh	B		-22.6	10.9	18.6	35.9	12.6	3.3
<u>94200/94400</u>			Kien-Urech river, Omoloy river basin (Northern Yakutia)	B	<u>humerus/radius</u>	<u>-22.6</u>	<u>9.1</u>	<u>17.7</u>	<u>41.5</u>	<u>15.4</u>	<u>3.2</u>
94800			Singnigese-Urech river (Central Yakutia)	B	scapula	-20.7	8.1	11.2	37.5	14.6	3.0
95000			East of Tchokourdakh, Indiguizka river basin	B	vertebra	-21.8	10.8	16.8	41.9	15.3	3.2
95100			Kien-Ajaan river, Indigirka river basin (northern Yakutia)	B	skull	-22.7	8.8	21.8	41.2	15.6	3.1
95300			East of Tchokourdakh, Indiguizka river basin	B	pelvis	-21.5	10.4	17.1	43.3	15.6	3.2
<u>95500/95600</u>			Bolshoj Ljachovskij Island	D/RD/C	<u>molar/skull</u>	<u>-22.3</u>	<u>9.7</u>	<u>21.0</u>	<u>44.5</u>	<u>16.0</u>	<u>3.3</u>
102100				B	bone	-21.6	11.4	22.0	42.1	15.5	3.2
95800				B	scapula	-21.3	7.2	18.4	39.6	15.1	3.1
102200				B		-19.9	5.8	27.6	42.2	15.5	3.2
PIN 3751-152			Yana Lowland	B		-20.5	7.4	4.1	43.6	16.0	3.2
ZIN 34770			Bolshoy Lyakhovsky Island	B		-20.7	8.2	18.4	44.9		3.3
PIN 3751-007			Yana Lowland	B		-20.2	6.5	5.6	43.1	15.9	3.2
GIN 367/117			Bol. Lyakhovsky Island	B		-21.4	8.0	6.0	44.9	16.4	3.2
PIN 3491-1			Kolyma Lowland	B		-20.0	5.2	8.9	44.0	16.1	3.2

GIN 772-123	Kolyma Lowland	B	-20.7	5.2	6.6	44.7	16.4	3.2
PIN 3492-067	Kolyma Lowland	B	-21.8	7.8	6.4	44.1	16.1	3.2
PIN 161-000	Indigirka Lowland	B	-19.5	9.3	5.1	43.5	16.0	3.2
GIN 367/105	Bol. Lyakhovsky Island	B	-20.2	8.8	8.8	43.6	15.7	3.3
ZIN 4546	Bolshoy Lyakhovsky Island	B	-20.8	6.7	7.1	44.7	16.5	3.2
PIN 199	Aldan	B	-19.8	7.3	6.0	44.7	16.5	3.2
ZIN 4565	Bolshoy Lyakhovsky Island	B	-21.2	5.2	7.5	44.4	16.3	3.2
ZIN 31264	Novaya Sibir' Island	B	-20.8	8.9	7.7	43.5		3.2
ZIN 4563	Bolshoy Lyakhovsky Island	B	-20.3	7.0	15.7	47.3		3.4
ZIN 4544	Bolshoy Lyakhovsky Island	B	-21.2	7.5	6.5	44.9	16.6	3.2
ZIN 5050	Bolshoy Lyakhovsky Island	B	-20.4	5.6	4.0	44.2	16.1	3.2
GIN 835-045	Kolyma Lowland	B	-19.6	5.2	6.0	45.4	16.5	3.2
ZIN 4562	Bolshoy Lyakhovsky Island	B	-21.0	6.7	4.2	42.8	15.9	3.2
ZIN 35434 (6)	Dm. Laptev Strait coast	B	-20.6	4.4	9.5	45.3	16.6	3.2
ZIN 64F- 35434 (7)	Dm. Laptev Strait coast	B	-21.7	7.5	5.8	43.5	16.0	3.2
ZIN 4227	Bolshoy Lyakhovsky Island	B	-21.4	7.2	9.7	45.0	16.5	3.2
PIN 2998-261	Kolyma Lowland	B	-20.4	4.4	2.5	44.2	16.0	3.2
PIN 3491-892	Kolyma Lowland	B	-21.2	6.9	9.2	44.8	16.2	3.2
ZIN 4226	Bolshoy Lyakhovsky Island	B	-21.5	4.1	5.5	45.3	16.6	3.2
PIN 3915-34	Indigirka Lowland	B	-20.9	8.7	4.8	44.1	16.2	3.2
PIN 3915-144	Indigirka Lowland	B	-21.2	6.2	5.7	46.5	16.4	3.3
PIN 3915-233	Indigirka Lowland	B	-20.1	4.3	4.9	44.7	16.4	3.2
ZIN 35434 (10)	Dm. Laptev Strait coast	B	-21.4	4.9	5.2	44.4	16.2	3.2
ZIN 35434 (13)	Dm. Laptev Strait coast	B	-20.0	6.7	5.2	42.8	15.7	3.2
ZIN 35434 (4)	Dm. Laptev Strait coast	B	-20.7	7.5	8.9	44.5	16.4	3.2
ZIN 4557	Bolshoy Lyakhovsky Island	B	-20.9	8.0	7.6	43.6	16.2	3.2
96000	Tchouraptcha (central Yakutia)	B	-20.6	8.4	13.6	40.5	15.0	3.2

*In Western Beringia, this would have been a reindeer, rather than a caribou. However, consistent naming of species is used in the thesis.

**These are approximate dates based on the cultural layer.

Average of repeat measurements on different tissues from the same specimen are underlined

Tissue: B = Bone; RD = Root dentin; C = Cementum; D = Crown dentin; T= Tusk dentin

References:

Bocherens, H., Pacaud, G., Lazarev, P.A., Mariotti, A., 1996. Stable isotope abundances (^{13}C , ^{15}N) in collagen and soft tissues from

Pleistocene mammals from Yakutia: implications for the palaeobiology of the Mammoth Steppe. *Palaeogeogr. Palaeoclimatol. Palaeoecol.* 126, 31–44.

- Debruyne, R., Chu, G., King, C.E., Bos, K., Kuch, M., Schwarz, C., Szpak, P., Gröcke, D.R., Matheus, P., Zazula, G., Guthrie, D., Froese, D., Buigues, B., de Marliave, C., Flemming, C., Poinar, D., Fisher, D., Southon, J., Tikhonov, A.N., MacPhee, R.D.E., Poinar, H.N., 2008. Out of America: ancient DNA evidence for a new world origin of late Quaternary woolly mammoths. *Curr. Biol.* 18, 1320–6. doi:10.1016/j.cub.2008.07.061
- Iacumin, P., Nikolaev, V., Ramigni, M., 2000. C and N stable isotope measurements on Eurasian fossil mammals, 40 000 to 10 000 years BP: herbivore physiologies and palaeoenvironmental reconstruction. *Palaeogeogr. Palaeoclimatol. Palaeoecol.* 163, 33–47.
- Iacumin, P., Matteo, A. Di, Nikolaev, V., Kuznetsova, T., 2010. Climate information from C, N and O stable isotope analyses of mammoth bones from northern Siberia. *Quat. Int.* 212, 206–212.
- Raghavan, M., Espregueira Themudo, G., Smith, C.I., Zazula, G., Campos, P.F., 2014. Musk ox (*Ovibos moschatus*) of the mammoth steppe: tracing palaeodietary and palaeoenvironmental changes over the last 50,000 years using carbon and nitrogen isotopic analysis. *Quat. Sci. Rev.* 102, 192–201. doi:10.1016/j.quascirev.2014.08.001
- Szpak, P., Gröcke, D.R., Debruyne, R., MacPhee, R.D.E., Guthrie, R.D., Froese, D., Zazula, G.D., Patterson, W.P., Poinar, H.N., 2010. Regional differences in bone collagen $\delta^{13}\text{C}$ and $\delta^{15}\text{N}$ of Pleistocene mammoths: implications for paleoecology of the mammoth steppe. *Palaeogeogr. Palaeoclimatol. Palaeoecol.* 286, 88–96. doi:10.1016/j.palaeo.2009.12.009

Appendix BB Results of the mathematical analysis on groups for each site and time period, with the time periods defined using binning approach A.

	SEA	SEA _c	TA	$\delta^{13}\text{C}$	$\delta^{15}\text{N}$	No.	First	Second	SEA _{bprop}	SEA _c overlap(1,2)	TA overlap(1,2)	SEA _c overlap(2,1)	TA overlap(2,1)
Alberta Pre-LGM													
Bison	1.9	2.2	3.3	-19.5	6.7	10	Bison	Caribou	0.0	0.0	0.0	0.0	0.0
Caribou	0.1	0.2	0.2	-18.7	4.8	7	Bison	Horse	0.2	0.0	0.2	0.0	0.3
Horse	1.0	1.1	2.4	-20.3	7.6	17	Bison	Mammoth	0.9	0.0	0.1	0.0	0.1
Mammoth	3.2	4.0	4.2	-20.7	8.1	6	Caribou	Horse	0.9	0.0	0.0	0.0	0.0
							Caribou	Mammoth	1.0	0.0	0.0	0.0	0.0
							Horse	Mammoth	1.0	0.8	0.6	0.2	0.4
Alberta Post-LGM													
Bison	0.5	0.6	0.9	-19.5	2.0	9	Bison	Horse	0.6	0.0	0.0	0.0	0.0
Horse	0.7	0.9	1.3	-20.5	0.7	9							
Fairbanks Pre-LGM													
Caribou	0.6	0.8	0.6	-19.4	3.1	5	Caribou	Horse	0.4	0.0	0.0	0.0	0.0
Horse	1.2	1.3	2.1	-21.2	2.7	10	Caribou	Mammoth	0.8	0.0	0.0	0.0	0.0
Mammoth	0.9	1.3	1.1	-20.8	6.7	5	Caribou	Mastodon	0.2	0.0	0.0	0.0	0.0
Mastodon	0.1	0.1	0.1	-21.0	4.4	5	Horse	Mammoth	0.9	0.0	0.0	0.0	0.0
							Horse	Mastodon	0.3	0.0	0.0	0.0	0.3
							Mammoth	Mastodon	0.1	0.0	0.0	0.0	0.0
Fairbanks Post-LGM													
Caribou	1.6	2.4	1.2	-19.5	3.5	4	Caribou	Horse	0.2	0.0	0.0	0.0	0.0
Horse	0.8	0.9	1.2	-21.0	3.5	8							
Klondike Pre-LGM													
Mammoth	0.5	0.5	1.8	-20.6	7.1	22	Mammoth	Mastodon	1.0	0.0	0.2	0.0	0.1
Mastodon	1.6	1.8	3.7	-20.6	4.4	12	Mammoth	Muskox	1.0	0.0	0.0	0.0	0.0
Muskox	2.1	2.4	4.2	-19.6	5.8	9	Mastodon	Muskox	0.8	0.0	0.1	0.0	0.1
Northwest Europe Pre-LGM													
Bison	0.9	1.0	2.5	-20.2	5.6	18	Bison	Caribou	0.9	0.0	0.2	0.0	0.1
Caribou	1.9	2.0	8.8	-19.2	4.2	44	Bison	Horse	1.0	0.8	1.0	0.3	0.2
Horse	3.2	3.3	16.0	-20.7	5.7	84	Bison	Mammoth	0.5	0.0	0.0	0.0	0.0

Mammoth	0.9	1.0	1.6	-21.4	8.0	10	Caribou	Horse	1.0	0.0	0.4	0.0	0.2
							Caribou	Mammoth	0.2	0.0	0.0	0.0	0.0
							Horse	Mammoth	0.0	0.0	0.1	0.0	0.7
Northwest Europe LGM													
Caribou	0.9	1.0	3.2	-19.3	3.9	23	Caribou	Horse	0.9	0.0	0.0	0.0	0.0
Horse	0.6	0.7	1.0	-21.1	2.8	9							
Northwest Europe Post-LGM													
Bison	0.1	0.1	0.0	-20.0	2.3	3	Bison	Caribou	0.1	0.3	1.0	0.0	0.0
Caribou	0.9	0.9	4.4	-19.6	2.7	93	Bison	Elk	0.4	0.5	0.9	0.0	0.0
Elk	1.5	1.6	5.7	-20.4	2.7	32	Bison	Horse	0.4	0.0	1.0	0.0	0.0
Horse	1.7	1.7	9.9	-20.8	2.2	88	Caribou	Elk	1.0	0.0	0.2	0.0	0.1
							Caribou	Horse	1.0	0.0	0.4	0.0	0.2
							Elk	Horse	0.5	0.5	0.9	0.4	0.5
Northwest Europe Holocene													
Elk	3.1	3.4	6.1	-22.2	4.5	12	Elk	Horse	0.8	0.8	0.3	0.2	0.5
Horse	5.8	11.6	3.2	-22.2	5.8	3							
North Slope Pre- LGM													
Bison	2.0	2.0	11.2	-20.1	4.6	58	Bison	Caribou	1.0	0.0	0.2	0.0	0.2
Caribou	3.6	3.7	14.0	-18.3	3.3	35	Bison	Horse	0.4	0.0	0.3	0.0	0.3
Horse	1.9	1.9	10.1	-21.0	6.1	52	Bison	Mammoth	0.1	0.0	0.0	0.0	0.0
Mammoth	1.6	1.6	7.8	-21.4	7.7	49	Bison	Mastodon	0.0	0.0	0.0	0.0	0.0
Mastodon	0.3	0.3	0.6	-20.9	3.1	12	Bison	Muskox	1.0	0.4	0.6	0.3	0.5
Muskox	3.1	3.1	12.0	-19.8	6.3	51	Caribou	Horse	0.0	0.0	0.0	0.0	0.0
							Caribou	Mammoth	0.0	0.0	0.0	0.0	0.0
							Caribou	Mastodon	0.0	0.0	0.0	0.0	0.0
							Caribou	Muskox	0.3	0.0	0.4	0.0	0.5
							Horse	Mammoth	0.1	0.1	0.5	0.2	0.6
							Horse	Mastodon	0.0	0.0	0.0	0.0	0.8
							Horse	Muskox	1.0	0.0	0.3	0.0	0.2
							Mammoth	Mastodon	0.0	0.0	0.0	0.0	0.0
							Mammoth	Muskox	1.0	0.0	0.0	0.0	0.0
							Mastodon	Muskox	1.0	0.0	0.0	0.0	0.0

North Slope LGM														
Bison	1.0	2.0	0.5	-20.1	4.9	3	Bison	Horse	0.0	0.0	0.2	0.1	0.1	
Horse	0.6	0.7	1.3	-20.6	5.8	12								
North Slope Post-LGM														
Bison	0.5	0.5	0.5	-20.3	3.0	8	Bison	Caribou	1.0	0.0	0.0	0.0	0.0	
Caribou	2.1	2.7	2.2	-19.0	5.1	5	Bison	Horse	0.9	0.0	0.0	0.0	0.0	
Horse	1.4	1.4	4.4	-20.8	5.9	19	Caribou	Horse	0.0	0.0	0.0	0.0	0.0	
North Slope Holocene														
Caribou	2.2	2.4	5.6	-18.5	2.2	13	Caribou	Moose	1.0	0.0	0.0	0.0	0.0	
Moose	3.9	4.6	6.9	-20.5	1.8	8	Caribou	Muskox	0.7	0.0	0.0	0.0	0.0	
Muskox	2.6	3.5	2.6	-19.6	4.9	5	Moose	Muskox	0.2	0.0	0.0	0.0	0.0	
Old Crow Pre-LGM														
Mammoth	1.2	1.5	1.5	-21.4	9.5	6	Mammoth	Mastodon	0.4	0.0	0.0	0.0	0.0	
Mastodon	1.1	1.6	0.8	-20.1	3.1	4								
Selawik Pre-LGM														
Horse	0.3	0.5	0.1	-21.1	3.5	3	Horse	Mammoth	0.3	0.0	0.0	0.0	0.0	
Mammoth	1.0	2.0	0.6	-21.8	7.4	3								
Taymyr Peninsula Pre-LGM														
Mammoth	1.5	1.6	3.2	-21.7	9.1	15	Mammoth	Muskox	0.3	0.0	0.0	0.0	0.0	
Muskox	1.2	1.3	2.9	-20.7	5.5	14								
Taymyr Peninsula Post-LGM														
Mammoth	1.2	1.8	0.9	-21.7	9.6	4	Mammoth	Muskox	0.3	0.0	0.0	0.0	0.0	
Muskox	2.0	2.2	5.3	-20.2	5.5	15								
Yakutia Pre-LGM														
Bison	3.2	6.3	1.7	-20.9	6.2	3	Bison	Mammoth	0.0	0.0	0.0	0.0	0.0	
Mammoth	1.2	1.2	4.4	-22.2	9.2	23	Bison	Muskox	0.4	0.4	1.0	2.2	0.4	
Muskox	2.9	3.0	9.4	-20.7	6.7	30	Mammoth	Muskox	1.0	0.0	0.0	0.0	0.0	

Legend

SEA

Standard ellipse area

SEA_c

Standard ellipse area corrected for small sample size

TA	Area of the total convex hull
$\delta^{13}\text{C}_{\text{Coll}}$	Average $\delta^{13}\text{C}$ value
$\delta^{15}\text{N}_{\text{Coll}}$	Average $\delta^{15}\text{N}$ value
No. of Samples	Number of samples
First	The group used as the 'first' group
Second	The group used as the 'second' group
$\text{SEA}_{\text{bprop}}$	The proportion of sites from the second group that are estimated to be larger than sites from the first group, based on Bayesian analysis.
$\text{SEA}_c \text{ overlap}_{(1,2)}$	The proportion of the SEA_c from the first group that overlaps with the second group.
$\text{TA overlap}_{(1,2)}$	The proportion of the TA from the first group that overlaps with the second group.
$\text{SEA}_c \text{ overlap}_{(2,1)}$	The proportion of the SEA_c from the second group that overlaps with the second group.
$\text{TA overlap}_{(2,1)}$	The proportion of the TA from the second group that overlaps with the first group.

Appendix CC Results of the mathematical analysis on groups for each site and time period, with the time periods defined using binning approach B.

	SEA	SEA _c	TA	$\delta^{13}\text{C}$	$\delta^{15}\text{N}$	No.	First	Second	SEA _{bropp}	SEA _c overlap(1,2)	TA overlap(1,2)	SEA _c overlap(2,1)	TA overlap(2,1)
Alberta Pre-LGM													
Bison	1.9	2.2	3.3	-19.5	6.7	10	Bison	Caribou	0.0	0.0	0.0	0.0	0.0
Caribou	0.1	0.2	0.2	-18.7	4.8	7	Bison	Horse	0.2	0.0	0.2	0.0	0.3
Horse	1.0	1.1	2.4	-20.3	7.6	17	Bison	Mammoth	0.9	0.0	0.1	0.0	0.1
Mammoth	3.2	4.0	4.2	-20.7	8.1	6	Caribou	Horse	0.9	0.0	0.0	0.0	0.0
							Caribou	Mammoth	1.0	0.0	0.0	0.0	0.0
							Horse	Mammoth	1.0	0.8	0.6	0.2	0.4
Alberta Post-LGM													
Bison	0.5	0.6	0.9	-19.5	2.0	9	Bison	Horse	0.6	0.0	0.0	0.0	0.0
Horse	0.7	0.9	1.3	-20.5	0.7	9							
Fairbanks Pre-LGM													
Caribou	1.0	1.3	1.2	-19.5	3.2	6	Caribou	Horse	0.2	0.0	0.0	0.0	0.0
Horse	1.1	1.2	3.4	-21.2	3.5	22	Caribou	Mammoth	0.8	0.0	0.0	0.0	0.0
Mammoth	0.9	1.3	1.1	-20.8	6.7	5	Caribou	Mastodon	0.2	0.0	0.0	0.0	0.0
Mastodon	0.1	0.1	0.1	-21.0	4.4	5	Horse	Mammoth	1.0	0.0	0.0	0.0	0.0
							Horse	Mastodon	0.4	0.1	0.0	0.7	1.0
							Mammoth	Mastodon	0.1	0.0	0.0	0.0	0.0
Fairbanks LGM													
Caribou	2.1	4.3	1.2	-19.5	3.5	3	Caribou	Horse	0.2	0.0	0.0	0.0	0.0
Horse	0.2	0.4	0.1	-21.1	3.0	3							
Klondike Pre-LGM													
Mammoth	0.7	0.7	2.5	-20.7	7.3	24	Mammoth	Mastodon	1.0	0.0	0.1	0.0	0.1
Mastodon	1.6	1.8	3.7	-20.6	4.4	12	Mammoth	Muskox	1.0	0.0	0.0	0.0	0.0
Muskox	2.1	2.4	4.2	-19.6	5.8	9	Mastodon	Muskox	0.8	0.0	0.1	0.0	0.1
Northwest Europe Pre-LGM													
Bison	0.9	1.0	2.5	-20.2	5.6	18	Bison	Caribou	0.8	0.0	0.2	0.0	0.1
Caribou	1.8	1.8	8.8	-19.2	4.3	50	Bison	Horse	1.0	0.8	1.0	0.2	0.1
Horse	3.4	3.4	17.5	-20.7	5.7	85	Bison	Mammoth	0.5	0.0	0.0	0.0	0.0

Mammoth	0.9	1.0	1.6	-21.4	8.0	10	Caribou	Horse	1.0	0.0	0.4	0.0	0.2
							Caribou	Mammoth	0.3	0.0	0.0	0.0	0.0
							Horse	Mammoth	0.0	0.0	0.1	0.0	0.7
Northwest Europe LGM													
Caribou	0.8	0.8	3.0	-19.3	3.6	27	Caribou	Horse	0.9	0.0	0.0	0.0	0.0
Horse	0.7	0.8	1.7	-21.0	2.9	10							
Northwest Europe Post-LGM													
Bison	0.1	0.1	0.0	-20.0	2.3	3	Bison	Caribou	0.1	0.3	1.0	0.1	0.0
Caribou	0.8	0.9	4.2	-19.6	2.6	80	Bison	Elk	0.4	0.5	0.9	0.0	0.0
Elk	1.5	1.6	5.7	-20.4	2.7	32	Bison	Horse	0.5	0.0	1.0	0.0	0.0
Horse	1.7	1.7	9.9	-20.8	2.2	86	Caribou	Elk	1.0	0.0	0.2	0.0	0.1
							Caribou	Horse	1.0	0.0	0.4	0.0	0.2
							Elk	Horse	0.6	0.5	0.9	0.4	0.5
Northwest Europe Holocene													
Elk	3.1	3.4	6.1	-22.2	4.5	12	Elk	Horse	0.8	0.8	0.3	0.2	0.5
Horse	5.8	11.6	3.2	-22.2	5.8	3							
North Slope Pre-LGM													
Bison	2.0	2.0	11.2	-20.1	4.6	60	Bison	Caribou	1.0	0.0	0.2	0.0	0.2
Caribou	3.7	3.8	14.0	-18.3	3.4	36	Bison	Horse	0.3	0.0	0.3	0.0	0.3
Horse	1.8	1.8	10.1	-20.9	6.0	64	Bison	Mammoth	0.1	0.0	0.0	0.0	0.0
Mammoth	1.6	1.6	8.1	-21.4	7.8	50	Bison	Mastodon	0.0	0.0	0.0	0.0	0.0
Mastodon	0.3	0.3	0.6	-20.9	3.1	12	Bison	Muskox	1.0	0.4	0.6	0.3	0.5
Muskox	3.1	3.1	12.0	-19.8	6.4	52	Caribou	Horse	0.0	0.0	0.0	0.0	0.0
							Caribou	Mammoth	0.0	0.0	0.0	0.0	0.0
							Caribou	Mastodon	0.0	0.0	0.0	0.0	0.0
							Caribou	Muskox	0.2	0.0	0.4	0.0	0.5
							Horse	Mammoth	0.3	0.1	0.5	0.1	0.6
							Horse	Mastodon	0.0	0.0	0.0	0.0	0.8
							Horse	Muskox	1.0	0.0	0.3	0.0	0.2
							Mammoth	Mastodon	0.0	0.0	0.0	0.0	0.0
							Mammoth	Muskox	1.0	0.0	0.0	0.0	0.0
							Mastodon	Muskox	1.0	0.0	0.0	0.0	0.0
North Slope LGM													
Caribou	0.9	1.8	0.5	-19.0	7.6	3	Caribou	Horse	0.1	0.0	0.0	0.0	0.0
Horse	0.8	0.9	1.1	-20.8	6.2	6							

North Slope Post-LGM														
Bison	0.5	0.6	0.5	-20.3	3.0	7	Bison	Caribou	0.7	0.0	0.0	0.0	0.0	0.0
Caribou	0.1	0.2	0.1	-19.0	3.0	3	Bison	Horse	0.9	0.0	0.0	0.0	0.0	0.0
Horse	1.6	1.8	4.4	-20.8	5.7	13	Caribou	Horse	0.7	0.0	0.0	0.0	0.0	0.0
North Slope Holocene														
Caribou	2.2	2.4	5.6	-18.5	2.2	13	Caribou	Moose	1.0	0.0	0.0	0.0	0.0	0.0
Moose	3.9	4.6	6.9	-20.5	1.8	8	Caribou	Muskox	0.7	0.0	0.0	0.0	0.0	0.0
Muskox	2.6	3.5	2.6	-19.6	4.9	5	Moose	Muskox	0.2	0.0	0.0	0.0	0.0	0.0
Old Crow Pre-LGM														
Mammoth	1.2	1.5	1.5	-21.4	9.5	6	Mammoth	Mastodon	0.4	0.0	0.0	0.0	0.0	0.0
Mastodon	1.1	1.6	0.8	-20.1	3.1	4								
Selawik Pre-LGM														
Horse	0.3	0.5	0.1	-21.1	3.5	3	Horse	Mammoth	0.3	0.0	0.0	0.0	0.0	0.0
Mammoth	1.0	2.0	0.6	-21.8	7.4	3								
Taymyr Pre-LGM														
Mammoth	1.5	1.6	3.2	-21.7	9.1	15	Mammoth	Muskox	0.1	0.0	0.0	0.0	0.0	0.0
Muskox	1.0	1.1	3.6	-20.6	5.6	27								
Taymyr Post-LGM														
Mammoth	1.5	3.0	0.8	-22.0	9.3	3	Mammoth	Muskox	0.4	0.0	0.0	0.0	0.0	0.0
Muskox	2.5	2.7	5.0	-20.3	5.3	11								
Yakutia Pre-LGM														
Bison	3.2	6.3	1.7	-20.9	6.2	3	Bison	Mammoth	0.0	0.0	0.0	0.0	0.0	0.0
Mammoth	1.2	1.3	5.0	-22.1	9.1	25	Bison	Muskox	0.4	0.4	1.0	0.9	0.2	
Muskox	2.9	3.0	9.4	-20.7	6.7	30	Mammoth	Muskox	1.0	0.0	0.0	0.0	0.0	

Legend is the same as the legend in Appendix BB

Appendix DD Results of the mathematical analysis on groups for each species and time period, with the time periods defined using binning approach A.

	SEA	SEA _c	TA	$\delta^{13}\text{C}$	$\delta^{15}\text{N}$	No.	First	Second	SEA _{bprop}	SEA _c overlap(1,2)	TA overlap(1,2)	SEA _c overlap(2,1)	TA overlap(2,1)
Bison Pre-LGM													
Alberta	1.9	2.2	3.3	-19.5	6.7	10	Alberta	North Slope	0.4	0.0	0.3	0.0	0.1
North Slope	2.0	2.0	11.2	-20.1	4.6	58	Alberta	Northwest Europe	0.1	0.0	0.2	0.1	0.3
Northwest Europe	0.9	1.0	2.5	-20.2	5.6	18	Alberta	Yakutia	0.8	0.2	0.0	0.1	0.0
Yakutia	3.2	6.3	1.7	-20.9	6.2	3	North Slope	Northwest Europe	0.1	0.2	0.2	0.5	0.9
							North Slope	Yakutia	0.8	0.4	0.1	0.1	0.3
							Northwest Europe	Yakutia	1.0	1.0	0.1	0.2	0.2
Caribou Pre-LGM													
Alberta	0.1	0.2	0.2	-18.7	4.8	7	Alberta	Fairbanks	0.9	0.0	0.0	0.0	0.0
Fairbanks	0.6	0.8	0.6	-19.4	3.1	5	Alberta	North Slope	1.0	1.0	1.0	0.0	0.0
North Slope	3.6	3.7	14.0	-18.3	3.3	35	Alberta	Northwest Europe	1.0	0.0	1.0	0.0	0.0
Northwest Europe	1.9	2.0	8.8	-19.2	4.2	44	Fairbanks	North Slope	0.8	0.0	0.9	0.0	0.0
							Fairbanks	Northwest Europe	0.4	0.5	1.0	0.2	0.1
							North Slope	Northwest Europe	0.0	0.1	0.5	0.2	0.8
Horse Pre-LGM													
Alberta	1.0	1.1	2.4	-20.3	7.6	17	Alberta	Fairbanks	0.7	0.0	0.0	0.0	0.0
Fairbanks	1.2	1.3	2.1	-21.2	2.7	10	Alberta	North Slope	0.8	0.0	0.5	0.0	0.1
North Slope	1.9	1.9	10.1	-21.0	6.1	52	Alberta	Northwest Europe	1.0	0.3	1.0	0.1	0.1
Northwest Europe	3.2	3.3	16.0	-20.7	5.7	84	Alberta	Selawik	1.0	0.0	0.0	0.0	0.0
Selawik	0.3	0.5	0.1	-21.1	3.5	3	Fairbanks	North Slope	0.5	0.0	0.4	0.0	0.1
							Fairbanks	Northwest Europe	0.9	0.0	0.5	0.0	0.1
							Fairbanks	Selawik	0.9	0.2	0.0	0.4	0.6
							North Slope	Northwest Europe	1.0	0.8	0.9	0.4	0.6
							North Slope	Selawik	0.9	0.1	0.0	0.3	0.8
							Northwest Europe	Selawik	0.7	0.0	0.0	0.3	0.8

**Mammoth
Pre-LGM**

Alberta	3.2	4.0	4.2	-20.7	8.1	6
Fairbanks	0.9	1.3	1.1	-20.8	6.7	5
Klondike	0.5	0.5	1.8	-20.6	7.1	22
North Slope	1.6	1.6	7.8	-21.4	7.7	49
Northwest Europe	0.9	1.0	1.6	-21.4	8.0	10
Old Crow	1.2	1.5	1.5	-21.4	9.5	6
Russian Plain	0.3	0.4	0.3	-20.0	9.5	5
Selawik	1.0	2.0	0.6	-21.8	7.4	3
Taymyr	1.5	1.6	3.2	-21.7	9.1	15
Yakutia	1.2	1.2	4.4	-22.2	9.2	23

Alberta	Fairbanks	0.4	0.2	0.2	0.6	0.6
Alberta	Klondike	0.0	0.1	0.4	1.0	0.9
Alberta	North Slope	0.0	0.0	0.3	0.1	0.2
Alberta	Northwest Europe	0.0	0.0	0.1	0.2	0.2
Alberta	Old Crow	0.1	0.1	0.1	0.3	0.3
Alberta	Russian Plain	0.0	0.0	0.0	0.0	0.0
Alberta	Selawik	0.2	0.0	0.0	0.0	0.0
Alberta	Taymyr	0.0	0.0	0.1	0.0	0.2
Alberta	Yakutia	0.0	0.0	0.0	0.0	0.0
Fairbanks	Klondike	0.0	0.2	0.5	0.5	0.3
Fairbanks	North Slope	0.0	0.0	0.6	0.0	0.1
Fairbanks	Northwest Europe	0.0	0.0	0.1	0.0	0.1
Fairbanks	Old Crow	0.2	0.0	0.0	0.0	0.0
Fairbanks	Russian Plain	0.1	0.0	0.0	0.0	0.0
Fairbanks	Selawik	0.3	0.0	0.0	0.0	0.0
Fairbanks	Taymyr	0.1	0.0	0.0	0.0	0.0
Fairbanks	Yakutia	0.0	0.0	0.0	0.0	0.0
Klondike	North Slope	1.0	0.0	0.5	0.0	0.1
Klondike	Northwest Europe	0.9	0.0	0.0	0.0	0.0
Klondike	Old Crow	1.0	0.0	0.0	0.0	0.0
Klondike	Russian Plain	0.8	0.0	0.0	0.0	0.0
Klondike	Selawik	1.0	0.0	0.0	0.0	0.0
Klondike	Taymyr	1.0	0.0	0.0	0.0	0.0
Klondike	Yakutia	0.9	0.0	0.0	0.0	0.0
North Slope	Northwest Europe	0.4	0.6	0.2	0.9	1.0
North Slope	Old Crow	0.9	0.2	0.1	0.2	0.6
North Slope	Russian Plain	0.4	0.0	0.0	0.0	0.0
North Slope	Selawik	0.8	0.5	0.1	0.4	1.0
North Slope	Taymyr	0.8	0.2	0.3	0.2	0.7
North Slope	Yakutia	0.3	0.0	0.3	0.0	0.5
Northwest Europe	Old Crow	0.8	0.3	0.3	0.2	0.3
Northwest Europe	Russian Plain	0.4	0.0	0.0	0.0	0.0

							Northwest Europe	Selawik	0.8	0.4	0.1	0.2	0.3
							Northwest Europe	Taymyr	0.8	0.3	0.5	0.2	0.2
							Northwest Europe	Yakutia	0.4	0.0	0.1	0.0	0.0
							Old Crow	Russian Plain	0.2	0.0	0.0	0.0	0.0
							Old Crow	Selawik	0.5	0.0	0.0	0.0	0.0
							Old Crow	Taymyr	0.3	0.5	0.7	0.5	0.3
							Old Crow	Yakutia	0.1	0.0	0.1	0.0	0.0
							Russian Plain	Selawik	0.8	0.0	0.0	0.0	0.0
							Russian Plain	Taymyr	0.8	0.0	0.0	0.0	0.0
							Russian Plain	Yakutia	0.5	0.0	0.0	0.0	0.0
							Selawik	Taymyr	0.3	0.2	0.6	0.2	0.1
							Selawik	Yakutia	0.1	0.0	0.3	0.1	0.0
							Taymyr	Yakutia	0.1	0.3	0.5	0.4	0.4
Mastodons Pre-LGM													
Fairbanks	0.1	0.1	0.1	-21.0	4.4	5	Fairbanks	Klondike	0.7	1.0	1.0	0.1	0.0
Klondike	1.6	1.8	3.7	-20.6	4.4	12	Fairbanks	North Slope	0.1	0.0	0.1	0.0	0.0
North Slope	0.3	0.3	0.6	-20.9	3.1	12	Fairbanks	Old Crow	0.8	0.0	0.0	0.0	0.0
Old Crow	1.1	1.6	0.8	-20.1	3.1	4	Klondike	North Slope	0.0	0.0	0.1	0.1	0.3
							Klondike	Old Crow	0.6	0.1	0.1	0.1	0.3
							North Slope	Old Crow	1.0	0.0	0.0	0.0	0.0
Muskox Pre-LGM													
Herschel Island	1.1	1.5	1.2	-19.2	6.9	5	Herschel Island	Klondike	0.6	0.5	0.8	0.3	0.2
Klondike	2.1	2.4	4.2	-19.6	5.8	9	Herschel Island	North Slope	0.6	0.4	0.9	0.2	0.1
North Slope	3.1	3.1	12.0	-19.8	6.3	51	Herschel Island	Taymyr	0.2	0.0	0.0	0.0	0.0
Taymyr	1.2	1.3	2.9	-20.7	5.5	14	Herschel Island	Yakutia	0.6	0.0	0.1	0.0	0.0
Yakutia	2.9	3.0	9.4	-20.7	6.7	30	Klondike	North Slope	0.5	0.7	1.0	0.6	0.3
							Klondike	Taymyr	0.1	0.0	0.0	0.0	0.0
							Klondike	Yakutia	0.5	0.0	0.3	0.0	0.1
							North Slope	Taymyr	0.0	0.0	0.1	0.0	0.5
							North Slope	Yakutia	0.4	0.1	0.4	0.1	0.5
							Taymyr	Yakutia	1.0	0.6	0.9	0.3	0.3
Caribou LGM													

South Central Siberia	0.5	0.6	0.7	-18.3	3.8	7	South Central Siberia	Northwest Europe	0.5	0.0	0.1	0.0	0.0
Northwest Europe	0.9	1.0	3.2	-19.3	3.9	23							
Horse LGM													
North Slope	0.6	0.7	1.3	-20.6	5.8	12	North Slope	Northwest Europe	0.9	0.0	0.0	0.0	0.0
Northwest Europe	0.6	0.7	1.0	-21.1	2.8	9							
Bison Post-LGM													
Alberta	0.5	0.6	0.9	-19.5	2.0	9	Alberta	North Slope	0.5	0.0	0.0	0.0	0.0
North Slope	0.5	0.5	0.5	-20.3	3.0	8	Alberta	Northwest Europe	0.8	0.0	0.0	0.0	0.0
Northwest Europe	0.1	0.1	0.0	-20.0	2.3	3	North Slope	Northwest Europe	0.8	0.0	0.0	0.0	0.0
Caribou Post-LGM													
Fairbanks	1.6	2.4	1.2	-19.5	3.5	4	Fairbanks	North Slope	0.8	0.2	0.1	0.2	0.1
North Slope	2.1	2.7	2.2	-19.0	5.1	5	Fairbanks	Northwest Europe	0.0	0.2	0.8	0.6	0.2
Northwest Europe	0.9	0.9	4.4	-19.6	2.7	93	Fairbanks	South Central Siberia	0.0	0.0	0.0	0.0	0.0
South Central Siberia	0.3	0.3	0.6	-18.6	1.8	14	North Slope	Northwest Europe	0.0	0.0	0.2	0.0	0.1
							North Slope	South Central Siberia	0.0	0.0	0.0	0.0	0.0
							Northwest Europe	South Central Siberia	0.2	0.0	0.0	0.0	0.1
Elk Post-LGM													
Klondike	0.0	0.1	0.0	-19.8	1.7	3	Klondike	Northwest Europe	0.4	0.0	0.2	0.0	0.0
Northwest Europe	1.5	1.6	5.7	-20.4	2.7	32							
Horse Post-LGM													
Alberta	0.7	0.9	1.3	-20.5	0.7	9	Alberta	Fairbanks	0.8	0.0	0.0	0.0	0.0
Fairbanks	0.8	0.9	1.2	-21.0	3.5	8	Alberta	North Slope	0.8	0.0	0.0	0.0	0.0
North Slope	1.4	1.4	4.4	-20.8	5.9	19	Alberta	Northwest Europe	0.8	0.1	1.0	0.1	0.1

Northwest Europe	1.7	1.7	9.9	-20.8	2.2	88	Fairbanks	North Slope	0.5	0.0	0.7	0.0	0.2
							Fairbanks	Northwest Europe	0.4	0.4	1.0	0.2	0.1
							North Slope	Northwest Europe	0.3	0.0	0.4	0.0	0.2
Mammoth Post-LGM													
Russian Plain	1.3	1.4	2.4	-20.1	5.9	11	Russian Plain	Taymyr	0.8	0.0	0.0	0.0	0.0
Taymyr	1.2	1.8	0.9	-21.7	9.6	4	Russian Plain	Yakutia	0.9	0.0	0.0	0.0	0.0
Yakutia	2.6	3.2	3.9	-21.8	8.6	7	Taymyr	Yakutia	0.6	0.5	0.7	0.3	0.2
Muskox Post-LGM													
Herschel Island	0.5	0.8	0.4	-19.7	8.5	4	Herschel Island	Taymyr	0.7	0.0	0.0	0.0	0.0
Taymyr	2.0	2.2	5.3	-20.2	5.5	15							
Moose Holocene													
Klondike	0.8	0.9	1.8	-20.5	2.2	11	Klondike	North Slope	1.0	1.0	1.0	0.2	0.3
North Slope	3.9	4.6	6.9	-20.5	1.8	8							
Muskox Holocene													
North Slope	2.6	3.5	2.6	-19.6	4.9	5	North Slope	Taymyr	0.3	0.0	0.0	0.0	0.0
Taymyr	0.8	1.0	0.9	-20.6	6.0	5							

Legend is the same as the legend in Appendix BB

Appendix EE Results of the mathematical analysis on groups for each species and time period, with the time periods defined using binning approach B.

	SEA	SEA _c	TA	$\delta^{13}\text{C}$	$\delta^{15}\text{N}$	No.	First	Second	SEA _{bprop}	SEA _c overlap(1,2)	TA overlap(1,2)	SEA _c overlap(2,1)	TA overlap(2,1)
Bison Pre-LGM													
Alberta	1.9	2.2	3.3	-19.5	6.7	10	Alberta	North Slope	0.4	0.0	0.3	0.0	0.1
North Slope	2.0	2.0	11.2	-20.1	4.6	60	Alberta	Northwest Europe	0.1	0.0	0.2	0.1	0.3
Northwest Europe	0.9	1.0	2.5	-20.2	5.6	18	Alberta	Yakutia	0.8	0.2	0.0	0.1	0.0
Yakutia	3.2	6.3	1.7	-20.9	6.2	3	North Slope	Northwest Europe	0.1	0.3	0.2	0.5	0.9
							North Slope	Yakutia	0.9	0.4	0.1	0.1	0.3
							Northwest Europe	Yakutia	1.0	1.0	0.1	0.2	0.2
Caribou Pre-LGM													
Alberta	0.1	0.2	0.2	-18.7	4.8	7	Alberta	Fairbanks	0.9	0.0	0.0	0.0	0.0
Fairbanks	1.0	1.3	1.2	-19.5	3.2	6	Alberta	North Slope	1.0	1.0	1.0	0.0	0.0
North Slope	3.7	3.8	14.0	-18.3	3.4	36	Alberta	Northwest Europe	0.9	0.0	1.0	0.0	0.0
Northwest Europe	1.8	1.8	8.8	-19.2	4.3	50	Alberta	South Central Siberia	0.7	0.0	0.0	0.0	0.0
South Central Siberia	0.5	0.6	0.7	-18.3	3.8	7	Fairbanks	North Slope	0.9	0.0	0.6	0.0	0.1
							Fairbanks	Northwest Europe	0.4	0.2	1.0	0.2	0.1
							Fairbanks	South Central Siberia	0.1	0.0	0.0	0.0	0.0
							North Slope	Northwest Europe	0.0	0.1	0.5	0.2	0.8
							North Slope	South Central Siberia	0.0	0.1	0.1	1.0	1.0
							Northwest Europe	South Central Siberia	0.2	0.0	0.0	0.1	0.5
Horse Pre-LGM													
Alberta	1.0	1.1	2.4	-20.3	7.6	17	Alberta	Fairbanks	0.5	0.0	0.0	0.0	0.0
Fairbanks	1.1	1.2	3.4	-21.2	3.5	22	Alberta	North Slope	0.7	0.1	0.5	0.0	0.0
North Slope	1.8	1.8	10.1	-20.9	6.0	64	Alberta	Northwest Europe	1.0	0.3	1.0	0.0	0.0
Northwest Europe	3.4	3.4	17.5	-20.7	5.7	85	Alberta	Selawik	1.0	0.0	0.0	0.0	0.0
Selawik	0.3	0.5	0.1	-21.1	3.5	3	Fairbanks	North Slope	0.8	0.0	0.4	0.0	0.3
							Fairbanks	Northwest Europe	1.0	0.1	0.8	0.0	0.2
							Fairbanks	Selawik	1.0	0.2	0.0	0.1	0.0

							North Slope	Northwest Europe	1.0	0.9	0.9	0.6	0.3	
							North Slope	Selawik	0.9	0.1	0.0	0.0	0.0	
							Northwest Europe	Selawik	0.7	0.1	0.0	0.0	0.0	
Mammoth Pre-LGM														
	Alberta	3.2	4.0	4.2	-20.7	8.1	6	Alberta	Fairbanks	0.4	0.2	0.2	0.6	0.6
	Fairbanks	0.9	1.3	1.1	-20.8	6.7	5	Alberta	Klondike	0.0	0.2	0.5	1.0	0.8
	Klondike	0.7	0.7	2.5	-20.7	7.3	24	Alberta	North Slope	0.0	0.1	0.4	0.1	0.2
	North Slope	1.6	1.6	8.1	-21.4	7.8	50	Alberta	Northwest Europe	0.0	0.0	0.1	0.2	0.2
	Northwest Europe	0.9	1.0	1.6	-21.4	8.0	10	Alberta	Old Crow	0.1	0.1	0.1	0.3	0.3
	Old Crow	1.2	1.5	1.5	-21.4	9.5	6	Alberta	Russian Plain	0.0	0.0	0.0	0.0	0.0
	Russian Plain	0.3	0.4	0.3	-20.0	9.5	5	Alberta	Selawik	0.2	0.0	0.0	0.0	0.0
	Selawik	1.0	2.0	0.6	-21.8	7.4	3	Alberta	Taymyr	0.0	0.0	0.1	0.0	0.2
	Taymyr	1.5	1.6	3.2	-21.7	9.1	15	Alberta	Yakutia	0.0	0.0	0.0	0.0	0.0
	Yakutia	1.2	1.3	5.0	-22.1	9.1	25	Fairbanks	Klondike	0.0	0.3	0.6	0.6	0.3
								Fairbanks	North Slope	0.0	0.0	0.7	0.0	0.1
								Fairbanks	Northwest Europe	0.0	0.0	0.1	0.0	0.1
								Fairbanks	Old Crow	0.2	0.0	0.0	0.0	0.0
								Fairbanks	Russian Plain	0.1	0.0	0.0	0.0	0.0
								Fairbanks	Selawik	0.3	0.0	0.0	0.0	0.0
								Fairbanks	Taymyr	0.1	0.0	0.0	0.0	0.0
								Fairbanks	Yakutia	0.0	0.0	0.0	0.0	0.0
								Klondike	North Slope	0.9	0.0	0.7	0.0	0.2
								Klondike	Northwest Europe	0.8	0.0	0.2	0.0	0.3
								Klondike	Old Crow	1.0	0.0	0.0	0.0	0.0
								Klondike	Russian Plain	0.7	0.0	0.0	0.0	0.0
								Klondike	Selawik	0.9	0.0	0.0	0.0	0.0
								Klondike	Taymyr	1.0	0.0	0.1	0.0	0.1
								Klondike	Yakutia	0.8	0.0	0.0	0.0	0.0
								North Slope	Northwest Europe	0.4	0.6	0.2	0.9	1.0
								North Slope	Old Crow	0.8	0.2	0.1	0.2	0.7
								North Slope	Russian Plain	0.4	0.0	0.0	0.0	0.0
								North Slope	Selawik	0.8	0.5	0.1	0.4	1.0
								North Slope	Taymyr	0.8	0.3	0.3	0.3	0.8
								North Slope	Yakutia	0.2	0.0	0.4	0.0	0.6

								Northwest	Old Crow	0.8	0.3	0.3	0.2	0.3
								Europe						
								Northwest	Russian Plain	0.4	0.0	0.0	0.0	0.0
								Europe						
								Northwest	Selawik	0.8	0.4	0.1	0.2	0.3
								Europe						
								Northwest	Taymyr	0.8	0.3	0.5	0.2	0.2
								Europe						
								Northwest	Yakutia	0.4	0.0	0.4	0.0	0.1
								Europe						
								Old Crow	Russian Plain	0.2	0.0	0.0	0.0	0.0
								Old Crow	Selawik	0.5	0.0	0.0	0.0	0.0
								Old Crow	Taymyr	0.3	0.5	0.7	0.5	0.3
								Old Crow	Yakutia	0.1	0.1	0.4	0.1	0.1
								Russian Plain	Selawik	0.8	0.0	0.0	0.0	0.0
								Russian Plain	Taymyr	0.8	0.0	0.0	0.0	0.0
								Russian Plain	Yakutia	0.5	0.0	0.0	0.0	0.0
								Selawik	Taymyr	0.4	0.2	0.6	0.2	0.1
								Selawik	Yakutia	0.1	0.1	0.3	0.1	0.0
								Taymyr	Yakutia	0.1	0.3	0.7	0.4	0.4
Mastodons Pre-LGM														
								Fairbanks	Klondike	0.7	1.0	1.0	0.1	0.0
								Fairbanks	North Slope	0.1	0.0	0.1	0.0	0.0
								North Slope	Old Crow	0.3	0.3	0.6	-20.9	3.1
								Old Crow	Klondike	1.1	1.6	0.8	-20.1	3.1
									North Slope	0.4	0.4	0.8	-21.0	4.4
									Old Crow	0.5	0.5	0.7	0.5	0.3
									Yakutia	0.1	0.1	0.4	0.1	0.1
									Selawik	0.8	0.0	0.0	0.0	0.0
									Taymyr	0.8	0.0	0.0	0.0	0.0
									Yakutia	0.5	0.0	0.0	0.0	0.0
									Taymyr	0.4	0.2	0.6	0.2	0.1
									Yakutia	0.1	0.1	0.3	0.1	0.0
									Yakutia	0.1	0.3	0.7	0.4	0.4
								Fairbanks	Klondike	0.7	1.0	1.0	0.1	0.0
								Fairbanks	North Slope	0.1	0.0	0.1	0.0	0.0
								North Slope	Old Crow	0.8	0.0	0.0	0.0	0.0
								Old Crow	Klondike	0.0	0.0	0.1	0.1	0.3
									North Slope	0.6	0.1	0.1	0.1	0.3
									Old Crow	1.0	0.0	0.0	0.0	0.0
									Old Crow	1.0	0.0	0.0	0.0	0.0
Muskox Pre-LGM														
								Herschel Island	Klondike	0.7	0.5	0.8	0.3	0.2
								Herschel Island	North Slope	0.8	0.4	0.9	0.1	0.1
								North Slope	Taymyr	0.1	0.0	0.0	0.0	0.0
								Taymyr	Yakutia	0.7	0.0	0.1	0.0	0.0
								Yakutia	Klondike	0.5	0.7	1.0	0.6	0.3
									North Slope	0.0	0.0	0.1	0.0	0.1
									Taymyr	0.5	0.0	0.3	0.0	0.1
									Yakutia	0.5	0.0	0.3	0.0	0.1
									Taymyr	0.0	0.0	0.2	0.0	0.6

							North Slope Taymyr	Yakutia Yakutia	0.4 1.0	0.1 0.8	0.4 0.9	0.1 0.3	0.5 0.3	
Caribou LGM														
Fairbanks	2.1	4.3	1.2	-19.5	3.5	3	Fairbanks	North Slope	0.4	0.0	0.0	0.0	0.0	
North Slope	0.9	1.8	0.5	-19.0	7.6	3	Fairbanks	Northwest Europe	0.0	0.2	0.9	1.0	0.3	
Northwest Europe	0.8	0.8	3.0	-19.3	3.6	27	North Slope	Northwest Europe	0.0	0.0	0.0	0.0	0.0	
Horse LGM														
Fairbanks	0.2	0.4	0.1	-21.1	3.0	3	Fairbanks	North Slope	0.4	0.0	0.0	0.0	0.0	
North Slope	0.8	0.9	1.1	-20.8	6.2	6	Fairbanks	Northwest Europe	0.4	0.6	0.9	0.3	0.1	
Northwest Europe	0.7	0.8	1.7	-21.0	2.9	10	North Slope	Northwest Europe	0.5	0.0	0.0	0.0	0.0	
Bison Post-LGM														
Alberta	0.5	0.6	0.9	-19.5	2.0	9	Alberta	North Slope	0.6	0.0	0.0	0.0	0.0	
North Slope	0.5	0.6	0.5	-20.3	3.0	7	Alberta	Northwest Europe	0.8	0.0	0.0	0.0	0.0	
Northwest Europe	0.1	0.1	0.0	-20.0	2.3	3	North Slope	Northwest Europe	0.7	0.0	0.0	0.0	0.0	
Caribou Post-LGM														
North Slope	0.1	0.2	0.1	-19.0	3.0	3	North Slope	Northwest Europe	0.1	0.1	1.0	0.0	0.0	
Northwest Europe	0.8	0.9	4.2	-19.6	2.6	80	North Slope	South Central Siberia	0.0	0.0	0.0	0.0	0.0	
South Central Siberia	0.3	0.3	0.6	-18.6	1.8	14	Northwest Europe	South Central Siberia	0.2	0.0	0.0	0.0	0.0	
Elk Post-LGM														
Klondike	0.0	0.1	0.0	-19.8	1.7	3	Klondike	Northwest Europe	0.4	0.0	0.2	0.0	0.0	
Northwest Europe	1.5	1.6	5.7	-20.4	2.7	32								
Horse Post-LGM														
Alberta	0.7	0.9	1.3	-20.5	0.7	9	Alberta	North Slope	0.9	0.0	0.0	0.0	0.0	
North Slope	1.6	1.8	4.4	-20.8	5.7	13	Alberta	Northwest Europe	0.8	0.1	1.0	0.1	0.1	
Northwest Europe	1.7	1.7	9.9	-20.8	2.2	86	North Slope	Northwest Europe	0.1	0.0	0.4	0.0	0.2	
Mammoth Post-LGM														
Russian Plain	1.3	1.4	2.4	-20.1	5.9	11	Russian Plain	Taymyr	0.8	0.0	0.0	0.0	0.0	
Taymyr	1.5	3.0	0.8	-22.0	9.3	3	Russian Plain	Yakutia	0.9	0.0	0.0	0.0	0.0	
Yakutia	2.6	3.2	3.9	-21.8	8.6	7	Taymyr	Yakutia	0.6	0.5	0.7	0.4	0.1	
Muskox Post-LGM														
Herschel Island	0.2	0.5	0.1	-19.9	8.7	3	Herschel Island	Taymyr	0.8	0.0	0.0	0.0	0.0	
Taymyr	2.5	2.7	5.0	-20.3	5.3	11								
Moose Holocene														

Klondike	0.8	0.9	1.8	-20.5	2.2	11	Klondike	North Slope	1.0	1.0	1.0	0.2	0.3
North Slope	3.9	4.6	6.9	-20.5	1.8	8							
Muskox Holocene													
North Slope	2.6	3.5	2.6	-19.6	4.9	5	North Slope	Taymyr	0.3	0.0	0.0	0.0	0.0
Taymyr	0.8	1.0	0.9	-20.6	6.0	5							

Legend is the same as the legend in Appendix BB

Appendix FF Results of the mathematical analysis on groups for each species and site, with the time periods defined using binning approach A.

	SEA	SEA _c	TA	$\delta^{13}\text{C}$	$\delta^{15}\text{N}$	No.	First	Second	SEA _{bprop}	SEA _c overlap(1.2)	TA overlap(1.2)	SEA _c overlap(2.1)	TA overlap(2.1)
Bison Alberta													
Pre-LGM	1.9	2.2	3.3	-19.5	6.7	10	Pre-LGM	Post-LGM	0.1	0.0	0.0	0.0	0.0
Post-LGM	0.5	0.6	0.9	-19.5	2.0	9							
Bison North Slope													
Pre-LGM	2.0	2.0	11.2	-20.1	4.6	58	Pre-LGM	LGM	0.8	0.8	0.0	0.8	1.0
LGM	1.0	2.0	0.5	-20.1	4.9	3	Pre-LGM	Post-LGM	0.1	0.1	0.0	0.3	1.0
Post-LGM	0.5	0.5	0.5	-20.3	3.0	8	LGM	Post-LGM	0.1	0.1	0.0	0.4	0.0
Bison Northwest Europe													
Pre-LGM	0.9	1.0	2.5	-20.2	5.6	18	Pre-LGM	Post-LGM	0.7	0.0	0.0	0.0	0.0
Post-LGM	0.1	0.1	0.0	-20.0	2.3	3							
Caribou Fairbanks													
Pre-LGM	0.6	0.8	0.6	-19.4	3.1	5	Pre-LGM	Post-LGM	0.7	1.0	0.8	0.3	0.4
Post-LGM	1.6	2.4	1.2	-19.5	3.5	4							
Caribou North Slope													
Pre-LGM	3.6	3.7	14.0	-18.3	3.3	35	Pre-LGM	Post-LGM	0.8	0.1	0.1	0.1	0.9
Post-LGM	2.1	2.7	2.2	-19.0	5.1	5	Pre-LGM	Holocene	0.1	0.3	0.2	0.5	0.5
Holocene	2.2	2.4	5.6	-18.5	2.2	13	Post-LGM	Holocene	0.0	0.1	0.2	0.1	0.1
Caribou South Central Siberia													
LGM	0.5	0.6	0.7	-18.3	3.8	7	LGM	Post-LGM	0.1	0.0	0.0	0.0	0.0
Post-LGM	0.3	0.3	0.6	-18.6	1.8	14							
Caribou Northwest Europe													
Pre-LGM	1.9	2.0	8.8	-19.2	4.2	44	Pre-LGM	LGM	0.0	0.4	0.4	0.9	1.0
LGM	0.9	1.0	3.2	-19.3	3.9	23	Pre-LGM	Post-LGM	0.0	0.1	0.3	0.1	0.6
Post-LGM	0.9	0.9	4.4	-19.6	2.7	93	LGM	Post-LGM	0.1	0.2	0.6	0.2	0.5
Elk Northwest Europe													
Post-LGM	1.5	1.6	5.7	-20.4	2.7	32	Post-LGM	Holocene	1.0	0.0	0.2	0.0	0.2

Holocene	3.1	3.4	6.1	-22.2	4.5	12								
Horse Alberta														
Pre-LGM	1.0	1.1	2.4	-20.3	7.6	17	Pre-LGM	Post-LGM	0.3	0.0	0.0	0.0	0.0	
Post-LGM	0.7	0.9	1.3	-20.5	0.7	9								
Horse Fairbanks														
Pre-LGM	1.2	1.3	2.1	-21.2	2.7	10	Pre-LGM	LGM	0.1	0.1	0.3	0.2	0.4	
LGM	0.6	0.7	1.6	-21.2	4.0	14	Pre-LGM	Post-LGM	0.5	0.4	0.4	0.6	0.7	
Post-LGM	0.8	0.9	1.2	-21.0	3.5	8	LGM	Post-LGM	0.9	0.6	0.4	0.5	0.5	
Horse North Slope														
Pre-LGM	1.9	1.9	10.1	-21.0	6.1	52	Pre-LGM	LGM	0.1	0.2	0.1	0.5	1.0	
LGM	0.6	0.7	1.3	-20.6	5.8	12	Pre-LGM	Post-LGM	0.5	0.6	0.4	0.7	1.0	
Post-LGM	1.4	1.4	4.4	-20.8	5.9	19	LGM	Post-LGM	0.9	0.7	0.7	0.3	0.2	
Horse Northwest Europe														
Pre-LGM	3.2	3.3	16.0	-20.7	5.7	84	Pre-LGM	LGM	0.1	0.0	0.0	0.0	0.6	
LGM	0.6	0.7	1.0	-21.1	2.8	9	Pre-LGM	Post-LGM	0.0	0.0	0.2	0.0	0.3	
Post-LGM	1.7	1.7	9.9	-20.8	2.2	88	Pre-LGM	Holocene	0.9	0.4	0.1	0.1	0.4	
Holocene	5.8	11.6	3.2	-22.2	5.8	3	LGM	Post-LGM	0.3	0.5	1.0	0.2	0.1	
							LGM	Holocene	1.0	0.4	0.0	0.0	0.0	
							Post-LGM	Holocene	1.0	0.1	0.0	0.0	0.0	
Mammoth Russian Plain														
Pre-LGM	0.3	0.4	0.3	-20.0	9.5	5	Pre-LGM	Post-LGM	0.7	0.0	0.0	0.0	0.0	
Post-LGM	1.3	1.4	2.4	-20.1	5.9	11								
Mammoth Taymyr														
Pre-LGM	1.5	1.6	3.2	-21.7	9.1	15	Pre-LGM	Post-LGM	0.8	0.5	0.1	0.4	0.5	
Post-LGM	1.2	1.8	0.9	-21.7	9.6	4								
Mammoth Yakutia														
Pre-LGM	1.2	1.2	4.4	-22.2	9.2	23	Pre-LGM	Post-LGM	1.0	0.5	0.4	0.2	0.4	
Post-LGM	2.6	3.2	3.9	-21.8	8.6	7								
Muskox Herschel Island														
Pre-LGM	1.1	1.5	1.2	-19.2	6.9	5	Pre-LGM	Post-LGM	0.2	0.0	0.0	0.0	0.0	
Post-LGM	0.5	0.8	0.4	-19.7	8.5	4								
Muskox North Slope														
Pre-LGM	3.1	3.1	12.0	-19.8	6.3	51	Pre-LGM	Holocene	0.5	0.5	0.2	0.4	1.0	
Holocene	2.6	3.5	2.6	-19.6	4.9	5								

Muskox Taymyr

Pre-LGM	1.2	1.3	2.9	-20.7	5.5	14	Pre-LGM	LGM	0.1	0.3	0.5	0.5	0.6
LGM	0.8	0.8	2.3	-20.4	5.9	18	Pre-LGM	Post-LGM	0.9	0.4	0.8	0.3	0.5
Post-LGM	2.0	2.2	5.3	-20.2	5.5	15	Pre-LGM	Holocene	0.7	0.5	0.3	0.6	0.9
Holocene	0.8	1.0	0.9	-20.6	6.0	5	LGM	Post-LGM	1.0	0.7	0.9	0.3	0.4
							LGM	Holocene	0.9	0.7	0.3	0.5	0.9
							Post-LGM	Holocene	0.4	0.2	0.1	0.4	0.8

Legend is the same as the legend in Appendix BB

Appendix GG Results of the mathematical analysis on groups for each species and site, with the time periods defined using binning approach B.

	SEA	SEA _c	TA	$\delta^{13}\text{C}$	$\delta^{15}\text{N}$	No.	First	Second	SEA _{bprop}	SEA _c overlap(1,2)	TA overlap(1,2)	SEA _c overlap(2,1)	TA overlap(2,1)
Bison Alberta													
Pre-LGM	1.9	2.2	3.3	-19.5	6.7	10	Pre-LGM	Post-LGM	0.1	0.0	0.0	0.0	0.0
Post-LGM	0.5	0.6	0.9	-19.5	2.0	9							
Bison North Slope													
Pre-LGM	2.0	2.0	11.2	-20.1	4.6	60	Pre-LGM	Post-LGM	0.1	0.1	0.0	0.3	1.0
Post-LGM	0.5	0.6	0.5	-20.3	3.0	7							
Bison Northwest Europe													
Pre-LGM	0.9	1.0	2.5	-20.2	5.6	18	Pre-LGM	Post-LGM	0.7	0.0	0.0	0.0	0.0
Post-LGM	0.1	0.1	0.0	-20.0	2.3	3							
Caribou Fairbanks													
Pre-LGM	1.0	1.3	1.2	-19.5	3.2	6	Pre-LGM	LGM	0.8	1.0	0.6	0.3	0.6
LGM	2.1	4.3	1.2	-19.5	3.5	3							
Caribou North Slope													
Pre-LGM	3.7	3.8	14.0	-18.3	3.4	36	Pre-LGM	LGM	0.5	0.0	0.0	0.0	0.6
LGM	0.9	1.8	0.5	-19.0	7.6	3	Pre-LGM	Post-LGM	0.1	0.0	0.0	0.1	1.0
Post-LGM	0.1	0.2	0.1	-19.0	3.0	3	Pre-LGM	Holocene	0.1	0.3	0.2	0.5	0.5
Holocene	2.2	2.4	5.6	-18.5	2.2	13	LGM	Post-LGM	0.2	0.0	0.0	0.0	0.0
							LGM	Holocene	0.2	0.0	0.0	0.0	0.0
							Post-LGM	Holocene	0.7	0.2	1.0	0.0	0.0
Caribou South Central Siberia													
Pre-LGM	0.5	0.6	0.7	-18.3	3.8	7	Pre-LGM	Post-LGM	0.1	0.0	0.0	0.0	0.0
Post-LGM	0.3	0.3	0.6	-18.6	1.8	14							
Caribou Northwest Europe													
Pre-LGM	1.8	1.8	8.8	-19.2	4.3	50	Pre-LGM	LGM	0.0	0.3	0.3	0.7	1.0
LGM	0.8	0.8	3.0	-19.3	3.6	27	Pre-LGM	Post-LGM	0.0	0.0	0.3	0.0	0.6
Post-LGM	0.8	0.9	4.2	-19.6	2.6	80	LGM	Post-LGM	0.4	0.2	0.6	0.2	0.5
Elk Northwest Europe													
Post-LGM	1.5	1.6	5.7	-20.4	2.7	32	Post-	Holocene	1.0	0.0	0.2	0.0	0.2

Holocene	3.1	3.4	6.1	-22.2	4.5	12	LGM										
Horse Alberta																	
Pre-LGM	1.0	1.1	2.4	-20.3	7.6	17	Pre-LGM	Post-LGM	0.3	0.0	0.0	0.0	0.0				
Post-LGM	0.7	0.9	1.3	-20.5	0.7	9											
Horse Fairbanks																	
Pre-LGM	1.1	1.2	3.4	-21.2	3.5	22	Pre-LGM	LGM	0.7	0.3	0.0	0.7	1.0				
LGM	0.2	0.4	0.1	-21.1	3.0	3	Pre-LGM	Post-LGM	0.8	0.6	0.4	0.7	1.0				
Post-LGM	0.9	1.1	1.2	-21.0	3.5	7	LGM	Post-LGM	0.5	0.6	0.9	0.2	0.1				
Horse North Slope																	
Pre-LGM	1.8	1.8	10.1	-20.9	6.0	64	Pre-LGM	LGM	0.4	0.5	0.1	1.0	1.0				
LGM	0.8	0.9	1.1	-20.8	6.2	6	Pre-LGM	Post-LGM	0.9	0.7	0.4	0.7	1.0				
Post-LGM	1.6	1.8	4.4	-20.8	5.7	13	LGM	Post-LGM	0.8	0.9	1.0	0.5	0.2				
Horse Northwest Europe																	
Pre-LGM	3.4	3.4	17.5	-20.7	5.7	85	Pre-LGM	LGM	0.0	0.0	0.1	0.0	1.0				
LGM	0.7	0.8	1.7	-21.0	2.9	10	Pre-LGM	Post-LGM	0.0	0.0	0.3	0.0	0.5				
Post-LGM	1.7	1.7	9.9	-20.8	2.2	86	Pre-LGM	Holocene	0.8	0.4	0.1	0.1	0.4				
Holocene	5.8	11.6	3.2	-22.2	5.8	3	LGM	Post-LGM	0.5	0.7	1.0	0.3	0.2				
							LGM	Holocene	1.0	0.4	0.0	0.0	0.0				
							Post-LGM	Holocene	1.0	0.1	0.0	0.0	0.0				
Mammoth Russian Plain																	
Pre-LGM	0.3	0.4	0.3	-20.0	9.5	5	Pre-LGM	Post-LGM	0.7	0.0	0.0	0.0	0.0				
Post-LGM	1.3	1.4	2.4	-20.1	5.9	11											
Mammoth Taymyr																	
Pre-LGM	1.5	1.6	3.2	-21.7	9.1	15	Pre-LGM	Post-LGM	0.8	0.6	0.1	0.3	0.5				
Post-LGM	1.5	3.0	0.8	-22.0	9.3	3											
Mammoth Yakutia																	
Pre-LGM	1.2	1.3	5.0	-22.1	9.1	25	Pre-LGM	Post-LGM	1.0	0.6	0.4	0.2	0.5				
Post-LGM	2.6	3.2	3.9	-21.8	8.6	7											
Muskox Herschel Island																	
Pre-LGM	1.0	1.2	1.2	-19.3	7.0	6	Pre-LGM	Post-LGM	0.4	0.0	0.0	0.0	0.0				
Post-LGM	0.2	0.5	0.1	-19.9	8.7	3											
Muskox North Slope																	
Pre-LGM	3.1	3.1	12.0	-19.8	6.4	52	Pre-LGM	Holocene	0.5	0.5	0.2	0.4	1.0				

Holocene	2.6	3.5	2.6	-19.6	4.9	5								
MuskoxTaymyr														
Pre-LGM	1.0	1.1	3.6	-20.6	5.6	27	Pre-LGM	LGM	0.7	0.3	0.3	0.4	0.8	
LGM	0.8	0.9	1.4	-20.3	6.0	9	Pre-LGM	Post-LGM	1.0	0.6	0.8	0.2	0.6	
Post-LGM	2.5	2.7	5.0	-20.3	5.3	11	Pre-LGM	Holocene	0.9	0.6	0.2	0.7	1.0	
Holocene	0.8	1.0	0.9	-20.6	6.0	5	LGM	Post-LGM	0.9	0.9	0.8	0.3	0.2	
							LGM	Holocene	0.8	0.4	0.2	0.4	0.4	
							Post-							
							LGM	Holocene	0.3	0.2	0.1	0.4	0.6	

Legend is the same as the legend in Appendix BB

Appendix HH Results of the normality tests on all groups of data.

Site	Species	Time Bin	<i>p</i> -value (Bin A)	<i>p</i> -value (Bin B)	
Alberta	Bison	Pre-LGM	0.79	0.79	
		Post-LGM	0.00	0.00	
	Caribou	Pre-LGM	0.23	0.23	
	Horse	Pre-LGM	0.40	0.40	
Fairbanks	Mammoth	Post-LGM	0.52	0.52	
		Pre-LGM	0.15	0.15	
	Caribou	Pre-LGM	0.01	0.04	
		LGM		0.00	
	Horse	Post-LGM	0.02		
		Pre-LGM	0.66	0.08	
	Herschel Island	Mammoth	LGM	0.32	0.00
			Post-LGM	0.09	0.13
Mastodon		Pre-LGM	0.53	0.53	
Muskox		Pre-LGM	0.01	0.01	
Klondike	Muskox	Pre-LGM	0.18	0.16	
		Post-LGM	0.36	0.00	
	Elk	Post-LGM	0.00	0.00	
		Mammoth	Pre-LGM	0.40	0.12
		Mastodon	Pre-LGM	0.07	0.07
North Slope	Moose	Holocene	0.27	0.27	
		Muskox	Pre-LGM	0.12	0.12
	Bison	Post-LGM	0.00	0.01	
		LGM	0.00	0.00	
	Caribou	Pre-LGM	0.00	0.00	
		Holocene	0.00	0.00	
	Horse	Post-LGM	LGM	0.90	0.00
			LGM		0.00
		Pre-LGM	LGM	0.07	0.08
			Post-LGM	0.12	0.25
		Mammoth	LGM	0.01	0.27
			Pre-LGM	0.33	0.48
Pre-LGM			0.05	0.03	
Pre-LGM			0.77	0.77	
Muskox	Moose	Holocene	0.00	0.00	
	Holocene	0.03	0.03		
	Pre-LGM	0.11	0.10		
	Post-LGM	0.00	0.00		
Northwest Europe	Bison	LGM	0.00	0.00	
		Pre-LGM	0.53	0.53	
	Caribou	Post-LGM	0.08	0.29	
		LGM	0.46	0.74	
		Pre-LGM	0.04	0.02	

	Elk	Holocene	0.30	0.30
		Post-LGM	0.02	0.02
	Horse	Holocene	0.00	0.00
		Post-LGM	0.00	0.00
		LGM	0.03	0.11
		Pre-LGM	0.03	0.55
Old Crow	Mammoth	Pre-LGM	0.41	0.41
	Mammoth	Pre-LGM	0.02	0.02
	Mastodon	Pre-LGM	0.01	0.01
Russian Plain	Mammoth	Post-LGM	0.89	0.89
		Pre-LGM	0.01	0.01
Selawik	Horse	Pre-LGM	0.00	0.00
	Mammoth	Pre-LGM	0.00	0.00
South central Siberia	Caribou	Post-LGM	0.07	0.07
		LGM	0.77	
		Pre-LGM		0.77
Taymyr Peninsula	Mammoth	Post-LGM	0.01	0.00
		Pre-LGM	0.07	0.07
	Muskox	Holocene	0.84	0.84
		Post-LGM	0.14	0.31
		LGM	0.52	0.34
		Pre-LGM	0.59	0.16
Yakutia	Bison	Pre-LGM	0.00	0.00
		Post-LGM		
	Mammoth	LGM	0.23	0.23
		Pre-LGM	0.27	0.16
	Muskox	Pre-LGM	0.78	0.78

Appendix II Copyright release

Chapter 3 was published in Scientific Reports. The following is an excerpt from the Scientific Reports website, accessed December 6, 2015:

<http://www.nature.com/srep/journal-policies/editorial-policies#license-agreement>

Scientific Reports does not require authors to assign copyright of their published original research papers to the journal. Articles are published under a CC BY license (Creative Commons Attribution 4.0 International License). The CC BY license allows for maximum dissemination and re-use of open access materials and is preferred by many research funding bodies. Under this license users are free to share (copy, distribute and transmit) and remix (adapt) the contribution including for commercial purposes, providing they attribute the contribution in the manner specified by the author or licensor.

Images from Wikipedia and Biogrounds used in Chapter 6 were all published under the Creative Commons License, as noted on their respective webpages (accessed December 6, 2015).

Artwork commissioned from Katherine Allan was used with permission.

To whom it may concern,

Rachel Schwartz-Narbonne has permission to use any and all artwork commissioned from illustrator Katherine Allan for use in personal, commercial, and published works. This includes, but is not limited to, all commissioned animal drawings and maps.

Signed,

Katherine Allan

Curriculum Vitae

Name: Rachel Schwartz-Narbonne

Post-secondary Education and Degrees: University of Ottawa
Ottawa, Ontario, Canada
2005-2009 B.Sc.

The University of Western Ontario
London, Ontario, Canada
2009-2016 Ph.D.

Honours and Awards: Robert and Ruth Lumsden Graduate Awards in Science
2015

The University of Western Ontario Sustainability and Environment
Research Showcase: Best Faculty of Science Student Poster
2014

Advances in Earth Sciences Research Conference: Best Talk in
Environmental Science, Sustainability and Hydrology; The
University of Western Ontario
2013

8th International Isoecol Conference Student Award: Third-place
Oral Presentation
2012

Western Graduate Thesis Research Award
2011, 2010

Natural Sciences and Engineering Research Council, Postgraduate
Scholarship - Doctoral
2011-2014

Province of Ontario Graduate Scholarship
2010-2011

Natural Sciences and Engineering Research Council, Canada
Graduate Scholarship - Master's
2009-2010

Related Work Experience Teaching Assistant
The University of Western Ontario

2011-2013

Publications:

Schwartz-Narbonne, R., Longstaffe, F.J., Metcalfe, J.Z., and Zazula, G. Solving the woolly mammoth conundrum: amino acid ¹⁵N-enrichment suggests a distinct forage or habitat, *Scientific Reports*, 5, 9791 (2015)

McGilvray, K.L., Fasciani, C. Bueno-Alejo, C.J., **Schwartz-Narbonne, R.**, and J.C. Scaiano. Photochemical strategies for the seed-mediated growth of gold and gold-silver nanoparticles, *Langmuir*, 28, 46 (2012)

Scaiano, J.C., Netto-Ferreira, J.C., Billone, P., Alejo, C.J.B., Crites, C.O.L., Decan, M., Fasciani, C., Gonzalez-Bejar, M., Hallet-Tapley, G., Grenier, M., McGilvray, K.L., Pacioni, N.L., Pardoe, A., Rene-Boisneuf, L., **Schwartz-Narbonne, R.**, Silvero, M.J., Stampelcoskie, K.G., and T.L. Wee. Tuning plasmon transitions and their applications in organic photochemistry, *Pure and Applied Chemistry*, 83, 913 (2011)

Kyser, T.K., Deadea, M., Chipley, D., Alexandre, P., Raycroft, M., Vuletich, A., and **Schwartz-Narbonne, R.** Tracing progressive redox gradients and directions of hydrothermal flow using uranium and lithium isotopes. *Proceedings of the 24th International Applied Geochemistry Symposium* 1, 247 (2009)

+ five presentations and accompanying abstracts at one national and four international conferences since 2011 and two contributions to the LSIS Technical Memoranda series